Chemical Hydride Slurry for Hydrogen Production and Storage

Final Report

Project Title: Chemical Hydride Slurry for Hydrogen Production and Storage

Project Period: January 1, 2004 to June 30, 2008
Date of Report: September 30, 2008

Recipient: Safe Hydrogen, LLC
Award Number: DE-FC36-04GO14011

Working Partners: Hatch Technology LLC, Boston University, Metallurgical Viability, Inc., HERA Hydrogen Storage Systems, Inc.
Cost-Sharing Partners: Safe Hydrogen, LLC, HERA Hydrogen Storage Systems, Inc., Boston University, and Massachusetts Technology Collaborative

Principal Investigator: Andrew W. McClaine, 781-861-7016, AWMcClaine@SafeHydrogen.com

DOE Managers: *DOE HQ Technology Manager*: Grace Ordaz,
DOE Field Project Officer: Jesse Adams/James Alkire

i. Acknowledgements

The Safe Hydrogen team would like to thank the Department of Energy Hydrogen Program Office for the opportunity to evaluate Chemical Hydride Slurry for application as an automotive fuel. In particular, we would like to thank Sigmund Gronich, Sunita Satyapal, Grace Ordaz, Jesse Adams, and James Alkire for their support and advice.

1 Table of Contents

i. Acknowledgements 2
1 Table of Contents 3
ii. Table of Tables 6
iii. Table of Figures 9
2 Executive Summary: 15
3 Project Objective: 17
4 Background: 17
5 Discussion 20
5.1 Task 1 – Development of MgH_2 slurry using techniques developed for LiH slurry 20
5.1.1 Description 20
5.1.2 Summary 20
5.1.3 Discussion 20
5.1.3.1 Overview 20
5.1.3.2 Slurry performance objectives 20
5.1.3.3 MgH_2 Characterization 22
5.1.3.4 Initial Testing Results 27
5.1.3.5 Slurry stability 29
5.1.3.6 Slurry viscosity 29
5.1.3.7 Slurry pumpability 31
5.1.3.8 Hydride Milling 31
5.1.3.9 Bimodal Particle Size Slurry 34
5.1.3.10 Wet Milling 34
5.1.3.11 Evaluation of decomposition of dispersants during reaction 34
5.1.3.12 Slurry age performance 34
5.1.3.13 Task References 35
5.2 Task 2 - Development of slurry mixing system for production of hydrogen 36
5.2.1 Description 36
5.2.2 Summary 36
5.2.2.1 Continuous Mixer 36
5.2.2.2 Semi-Continuous Mixer 36
5.2.3 Discussion 36
5.2.3.1 Overview 36
5.2.3.2 Issues to address 37
5.2.3.3 Continuous Mixer 37
5.2.3.4 Semi-Continuous Mixer 57
5.2.3.5 Analytical and Control System Development 65
5.2.3.6 Estimation of System Energy Density 79
5.3 Task 3 – Slurry and Mixer Testing 84
5.3.1 Description 84
5.3.2 Summary 84
5.3.3 Discussion 84
5.3.3.1 Overview 84
5.3.3.2 Semi-Continuous Mixer Operation 84

5.3.3.3 Hydrogen and Byproduct Analyses 97
5.3.3.4 Residue Recovery 99
5.4 Task 4 – Recycle Slurry Organics 102
5.4.1 Description 102
5.4.2 Summary 102
5.4.3 Discussion 102
5.4.3.1 Solvent refining 102
5.4.3.2 Settling 103
5.4.3.3 Use of Recycled Oils 103
5.5 Task 5 – Produce Magnesium Hydride from Magnesium and Hydrogen 104
5.5.1 Description 104
5.5.2 Summary 104
5.5.3 Discussion 104
5.5.3.1 Current Hydriding Technology 104
5.5.3.2 Initial Hydriding Tests 105
5.5.3.3 Hydriding Mg powder and MgH_2 powder 106
5.5.3.4 Conclusion 106
5.6 Task 6 – Preliminary Designs and Economic Evaluations of $Mg(OH)_2$ Reduction Processes 107
5.6.1 Description 107
5.6.2 Summary 107
5.6.3 Discussion 108
5.6.3.1 Overview of Magnesium Reduction Technologies 108
5.6.3.2 Nozzle Based Carbothermic Process 114
5.6.3.3 Magnesium Chloride Process 133
5.6.3.4 SOM Process 147
5.6.3.5 Initial Magnesium Slurry Process Economic Analyses 158
5.6.3.6 COMPARISON OF ANALYSES 187
5.6.3.7 Efficiency Comparison 200
5.6.4 Conclusions 205
5.7 Task 7 – Experimental Evaluation of the SOM Process – 100 g/day (Provided by Boston University) 207
5.7.1 Description 207
5.7.2 Summary 207
5.7.3 Discussion 207
5.7.3.1 Introduction 207
5.7.3.2 Initial Experiments and Results 208
5.7.3.3 Characterization of Flux Properties 217
5.7.3.4 Proof of Concept for the Low Temperature Flux (LTF) System 220
5.7.3.5 Membrane Stability Using Flux Modification 225
5.7.3.6 Flux Volatility, Conductivity and Viscosity Measurement 226
5.7.3.7 Dissolution Rate of MgO in LTF system 231
5.7.3.8 SOM Process Using Hydrogen Reductant and Tin Anode 232
5.7.3.9 Validation of SOM Process for Continuous Magnesium Production and SOM Process without Reductant 238

5.7.3.10 Scale-up Modeling of SOM Process for Continuous Magnesium Production 253
5.7.3.11 Modeling the 1-tube SOM cell: 257
5.7.3.12 Generation of MgH_2 using Mg-SOM process 262
5.7.3.13 Scale-up Modeling of SOM Process for Continuous Magnesium Production 268
5.7.3.14 Three Tube Design 273
5.7.3.15 Lanthanum Strontium Manganite Coating (LSM) Coating Development 278
5.8 Task 8 – Experimental Evaluation of the SOM Process – 1-5 kg/day 279
5.8.1 Description 279
5.8.2 Accomplishments 279
5.8.3 Discussion 279
5.8.3.1 Boundary Element Method (BEM) 3-D mathematical modeling 279
5.8.3.2 Mg-SOM: Periodic Potentiodynamic Scans 284
5.8.3.3 Determining the source of electronic conductivity in Mg-SOM experiments 285
5.8.3.4 Modeling and Support Experiments 286
5.8.3.5 Scale-up Experiment #1 289
5.8.3.6 Scale-up Experiment #2 295
5.8.3.7 Analysis 298
5.8.3.8 Force Calculation 298
5.8.3.9 Conclusions 299
5.8.3.10 Future Work: 299
5.9 Task 9 – Experimental Evaluation of the Carbothermic Process – 100 gm/day 300
5.9.1 Description 300
5.9.2 Discussion 300
5.10 Task 10 – Experimental Evaluation of the Carbothermic Process – 1-5 kg/day 301
5.10.1 Description 301
5.10.2 Discussion 301
5.11 Task 11 – Recycling Cost Reduction Evaluation 302
5.11.1 Description 302
5.11.2 Summary 302
5.11.3 Discussion 302
5.11.3.1 SOM Process Description 302
5.11.3.2 Automated Recycle of ZrO Tubes 303
5.11.3.3 Use of LSM Coating to Produce Oxygen 303
5.11.3.4 Design for Plant Efficiency 303
5.11.3.5 Magnesium Condensation Process 304
5.11.3.6 Process Modeling 304
5.12 Task 12 – Program Management and Reporting 305
5.12.1 Description 305
5.12.2 Summary 305

6 Key Issues and Future Work 306
6.1 What we have accomplished 306
6.2 Issues and Future Work 307
6.2.1 Water on board vehicle 307
6.2.2 Slurry pumpability in cold climates 308
6.2.3 Size of hydrogen release system 308
6.2.4 Improved definition of costs for hydrogen, slurry, mixer, storage, delivery, distribution, and recycle 308
6.2.5 Byproduct handling within the mixer 309
6.2.6 Reuse of dispersant 309
6.2.7 Slurry pump selection 309
6.2.8 SOM process development 309
6.2.9 Hydrider development 309
7 Patents: 311
8 Publications/Presentations: 312
9 Nomenclature 315
10 References 316
11 Appendixes 318
11.1 Statement of Objectives 318
11.2 Nozzle Based Carbothermic Magnesium Process by Robert Odle PhD, Metallurgical Viability 325
11.2.1 Appendix for Nozzle Based Carbothermic Magnesium Process .. 375

ii. Table of Tables

Table 1 - Calculation of Hydrogen Reacted 60
Table 2 - Chemical Hydride Slurry System Mass and Volume 80
Table 3 - H_2 Sample taken at 14,776 seconds 97
Table 4 - H_2 Sample taken at 20,600 seconds 98
Table 5 - Byproduct Sample #2, Time 19,500 seconds 98
Table 6 - Byproduct Sample #3, Time 21,000 seconds 98
Table 7 - Impurities in the Magnesium (ppm) Produced in the Bench Scale Reactor .. 117
Table 8 - Equipment Costs Grouped by Equipment Types for the NBC Magnesium Plant, part 1 121
Table 9 - Equipment Costs Grouped by Equipment Type for the NBC Magnesium Plant, part 2 122
Table 10 - Installed Equipment Costs by Plant Area, Calcining Plant 123
Table 11 - Installed Equipment Costs for the NBC Magnesium Plant Area by Plant Area, Furnace Plant 124
Table 12 - Installed Equipment Costs for the NBC Magnesium Plant by Plant Area, Utilities. 125
Table 13 - Greenfield Capital Costs and Unit Capital Cost for Making Magnesium via the NBC Magnesium Process 126
Table 14 - Electrochemical Plant Process Flows Summary 134
Table 15 – Financial Inputs 148
Table 16 - Cost Inputs - Capital Costs 149

Table 17 – Cost Inputs – Depreciable and Non-Depreciable Capital Costs 150
Table 18 - Cost Inputs - Fixed O&M 150
Table 19 - Cost Inputs – Feedstock Costs 151
Table 20 - Cost Inputs – Other Raw Materials and Utility Costs 151
Table 21 - Cash Flow Analysis Results 152
Table 22 - Bureau of Mines Study on Carbothermic Reduction of Magnesium – Ore Handling 160
Table 23 - Bureau of Mines Study on Carbothermic Reduction of Magnesium – Magnesium Reduction 161
Table 24 - Bureau of Mines Study on Carbothermic Reduction of Magnesium – Magnesium Refining 162
Table 25 - Bureau of Mines Study on Carbothermic Reduction of Magnesium - Summary 163
Table 26 - Bureau of Mines Study Operating Costs 1966 164
Table 27 - Bureau of Mines Study Operating Costs 1966 Continued 165
Table 28 - Bureau of Mines Study Operating Costs 2002 166
Table 29 - Bureau of Mines Study Operating Costs 2002 Continued 167
Table 30 - Safe Hydrogen Slurry Process Plant Design 169
Table 31 - Safe Hydrogen Slurry Process Plant Design 170
Table 32 - Safe Hydrogen Slurry Process Plant Design 171
Table 33 - Safe Hydrogen Slurry Process Plant Design 172
Table 34 - Safe Hydrogen Process Operating Costs 173
Table 35 - Safe Hydrogen Process Operating Costs Continued 174
Table 36 – Summary of Bureau of Mines Study 175
Table 37 - Safe Hydrogen Recycle Plant Compared to Updated BOM Study 176
Table 38 - Comparison of Bureau of Mines Study and Three $MgCl_2$ Plants 179
Table 39 - Scaling of Bureau of Mines Process 180
Table 40 - Scaling of the Magnesium Alloy Corporation Process 181
Table 41 - Scaling of the Australian Magnesium Corporation Process 182
Table 42 - Scaling of the Noranda Magnola Plant 183
Table 43 - Summary of Costs and Plan Costs 184
Table 44 - Table of Assumptions 188
Table 45 - Process Comparison 192
Table 46 - Magnesium Chloride Process Analysis 193
Table 47 - Magnesium Chloride Hydrogen Cost Calculation 193
Table 48 - SOM Cell Design Assumptions 194
Table 49 – SOM-LSM Based MgH_2 Slurry Plant Magnesium Sub-Process 195
Table 50 - Comparison of SOM Design Options Capital Costs 196
Table 51 - Comparison of SOM Plant Design Options Operating costs 196
Table 52 - Comparison of SOM Plant Design Options Labor costs 197
Table 53 - Comparison of SOM Plant Design Options Cost of Hydrogen 197
Table 54 - Capital and Operating Costs for SOM LSM Plant 198
Table 55 - Labor and Cost Estimate for SOM LSM Plant 198
Table 56 - Transportation Costs 199
Table 57 - Assumptions for H_2 Production and Storage 201
Table 58 - Transportation Assumptions 202

Table 59 - Electrical Energy Generation and Transmission Assumptions 203
Table 60 - Comparison of Efficiencies 204
Table 61 - Comparison of Energy Used by the Process and Greenhouse Gas Emissions 205
Table 62 – Compositions of flux used for membrane stability experiments 225
Table 63 - Constant Model Dimensions Based on the 3-tube SOM Reactor 254
Table 64 - Total Current Density 255
Table 65 - Data used for Figure 142 260
Table 66 - Dimensions Used in Altered Cross-section Geometry 275
Table 67 - Dimensions Used in the Single Tube Model 282
Table 68 - Lead Wire Resistance Averages 287
Table 69 - Dimensions Used in the Single and Triple Tube Models 288
Table 70 - Specifications - Comparison of Single Tube and Triple Tube Mg-SOM Experiment 291

iii. Table of Figures

Figure 1 - Lithium Hydride slurry prepared during previous chemical hydride slurry development program 18
Figure 2 - Lithium Hydride slurry laboratory mixing system mounted in the bed of a Ford Ranger pickup truck to demonstrate its ability to provide hydrogen for a modified IC engine 19
Figure 3 – Typical Slurry Comparison 21
Figure 4 - 70% Magnesium Hydride Slurry Pouring 22
Figure 5 - X-ray diffraction pattern of the “Tego Magnan” powder (Red bars indicate peaks of MgH_2, Green bars indicate peaks of Mg) 24
Figure 6 - Enlarged range of the x-ray diffraction pattern showing major peaks of MgH_2 and Mg 25
Figure 7 - SEM micrograph of the MgH_2 powder 26
Figure 8 - SEM micrograph of the MgH_2 powder 26
Figure 9 - SEM micrograph of the MgH_2 powder 27
Figure 10 - Parr Autoclave Reaction Rate Testing Apparatus 28
Figure 11 - Magnesium Hydride Slurry Pouring 29
Figure 12 - Viscosity Measurements - Reduced Scale 30
Figure 13 - Viscosity Measurement Results Showing Low Temperature Results 30
Figure 14 - MgH_2 powder as received from vendor 32
Figure 15 - After 1 hour of ball milling 32
Figure 16 - After 15 hours of ball milling 33
Figure 17 - Summary of particle size reduction tests 33
Figure 18 - Prototype Continuous Reactor 38
Figure 19 - Positive Displacement Pump System 39
Figure 20 - Second Prototype Continuous Reactor 42
Figure 21 - Continuous Reactor Test Vessel 43
Figure 22 - Continuous Mixer Test Apparatus 44
Figure 23 - Continuous Mixer Design Preheating Both Water and Slurry 45
Figure 24 - Modified Slurry Reactor With Only Water Preheat 48
Figure 25 - Model 2 Continuous Mixer 50
Figure 26 - Model 3 Continuous Mixer 51
Figure 27 - Hydrogen Generation with Continuous Mixer 52
Figure 28 - Continuous Mixer System 53
Figure 29 - Reaction Results from Parr Autoclave Experiment 54
Figure 30 - Reaction Results from Continuous Mixer Experiment 55
Figure 31 - Startup of Continuous Mixer Experiment 56
Figure 32 - Shutdown of Continuous Mixer Experiment 56
Figure 33 - Slurry Piston Pump 58
Figure 34 - Slurry Piston Pump with Parr Autoclave Apparatus 59
Figure 35 - Temperature and Pressure Data from Test 200611291 60
Figure 36 - Schematic of Level Probe 64
Figure 37 - Equivalent Circuit for Level Probe 64
Figure 38 - Comparison of Perfect Gas Law and NIST Data - T vs Difference 66
Figure 39 - Comparison of Perfect Gas Law and NIST Data - P vs Difference 67
Figure 40 - Effect of Compressibility Factor - T vs density 68

Figure 41 - Effect of Compressibility Factor - P vs density 68
Figure 42 - T vs Density using Z Factor derived from 398.15°K Data 69
Figure 43 - P vs Density using Z Factor derived from 398.15°K Data 69
Figure 44 - Notes Tab for the Data Acquisition and Control Program 70
Figure 45 - Auxiliary Oven Control Tab 71
Figure 46 - Shakedown Tab 72
Figure 47 - Control Tab for Control Selection and Data Display 73
Figure 48 - System Diagram Provides and Alternate Display 74
Figure 49 - Diagnostics Tab Provides Array and Error Displays 75
Figure 50 - Control Settings Tab 76
Figure 51 - Second Control Settings Tab 77
Figure 52 - Indices Settings Tab 78
Figure 53 - Effect of Amount of Stored H2 on Gravimetric Energy Density 81
Figure 54 - Effect of Amount of Stored H2 on Volumetric Energy Density 81
Figure 55 - Relative Mass Comparison of Slurry System with Water Recovery 82
Figure 56 - Relative Mass Comparison Excluding Byproduct Mass of Slurry System with Exhaust Water recovery 82
Figure 57 – Relative Mass Comparison of Slurry System in which All Water is Carried 83
Figure 58 - Relative Volume Comparison of a Slurry System in which all Water is Carried 83
Figure 59 - Schematic of the Semi-Continuous Mixer System 86
Figure 60 - Semi-Continuous Mixer System – Front View 88
Figure 61 - Semi-Continuous Mixer - View from Right 89
Figure 62 - Semi-Continuous Mixer - Rear View 90
Figure 63 - Semi-Continuous Mixer - Close-up of Byproduct Recovery Apparatus 91
Figure 64 - Reactor Temperature, System Pressure, and Slurry Injection 92
Figure 65 - Reactor Temperature, Accumulator Temperature, Accumulator Heater, and Reactor Heater 92
Figure 66 - Comparison of Measured and Calculated Hydrogen Production Slurry Flow 2.78 gm/injection 93
Figure 67 - Comparison of Measured and Calculated Hydrogen Production Slurry Flow 3.1 gm/injection 94
Figure 68 – Temperatures 95
Figure 69 - Treactor, Tlevel, and ValveSlurry 95
Figure 70 - Treactor, Pbuffer, H_2 Flow, and ValveSlurry for a Single Cycle 96
Figure 71 - Discharging and Charging of MgH_2 Powder 105
Figure 72 - The Impact of Energy Costs on the Operating Costs 127
Figure 73 - The Impact of the Vacuum Level in the Salt Box Furnace on the Operating Costs 128
Figure 74 - Energy Complex for the Safe Hydrogen Project 130
Figure 75 - Reception and Calcining Processes 140
Figure 76 - MgO Briquetting Process 140
Figure 77 - MgO Chlorination Process 140
Figure 78 - $MgCl_2$ Electrolysis Process 141
Figure 79 - Cost of Hydrogen Using H2A Framework 153
Figure 80 - Tornado Chart with Baseline Cost of Electricity of $0.029/kWh 155

Figure 81 - Tornado Chart with Baseline Cost of Electricity of ~$0.055/kWh 156
Figure 82 – Summary of Costs 184
Figure 83 - Production Cost Drivers 186
Figure 84 - Magnesium Hydride Slurry Process 190
Figure 85 - Magnesium Hydride Slurry Production Process 191
Figure 86 - Cross-sections of the representative areas of the YSZ membranes in contact with the MgF_2-based flux systems at 1300°C 209
Figure 87 - Cross-sections of the representative areas of the YSZ membranes in contact with the MX_2-MgF_2-based flux systems at 1150°C 210
Figure 88 - Schematic of experimental apparatus for measuring current-potential profile as function of various process parameters 211
Figure 89 - Current-potential profile of thesame MgF2-MgO flux system as a function of Argon bubbling rate at 1300°C 211
Figure 90 - Current-potential profile of the MgF_2-MX_2-MgO flux system at 1150°C 212
Figure 91 - Effect of oxygen partial pressure on residual current below the MgO dissociation potential for the system at 1300°C 213
Figure 92 - Effect of cathode area on residual current below the MgO dissociation potential for the system at 1300°C 214
Figure 93 - Cross-sections of the membranes after the experiments conducted with the flux system at 1150°C and 1300°C 215
Figure 94 - Impedance of the cell system measured during the experiment with the flux system at 1150°C 215
Figure 95 - Density of fluoride flux compositions 218
Figure 96 - - Magnesium Fluoride - Calcium Fluoride Phase diagram 218
Figure 97 - Cooling curves for base composition as a function of MgO 219
Figure 98 - Experimental Setup for SOM electrolysis for LTF system 221
Figure 99 - Effect of Partial pressure of magnesium vapor in the SOM reactor on the stability of zirconia 221
Figure 100 - Slow potentio-dynamic scan to estimate the dissociation potential of MgO in LTF system 222
Figure 101 - Fast potentio-dynamic Scan (5mv/sec) for LTF system 223
Figure 102 - Current response during electrolysis at 3 V for LTF system 223
Figure 103 - Periodic Impedance measurements of cell in LTF system (The dotted line indicates the average of measured impedance values) 224
Figure 104 - a) Magnesium Deposit inside condenser b) Chemical analysis (EDAX) of Magnesium deposit in LTF system 224
Figure 105 - Cross-section of YSZ membrane a) before b) after experiment 225
Figure 106 - Cross-sections of the representative areas of the YSZ membranes in contact with the flux compositions 227
Figure 107 - WDS analysis of yttrium content across the membrane cross-section as a function of YF_3 in HTF system (MgF_2-10% MgO) exposed for 40 hours at 1300°C 228
Figure 108 - WDS analysis of magnesium content across the membrane cross-section as a function of YF_3 in HTF system (MgF_2-10% MgO) exposed for 40 hours at 1300°C 228

Figure 109 - WDS analysis of yttrium content across the membrane cross-section as a function of YF_3 in LTF system ({55.5% MgF_2- CaF_2} - 10% MgO) exposed for 40 hours at 1150°C 229
Figure 110 - WDS analysis of Magnesium content across the membrane cross-section as a function of YF_3 in LTF system ({55.5% MgF_2- CaF_2} - 10% MgO) exposed for 40 hours at 1150°C 229
Figure 111 - Experimental setup for high-temperature viscosity measurement 230
Figure 112 - Temperature dependence of viscosity of HTF and LTF system 231
Figure 113 - - Comparison of dissociation potentials of MgO with carbon and hydrogen as reductant at 1150°C 233
Figure 114 - Comparison of vapor pressures of liquid tin and copper 233
Figure 115 - Experimental setup for long-term experiments 234
Figure 116 - Removal of oxygen impurities from the cell after MgO additions 235
Figure 117 - Potentio-dynamic response of SOM cell with liquid Sn anode 236
Figure 118 - Potentio-static response at 3V of SOM scale-up cell 236
Figure 119 - Magnesium deposit from scale-up experiment 237
Figure 120 - Chemical analysis (EDAX) of deposit 237
Figure 121 - Schematic of the SOM experiment reactor 239
Figure 122 - Comparison of dissociation potentials of MgO with carbon and hydrogen as reductant at 1150°C 240
Figure 123 - Comparison of vapor pressures of liquid tin and copper Ohmic resistance of the SOM setup 241
Figure 124 - Equivalent circuit of the SOM cell 241
Figure 125 - Rohmic measurement results by impedance spectroscopy 243
Figure 126 - Removal of oxygen impurities from the cell after MgO addition 244
Figure 127 - Magnesium deposit from scale-up experiment 244
Figure 128 - Chemical analysis (EDAX) of deposit 245
Figure 129 - Schematic of the reactor section of the experiment setup 246
Figure 130 - Comparison of oxygen solubility in copper, tin and silver 247
Figure 131 - Comparison of oxygen diffusivity in liquid copper, tin and silver 247
Figure 132 - Dissociation potentials of MgO without reductant at 1150°C 248
Figure 133 - Potentiostatic response of the SOM cell 249
Figure 134 - Magnesium collected inside the condenser 249
Figure 135 - Dimension A 254
Figure 136 - Total current density for A=0.7in 255
Figure 137 - Total current density for A=0.87in 256
Figure 138 - Total current density for A=1.0in 256
Figure 139 - Total current density for A=1.2in 257
Figure 140 - Detail of the 1-tube cell simulation dimensions 258
Figure 141 - Total current density in the 1-tube SOM cell model (scale to left and bottom of image in meters) 259
Figure 142 - A graph of potential versus calculated total current for the 1-tube Mg SOM cell 260
Figure 143 - Fast potentiodynamic scan (5 mv/s) of a single tube Mg SOM cell 261
Figure 144 - A detailed image of the YSZ membrane subdomain from the 2-D model of a 1-tube Mg SOM cell (scale to left and bottom of image in meters) 262

Figure 145 - Condenser Apparatus 263
Figure 146 - Temperature Profile for the hydrogen feed tube insulated by ceramic shielding 264
Figure 147 - Temperature Profile Comparison 265
Figure 150 - Potentiodynamic Scan (before electrolysis) 266
Figure 151 - Electrolysis Scan 267
Figure 152 - XRD scan of condenser residue 267
Figure 153 - Modeled and Experimental I-V Plot - Single Tube SOM Cell 268
Figure 154 - Schematic of 2-D cross section of cylindrical triple tube cell geometry 269
Figure 155 - Comparison of modeled I-V curves for varying 'A' values 269
Figure 156 - Proposed SOM Reactor (Top and Side Views) 270
Figure 157 - Schematic of 2-D cross section of hexagonal triple tube cell geometry 271
Figure 158 - Cylinder vs. Hexagonal Cathode Geometry – A = 0.7” 271
Figure 159 - Cylinder vs. Hexagonal Cathode Geometry – A = 0.87” 271
Figure 160 - Cylinder vs. Hexagonal Cathode Geometry - A = 1" 272
Figure 161 - Cylinder vs. Hexagonal Cathode Geometry - A = 1.2" 272
Figure 162 - Difference in Total Current between Cylindrical and Hexagonal Cathode Geometries vs. Applied Potential (V). Legend at right indicates ‘A’ value and corresponding color in plot 273
Figure 163 - Dimension ‘A’ in previously modeled triple-tube Mg-SOM cell design 274
Figure 164 - Dimensions 'B' and 'C' in new triple-tube Mg-SOM cell design 274
Figure 165 - Current Density Distribution at B = 1.065"and C = 1.42" (New cell design) 276
Figure 166 - Current Density Distribution at A=1.0" (Old cell design) 276
Figure 167 - Exterior of the triple-tube Mg-SOM cell assembly 277
Figure 168 - Interior of the triple-tube Mg-SOM cell assembly 278
Figure 169 - Mg-SOM 3-D Model Geometry: Single Tube 280
Figure 170 - Mg-SOM 3-D Model Geometry: Triple Tube 280
Figure 171 - Potentiodynamic Scan from Mg-SOM Experiment 281
Figure 172 - Calculated Values for Anode Current using Single Tube BEM Model 282
Figure 173 - Depth of Bubbling Tube Immersion vs. Current Density Difference 283
Figure 174 - Bubbling Tube at 1 inch Immersion 283
Figure 175 - Bubbling Tube at 2 inch Immersion 284
Figure 176 - Periodic Potentiodynamic Scans during Mg-SOM Electrolysis 285
Figure 177 - Plot of Resistance of Components of Experimental Setup 287
Figure 178 - Potentiodynamic Scan from Mg-SOM experiment with single-tube 289
Figure 179 - Calculated Values for Anode Current using Triple Tube BEM Model 289
Figure 180 - Completed Mg-SOM Setup Furnace 290
Figure 181 - Mg-SOM Cell Setup Inside 290
Figure 182 - Cutaway Schematic of the Triple Tube Mg-SOM Setup 291
Figure 183 - Potentiodynamic Scan before Electrolysis 291
Figure 184 - Plot of Current and Time for Electrolysis 292
Figure 185 - Plot of Current and Time for Electrolysis 2 293
Figure 186 - Magnesium Metal Captured in Condenser 294
Figure 187 - Magnesium Deposit on Floor of Condenser 294
Figure 188 - Pre Electrolysis 295

Figure 189 - Potentiodynamic Scan showing Dissociation Potential 296
Figure 190 - Potentiodynamic Scans 296
Figure 191 - Electrolysis Scans 297

2 Executive Summary:

The purpose of this project was to investigate and evaluate the attractiveness of using chemical hydride slurry as a hydrogen storage, delivery, and production medium for automobiles. We focused our attention during this project on the use of magnesium hydride as the chemical hydride to use in the slurry. Two previous projects, performed by Thermo Power Corporation and supported by the Department of Energy, Southern Illinois University, and the California Air Quality Management District evaluated the use of lithium hydride.

To fully evaluate the potential for magnesium hydride slurry to act as a carrier of hydrogen we needed to evaluate potential slurry compositions, potential hydrogen release techniques, and the processes (and their costs) that will be used to recycle the byproducts back to a high hydrogen content slurry. This project was designed to perform these functions and to identify any “show stopper” issues.

The project was quite successful. We achieved or nearly achieved all of our project objectives.

We demonstrated a 75% MgH_2 slurry, just short of our goal of 76%. This slurry is pumpable and storable for months at a time at room temperature and pressure conditions. It has the consistency of paint.

We demonstrated two techniques for reacting the slurry with water to release hydrogen. The first technique was a continuous mixing process that proved to be too complex to reduce to practice in the time available. We tested a continuous mixer system for several hours at a time and demonstrated operation without external heat addition. However, further work will be required to reduce this design to a reliable, robust system. The second technique was a semi-continuous process that can be readily scaled. It was demonstrated on a 2 kWth scale. This system operated continuously and reliably for hours at a time. It was reliably started and stopped. This process could be readily reduced to practice for commercial applications.

We evaluated the processes and costs associated with recycling the byproducts of the water/slurry reaction. This included recovering and recycling the oils of the slurry, reforming the magnesium hydroxide and magnesium oxide byproduct to magnesium metal, hydriding the magnesium metal with hydrogen to form magnesium hydride, and preparing the slurry. We found that the SOM process, under development by Boston University, offers the lowest cost alternative for producing and recycling the slurry. We estimate, using the H2A framework, a total cost of production, delivery, and distribution of $4.50/kg of hydrogen delivered or $4.50/gge. Experiments performed at Boston University have demonstrated the technical viability of the process and have provided data for the cost analyses that have been performed. We also concluded that a carbothermic process could also produce magnesium at acceptable costs.

During the performance of this project, the price of gasoline, the primary competition for hydrogen, has steadily risen. During the summer of 2008 it exceeded $4.00/gallon. The cost estimate for a mature large-scale magnesium hydride slurry system of $4.50 looks quite attractive. The magnesium hydride slurry system is particularly attractive when one recognizes that it is a very low carbon fueling system and relies only on widely available magnesium, water, and electricity that can be produced by renewable sources or nuclear power plants. Magnesium is either the sixth or the eighth most abundant element in the earth’s crust depending on the reference

used. It makes up about 2.9%wt of the crust and about 0.133%wt of seawater. It is widely available. (Reference 1, 2, 3)

The use of slurry as a medium to carry chemical hydrides has been shown during this project to offer significant advantages over alternative techniques for storing, delivering, and distributing hydrogen:

- Magnesium hydride slurry is stable for months and pumpable.
- The oils of the slurry minimize the contact of oxygen and moisture in the air with the metal hydride in the slurry. Thus reactive chemicals, such as lithium hydride, can be handled safely in the air when safely encased in the oils of the slurry.
- Though magnesium hydride offers an additional safety feature of not reacting readily with water at room temperatures, it does react readily with water at temperatures above the boiling point of water. Thus when hydrogen is needed, the slurry and water are heated until the reaction begins, then the reaction energy provides heat for more slurry and water to be heated. In a properly designed system, this process can be used to produce hydrogen as needed.
- The reaction system can be relatively small and light and the slurry can be stored in conventional liquid fuel tanks. When transported and stored, the conventional liquid fuel infrastructure can be used.
- The particular metal hydride of interest in this project, magnesium hydride, forms benign byproducts, magnesium hydroxide (“Milk of Magnesia”) and magnesium oxide.
- We have estimated that a magnesium hydride slurry system (including the mixer device and tanks) could meet the DOE 2010 energy density goals.

During the investigation of hydriding techniques, we learned that magnesium hydride in a slurry can also be cycled in a rechargeable fashion. Thus, magnesium hydride slurry can act either as a chemical hydride storage medium or as a rechargeable hydride storage system. Hydrogen can be stored and delivered and then stored again thus significantly reducing the cost of storing and delivering hydrogen. The further evaluation and development of this concept falls outside the scope of this project and will be performed under another project. However, since the cost of reducing magnesium from magnesium oxide makes up 85% of the cost of the slurry, if hydrogen can be stored many times in the slurry, then the cost of storing hydrogen can be spread over many units of hydrogen and can be significantly reduced from the costs of a chemical hydride system. This may be the most important finding of this project.

If the slurry is used to carry a rechargeable hydride, the slurry can be stored in a conventional liquid fuel tank and delivered to a release system as hydrogen is needed. The release system will contain only the hydride needed to produce the hydrogen desired. This is in contrast to conventional designs proposed for other rechargeable hydride systems that store all the hydride in a large and heavy pressure and heat transfer vessel.

3 Project Objective:

Demonstrate that magnesium hydride slurry can meet the cost, safety, and energy density targets for on-board hydrogen storage of hydrogen fueled fuel cell vehicles.

- Develop stable and pumpable magnesium hydride slurry with energy density of 3.9kWh/kg and 4.8kWh/L
- Develop a compact robust mixing system to produce hydrogen from the slurry and to meet the 2kWh/kg and 1.5kWh/L system targets
- Define and assess the capital and operating costs of the recycling system required to make new magnesium hydride slurry from the materials remaining after the hydrolysis of magnesium hydride slurry and water

4 Background:

Chemical hydride slurry provides a promising means for storing, transporting, and producing hydrogen. As a pumpable medium, it can be easily moved from tank to tank, can be easily metered and can be transported with the existing liquid fuel infrastructure. Magnesium hydride slurry has a high energy density on a materials basis (twice the volumetric energy density of liquid hydrogen and 11.7% hydrogen by mass) and provides significant safety features. The slurry is slow to ignite and is protected from unwanted reaction with ambient moisture by the oil coating on the metal hydride particles. When hydrogen is needed, the chemical hydride slurry is metered into a chemical reaction vessel with water. The reaction between the water and the chemical hydride produces hydrogen. Heat and a hydroxide of the original hydride are byproducts.

$$MgH_2 + 2H_2O \rightarrow Mg(OH)_2 + 2H_2$$

After shedding hydrogen, the hydroxide slurry is returned to a large recycle plant in the vehicles that originally delivered the hydride slurry. Unlike the delivery of gasoline and diesel fuel where tanker trucks return empty, the slurry tanker trucks are full in both directions. In the optimal approach, there should be little additional cost to return the hydroxide slurry. At the recycle plant where large scale processing takes advantage of economies of scale to reduce costs, the hydroxide is separated from the slurry oils, it is reduced to metal, the metal is hydrided to the original chemical hydride, and the chemical hydride is incorporated into new slurry using the original oils. Full cycle efficiency has been estimated to be comparable to liquid hydrogen and significantly better than compressed hydrogen production, storage, and delivery systems. In addition to its use for on-board vehicular storage, the proposed approach may be even more applicable to off-board storage systems, where there are fewer constraints for the additional weight and volume for the water reactant.

Previous work, performed by Thermo Power Corporation, demonstrated that lithium hydride slurry is pumpable, easily metered, stable for months, and much easier to handle than dry powders. Figure 1 displays lithium hydride slurry used in the prior chemical hydride development projects. A simple mixing system was built to demonstrate the capability of producing hydrogen at a wide range of rates sufficient to supply a hydrogen-fuelled vehicle. Figure 2 displays the mixing system mounted in the

bed of a Ford Ranger pickup truck with an IC engine modified to use hydrogen. Since the slurry is easily metered the design of the mixing system is dependent only on the maximum rate required and the minimum amount metered. At the conclusion of the project, the assumptions and design criteria were reviewed to determine if they should have been changed. We concluded that the system could be safer if the reaction between the hydride and water proceeded slowly at room temperature; that the use of a cheaper metal would help the technology to be competitive at a smaller scale; and that the byproduct would be safer if it is less caustic. Some additional experiments indicated that MgH_2 could potentially meet these additional design criteria.

Figure 1 - Lithium Hydride slurry prepared during previous chemical hydride slurry development program

Figure 2 - Lithium Hydride slurry laboratory mixing system mounted in the bed of a Ford Ranger pickup truck to demonstrate its ability to provide hydrogen for a modified IC engine

5 Discussion

5.1 Task 1 – Development of MgH_2 slurry using techniques developed for LiH slurry

5.1.1 Description

The objective of this task is to develop magnesium hydride slurry. Techniques learned during the development of lithium hydride slurry will be applied to the development of magnesium hydride slurry. This task will begin with a study to define the critical issues affecting the feasibility of MgH_2 slurry (ie. agglomeration of particles, hydroxide shells around hydride particles, options for assuring adequate reaction of the MgH_2). A slurry production apparatus will be built and the slurry properties will be monitored and improved during the development effort. Slurry compositions will be evaluated and tested to achieve the same or better slurry stability as previously demonstrated with lithium hydride slurry. At the conclusion of the development effort, a design for an early commercial slurry production facility will be prepared.

5.1.2 Summary

- Slurries of magnesium hydride, light mineral oil or alkanes, and dispersants were prepared and observed over periods up to several months to determine their stability. Some compositions remained fluid and in suspension for several months.
- Slurry compositions as high as 75% MgH_2 have been prepared. Most of our experience is with slurries of 70% MgH_2.
- Slurry viscosities were measured to be similar to SAE 30 oil at room temperature. It has the consistency of paint. Slurry pumping capability was demonstrated over a temperature range of 12° to greater than 80°C.

5.1.3 Discussion

5.1.3.1 Overview

This section describes the work performed and the experience gained in the development of magnesium hydride slurry. We begin with a discussion of what we were looking for in the slurry. This is followed by a discussion of the as delivered MgH_2 powder that was purchased from Goldschmidt in Germany. This is followed by discussions about some of our early test results, slurry stability, viscosity, pumpability, hydride milling, bimodal particle size slurry, wet milling, dispersants, and slurry composition performance.

During the development project, we have achieved slurries of 75% MgH_2. Slurries of 70% MgH_2 have been demonstrated to remain in suspension for months at a time. The slurry is flowable, pumpable, and stable.

5.1.3.2 Slurry performance objectives

To be useful, slurry should be fluid enough to be pumped and stable enough that it will not settle within the time that it is to be used. Some settling can be allowed if the

slurry can be remixed readily with little energy input. If the slurry flows readily, it will flow to the pump inlet and it will be easier to pump.

Slurries are a suspension of solid particles that stay in suspension with the aid of dispersants and/or surfactants. The dispersants/surfactants attach themselves to the particles and keep the particles from agglomerating. When particles in slurries settle, the sample will form either a hard pack or soft pack on the bottom of the vessel with a layer of oil over the pack. Hard pack is dense and difficult to reincorporate back into the slurry. Soft pack is diffuse and easily reincorporated. The layer of oil over the pack will also vary in depth depending on the slurry composition.

During the development of the slurry, we have relied on observable measures to evaluate the capability of the slurry. We have been looking for a slurry that stays in suspension for several days to several weeks or which forms a soft pack that can be readily remixed when it does settle. We have not required sophisticated measurements of the slurry because most of our testing has provided fairly obvious results.

Our initial experience with mixing magnesium hydride powder with mineral oil was that the powder would settle relatively rapidly and form a hard pack that required substantial scraping and stirring to re-entrain the particles. By application of certain dispersants, we first achieved a soft pack settling and then increasing duration of maintaining the particles in suspension. The use of milled magnesium hydride allowed us to increase the concentration of the slurry from 50% to 70% solids loading. Figure 3 displays a typical comparison. Both slurries have been undisturbed for two months. The slurry on the left has a thin layer of oil on the surface. The slurry on the right has a deeper layer of oil on the surface. The slurry on the left is judged to be the better slurry.

Figure 3 – Typical Slurry Comparison

Other characteristics that we observe are that the slurry on the right has formed a soft pack that is readily re-entrained into the slurry when stirred. This is observed by dipping a rod into the slurry and feeling the resistance of the settled material. The slurry on the left did not feel different as the rod was pushed from the top to the bottom. The slurry on the right resisted the rod a bit more toward the bottom.

As we have developed and tested various pump systems, we have observed a variety of characteristics in the slurry performance. Some slurries appear to flow readily and cleanly from storage bottles. Others appear to leave a coating of slurry on the walls of the container. The coatings do not appear to grow in thickness.

We have been evaluating the pumpability of the slurry by testing it with our pumps. As a result, we have not needed to measure the viscosity of the material. The viscosity measurements that we have taken indicate that the slurry is slightly less viscous at room temperature than SAE 30 motor oil at the same temperature. Figure 4 is a picture of a 70% magnesium hydride slurry being poured from a storage bottle into a beaker. The slurry has a fine, smooth texture.

Figure 4 - 70% Magnesium Hydride Slurry Pouring

5.1.3.3 MgH_2 Characterization

Characterization was performed on a batch of magnesium hydride powder sent to HERA Hydrogen Storage Systems by Safe Hydrogen. This section was provided by

HERA Hydrogen Storage Systems. The powder of MgH_2 was produced by Goldschmidt GmbH (product name Tego Magnan, #14E019-000).

5.1.3.3.1 X-ray diffraction

Crystallographic structure of the material was determined by x-ray diffraction. The measurements were performed using a multi-sample BRUKER D8 Discover diffractometer, operating with Cu radiation. The measurements were performed in the 2Theta range between 15 and 80 degrees.

Figure 5 shows the recorded x-ray diffraction pattern, which was interpreted using an ICDD (International Center for Diffraction Data) database. Crystallographic structure of the powder was identified as corresponding to the magnesium hydride, MgH_2. No presence of other phases was detected, apart from a relatively small signal coming from the structure of magnesium (Figure 6). Therefore, it can be concluded that the significant majority of the material consists indeed of magnesium hydride, with a relatively small amount of the un-hydrogenated magnesium.

5.1.3.3.2 Scanning Electron Microscopy

Particle size of the powder of magnesium hydride was determined with the use of a scanning electron microscope (Phillips SM515, operating at the voltage of 15 kV). Figure 7 to Figure 9 show micrographs of the MgH_2 powder. The particle size distribution is relatively homogeneous, with the majority of the particles being smaller than 50 micrometers. There is an interesting feature of elongated shapes of some of the particles, which could be possibly explained by fracturing (or "flaking") of the particles during hydrogenation due to the material expansion. The "flaking" feature can be seen in more detail in the micrograph in Figure 9.

5.1.3.3.3 Surface Area Analysis

The surface area of the MgH_2 powder was measured by using BET Instrument Autosorb 1 from Quantachrome Instruments.

The analysis was performed under the following conditions:
Sample mass: 2.035g
Outgas temperature 120°C
Outgas time: 20hrs
Adsorbate: Nitrogen (cross sectional area=16.2 square angstroms)
11 adsorption points were used in the BET methods

The measured specific surface area of this material is 0.63m^2/g.
The correlation coefficient of the measurement: 0.99962.

It is interesting to note that a similar powder of MgH_2 provided by the same supplier about two years ago exhibited a significantly larger surface area (measured under identical conditions), i.e. 2.5 m^2/g.

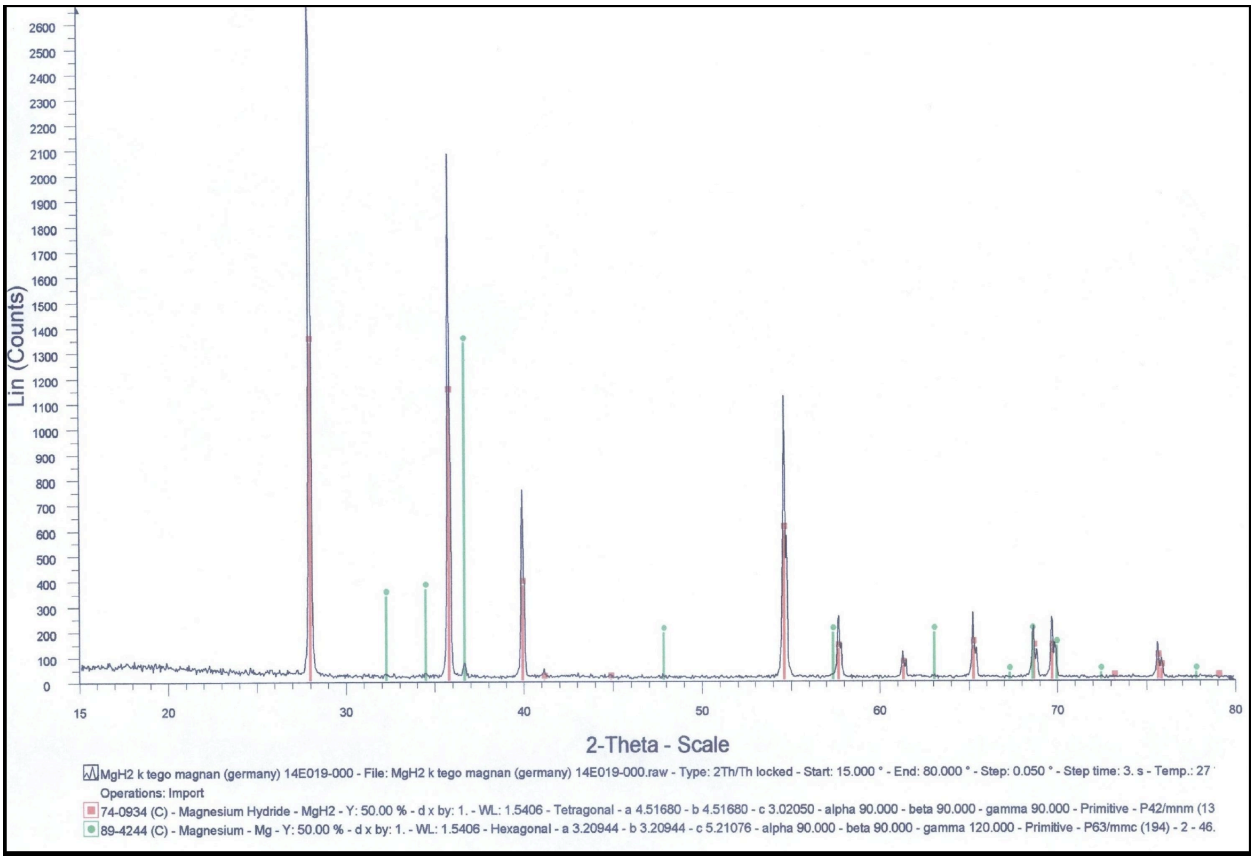

Figure 5 - X-ray diffraction pattern of the "Tego Magnan" powder (Red bars indicate peaks of MgH_2, Green bars indicate peaks of Mg)

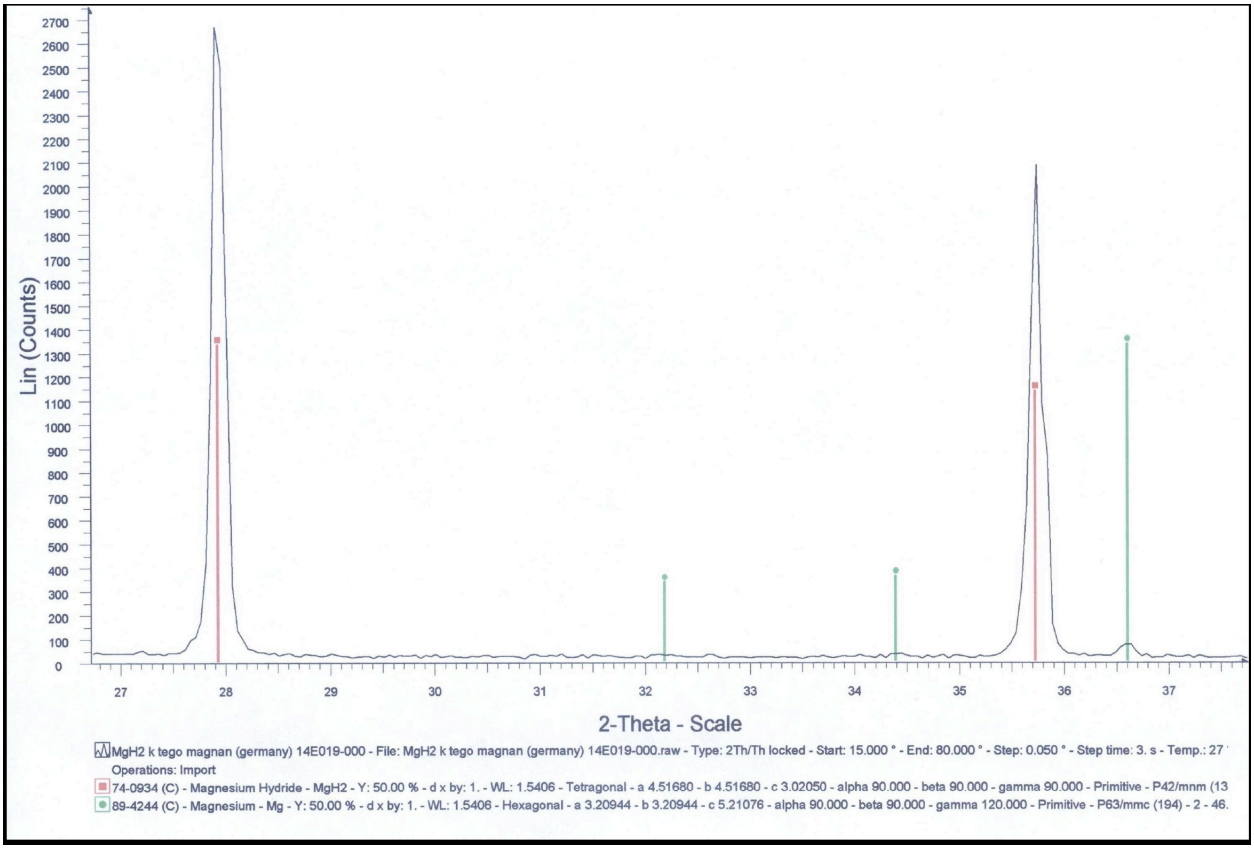

Figure 6 - Enlarged range of the x-ray diffraction pattern showing major peaks of MgH_2 and Mg

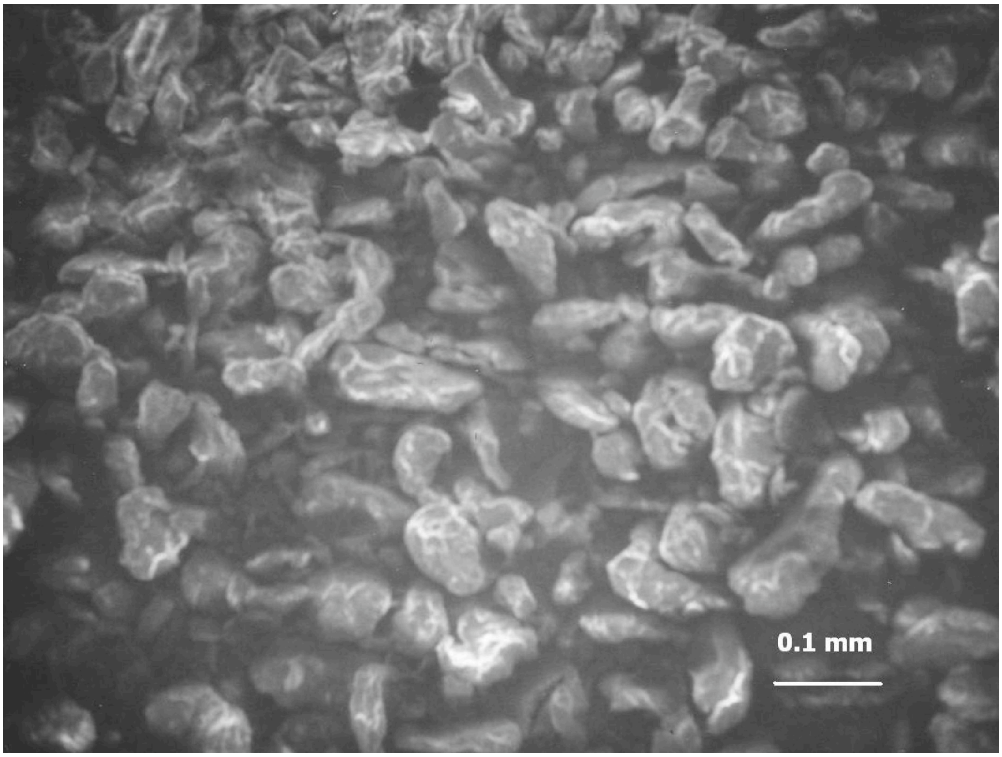

Figure 7 - SEM micrograph of the MgH_2 powder

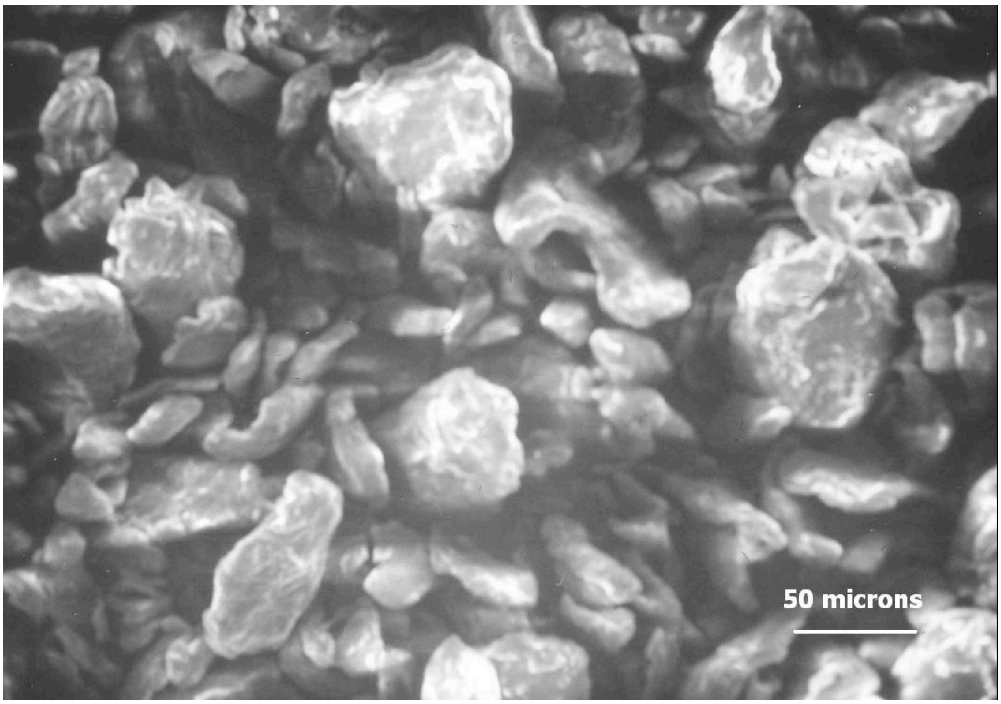

Figure 8 - SEM micrograph of the MgH_2 powder

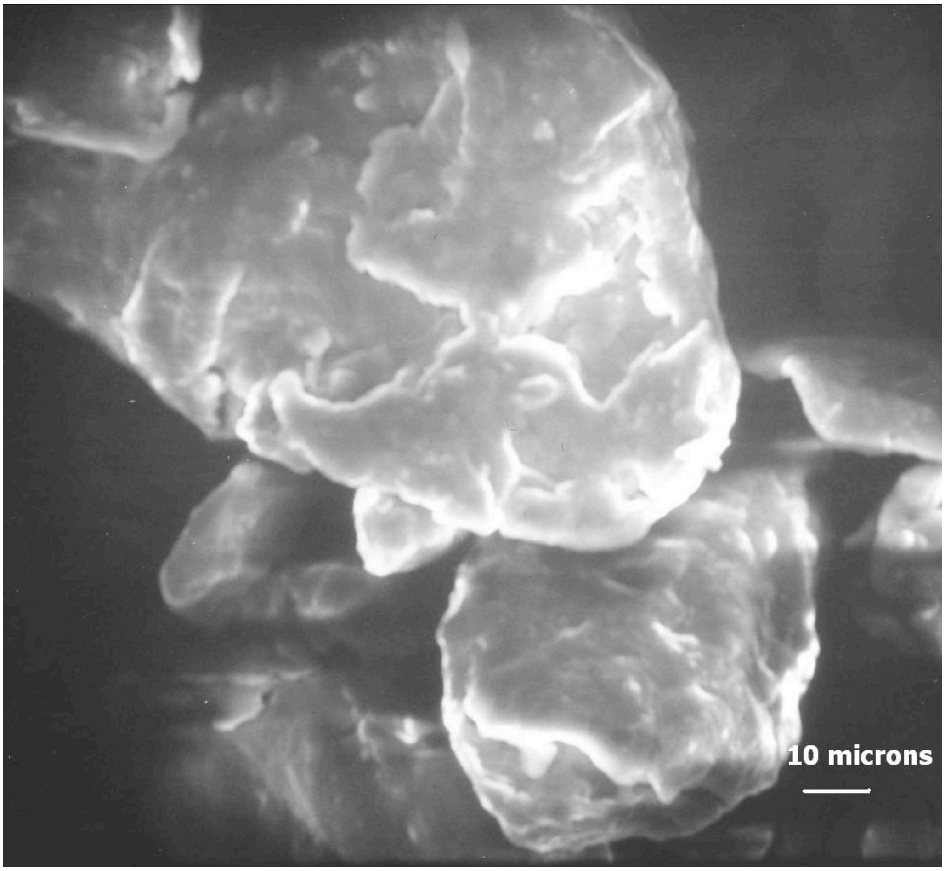

Figure 9 - SEM micrograph of the MgH_2 powder

5.1.3.4 Initial Testing Results

5.1.3.4.1 Slurry Development

The development of slurry is necessarily an iterative process. A slurry composition must be tested for stability and flowability in the slurry laboratory. When a prospective slurry composition is identified, the slurry is tested for reactivity in the Parr autoclave apparatus and then, if the reaction rates are satisfactory, they are tested in the continuous mixer apparatus.

Tests of viscosity, flow-ability, and settling are performed. Slurry compositions consist of magnesium hydride, mineral oil, and one or two dispersants. Our goal is a slurry composition of 76% magnesium hydride by weight. This goal was set based on the results of earlier work performed on lithium hydride slurry. It is based on assumptions that the slurries will be comparable in void fraction and that differences will be due to the differences in particle density. We began our testing of slurries with 50% to 65% magnesium hydride by weight. The choices of dispersants have enormous effects on the slurry composition and performance.

5.1.3.4.2 Dispersant Choice Affects Reaction Rate

The choice of dispersant can affect the reaction rate of the slurry both in a positive and negative manner. Some dispersants are observed to increase the reaction rate between slurry and water. Other dispersants are observed to delay or slow the reaction rate. This effect will influence the design of the continuous mixer by changing the residence time needed in the reactor. So far the reaction rates tested appear to be fast enough to allow compact continuous mixer designs.

Figure 10 displays the Parr autoclave reaction rate testing apparatus. The autoclave is charged with about 12 grams of slurry and 50 grams of water. A rotor is turned at about 400 rpm to stir the mixture and the temperature of the system is increased to a set point of 140°C. A cooling pump cools the contents when the temperature exceeds 150°C. The controller holds the temperature between these two temperatures. The pressure, temperature, and flow rates of hydrogen are monitored during the tests. This information is used to define the reaction rates of the samples.

Figure 10 - Parr Autoclave Reaction Rate Testing Apparatus

5.1.3.4.3 Dispersant Choice Affects Flow-Ability

We have observed that some slurry compositions leave a residue of slurry in the container when poured out and other compositions leave a relatively clean clear bottle. These are flow-ability characteristics.

Figure 11 displays a typical slurry pouring. This sample leaves a residue on the bottle walls. Our continuous mixer tests indicate that the clean wall slurries flow more easily through the mixer.

Figure 11 - Magnesium Hydride Slurry Pouring

5.1.3.4.4 Reaction Completion

With sufficient water, the reaction between water and slurry runs to completion. This was an issue of particular interest as there was an original concern that magnesium hydroxide might form a water impervious shell around unreacted particles within the shell. Measurements of the hydrogen produced from the reaction show that the reaction precedes to completion. The hydrogen measured compares well with that anticipated from the magnesium hydride tested. The measurement of the hydrogen is performed in a water displacement bottle. Corrections to the volume are made for temperature, pressure, and water vapor in the bottle. The resulting hydrogen measured is consistent with the hydrogen anticipated from the mass of magnesium hydride tested.

5.1.3.5 Slurry stability

The slurries that we developed and explored during the course of this project were quite stable. The particles remained in suspension for weeks to months and if there was settling, the particles formed a very diffuse soft pack that flowed readily and could be pumped.

5.1.3.6 Slurry viscosity

The viscosity of the slurry was measured over a range of -43°C to 62°C. Slurry samples were cooled in the freezer for several hours and then viscosity measurements using a Brookfield Model LVDVE115 viscometer. Figure 12 and Figure 13 display the results of the measurements. The viscosity is similar to SAE 30 oil. Two spindles and two rotational speeds were used to span the large temperature range of interest.

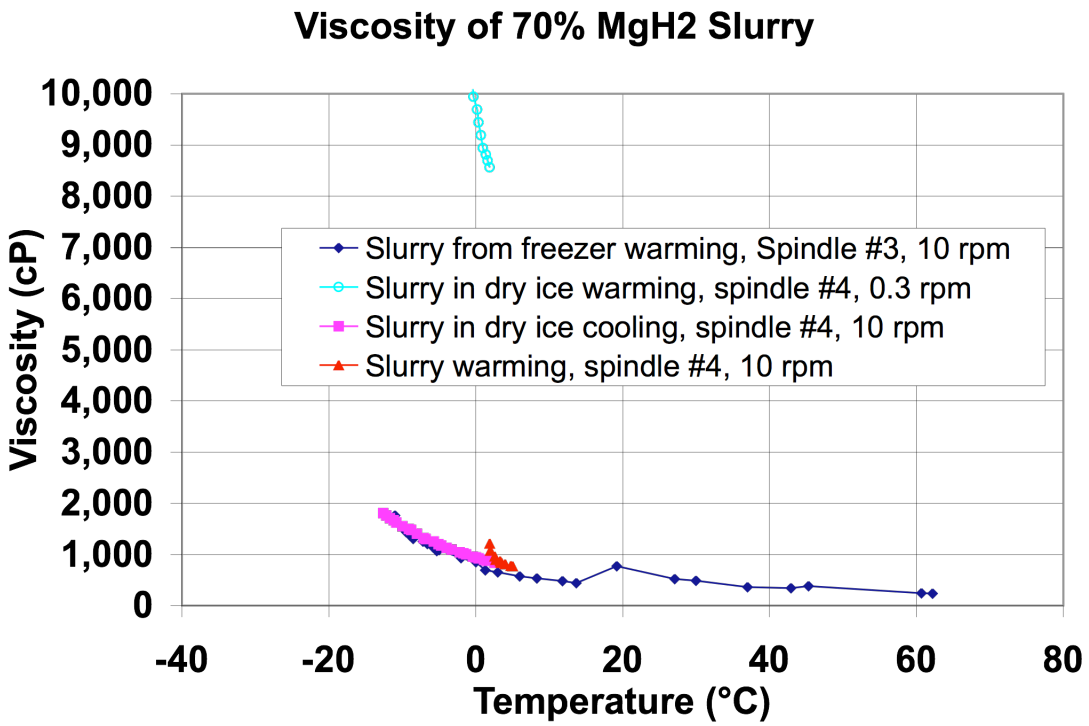

Figure 12 - Viscosity Measurements - Reduced Scale

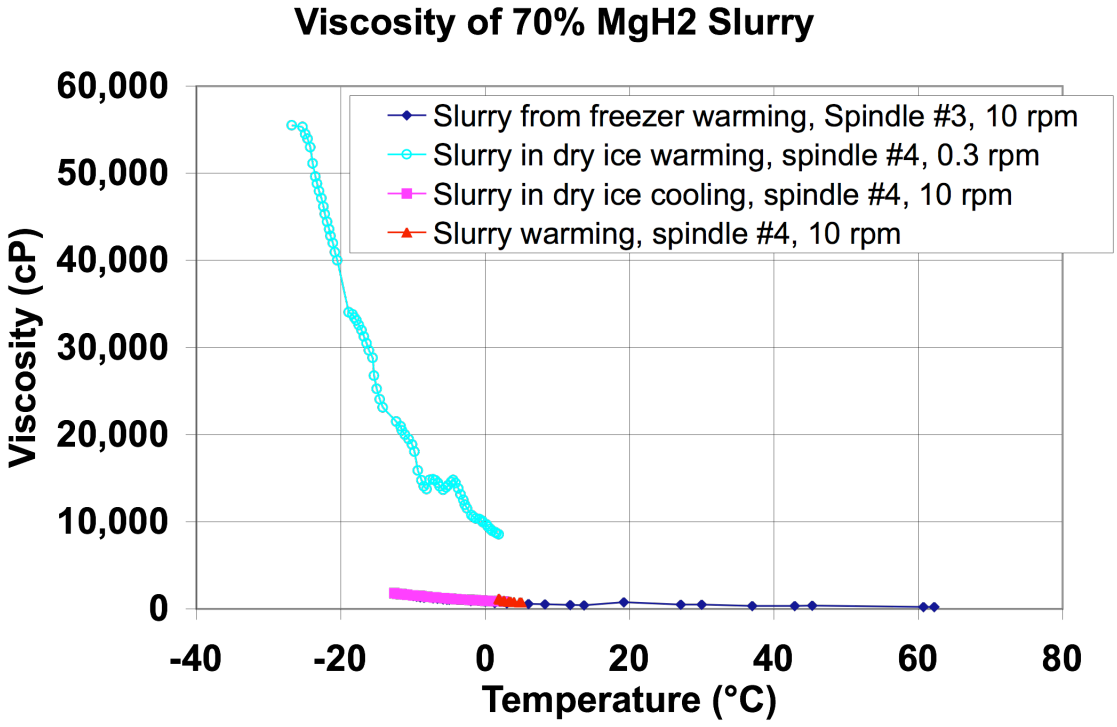

Figure 13 - Viscosity Measurement Results Showing Low Temperature Results

The viscosity measurements indicate that the slurry is a non-Newtonian fluid. A Newtonian fluid would exhibit a consistent viscosity with temperature. The Brookfield guide More Solutions to Sticky Problems, A Guide to Getting More from Your Brookfield Viscometer, defines viscosity as "the internal friction of a fluid, caused by molecular attraction, which makes it resist a tendency to flow." Our Brookfield viscometer measures the shear between layers of slurry as the spindles turn.

A Newtonian fluid follows the relationship:

Viscosity = η = shear stress/shear rate = $\tau/(d\gamma/dt)$

As the shear stress increases at constant shear rate, the viscosity will increase or as the shear rate increases at constant shear stress, the viscosity will decrease. In Newtonian fluids, the shear rate is independent of the viscosity at a given temperature. Water is an example of a Newtonian fluid. In a Newtonian fluid, the viscosity will remain constant despite changes in spindle size or rotational speed.

In non-Newtonian fluids, the shear stress doesn't vary in proportion to the shear rate and the viscosity can change with the selection of spindle size and rotational speed. Reference 4 notes that "Non-Newtonian flow can be envisioned by thinking of any fluid as a mixture of molecules with different shapes and sizes. As they pass by each other, as happens during flow, their size, shape, and cohesiveness will determine how much force is required to move them. At each specific rate of shear, the alignment may be different and more or less force may be required to maintain motion". From the data collected, it appears that the MgH_2 slurry is a pseudo-plastic fluid. The viscosity decreases with increasing shear rate. This is a common characteristic of paints, emulsions, and dispersions. Reference 4 describes these fluids as "shear thinning".

5.1.3.7 Slurry pumpability

A pump system was developed using two cylinders with the pistons joined by a common shaft. The larger diameter cylinder was driven by air to cause the smaller cylinder to pump slurry in and out. This arrangement allowed us to provide extra force on the slurry when needed. This pump system was used to move both water and slurry in our semi-continuous mixer system. It will be described in more detail in that section.

Slurry pumpability has been tested from about 12°C to greater than 80°C without difficulty.

5.1.3.8 Hydride Milling

Magnesium hydride powder has been milled in a 0.5 gallon ball mill using zirconia grinding media that is shaped as cylinders 0.375" diameter by 0.375" tall. The milling process has been performed in steps ranging from 1 hour to 5 hours. At the completion of each step, the mill was opened and a sample of the powder was removed for particle size analysis using a Horiba LA-910 Particle Size Distribution Analyzer. Figure 14 through Figure 16 display the particle size frequency vs size as received, after 1 hour, and after 15 hours. The initial sample showed two particle size peaks at 100 and 400 microns. After 1 hour the 400 micron particles were removed from the powder. After 15 hours, the particle size of the material was reduced to less than 4 microns. Figure 17 displays a summary of the results obtained in these measurements. It appears that the particles are continuing to be reduced in size with continued milling.

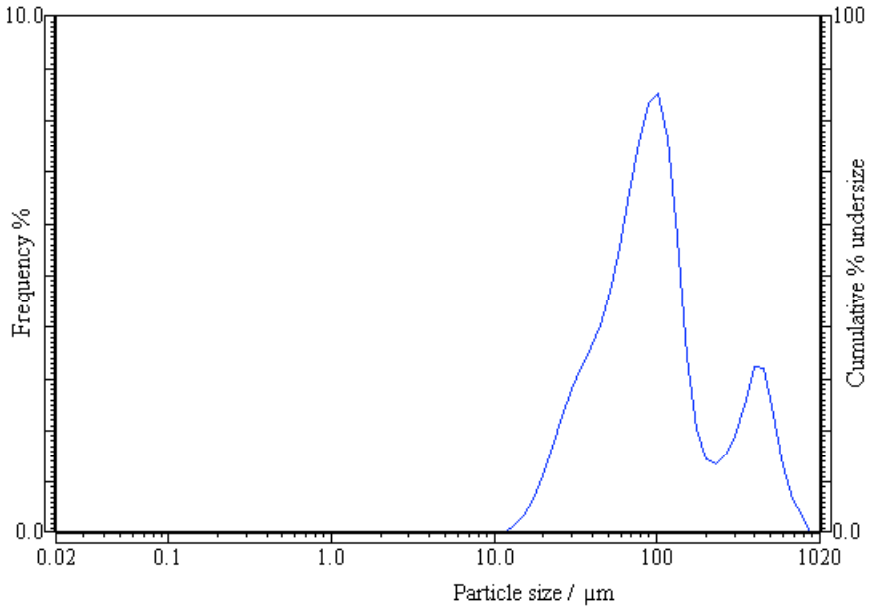

Figure 14 - MgH_2 powder as received from vendor

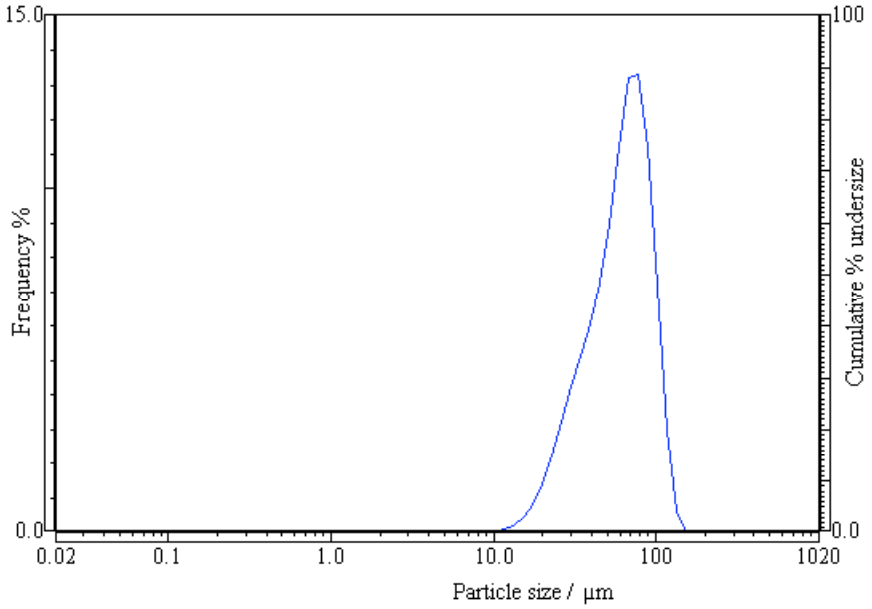

Figure 15 - After 1 hour of ball milling

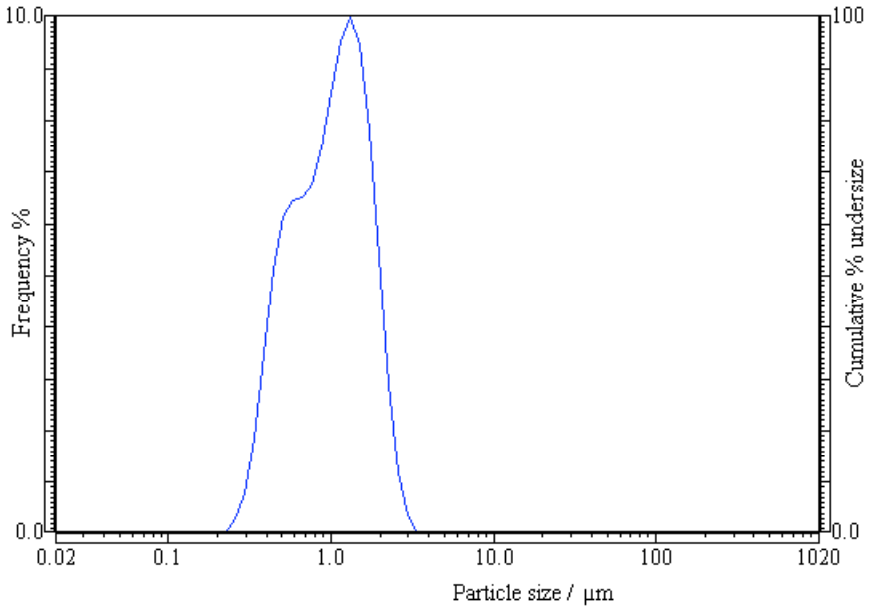

Figure 16 - After 15 hours of ball milling

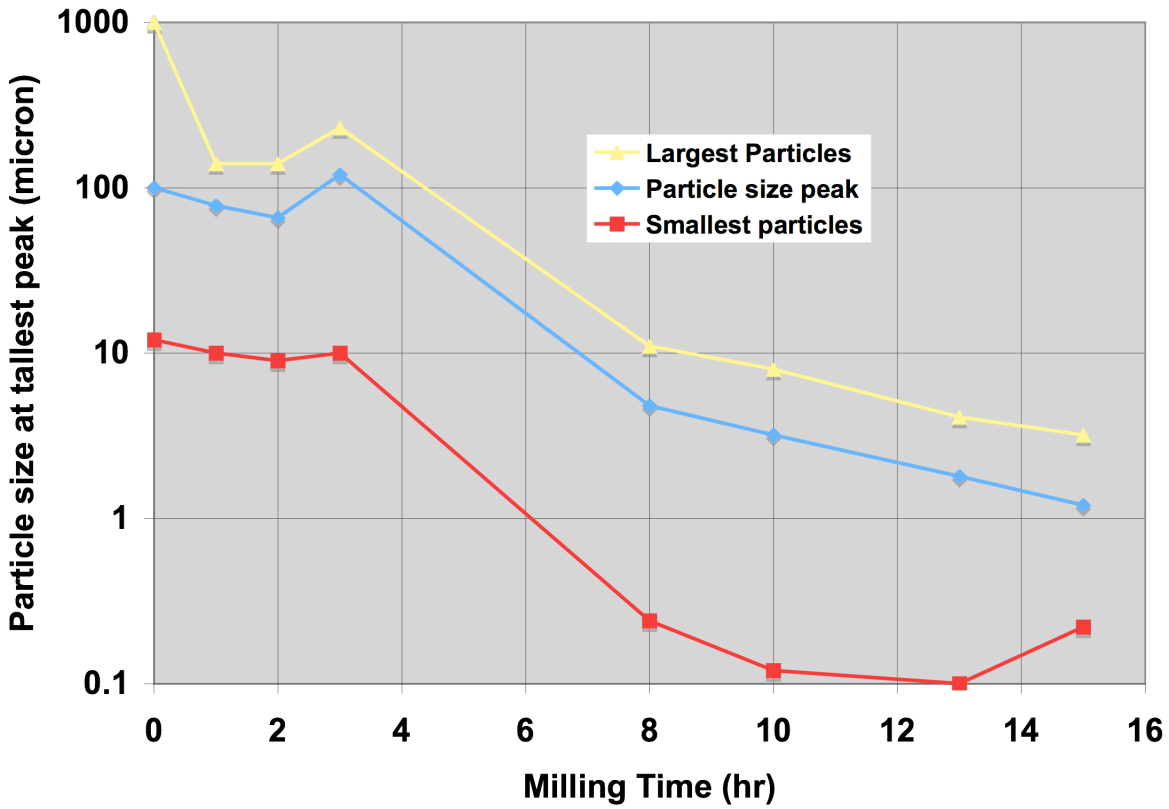

Figure 17 - Summary of particle size reduction tests

After 15 hours, the milling test was stopped to evaluate the effect of milling on slurries of the milled particles. The milling had a significant effect on the stability of the

slurry produced using one of the favored compositions. This slurry has remained in suspension for several months.

5.1.3.9 Bimodal Particle Size Slurry

We also prepared slurries with bimodal particle size distributions. We tested slurries made with milled powders that had been milled for periods of 1 hr, 3 hrs, and 5 hrs. These milled powders were mixed with unmilled powder. All of the bimodal powder combinations have stratified after a week. The 70% slurries made with powder milled for 5 hours have remained in suspension for several weeks. We also observed that the bimodal slurries were sticking to the sides of the container if there was more than 50% of milled powder in the mixture.

5.1.3.10 Wet Milling

A cost saving option of slurry preparation involves milling the "wet" ingredients for the slurry. Wet milling promised to offer advantages to the slurry production system by allowing coarsely milled MgH_2 to be incorporated into a slurry so that it could be pumped into and out of the ball mill apparatus. Such a system might be cheaper than a dry milling system since it would involve pumps rather than dry powder handling systems. We found that we could not save time by doing this as it appears that the milling times are longer. Also, it proved difficult to remove the thinning agent, hexane, from the slurry when the MgH_2 was reduced in size. Hexane was added to the slurry to reduce the viscosity of the larger particle slurry so that it would flow within the ball mill. The plan was to remove the hexane after the particle sizes were reduced sufficiently to form the 70% slurry.

Further, discussion about size reduction systems identified a system that may be as simple as the wet milling concept. A flow-through ball mill can be used to mill large particle MgH_2. A flow of non-reactive gas, such as argon, through the mill should carry milled MgH_2 out of the mill and into a cyclone separator where it can be separated and mixed with oil and dispersants to form the final slurry.

5.1.3.11 Evaluation of decomposition of dispersants during reaction

During our testing of slurry in the semi-continuous reactor, we have observed that sometimes the byproducts of the reaction are grey to black and sometimes they are white. To evaluate this effect, we performed a test using 50% MgH_2 slurries. One was with no dispersant, one was with only our first dispersant, and one was with only our second dispersant. The slurry with no dispersant and the slurry with our first dispersant produced white byproduct. The slurry with our second dispersant produced black byproduct. We changed the standard slurry for testing to use only our first dispersant.

5.1.3.12 Slurry age performance

Several batches of slurry were made for reactor testing. The hydrogen produced in the reactor depended only on the amount of slurry injected. Slurries made months before or made from MgH_2 that was milled months before behaved the same as slurries made with fresh ingredients.

5.1.3.13 Task References

4. More Solutions to Sticky Problems, A Guide to Getting More from Your Brookfield Viscometer, Brookfield Engineering Laboratories, Inc.

5.2 Task 2 - Development of slurry mixing system for production of hydrogen

5.2.1 Description

The objective of this task is to improve the performance of the mixing system originally prepared for lithium hydride slurry and to extend its use for magnesium hydride slurry. Specific targets are to reduce the size of the system, to improve the handling of materials within the system, and to modify the system for use with magnesium hydride slurry. Starting with the existing mixing system, an experimental development effort will be carried out to test alternate mixing technologies and material handling techniques. Two mixer designs are planned for this task. The first design will take advantage of the results of the initial experiments. The second design will improve upon the first for robustness and reliability. This task will be performed over two years. During the first year, testing of the model #3 mixing system will be completed.

5.2.2 Summary

5.2.2.1 Continuous Mixer

- Performed tests where both water and slurry were heated from the reaction heat
- Performed tests where only water was heated from reaction heat
- Showed that slurry can be turned on and off reliably
- Experimented with variations on the mixing section

5.2.2.2 Semi-Continuous Mixer

- Tested semi-continuous mixer for several multi-hour tests
- Demonstrated design condition of greater than 10 L/min hydrogen production
- Demonstrated operation with no additional heat after startup
- Tested water reclamation from byproducts
- Tested oil and solids reintegration

5.2.3 Discussion

5.2.3.1 Overview

After review of the original mixing system used in the lithium hydride slurry project, the design team decided to experiment with a modification of the continuous mixer system originally developed for lithium hydride slurry. The new system was designed for a 2 kWth hydrogen production rate. This is equivalent to about 10 L/min of hydrogen production. This apparatus demonstrated the capability of the concept. However, difficulties in the design of the mixing section involving two-phase flow prevented us from achieving reliable and consistent operation. Additional design work will be required to define ways of moving the liquid and gaseous components of the system through the mixer continuously. The continuous mixer system was set aside while a second design, referred to as the semi-continuous mixer, was tested and verified. The continuous mixer system offers compactness. More design will be required to reduce it to practice however.

The semi-continuous mixer was demonstrated to be consistent and reliable. It is not as compact as the continuous system but allowed us to produce hydrogen consistently and to investigate methods of handling the byproducts of the reaction. Byproduct handling was an issue that was not addressed during the LiH slurry project.

5.2.3.2 Issues to address

For the production, delivery, and distribution of hydrogen, chemical hydride slurry offers significant safety, density, and cost advantages. Magnesium hydride slurry has very slow reaction rates at normal temperatures and pressures. This means that spills will not produce large quantities of hydrogen and that the charged slurry is not a reactive hazard. The byproducts of reaction are benign consisting of magnesium oxide and magnesium hydroxide (Milk of Magnesia) and mineral oil. The slurry carries a high energy density of stored hydrogen. At 70% MgH_2, the slurry has a gravimetric energy density of 12.8 MJ/kg and a volumetric energy density of 15.3 MJ/L. Because it can be transported using conventional liquid fuels infrastructure, the cost of moving the slurry around is low. TIAX estimated about \$0.25/kg H_2 per 100 km.

For automotive applications, chemical hydride slurry using magnesium hydride slurry should be capable of meeting the DOE 2010 energy density goals. These goals require that the slurry system, including all slurry, water, and tanks meet the goals. As the program progressed, the automobile industry developed other criterion that have not been fully addressed by this project.

It was important in this task to investigate and demonstrate that magnesium hydride based chemical hydride slurry can produce hydrogen as needed by mixing the slurry with water. Since some of the safety characteristics of magnesium hydride slurry rely on its very very slow reactivity at normal temperatures and pressures, it is necessary to show how the reaction temperatures can be maintained at reaction conditions. It is also necessary to evaluate how much energy is required to achieve stable operation.

It is also necessary to show how the system will maintain its water balance and how the byproducts can be handled.

There are a considerable number of other issues that remain to be addressed. But this project has achieved the goals that it set out to accomplish.

5.2.3.3 Continuous Mixer

5.2.3.3.1 First Model Continuous Mixer System Design And Operation

INTRODUCTION

The original concept of the continuous mixer was to inject the slurry and water through a nozzle to promote mixing and to react the mixed reactants in a tube downstream of the nozzle. The prototype reactor was constructed from stainless steel tubes mounted concentrically in standard compression fittings so that water needed for the reaction was conducted through an annulus surrounding the reaction zone (see Figure 18)

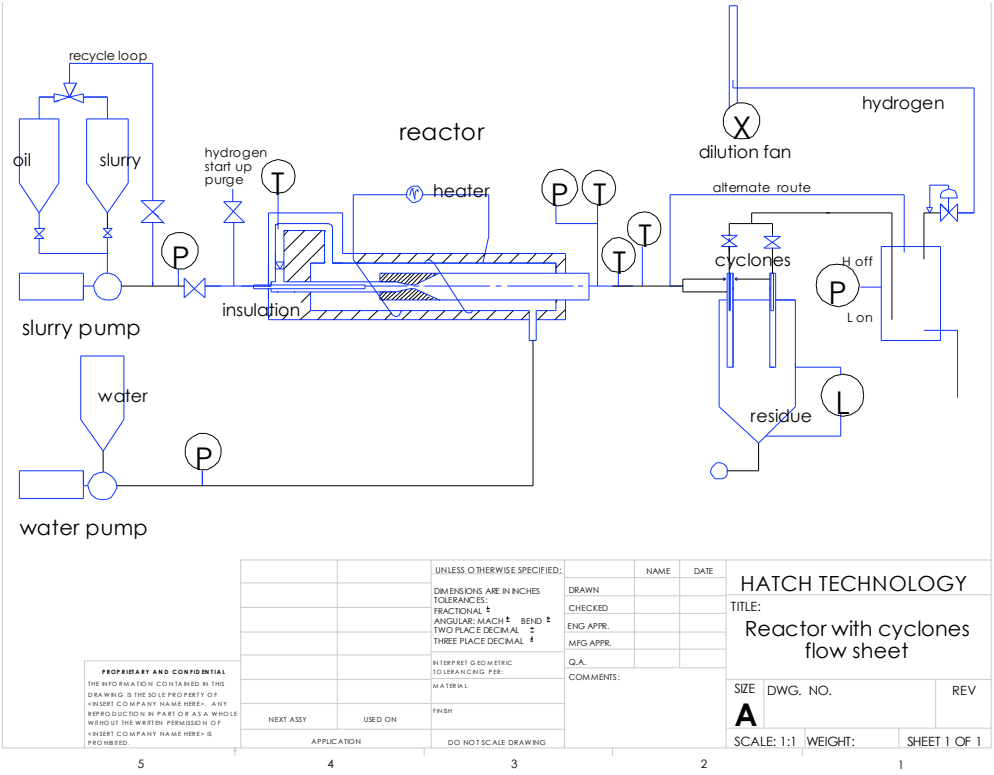

Figure 18 - Prototype Continuous Reactor

The purpose of this initial set up was to try to achieve a self-sustaining continuous reaction between slurry and water where the heat of reaction was collected and used to preheat the incoming reactants to a temperature for fast evolution of hydrogen.

The magnesium hydride slurry was added to the reactor through an injection tube that passed through the heated water for temperature equalization before being released for mixing in the reaction zone. The reacting components progressed through the discharge tube into the separating vessel where spent solid residue was collected and the hydrogen released through a back pressure control valve to discharge to atmosphere through a forced air dilution pipe.

EQUIPMENT DESCRIPTION

PUMP SECTION

Two electrically driven progressive cavity pumps, one for water the other for slurry were mounted on a structural framework which also held reservoirs for water, slurry and mineral oil (Figure 19). The water was delivered to a connection near the discharge end of the reactor. The slurry pump was connected to the injection tube at the start of the reactor. Interconnecting tubing and valves allowed the slurry pump to draw from the oil reservoir and from the slurry reservoir. A return loop in front of the reactor allowed the slurry pump to recycle back to the reservoirs. After a run, if an extended shut down was anticipated, the lines and pump could be cleared of slurry and filled with oil.

These pumps have a positive displacement characteristic where the volume flow rate is directly proportional to the pump speed. A variable frequency drive control was used for each pump so that after calibration checks, the flow rate for each reactant could be closely and independently controlled.

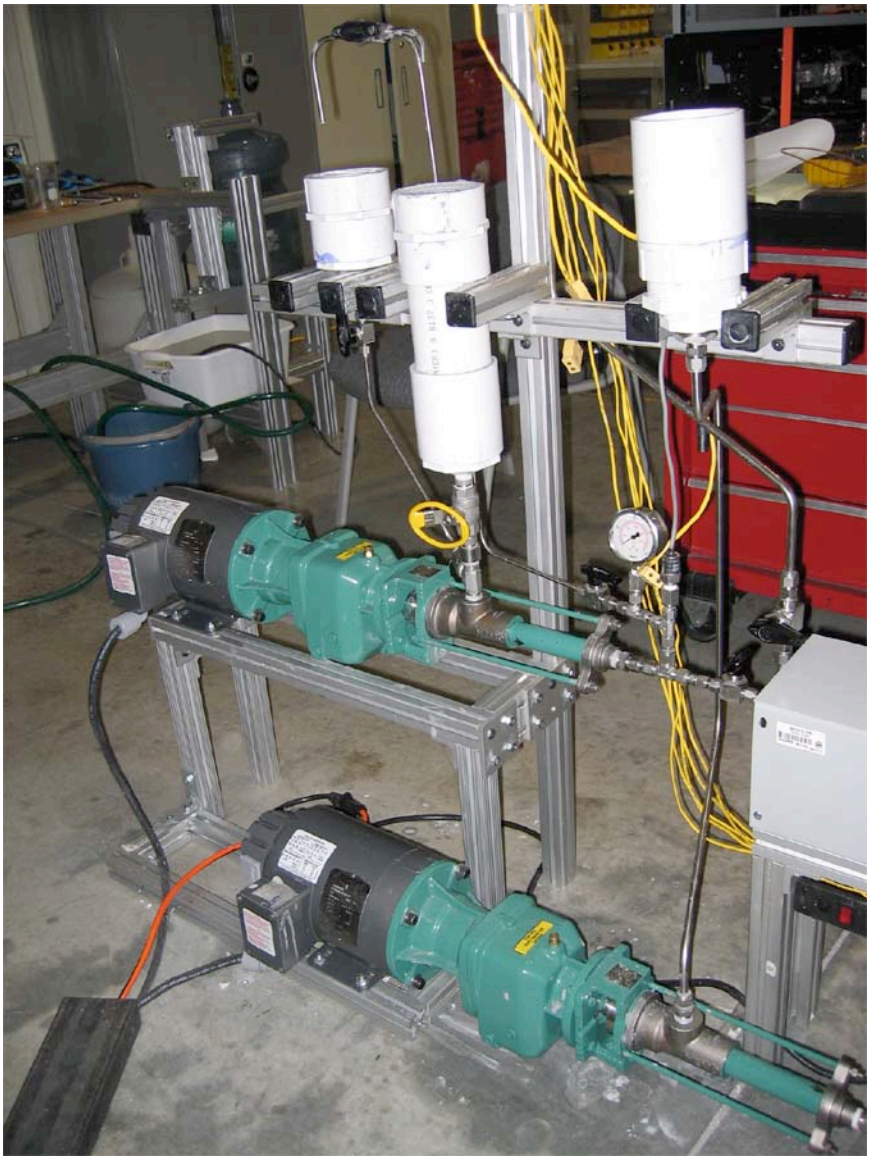

Figure 19 - Positive Displacement Pump System

REACTOR SECTION

Slurry entered the reaction zone after traveling along to the exit holes at the end of a 0.125” diameter tube mounted concentrically with the 0.25” diameter reaction tube. Preheated water fed to the 0.25” diameter tube traveled along the outside of the injection tube to heat up the slurry before the two reactants met. The reacting components passed through a venturi shaped nozzle to promote further turbulence for mixing and continuation of the reaction within the 0.375”diameter discharge tube. Heat

from the exothermic reaction passed through the walls of the discharge tube into an annulus formed between it and a 0.5”diameter concentric tube containing the incoming water which was transported to the inlet end of the reactor. A 130W heating tape was wrapped around the 0.5” diameter tube for preheating the system at start up.

The reactor section was set in a steel box and packed around with insulation to reduce heat losses from the system. The discharge tube leading from the box was fitted with an insulation sleeve for personnel protection.

A thermocouple measured the water temperature after its preheat and was used to control a relay to switch off of the electrical heater after its preset temperature had been reached. Three more thermocouples at intervals in the discharge tube were used to measure the temperature of the reaction materials as they moved towards the separation section.

SEPARATION SECTION

It was intended that the products of the reaction would be lead into cyclone separators for collection of the solid residue and for passing just gaseous hydrogen saturated with water vapour into a hydrogen storage vessel. For initial simplicity of equipment operation it was decided to omit the cyclones and lead all the reaction products directly to the storage vessel. It is intended to reintroduce the cyclones when the initial reaction process is better defined.

The 0.375” diameter discharge tube turns down in the top of the storage vessel, which promotes the separation and collection of solid and liquid components in the bottom of the storage tank. A thermocouple measures the temperature in the storage vessel.

Hydrogen leaves at the top of storage vessel through a backpressure regulator and water trap. It was disposed of to the atmosphere at low pressure through the side of a 3” pipe. A ventilation fan was connected to the 3” pipe to provide dilution air to ensure the discharge was well below the flammable limits for hydrogen. Dilution of the hydrogen in the air reduces the concentration of hydrogen in air below the lower ignition level.

INITIAL OPERATION

SAFETY CHECK

The system component with the lowest allowable working pressure is the separation vessel at 135 psig. Prior to operating with slurry the whole system was filled with water and the positive displacement water pump was used to raise the pressure to 205 psig, 1.5 times the allowable working pressure, and held for 1 hour. This confirmed that the available maximum pressure for safe system operation would be 135 psig. During operation, the water is forced out of the system with bottled hydrogen and kept tight to avoid the production of a combustible mixture of hydrogen with air.

FIRST PROTOTYPE CONCLUSIONS

The electrical heater raised the temperature of the water so that when the hot water passed over the injection tube carrying the magnesium hydride slurry the temperature of the slurry and water when mixed together was sufficient to cause the reaction to produce hydrogen. The hydrogen together with reacting components and residue from the reaction passed along the reactor tube to the separation vessel. However it was found that the mixed temperature was not high enough to allow enough

of the exothermal reaction to be completed within the concentric tube heat exchanger for the reaction to continue without intermittent application of the electrical heater.

From thermocouple measurements located downstream of the heat exchanger section, it was evident that the reaction was continuing beyond the heat exchanger and through to the separator vessel.

In order to obtain a high enough mixed temperature without causing the water to boil at the system operating pressure it was concluded that the slurry also needed to be heated.

MODIFIED PROTOTYPE FIRST MODEL

A copper coil of ¼ tube was wound around the heat exchanger section together with the electrical heater. The slurry was pumped though the copper coil and then into the injection tube. This allowed heat to be picked up by both slurry and water before being mixed in the reaction section.

After start up with the electrical heater the duration of unheated continuous reaction was improved but it was evident that too much of the exothermic reaction was taking place beyond the heat exchanger. It was concluded that more information was required on the temperatures within and immediately down stream of the heat exchanger in order to judge the extent of completion of the reaction as the reactants moved towards the separation vessel.

5.2.3.3.2 Second Model Continuous Mixer System Design And Operation

EQUIPMENT DESCRIPTION

A second reactor was built with larger diameter tubes. The configuration is illustrated in the flow sheet (see Figure 20). A picture of the second reactor is displayed in Figure 21.

The mixing section was increased to 3/8” diameter with a 3/16” slurry injection tube.F The throat diameter of the mixing nozzle was kept the same at 0.120 inch but downstream the tube was increased to 1/2". This increased the cross sectional area which allowed room for a 36” long 3/16” diameter thermocouple probe which contained six thermocouples spaced at 3.5” intervals along its length to allow a thermal profile to be generated for investigation of the proportion of reaction completion along the discharge tube. A splitter block was added so that the profile probe could be mounted axially with the reactor tubes. Exhaust products were directed from the splitter at an angle towards the separator vessel.

The heat exchanger section was lengthened and made from two concentric tubes at 5/8” and 3/4" around the reactor tube. The two annular passages created were used for water next to the reactor tube and slurry around the outside. The recycle loop was modified by adding a three-way valve so that slurry passing through the heating annulus could be returned to the reservoir before entering the injection tube.

The electrical heater was increased to 272W with the addition of a second heating tape and as with the first prototype the whole system was surrounded with thermal insulation in the steel container.

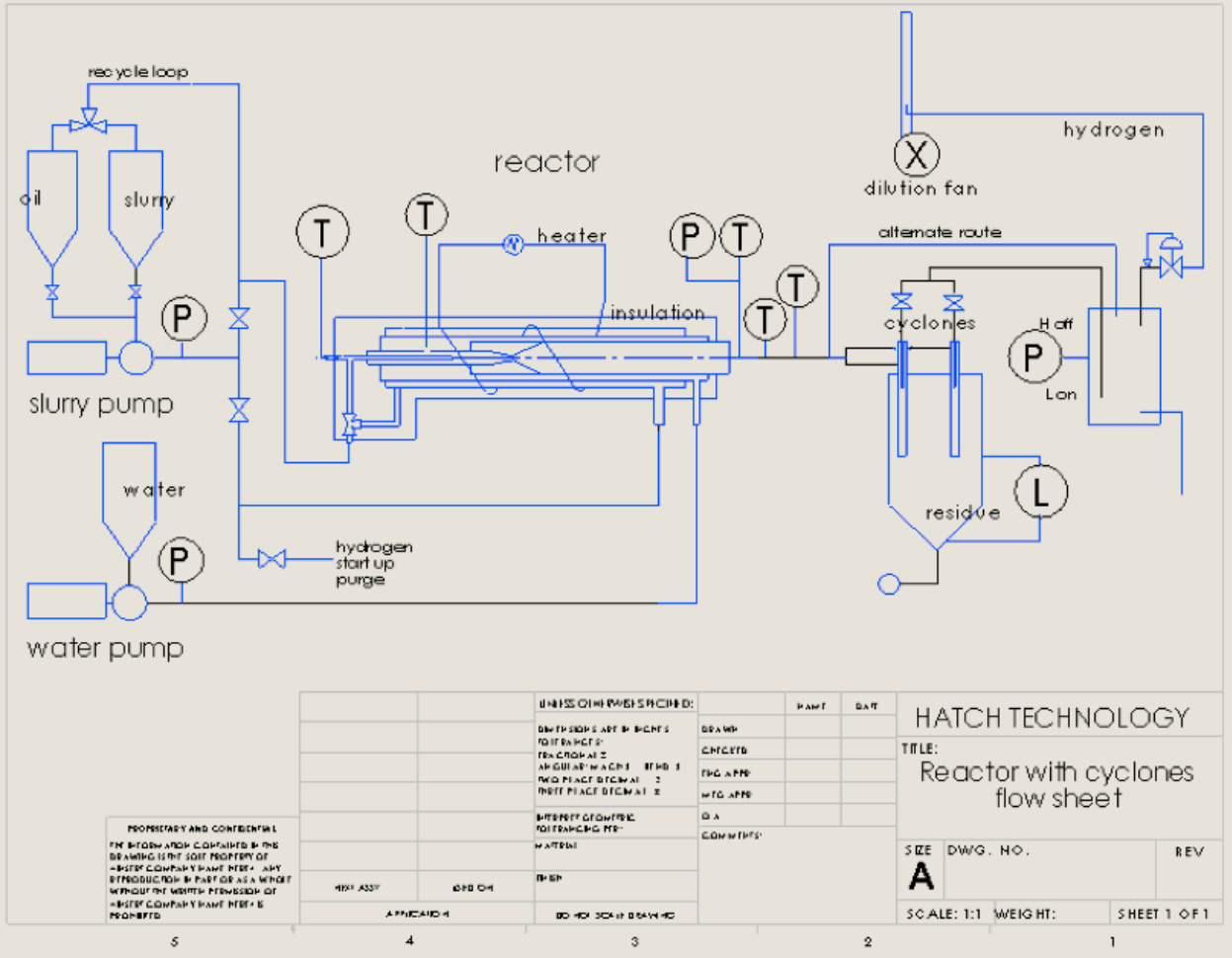

Figure 20 - Second Prototype Continuous Reactor

Figure 21 - Continuous Reactor Test Vessel

The electrical heater was increased to 272W with the addition of a second heating tape and as with the first prototype the whole system was surrounded with thermal insulation in the steel container.

INITIAL RESULTS

After small modifications to improve the slurry flow path to avoid plugging it was found that the slurry could be pumped reliably through the annular heating section and into the injection tube.

The improved heat exchange, allowing both reactants to be heated before mixing, raised the mixed temperature to a point where continuous production of hydrogen was achieved without requiring electrical heating after that required for the start.

A number of runs were carried out where the reaction was continued for several hours; variations in slurry flow rates and mixture ratios between slurry and water were explored.

A picture of the continuous mixer test apparatus is shown in Figure 22

Figure 22 - Continuous Mixer Test Apparatus

FURTHER RESULTS

Changes in the slurry and water flow rates together with changes in the ratio between slurry and water were made to try to establish the characteristics of the process operation in this equipment configuration. As more was learned, various equipment modifications were made and improvements in data collection and system control were carried out. This work resulted in the conceptual design of a more compact slurry water mixing head that will be built and operated in the next period.

Continuous operation of the mixer produced byproducts from the hydrogen generation process; solid powdered residue, oil from the slurry, and the excess water. Preliminary observations indicated that the majority of the oil would separate easily from the water and solids by gravity settlement and could be recovered for reuse.

EQUIPMENT DESCRIPTION

Figure 23 shows the configuration of the continuous mixer system including the slurry and water pumps, the reaction section, the instrumentation, the byproduct separation section, and the hydrogen disposition. The reaction section shown consists of an inner reaction region with two annular regions around it. Water flows through the inner annular space and slurry flows through the outer annular space. The water and slurry flowing through the annular spaces are preheated prior to being mixed in the reaction section. The reaction section consists of an injection volume followed by a mixing nozzle and then an open reaction tube.

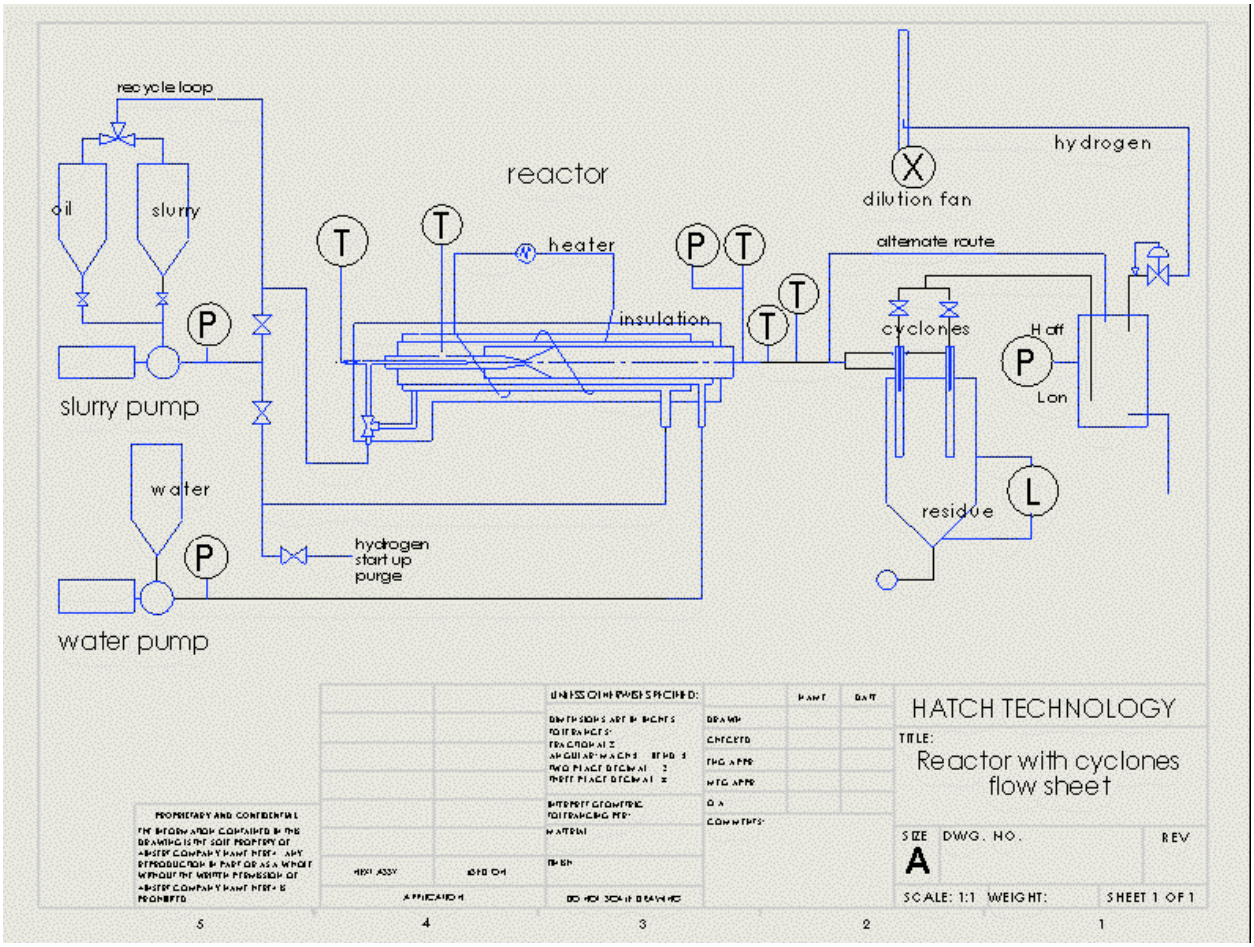

Figure 23 - Continuous Mixer Design Preheating Both Water and Slurry

PUMP SECTION

The pump system configuration remained unchanged throughout the period with the water pump and slurry pump supplying connections at the down stream end of the

heat exchange section of the reactor. Several replacement stators were required for the slurry pump. For these smaller sizes of progressive cavity pump the rotor stator contact is critical for achieving the required pressures and it proved too easy for the stator to be worn down by high frictional contact with the slurry. The heat generated by this contact worsened the situation by increasing the friction due to expansion of the rubber stator within the confines of its steel sleeve. The stators are easily exchanged but an investigation will be made to choose a better stator material for the slurry pump.

REACTOR SECTION

The second prototype reaction section was operated initially with a 3/8" mixing section in front of a 1/8" throat venturi nozzle. The reaction was continued down stream in a 1/2" discharge tube. Some cross sectional area was lost with the introduction of a 3/16" diameter, 36" long temperature probe mounted concentrically with the discharge tube. The probe contained six thermocouples spaced at 3 1/2" intervals in order to track the progress of the reaction along the heat exchange section of the reactor. A flow diverter block allowed the byproducts to be led away in a 3/8" tube to the separation vessel. The diverter block enables us to insert the long thermocouple and divert the flow at a slight angle to the side. Three thermocouples were sited just downstream of the diversion block at 3" intervals.

After running several tests it was decided to give more space for the initial mixing of the components by removing the 1/8" venturi nozzle and extending the 1/2" discharge tube upstream to replace the original 3/8" reaction section. The water was fed into the reaction section through a very fine nozzle hole, 0.010" diameter, in the side of the 1/2" tube so that a jet of hot water impinged on the slurry as it flowed from the 3/16" injection tube. A spacer piece surrounded the injection tube to fill the section of the 1/2" tube upstream of the impingement point to prevent deposition of solid residue upstream and to encourage the reaction materials to move forwards.

Occasional plugging of the slurry line at the entrance to the outer heat exchange annulus led to the implementation of a bypass route for direct injection of the slurry without preheating so that operation could continue. It was found that the impingement of the jet of hot water on the cooler slurry was still sufficient to start the reaction to release hydrogen and that the release of heat from the exothermic reaction into the heat exchange section could heat up the incoming feed water.

It was decided to simplify the reactor to use the direct injection only and to remove the slurry annulus tube. The start up heating tape was spread along a greater length of water heat exchange annulus and around the mixing section to speed the starting by providing heat to the more massive metal components in that area.

SEPARATION SECTION

The use of the simple separation system was continued. A change of direction of the products of the reaction within the separation vessel collected solids and liquids in the bottom of the vessel and allowed hydrogen with some water vapor to exit through a filter at the top. A backpressure control valve controlled the pressure within the reactor and passed the gaseous product through a cold-water trap to the dilution exhaust fan system to atmosphere as before.

OPERATION

SAFETY

Prior to each experimental run, where the system had previously been opened for removal of byproducts, the system was pressurized with hydrogen to about 100 psig for leak checking and then vented through the exhaust fan down to about 30 psig before repressurizing to the initial operational pressure of 100 psig. The cycling of pressure prior to start up served to take the composition of the contained hydrogen well above the flammable range for hydrogen.

Hydrogen is flammable in air from 4% to 74%. When the system is pressurized with hydrogen to 100 psi, the concentration of hydrogen in the air is 88%. So the hydrogen concentration is above the upper flammability limit.

INITIAL TESTS

The water pump and slurry pump were switched on to fill the pipelines and annular heat exchanger passages then the electrical heater was turned on to heat up the feed fluids through the walls of the heat exchanger section of the reactor. Low flow rates were used to limit the quantity of unreacted slurry in the reaction tube. The heat capacity of the metal reactor components slowed the heating up of the reactants. The initial hydrogen production rate was less than that which could be expected from the slurry flow rate. However, as the reactor and feed flows heated up, the hydrogen flow increased until the exothermic reaction rate was sufficient to heat up all the materials. During some periods of the test cycle, hydrogen was produced at rates greater than theoretically expected as the previously unreacted slurry was consumed. It was observed that the thermocouples down stream of the heat exchanger section sometimes showed increasing temperature in the direction of the separator during this period, which indicated that the reaction was still progressing outside the heat exchange section.

The backpressure control valve on the separator vessel maintained pressure in the system around 120 psig. This pressure kept the water below saturation to prevent boiling allowing the reactants to mix in liquid form.

After complete warm up of the system for steady flow rates of water and slurry there were still variations in hydrogen production both above and below theoretical expectations although the average was close to theoretical.

Variations of the molar ratio between the flow rate of magnesium hydride in the slurry and water showed little change in hydrogen production at ratios from 1.5 to 2 times the stoichiometric water needed to produce magnesium hydroxide. At lower ratios, although theoretically in excess of that needed for magnesium hydroxide production and full hydrogen release, there was a reduction in hydrogen production indicating that sufficient excess water is required for adequate mixing and full reaction using this design of mixer. There were also occasional brief flow stoppages, which indicated that excess liquid water was also needed to help smooth the flow of solids through the venturi nozzle and along the discharge tube.

Periods of several hours of continuous running showed flow variations of the slurry while maintaining constant molar relationship between magnesium hydride and water produced proportionate changes in average hydrogen production. It was also

shown that the process could be stopped and started easily with the system in the fully warmed up condition.

A number of test runs were prematurely curtailed due to plugging of the slurry supply line near the entrance to the very narrow annulus of the heat exchange section despite the attempts to improve the flow path.

A bypass to the slurry heating section showed that the process could be run without preheating the slurry. However, it appeared that the reaction started further downstream and continued beyond the water heat exchange section and help was required from the electric heater to keep temperatures up and maintain full hydrogen production.

CONTINUING OPERATION

MODIFIED SECOND PROTOTYPE

As a result of the forgoing tests it was decided to simplify the reactor by removing the slurry preheating annulus and injecting the slurry directly. To promote early reaction with hot water and initiate mixing the water was fed into the reaction tube through a fine orifice to create a jet impinging on the slurry as it enters The configuration is illustrated in the flow sheet see Figure 24.

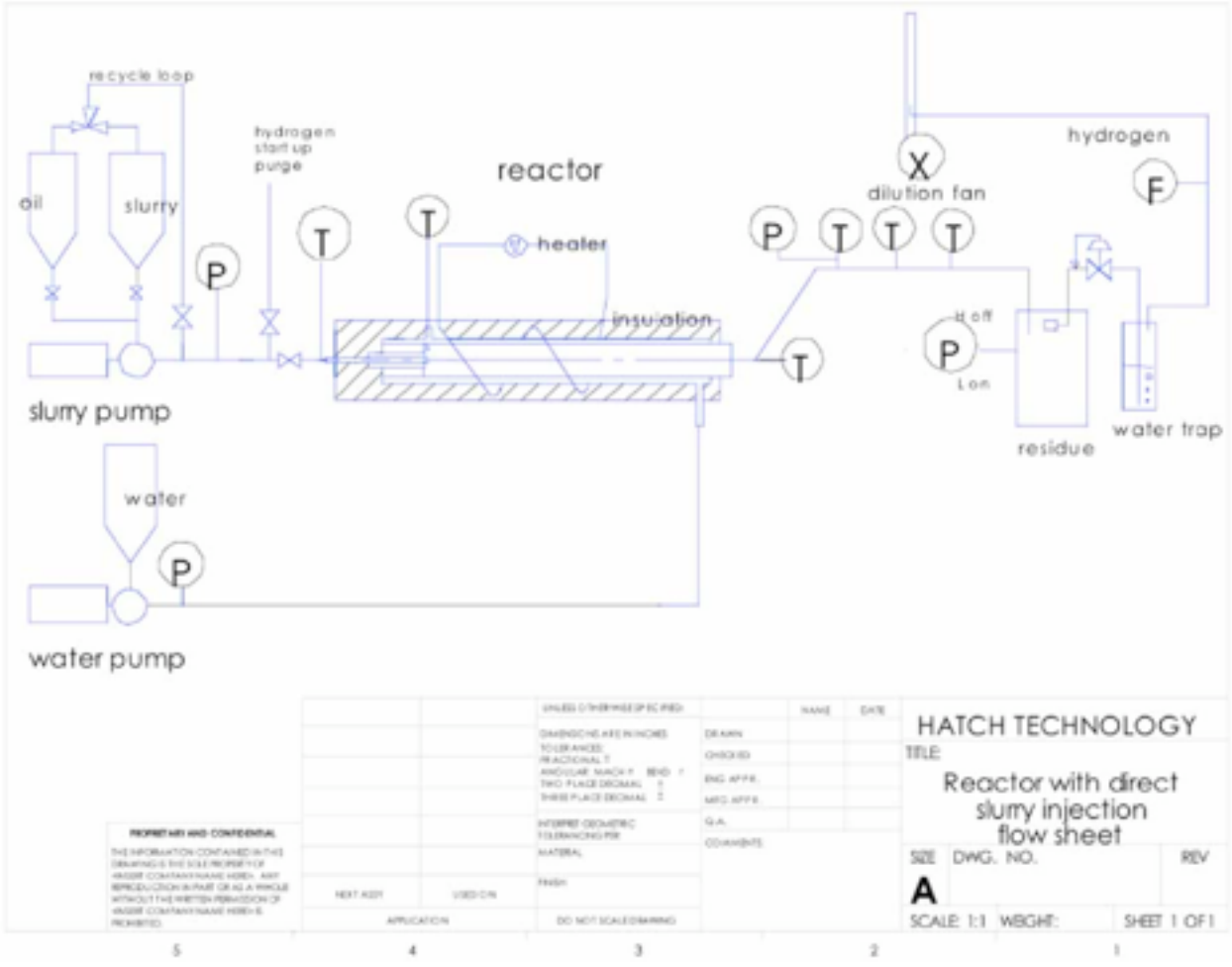

Figure 24 - Modified Slurry Reactor With Only Water Preheat

The mixing section was increased to 1/2” diameter by the removal of the venturi nozzle. The 3/16” slurry injection tube was retained. The purpose of the increased space at the point of mixing was to encourage completion of the exothermic reaction within the water heat exchange section. This was deemed important because the water would become the main means for carrying sufficient heat to ensure that both reactants reached the temperature required to give a good reaction rate.

INITIAL RESULTS

The modified construction gave much more reliable pumping of the slurry with the direct injection.

When the reactor was warmed up there was a little preheating of the slurry as it entered the reaction zone. This was due mainly to the conduction of heat along the metal components from the reaction zone. The start up heater tape also aided in this preheating process by being wrapped around the area of initial mixing.

The reaction volume inside the heat exchange area was increased by lengthening the water jacket and replacing the 3/16” diameter temperature probe with a 1/16” diameter single point thermocouple. This too was 36” long and was capable of being slid along through its mounting fitting to different positions to investigate the temperature profile along the inside of the reaction zone. Despite the extra volume within the heat exchange zone, it was evident that the reaction continued in the tube leading to the separation vessel.

Long continuous runs of the reactor allowed various flow rates to be stopped and started with molar ratios of magnesium hydride to water over the 1.5 to 2 times stoichiometric water to produce magnesium hydroxide range.

CONCLUSIONS FROM TESTS

With the relatively consistent behavior of the reactor it was concluded that this could be the basis for further improvements. One of the main objectives would be obtained by making the mixing zone more compact by using the hot water impingement on the slurry stream as the means of rapid initiation of the reaction. It is proposed to use a standard atomization nozzle for this purpose. The pressure drop across this nozzle will allow water to be heated to high temperature without boiling so giving a rapid start up.

The water nozzle with its inlet filter will be mounted in the compact mixing head where a small reservoir of water fed from a heat exchange annulus around the reaction discharge tube will be heated for rapid start up by a small cartridge heater. Slurry will be injected directly through twin injection tubes. Some preheating of the slurry will occur as the injection tubes pass through the heated water.

The mixing head will be adaptable to different discharge and heat exchange sections. The first assembly will incorporate static inline mixing within the discharge tube to promote completion of the exothermic reaction in a short length by ensuring good contact between the water and any unreacted slurry. As before, the feed water will run in an annulus surrounding the discharge tube in order to pick up heat from the reaction.

Observations of the behavior of the residue and excess water removed from the separator vessel after test runs had been completed, indicated that the mineral oil could easily be separated from the solids and water. An objective for the next quarter will be the investigation of means for removal of the by products from the pressurized

separator vessel to containment at atmospheric pressure and the preparation for separation and recovery of the oil.

5.2.3.3.3 Continuous Mixer Injection Head Modifications

EQUIPMENT DESCRIPTION

In the prior design, shown in Figure 25, the continuous mixer was assembled from purchased fittings and tubes.

This design allowed us to easily incorporate variations in the heat recovery system. We explored having the water heated by the reaction products in an annulus around the reaction chamber. We also explored having the water and slurry heated in two annulus's around the reaction chamber. This information was used to design the unit shown in Figure 26.

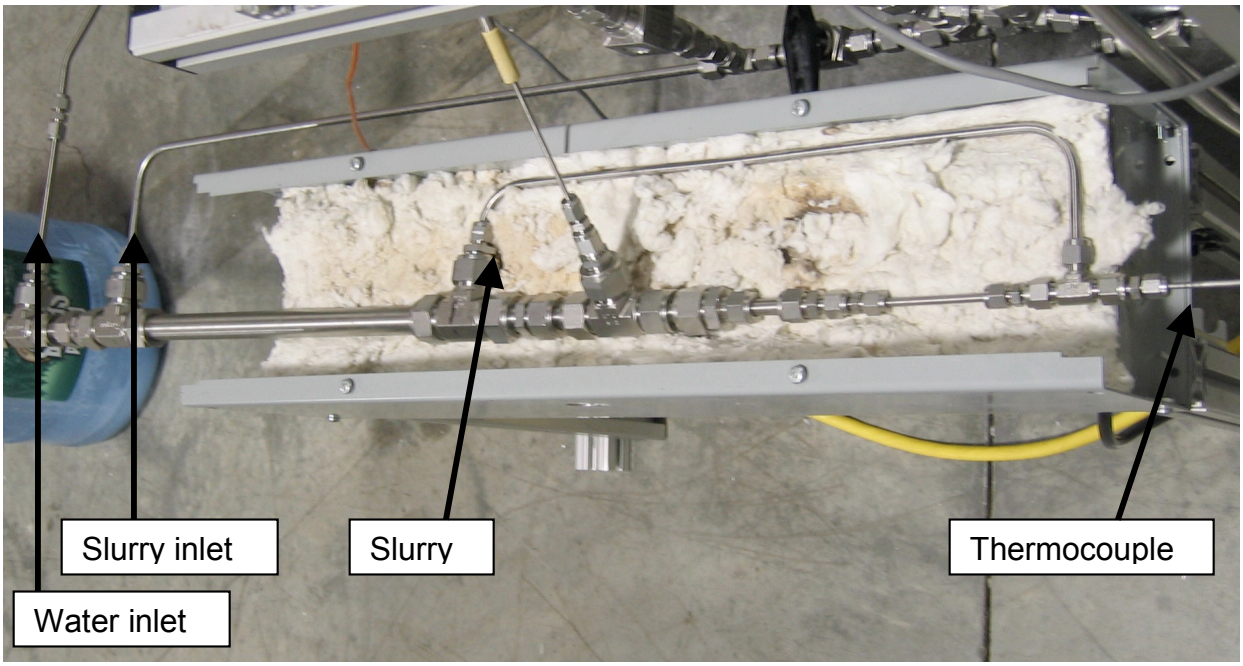

Figure 25 - Model 2 Continuous Mixer

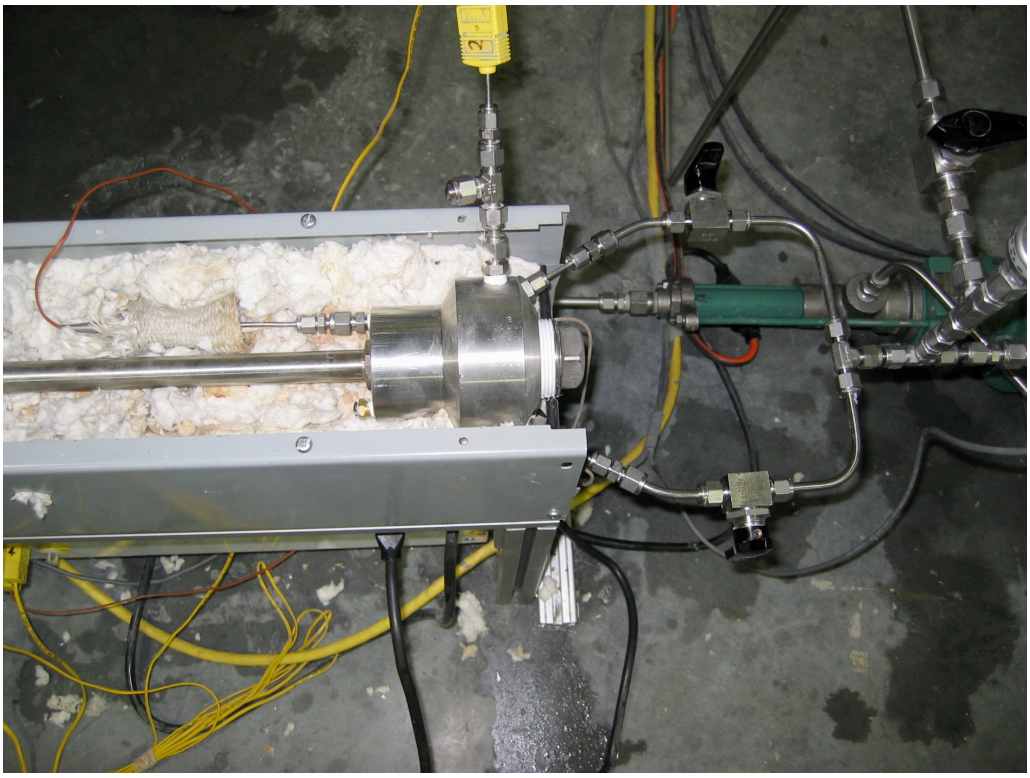

Figure 26 - Model 3 Continuous Mixer

The new design makes the system more compact and reduces heat losses. The movement of the water from the annulus around the reaction zone is accomplished within the head block rather than via external tubing. A cartridge heater is built into the head water reservoir to provide initial heating of the system. A nozzle between the reservoir and the reaction section provides back pressure to increase the boiling point of the water in the reservoir and to provide some velocity to the water in the mixer to aid in the mixing process.

Slurry in injected into the mixing zone next to the nozzle through two injectors. Each injector is valved to allow us to better control the flow of the slurry into the mixer.

The final modification in this design is the use of in-line mixer inserts into the reaction zone. These inserts split the flow and turn it. With several inserts in line, the two flow streams are thoroughly mixed and reaction is rapid.

OPERATION

The performance of the system during the shakedown testing with the in-line mixer is shown in Figure 27. This chart shows the hydrogen production rising and falling with changes in the slurry flow rate. Changes in the water flow rate were also made during this test. The changes in the water and slurry flow rates are noted by the pump control setting. We do not have flow meters on the slurry and water.

The light blue trace is the temperature of the water within the water reservoir. The cartridge heater was cycling frequently to maintain this temperature. The red trace is the temperature at the exit if the reaction zone as the flow leaves the in-line mixers. This temperature represents the temperature of the byproducts after some of the reaction heat has been transferred to the water. The yellow trace represents the

temperature of the water leaving the annulus heat exchanger. Changes in the water flow rate are observed to affect this temperature. The hydrogen flow rate is represented by the green trace. This flow is measured between a backpressure regulator on the separation chamber and exhaust to a dilution fan. Hydrogen leaves a 20L separation chamber through the backpressure regulator passes through a bubble chamber and then through a desiccant to the flow meter. When hydrogen production begins, the hydrogen flow rate lags a bit because the pressure in the separation tank must rise to activate the backpressure regulator.

At about 2200 seconds, the temperature at the cartridge heater was dropped. The temperature of the water from the annulus dropped shortly afterward indicating that the insulation around the reaction zone is probably insufficient.

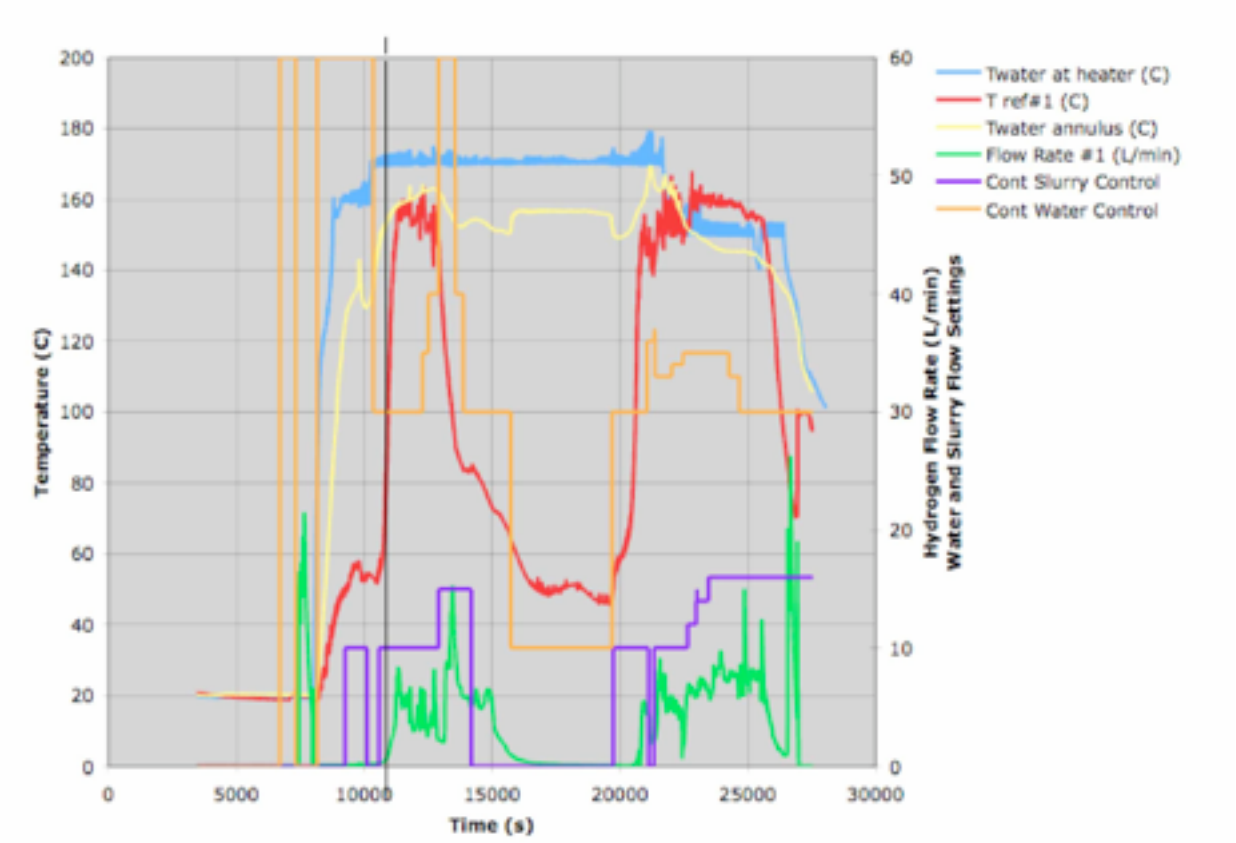

Figure 27 - Hydrogen Generation with Continuous Mixer

CONCLUSIONS FROM TEST

This was a shakedown test of the new mixer system. The measured hydrogen flow rates were slightly more than what we thought we should be producing and the flow rate stopped shortly after the slurry was stopped indicating that the reaction was reaching completion within reaction zone.

We were quite pleased with these results. There is much to learn and improve however. We need to improve the reliability and reduce the heat losses. We need to determine how much water is needed at different flow rates. In addition, we need to focus attention on the removal of the byproducts from the separator section and recycle the excess water used in the system.

FURTHER TEST RESULTS

Since the previous section, we performed 12 tests of the continuous mixer system. During this time, we increased the concentration of the solids in the slurry from 50% to 70%, and tested the mixer with an in-line passive mixing system. The performance with the in-line mixer was markedly improved and predictable over the performance with a straight smooth tube. The performance with 70% slurry has also been quite good.

Figure 28 displays the continuous mixer system. The system consists of a slurry pump with two reservoirs; one for slurry and the other for oil. The slurry pump pumps slurry into a T-connection that splits the flow to two injector tubes.

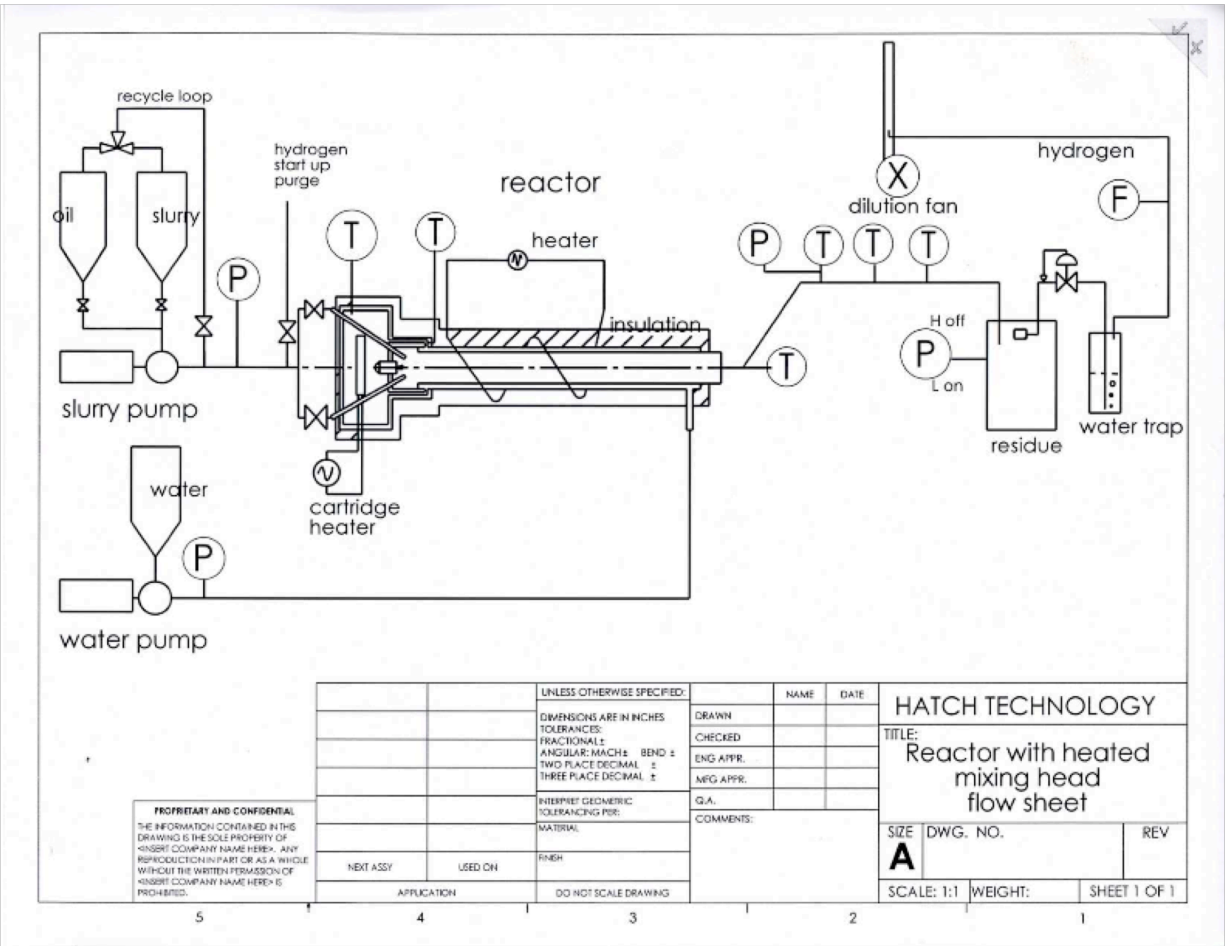

Figure 28 - Continuous Mixer System

Water is pumped with a second pump through an annulus around the mixer tube to capture heat from the reaction. The water flows into a reservoir in the head of the mixer, through a nozzle, and sprays across the slurry injectors in the front end of the mixer. The nozzle creates backpressure that enables the water to be heated to a higher temperature than it might if the pressure was limited to the operating pressure of the system. The slurry and water mixture flows through an in-line mixer where it is cut and turned once each half inch. The mixer results in a thoroughly mixed composition. The byproduct flows into a separation tank where the gases are separated from the solids

and liquids. The separation tank has been cooled for the tests performed during the past quarter. The hydrogen and steam leaving the separator are bubbled through a moisture trap, led through a desiccator, flow through a flow meter, and then pass into a stream of air where they are diluted to a concentration less than the lower flammability limit of hydrogen.

Several important design issues are addressed in this section: the reaction rate of the slurry and water, the time required to start the system, and the time that the reaction proceeds after the slurry is stopped. Figure 29 displays the reaction temperature and the hydrogen mass calculated from the pressure and temperature recorded in the Parr autoclave. For this experiment, measured quantities of magnesium hydride and water were placed in the autoclave pressure vessel. The vessel was purged 5 times to a pressure of 150psia to reduce the concentration of oxygen in the vessel to a few parts per million (comparable to the specified concentration of oxygen in the purchased hydrogen). The pressure vessel was then heated to 140°C. Above 150°C, the control system began cooling the reactants with a U-tube cooler. For this test, the reaction began at a temperature of about 80°C. When the temperature reached 140°C the reaction was so rapid that the cooler could not hold the temperature at the set point. The temperature overshot. At 180°C, the reaction rate slowed and the reactants cooled.

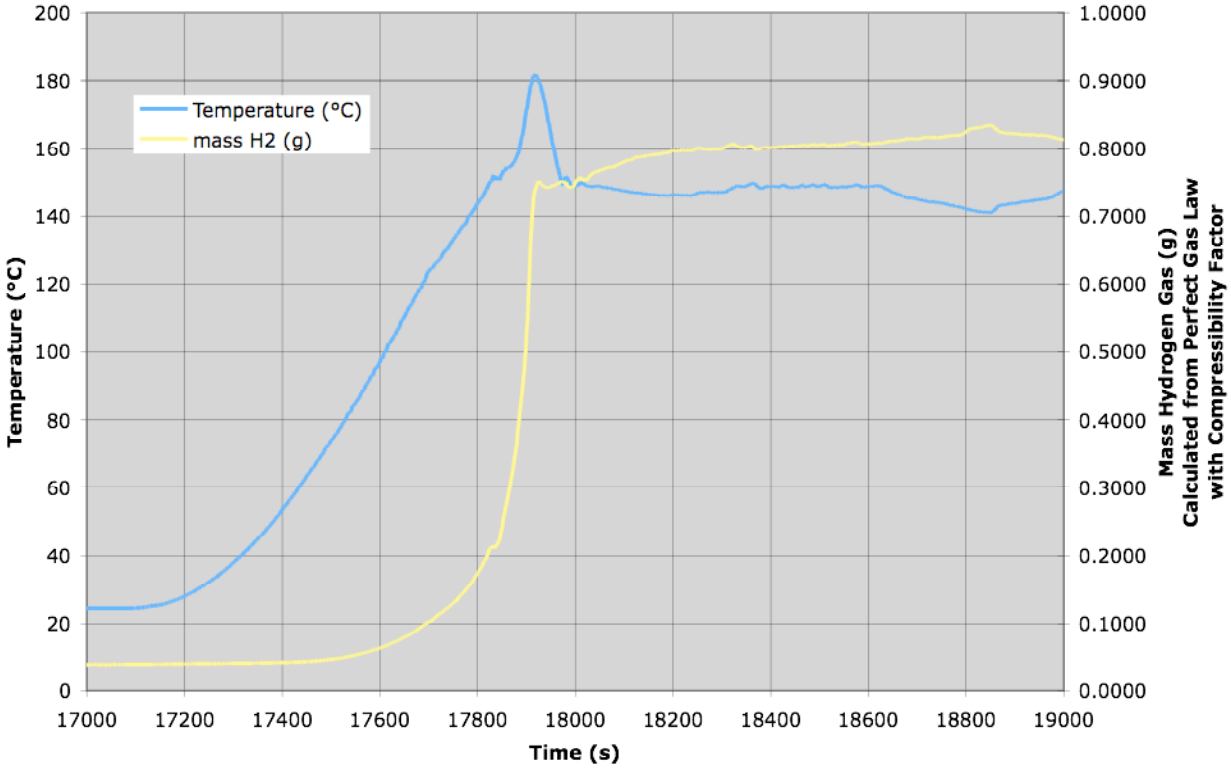

Figure 29 - Reaction Results from Parr Autoclave Experiment

The time scale is high because the data acquisition and control system had been running for several hours on another experiment prior to the start of this experiment. The calculation of hydrogen corrects for pressure, temperature, and steam in the system. The quantity of hydrogen calculated was measured at the end of the test by flowing the hydrogen into an inverted bottle filled with water.

From experiments such as these, the reaction rate was judged to be sufficiently fast at 140°C to meet the needs of an automobile.

Figure 30 shows temperatures, pressures, and flow rates for several parameters measured during one of our continuous mixer tests. The test ran for just under 5 hours. The slurry was turned on at about 8400s and then again at about 8800s. It was turned off at about 21,800s. The hydrogen flow throughout the test was measured at 7 to 10L/min. Hydrogen leaves the separation chamber through a back flow regulator. The backflow regulator is a mechanical device that adjusts the flow in increments and results in fluctuating flow signals. A thermocouple probe was located at the downstream end of the in-line mixer. Other thermocouples were located in the water reservoir in the head of the mixer, in the annulus water at the head of the mixer, and in the separator. Slurry pressure and the slurry control are used to tell when the slurry was pumping into the mixer.

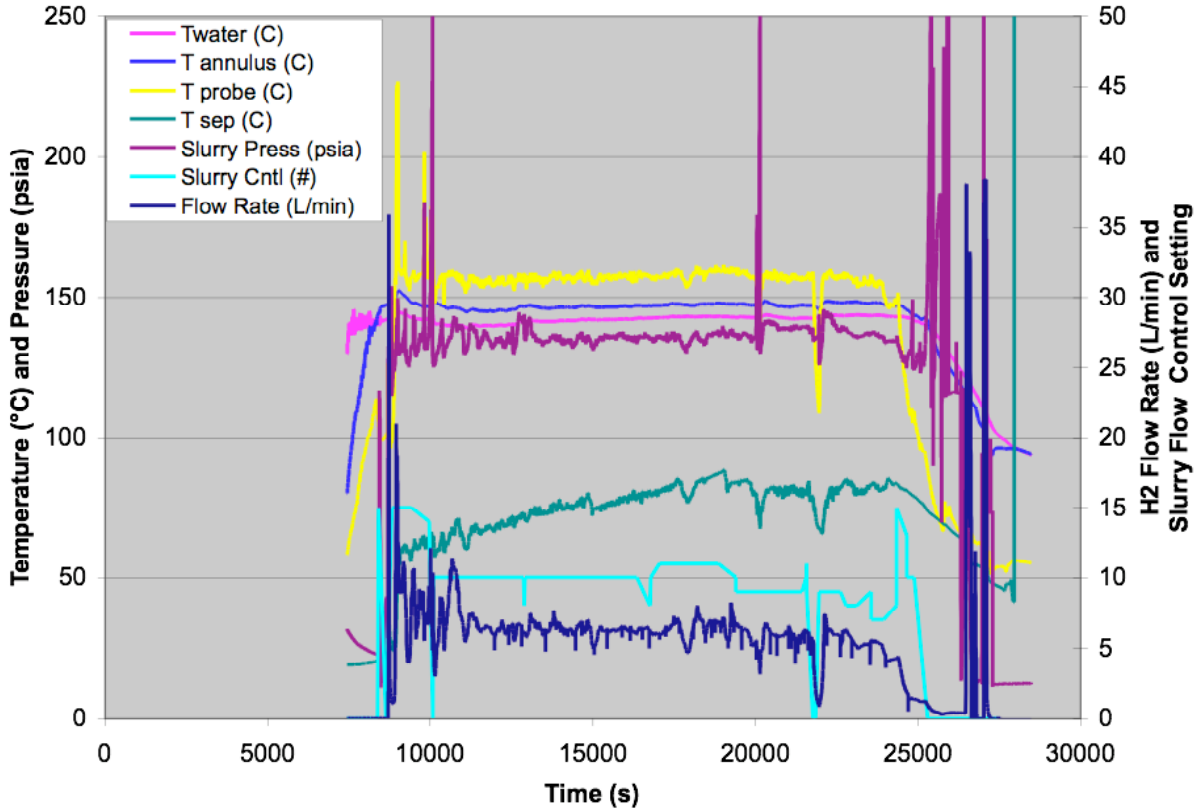

Figure 30 - Reaction Results from Continuous Mixer Experiment

Figure 31 shows the startup of the system and Figure 32 shows the shutdown response when the slurry was turned off. For this experiment, at the startup, the slurry was turned on for a few seconds and then turned off. When it was turned on the second time, the probe temperature began to rise rapidly indicating a reaction in the mixer.

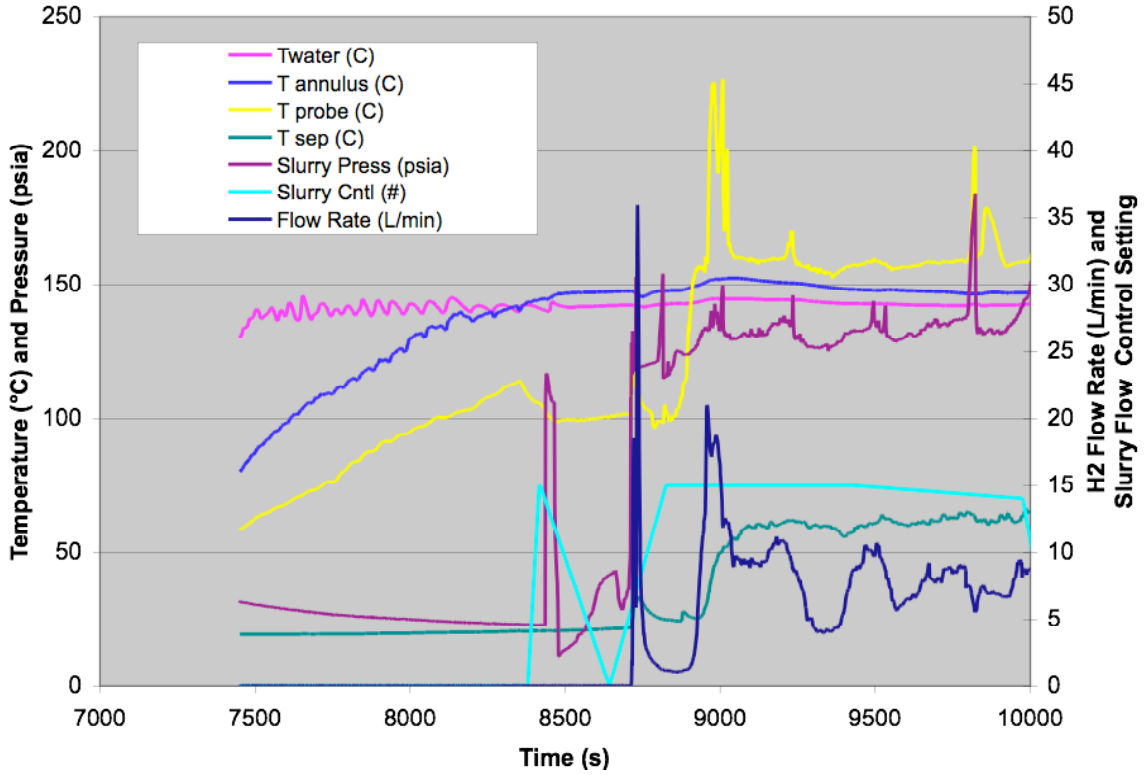

Figure 31 - Startup of Continuous Mixer Experiment

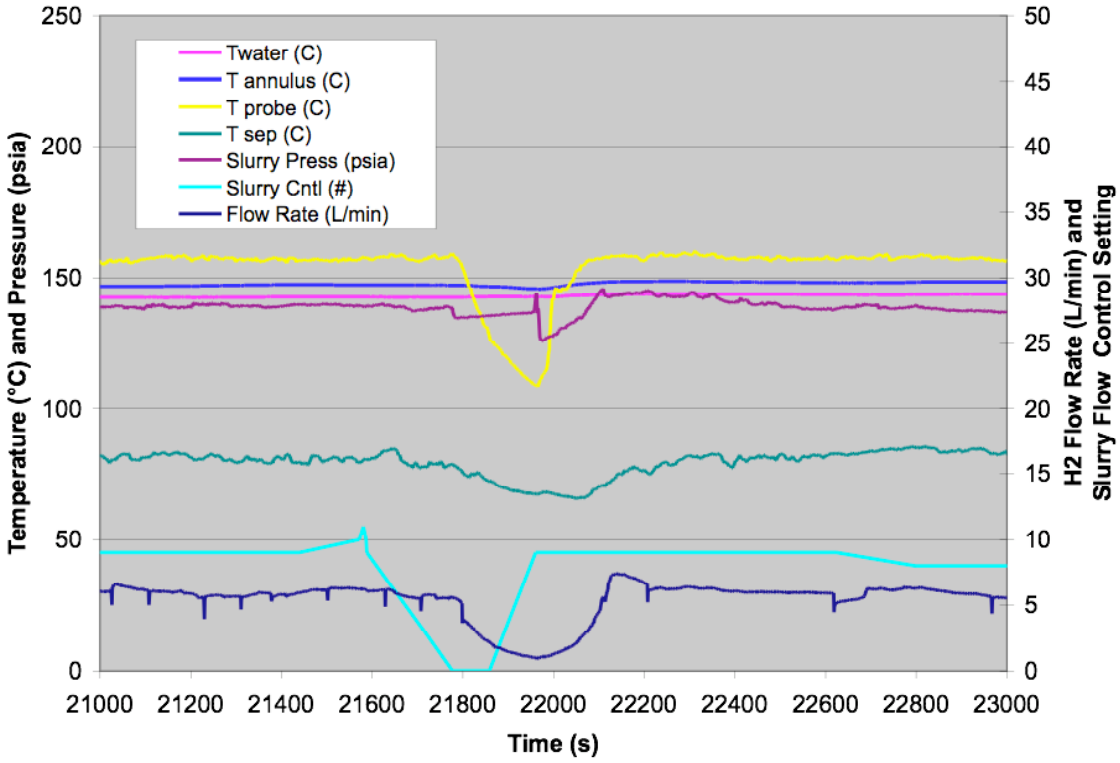

Figure 32 - Shutdown of Continuous Mixer Experiment

In Figure 32, the slurry was shut off just before 21,800s. The flow rate began to drop very shortly afterward and the temperature at the probe (end of the reactor) also dropped rapidly until the slurry flow was turned back on just before 22,000s. For automotive application, when the hydrogen flow is stopped, the slurry would need to be stopped and a hydrogen accumulator would rise in pressure for a few minutes after the slurry was stopped until the reaction had completed.

Good progress is being made on the mixer system. During the next quarter, we will be focusing attention on the byproduct removal and hydrogen composition.

CONCLUSIONS FROM TESTS

Continuous mixer tests were performed in July with 70% MgH_2 slurry using our continuous mixer apparatus. Some of the tests used an inline mixer in the reactor. These tests were compared to tests performed with a smooth tube reactor. The reactions in these tests proceeded readily. The tests with the inline mixer appeared to proceed more readily and with greater repeatability than those without the inline mixer. The 70% slurry mixed well and reacted readily with water in the mixer. However, there was some evidence that some of the reactants were reacting in the separation volume. This would be an undesirable feature of the design. We would very much like to separate these functions in order to be better able to design components for the individual functions. As a result of these tests, we decided that we needed to develop a computer model to aid in the design of the continuous mixer process and other possible mixer designs. We need the capability of understanding the conditions of the reactants and the products at the various stages of the reaction. The modeling effort will be described later in this section.

The tests with the continuous mixer have shown that the 70% MgH_2 slurry reacts readily with water in our current mixer design. They also showed that after several tests, the in-line mixer was showing signs of partial plugging.

5.2.3.4 Semi-Continuous Mixer

5.2.3.4.1 Introduction

The semi-continuous mixer was designed to allow the team to achieve a reliable and consistent mixer reaction as well as to begin investigating byproduct handling. This section describes some of the tests and development of the semi-continuous mixer.

5.2.3.4.2 Paint Pump Tests

An airless paint pump was purchased to evaluate its capability to pump slurry. We found that the pump performed acceptably with the 70% slurries and readily moved slurry between tanks. This demonstrates that a low cost commercially available pump can be used for this purpose. The pump is a piston pump that is designed to pump paint up to 0.91 L/min at a pressure of up to 2800 psi. We are interested in using the pump to inject slurry into the mixer.

5.2.3.4.3 Semi-continuous mixer development

PARR PISTON PUMP

In order, to complete a prototype of the MgH_2 slurry mixer system, we decided that we needed to change our approach. We have had consistent operation of the batch

mode Parr Autoclave experiments. We decided to evaluate how this system could be automated to fill and empty the batch reactor. This has been the basis of the new design. Our success with the paint pump has led us to review the operation of the slurry piston pump used in the LiH slurry development project. Figure 33 displays the slurry piston pump used in the LiH mixer development.

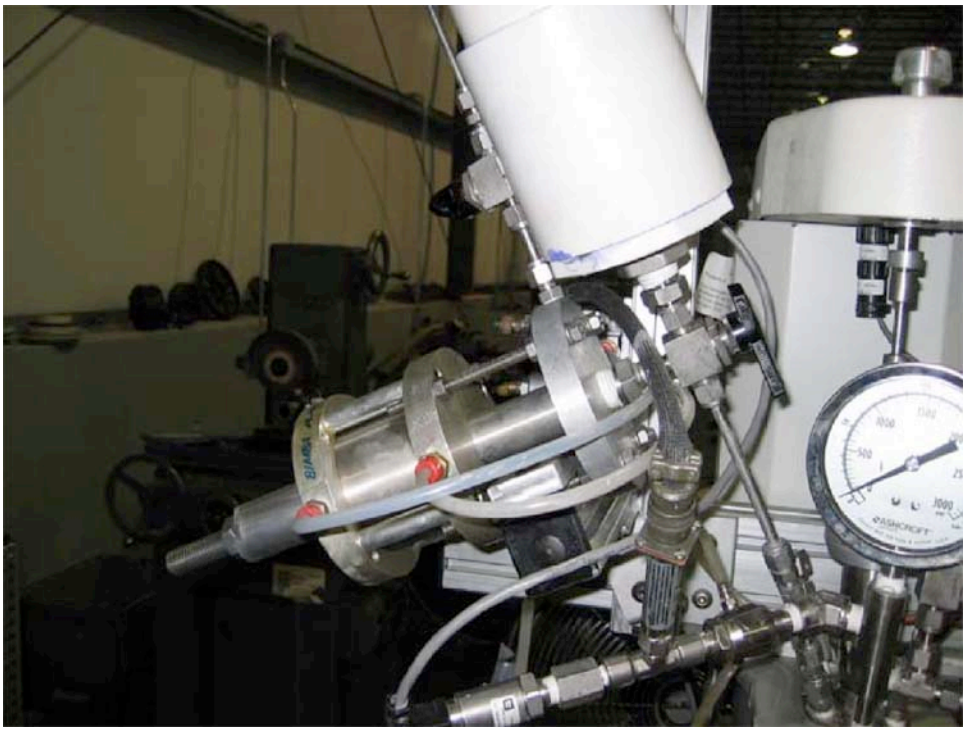

Figure 33 - Slurry Piston Pump

The commercial paint pump performed adequately but not as well as required. It appears that some of the chambers inside the pump were getting clogged with some of the larger slurry particles. The slurry particles are larger than paint particles. However, the design of the paint pump was similar to that of the piston pump previously developed. We decided to use the piston pump design for our tests with the Parr Autoclave. Figure 34 displays the slurry piston pump on the Parr Autoclave apparatus.

Figure 34 - Slurry Piston Pump with Parr Autoclave Apparatus

We were able to use this apparatus to test the reaction of the slurry in a batch mode operation. Slurry was injected into the Parr vessel five times at times: 4112s, 5425s, 6080s, 6844s, and 7470s. The Parr vessel was sealed on the first, third, fourth, and fifth injection. It was open to the 20L vessel on the second injection. Figure 35 shows the pressure and temperature data collected during this test. The release of hydrogen from the Parr is shown by the rise of the pressure Pseparator. (Pseparator refers to the pressure in the large vessel that was previously used as the separator pressure. The test was terminated shortly after the fifth injection because the injector was plugged (possibly because the fifth injections was made into a pressurized Parr vessel.

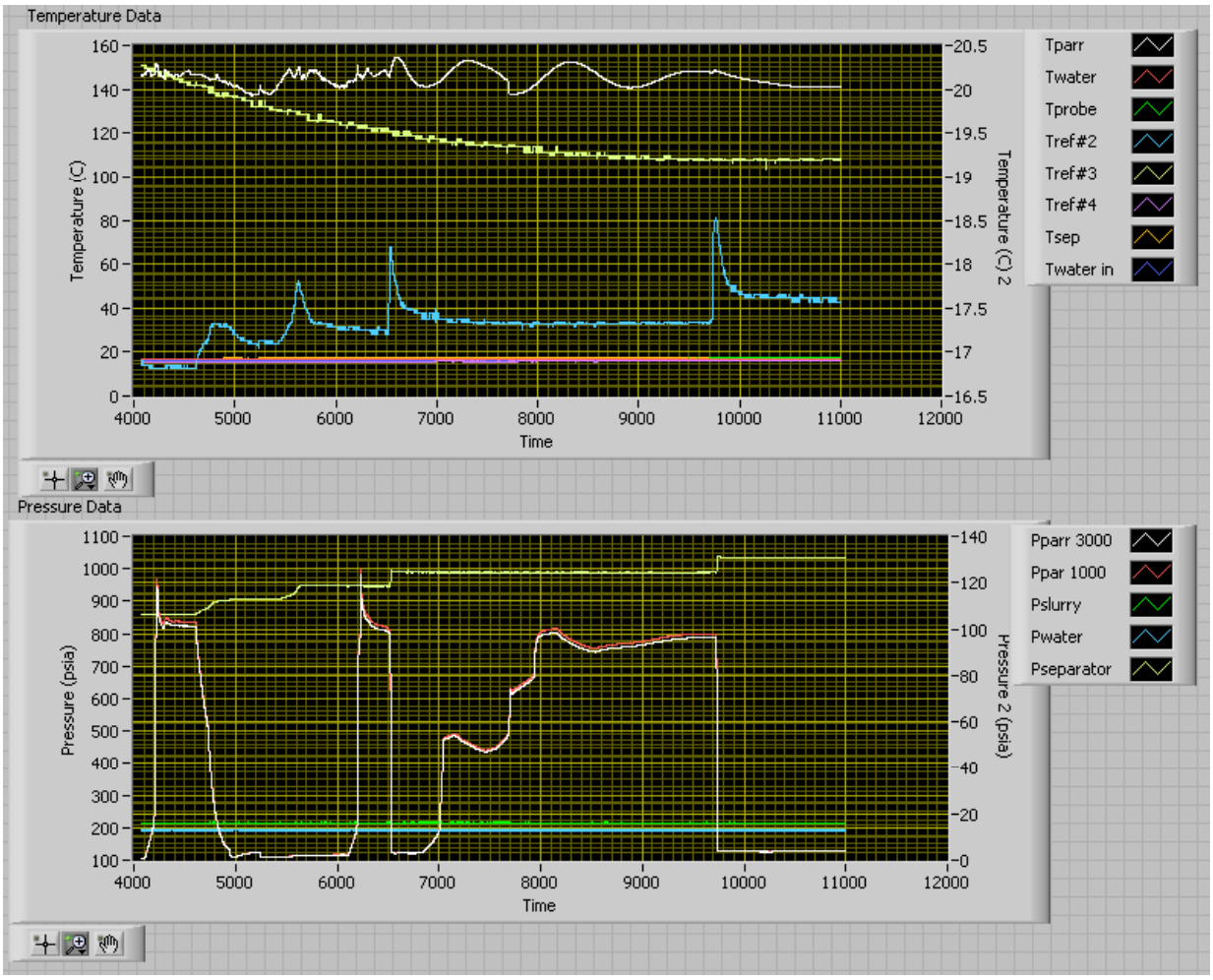

Figure 35 - Temperature and Pressure Data from Test 200611291

From the pressure rise in the large vessel, we can calculate the amount of hydrogen required to raise the pressure and from this the amount of MgH_2 required to react with water as shown in Table 1.

Table 1 - Calculation of Hydrogen Reacted

Time	Inj. #	P	T	H2 calc	H2 prod.	MgH2 req.
sec		Psia	°C	sL	g	g
4100		105.5	106.1	16.6	12.3	
5000	1	110.1	16.6	123.0	0.4	2.61
5800	2	116.1	16.8	130.7	0.7	4.57
6800	3	122.7	16.8	139.1	0.8	5.22
10000	4 & 5	127.2	17.1	144.7	0.5	3.26

The slurry pump injection amounts were measured prior to the test at about 5.5 g of MgH_2 per injection. The hydrogen production indicated that the slurry pump was

pumping less than expected. This might be explained if there was a bubble of air in the line that compressed at the higher pressure of the experiment.

Another interesting feature of the tests was the apparent two stage reaction. After injection, a slow reaction period occurred followed by a rapid reaction period. It appears that the slurry/water mixing rate is slow at first and retard the reaction initially. It is also interesting to note that the peak pressure reached in the sealed Parr vessel was about the same for the fist and third injections. This is in contradiction with the pressure observed in the system after the Parr pressure was released to the large vessel.

5.2.3.4.4 SEMI-CONTINUOUS MIXER SYSTEM DESIGN

PROCESS DESCRIPTION

Discrete slugs of Magnesium Hydride slurry will be injected into a bath of hot water contained in a pressure vessel to react individually. The hydrogen produced will be passed through a cooled condensing section to remove water vapor and entrained water droplets. The reaction bath will be allowed to settle so that solid residue may be accumulated. Solids together with accompanying water will be removed occasionally. Water will be returned to the reaction vessel to restore original fluid levels ready for the next batch of slurry reactions. For continuity of hydrogen production a number of these reactors will be coupled and operated consecutively to feed into a common storage which will use pressure to initiate injection sequences in response to hydrogen demand. Heat from the highly exothermic reactions will be distributed to bring the system to operating temperature and the surplus rejected. Cooled fluid will be used to promote condensation of water vapor to help dry the hydrogen product.

EQUIPMENT DESCRIPTION

The batch reactor will be constructed in sections that will facilitate development aimed at optimizing specific process operations.

REACTION CHAMBER

The main reaction chamber will be a pressure rated vertical cylinder with branch connections at lower levels for slurry injection, a heating device for start up, a tube for fluid for heat management, and a thermocouple probe for control information. A weir outlet above the reaction zone connected to a collection vessel will allow consistent fluid levels to be achieved for the start of each batch of reactions.

A baffle arrangement will be set immediately above the start up heater to constrain the reactants and promote settlement of the solid residue from the reaction. The lower section of the baffle will be a divergent cone shape with the injector discharging batches of slurry at the center of the narrow bottom just above the startup heater. It is expected that hydrogen and heat from the reaction will cause an expanding rising current of fluid within the cone.

The upper section of the baffle will be a cylinder of larger diameter than the base of the cone so that a space is made for the downward current of fluid necessary to recirculate the fluid lifted by the reaction. A wire mesh will be fixed across the top of the cylinder and this will be set below the level of the reactor liquid to encourage unreacted slurry particles to complete their reaction in the water without reacting in the head space above the liquid. It has been theorized that reactions in the gas, which has relatively low heat capacity and conductivity compared with the liquid, can allow the occurrence very

high temperature hot spots from the heat released during the reaction and that this can cause decomposition of some of the oils and dispersants used in making the slurry.

The cylinder will create an annular gap with the wall of the reaction chamber so that liquid passing through the screen has a preferred route for recirculation back to the bottom of the reactor. Longitudinal spacers attached to the outside of the upper cylindrical baffle will hold the baffle system concentric to the reaction chamber.

SETTLEMENT SECTION

A conical settlement section will be coupled to the bottom of the main reaction chamber. This will create a relatively quiescent zone where the higher density solid residue particles can settle and concentrate towards the valve at the narrow outlet. Outside this section further dewatering of the residue can be carried out so that space required for residue storage can be minimized and the removed water can be returned to the process.

GAS REMOVAL SECTION

A cylindrical section will be coupled to the top of the main reaction chamber. The headspace will allow small droplets and solid particulate to coalesce and fall back into the reaction fluid while the product gas is removed to a condenser section where water vapor can be removed. The gas outlet will be baffled to reduce entrainment of liquid droplets in the product gas stream. The water required to return the fluid to its operational level, after some has been removed with the settled solids and some with reaction, will be sprayed into the gas space and will help clear residue that may have stuck to the baffle screen during the reaction.

CONDENSER SECTION

The product gas, possibly from a number of sequenced reactor chambers, will pass into the condenser section where it will flow through a bed of stainless steel packing. Cooling water will be fed from a distribution tube embedded in the packing and this water together with water vapor condensed from the product gas will fall into the coupled water level control section.

WATER LEVEL CONTROL SECTION

This section, also common to a number of sequenced reactors, will be used to monitor all the process water in the system. Water level monitoring equipment will determine water quantities that will be required from storage to offset that used in the reaction to release hydrogen, that carried away as vapor or liquid in the product hydrogen, and that removed to store with the solid residue. As part of the sequence of operation of any attached reactor, water from the control section will be used to refill to the weir level after reaction and solids removal have occurred. The level monitoring equipment will indicate when flow over a weir stops the fall in level in the control section and so indicate when a reactor has been re-supplied to its operational level.

Oil that has been used to make the Magnesium Hydride slurry tends to separate from the particulate during the reaction and float on the water. During the restoration of level in any reactor the oil is swept over the weir into the level control section. The oil from the connected reactor chambers can be recovered from the control section by adjusting water level so that the interface with the recoverable oil is set just below an outlet valve in the wall of the control section. This oil may be added to the dewatered solids residue to maintain its ability to be pumped during recycling processes.

SOLIDS REMOVAL SECTION

A conical section connected to the bottom of the level control system will be similar to the settlement section attached to the reaction chamber. This too will allow settlement of solids carried by liquid overflowing the weir from the reaction chamber. The solids will be removed occasionally and treated in the same way as those from the reaction chamber and may share the dewatering equipment so that recovered water is returned to the process.

5.2.3.4.5 Level Detector Development

In order to provide a signal for the control system to define the water level in the level vessel, we have implemented a level detection system. The system consists of a central rod that is separated from two concentric tubes by non-conductive PFA plastic tubing. An alternating current transformer is wired between the central rod and each of the concentric tubes. When the water level rises to the first concentric tube, an alternating current signal is observed at an AC measurement sensor because the liquid in the vessel is conductive. When the water level rises to the second concentric tube, an alternating current is observed on a second AC measurement sensor. A schematic of the apparatus is shown in Figure 36. The system uses an AC transformer to produce a low voltage source between the two tubes and the central rod. It also uses two signal conditioners to measure the AC current and provide a DC current signal for our data acquisition system. Figure 37 displays the equivalent circuit of the system.

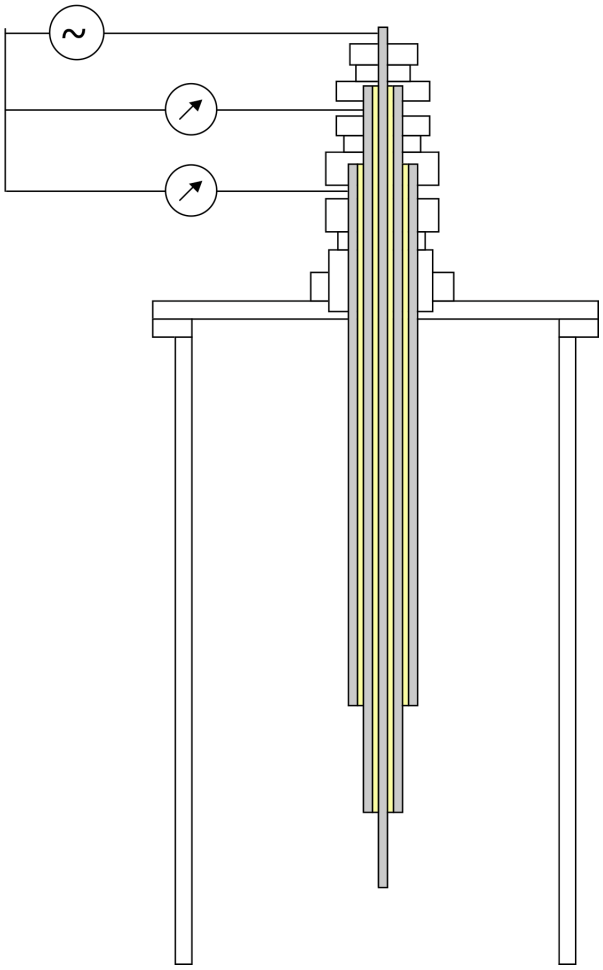

Figure 36 - Schematic of Level Probe

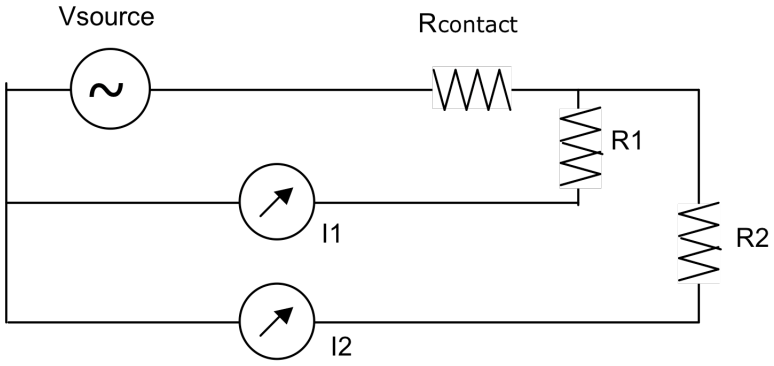

Figure 37 - Equivalent Circuit for Level Probe

The signals produced are quite distinct but not without some confusion. When the upper measurement point starts to conduct, we are observing that the lower point measurement declines. We are also observing that after operating for a few cycles, the current measured begins to increase in both probes. Based on the equivalent circuit diagram, we note that the probe contact resistance is common to both probe points.

This resistance will increase as the current increases which will affect both measurements.

We are currently using the measured signals to indicate the levels in the level vessel and then we manually change the process. We have not yet defined how the measurements should be used to automatically define the operation changes.

We also use a sight glass on the outside of the level vessel to display the water level inside the vessel. This measurement is fairly reliable, but we have observed that it can be plugged by foam that is carried into the upper connection due to our choice for the upper connection point.

Neither of these measurement issues affects the primary purpose of the mixer system testing which is to demonstrate how a semi-continuous system can be operated and to provide data for use in estimating the mass and volume of a full-scale system.

5.2.3.4.6 Testing of the Semi-Continuous Mixer System

Many tests of the semi-continuous mixer apparatus were performed during the summer and fall of 2007. These tests culminated in the test in which samples of the hydrogen and byproducts were analyzed. This test is described in Task 3.

5.2.3.5 Analytical and Control System Development

5.2.3.5.1 Hydrogen State Points Estimation

Our modeling activity began with the goal of modeling the reaction within the Parr Autoclave. In these experiment, slurry and water are heated to above 100°C in an atmosphere of hydrogen. (We have found that the reaction proceeds well even with air present however then the hydrogen is contaminated with oxygen and nitrogen). As the water is heated the amount of water vapor in the vessel increases and the pressure increases with the additional water vapor and the pressure rise of the initial atmosphere of hydrogen. When the reaction begins, the pressure rises rapidly due to the additional hydrogen present and due to the production of additional water vapor due to the heat release during the reaction.

One of our first challenges was to calculate the hydrogen mass as a function of temperature, pressure, and volume. Hydrogen is known to be a non-perfect gas; it does not behave as a perfect gas would behave. There are several functional relations that have been developed to calculate the pressure of hydrogen as a function of temperature. One of these relations uses a compressibility factor and modifies the perfect gas law; ie PV=znRT. We compared the results of various algorithms with data provided by the NIST Chemistry WebBook (http://webbook.nist.gov). We built a table lookup routine to allow easy comparisons with our models. The table lookup routine, though providing the most accurate values, only provides data to 398.15°K. The reactions between MgH_2 and water that we are studying typically operate in a range of 373.15°K to 473.15°K (100°C to 200°C). We are also interested in some reactions between magnesium and hydrogen that occur at temperatures between 553°K and 673°K (280°C to 400°C).

Figure 38 and Figure 39 display the fractional difference (Tcalc-Tmeas)/Tmeas*100) for the perfect gas law and the NIST data as functions of

temperature and pressure. The perfect gas law over the range of interest up to 125°C is fairly accurate at normal pressure but as the pressure rises the calculation is less accurate with an inaccuracy of 7.5% in the pressure range of interest.

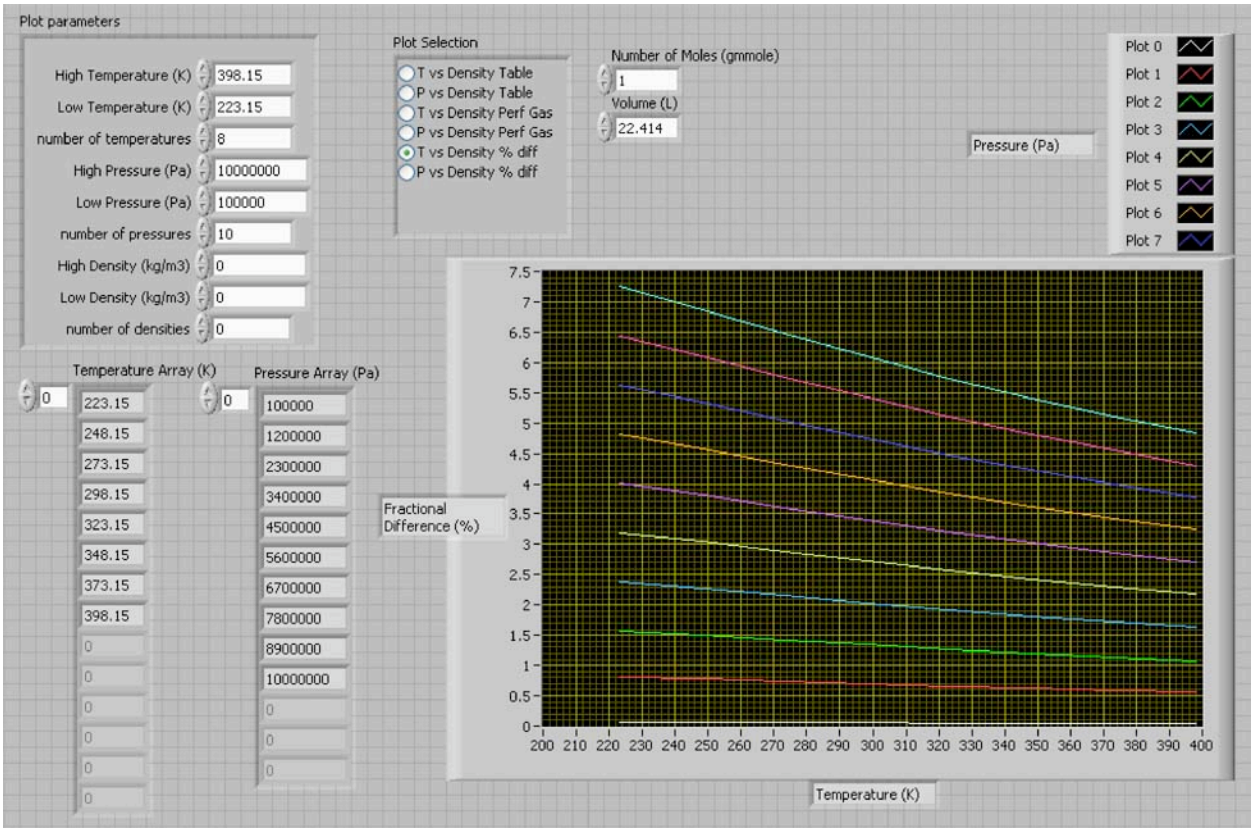

Figure 38 - Comparison of Perfect Gas Law and NIST Data - T vs Difference

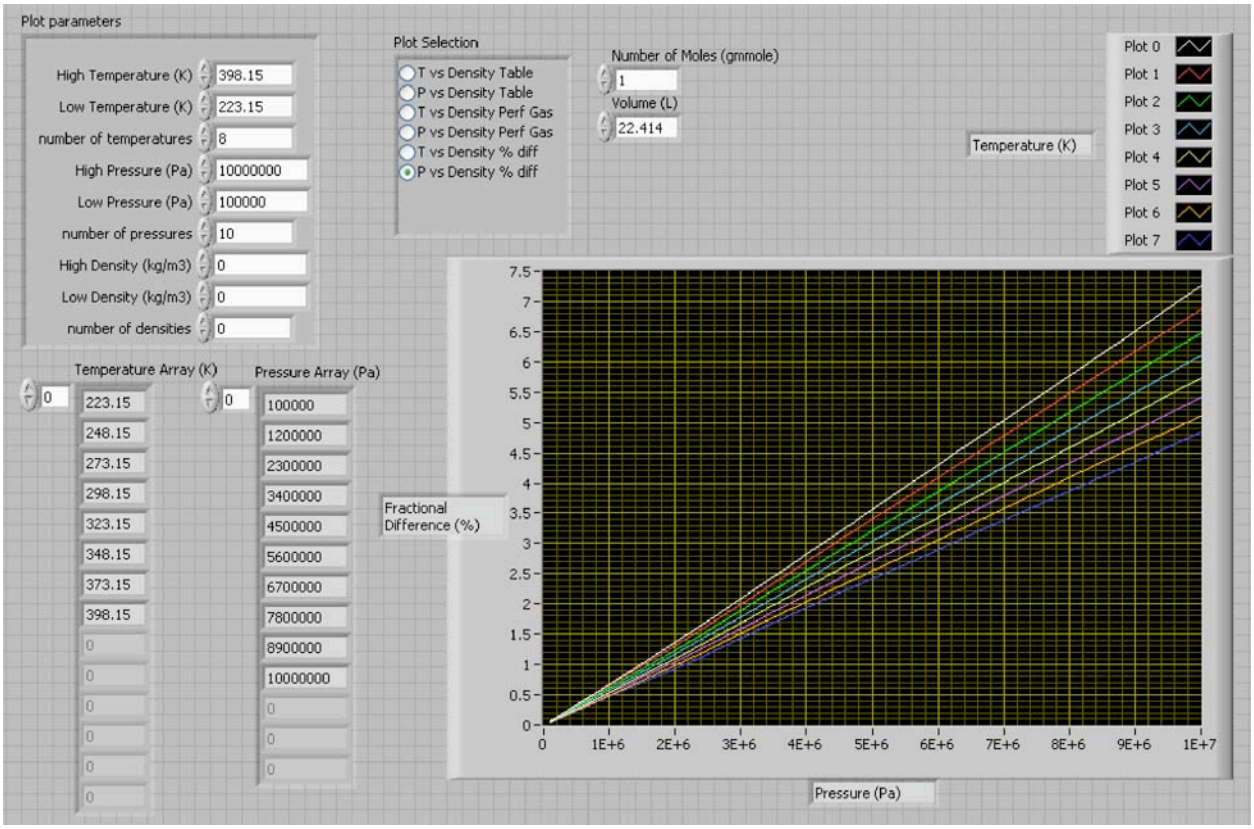

Figure 39 - Comparison of Perfect Gas Law and NIST Data - P vs Difference

Using the compressibility factor (Z factor) suggested by the American Society of Heating, Refrigeration and Air Conditioning Engineers, the accuracy is better, as shown in Figure 40 and Figure 41, improving with a peak inaccuracy of 1.2% over the data range. However, the gas law is most accurate for normal pressure and our system is intended to operate at a slightly elevated pressure of about 10 atmospheres. To compensate for this, we have modeled the compressibility factor using the highest temperature data rather than the room temperature data. Figure 42 and Figure 43 compare the calculated results to the measured data using this new compressibility factor. The peak inaccuracy is the same as with the room temperature compressibility factor now the most inaccurate points occur with the low temperature calculations. The compressibility factor for this calculation is determined from the following equation:

$$Z = -7.88273568E\text{-}09x^3 + 1.35405475E\text{-}06x^2 + 4.80543792E\text{-}03x + 1.00005153E+00$$

The coefficient of determination, R^2, indicates how closely the trendline corresponds to the data. This trendline matches the data well with a value of 0.999999774.

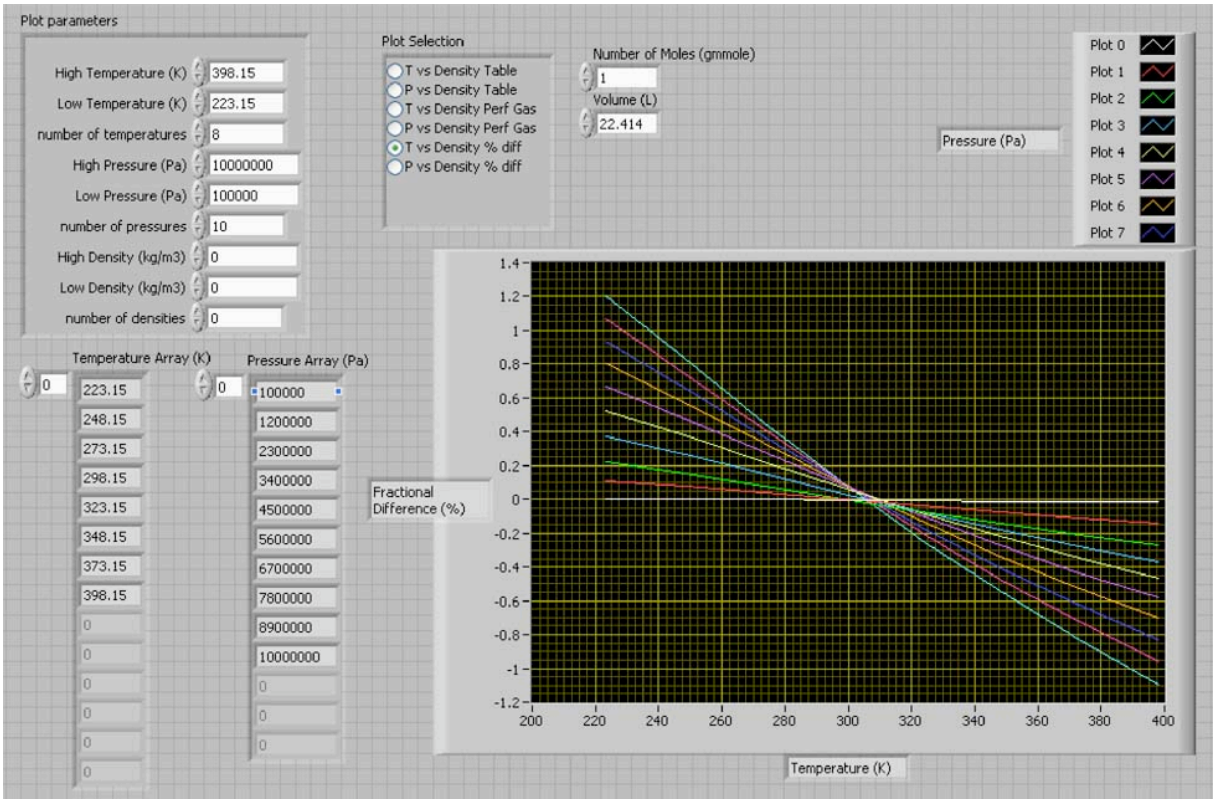

Figure 40 - Effect of Compressibility Factor - T vs density

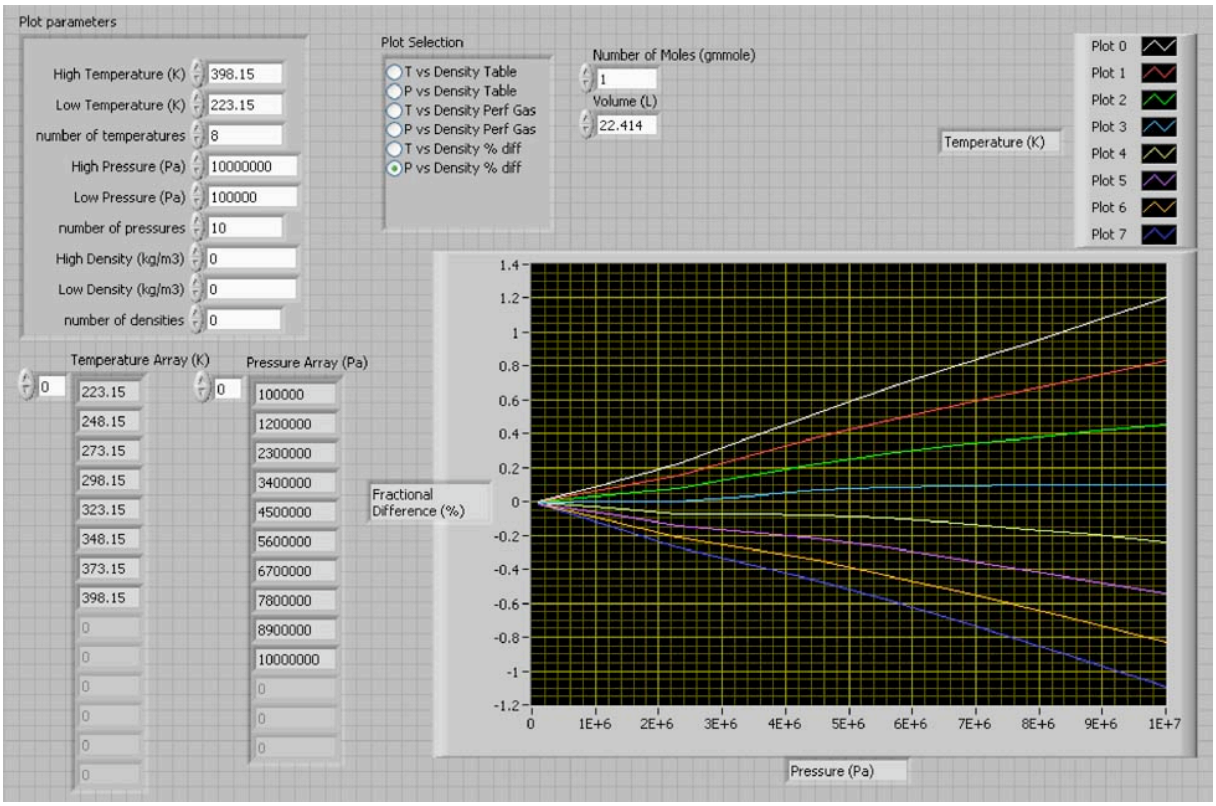

Figure 41 - Effect of Compressibility Factor - P vs density

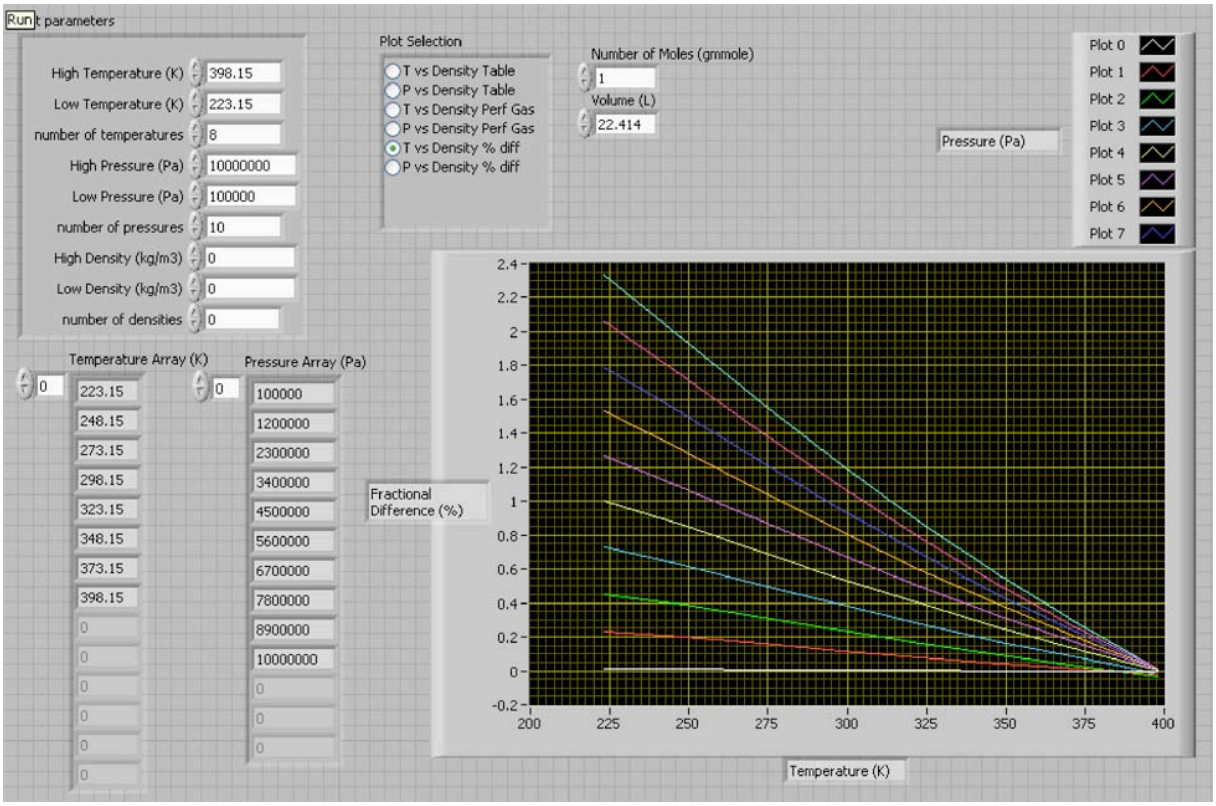

Figure 42 - T vs Density using Z Factor derived from 398.15°K Data

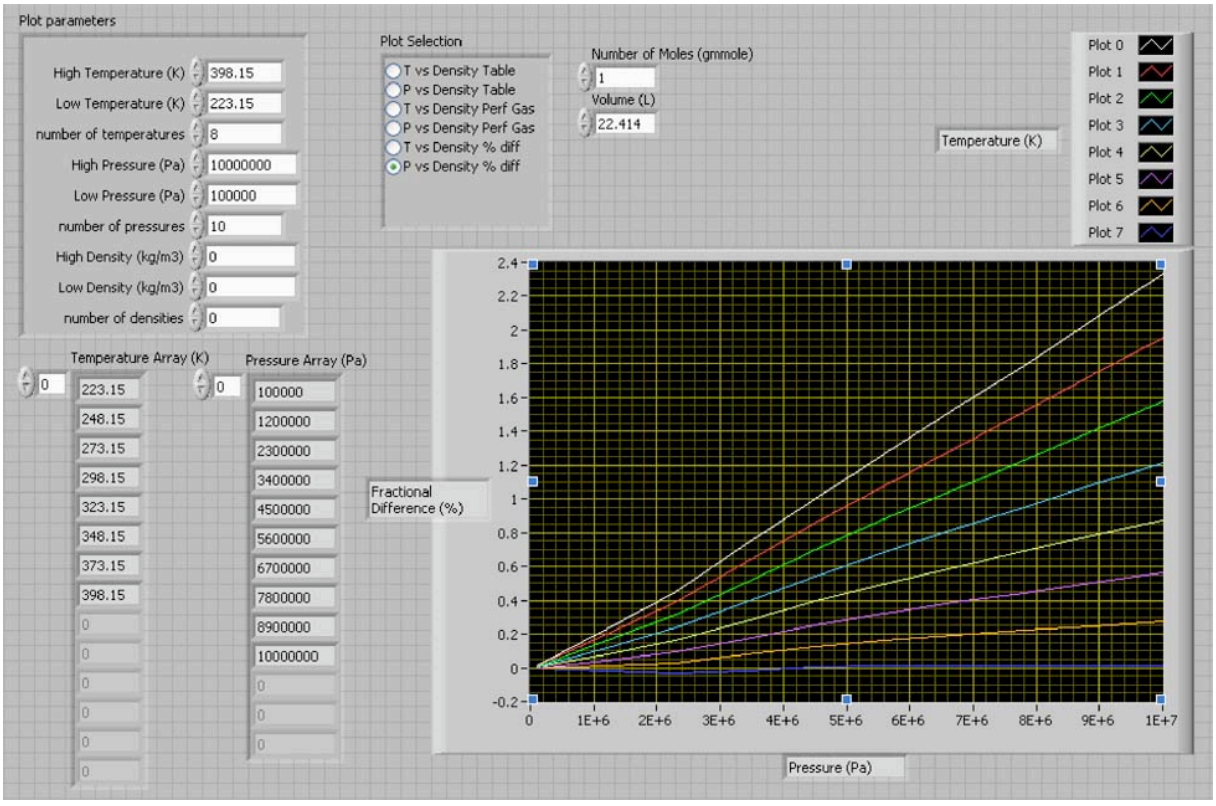

Figure 43 - P vs Density using Z Factor derived from 398.15°K Data

Presumably, the error will fan out in the negative direction as the temperatures are increased to about 125°C in a similar manner to how it increases with decreasing temperature. Thus at our highest temperatures of about 175°C, we should expect that we will have an error of -0.6% or less.

We attempted to measure the density as a function of temperature in the Parr Autoclave but discovered that the temperature of the gas within the autoclave varies from a hot zone at the bottom of the vessel to a much cooler head zone. Without a relatively constant hydrogen temperature, we felt that the uncertainty of our data would exceed the error that we have estimated from the corrected perfect gas law.

5.2.3.5.2 Control System Development

The object of the control program is to automate the process, collect data for post test review, and perform some data reduction to inform the operators. The program display is broken into nine tabs. The first tab, Figure 44, displays notes that are used to describe some of the functions and settings. It has been used to remind the operators of decisions made for the control program that might not be evident in the following tabs.

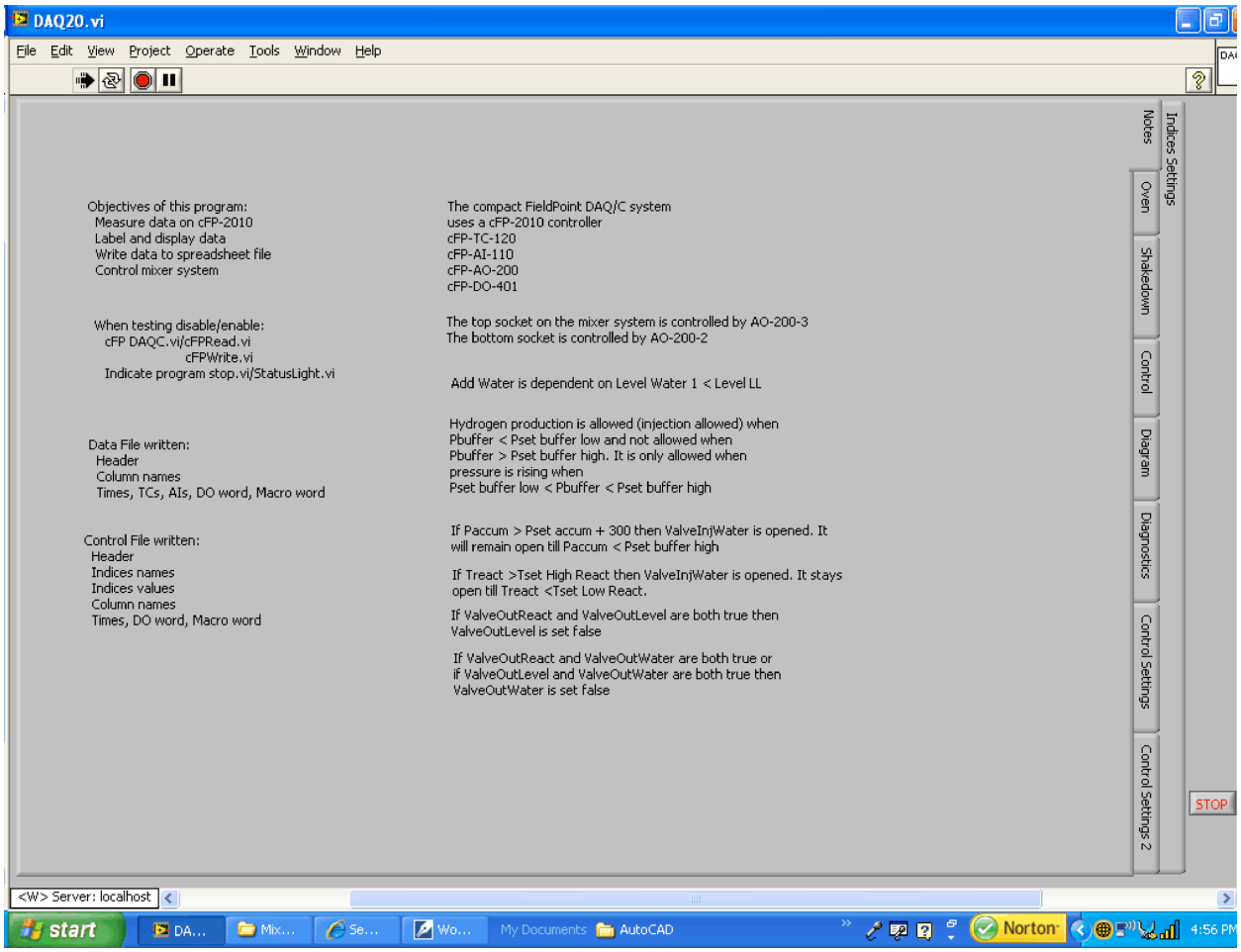

Figure 44 - Notes Tab for the Data Acquisition and Control Program

The Oven tab, Figure 45, provides a control for an auxiliary oven or it can be used to control a hot plate. It does not relate to the mixer system control but is helpful for other experimental needs.

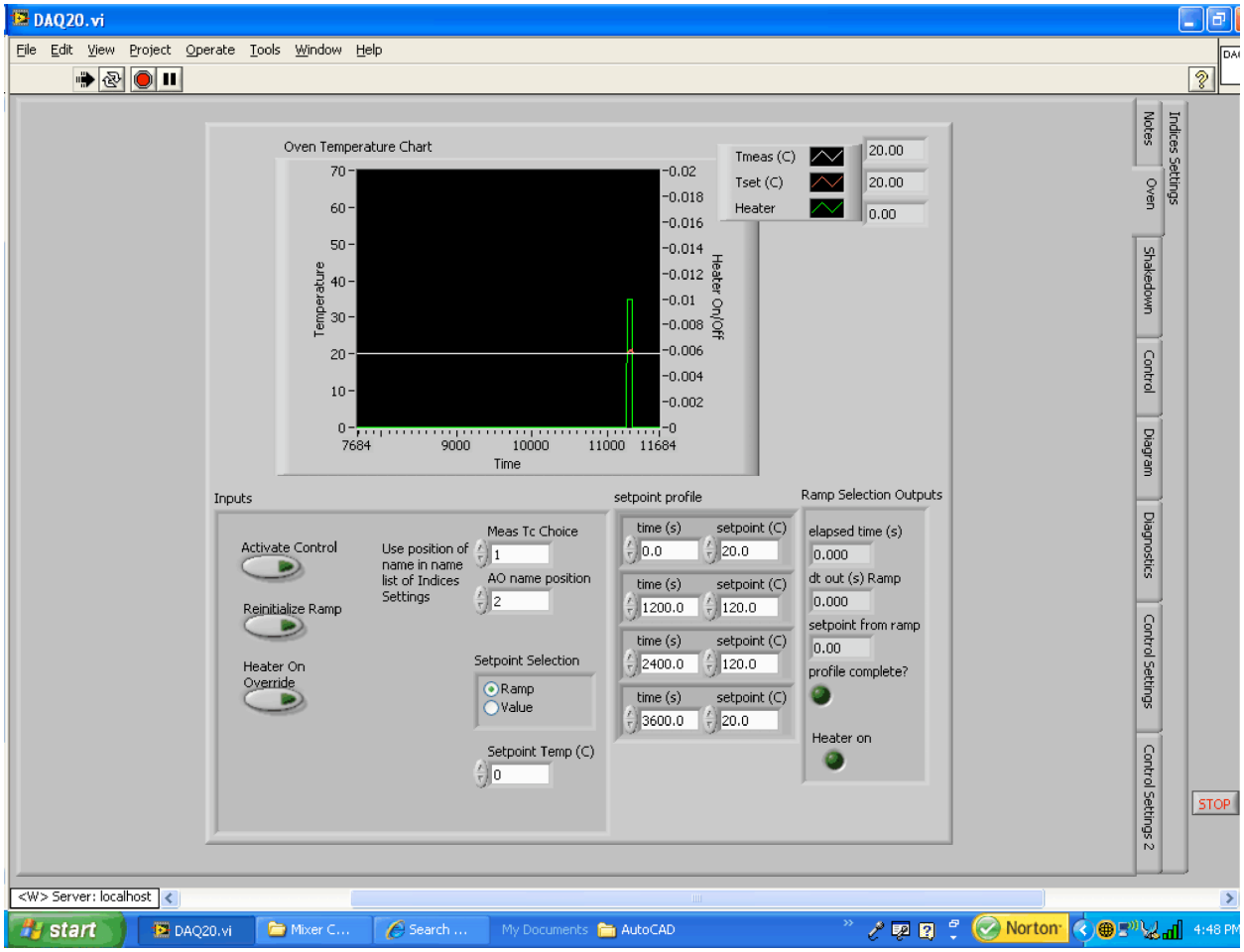

Figure 45 - Auxiliary Oven Control Tab

The Shakedown Tab, Figure 46, is used to operate specific valves, heaters, fans, or pumps. It also displays the thermocouple outputs and the pressure, hydrogen flowrate, and level sensor outputs. It is useful for debugging the control program and the various control sequences.

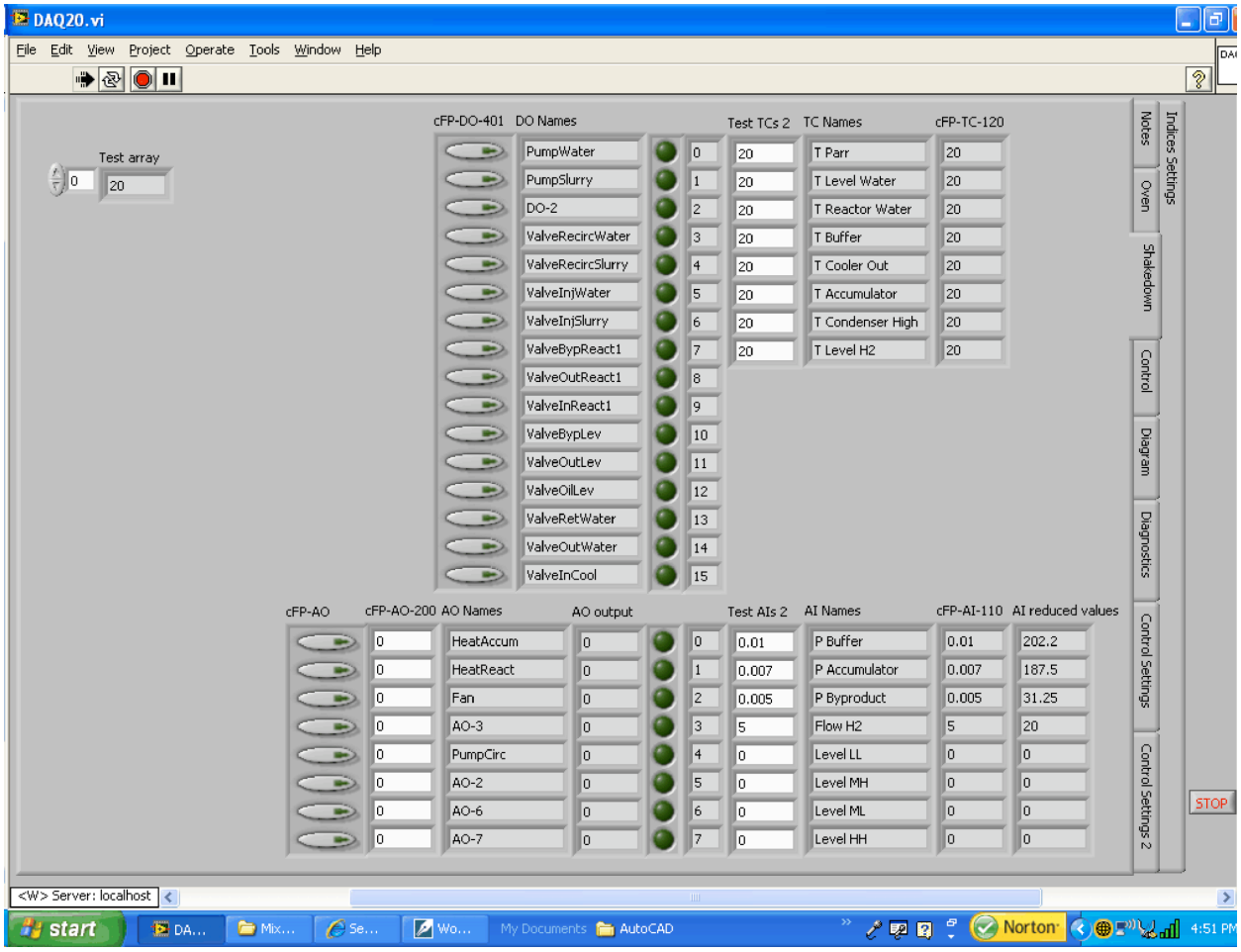

Figure 46 - Shakedown Tab

The Control Tab, Figure 47, is the primary control and data display page. On the left top is the space where the data file name is input as well as a radio button to turn the file write function on or off. There is a display of the time and time from reset and a button to reset the time to zero. Below that is a list of Macro Control buttons. Each button performs a separate process in the control sequence. There is a light that indicates if any switches have been set from the Shakedown tab. We had some troubles that resulted from forgetting that we had set some of the switches. The light helps to identify that switches have been set. This tab also has plots for the temperatures, pressures, hydrogen flow rate, and level probe currents. The program integrates the hydrogen flow, so there is also a pair of switches to zero the total flow and hydrogen production. Since some of the hydrogen flow may be due to pressure reductions in the buffer volume, the hydrogen production output displays the difference between the flow and the reduction in pressure.

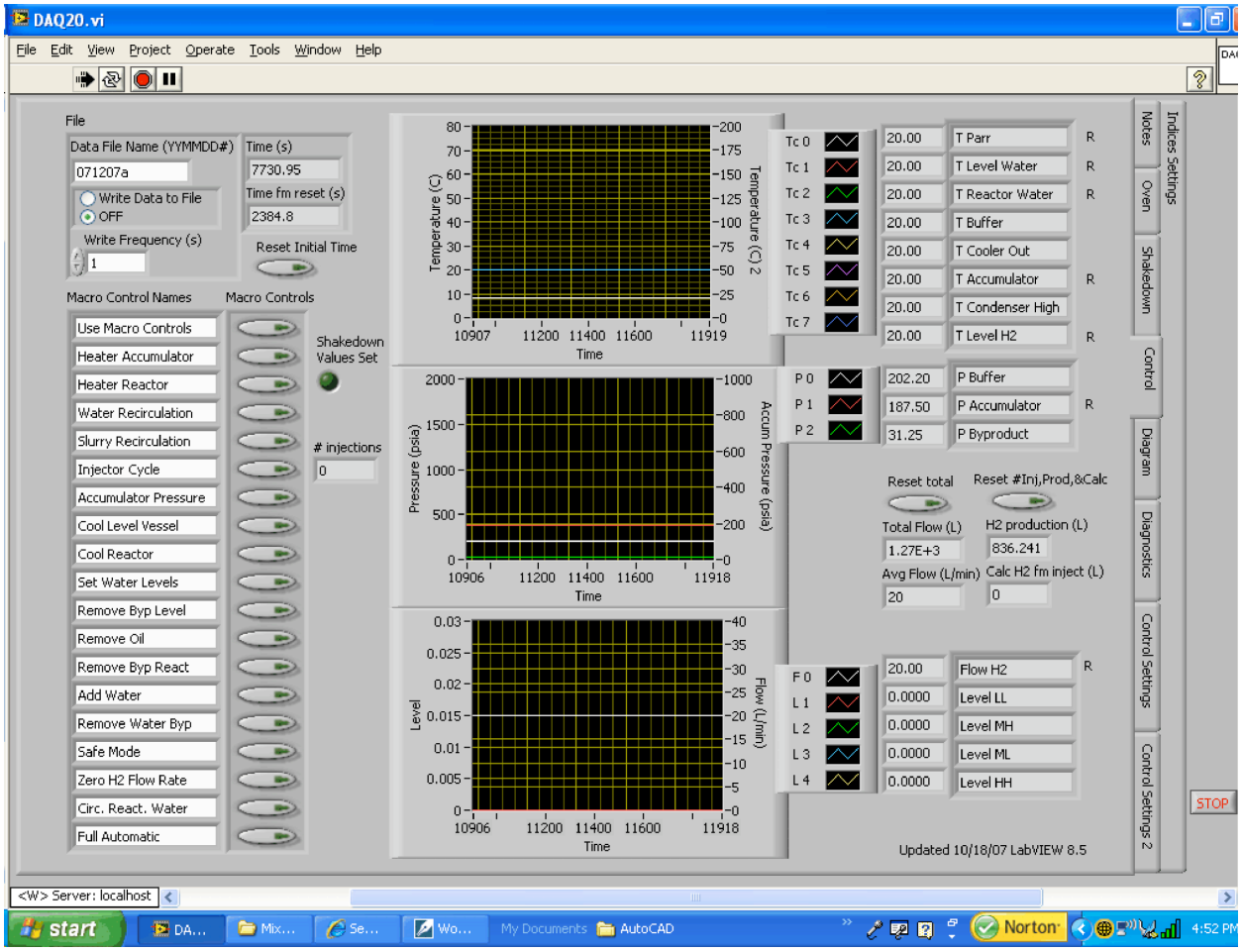

Figure 47 - Control Tab for Control Selection and Data Display

The diagram tab, Figure 48, provides an alternate display of the system. It is used primarily to observe the valve turning, pump, and heater sequences that the system is controlling.

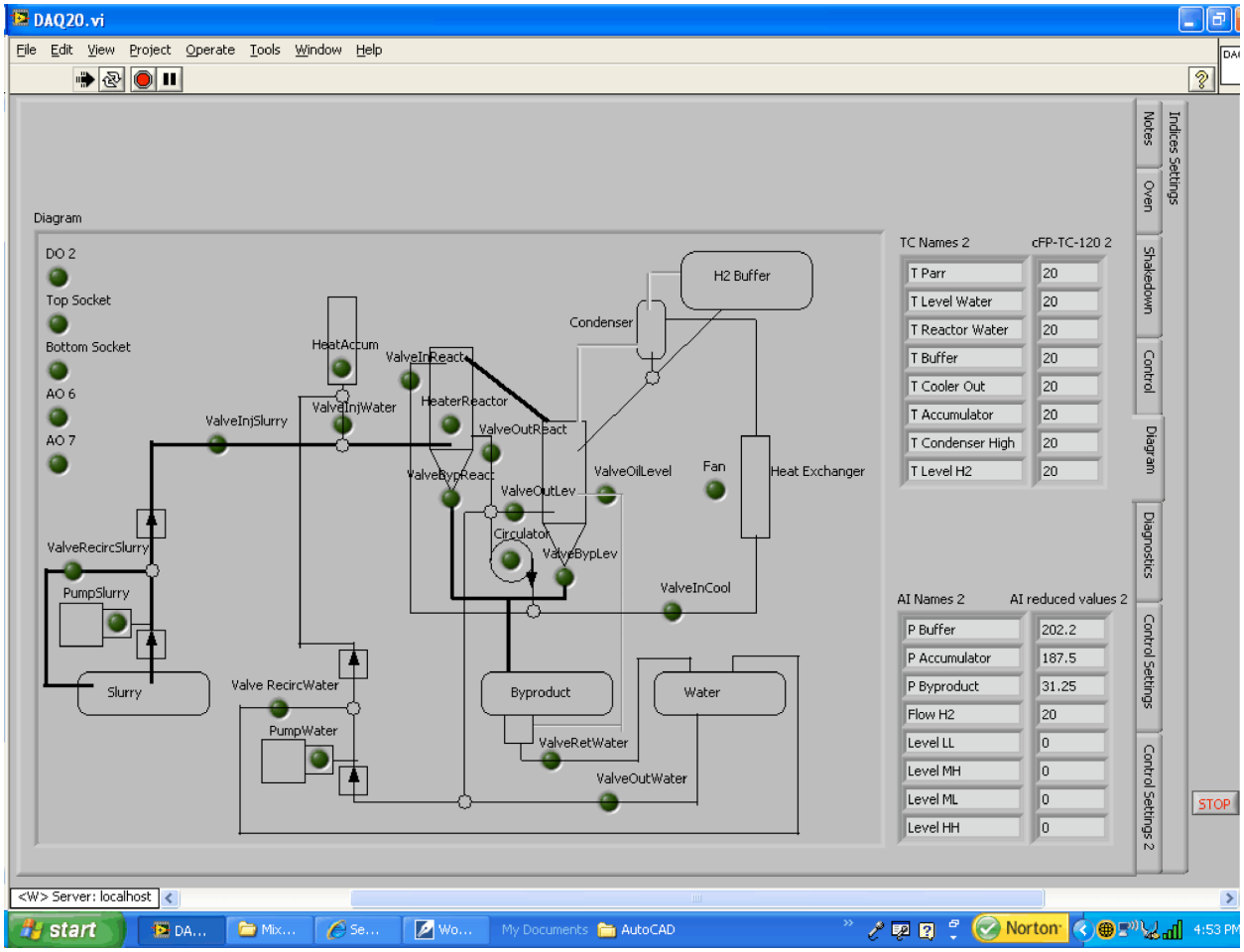

Figure 48 - System Diagram Provides and Alternate Display

The diagnostics tab, Figure 49, displays the values in the data array, the control array, the names array, and error messages from the two loops of the program.

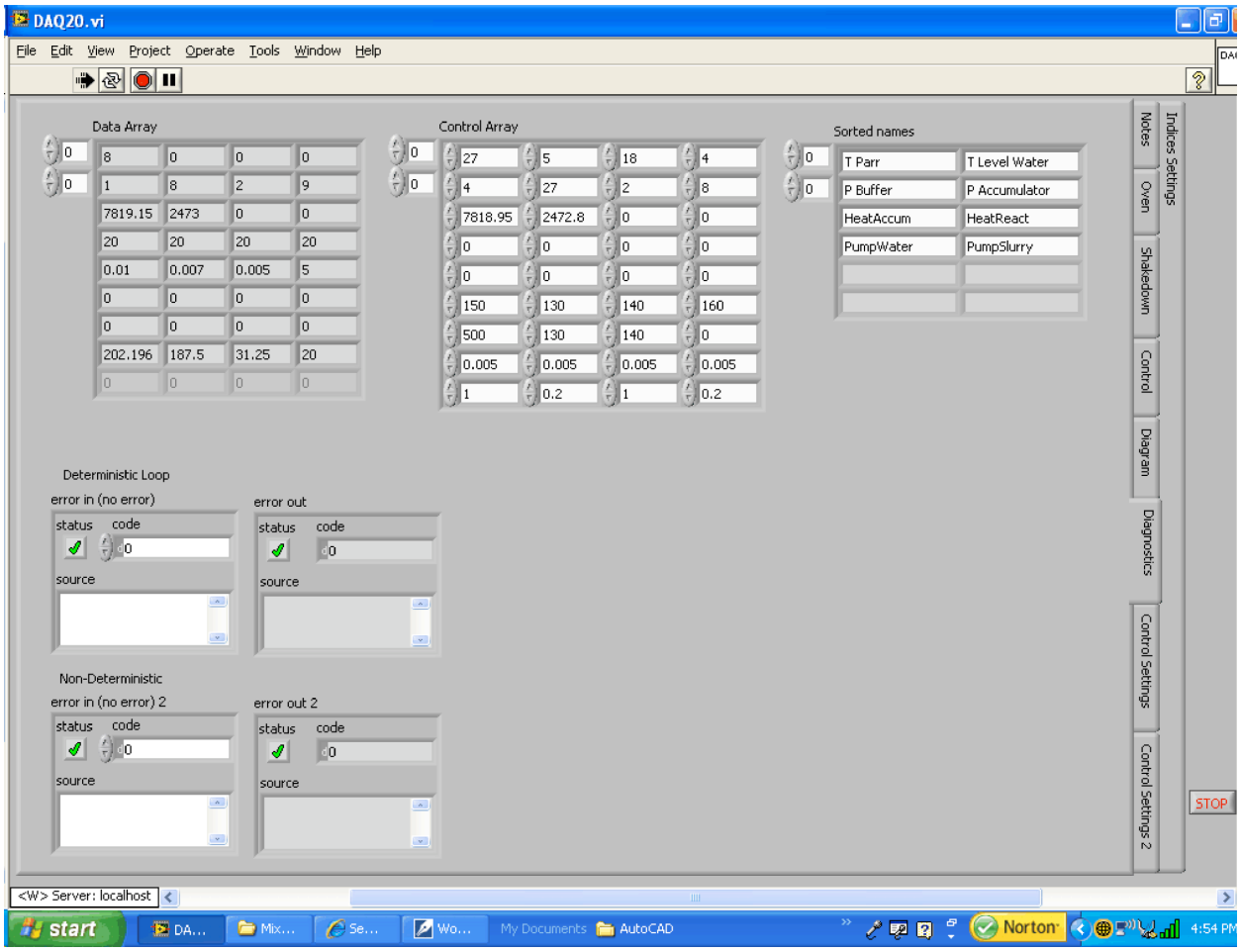

Figure 49 - Diagnostics Tab Provides Array and Error Displays

The Control Settings tab and the Control Settings 2 tab, Figure 50 and Figure 51, provide a means to set variables used in the control program. Most of the variables are time settings to define the time between the sequences of the control system.

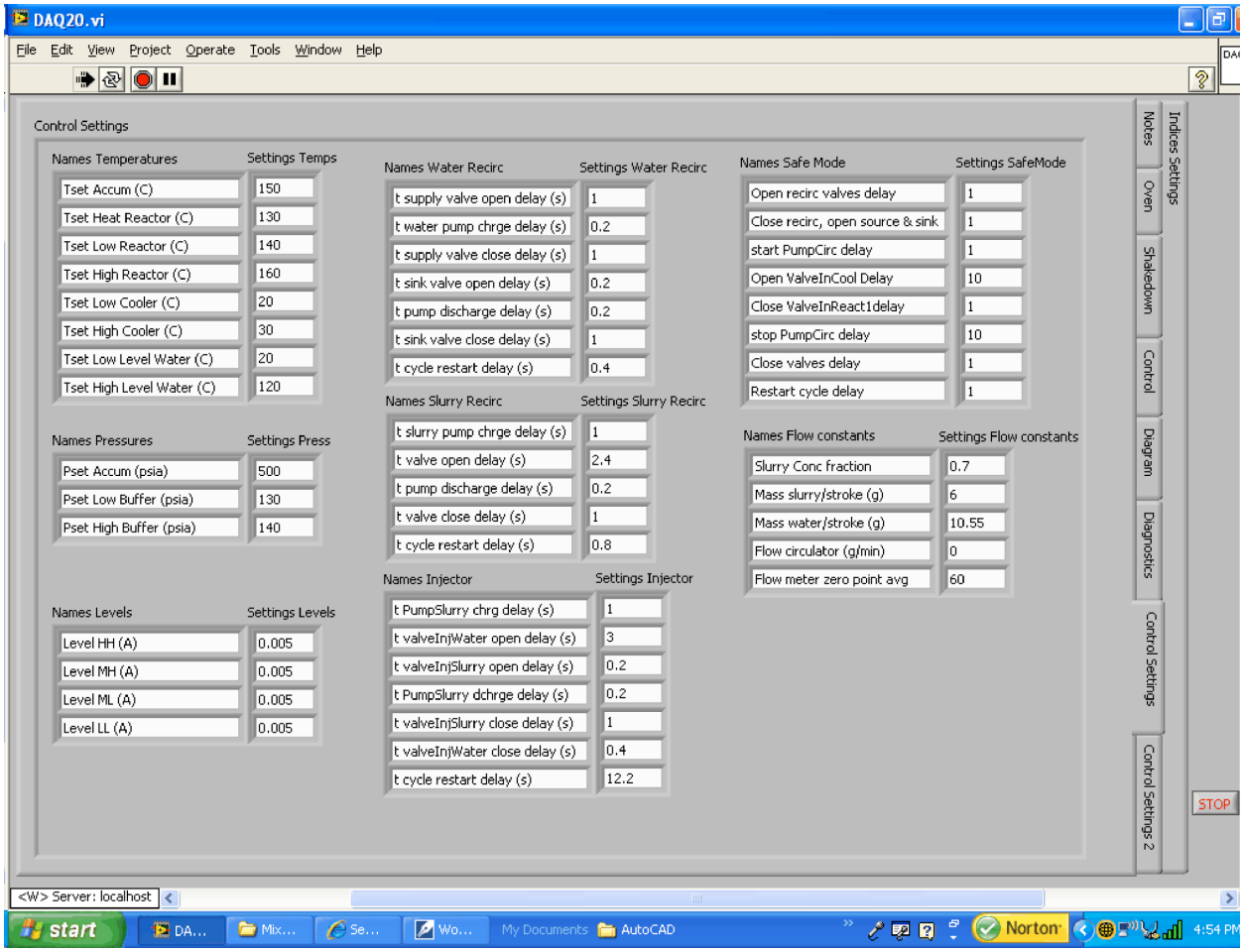

Figure 50 - Control Settings Tab

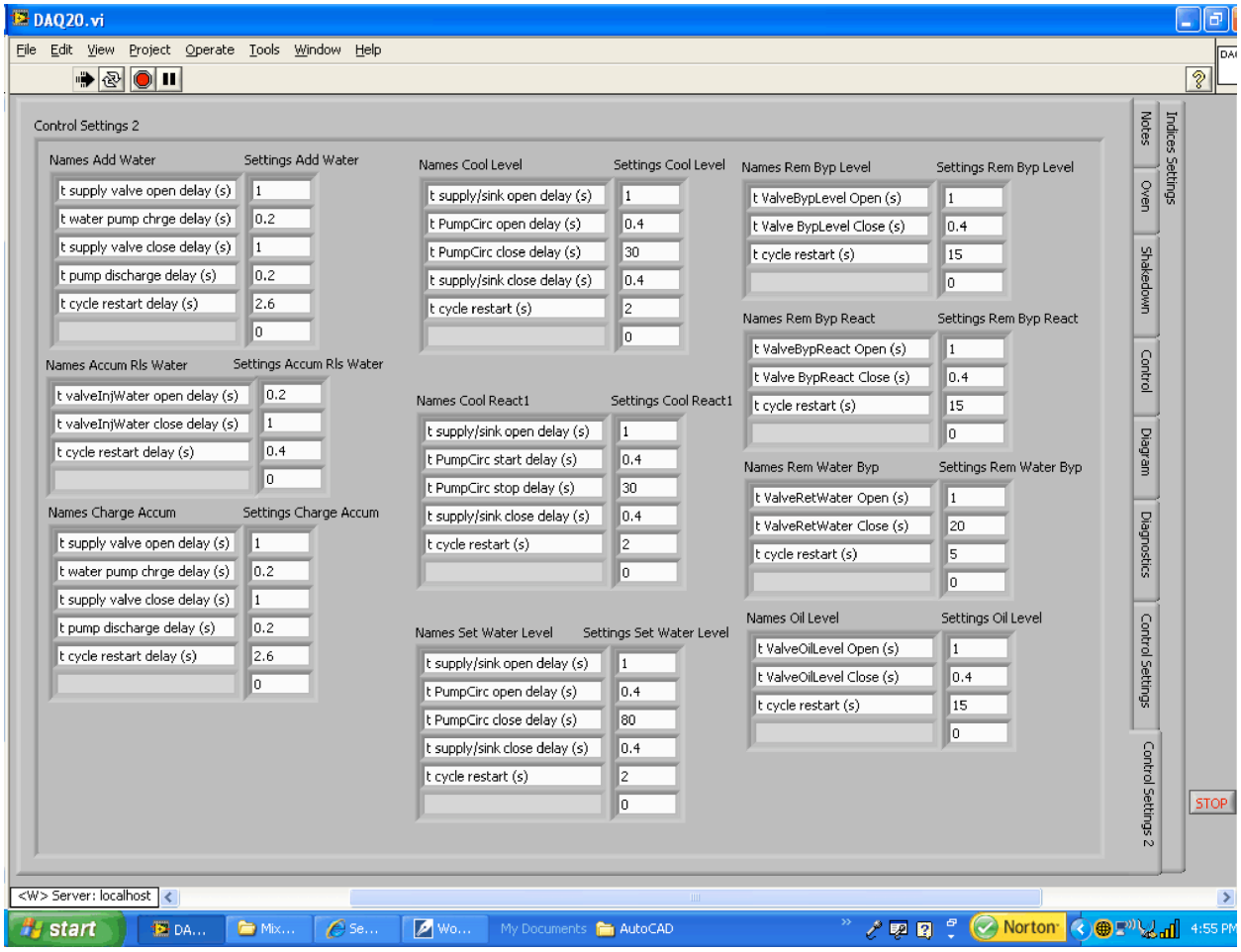

Figure 51 - Second Control Settings Tab

The Indices Settings tab, Figure 52, provides a means for defining the indices of the physical data acquisition and control system to the control program. The control program was written with the assumption that each of the measured variables and control variables were in the order of the displayed arrays. The indices define how they are actually connected to the sensor banks of the control system. There are four cards in the control system: a thermocouple input card, an analog input card, an analog output card, and a digital output card. This system provides a means for defining the actual connections in the event that the wiring gets changed.

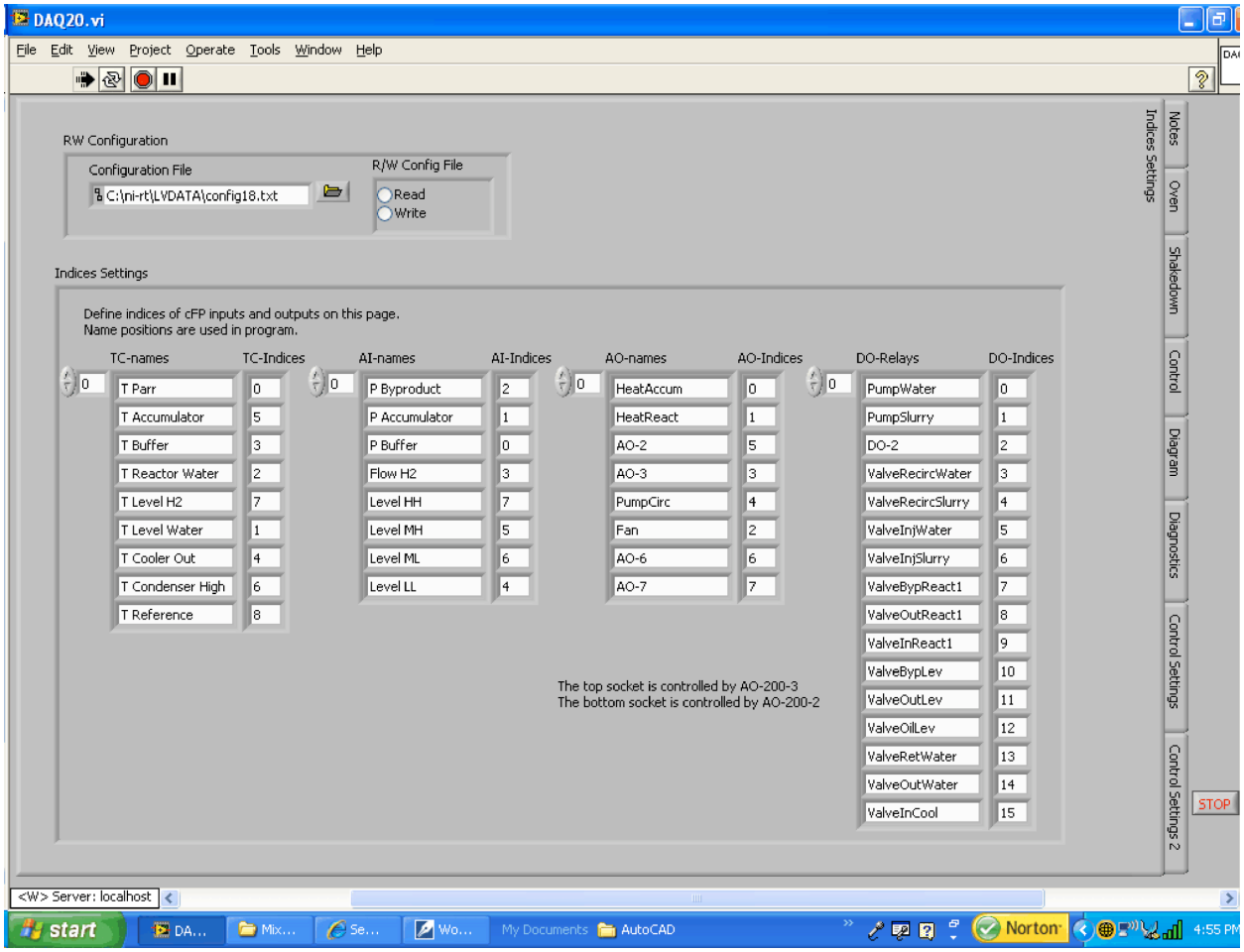

Figure 52 - Indices Settings Tab

The control sequence consists of:

Pumping water from the level vessel into the reactor to bring the temperature of the reactor into the reaction temperature range. This raises the level of the water in the reactor until it flows over a weir and back into the level vessel. If the level vessel gets too hot, water is pumped from the level vessel through the heat exchanger. Also if the level in the level vessel drops too low (using the low level sensor) during this process, water is drawn from the water storage and pumped into the level vessel.

Setting the level in the reaction vessel by pumping water from the reaction vessel into the level vessel until the high level sensor registers water level.

Heating the reaction vessel to the control setting.

Charging the accumulator to the set pressure.

Injecting water and slurry into the reaction vessel. We are finding that several injections can be performed in quick succession.

When a given number of injections have been performed, the byproducts are removed from the reaction vessel and the level vessel to the byproduct vessel. Then the reaction vessel is filled and cooled with water from the level vessel.

The process then repeats.

After the byproducts have been sent to the byproduct vessel, the pressure in the byproduct vessel is elevated enough to drive a water separation process. A valve at the bottom of the byproduct vessel is opened to allow water to flow through a sand filter and to the water storage tank.

After several cycles, oil will collect in the level vessel. This is determined by monitoring levels inside the level vessel and in a water level tube outside the level vessel. The water level tube only contains water as it is connected to the bottom of the level vessel and the hydrogen exhaust from the level vessel. The level observed in the water level vessel will be different from the level observed in the level vessel because the layer of oil is less dense than water. When the oil level is sufficiently deep, oil is removed from the level vessel and injected into the byproduct vessel to back flush the sand filter. When properly sized, we anticipate that we will be able to recover the water from the byproduct vessel and concentrate the solids and oils into a paste.

Hydrogen produced from the reaction flows from the reaction vessel through the weir to the level vessel and then up to a condenser. The condenser consists of a chamber with packing through which the hydrogen flows. The packing is maintained at a relatively cool temperature by the water flow from the heat exchanger. Hydrogen is cooled as it flows through both the level vessel and the condenser. Water recovered is returned to the level vessel. Hydrogen flows to the buffer volume. Hydrogen is removed from the system through the buffer volume. Any water condensing in the buffer volume is returned to the level vessel.

5.2.3.6 Estimation of System Energy Density

The system energy density was estimated by calculating the mass and volume of the components that will be required for tanks, valves, mixing vessels, condensers, and pumps. The chemical hydride slurry system will require a tank in which to store the slurry, the water, and the byproducts. We have assumed that these materials will be stored in the same vessel within separate bladders and that this vessel will be fabricated from thin wall sheet metal. As the slurry and water are consumed, their bladders will be reduced in volume while the bladder for the byproduct will increase in volume. Since the byproduct is made up of magnesium hydroxide and magnesium oxide, we have calculated the volume based on 50% molar magnesium hydroxide and 50% molar magnesium oxide, which is what we have been measuring. The containment tank has been sized to contain the maximum volume of water, slurry, and byproduct depending on the conditions assumed. We have assumed that the mixer system will be built to minimize mass and volume, that the pumps will be incorporated into a single block, that the valves will be of a spool type construction that can also use the pump block for structure, and that the reactor vessels will share a common block to also share structure. We have sized the reaction vessel condenser and the condenser for exhaust

to be appropriate for the conditions. All masses and volumes are estimates to give us an idea of the system energy density.

The system mass and volume has been estimated for a peak hydrogen flow rate of 3.0 kg/hr. This peak flow defines a particular size for the reaction vessel, the pumps, and valves. With a 50% efficient fuel cell, a fuel consumption rate of 3 kg/hr will provide about 50 kW of power to the vehicle.

To see what the effect might be of including a condensation system to recover water from the fuel cell, we have estimated the size of such a condensation system for each of these cases. We have assumed that the water vapor leaving the fuel cell will be carried by an air flow rate of 200% excess air. With this condition and a cooling temperature of 31°C, we are estimating a recovery of 88% of the water produced in the fuel cell. Guidance from Daimler Chrysler indicates that they plan to flow a significantly greater amount of excess air through the fuel cell to help keep the fuel cell dry. This design will preclude the use of a condensation water recovery system.

Not having any guidance for the amount of hydrogen to store, we have calculated systems for four storage volumes, 5, 10, 15, and 20 kg of hydrogen.

Table 2 displays the results of our estimates for 5, 10 and 20 kg of stored hydrogen. We have highlighted in red the energy density and the specific energy density of the system for 10 kg of hydrogen stored in a system in which all the water is stored. The gravimetric energy density is estimated to be 1.8 kWh/kg and the volumetric energy density is estimated to be 1.7 kWh/L. These values compare favorably to the DOE 2010 goals of 2.0 kWh/kg and 1.5 kWh/L.

Table 2 - Chemical Hydride Slurry System Mass and Volume

	Condense Exhaust		Carry water		Condense Exhaust		Carry water		Condense Exhaust		Carry water	
H2 Stored (kg)	5.0		5.0		10.0		10.0		20.0		20.0	
H2 Peak Flow Rate (kg/hr)	3.0		3.0		3.0		3.0		3.0		3.0	
Item	Mass kg	System Volume L	Mass kg	System Volume L	Mass kg	System Volume L	Mass kg	System Volume L	Mass kg	System Volume L	Mass kg	System Volume L
Fuel Tank	1.5	51.4	1.9	81.4	2.2	101.5	2.9	161.4	3.3	201.7	4.5	320.8
Balloons or bladders for water	0.2		0.8		0.3		1.1		0.5		1.7	
Balloons or bladders for slurry	0.9		0.9		1.3		1.3		2.0		2.0	
Balloons or bladders for byproduct	0.9		0.9		1.3		1.3		2.0		2.0	
Fuel/Water Pump	0.3	0.3	0.3	0.3	0.3	0.3	0.3	0.3	0.3	0.3	0.3	0.3
Heater	0.1	0.1	0.1	0.1	0.1	0.1	0.1	0.1	0.1	0.1	0.1	0.1
Mixer Section	1.2	2.3	1.2	2.3	1.2	2.3	1.2	2.3	1.2	2.3	1.2	2.3
Mixer motor/stirrer	0.3	0.3	0.3	0.3	0.3	0.3	0.3	0.3	0.3	0.3	0.3	0.3
Gas Separator Tank	2.3	9.4	2.3	9.4	2.3	9.4	2.3	9.4	2.3	9.4	2.3	9.4
Separator Mixer Motor	0.5	0.3	0.5	0.3	0.5	0.3	0.5	0.3	0.5	0.3	0.5	0.3
Condenser for cooling	5.0	15.0	5.0	15.0	5.0	15.0	5.0	15.0	5.0	15.0	5.0	15.0
Filter/separator	0.7	1.6	0.7	1.6	0.7	1.6	0.7	1.6	0.7	1.6	0.7	1.6
By-product Valve	0.1	0.1	0.1	0.1	0.1	0.1	0.1	0.1	0.1	0.1	0.1	0.1
Water Valve	0.1	0.1	0.1	0.1	0.1	0.1	0.1	0.1	0.1	0.1	0.1	0.1
Piping/fittings	0.3	1.0	0.3	1.0	0.3	1.0	0.3	1.0	0.3	1.0	0.3	1.0
Condenser for Exhaust	5.0	15.0	0.0	0.0	5.0	15.0	0.0	0.0	5.0	15.0	0.0	0.0
Pump for exhaust water	0.3	0.3	0.0	0.0	0.3	0.3	0.0	0.0	0.3	0.3	0.0	0.0
Subtotal	19.5	96.9	15.2	111.7	21.2	147.1	17.4	191.8	23.9	247.2	20.9	351.1
Slurry			51.5				103.0				206.1	
Reaction Water to Carry			33.5				67.0				134.0	
Byproduct Water to Carry			0.0				0.0				0.0	
Byproduct	80.0				160.1				320.1			
Total	99.6	96.9	100.3	111.7	181.3	147.1	187.5	191.8	344.0	247.2	361.1	351.1
Stored Energy, kWhrth	**166.6**		**166.6**		**333.1**		**333.1**		**666.3**		**666.3**	
Specific Energy, kWh/kg, kWh/L	**1.7**	**1.7**	**1.7**	**1.5**	**1.8**	**2.3**	**1.8**	**1.7**	**1.9**	**2.7**	**1.8**	**1.9**

Figure 53 and Figure 54 display the Gravimetric and Volumetric Energy Densities calculated for the cases varied by hydrogen stored mass and by whether water is recovered from the fuel cell or carried by the vehicle. Both gravimetric and volumetric energy densities would be higher if water is condensed. For the gravimetric energy density, the advantage is not great. The advantage of condensing water from the exhaust appears to be greater for the volumetric energy density. The figures also show the improvement to the energy density figures of merit as the volume of stored hydrogen is increased. Again the gravimetric advantage is not great but the volumetric advantage is more noticeable.

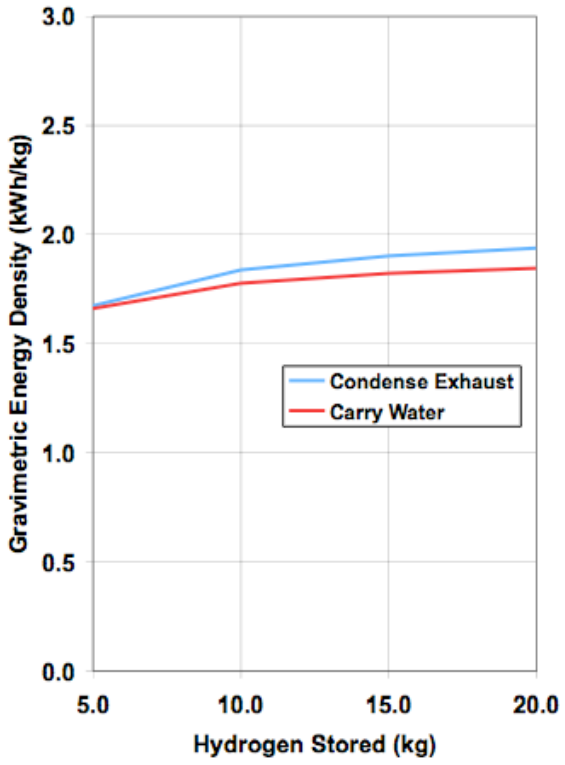

Figure 53 - Effect of Amount of Stored H2 on Gravimetric Energy Density

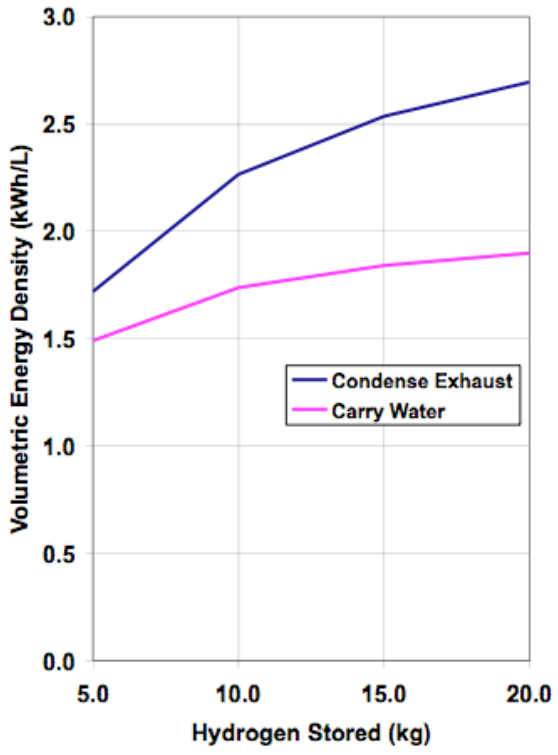

Figure 54 - Effect of Amount of Stored H2 on Volumetric Energy Density

It should be noted that the mass of the system is largest for the system when the system is full for the system with water recovery and when the system is empty for the system in which all the water is carried.

Figure 55 displays the relative masses of the system in which water is condensed. The byproduct makes up the largest fraction of the total mass of the system. Figure 56 displays the relative masses of this same system without the mass of the byproducts. The condensers are the largest mass components. Figure 57 displays the relative masses of the components of the system in which all the water is carried. Figure 58 displays the relative volumes of the components of the system in which all the water is carried. As with the case in which water is condensed, most of the mass is in the reactants or byproducts. For all these figures, the mass and volume of the reactants

and products are for 5 kg of stored hydrogen. The relative differences between the stored reactants and products and the rest of the system gets bigger as the stored mass increases.

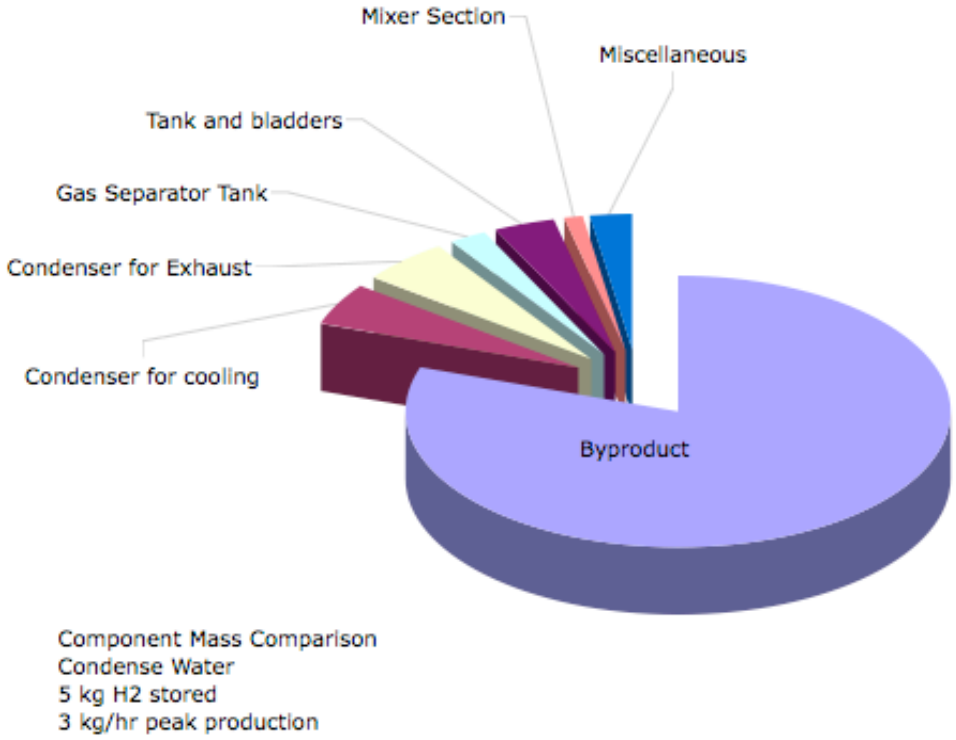

Figure 55 - Relative Mass Comparison of Slurry System with Water Recovery

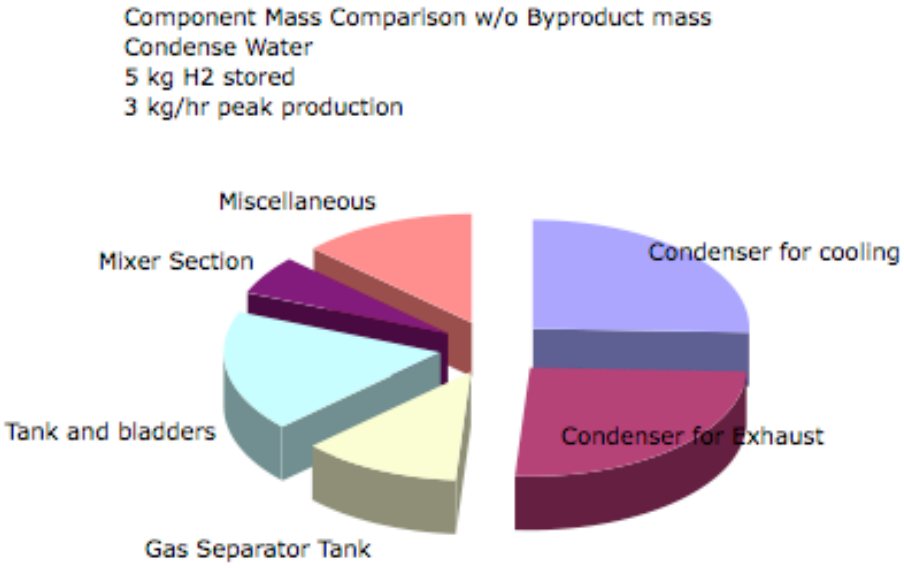

Figure 56 - Relative Mass Comparison Excluding Byproduct Mass of Slurry System with Exhaust Water recovery

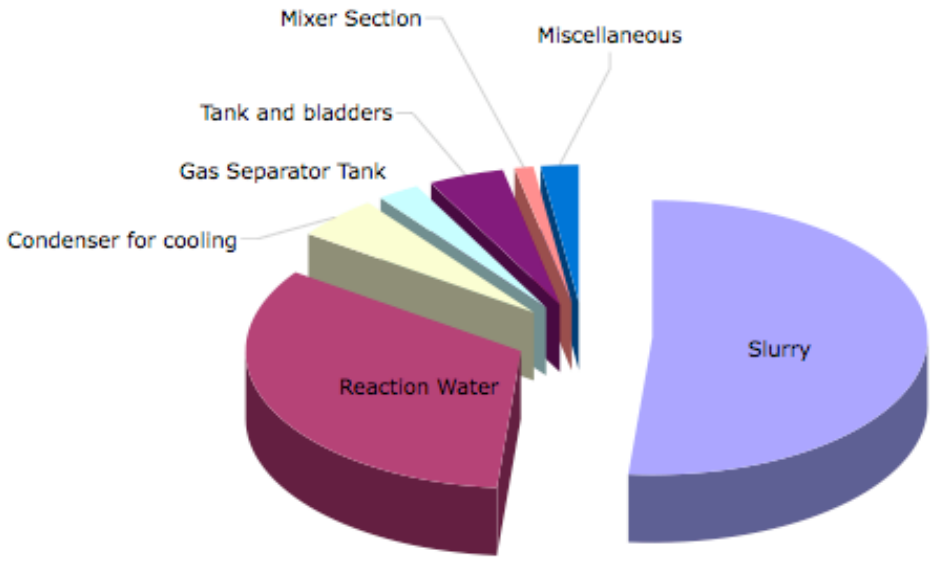

Figure 57 – Relative Mass Comparison of Slurry System in which All Water is Carried

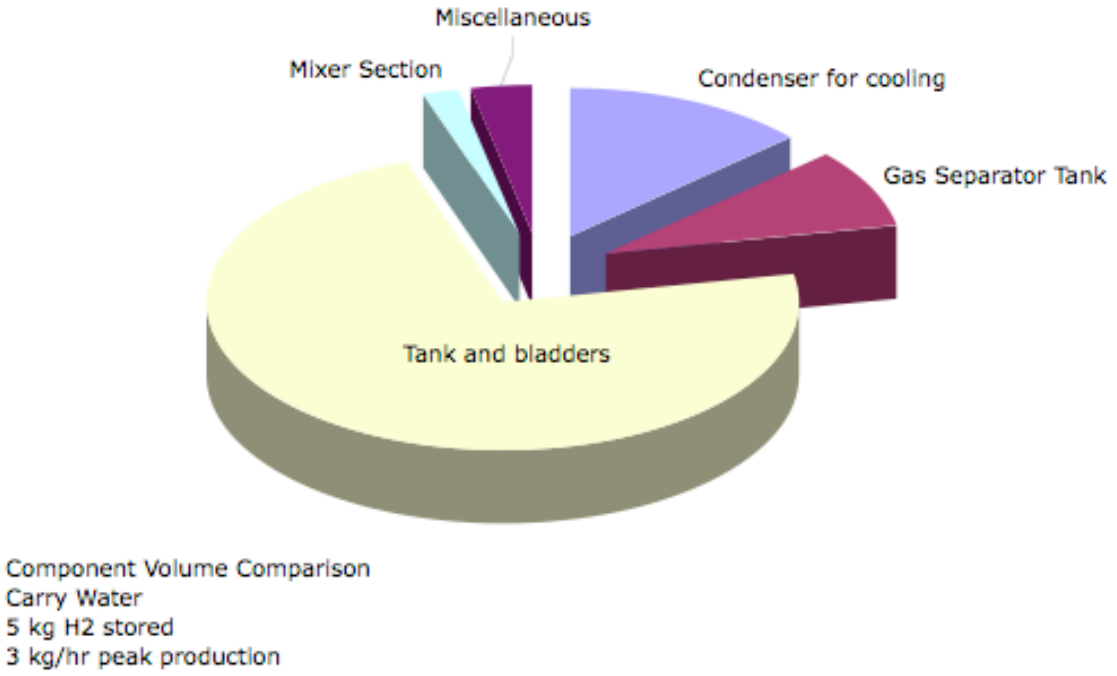

Figure 58 - Relative Volume Comparison of a Slurry System in which all Water is Carried

5.3 Task 3 – Slurry and Mixer Testing

5.3.1 Description

An important issue related to the use of chemical hydride slurry is to prove its ability to supply hydrogen to fuel cells. This task will be focused on the testing of a MgH_2 slurry hydrogen storage system to measure purity of H_2, stability of the slurry, and performance of the slurry/mixer system over time. Slurry stability of at least one month is desired. The results of these tests will guide further development effort and testing to be performed on the slurry and mixer. Examples of further testing will be the use of impurities in the water supply, freeze protection, and on-board vs off-board applications.

5.3.2 Summary

- A semi-continuous mixer design was demonstrated to start and stop reliably and to produce hydrogen with no additional heat input besides initial startup heat.
- The hydrogen produced was tested for quality and found to have only trace contaminants below 10 ppm levels. Mineral oil levels were found to be less than 0.1 ppm.
- The slurry performed well, remaining in suspension for months and pumping easily
- The byproduct handling system demonstrated the capability of recovering excess water for reuse by the system and concentrating the solids and oils in the byproduct storage tank.
- Further work is required on the byproduct storage. The filtering system needs to be scaled up to fit the scale of hydrogen production and slurry use. The tested system was found to be undersized. The handling of the oil and solids byproduct also needs additional development.
- Byproduct analysis confirms that MgO is being formed during the reaction. The byproduct solids were found to be 45 to 48% molar MgO. This is an important observation because less water will need to be carried if MgO is formed rather than $Mg(OH)_2$.

5.3.3 Discussion

5.3.3.1 Overview

A definitive test of the semi-continuous mixer system was performed on 7 November 2007. During this test, samples were taken of the hydrogen and the byproducts to determine the quality of the hydrogen and the completeness of reaction of the magnesium hydride. The result of this test are discussed in this section. We will begin with a discussion of the semi-continuous mixer operation followed by a discussion of the hydrogen quality results and then a discussion of the byproduct recovery system.

5.3.3.2 Semi-Continuous Mixer Operation

5.3.3.2.1 Summary

The semi-continuous mixer system was designed and built to demonstrate the simplicity of the slurry water mixing system using a batch reaction process. The design

concept is to react small quantities of slurry with water in pools of water. Multiple reactors can be clustered around the support apparatus to provide continuous and large hydrogen production rates. One batch reactor was built for this apparatus to test and demonstrate the concept. In a commercial system, many batch reactors could be operated at intervals to produce hydrogen at any rate required. The operation of this apparatus also demonstrates the reaction rates and the byproduct management. Since we did not have much prior experience with the byproduct handling, this apparatus provided us with our initial design data for byproduct management.

The apparatus performed well. Hydrogen was produced at rates exceeding the design of 10 L/min. Temperatures were controlled though some temperature excursions during the reactions were recorded. Byproduct was captured and water was removed from this byproduct and returned to the water storage vessel. The apparatus accomplished all our goals and demonstrated semi-continuous mixer design approach for reacting slurry and water to produce hydrogen. (Our first approach was discussed in the previous section and is labeled the continuous mixer system. The development of the continuous mixer system was postponed because we decided that a complete understanding of the process to achieve a stable and robust apparatus would exceed the program resources for its development).

5.3.3.2.2 Operation

The semi-continuous mixer is shown, in schematic form, in Figure 59. The heart of the mixer design is the reaction vessel. In a commercial system, several reaction vessels would operate around a common level control vessel. Slurry and water are injected into the reaction vessel together through a nozzle to achieve further mixing with the water in the reaction vessel and to spread the reacting magnesium hydride throughout the reaction zone of the vessel. As the reaction proceeds, hydrogen rises to the surface of the water within the reaction vessel and byproducts fall to the bottom of the vessel. The reaction vessel and the level control vessel are connected so that gas can flow into to the level control vessel as it is produced in the reaction vessel. From the level control vessel, the produced hydrogen flows through the condenser and to the hydrogen buffer storage volume. We have used a backpressure regulator to hold the pressure within the buffer tank to 150 psia. Our flow measurements are of the hydrogen flow that is released from the buffer tank.

In a typical production cycle, several injections are performed in succession to allow the heat of reaction to warm the cool slurry and bring the reactants up to reaction temperatures. Water from the reaction vessel is used with each injection to provide this heat and to mix with the slurry in a turbulent flow as it enters into the reaction vessel. An accumulator is filled with the reaction water to provide a high-pressure injection of the slurry and water through the injection nozzle.

Periodically, the byproduct valve at the bottom of the reaction vessel cone is opened to allow pressure from within the reaction vessel to push settled byproduct into the byproduct storage system.

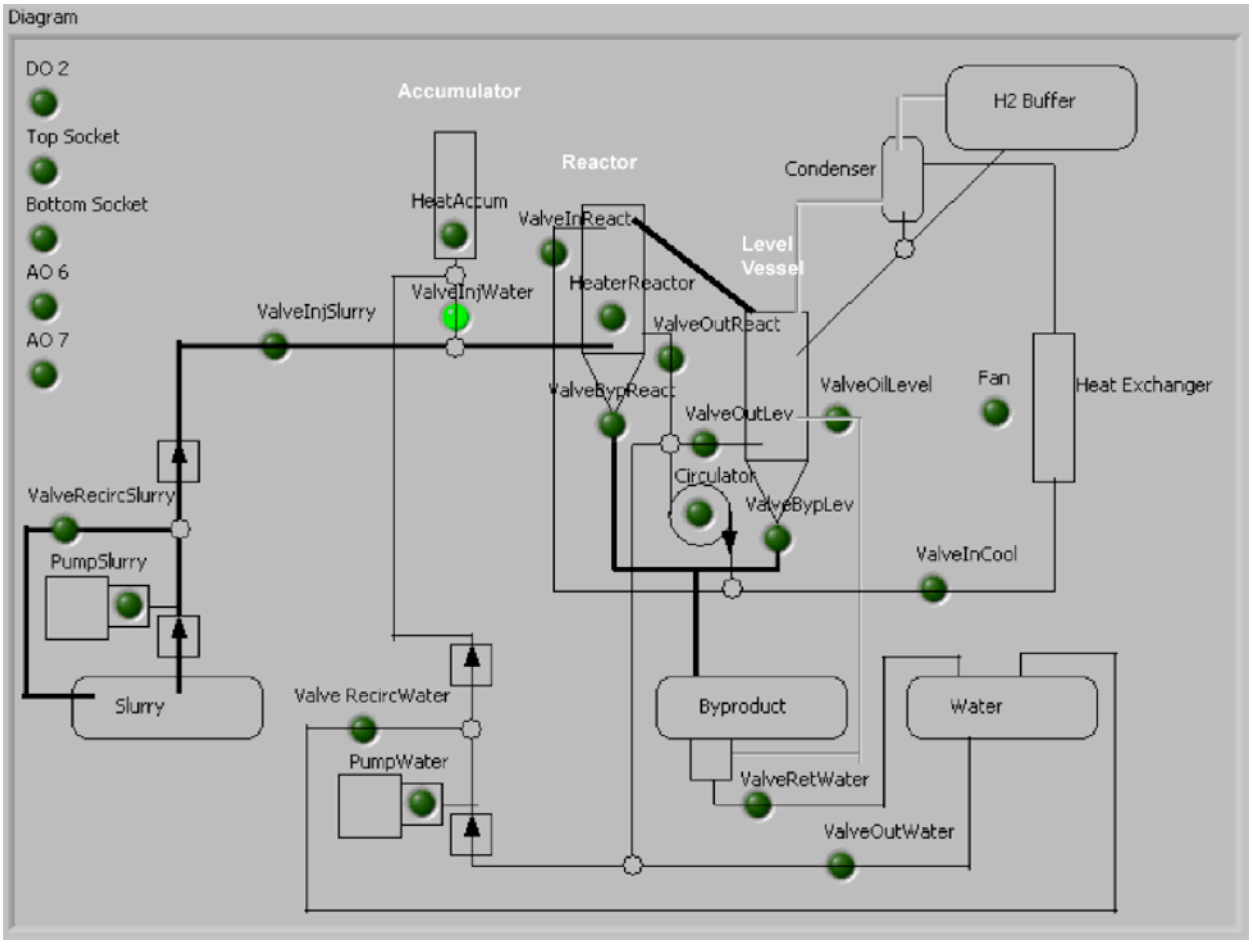

Figure 59 - Schematic of the Semi-Continuous Mixer System

When the water within the reaction vessel exceeds the design temperature, the injections are stopped and the water within the reactor is circulated from the reaction vessel, through a heat exchanger, and back to the level control vessel. After a defined period of time, water from the level vessel is circulated back into the reaction vessel until the water in the reaction vessel reaches the weir tube and the level in the level control vessel ceases to fall. Then water is removed from the reaction vessel to set a level about 1” below the weir. This prevents reactants from flowing into the level control vessel during the reaction.

Hydrogen from the reaction flows through the weir tube, into the level control vessel, then through a condenser and into a hydrogen buffer storage. Water condensed in the condenser is returned by gravity to the level control vessel. The condenser is cooled using the water leaving the heat exchanger.

After several cycles of reaction and level setting, the byproducts are removed from the reaction vessel cone and the level control vessel cone. The byproducts flow into a byproduct vessel as a mixture of solid byproducts and water. Much of the oil from the slurry has separated from the byproduct solids by this time and has been collected within the level control vessel. When the oil layer is sufficiently thick, and the water level in the level control vessel is below the oil removal port, the oil is removed from the level control vessel to the byproduct vessel to be stored with the byproduct solids.

Within the byproduct vessel, water is filtered through a sand filter into the low pressure water storage vessel. When the oil is removed from the level control vessel, it passes through the sand filter in the reverse direction of the water to clear the sand of the very small byproduct particles. This oil and byproduct mixture is removed from the byproduct vessel periodically. In a commercial apparatus, it would be stored in a bladder within the slurry storage vessel. Samples of this material were taken during our testing.

5.3.3.2.3 Results

APPARATUS AND OPERATION

The 7 November 2007 test ran for about 6 hours. Pictures of the apparatus are shown in Figure 60 through Figure 63. The apparatus is pneumatically actuated and it uses a National Instruments compact Fieldpoint Data Acquisition and Control system. It is instrumented with pressure and temperature transducers. It uses a backpressure regulator to maintain the pressure in the buffer volume tank at about 150 psia. Hydrogen flow from the backpressure regulator is measured by an Aalborg hydrogen flow meter with a range of 0 to 20 standard Liters per minute of hydrogen.

Figure 60 - Semi-Continuous Mixer System – Front View

Figure 60 shows the buffer tank at the top of the apparatus. The control box is on the left. The water tank is the white plastic vessel in the middle. The level control vessel is right of the middle of the picture. It is a 3” stainless steel tube and cone assembly with a water level gauge. The 3” stainless steel T with a cone on the far right is the byproduct recovery assembly.

We experimented with some level detectors within the level control vessel but had mixed results. We observed the signal rising and falling with the level of the water but the level was not consistent. For this test, we relied on both the level probe measurements and the level gauge. Pneumatic ball valves were used to control the flow of slurry, water, and byproducts.

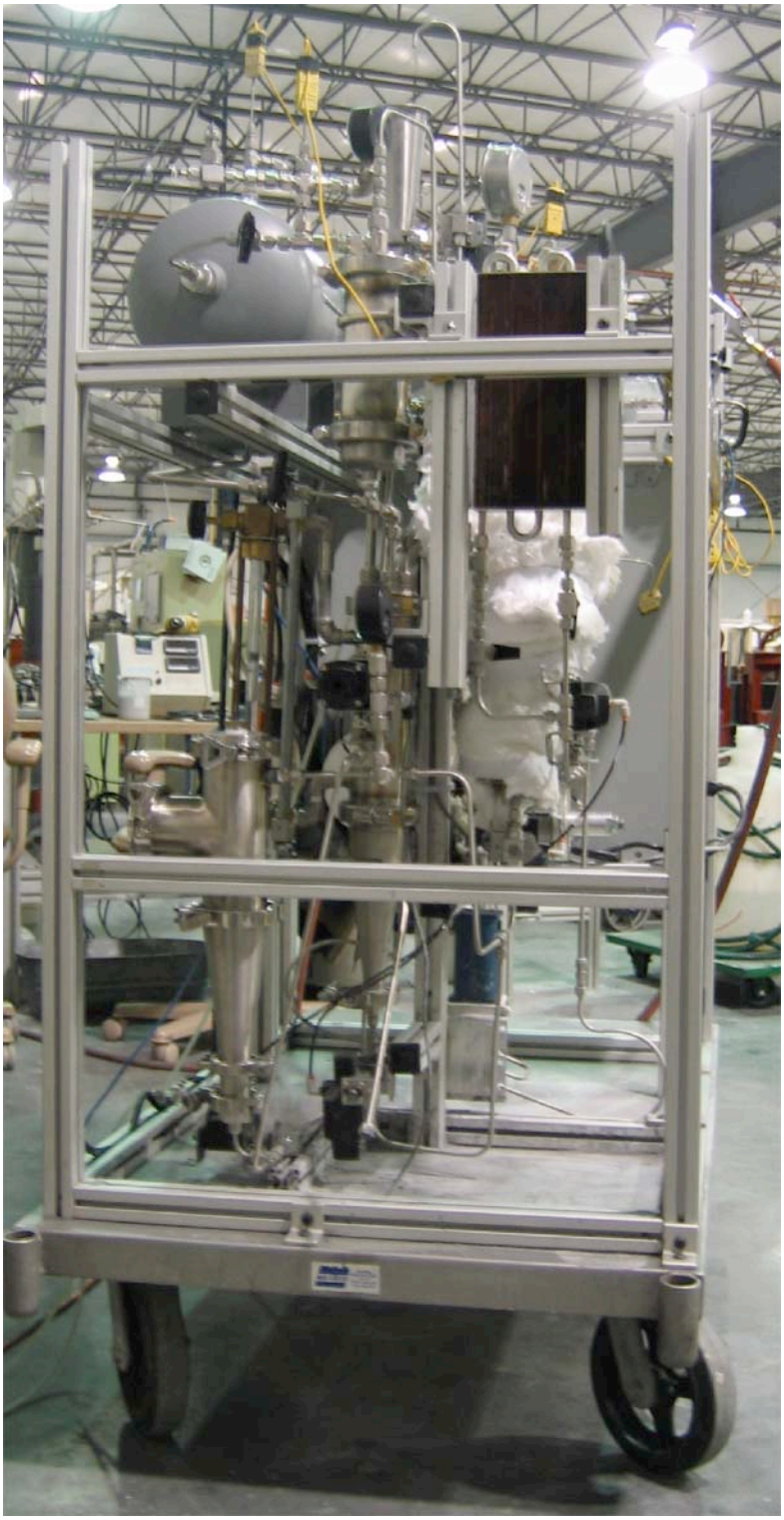

Figure 61 - Semi-Continuous Mixer - View from Right

The right side view, Figure 61, shows the heat exchanger used to reject heat from the system (top right) and the byproduct recovery assembly (bottom left).

Figure 62 - Semi-Continuous Mixer - Rear View

The rear view, Figure 62, shows the water pump (lower center) and the slurry pump (upper center). The reaction vessel and the accumulator are wrapped in insulation. At the bottom of the apparatus is the blue circulation pump that is used to move water between the reactor, level control vessel, and the heat exchanger.

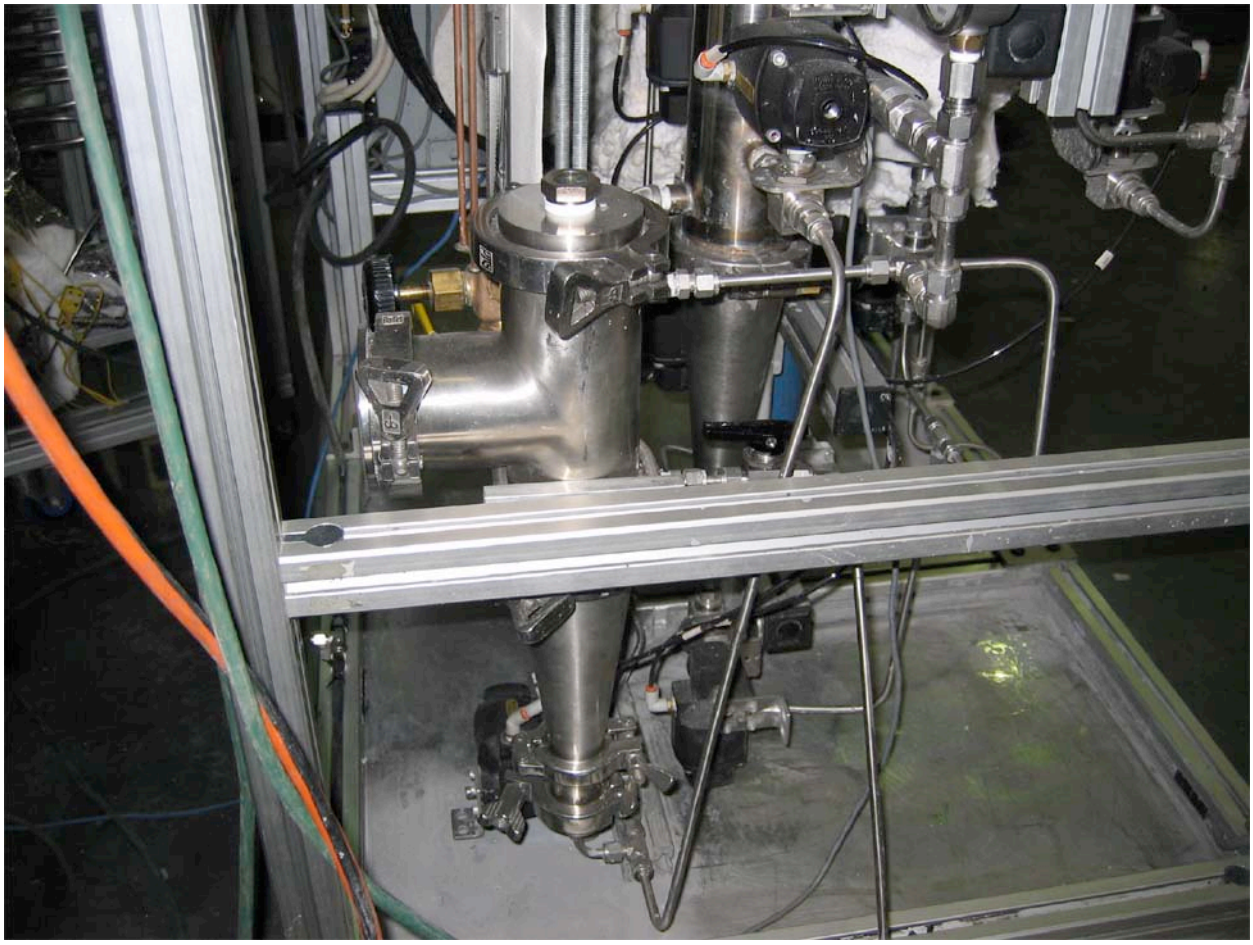

Figure 63 - Semi-Continuous Mixer - Close-up of Byproduct Recovery Apparatus

The test was begun with the purging of the gaseous portion of the apparatus with hydrogen. Hydrogen from the buffer volume was used for this purpose. Figure 64 displays the reactor temperature, the system pressure (measured in the buffer volume) and the slurry injection signal. The pressure reduction in the system is noted by the green curve. The electric heater in the reaction vessel was on during the purge process to bring the reaction vessel up to operating conditions. When the reaction vessel had achieved about 110°C, the injector was cycled a couple times to test the reaction and to add additional heat to the reaction vessel. Hydrogen flow measured by the flow meter and the hydrogen pressure rise indicates that the reaction began with the first injection (see Figure 66). The temperature of the reaction vessel is also seen to be disturbed during the injection.

Figure 65 shows the temperatures measured in the reactor and accumulator along with the control signals for the accumulator and reactor heaters. We used both heaters at the startup to bring the temperature of the system up rapidly. Upon achieving stable reaction, we found that we could turn off the accumulator heater. We found that we could operate without the reactor heater but that the system performed with more stability when we started the injection cycle with the reactor heater on. This is an issue that will require more development.

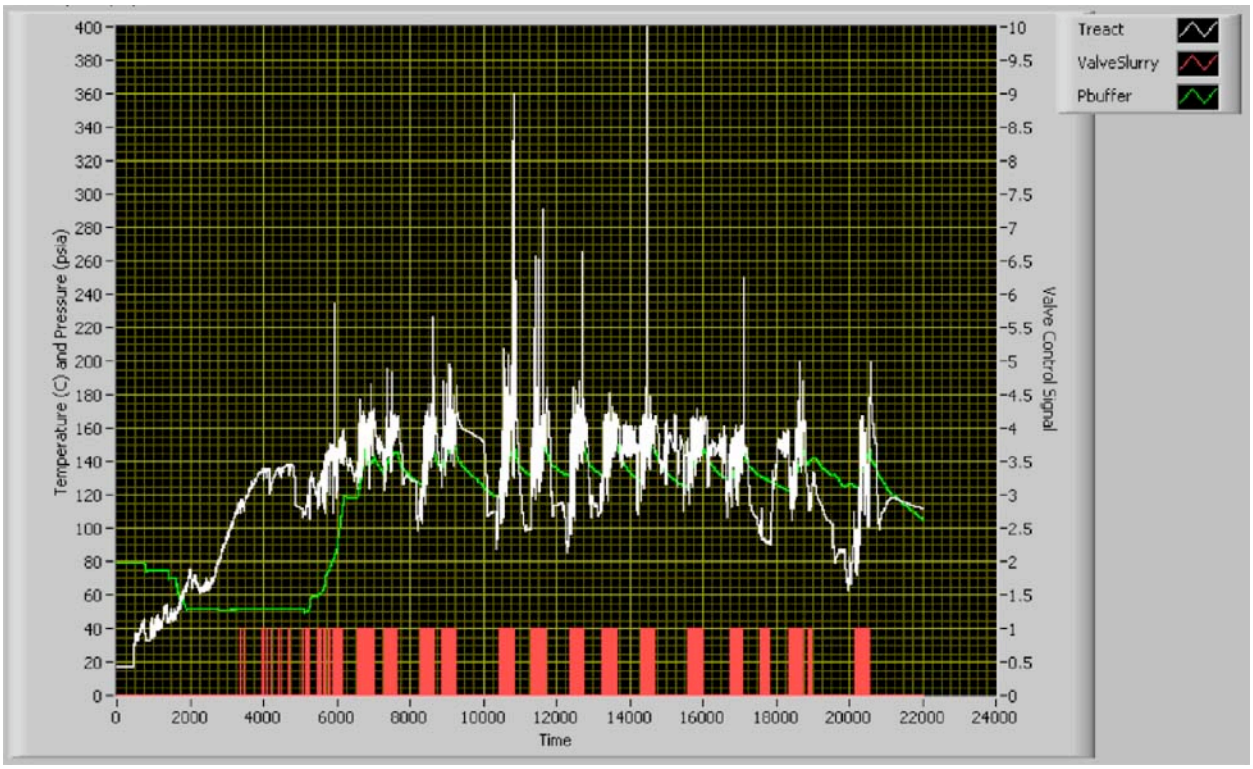

Figure 64 - Reactor Temperature, System Pressure, and Slurry Injection

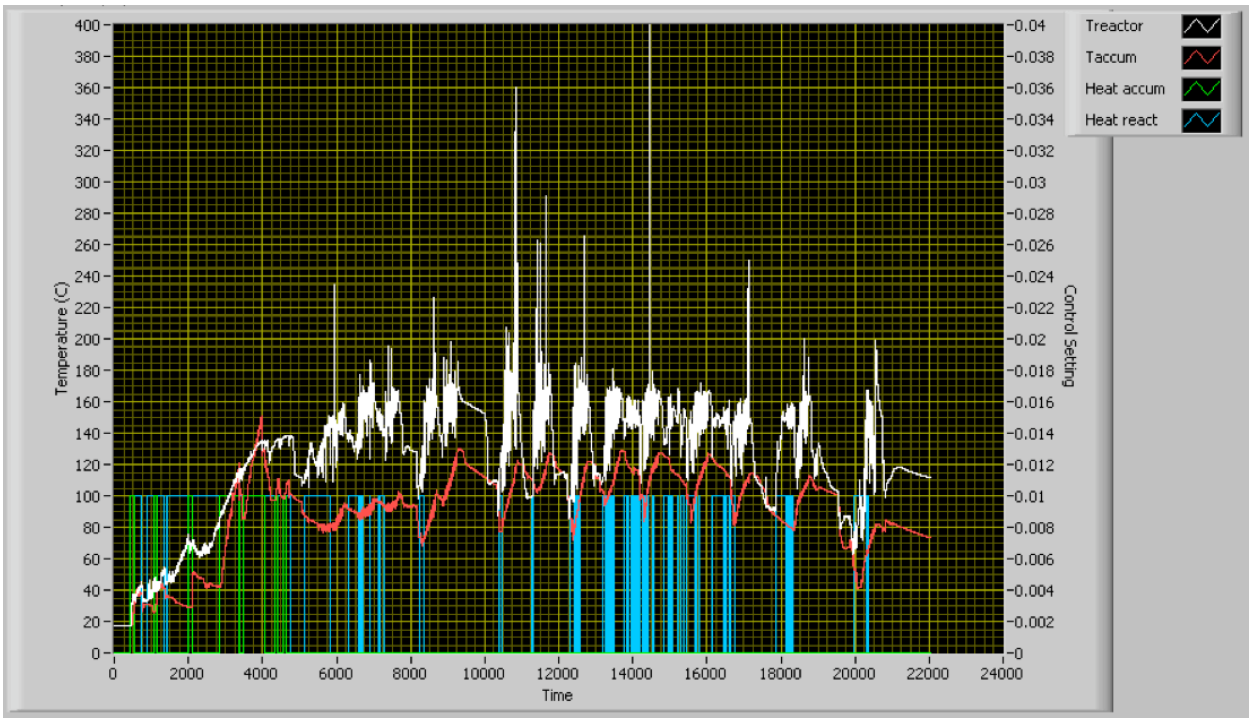

Figure 65 - Reactor Temperature, Accumulator Temperature, Accumulator Heater, and Reactor Heater

HYDROGEN PRODUCTION

The flow of hydrogen was calculated by measuring the hydrogen flow through the flowmeter and by calculating the amount of hydrogen accumulating in the buffer tank which exhibited itself in a rise in pressure. By calculating the hydrogen flow after the system purge, we can compare the amount of hydrogen actually measured with the amount expected from the slurry that was injected.

We had measured the injection flow rate prior to the test by cycling the pump into a small tray to collect the slurry pumped. This technique circulates the slurry from the slurry tank through the pump and back to the slurry tank. We use the recirculation approach to purge the slurry pump of air. (Air can accumulate in the piston pump due to leakage by the seals on the piston). The comparison shows that the calculated hydrogen production is less than the total measured hydrogen production. The initial production was actually lower than the measured but then the actual production increased.

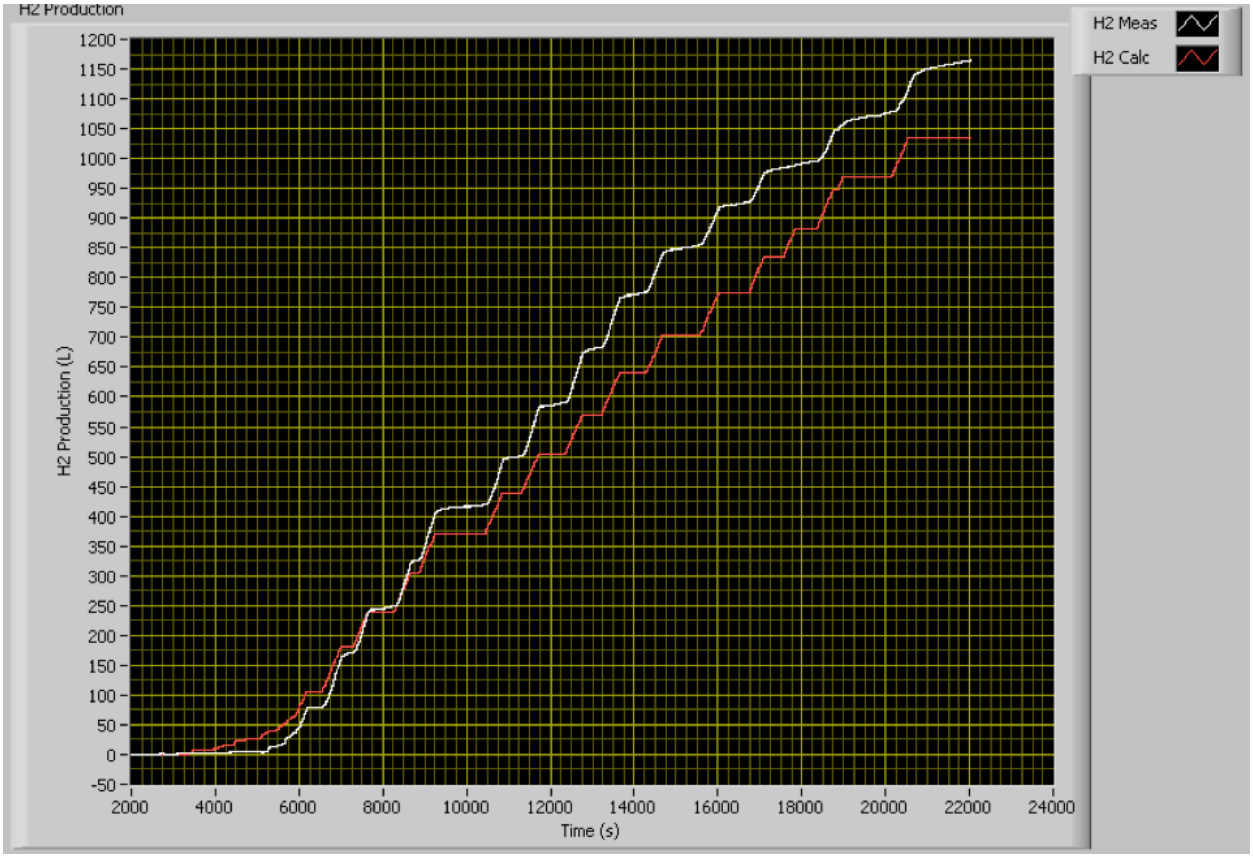

Figure 66 - Comparison of Measured and Calculated Hydrogen Production Slurry Flow 2.78 gm/injection

By increasing the amount of slurry pumped per stroke, we can match the total hydrogen produced. We had originally measured the slurry pumped per stroke as 2.78 gm/injection. By using a value about 11% higher (3.1 gm/injection), we can match the measured and calculated data (see Figure 67).

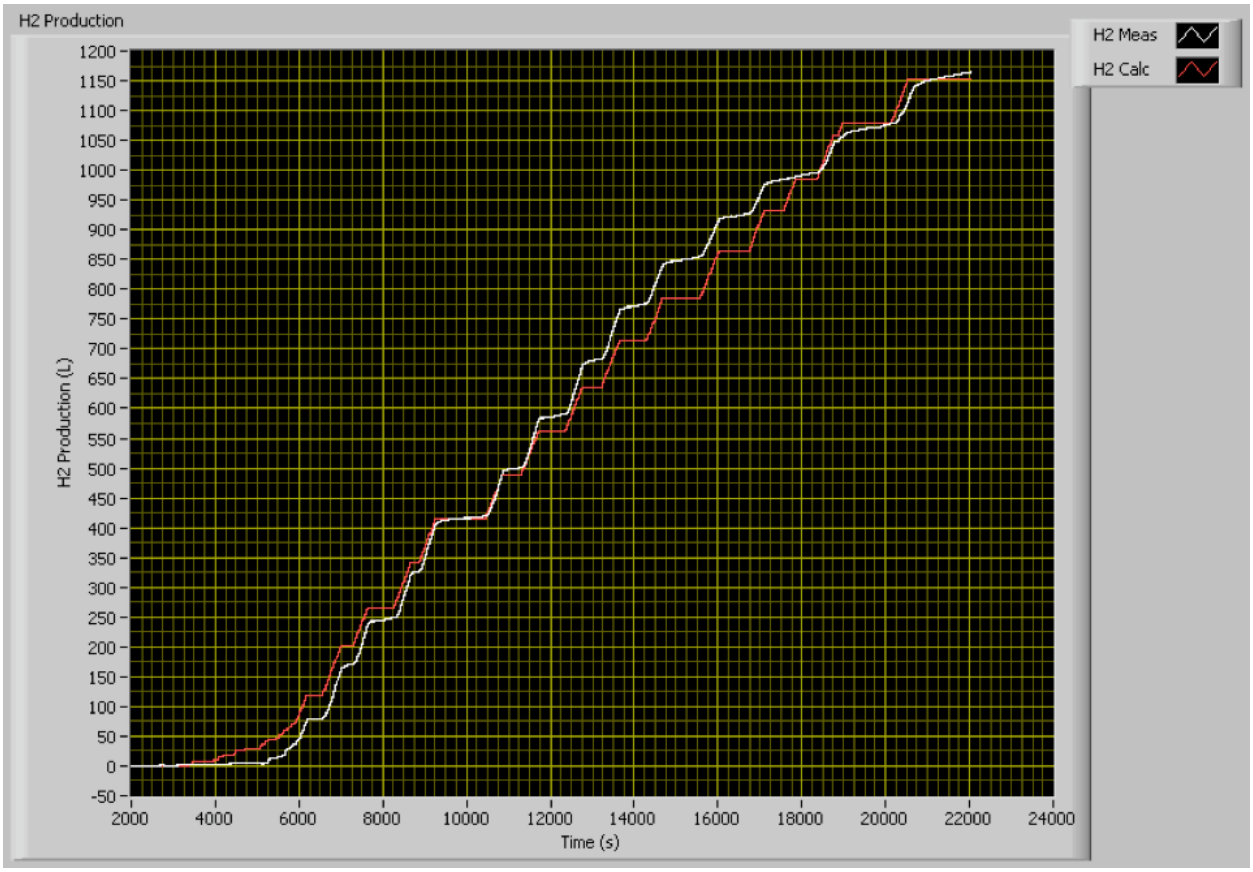

Figure 67 - Comparison of Measured and Calculated Hydrogen Production Slurry Flow 3.1 gm/injection

It is interesting to note that the calculated and measured hydrogen production do not match throughout the test however. It is not clear why this occurs.

TEMPERATURES

Figure 68 displays the temperatures measured during the test sequence. The level control vessel temperature rises when the water is circulated. Figure 69 displays the relationship between the level vessel temperature, the reactor temperature, and the injection timing. The level vessel temperature rises when the injection sequence is completed and the reactor water is cooled and falls during the injection sequence when there is no water coming from the hot reactor.

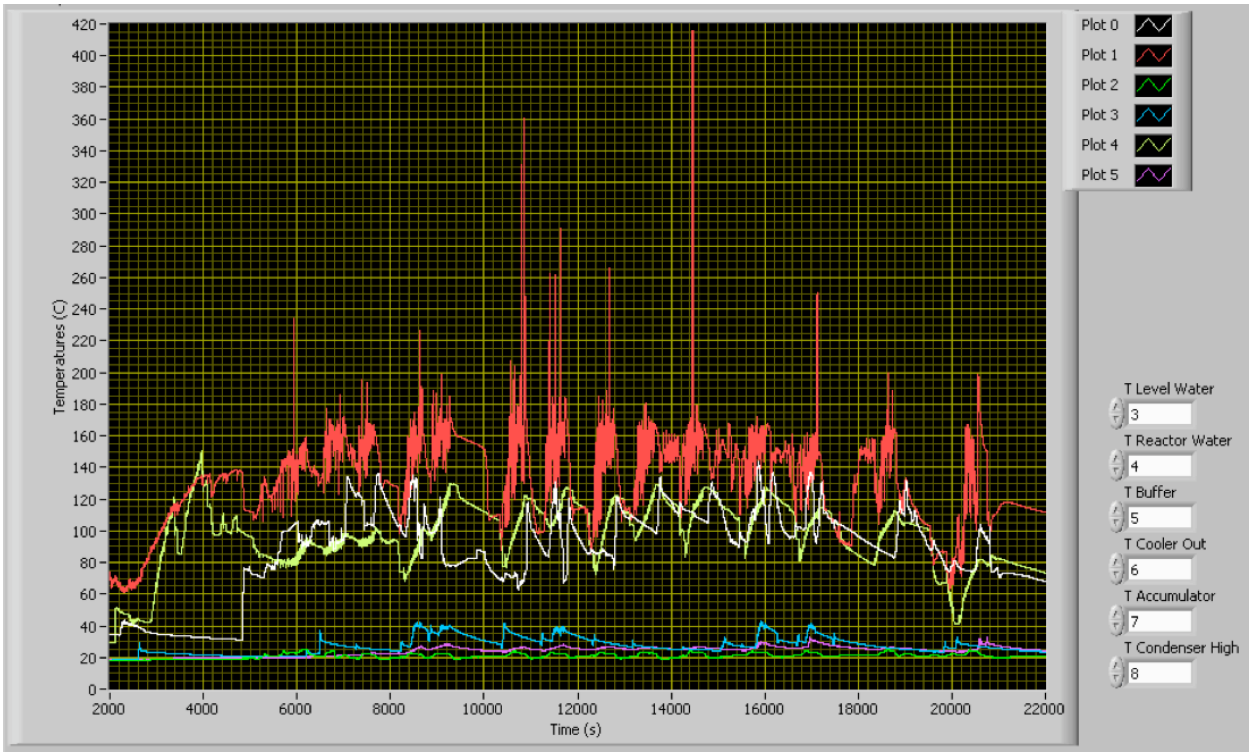

Figure 68 – Temperatures

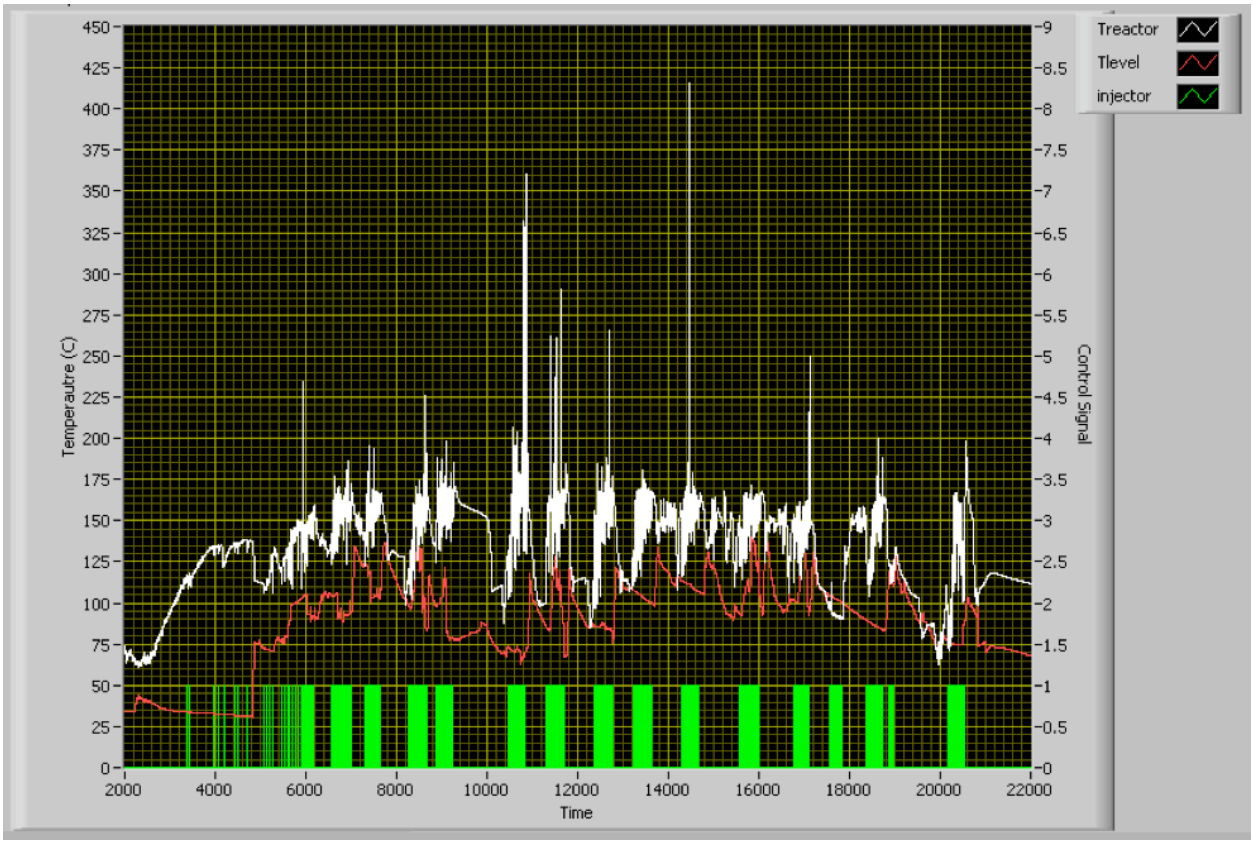

Figure 69 - Treactor, Tlevel, and ValveSlurry

TYPICAL CYCLE

Figure 70 displays the temperature of the reactor, the pressure of the buffer tank, the hydrogen production, and the slurry valve actuation for a single cycle of the apparatus. When the slurry valve is opened, slurry flows into an already moving stream of water coming from the accumulator. The water from the accumulator comes from the reaction vessel so it is hot. The slurry mixes readily with the moving stream of water and the force of the injection in the reaction vessel stirs the slurry further with the water in the reaction vessel. The result is a sharp decline in temperature, due to the mixing, followed by a sharp rise in temperature due to the reaction. The injections were timed to inject the slurry into an already reacting pool in order to temper the reaction zone and to heat the slurry. About 20 injections were performed in each cycle. About 90 liters of hydrogen were produced in this time. The reaction was adequately fast.

On the 16th injection, the temperature in the reaction vessel rose rapidly to a peak temperature exceeding 260°C. This indicates to us that there is a need to improve the stirring and mixing of the materials in the reaction vessel. The peak temperature was reduced by the following injection that succeeded in stirring the mixture again. The typical injection does not have a temperature spike as shown in the last injection.

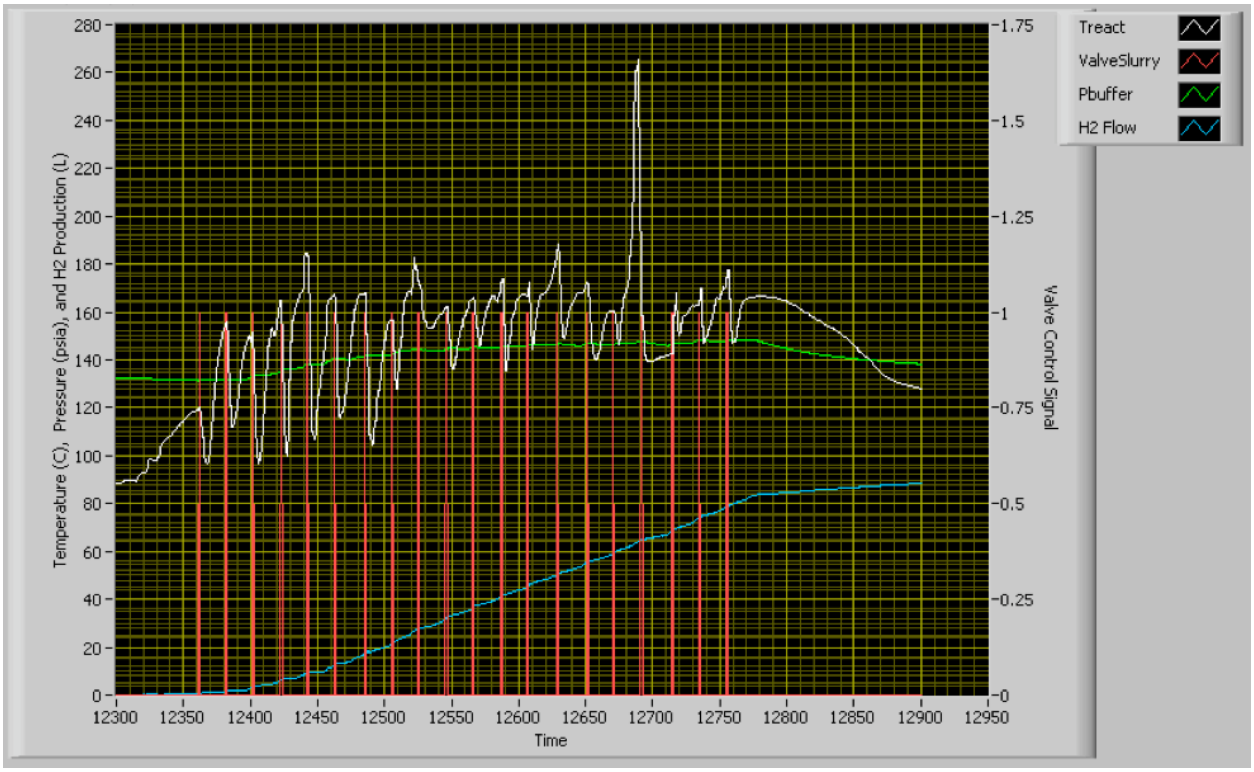

Figure 70 - Treactor, Pbuffer, H_2 Flow, and ValveSlurry for a Single Cycle

5.3.3.2.4 Conclusions

This experiment has provided us with valuable scaling data that can be used in the next design to improve the designs the various components to work better together. We envision that a full-scale system will consist of the various vessels assembled with shared walls in a compact form that will minimize mass and volume. Valving will be

performed with ganged valve systems that will direct the flows of slurry, water, oil, and byproducts in a compact ganged valve block. With proper sizing of the slurry and water pumps so that the water pump can provide all the water needed for the injection and mixing in one stroke, the time between injections can be reduced and the accumulator can be eliminated.

This apparatus was driven by compressed air. In a commercial system, we envision that the system can be driven by compressed hydrogen provided by the hydrogen in the buffer tank.

The operation was reliable and consistent. A two or three reactor system could produce a continuous flow of hydrogen at a flow rate of at least 10 liters per minute with this apparatus scale. Improvements in the reaction vessels could reduce the size of the reactors and improve the slurry injection rate. Improvements in the mixing would allow larger slurry injection quantities.

5.3.3.3 Hydrogen and Byproduct Analyses

Analytical tests were performed by Dr. Robert Sacher, Ph.D. of Ressel Scientific Co. Several samples of hydrogen and byproducts were taken during the middle and end of the test. Samples of hydrogen were taken upstream and downstream of a carbon filter. Samples of the components of the slurry were also provided to Dr. Sacher so that he would be able to look for the specific compounds.

We asked Dr. Sacher to analyze the hydrogen gas for the presence of contaminants and to analyze the solid byproducts for their composition. Dr. Sacher performed the tests using:

1) Gas Chromatography-Mass Spectroscopy Analysis
2) Fourier Transform Infrared Spectroscopy Analysis
3) Total Magnesium Analysis

His reported results for the hydrogen samples follow:

Table 3 - H_2 Sample taken at 14,776 seconds

Contaminant	Upstream of Carbon Filter (ppm)	Downstream of Carbon Filter (ppm)
Carbon Monoxide	1.6	1.0
Carbon Dioxide	2.0	2.0
Methane	1.2	0.1
Ethane	0.5	0.4
Propane	0.2	0.2
Mineral Oil	0.1	0.08
Oxygen	9	4
Nitrogen	35	32
Magnesium Oxide	0.3	0.2
Magnesium Hydroxide	0.5	0.5

Table 4 - H_2 Sample taken at 20,600 seconds

Contaminant	Upstream of Carbon Filter (ppm)	Downstream of Carbon Filter (ppm)
Carbon Monoxide	1.5	1.0
Carbon Dioxide	2.5	2.0
Methane	1.5	0.2
Ethane	0.5	0.2
Propane	0.2	0.1
Mineral Oil	0.08	0.07
Oxygen	10	5
Nitrogen	40	30
Magnesium Oxide	0.3	0.2
Magnesium Hydroxide	0.5	0.2

Table 5 - Byproduct Sample #2, Time 19,500 seconds

Chemical Component	Approximate Concentration,%
Water	28
Mineral Oil	22
Magnesium Hydroxide	32
Magnesium Oxide	18

Table 6 - Byproduct Sample #3, Time 21,000 seconds

Chemical Component	Approximate Concentration,%
Water	52
Mineral Oil	12
Magnesium Hydroxide	22
Magnesium Oxide	14

The hydrogen composition results are much like the results obtained for the hydrolysis of lithium hydride performed several years ago as part of the Thermo Power Corporation project. The hydrogen samples were found to be relatively pure. The largest impurity was from oxygen and nitrogen. This was probably an impurity of air introduced into the vessel during the sampling procedure. The oxygen concentration declined as it passed through the carbon filter. There were also some minor impurities from magnesium oxide and magnesium hydroxide. One of the most important findings was that mineral oil is a very minor component. This was a concern voiced by some of the fuel cell manufacturers. The concern was that mineral oil might accumulate on the fuel cell plate and block flow of hydrogen to the cell.

The byproduct compositions showed that there was no observable magnesium hydride. It also showed that there is magnesium oxide production rather than all magnesium hydroxide. The early sample had 45 molar % MgO. The later sample had 48 molar % MgO. This is consistent with the results that we had estimated in the laboratory of approximately 50% MgO. This finding reduces the total mass of the byproduct and it reduces the amount of water that must be carried for reaction.

The two samples that were analyzed contain more oil than was in the original slurry. After calculating the amount of magnesium hydride that produced the magnesium hydroxide and magnesium oxide, we note that the byproducts represent 54% MgH_2 slurry and 61% MgH_2 slurry respectively. This indicates that the oil recovered from the system is migrating closer to the top of the byproduct system as it was intended to do.

Both samples contained quite a bit of water indicating that improvements in the system would be needed to minimize the water concentration stored. This point has been recognized as the filter performance had demonstrated that it was too small for this system.

5.3.3.4 Residue Recovery

5.3.3.4.1 Residue Recovery Process

The residue from reacted Magnesium Hydride slurry is removed through a pneumatically actuated ball valve at the bottom of the reactor cone to the top of a closed collection vessel. A similar system allows the removal of residue from the bottom of the level control vessel. The higher pressure within the reactor and level control system forces out the partially settled solids to the lower pressure collection vessel. As the closed collection vessel fills, its pressure rises.

The solids in the transferred materials settle further in the collection vessel. Dewatering of the residue is improved by the raised pressure within the collection vessel forcing water through a sand filter contained between two mesh screens at its base. The water leaves the sand filter through a pneumatically actuated ball valve, which discharges back to the system water reservoir at atmospheric pressure.

Oil from the slurry collects within the level control vessel and may be removed through a pneumatically actuated ball valve up on the side of the level control vessel. For oil removal the level of fluid in the level control vessel is adjusted so that the interface between water and the collected oil is just below the side exit port. The oil is fed to the bottom of the residue collection vessel and passes up through the sand filter and settled solids.

The settled solids are extruded through a dip tube by the built up pressure within the collection vessel and may be recovered in an open container. The end of the dip tube was sited about half an inch above the sand filter.

5.3.3.4.2 Residue Recovery Operation

After a number of injection cycles into the reactor, generally twenty, the water levels were adjusted and if required, water was added from the reservoir to compensate for that used to generate hydrogen. Occasionally after it was estimated that enough solids residue had been built up, it was transferred to the collection vessel. A similar assessment was made for the level control vessel. This removal of solids and liquid was also compensated by the level adjustment and water addition procedure.

Removal of residue from the bottom of the reactor occurred when its ball valve was operated through a selected timed automatic cycle. A one second open time in a fifteen second cycle was chosen. One or two cycles successfully transferred partially settled solids to the collection vessel. A similar timed cycle was used to transfer residue from the level control vessel.

Water recovery was successfully carried out through the sand filter. The recovered water was relatively clear and could easily be reused within the reactor system. However, the recovery rate was slow and indicated that a larger area sand filter would be required in a properly sized system.

After a period of settlement a manual ball valve was opened in the dip tube discharge. It was found that the settled solids could be removed as a stream of the consistency of toothpaste. As the discharge continued it was generally followed by a stream of water from above the settled solids. If the settled solids became too thick to be pushed out by the pressure within the collection vessel the solids could be loosened by an oil injection from the level control vessel through the sand filter.

5.3.3.4.3 Clean out examination

After operating for many injection periods the residue collection vessel was depressurized and disassembled for examination.

- The dip tube had run with mainly water after the thickened solids in paste form had ceased to flow. However it was observed that the level of thick solids was about four inches above the entrance to the dip tube.
- It was concluded that after thickened solids near the tube end had been removed the thickened solids above that level had not slumped down evenly in the conical section of the collection vessel. The solids immediately around the vertical dip tube had moved down preferentially to be followed by water from above the settled solids leaving much of the settled residue clinging to the sides of the cone.
- The main body of the remaining solids was scooped out. It appeared to be of a similar toothpaste consistency as that extruded through the dip tube.
- Below the pasty solids and below the level of the dip pipe entrance a layer of much stiffer solids formed a cake on the top of the sand filter screen. This was broken up and scraped out with a spatula.
- The material from this layer was much lighter in color than the paste solids yet appeared to consist of fine particles like the paste solids but more tightly packed. It was proposed that some differential settlement had occurred with higher density particles of Magnesium Oxide had settled

faster than particles of Magnesium Hydroxide and that this effect would be enhanced by the bottom stirring created by the oil recovery injections. Alternatively, early operations of the reactor with cooler water present produced a lighter color residue because the hydrocarbons present in the slurry oil and dispersants would be less likely to carbonize. However, it has been observed that discrete areas of white residue were present in the solids remaining in the reactor vessel when it was disassembled for clean out.

- Samples of both light and dark material were collected for further examination.

5.3.3.4.4 Conclusions and Recommendations

In general a successful method of residue recovery from the process was demonstrated.

- The use of a pressurizable container for collection of partially settled residue from reactor and level control vessels was a viable method of removal of residue from the system at times which suit the operation of these vessels.
- The further settlement allows for more compact storage of such residue.
- The sand filter successfully recovers excess water in the residue back to the process.
- Oil was also be recovered from the process and added to the residue to maintain its flow characteristics.
- Pressure within the collection vessel can be used to recover residue material for later recycling.
- The dip tube was an unreliable method of settled solids removal, which left much of the residue behind.

Although successful in principle, improvements to the system could be investigated.

- The filtration process could be improved by increased area and better media selection to increase the recovery rate of water to the process.
- Better control of pressure, possibly using a differential between stored hydrogen pressure and user pressure requirement, could give more control for the removal of partially settled solids from the reactor and level control vessels also for the subsequent discharge of the dewatered solids from the residue collection vessel.
- The solids removal system could be improved, possibly by using a much more direct route from the bottom of the collection vessel and a better shaped collection device. This device would encourage the recovery of the solids so that less was left behind. A mechanical device such as an auger could give a positive withdrawal method and encourage better distribution of the recovered oil in the residue for improved subsequent handling of the residue during the recycling process.

5.4 Task 4 – Recycle Slurry Organics

5.4.1 Description

The first step in the recycle process is the separation of the organics contained in the spent slurry. Experiments have indicated that a solvent refining process can be used to recover the organics without damage to the oil or dispersant. A laboratory scale process will be designed, fabricated, and tested to demonstrate this process on a continuous basis. Upon successful completion of this testing, a design will be prepared for an early commercial stage process. Capital costs and operating costs will be estimated for this design. During year 2, the first laboratory scale process will be developed. This system will be refined and an early commercial scale design will be prepared in year 3.

5.4.2 Summary

- Observed that oils separate readily from the water and solids when allowed to stand
- Oils can be removed by oil skimming
- Solids and water can be removed by pumping
- Recycled oils have been used to prepare slurry. The resulting slurry exhibits characteristics of original slurry and dispersant combinations.
- Some reaction observed with the MgH_2 producing small bubbles in the slurry
- Solvent refining can be used to separate the oils from the solids

5.4.3 Discussion

One of the issues related to the recycling of the byproducts of the magnesium hydride slurry system is the issue of recovering the oil for reuse. During the performance of this project, we evaluated two separation techniques: solvent refining and settling. The byproducts from the process should return with minimal water. The byproducts should be oil, magnesium oxide, and magnesium hydroxide. During the testing of the mixing system, we demonstrated in principle that the water can be separated from the oil and solids. It will be necessary to refine this technique to minimize the amount of water that returns to the main recycling plant with the slurry byproducts.

5.4.3.1 Solvent refining

In solvent refining, a lighter oil is mixed with the byproduct slurry. Once mixed, the solids tend to separate readily and settle on the bottom of the container where they can be concentrated and removed from the vessel as a thick paste. After draining this paste and returning the drained material to the liquids recovery system, the solids can be fed to a calciner where the magnesium hydroxide in the system is converted to magnesium oxide.

The liquids from the system can be heated to separate the light fraction from the heavy fraction. This process was tested with hexane. The solids could be removed but there was always a smell of hexane with the light mineral oil indicating that the light fraction was only reduced in the light mineral oil.

5.4.3.2 Settling

Initial experiments with the byproducts from the Parr autoclave experiments showed that the oils can be recovered by washing with pentane and then boiling the pentane from the oil.

Recent experiments with the byproducts from the continuous mixer have shown that the oils separate readily from the solids and water when allowed time to do so. The oils recovered from this separation have been used to make new slurry. The characteristics of this slurry are similar to those of slurries made with dispersants indicating that at least some of the dispersants have been recovered with the oil.

Oils recovered from the continuous mixer experiments appear clear and nearly indistinguishable from the original oils.

Several tests have been run with the byproducts. The byproducts were allowed to settle. During the settling, which was fairly rapid, the oils rose to the top and a sludge of solids and water was below. The oils could be collected readily with oil skimming techniques.

5.4.3.3 Use of Recycled Oils

Recycled oils were used in several of the slurries that were used in the continuous mixer tests. The slurries performed well. However, there was some evidence of water in the oil that was reacting with the magnesium hydride. Bubbles in the slurry indicated that some hydrogen was being released from the slurry. Bubbles were not observed in the slurries prepared with fresh mineral oil. The recycled oil had been baked at 120°C for several hours prior to being used. We need to have some analyses performed to compare the original oil with the recovered oil. Perhaps there has been a chemical change to the oil that is retaining some water.

5.5 Task 5 – Produce Magnesium Hydride from Magnesium and Hydrogen

5.5.1 Description

Once the magnesium has been reduced from the magnesium hydroxide byproduct, it will be necessary to produce magnesium hydride. The early commercial production of slurry may use purchased magnesium and hydrogen to make magnesium hydride for the slurry until the production needs of the process become large enough to warrant the investment in a magnesium reduction plant. The objective of this task will be to demonstrate the process that will be needed to produce magnesium hydride from magnesium and hydrogen. A laboratory scale process will be prepared and tested. The final design of this equipment will be used to produce an early commercial scale design. Capital and operating costs will be estimated from this design. During year 1, a laboratory scale device will be tested. During year 3, this device will be modified, tested, and a design for an early commercial device will be prepared.

5.5.2 Summary

- A mixture of magnesium and magnesium hydride was heated under an atmosphere of hydrogen to form magnesium hydride.
- The magnesium hydride formed was tested in the Parr Autoclave to confirm that a high grade magnesium hydride had been formed.
- The requirement in preparing magnesium hydride using the Goldschmidt process is temperature control, pressure control, and agitation.

5.5.3 Discussion

5.5.3.1 Current Hydriding Technology

Magnesium hydride is the thermodynamically preferred compound of the reaction between magnesium and hydrogen at room temperature. However, this reaction generally occurs slowly. To accelerate the process, the elements can be heated and pressurized but the process is still anticipated to be slow for our application and the pressure will add expense that should be avoided if possible.

A patent was issued for a process (U.S. Patent Number 5,198,207) that notes that the reaction between magnesium and hydrogen is self-catalyzed in the presence of a small fraction of magnesium hydride. The use of this process promises to reduce the cost of producing magnesium hydride by an order of magnitude.

Currently the price of magnesium hydride is 100 to 200 times the cost of the magnesium and hydrogen that is used to make the compound. We need to understand what is causing this high price and to explore other methods of producing magnesium hydride in large quantities. The probable reason for the high price today is that the compound is not in large demand. As a result, the production of magnesium hydride occurs in small quantities and the cost is dominated by the high cost of labor.

5.5.3.2 Initial Hydriding Tests

The testing method has been to confirm that we can decompose an existing sample of magnesium hydride, then to show that we can hydride the existing sample. Once this was accomplished, we attempted to hydride magnesium to magnesium hydride.

The first test was to measure the decomposition of magnesium hydride powder in the Parr Autoclave. A sample of magnesium hydride was deposited in the Parr Autoclave. The autoclave was purged 5 times at a pressure of 150 psia to reduce the oxygen composition within the vessel to the concentration of oxygen within the compressed hydrogen, >5ppm O2. Decomposition was observed with temperatures between 365°C and 400°C. About 92% of the hydrogen theoretically contained in the magnesium hydride was observed. This is consistent with literature supplied by the manufacturer.

Next, hydrogen was supplied under pressure to the discharged hydride. The magnesium hydride was observed to absorb hydrogen. Absorption rate was increased when the temperature was reduced slightly. Figure 71 displays the temperatures and pressures observed during this test. This behavior was expected based on data provided by the manufacturer.

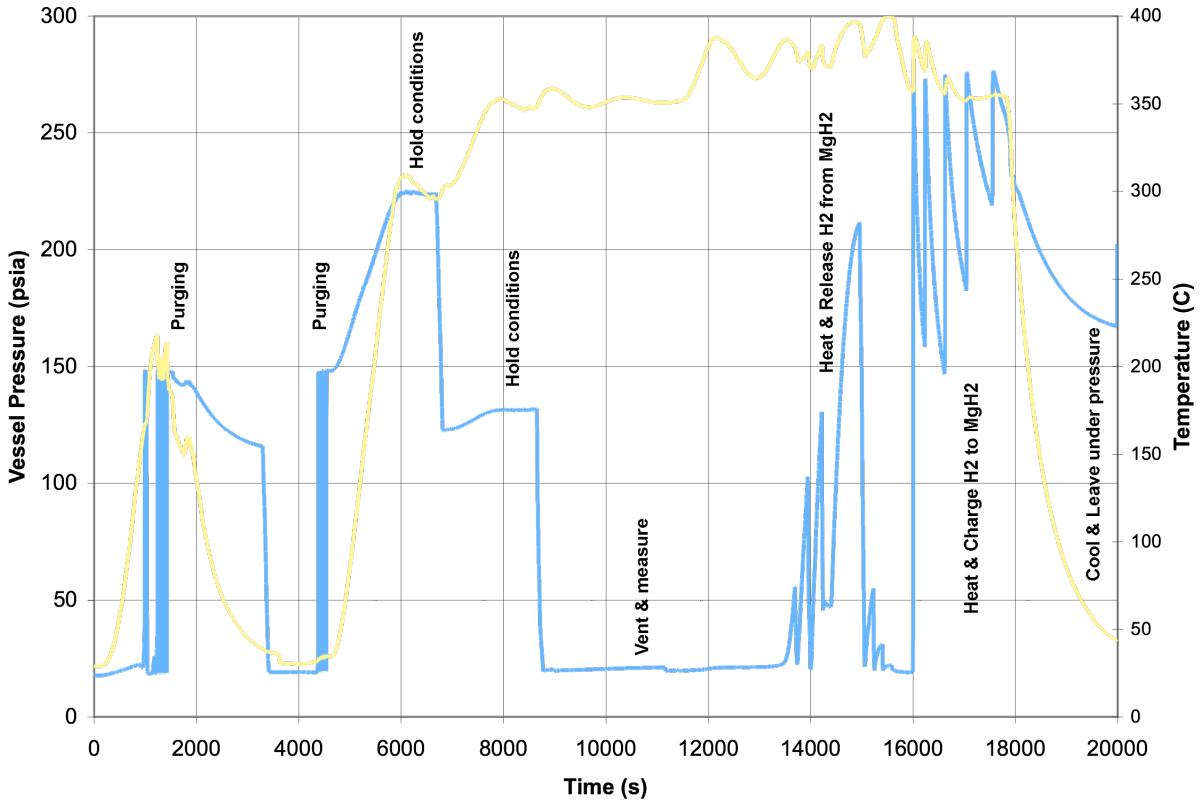

Figure 71 - Discharging and Charging of MgH_2 Powder

5.5.3.3 Hydriding Mg powder and MgH_2 powder

The next test measured the absorption rate of hydrogen into magnesium. A sample of powdered magnesium metal was placed in the Parr Autoclave with magnesium hydride. The vessel was purged and heated under hydrogen pressure. At about 370°C, hydrogen pressure began to drop indicating that hydrogen was being absorbed. Upon declining absorption rates, the hydride was discharged. Hydrogen produced by the discharge was collected in a displacement bottle. About 85% of the hydrogen theoretically possible, based on the weight of the sample, was recovered. This is a typical value for recovery based on the manufacturers data. When a slurry of this magnesium hydride was mixed with water about 85% of the hydrogen anticipated based on the weight of the sample was recovered. This test indicated that the hydriding had not completed.

In a later test, a larger sample of magnesium powder and magnesium hydride powder was hydrided. During this test, significant sintering was observed. The sintered material formed a block at the bottom of the glass liner in the Parr Autoclave.

5.5.3.4 Conclusion

Our conclusion from these tests is that production of magnesium hydride is relatively easy. The variables are temperature, pressure, and agitation.

5.6 Task 6 – Preliminary Designs and Economic Evaluations of $Mg(OH)_2$ Reduction Processes

5.6.1 Description

The magnesium hydride slurry concept relies on recycling the byproduct back to new slurry in a large-scale production facility. The large scale allows the process costs to benefit from economies of scale. Recycling of the byproduct is assumed since the scale of the automotive market is so large that mountains of byproduct would be built which would then be mined for raw materials anyway. Several methods of recycling have been identified. Both lithium and magnesium are currently produced by melting lithium chloride or magnesium chloride and electrolytically separating the metal from the chlorine. Chlorine gas produced in the electrolysis is used to make hydrochloric acid, which in turn is used to make lithium chloride and magnesium chloride from lithium hydroxide and magnesium hydroxide.

Three alternate processes have been identified that promise significant cost reductions in the production of magnesium. Two are carbothermic reduction processes and the third is a new technology using a solid-oxide-oxygen-ion-conducting membrane (SOM) technology.

We are evaluating these processes for their potential cost reduction capability. This evaluation will include experimental development at the laboratory scale, design analysis at a production scale, and an economic evaluation of the cost of hydrogen resulting from each process. Information will be collected to perform a similar design and analysis of an electrochemical process so that the cost comparisons of the systems can be made.

Separation of the metal hydroxide from the oil/dispersant/water of the byproduct of the hydrolysis reaction will be a common part of each system design. Similarly, the production of hydride slurry from the reduced metal will be a common part of each design.

5.6.2 Summary

- Evaluations of carbothermic, magnesium chloride electrolysis, and the SOM processes were performed determine the rough costs of the systems.
- The carbothermic process should be able of producing magnesium, using modern control techniques, for $1.15/kg ($0.52/lb) at a scale of 90,000 mtpy. This cost is made up of $0.75/kg ($0.34/lb) of operating costs and $0.40/kg ($0.18/lb) of capital recovery costs.
- The magnesium chloride electrolysis process was, until recently, the primary method used to make magnesium. The operating costs of this system were reported to be about $1.32/kg ($0.60/lb). Capital recovery and profit requirements required a selling price of about $2.76/kg ($1.25/lb).
- The SOM process, when incorporated into a magnesium hydride slurry system, are estimated to provide hydrogen for about $4.50/kg. This cost consists of a cost to make the slurry of about $3.89/kg hydrogen and $0.62/kg hydrogen for delivery and distribution. The operating cost for magnesium production is estimated to be about $0.59/kg ($0.27/lb) of magnesium. The total cost to return

10% on the invested capital would be $0.65/kg ($0.29/lb) of magnesium because the capital costs are quite low for a 731,000 mtpy scale.

- Comparisons were made between various magnesium production methods to define opportunities. The SOM process appears to offer the lowest cost option primarily due to its low capital cost but also because of its lower operating costs.

5.6.3 Discussion

5.6.3.1 Overview of Magnesium Reduction Technologies

A preliminary survey of processes for the extraction of magnesium revealed a number of potential routes for recovering magnesium from the byproducts of magnesium hydride slurry after its use in the generation of hydrogen. Conceptual and experimental processes along with established industrial methods were included.

The two main process families are based on electrolysis and thermal reduction. Major industrial plants for the extraction of magnesium, where electrical power is economically available, are based on the electrolysis of magnesium chloride with chlorine being recycled within the plant to form magnesium chloride from the incoming hydroxide feed material. Thermal reduction of magnesium oxide with carbon as the reductant is also a large-scale industrial process and uses magnesium oxide derived from the thermal decomposition of the hydroxide feed material.

A preliminary extrapolation of historical costs scaled to 100,000 tons per year of magnesium production indicated that the electrolytic process plant capital cost was likely to be approximately 35% more than the carbothermic process plant.

Developing electrolytic processes such as the SOM (solid-oxide-oxygen-ion-conducting membrane) process and the FFC (Fray-Farthing-Chen Cambridge) process show promise in that they process the oxide directly without the complexity of recycling chlorine.

Other industrial thermal processes use alternative reductants such as silicon or aluminum. Their promise may lie in the production of magnesium for making magnesium hydride without the potential contamination of carbon. However, some added complexity might result from the recycling of the reductant metal. In the case of aluminum, the oxide formed in the reduction of magnesium could be recycled through the normal industrial electrolysis process for aluminum by coupling the processes together.

5.6.3.1.1 Chlorination and electrolysis

In this process magnesium hydroxide is dissolved in hydrochloric acid to form magnesium chloride and water. The water is driven off and the magnesium chloride is heated to its molten state. Magnesium metal is separated from the chlorine by electrolysis with the chlorine being recycled to form hydrochloric acid while the molten magnesium is removed for forming the magnesium hydride powder for use in the slurry.

This is a well-proven industrial scale process and is well established. However, although the total energy usage is similar to that used for carbothermic reduction, a very high proportion of the energy is supplied as electrical energy which dictates that plant locations are generally sited where electrical power is cheap and plentiful.

The electrolysis process produces relatively clean metal for making the metal hydride.

The recycling of chlorine in the process, both as chlorine gas and hydrochloric acid, could pose a chemical hazard in the event of equipment damage. A further hazard is the formation of poisons if the magnesium hydroxide is contaminated with oil as it will be with the magnesium hydride slurry cycle.

5.6.3.1.2 Carbochlorination

In the carbochlorination process magnesium hydroxide is heated until it decomposes to magnesium oxide and water. A mixture of chlorine gas and carbon monoxide gas reacts with the magnesium oxide to form magnesium chloride, which is drained as liquid from the reactor while the carbon monoxide reacts with the released oxygen to form carbon dioxide. Liquid magnesium is separated from magnesium chloride by electrolysis while the chlorine is recycled to the chlorination reactor. This process was developed on an industrial scale but still has problems preventing its large-scale adoption.

The manufacture of magnesium chloride directly from solid magnesium oxide requires less energy than that needed to drive off water from that made by dissolving magnesium hydroxide with hydrochloric acid. However, the process taking magnesium carbonate ore to magnesium oxide in the same reactor proved difficult to operate at steady state and had a high refractory material usage. No doubt these problems could have been solved eventually but this was too great a financial burden on the industrial scale plant in Alberta, Canada, which closed down.

Separating the hydroxide decomposition to the oxide and water and chlorinating directly the magnesium oxide is simpler to operate and is operated at an industrial scale by Norsk Hydro. Carbon is added with the magnesium oxide by pelletizing, the pellets being bound together by the hydration of the magnesium oxide and the formation of magnesium oxychlorides. The resulting off gas contains CO, CO_2 and some HCl. The anhydrous magnesium chloride is formed as a hot liquid, melting point 714°C, then the magnesium reacts with injected chlorine gas and is filtered through a bed of carbon briquettes before being tapped from the base of the reactor into an insulated container to allow hot transfer to the electrolysis cells. The carbon briquettes are also used as resistance heaters by passing a high current through them from carbon electrodes inserted through the sides of the reactor. The injected chlorine gas from the subsequent electrolysis process is preheated as it passes up through the carbon briquettes. The recycling of chlorine from the electrolysis step closes the chlorine loop. As with other processes the handling of chlorine requires care as it poses a potential chemical hazard.

5.6.3.1.3 Thermal reduction

In thermal reduction processes, magnesium oxide is reduced by silicon and or aluminum metal at temperatures over 1200°C and is removed as a vapor for subsequent condensation. Heating of the furnace is required. Various versions of this process have been developed; the Pigeon process uses an externally heated retort; while other processes use internal electric resistance, submerged or open arc heating. Sometimes the furnaces are run under vacuum. Generally the processes are lower in

capital cost than the ones involving electrolysis but operating costs are highly dependent on reduction materials and power costs in the area. Recent developments in South Africa indicate that a large D.C. arc furnace operating at atmospheric pressure may prove to be a cost effective embodiment of this class of reduction process and could be applied with magnesium hydroxide or magnesium oxide as the initial feedstock. The Chinese are said to be producing magnesium on a large scale using a ferrosilicon thermal reduction process.

The reduction with aluminum takes place at a lower temperature than with carbon but silicon is a little higher. The vapor pressure of these metals and their oxides is very low at the operating temperature of this process so the clean removal of magnesium vapor with no back reaction is highly likely assuming that entrained particulate is removed close to the furnace.

The oxides of the reductants will form a slag that can be tapped as a liquid from the furnace. The addition of some calcium oxide to the aluminum and silicon oxide slag will allow the composite slag to be liquid at temperatures around 1300°C rather than the much higher melting points of the individual oxide components or even the best combination of alumina and silica.

The main disadvantage of this process, especially when scaled up to the level envisaged for large-scale hydrogen distribution, is the use of the relatively expensive reductant materials although the purity of the metals used should not be critical when used for this purpose. On a large scale integrated plant for magnesium hydroxide treatment it would be expected that the aluminum would be recovered as an oxide and recycled through a reduction process hence minimizing the requirement for new aluminum metal. Energy losses between process steps would be reduced by close coupling the processes.

5.6.3.1.4 Carbothermic

In the carbothermic process, magnesium hydroxide is heated to form magnesium oxide and water. An intimate mixture of the magnesium oxide and carbon, a relatively economic reductant, is reacted at high temperature to form magnesium metal vapor and carbon monoxide. To minimize the back reaction where the magnesium vapor may react with the carbon monoxide to re-form magnesium oxide, the vapor stream is rapidly cooled and diluted. This process is well proven on an industrial scale. Variations in quenching and metal recovery have been used. Also variations in the reduction process have been used where the feed is reacted in an electric arc.

The main reduction process to produce the magnesium vapor is relatively straightforward. The critical step is the rapid quenching of the gas stream to prevent the reforming of magnesium oxide from magnesium metal and carbon monoxide. Impurities of oxide carried through to the hydride formation would act as a dead load in the hydrogen-producing reactor.

This process can minimize the electrical energy usage by utilizing energy from primary sources such as carbon from coal.

The reduction normally takes place in an electric arc furnace. The furnace temperature is kept between1950°C and 2050°C. Equilibrium temperature for this reaction is a little higher than 2050°C but no doubt the temperature in the reaction zone at the arcs is much higher and promotes a speedy reaction.

A significant problem with this process is the carry over of dust and gas with the product metal vapor. The dust contains unreacted magnesium oxide and carbon; also the carbon monoxide gas from the reaction may react in a reverse manner to create more magnesium oxide. Dilution gas and rapid quenching of the stream as it leaves the arc furnace minimizes the back reaction but still leaves unwanted magnesium oxide and carbon in the product stream. The condensed magnesium metal requires separation from the unwanted dusts. These can be returned to the reduction process but this recycled load represents a waste of energy and potential contamination of the product stream.

Above 1850°C re-oxidation is not preferred. Below 1850°C re-oxidation is preferred so it is important to quench and cool down the stream as rapidly as possible to slow down and minimize the back reaction.

Reducing the concentration of oxidizing gas such as the carbon monoxide by the introduction of dilution gases such as hydrogen and natural gas also reduces the oxidation rate and helps with the cooling.

In the cooled state, particulate can be filtered from the stream and removed from the oxidizing gas. The magnesium can be released from the solid particulate by heating to its liquid or gaseous state and draining or flowing away from the residue.

Magnesium is liquid from 650°C to 1110°C. It may be sprayed in this state in hydrogen to form the hydride as a solid and cooled below the hydride decomposition temperature of 287°C as a white crystalline solid. This may be separated from unreacted magnesium particles by density with the metallic magnesium being recycled.

Fluidized bed flotation and gas deflection are potential means for continuous separation of the lower density hydride (SG 1.45) from metal (SG 1.74).

The processes are generally closed and shielded with an appropriate dry gas to prevent air in leakage and potential reaction with atmospheric moisture.

5.6.3.1.5 Iron carbide bath

A suggested variation on the carbothermic process is the injection of magnesium hydroxide or oxide beneath the surface of a liquid iron bath saturated with carbon. The resulting gas leaving the bath will be magnesium metal vapor together with carbon monoxide and water vapor from the decomposition of the hydroxide. Some of the water is also likely to decompose in the presence of the hot iron to form hydrogen. If a hydrocarbon is also injected to help replenish the bath carbon then more hydrogen will also be released with the gas leaving the bath. Rapid quenching will recover the magnesium metal. Various aspects of this process have been proven at a large industrial scale with the injection of powdered materials and hydrocarbons into an iron bath with high carbon content as part of a bulk steelmaking process.

This process is very similar to the carbothermic process using solid carbon reductant but offers a convenient way of carbon contacting the magnesium oxide because the carbon is dissolved in solution with the iron. Used carbon is easily replaced by dissolving more carbon in the bath as it becomes depleted.

The reduction process is endothermic so heat must be provided to keep the process going. Heat will also be required to melt the initial iron bath and dissolve the carbon.

Rapid quenching will be required as with the standard carbothermic reduction.

Large-scale iron baths exist in the steel industry with various means of heating. A promising method may involve the use of induction furnaces. The coreless type tends to be limited in scale because the induction coil surrounds the whole bath. However much larger bath capacities are heated by channel type furnaces mounted outside the shell of the main bath. Each channel furnace draws metal from the bath through the leg of a “U” shaped channel and returns it to the bath through the other leg. Heating and motive force is applied to the stream by an induction coil wound round the base of the “U”.

An alternative heating method is by passing the feed materials into the bath through graphite electrodes with a direct arc struck from the tip of each electrode to the bath to provide a local high-temperature processing zone and heat to the bath. The feed may be to the hot zone between electrodes as with the carbothermic process or may be fed through hollow graphite electrodes.

Each of these feeding methods has the disadvantage of delivering the feed materials on top of a very dense bath where they will float. A more efficient method of ensuring contact with the bath carbon is by injecting the feed through the bottom of the bath similar to the powdered lime injection of the OBM/Q-BOP steelmaking process.

The process will evolve large quantities of gas that may carry solid dust particles, such as iron and carbon from the bath. If this follows the example of the steel industry process, less dust will be formed than from the top feeding or from the dry processing of the carbothermic process.

A potential major problem with this process is that the equilibrium temperature for the reduction of magnesium oxide by carbon is around 2100°C which is excessive for normal steelmaking refractory materials apart from graphite. However, a localized hot zone at the arc location could allow the main bath to be cooler and operate at a similar temperature to the carbothermic process without an iron bath.

5.6.3.1.6 SOM

In the SOM process, magnesium oxide is dissolved in a melt of magnesium chloride and Neodymium chloride ($NdCl_3$) at 1200°C-1400°C. The melt is separated by a membrane of solid-oxygen-ion-conducting stabilized zirconia. Voltage is applied between an inert cathode in the melt and an anode on the other side of the membrane. Oxygen ions are conducted through the membrane while reduced magnesium metal is collected at the cathode and leaves as a vapor to be retrieved by condensation. Proof of concept for this process has been claimed after laboratory scale research work at Boston University. Further development is required for industrial scale application.

The oxide status of zirconia is preferred to magnesia above 1395°C. So although the separated magnesium metal may be removed as a vapor it may well promote longer life of the membrane structure if temperature is kept above this during process operation.

A significant advantage of this process is that once separated the magnesium metal is no longer in any danger of re-oxidation and can be passed directly to the magnesium hydride forming process.

5.6.3.1.7 Hydrogen Plasma Reduction

At the high temperatures achievable within a heated ionized stream of hydrogen gas, magnesium oxide/hydroxide will be reduced to magnesium metal vapor and water

vapor. Rapid quenching will prevent the back reaction and allow the magnesium to be separated from the steam and hydrogen stream. Further quenching of the magnesium in a stream of hydrogen will promote the formation of magnesium hydride. This process is at the conceptual stage.

A potential advantage of this process is that the reduction does not involve carbon and carbon monoxide. This should produce a cleaner product more suitable for forming the hydride.

The back re-oxidation of magnesium with water vapor is favored below about 2950°C so again rapid quenching is required to arrest this process. Higher temperatures, 20,000°K, are easily achieved within the plasma stream which will promote very rapid reduction of the magnesium oxide since it is well above the 2950°C equilibrium temperature for this process.

Quenching to below 1110°C condenses the magnesium metal which remains liquid above 650°C. In this state it can be separated from the water vapor and introduced to the hydriding process.

Hydrogen plasma equipment is well established at the scale of metal cutting so the process could be tested conceptually. However, large scale processing would require significant development time.

5.6.3.1.8 FFC Cambridge Process

The Fray-Farthing-Chen (FFC) Cambridge Process, a recently developed process applied to titanium oxide reduction, uses electrolysis of the oxide from the solid state. The solid oxide is the cathode in a molten salt electrolyte and after the oxygen has migrated to the anode the solid metal is removed as a sponge. A variation of this process could be applied to magnesium oxide where the metal can be removed from the bath as a solid or liquid without the need of a separating membrane.

Further work, under the sponsorship of DARPA, is being carried out at Berkeley.

If the magnesium is to remain as a solid, as in the titanium process, it is relatively well protected against re-oxidation below its melting temperature of 650°C. If the process is run at a higher temperature with the magnesium as a liquid, it is likely to float to the surface of the electrolyte. The calcium chloride bath is used for titanium melts at 772°C and has a density of 2.16g/cc compared with magnesium melting at 650°C with a density of 1.74g/cc. It is important to keep the oxygen at the anode from contacting the liquid magnesium.

Shaping a submerged shield around the anode will separate the oxygen gas at the anode from the magnesium metal floating to the surface of the bath.

The hot metal may be removed as a liquid but should be protected by a shield gas. Hydrogen may commence the hydriding process with advantage.

A combination of SOM and FCC may utilize the electrolysis of the solid oxide and the membrane filter for separating the anode gas. This would allow the process to operate at a lower temperature than the straight SOM method enabling the magnesium to be more conveniently removed as a liquid.

5.6.3.2 Nozzle Based Carbothermic Process

5.6.3.2.1 Prior Development Of The Carbo-Thermal Magnesium Process

INTRODUCTION

The carbothermal magnesium process for making magnesium has been known as a viable means of making magnesium for four decades. In this process a magnesium oxide is heated with a carbon source to produce magnesium gas and carbon monoxide according to this reaction:

MgO + C --> Mg(g) + CO(g) Reaction #1

Magnesium Technology Limited (MTL) has a patented technology in which a Lavalle nozzle is used to cool the gases in a few fractions of a millisecond to condense the magnesium and separate it from the CO before the back reaction can occur. This nozzle-based carbothermal magnesium (NBC Mg) process has been demonstrated on a bench-scale where a few grams of metal were made. A furnace to demonstrate the process at the 1 kg/hour rate is currently under design by BAM, Inc. in Knoxville, TN. Techno-economic modeling has shown that the cost of producing a pound of magnesium by the nozzle-based carbothermal magnesium process could be as low as $0.30 a pound when the magnesium plant is part of an energy complex (Minimizing the Cost of Making Magnesium) with electric costs of $0.02 per kwh. Such technology could revolutionize the magnesium industry and contribute significantly to making magnesium hydride a low cost alternative for using hydrogen in automotive transportation.

A detailed capital cost estimate has been carried out for a production plant using the NBC Mg process. The estimate was incorporated into the techno-economic model. The model allows the user to select the Design Criteria for the project under consideration, including the plant capacity. The model then carries out a material and energy balance and estimates the income statement for the process and the capital costs. The model allows the optimization of the total cost of making magnesium including amortization of the facility. Amortization cost is on the order of $0.10 per pound of magnesium for a 90,000 mtpy plant.

The carbothermal method of producing magnesium has always promised to be a low cost method of making magnesium. In concept, the process is very simple: 1) react carbon and a magnesium oxide mineral together at an elevated temperature to produce magnesium gas and carbon monoxide, then 2) cool the gases rapidly and collect the magnesium. The first step has been done and can be accomplished by those skilled in high temperature metallurgical furnaces, such as electric arc furnaces used in the steel industry. A recent patent by Engell, et al, U.S. Patent No. 5,803,947 in September 8, 1998 defines a process in which the gases from the carbothermal process are cooled rapidly by passing through a lavalle nozzle. Very high conversion rates to magnesium metal were observed in bench scale demonstrations of the process by Mineral Development International A/S (MDI), Birkerod, DK. The experimental results referred to in this report were carried out by MDI.

The methodology used by major engineering firms to evaluate new technology has been incorporated into a techno-economic model. This model has been used to

bring together the design criteria, process flow diagrams, material and energy balances, and the income statement into a single format to evaluate the viability of the proposed NBC Mg Process.

In the industrialized “western” world, the majority of magnesium is currently produced by electrolytic refining of magnesium from a molten salt bath containing a significant portion of magnesium chloride. These electrolytic cells are fed with anhydrous magnesium chloride, which requires a capital-intensive process to produce a grade that will operate efficiently in modern cells. This technology also requires the handling of chlorine gas.

In recent years, a significant amount of magnesium is produced by metallo-thermic reduction of calcined dolomite. Alloys and carbides of aluminum, calcium, and silicon are good reductants of magnesium oxides and magnesium silicates. Ferro-silicon is used extensively in China, the world's largest producer. These reactions have one inherent advantage over the carbo-thermal reduction route in that only magnesium vapor (no carbon monoxide) is produced. Their inherent disadvantages are that (1) all of these reductants are expensive, (2) as batch processes under vacuum they are labor intensive, and (3) the metal is collected as a mixture of fine crystals and powder for subsequent processing into metal.

For a historical perspective, a carbothermal reduction process was operated in Permanente, USA in the late 1940’s. An arc furnace was used to carry out the main reactions and large quantities of natural gas were used to quench the magnesium and carbon monoxide to reduce the back reaction. The cooling method employed frequently produced pyrophoric magnesium particles. Plants were also operated in Swansea, Wales and Konan, Korea based on a similar approach by Austro-American Magnesite Corporation. Because of the production of pyrophoric magnesium and the difficulty of suppressing the back reaction, the carbothermal process, in any form, is not currently used for the production of magnesium.

NBC MAGNESIUM PRODUCTION

In the NBC Mg Process, a mixture of coke and magnesia, or magnesium silicate, or any other oxide based magnesium ore, is fed into the hot zone of an air-tight furnace and heated to above 1500°C, typically in the range of 1800°C. The carbon reacts with the magnesium oxide to produce magnesium metal and carbon monoxide in a highly endothermic reaction, see Reaction #1.

Electric arc, or submerged arc furnaces traditionally furnish this heat, but, induction furnaces, plasma arc or any other convenient means may be used. To recover the magnesium metal from this gas mixture, the gas mixture has traditionally been cooled as rapidly as possible below the freezing point of magnesium to avoid a reversal of the reaction. Past uses of carbothermal technology have never been able to cool the gases rapidly enough to avoid significant losses of magnesium by reversion to magnesia. Most approaches have involved mixing the Mg/CO mixture with large quantities of inert gases such as nitrogen or reducing gases such as methane. Such techniques depend on forming an intimate mixture of the diluting gas quickly and the transfer of heat to those gases, not a trivial task.

The new technology provides near instantaneous cooling of the gas by an adiabatic expansion of the gas through a lavalle nozzle. In prior technology, the cooled magnesium is dispersed and must be collected over a correspondingly large surface

area. With the current technology, condensation is focused near the exit of the lavalle nozzle that should facilitate its collection on a cold surface or perhaps in or on a bath of liquid magnesium or fused salts. The carbon monoxide must be removed from the collection area via a vacuum, possibly maintained by steam ejectors.

A well-known phenomenon is that if a constriction is placed in a closed channel carrying a stream of fluid, there will be an increase in velocity, and an increase in kinetic energy at the point of constriction. From energy balance considerations, there must also be a reduction in pressure. If the fluid is a gas, there is a subsequent expansion and cooling of the gas after the nozzle corresponding to the pressure drop. If the pressure difference over the nozzle becomes higher than a threshold value, the gas flow through the nozzle changes from sonic to supersonic. With a given gas composition, the amount of gas passing through the nozzle depends on the cross sectional area of the constriction and the pressure differential across the nozzle.

The pressure upstream of the nozzle is set by the vapor pressure of the magnesium and carbon monoxide, which in turn is set primarily by the temperature maintained in the reaction zone in the furnace, which in turn, is maintained by the heat input rate into the charge. The temperature of gas downstream of any given nozzle is proportional to the initial temperature of the gas and the pressure differential across the nozzle.

In the jet age, the physical chemistry and thermodynamics of how gases are cooled by adiabatic expansion through a nozzle is well understood and commonly observed.

BENCH SCALE RESULTS

The nozzle was demonstrated at a rate of magnesium metal production up to a rate of 0.116 gram/min through a lavalle nozzle with a throat area of 10.18 mm^2. Forsterite, a relatively pure form of magnesium silicate ore, was used in these tests.

Aside from the desired reaction in the reaction chamber of producing Mg (v) and CO (Reaction #1), there are several other potential side reactions. If a silica or silicate is present in the magnesium feedstock, it will also react with the carbon in the bed to produce SiO according to Reaction #2 below. This reaction is more significant the higher the temperature.

$SiO_2 + C \rightarrow SiO + CO$ Reaction #2

SiO gas is also evolved in the reaction chamber along with magnesium and carbon monoxide vapors. With the reaction chamber at 1500oC, if SiO was allowed to proceed in the gas phase to the lavalle nozzle, about 1 to 3% silicon was reported to the magnesium metal. Therefore, a condenser was placed down stream from the reactor operating at 1300°C, a lower temperature than the reaction zone. This condenser is a carbon source that converts the SiO produced to SiC according to this reaction:

$SiO + C \rightarrow SiC + CO$ Reaction #3

A potential negative effect of this condenser is that the lower temperature shifts the equilibrium for Reaction #1 slightly to the left with the possible result that some MgO(s) may condense in the second condenser if conditions in the system are not well

controlled. The extent of this back reaction can be approximated from thermodynamics. Therefore, for optimum results, the condenser must be operated above a temperature at which significant reversal of Reaction #1 will occur. Their subsequent experimental results lend support to the accuracy of their theoretical model.

Finally, there is the reaction of metals in the feedstock with carbon to produce elemental metals according to the general reaction:

$Me_xO_y + y\ C \rightarrow x\ Me + y\ CO$ Reaction #4

Where Me can be iron, copper, nickel, phosphorus, sodium, lead, etc. Small iron droplets form and remain in the charge and contain most of the less volatile elements like nickel and copper while the vapor phase will contain all or part of the more volatile elements like zinc, lead, phosphorus, and sodium. In fact, much of the silica may also react to produce some silicon that will be dissolved in the iron droplets. Similar reactions occur in all metallothermic systems for magnesium production. The composition of the feedstock must be controlled for these volatile elements to control the quality of the magnesium metal produced.

EXPERIMENTAL RESULTS WITH SiO CONDENSER IN PLACE

Eleven experiments were carried out with an improved bench scale reactor that included a condenser for SiO. Temperature of the reactor was varied between about 1260 to 1550°C. A nozzle with a 10.18 mm^2 diameter nozzle was used, which processed about 90 to 285 grams of feed in a period ranging from about 100 to 400 minutes.

In the best test in the bench scale reactor, more than 99% of the total magnesium content of the charge was recovered as magnesium metal. In five other runs the recovery was between about 70 and 80%. These results indicate that the process is technically viable when careful attention is paid to excluding leaks from the system, a task somewhat easier in larger systems. Further, the work demonstrates the value of the lavalle nozzle for rapid cooling of magnesium and carbon monoxide to produce magnesium metal.

QUALITY OF THE METAL PRODUCED

The bench scale reactor with the condenser produced magnesium metal with the following average impurities:

Table 7 - Impurities in the Magnesium (ppm) Produced in the Bench Scale Reactor

Al 110	Ca 21	Zn 35	P 15
Mn 77	Na 150	Si 80*	Fe 15
K 240	Ni <5		
*Results for Si only shown for one run.			

This analysis classifies the metal as meeting 9980A ASTM B92M-83 but not 9990A or higher; secondary refining may further improve metal quality. As important, on the runs with high metal yields skeletal growth of cm-sized whiskers was observed. These whiskers were not pyrophoric. The condenser appeared to remove most of the SiO from the gas phase and reduce the concentration of silicon in the magnesium.

However, results for Si are only shown for one sample of metal in the report. Melting of this metal would get rid of most of the alkali metals. Iron is removable by conventional settling near the melting point.

5.6.3.2.2 Safe Hydrogen Process

Safe Hydrogen, Inc. is studying the feasibility of using magnesium hydride, MgH_2, as a means of distributing hydrogen, primarily in the transportation sector. MgH_2 in an oil slurry is reacted with water inside of an automobile to produce hydrogen, via the equation below, which is then used to power the vehicle via an internal combustion engine.

$MgH_2 + 2H_2O \rightarrow Mg(OH)_2 + 2H_2$ Reaction #5

The magnesium hydroxide ($Mg(OH)_2$) produced by this reaction is returned in an oil-water slurry for reprocessing back to magnesium metal. Safe Hydrogen employs a solvent extraction process to remove most of the oil and leaving a moist, high purity magnesium hydroxide for recycling back to magnesium metal. The chemical hydride slurry has the potential of generating twice as much volume of hydrogen as a similar volume of cryogenically cooled liquid hydrogen. Liquid hydrogen is a proven method of storing hydrogen, but it takes substantial energy to liquefy the hydrogen and there is continual "boil off" of hydrogen during storage. Slurry, on the other hand, is stored at normal temperature and normal pressure.

A major cost advantage of this technology is based on the characteristics of the slurry. The slurry is a non-explosive, non-corrosive, environmentally safe, pumpable "hydrogen fuel". Slurry can be stored, transported, and pumped with existing tanks, pumps and pipelines and can therefore distribute hydrogen to the market utilizing the existing fossil fuel infrastructure. The only difference from current fuel delivery systems is that the delivery devices such as trucks or rail tankers don't return empty. They are fully loaded in both directions. They return from delivery runs, loaded with depleted slurry for recycling.

Since virtually all the magnesium would be recycled, the cost of the magnesium hydroxide that would be fed into the carbo-thermal magnesium process would only be the cost of makeup magnesium feedstock. A somewhat arbitrary cost of magnesium hydroxide was set at $2/tonne for the base case to reflect that most of the magnesium hydroxide produced by Reaction #5 would be recycled and only a nominal cost would be incurred from the inefficiencies in recycling. This affords a significant advantage, quantified subsequently, to the cost structure for the Safe Hydrogen approach compared to the normal approach where the entire feedstock has to be mined and shipped to the magnesium smelter.

The ultimate price of the Safe Hydrogen approach for delivering hydrogen economically will depend in part on the optimum placement of magnesium recycling centers near affordable power plants. In addition, a viable system will require minimizing the transportation costs of moving the MgH_2 slurry to the filling stations and the $Mg(OH)_2$ slurry from the stations back to the magnesium recycling centers. Safe Hydrogen envisions that a mature system will be sized to use all the power from a large

scale power plant thus operating the power plant as a base load plant and minimizing the distribution costs because the power plant will be part of the slurry recycling plant.

5.6.3.2.3 Techno-Economic Modeling on NBC Process

The question arises, how would a modern carbothermal process that uses the lavalle nozzle compete with existing technology, specifically the Pidgeon Process as practiced by the Chinese. Based on prior pricing, one would expect a new process would be competitive if it could produce magnesium with operating costs in the $0.50 to $0.75 per pound range. At the low end of this range one would speculate that the Pidgeon Process could be supplanted, at the high end of this range the management of capital costs would become critical. Even lower costs have to be realized to make Safe Hydrogen's methodology for delivering hydrogen viable. The advantage Safe Hydrogen has in its approach are the lower costs possible with the economies of scale associated with very large facilities, which would be necessary with their vision.

A techno-economic model has been created that simulates all the unit operations of a magnesium facility. A complete material and energy balance is carried out for the magnesium facility based on the design criteria selected by the user of the model. This allows the model to be used for a variety of project conditions and it allows the identification of design criteria that are critical in keeping the operating costs for the facility to a minimum. The usefulness and flexibility of the model is illustrated herein by considering a project for Safe Hydrogen, Inc. With relatively small modifications, the model could be used for many other projects employing the nozzle-based carbothermal magnesium technology.

DESIGN CRITERIA

The Design Criteria have been developed for the following key steps in carbothermal magnesium process:

- General
- Calcining
- Electric Arc Furnace
- Salt Box Furnace
- Ingot Casting

OPERATING COSTS ESTIMATE FOR THE NBC MAGNESIUM PROCESS

In Metallurgical Viability's Final Report, displayed in Appendix B, the method for determining the operating costs is discussed in detail. The method was to prepare process flow diagrams of the separate sub-processes and then to calculate the amount of material that flowed through these sub-processes including the heat losses and heat recovery possible and the labor required to operate the processes.

THE COST ESTIMATE FOR THE NBC MAGNESIUM PROCESS

All of the equipment costs have been estimated for the NBC Magnesium Process. Even items that require design, such as the salt-bath furnace have been estimated by completing a preliminary design and then the cost estimated from the weight of the containment box and algorithms used for estimating the cost of low pressure vessels based on their weight.

The cost of the NBC Mg Plant could be reduced by some process changes in the Utility area of the plant. Specifically, replacing the scrubbing circuit for carbon monoxide

with ESP (electrostatic precipitators) could lower the cost. This would probably also lower the operating costs slightly.

GREENFIELD CAPITAL COST

The installed equipment costs are shown in Table 8 and Table 9 sorted by equipment type. The most expensive equipment are the electric furnaces at $100 million, the boilers to make steam, primarily for the vacuum ejectors at $44 million, and the kilns for calcining the $Mg(OH)_2$ at $32 million. These three items make up more than half the cost of the plant. This equipment would be optimized during engineering for any potential costs savings.

The installed equipment costs, sorted by Plant Areas, are in shown in Table 10, Table 11, and Table 12. The Furnace Plant at $116 million is the most expensive, the Utilities at $80 million are the second most expensive, while the Calcining Plant costs about $26 million.

The total installed equipment cost for an NBC Magnesium Plant making 90,000 metric tons of magnesium a year is about $223 million dollars. With contingency and fees, the total plant costs are estimated at $305 million. The factored Greenfield Costs are estimated to be about $400 million, Table 13. The estimated capital costs per tonne of capacity of about $4500 compares with Alan Donaldson and Ronald Cordes estimate of $3200/metric tonne for their the rapid plasma quenching process. There are some references in the literature for the Western Pidgeon process of about $6000/metric tonne. However, none of these studies have been done as comprehensively as the present; a lack of thoroughness generally leads to an under-estimation of costs.

Table 8 - Equipment Costs Grouped by Equipment Types for the NBC Magnesium Plant, part 1

Equipment Costs		Case No.:	2159		Capital		
Equipment Name	ID	Item Cost	No.of Units	Total Item Cost	Installation Factor	Materials or Pressure Factor	Installed Cost
MgOH2/Dust Blender	BD-01A	$ 56,870	2	$ 113,739	3.0	1.00	$ 341,218
BLENDERS		Subtotal		$ 113,739			$ 341,218
Calciner Baghouse	BH-01A	$ 32,616	1	$ 32,616	1.5	3.50	$ 171,237
BAGHOUSE		Subtotal		$ 32,616			$ 171,237
Baghouse Exhaust Blower	BL-01A	$ 180,640	1	$ 180,640	3.0	1.00	$ 541,921
Oxygen Blower to Calcine Circuit	BL-02A	$ 129,525	1	$ 129,525	3.0	1.00	$ 388,576
CO Blower from Coke Preheater	BL-03B	$ 132,263	1	$ 132,263	3.0	1.00	$ 396,790
Gases from Caster Blower	BL-04B	$ 34,635	1	$ 34,635	3.0	1.00	$ 103,906
Air Blower for Boiler	BL-05C	$ 309,615	1	$ 309,615	3.0	1.00	$ 928,845
CO Compressor	CM-01B	$ 1,139,613	1	$ 1,139,613	2.5	1.00	$ 2,849,033
Stack Blower	BL-06C	$ 537,506	1	$ 537,506	3.0	1.00	$ 1,612,518
BLOWERS		Subtotal		$ 2,463,799			$ 6,821,590
Central Boiler	BP-01C	$ 8,886,069	2	$ 17,772,139	2.5	1.00	$ 44,430,347
BOILERS		Subtotal		$ 17,772,140			$ 44,430,348
MgOH2 Conveyor from SH	CN-01A	$ 194,236	1	$ 194,236	2.5	1.00	$ 485,590
MgOH2 Conveyor to Calcine	CN-02A	$ 98,558	1	$ 98,558	2.5	1.00	$ 246,395
MgO Product Conveyor	CN-03A	$ 194,236	1	$ 194,236	2.5	1.00	$ 485,590
Coke to Boiler Conveyor	CN-04C	$ 194,236	1	$ 194,236	2.5	1.00	$ 485,590
Coke to Preheater Conveyor	CN-05B	$ 98,558	1	$ 98,558	2.5	1.00	$ 246,395
Preheated Coke Conveyor	CN-06B	$ 98,558	1	$ 98,558	2.5	1.00	$ 246,395
Salts Conveyor	CN-07B	$ 98,558	1	$ 98,558	2.5	1.00	$ 246,395
Lime Conveyor	CN-08B	$ 98,558	1	$ 98,558	2.5	1.00	$ 246,395
CONVEYORS		Subtotal		$ 1,075,498			$ 2,688,744
Cooling Tower	CT-01C	$ 3,269	1	$ 3,269	2.5	1.00	$ 8,173
Cooling Tower		Subtotal		$ 3,270			$ 8,172
Ingot Casting Machine	IC-01B	$ 345,000	1	$ 345,000	1.5	1.00	$ 517,500
INGOT CASTING		Subtotal		$ 345,000			$ 517,500
Boiler Demin. Plant	DM-01C	$ 1,198,838	1	$ 1,198,838	1.5	1.00	$ 1,798,257
Demineralizer		Subtotal		$ 1,198,838	3.0	1.00	$ 1,798,256
Boiler Feedwater Pump	PM-01C	$ 8,522	1	$ 8,522	3.0	1.00	$ 25,565
CO Scrubber Pump	PM-02C	$ 22,462	11	$ 247,078	3.0	1.00	$ 741,234
Caustic Pump	PM-03C	$ 1,202	1	$ 1,202	3.0	1.00	$ 3,606
Caster Scrubber Pump	PM-04C	$ 13,289	1	$ 13,289	3.0	1.00	$ 39,868
Cooling Water Pumps	PM-05C	$ 4,877	1	$ 4,877	3.0	1.00	$ 14,632
PUMPS		Subtotal		$ 274,970	2.0	1.00	$ 824,900

Table 9 - Equipment Costs Grouped by Equipment Type for the NBC Magnesium Plant, part 2

MgOH2 Blender Hopper	SI-01A	$ 12,285	1	$ 12,285	2.0	1.00	$ 24,571
Coke Day Bin	SI-02A	$ 20,217	1	$ 20,217	2.0	1.00	$ 40,434
Salt Week Bin	SI-03B	$ 5,340	1	$ 5,340	2.0	1.00	$ 10,681
Quick Lime Storage Bin	SI-04B	$ 4,331	1	$ 4,331	2.0	1.00	$ 8,661
Dust Transport Hoppers	HP-01A	$ 2,033	1	$ 2,033	2.0	1.00	$ 4,067
Dust Disposal Supersacks	HP-02A	$ 1,823	1	$ 1,823	2.0	1.00	$ 3,645
BINS		Subtotal		$ 46,028			$ 92,056
Plant Stack	ST-01C	$ 358,402	1	$ 358,402	2.0	1.00	$ 716,805
PLANT STACK		Subtotal		$ 358,402			$ 716,804
Vacuum Steam Ejectors	EJ-01B	$ 55,666	10	$ 556,661	2.5	1.00	$ 1,391,651
Vacuum Steam Ejectors		Subtotal		$ 556,660	2.5	1.00	$ 1,391,652
CO Gas Cooler	HX-01B	$ 57,469	1	$ 57,469	2.5	1.00	$ 143,673
Boiler H2O Preheater	HX-02C	$ 56,155	1	$ 56,155	2.5	1.00	$ 140,387
Compressed CO Cooler	HX-03C	$ 94,764	17	$ 1,610,982	2.5	1.00	$ 4,027,455
HEAT EXCHANGERS		Subtotal		$ 1,724,606	2.1	1.00	$ 4,311,516
Boiler Feedwater Tank	TK-01C	$ 92,582	2	$ 185,164	2.1	1.00	$ 388,844
CO Scrubber Tank	TK-02C	$ 130,852	22	$ 2,878,734	2.1	1.00	$ 6,045,341
Stack Scrubber Tank	TK-03C	$ 73,889	1	$ 73,889	2.1	1.00	$ 155,168
TANKS		Subtotal		$ 3,137,788			$ 6,589,352
CO Buffer Storage Vessel	VS-01C	$ 483,502	1	$ 483,502	2.1	1.00	$ 1,015,355
PRESSURE VESSELS		Subtotal		$ 483,502	3.0	1.00	$ 1,015,352
CO Scrubber	SC-01C	$ 24,626	1	$ 24,626	3.0	1.00	$ 73,877
Caster Scrubber	SC-02B	$ 42,625	1	$ 42,625	3.0	1.00	$ 127,874
SCRUBBERS		Subtotal		$ 67,250	1.0	1.00	$ 201,752
MgOH2 Calciner	KN-01A	$ 11,651,147	1	$ 11,651,147	2.0	1.00	$ 23,302,293
Coke Preheater	KN-02B	$ 4,568,909	1	$ 4,568,909	2.0	1.00	$ 9,137,819
KILNS		Subtotal		$ 16,220,054			$ 32,440,112
Salt Box Furnace	SF-01B	$ 181,458	1	$ 181,458	3.0	1.00	$ 544,373
SALT BOX FURNACE		Subtotal		$ 181,456			$ 544,376
Electric Smelting Furnace	EF-01B	$ 100,361,104	1	$ 100,361,104	1.0	1.00	$ 100,361,104
Electric Arc Furnaces		Subtotal		$ 100,361,104			$ 100,361,096
Waste Water Treatment Plant	WWTP-01C	$ 2,683,649	1	$ 2,683,649	1.5	1.00	$ 4,025,474
Wastewater Treatment Plant		Subtotal					$ 4,025,472
Cryogenic O2 Plant	OP-01C	$ 4,444,466	2	$ 8,888,931	1.5	1.00	$ 13,333,397
Cryogenic O2 Plant		Subtotal		$ 8,888,928			$ 13,333,392
Total Equipment Costs				$ 157,989,296			$ 222,624,896

Table 10 - Installed Equipment Costs by Plant Area, Calcining Plant

Equipment Costs		Case No.:	2159				
Calcining Plant Costs							
Equipment Name	**ID**	**Item Cost**	**No.of Units**	**Total Item Cost**	**Installa-tion Factor**	**Materials or Pressure Factor**	**Installed Cost**
MgOH2/Dust Blender	BD-01A	$56,870	2	$113,739	3	1	$341,218
Calciner Baghouse	BH-01A	$32,616	1	$32,616	1.5	3.5	$171,237
Baghouse Exhaust Blower	BL-01A	$180,640	1	$180,640	3	1	$541,921
Oxygen Blower to Calcine Circuit	BL-02A	$129,525	1	$129,525	3	1	$388,576
MgOH2 Conveyor from SH	CN-O1A	$194,236	1	$194,236	2.5	1	$485,590
MgOH2 Conveyor to Calcine	CN-O2A	$98,558	1	$98,558	2.5	1	$246,395
MgO Product Conveyor	CN-03A	$194,236	1	$194,236	2.5	1	$485,590
MgOH2 Blender Hopper	SI-01A	$12,285	1	$12,285	2	1	$24,571
Coke Day Bin	SI-02A	$20,217	1	$20,217	2	1	$40,434
Dust Transport Hoppers	HP-01A	$2,033	1	$2,033	2	1	$4,067
Dust Disposal Supersacks	HP-02A	$1,823	1	$1,823	2	1	$3,645
MgOH2 Calciner	KN-01A	$11,651,147	1	$11,651,147	2	1	$23,302,293
		Equip.Cost		**$12,631,055**		**Installed Cost**	**$26,035,536**

Table 11 - Installed Equipment Costs for the NBC Magnesium Plant Area by Plant Area, Furnace Plant

Furnace Plant Area							
Equipment Name	**ID**	**Item Cost**	**No.of Units**	**Total Item Cost**	**Installa-tion Factor**	**Materials or Pressure Factor**	**Installed Cost**
CO Blower from Coke Preheater	BL-03B	$132,263	1	$132,263	3	1	$396,790
Gases from Caster Blower	BL-04B	$34,635	1	$34,635	3	1	$103,906
CO Compressor	CM-01B	$1,139,613	1	$1,139,613	2.5	1	$2,849,033
Coke to Preheater Conveyor	CN-05B	$98,558	1	$98,558	2.5	1	$246,395
Preheated Coke Conveyor	CN-06B	$98,558	1	$98,558	2.5	1	$246,395
Salts Conveyor	CN-07B	$98,558	1	$98,558	2.5	1	$246,395
Lime Conveyor	CN-08B	$98,558	1	$98,558	2.5	1	$246,395
Ingot Casting Machine	IC-01B	$345,000	1	$345,000	1.5	1	$517,500
Salt Week Bin	SI-03B	$5,340	1	$5,340	2	1	$10,681
Quick Lime Storage Bin	SI-04B	$4,331	1	$4,331	2	1	$8,661
Vacuum Steam Ejectors	EJ-01B	$55,666	10	$556,661	2.5	1	$1,391,651
CO Gas Cooler	HX-01B	$57,469	1	$57,469	2.5	1	$143,673
Caster Scrubber	SC-02B	$42,625	1	$42,625	3	1	$127,874
Coke Preheater	KN-02B	$4,568,909	1	$4,568,909	2	1	$9,137,819
Salt Box Furnace	SF-01B	$181,458	1	$181,458	3	1	$544,373
Electric Smelting Furnace	EF-01B	$100,361,104	1	$100,361,104	1	1	$100,361,104
		Equip.Cost		**$107,823,640**		**Installed Cost**	**$116,578,647**

Table 12 - Installed Equipment Costs for the NBC Magnesium Plant by Plant Area, Utilities.

Utilities							
Equipment Name	ID	Item Cost	No.of Units	Total Item Cost	Installa-tion Factor	Materials or Pressure Factor	Installed Cost
Air Blower for Boiler	BL-05C	$309,615	1	$309,615	3	1	$928,845
Stack Blower	BL-06C	$537,506	1	$537,506	3	1	$1,612,518
Central Boiler	BP-01C	$8,886,069	2	$17,772,139	2.5	1	$44,430,347
Coke to Boiler Conveyor	CN-04C	$194,236	1	$194,236	2.5	1	$485,590
Cooling Tower	CT-01C	$3,269	1	$3,269	2.5	1	$8,173
Boiler Demin. Plant	DM-01C	$1,198,838	1	$1,198,838	1.5	1	$1,798,257
Boiler Feedwater Pump	PM-01C	$8,522	1	$8,522	3	1	$25,565
CO Scrubber Pump	PM-02C	$22,462	11	$247,078	3	1	$741,234
Caustic Pump	PM-03C	$1,202	1	$1,202	3	1	$3,606
Caster Scrubber Pump	PM-04C	$13,289	1	$13,289	3	1	$39,868
Cooling Water Pumps	PM-05C	$4,877	1	$4,877	3	1	$14,632
Plant Stack	ST-01C	$358,402	1	$358,402	2	1	$716,805
Boiler H2O Preheater	HX-02C	$56,155	1	$56,155	2.5	1	$140,387
Compressed CO Cooler	HX-03C	$94,764	17	$1,610,982	2.5	1	$4,027,455
Boiler Feedwater Tank	TK-01C	$92,582	2	$185,164	2.1	1	$388,844
CO Scrubber Tank	TK-02C	$130,852	22	$2,878,734	2.1	1	$6,045,341
Stack Scrubber Tank	TK-03C	$73,889	1	$73,889	2.1	1	$155,168
CO Buffer Storage Vessel	VS-01C	$483,502	1	$483,502	2.1	1	$1,015,355
CO Scrubber	SC-01C	$24,626	1	$24,626	3	1	$73,877
Plant	01C	$2,683,649	1	$2,683,649	1.5	1	$4,025,474
Cryogenic O2 Plant	OP-01C	$4,444,466	2	$8,888,931	1.5	1	$13,333,397
		Equip.Cost		**$37,534,605**		**Installed Cost**	**$80,010,737**
Totals for Entire Plant		**Ttl. Equip.Cost**		**$157,989,300**		**Ttl. Installed Cost**	**$222,624,920**

Table 13 - Greenfield Capital Costs and Unit Capital Cost for Making Magnesium via the NBC Magnesium Process

Capital Cost Estimate		Case Code	2159
Magnesium Production, mtpy		90,000	
Description		**Costx 10^6**	
Installed Equipment Costs		$ 223	
Contingency Cost	30%	$ 67	
Engr.Project Fees	7%	$ 16	
Total Plant Cost		$ 305	
Total Greenfield Cost/Auxilaries	30%	$ 396	
Interest rate, annual	9%		
Plant life, months	300		
Amount Financed, 90% of above	356.85	millions	
Monthly payment	($2.99)	millions	
Annual Payment	($35.94)	millions	
Amorization cost, per pound	**$ (0.18)**	**per pound**	

5.6.3.2.4 Unit Costs Of Making Magnesium By The Nbc Magnesium Process

From Appendix B, the total operating cost of making magnesium was about $0.34 per pound. Coupled with the capital cost of $0.18 per pound, the total cost of making magnesium including operating and capital costs is about $0.52 per pound. The price of magnesium in 2006 ranged from about $0.90 to $1.00 per pound. This implies about a two-year pay back and about a 50% return on investment for a new NBC Magnesium Plant.

5.6.3.2.5 Model Predictions and Insights

EFFECT OF COST OF ELECTRICITY

A base case has been somewhat arbitrarily been set by the author for the model. The user of the model can typically enter values above and below the base values within reason. Values entered outside of the allowed range, shown for each variable, are reset to the base value. The team evaluating the carbothermal magnesium process must set the base case to be in agreement with reality for a given project as much as is possible. Typically, the base case is executed and then other cases are run varying one or more of the other design or cost variables to arrive at a new income statement and a new estimated unit cost for making magnesium.

Using this approach, the cost of making magnesium via the carbothermal magnesium process described herein, as a function of energy costs (electric power and

coke) is shown in Figure 72. The model predicts operating costs between about $0.36 an $0.70 a pound. The base case and even the configuration of the model is still varying. Therefore, these estimates of operating costs should not yet be considered the final estimate. An example of the type of changes expected is illustrated in the next example.

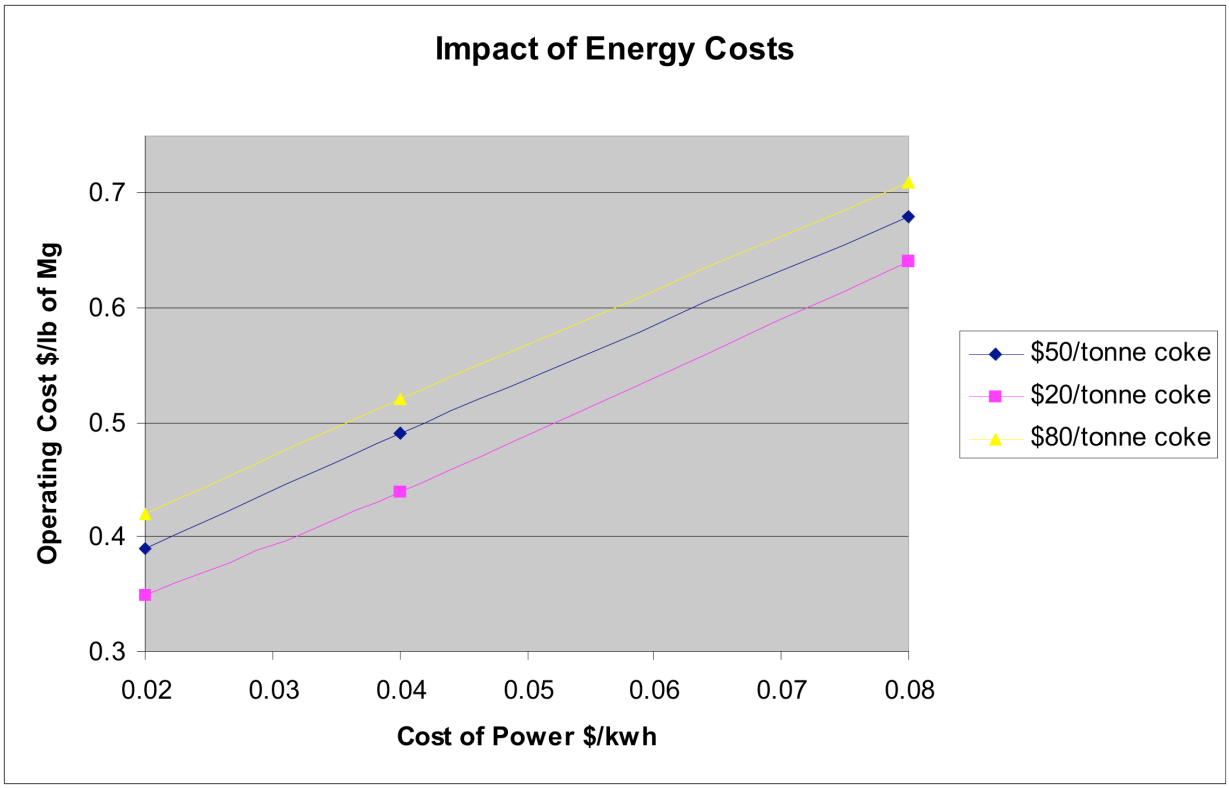

Figure 72 - The Impact of Energy Costs on the Operating Costs

EFFECT OF THE VACUUM LEVEL

The model was used to estimate the impact of the vacuum level in the salt box furnace (downstream of the lavalle nozzles) on the operating costs, Figure 73. The model showed the operating costs are very sensitive to vacuum levels. The vacuum is currently established by a two stage steam ejector system. Such a system is effect down to a level of about 0.1 atmospheres, below this the consumption of steam begins to rise rapidly. The model further showed that stronger vacuums were required to reach the desired temperature ranges in the salt box furnace. The model has in effect shown that the vacuum system needs to be upgraded. Combination systems using steam ejectors and mechanical pumps are required to go efficiently to these stronger vacuums. Also, the efficiency of the steam ejectors can be improved by cooling the gases between stages and removing condensables.

Another thing learned from the initial modeling runs is that natural gas as priced is more cost effective that the combination of coke and purchased oxygen in calcining the magnesium hydroxide and the in making steam.

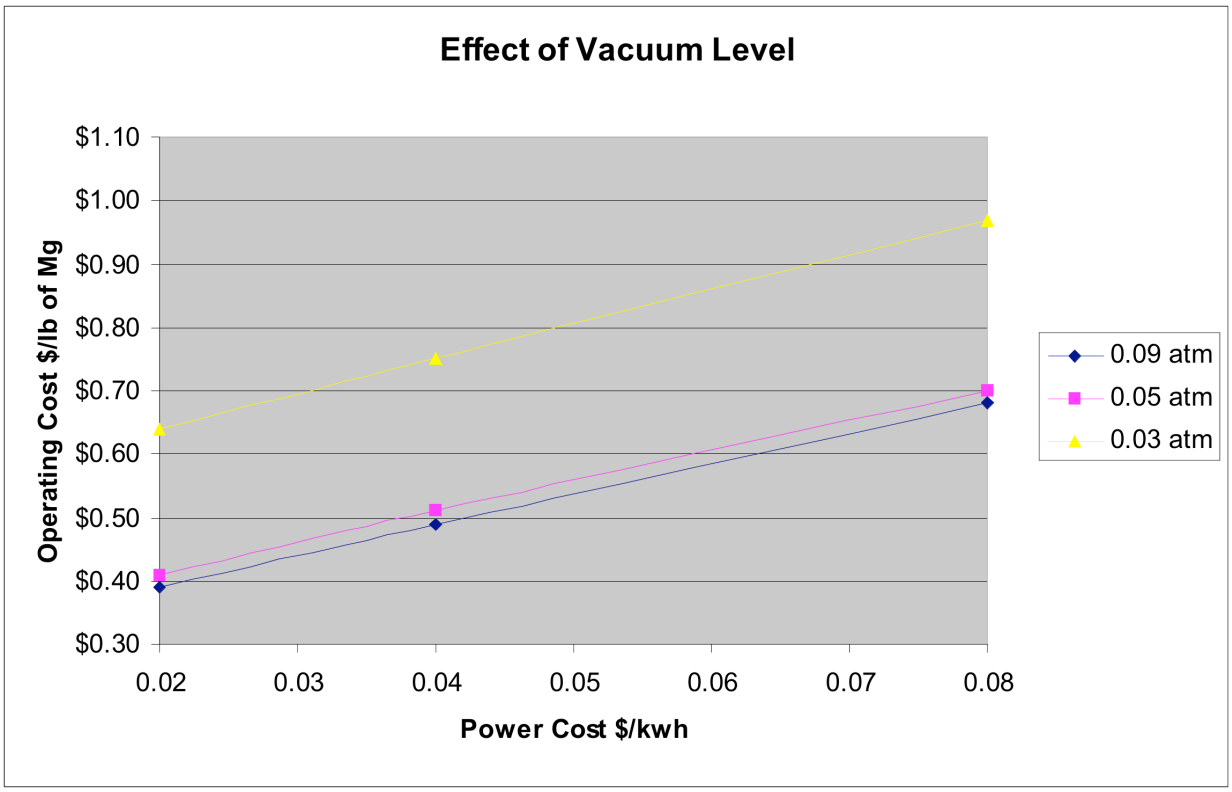

Figure 73 - The Impact of the Vacuum Level in the Salt Box Furnace on the Operating Costs

For those who hope to use such a model to optimize the economics of a process, the above effort represents the first step in defining the economic sensitivities of the process and those areas where conceptual improvements are required. For those whose primary purpose is the establish the approximate operating cost of making magnesium by the carbothermal process, the above serves as a good first estimate. A large part of the value of such models is the knowledge gained by its construction. These models in effect provide an estimate of the operating costs if the process performs according to the best knowledge available on the process. The best knowledge available (to the author) on the carbothermal process indicates that it could be the lowest cost method of making magnesium.

ENERGY COMPLEX

In an actual application of the Safe Hydrogen concept, a magnesium plant would be part of an energy complex, Figure 74, in which these factors of production would be clustered around a coal mine:

- Coal-fired Electrical Power Plant
- Coke Plant
- Oxygen Plant
- Hydrogen Plant
- Steam Boiler Plant

- Magnesium Plant
- Magnesium Hydride Plant

The end product of this complex would be magnesium hydride slurry, which would be transported to distribution complexes in population centers via rail or trucks in the most cost effective manner possible. The magnesium hydride would be made into a oil-based slurry and distributed to gas stations by the same or similar infrastructure that currently distributes gasoline. The spent fuel, i.e., the magnesium hydroxide slurry, would be returned to the distribution complexes, probably filtered and dried to produce magnesium hydroxide cakes which would be returned to the energy complex. This scenario makes the assumptions that the cost savings released in the energy complex, discussed below, would more than offset the transportation costs of transporting magnesium hydride to the distribution centers and the magnesium hydroxide from the distribution centers back to the energy complex. Given the author's understanding of the costs involved, this seems obvious, but granted, it has not been demonstrated by the appropriate modeling and cost gathering and is outside of the current scope of this effort.

Estimating the efficiency of an energy complex as presented in Figure 74 is also outside the scope of this current effort except in the form of preliminary assumptions. We have assumed the magnesium plant would be located in such an energy complex and would have access to the low cost commodities, including power, that such a complex would make possible. This efficiency of such a complex is expected to be achievable by a CHP (combined heat and power plant) since byproducts from one product are used by the other plant. In particular, technologies that produce hydrogen from coal or coke, such as Alchemix's (www.alchemix.net) would be expected to work particularly well in such an energy complex.

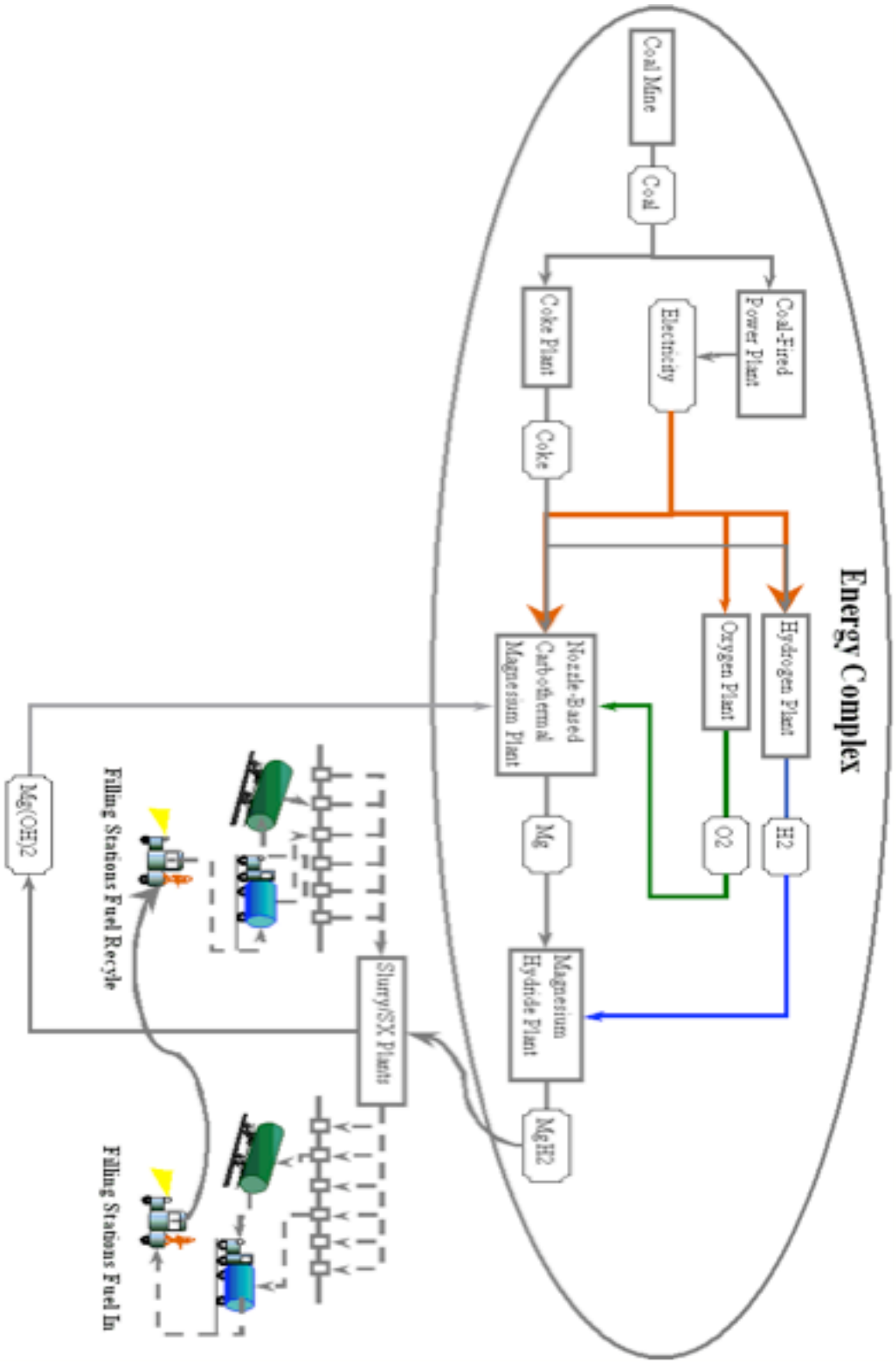

Figure 74 - Energy Complex for the Safe Hydrogen Project

POWER COSTS

The lowest cost electricity is made from nuclear power plants followed closely by power plants fired with coal and/or coke (reference 5) For example, the average price paid for natural gas by electricity generators in October 2004 was $5.82 per MMBtu , whereas the average price paid for coal sold to electricity generators in October was only $1.41 per MMBtu. The average industrial price for electricity was $0.049 per kWh for this same time period.

Electricity production costs are a function of the costs for fuel, operations and maintenance, and capital. For a new coal fired plant built today, fuel costs would represent about one-half of the total operating costs. Delivered coal prices are expected to remain about $1.20 per MMBTU for the next ten years, or about $30/ton. New coal technology requires about 7200 BTU to generate a kWh of electricity, or about $0.0086 per kWh. Since coal represents about half of the operating costs, this corresponds to about $0.017 per kWh. Given that our Energy Complex is located next to the mine, the cost of coal/coke is expected to be on the order of $18/ton, or $20/tonne (in the MV model). This corresponds to a power cost of about $0.014 per kWh. Given that the load factor in an industrial power plant is typically only 60 to 70%, and sometimes as low as 50%, keeping the plant on line more than 90% of the time to supply power for a magnesium facility would reduce costs even further.

LOAD SHARING

One way to reduce power demand is to use a procedure called load shifting, in which some electrical loads are operated only during off-peak periods-when demand for and the cost of electricity are relatively low. With such an approach, power costs could be reduced further by designing the magnesium facility to operate at two levels: (1) a maintenance level during peak load periods, and (2) a production level during off-peak periods.

In the maintenance level, enough energy would be required to keep furnaces at temperature, or about 10% of the normal demand. Additional energy would be used if available from the power plant to produce magnesium at a lower than normal production level. At the production level, the magnesium plant would help to keep the power plant at full load during off-peak periods with still some capabilities of cutting back if required. Enron, before its demise, was considering the aluminum and magnesium industry as a means of converting excess power into a bankable commodity with such an approach.

OXYGEN PRODUCTION COSTS

Oxygen costs used in our study were derived from the H2A (Hydrogen Analysis) study performed by NREL (National Renewable Energy Laboratory) and from the presentation by Gary J. Stiegel of NETL (National Energy Technology Laboratory) (reference 5). The H2A model uses an assumption of $0.02/kg of O_2 for a cost of oxygen.

A report by Praxair addressed the cost of oxygen using a new OTM (oxygen transport membrane) technology (reference 6). However, they did not state the cost of power in presenting their costs for making oxygen. If their cost of electricity was $0.05/kWh, then the cost of the OTM (oxygen transport membrane) oxygen due to electricity is about $0.0049/kg of O_2 and the cost of Cryogenic oxygen is $0.0079/kg of O_2 based on power consumption presented in their literature. Assuming that the basis of cost for their electricity was $0.05/kWhr, and assuming that the return on capital

required was 10% of the capital cost, the net operating costs with lower cost electricity ($0.03/kwh) would be about $0.0037/kg O_2. Thus the lower total cost of OTM O_2 would be about $0.0125/kg O_2. (The value from NREL of $0.02/kg for oxygen was used in the model.)

5.6.3.2.6 Task References

5. Gasification – Versatile Solutions, Overview of Gasification Technologies, By Gary J. Stiegel, Technology Manager – Gasification, National Energy Technology Laboratory, US Department of Energy, Presented at the Global Climate and Energy Project Advanced Coal Workshop, March 15, 2005

6. CO_2 Reduction by Oxy-Fuel Combustion: Economics and Opportunities, by H. Sho Kobayashi, and Bart Van Hassel of Praxair, Inc., Presented at the GCEP Advanced Coal Workshop, Provo, Utah, March 15, 2005

7. Hydrogen Delivery Component Model prepared by researchers at National Renewable Energy Laboratory, Golden, CO. Electric Power Monthly, February 2005, Energy Information Administration, Office of Coal, Nuclear, Electric and Alternative Fuels, U.S. Department of Energy, Washing DC 20585. Available at: http://www.eia.doe.gov/cneaf/electricity/epm/epm_sum.html. Also private communications with Matthew Ringer of NREL.

8. The Annual Energy Outlook 2005 (AEO2005) prepared by the Energy Information Administration (EIA), National Energy Information Center, EI_30, Forrestal Building, Washington, DC 20585.

5.6.3.3 Magnesium Chloride Process

5.6.3.3.1 Chlorination and Electrochemical Plant Based on 500 kA Electrolytic Cells

INTRODUCTION

As part of the economic evaluation of the various potential means of reduction of magnesium hydroxide and the subsequent manufacture of magnesium hydride for the production of slurry, a process plant design was estimated. The plant design was based on calcining the magnesium hydroxide, chlorination, and electrolysis of magnesium chloride to recover the magnesium metal. These operations are based on existing large scale industrial equipment with a magnesium throughput of 100,000 T/Y. Electrolysis is based on the use of 500 kA electrolytic cells. All ancillary equipment and supplies are based on supporting this throughput and enable operating costs and manning levels to be estimated. Although future economies of scale are likely to improve capital and operating costs, it is likely that this plant scale will form a good basis for economic evaluation.

The purpose of this plant is to receive recovered slurry arriving in tanker trucks from vehicle filling stations, process the materials and return them as Magnesium Hydride slurry for distribution back to the filling stations. The main process central to the operation of this plant will be based on the electrolytic reduction of magnesium chloride to magnesium metal in 500 kA cells. Although these units are regarded as the largest currently available, it is expected that future development would lead to larger sizes as demand increases. This would also apply to other elements of the plant such as the chlorinators. However for this example, scale-up is achieved by using multiple units of the largest currently envisaged. The following describes the plant areas and their functions in support of this operation based on a production throughput of 100,000 T/Year of Magnesium. Table 14 summarizes the design. The discussion that follows describes the individual process steps. 100,000 T/year of magnesium will carry about 18 million kg of hydrogen per year. This is about 0.03% of the projected US hydrogen automotive demand.

Figure 75 to Figure 78 display schematics of the major plant processes.

Table 14 - Electrochemical Plant Process Flows Summary

100,000T/Y MAGNESIUM METAL
500kA ELECTROLYTIC CELLS

PLANT AREA	MAIN FEATURES	VALUE
MATERIALS RECEPTION AND STORAGE	Magnesium metal content	350T/day
		14.6T/hr
	As Magnesium oxide MgO	583T/day
		24.3T/hr
	Alternatively	
	As Magnesium Hydroxide $Mg(OH)_2$	846T/day
		35.2 T/hr
COKE PREPARATION	Coke use rate	175T/day
	(design based on 78% utilization)	
	Storage	5 days
	Bulk density	(30lb/cu ft)
		0.48g/cc
	Storage	$1825m^3$
MAGNESIUM OXIDE PREPARATION	Magnesium oxide use rate	585T/day
	(design base 78% utilization)	
	Density	3.65g/cc
	Storage	5 days
	Bulk density	1.6g/cc
	Storage volume	$1825m^3$
CHLORINATOR FEED PREPARATION	Briquette rate	760T/day
	Press rate	35T/hr
	(10% recirculation)	
	Bulk density	2.2g/cc
	Day storage	$345\ m^3$
CHLORINATION	Reactors	55
	Production Magnesium Chloride	5300T/y-5900T/y each
	Tapping	3 times /day
	Tap weight	8.5T max
CHLORINATOR GAS SUPPLY	Chlorine rate	$14{,}000Nm^3/hr$
	Reactor rate	$275Nm^3/hr$
	Recycled from cells	$11{,}000Nm^3/hr$
	New Chlorine	$3{,}000Nm^3/hr$
CHLORINATOR OFF GAS HANDLING		
LIQUID MAGNESIUM CHLORIDE TRANSPORT	Ladle capacity	8.5T
	Number of ladles	18
	Volume inside refractory	$4m^3$ including freeboard
ELECTROLYSIS	Number of cells	65
	Cell liquid capacity	85T
LIQUID MAGNESIUM HANDLING AND STORAGE	Container capacity	2T
	Number of containers	20
	Volume inside refractory	$1.3m^3$including freeboard
	Heated mixer capacity	500T
	Volume inside refractory	$325m^3$including freeboard
CHLORINE RECYCLING TO CHLORINATORS	Chlorine recovery rate	650kg/hr

Plant areas

MATERIALS RECEPTION AND STORAGE

Process Materials

Magnesium

Magnesium metal content	350 T/day
	14.6 T/hr
As Magnesium oxide (MgO)	583 T/day
	24.3 T/hr
As Magnesium Hydroxide ($Mg(OH)_2$)	846 T/day
	35.2 T/hr

Tanker trucks will arrive and have their contents checked by weight and sampled for accounting as they are discharged into a reception hopper. The Magnesium oxide/hydroxide collected from filling stations will be transferred to bulk storage to maintain continuity of operation for the processing plant. About five days' stock is anticipated. Slurry oil settling out will be recovered from the received materials and collected for reuse with the outgoing Magnesium Hydride slurry product. More oil may be recovered by pressing or vacuum filtration in preparation for chlorination.

New oil will be required to make up the total requirement for forming Magnesium Hydride slurry as well as for start up and expansion.

New Magnesium Oxide powder will be received into the plant for start up, expansion, and occasionally to make up for system losses.

Carbon. Petroleum coke will be checked for weight and sampled before being conveyed to buffer storage. About one weeks' stock will be required to provide continuity from outside suppliers.

Hydrogen for hydriding magnesium metal. Generated on site from natural gas.

Chlorine make up for losses.

Nitrogen for purge and sealing. Evaporation and distribution system required. Also nitrogen may be used for instrumentation actuation and control.

Gas cleaning water neutralization: Caustic soda NaOH

Plant Consumable Materials

Various materials will be received into the plant, checked and placed in appropriate storage until required for use as replacement for worn out materials.

Refractory

Lining for chlorinators. High Alumina

Lining for hot transport ladles. High Alumina working face; bubble alumina insulation backing; light weight insulation for ladle covers.

Lining for electrolysis cells.

Liquid magnesium holding vessel. Chrome magnesite, insulation backing.

Recirculating fluid bed hydriding reactors. Strategically placed abrasion resistant areas.

Carbon briquettes for chlorinator resistance heating and liquid magnesium chloride filtration.

Chemicals for electrolyte in cells

Sodium chloride NaCl

Potassium Chloride KCl

Lithium Chloride LiCl

Barium Chloride BaCl2
General maintenance materials
Lubrication oils and greases
Replacement bags for fabric filters.

COKE PREPARATION

Coke use rate	175 T/day (design based on 78% utilization)
Storage	5 days
Bulk density	0.48 g/cc (30lb/cu ft)
Storage	1825 m^3

Petroleum coke will be received into the plant, screened to remove tramp material, and crushed to a suitable size for blending with the magnesium oxide. Storage bins with weigh feeders will dispense the coke at the appropriate rate for mixing with the magnesium oxide.

MAGNESIUM OXIDE PREPARATION

Magnesium oxide use rate	585 T/day (design base 78% utilization)
Density	3.65 g/cc
Storage	5 days
Bulk density	1.6 g/cc
Storage volume	1825 m^3

Magnesium oxide together with any oil will be fed to vacuum disc filters for oil recovery. The magnesium oxide cake will be fed to a collecting belt for delivery and metering with the coke to the blending system.

CHLORINATOR FEED PREPARATION

Coke and magnesium oxide metered in batches will be delivered to mixers for blending together. The blended material will then be sent to bins for subsequent feeding to briquetting presses. The briquettes will be sent to storage bins for distribution to the chlorinators. Fines from the briquetting and storage will be recycled to the briquetting feed bins. Briquettes will be metered out of the storage bins and fed in batches to the inlet lock hoppers of the chlorinators by the conveyor distribution system.

Briquette rate	760 T/day
Press rate	35 T/hr (10% recirculation)
Bulk density	2.2 g/cc
Day storage	345 m3

CHLORINATION

Reactors	55
Production	5300 T/y-5900 T/y each Magnesium Chloride $MgCl_2$
Tapping	3 times /day
Tap weight	8.5 T max

A batch of briquettes will be diverted from the distribution conveyor system to the empty top hopper of a chlorinator as the lower hopper discharges its batch into the chlorinator reactor. The top lock hopper will be closed and sealed, purged and raised to reactor pressure. When the lower hopper reaches a level when there is sufficient room for the new batch it will be transferred from the top hopper to the lower hopper. The empty top hopper will be de pressurized to await the need for a new batch of feed.

The briquettes from the hoppers will be fed to the top of the burden inside the reactor and will react with the carbon and the hot chlorine gas flowing up from the layer of carbon briquettes in the base of the reactor vessel. The feed rate will be based on maintaining a steady level of burden in the reactor, replacing material as it gravitates to the reaction zone where gaseous and liquid products form. As the reaction proceeds carbon monoxide and magnesium chloride will be the products. The carbon monoxide will leave the reactor through the off gas duct while the liquid magnesium chloride will drain to the bottom of the reactor and occupy the voids in the carbon briquettes in the base of the reactor. Although the reaction is exothermic and provides more than enough heat to heat the reacting materials and the products to the appropriate temperature, the carbon briquettes at the bottom of the reactor will also be used as resistance heating elements to provide heat during start up to raise the reactor temperature to the desired operating range and to offset thermal losses through the reactor walls during steady state processing. Varying this heat input will provide a degree of process control. These carbon briquettes will also serve as a gas distributor for the injected chlorine and a physical support for the solid burden to allow the liquid product to filter down to the bottom of the reactor.

CHLORINATOR GAS SUPPLY

Chlorine rate	14,000 Nm^3/hr
Reactor rate	275 Nm^3/hr
Recycled from cells	11,000 Nm^3/hr
New Chlorine	3,000 Nm^3/hr

Chlorine gas collected from the electrolytic cells will be filtered to remove particulate and compressed for buffer storage and injection through the base of the reactors. Extra chlorine will be added into this system to make up for losses.

CHLORINATOR OFF GAS HANDLING

Carbon monoxide generated in the reaction will be removed from the reactor through a duct to a wet gas cleaning system that will also be treated with sodium hydroxide to neutralize chlorine that may be carried over. The off gas system will also provide a means of controlling the reactor pressure. Higher operating pressure will improve the operating rate and reduce the carry over of magnesium chloride as vapor.

LIQUID MAGNESIUM CHLORIDE TRANSPORT

Ladle capacity	8.5 T
Number of ladles	18
Volume inside refractory	4 m^3 including freeboard

Liquid magnesium chloride will accumulate at the bottom of each reactor and will be tapped off in batches into insulated transport ladles. Each ladle will be fitted with an insulated cover and will be purged out with inert gas in order to prevent contact with atmospheric moisture. The ladles will be transported through a flexible system of transfer cars or overhead cranes so that ladles may be sent from various chlorinators to different electrolysis cells.

ELECTROLYSIS

Number of cells	65
Cell liquid capacity	85 T

Each 500 kA cell will produce magnesium metal at a rate of 220 kg/hr. The incoming magnesium chloride feed will be dissolved in an electrolyte bath where it will represent 5% to 15% of the bath composition. The remainder will be various combinations of metal chlorides such as sodium, potassium, lithium, calcium, and barium. The combination of potassium chloride with the lighter lithium chloride may be adjusted to give an electrolyte density that allows the magnesium metal to accumulate at the bottom of the cell where it is tapped off. Lithium chloride also increases the conductivity of the melt. For higher density melts the magnesium metal accumulates at the surface and is pumped away.

LIQUID MAGNESIUM HANDLING AND STORAGE

Container capacity	2 T
Number of containers	20
Volume inside refractory	1.3 m^3 including freeboard
Heated mixer capacity	500 T
Volume inside refractory	325 m^3 including freeboard

Liquid magnesium from the cells will be transported in insulated containers and added to a large heated storage vessel where temperature of the metal will be equalized and controlled for feeding to the hydriding reactors. The mixer will be shrouded to prevent contact between the magnesium and air. Liquid metal pumps may be used to aid metal transfer to and from the mixer vessel.

ELECTROLYSIS ELECTRICAL CONTROL

Efficient operation of the cells will rely on monitoring bath parameters to adjust voltage and currant to maintain magnesium metal production rate and bath temperature at optimum levels.

CHLORINE RECYCLING TO CHLORINATORS

Chlorine recovery rate	650 kg/hr
	205 Nm^3/hr

Chlorine gas, which will be released at the anodes of the cell, will be extracted through a fabric filter to remove entrained particulate before being compressed into a storage vessel for distribution to the chlorinators. The particulate may be returned to the electrolysis cells by adding to the empty magnesium chloride transfer ladles prior to tapping the magnesium chloride from the chlorinators.

HYDRIDING REACTORS

Liquid magnesium is too hot to react with hydrogen to form magnesium hydride as it is above the decomposition temperature. However, the liquid magnesium will likely be atomized with cold hydrogen and sprayed into the hydriding system. The product will be removed from the hydriding system and fed to a storage hopper for subsequent metering and blending with the slurrying oil.

HYDROGEN GENERATION AND SUPPLY

Hydrogen generation	9000 T/year
	100.106 Nm^3 /year
	370,000 Nm^3 /day

An important part of the plant economy will be the generation of hydrogen. The method used will depend on local economy. If electrical power is relatively cheap then

electrolysis may be used as opposed to steam reforming of natural gas. Other methods under development include gas from biomass reformed as with natural gas and direct separation from water using energy from sunlight. The daily generation rate is based on 10% loss and a plant availability of 75%.

MAGNESIUM HYDRIDE HANDLING

Hydride storage	8 hr
	100 T
Storage volume	140 m^3
Bulk density	0.7 g/cc

The storage weigh hoppers will be blanketed with protective gas to prevent reaction with moisture. The hydride powder will be blended with slurry oil and pumped to product storage tanks ready for dispensing into transport tankers for delivery to filling stations.

MINERAL OIL BLENDING SLURRY MANUFACTURE AND STORAGE

Product storage	5 days
Solids proportion	60%
Density	0.87 g/cc

Mineral oil recovered from returned material reception will be mixed with oil from storage tanks and added to magnesium hydride powder and sent to product stock tanks. Agitation will be applied to the stock tanks to prevent settlement and maintain product homogeneity.

SLURRY PRODUCT DISPENSING AND LOADING ON TO TRANSPORT.

After ensuring that tanker trucks with returned magnesium oxide for recycling have been certified as empty and dry they will be filled from the product stock tanks. Product quantity and hydride and additive content will be ascertained and recorded for accounting.

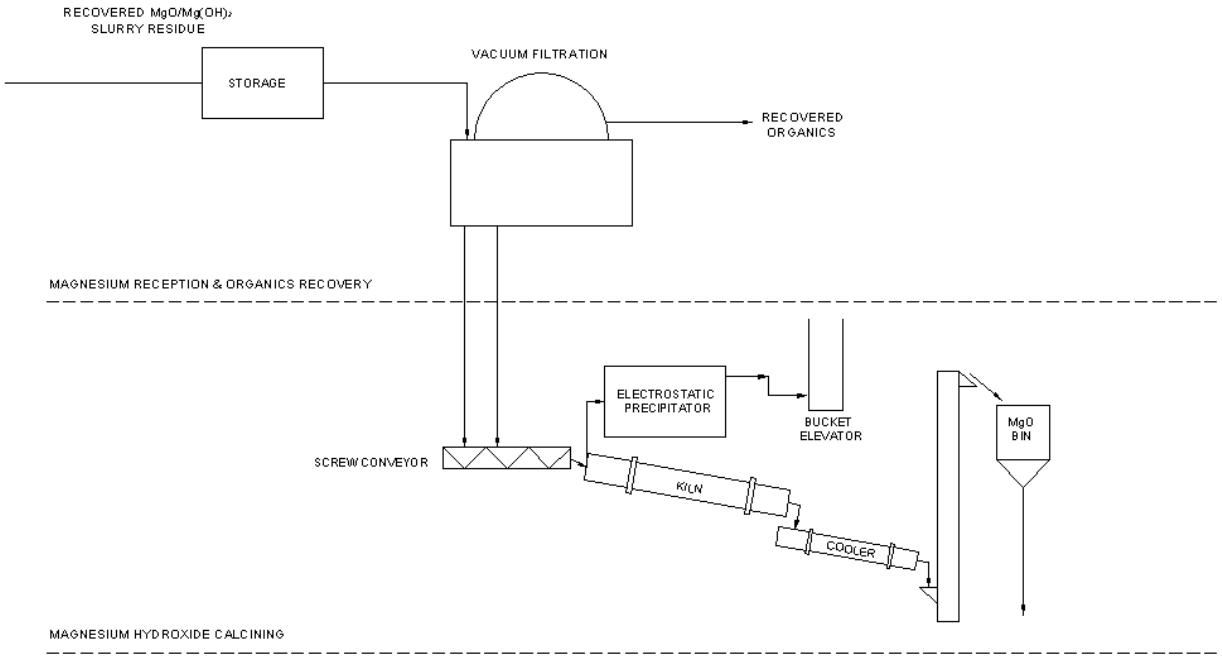

Figure 75 - Reception and Calcining Processes

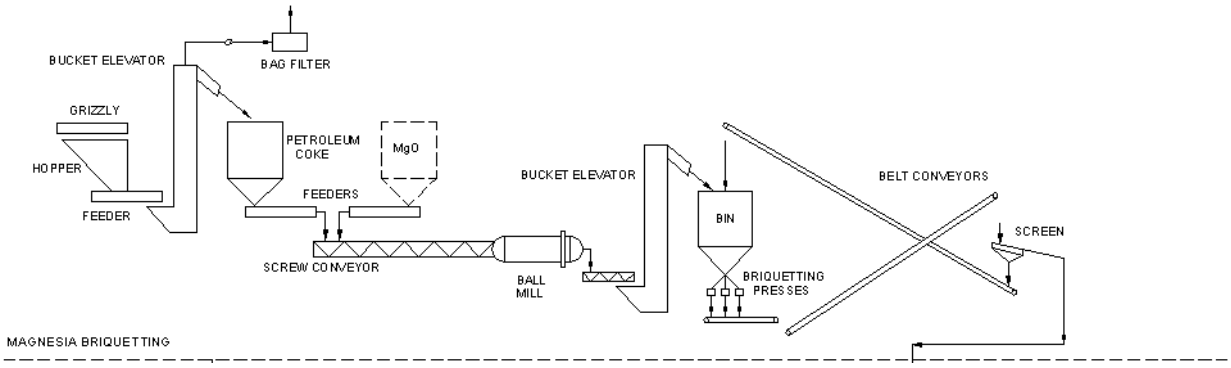

Figure 76 - MgO Briquetting Process

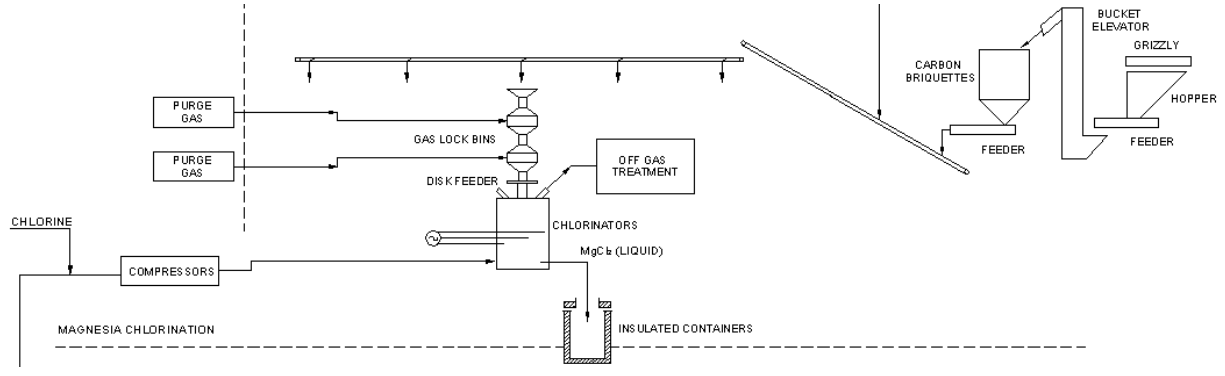

Figure 77 - MgO Chlorination Process

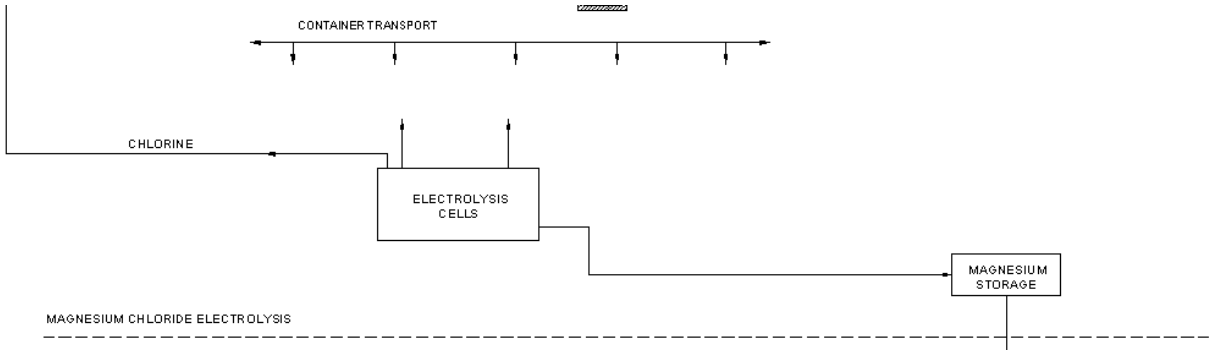

Figure 78 - $MgCl_2$ Electrolysis Process

5.6.3.3.2 Magnesium Chloride Electrolytic Process Analysis

The viability of the large-scale use of Magnesium Hydride slurry as a means of transporting and storing hydrogen is benefited by recycling the magnesium metal from the collected residue from used slurry that has been exchanged for new slurry distributed to the users. It is envisaged that large recycling plants would be strategically sited to suite the fuel distribution infrastructure.

Central to the recycling process will be a means for reducing Magnesium Hydroxide and Magnesium Oxide to Magnesium metal ready for hydriding to produce new slurry. A number of processes exist for carrying out this reduction process. Comparison of plant capital and operating costs for the different processes will help in selecting which process would be best suited to utilize the resources available in a chosen area and hence determine the overall costs associated with using a Magnesium Hydride slurry system.

Cost estimates have indicated that the capital cost of a recycling plant based on the electrolysis of Magnesium Chloride is likely to be 35% more expensive than a plant based on the carbothermic reduction of Magnesium Oxide. However, plant locations close to the production of cheap electrical energy such as at a geothermal field, hydroelectric power source, or with a captive nuclear power generating plant, all of which minimize transmission losses; may have operating costs which will allow the convenience of using electrical energy to offset the capital cost differential.

A plant design based on an annual throughput of 100,000 tons has been used as a model for developing an assessment of both capital and operating costs including manpower and energy requirements. This plant size has been chosen because it is in line with the maximum size of Magnesium metal producing plants currently in operation. However, Magnesium hydride as a major part of a Hydrogen fuel system for vehicles is likely to benefit from further economies of scale through being processed in much larger facilities.

Major areas of the plant and some unit process operations would be common to all recycling plants. These include the reception and storage of recovered residue from the used Magnesium Hydride slurry, recovery and reuse of oils from the slurry, manufacture of Magnesium Hydride from the Magnesium metal reduced from the residue, blending the Hydride with oil to make new slurry, and storage and redistribution of the Magnesium Hydride slurry to the users.

Hatch Technology has the portion of this task which covers the economic evaluation of the recycling process using chlorination with the subsequent electrolysis of

Magnesium Chloride. The evaluation is in progress and is based on estimating manpower requirements and calculating energy needs of the individual plant areas and the unit process operations. The plant area subdivisions are those indicated in the plant flow table used for capital cost estimation. For each area electrical and other energy needs have been assigned, operational manning has been estimated, and for hot operational and transfer equipment heat losses have been estimated. These elements will be used to compare alternative means of recycling spent slurry as well as forming sections of the overall cost build up for the energy delivered to vehicle wheels.

ENERGY

Energy requirements in each area are expressed as a continuous power rating in kW needed to maintain a plant throughput based on 100,000 tonnes a year of Magnesium and applies to both electrical and other forms of energy such as the heating power of fuel.

MATERIALS RECEPTION AND STORAGE

A significant power use in this area will for the running of mechanical equipment such as pumps and conveyors for receiving materials, especially the returned residue from used slurry. This will be pumped from tankers to storage and then to treatment for oil recovery. Energy will be required at a much greater rate for the evaporation of solvent for oil recovery but it is likely that such low grade heat, at say 50°C, would be recoverable from other plant areas.

Pumping, material handling etc.	15 kW
Solvent evaporation (received from Hydriding)	(3,520 kW)

COKE PREPARATION

The petroleum coke will require screening to maintain consistent size and to remove any tramp materials before delivery to the chlorination feed preparation area.

Screens, conveyors, feeders.	10 kW
Dust extraction, say 300 m^3/min	35 kW

MAGNESIUM OXIDE PREPARATION

Conveyers and feeders will deliver the solvent washed recovered residue to the calcining process where it will be heated to decompose any Magnesium Hydroxide to Magnesium Oxide. The major energy consumption will be heat for calcining but this is also potentially recoverable from other plant areas since the decomposition temperature is about 270°C and process heat could be recovered at more than 350°C. Calciner exhaust gases would require particulate removal before discharge.

Conveyors, feeders.	25 kW
Exhaust treatment, say 1000 m^3/min	75 kW
Calcining, 60% $Mg(OH)_2$	6,450 kW

CHLORINATOR FEED PREPARATION

Mixing and pressing the Magnesium Oxide with the coke to form briquettes for convenient feeding to the calciner, together with screening and recycling of undersize will require operating power. Dust extraction will also be required.

Mixers, briquetting, screening and conveying	40 kW
Dust extraction, say, 200 m^3/min,	25 kW

CHLORINATION

The main energy requirement is represented by the coke included in the feed materials. The resulting chlorination reaction produces excess heat, more than that required to raise the feed materials to reaction temperature and then deliver the Magnesium Chloride product in liquid form at about 850°C. However, some external heat is required for start up and may be applied electrically but this represents a negligible quantity when considered as a continuous demand. There is potential for some heat recovery from the reaction process but there may be more convenient sources in the plant than from this type of reactor.

Coke in feed, based on calorific value	27,000 kW

CHLORINATOR GAS SUPPLY

The majority of the chlorine gas for the chlorinators is recovered from the Magnesium Chloride electrolysis. It is assumed that make up gas is required to offset losses and incomplete recovery. This is generated by the electrolysis of aqueous Sodium Chloride. This process will also produce hydrogen simultaneously at the same rate.

Chlorine make up, say 10% at 3,000 kWh/ton	10,000 kW

CHLORINATOR OFF GAS HANDLING

Waste gas from the chlorination process may be treated by wet scrubbing with neutralization of any acid carried over with the waste gas.

Process gas 3500 Nm^3/min	1,230 kW

LIQUID MAGNESIUM CHLORIDE TRANSPORT

Although energy will be required to keep the transport ladles up to temperature this heat quantity will be small in view of the insulation of the containers. Ladle heaters will be needed to dry newly lined ladles and bring them up to service temperature but the low frequency of these tasks do not constitute a significant mean energy demand.

Ladle heating (negligible)	0.6 kW

ELECTROLYSIS

The most significant quantity of electrical power will be for the electrolysis of liquid Magnesium Chloride to form liquid Magnesium and Chlorine gas.

Electrolysis (12 kWh/kg)	137,000 kW

LIQUID MAGNESIUM HANDLING AND STORAGE

The ladles of liquid Magnesium will be collected and poured into a heated storage vessel to give consistent temperature and availability of feed to the subsequent Hydriding process. The energy usage will be based on compensating for the heat losses from the insulated storage vessel.

Vessel heating (shell 300 m^2 at 100°C)	30 kW

CHLORINE RECYCLING TO CHLORINATORS

The chlorine recovered from the electrolytic cells will be drawn off and compressed into storage with newly made make up Chlorine for distribution to the chlorinators.

Compression of chlorine gas (4.5 bar)	1,700 kW

HYDRIDING REACTORS

Liquid magnesium metal at about 700°C will be pumped and sprayed into a recirculating pressurized stream of hydrogen gas which will cool the droplets and react to form Magnesium Hydride at about 250°C. The particulate will circulate within the system such that the Magnesium Hydride can be separated from any unreacted Magnesium metal particles by density. The Magnesium Hydride will be removed as product while unreacted Magnesium metal continues to circulate until the reaction is complete. The hydriding reaction is exothermic so this energy together with excess sensible and latent heat from the liquid Magnesium feed must be removed. Although low grade this heat is more than enough to meet the needs of the solvent evaporation for oil recovery.

Hydriding reaction heat available	(10,000 kW)

HYDROGEN GENERATION AND SUPPLY

Various means of hydrogen generation exist but in this plant where electrolysis is the major process it is likely to be used throughout. It is assumed that about 10% of the hydrogen need will be met from the Aqueous Sodium Chloride electrolysis for chlorine production.

H_2 electrolysis 10,000 Nm^3/h at 4.2 kWh/Nm^3	42,000 kW
Compression to 5bar	2,000 kW

MAGNESIUM HYDRIDE HANDLING

Collection of the Magnesium Hydride from the hydriding reactors will be through pressurized lock hoppers using nitrogen as a protective sealing gas. Closed conveyors will deliver it to storage facilities. This area will have insignificant energy consumption.

Material handling equipment	10 kW

MINERAL OIL BLENDING SLURRY MANUFACTURE AND STORAGE

Magnesium Hydride powder with metered quantities of recovered mineral oil together with new oil to cover short fall through losses will be mechanically mixed to form a pumpable slurry.

Mixing and feeding	10 kW

SLURRY PRODUCT DISPENSING AND LOADING ON TO TRANSPORT

The slurry will be pumped to storage tanks to await discharge to tankers for distribution. The tankers will be those used for bringing into the reception area the residue from used slurry.

Pumping and stirring	15 kW
Total energy requirements	**227,670 kW**
Production throughput average tonnes/year Mg	**100,000**
Tonnes/hour	**11.4**
Specific energy consumption	**20 kWh/kg**

MAN LOADING

The plant will be subdivided into areas of similar character so that expertise can be developed in maintenance and supervisory teams as well as operators.

MATERIALS HANDLING

The storage handling and treatment equipment associated with incoming materials and product export will be similar in nature and likely to be in close proximity. A supervision and maintenance team will look after the whole area.

Area manager	1	Shift supervisor	1	Total	5
Maintenance manager	1	Shift technician	5	Total	21

MATERIALS RECEPTION AND STORAGE

Shift operator	4	Total	16

COKE PREPARATION

Shift operator	3	Total	12

MAGNESIUM OXIDE PREPARATION

Shift operator	6	Total	24

CHLORINATOR FEED PREPARATION

Shift operator	4	Total	16

MAGNESIUM HYDRIDE HANDLING

Shift operator	2	Total	8

MINERAL OIL BLENDING SLURRY MANUFACTURE AND STORAGE

Shift operator	1	Total	4

SLURRY PRODUCT DISPENSING AND LOADING ON TO TRANSPORT

		Shift operator	1	Total	4
		Area Total			110

CHLORINATION

The chlorination reactors together with their gas supply systems and off gas handling trains will form a large integrated area of the plant.

Area manager	1	Shift supervisor	1	Total	5
Maintenance manager	1	Shift technicians	6	Total	24

CHLORINATION

		Shift operator	11	Total	88

CHLORINATOR OFF GAS HANDLING

		Shift operator	4	Total	16
		Area Total			133

GAS GENERATION

The production of new chlorine, the recycling of chlorine from the Magnesium Chloride, the generation of hydrogen from the chlorine operation as well as the main new hydrogen production will comprise a single operational area.

Area manager	1	Shift supervisor	1	Total	5
Maintenance manager	1	Shift technicians	6	Total	24

CHLORINATOR GAS SUPPLY

		Shift operator	2	Total	8

CHLORINE RECYCLING TO CHLORINATORS

		Shift operator	2	Total	8

HYDROGEN GENERATION AND SUPPLY

		Shift operator	2	Total	8
		Area Total			53

HOT OPERATIONS

Hot liquid handling demands specific skills for safe operations. The combination of the supply of incoming materials and handling of the hot metal product with the running of the electrolysis cells will promote efficient operation of this critical area of the plant.

Area manager	1	Shift supervisor	1	Total	5
Maintenance manager	1	Shift technicians	6	Total	24

LIQUID MAGNESIUM CHLORIDE TRANSPORT					
		Shift operator	13	Total	52
ELECTROLYSIS					
		Shift operator	26	Total	104
LIQUID MAGNESIUM HANDLING AND STORAGE					
		Shift operator	13	Total	52
		Area Total			237

FLUIDISED BED OPERATION

This specialist area of the plant will play a key role in controlling the quality and availability of the finished product.

Area manager	1	Shift supervisor	1	Total	5
Maintenance manager	1	Shift technicians	3	Total	12

HYDRIDING REACTORS					
		Shift operator	4	Total	16
		Area Total			33

Plant operation, maintenance and supervision **566**

5.6.3.4 SOM Process

5.6.3.4.1 SOM Based Slurry Byproduct Reduction Process Based on H2A Analysis Framework

Introduction

The results of the first evaluation of one of the SOM processes in the H2A format is discussed in this section. The cost of hydrogen resulting from this analysis with the H2A analysis framework is $3.89/kg of hydrogen delivered. TIAX has recommended that we take credit for the oxygen byproduct since oxygen is anticipated to be needed as a feedstock for biomass applications.

H2A Analysis of the SOM/LSM Process

The Department of Energy has been developing a framework to help researchers evaluate hydrogen production and delivery concepts with a set of similar assumptions. The analyses described above for the SOM/LSM option has been recast in the H2A Production Analysis format starting with the template “h2a_central_model_tool.xls”. This template is used with Microsoft Excel and has several tabs to describe the assumptions of the model.

The assumptions made in this analysis for the Financial Inputs are shown in Table 15. This analysis is performed assuming that a GT-MHR GEN IV nuclear power plant will supply 2,400 MWth of energy. 1,854 MWth will produce 835 MWe for the SOM electrolysis of MgO to Mg. 545 MWth will produce 60,629 metric tonne/year of hydrogen needed to make the MgH_2. The slurry will produce 121,257 metric tonne of hydrogen when mixed with water.

The values for several of the inputs on this tab were taken from the sample analysis of the coal fired production facility with sequestration, "h2a_central_coal_sequestration_current_final.xls".

Table 15 – Financial Inputs

	Base Case	H2A Guidelines	Values in Reference Study	Comments
Reference $ Year	2005	Half-decade increments, beginning with the most recent half-decade (e.g., 2005)		
Assumed Start-up Year	2005			
After-Tax Real IRR (%)	10%	10%		
Depreciation Type (MACRS, Straight Line)	MACRS	MACRS		
Depreciation Schedule Length (No. of Years)	20	20		
Analysis Period (years)	40	40		
Plant Life (years)	40	40		
Assumed Inflation Rate (%)	1.90%	1.90%		
State Income Taxes (%)	6.0%	6%		
Federal Income Taxes (%)	35.0%	35%		
Effective Tax Rate (%)	38.9%			
Design Capacity at 100% Capacity (kg of H2/day)	332,211.00			
Operating Capacity Factor (%)	100%	Varies according to case		
Plant Output (kg H2/day)	332,211.00			production based on size of power plant and Mg production requirments
Plant Output (kg H2/year)	121,257,015.00			
% Equity Financing	100%	100%		
% Debt Financing	0%	0%		
Debt Period (years)	0	N/A; zero debt assumed in H2A guidelines		
Interest Rate on Debt, if applicable (%)	0.0%	N/A; zero debt assumed in H2A guidelines		
Length of Construction Period (years)	3	Varies according to case		h2a_central_coal_sequestration_current_final.xls
% of Capital Spent in 1st Year of Construction	40%	Varies according to case		h2a_central_coal_sequestration_current_final.xls
% of Capital Spent in 2nd Year of Construction	35%	Varies according to case		h2a_central_coal_sequestration_current_final.xls
% of Capital Spent in 3rd Year of Construction	25%	Varies according to case		h2a_central_coal_sequestration_current_final.xls
		Varies according to case		
Start-up Time (years)	2	Varies according to case		h2a_central_coal_sequestration_current_final.xls
% of Revenues During Start-up (%)	50%	Varies according to case		h2a_central_coal_sequestration_current_final.xls
% of Variable Operating Costs During Start-up (%)	75%	Varies according to case		h2a_central_coal_sequestration_current_final.xls
% of Fixed Operating Costs During Start-up (%)	75%	Varies according to case		h2a_central_coal_sequestration_current_final.xls
Salvage Value of Capital (% of Total Capital Investment)	10%	10%		h2a_central_coal_sequestration_current_final.xls
Decommissioning Costs (% of Depreciable Costs)	10%	10%, equal to salvage value		

Table 16 displays the capital costs of the system. The costs of the nuclear power plant are not included because the costs of hydrogen and electricity are provided as though the plant was located next door to the magnesium hydride slurry plant. The uninstalled costs represent the costs of the equipment called out in our analysis. The installed costs represent the cost of the equipment plus the labor estimated for installation plus allowances for foundations, structures, buildings, insulation, instrumentation, electrical work, piping, painting, and miscellaneous.

Table 16 - Cost Inputs - Capital Costs

CAPITAL INVESTMENT (Inputs REQUIRED in Reference Year, 2005 $)			
Major pieces/systems of equipment	Uninstalled Costs	Installation Cost Factor	Installed Cost
Tank storage- Spent Hydroxide Slurry: Pumps, Mixers, Tanks	1,736,421	2.982499155	5,178,875
Solvent Separation: Tanks, Pumps, Filters, Mat'l Handling Equip	5,011,329	2.375641977	11,905,125
Calcining: Rotary Kiln, Electrostatic precipitator, Exhaust Blower, damper, stack, Rotary cooler, Bins and tanks, miscellaneous pumps, materials handling equip	17,070,310	2.34356809	40,005,433
Magnesia Reduction - SOM cell components, gas lock, heat exchanger, bag filter, centrifugal compressor, bins and hoppers materials handling equipment	51,353,162	1.776548532	91,231,385
Hydride Process: Gas lock, fluidized bed reactor, centrifugal compressor, bins and hoppers, materials handling equipment	11,804,065	2.170093427	25,615,924
Slurry Production: Pumps, tanks, grinders, mixers, augers	4,045,651	2.632234491	10,649,103

Table 17 displays the costs of the installed direct capital and costs for site preparation, Engineering & design, contingency and permitting following the values used in the coal to hydrogen plant. Some of these costs, such as site preparation, and engineering & design, may have been included in the previous analysis but have been called out specifically in this analysis.

Table 17 – Cost Inputs – Depreciable and Non-Depreciable Capital Costs

TOTAL DIRECT CAPITAL INVESTMENT (DEPRECIABLE)	$ 184,585,843.87			
Indirect Depreciable Capital Costs				
Site preparation ($)	1,820,419		2% of uninstalled costs. This factor may be double counted from the original analysis.	h2a_central_coal_sequestration_current_final.xls
Engineering & design ($)	18,458,584		10% of installed costs. This factor may be double counted from the original analysis.	h2a_central_coal_sequestration_current_final.xls
Process contingency ($)				
Project contingency ($)	27,687,877		15% of installed costs	h2a_central_coal_sequestration_current_final.xls
Other ($)				
One-time licensing fees ($)				
Up-front permitting costs ($)	13,653,141		15% of uninstalled costs	h2a_central_coal_sequestration_current_final.xls
TOTAL DEPRECIABLE CAPITAL COSTS ($)	$246,205,864			
Other (Non-Depreciable) Capital				
Land required (acres)	10		Estimated land requirement	
Cost of land ($/acre)	$5,000.00	**Without a reference to a case-specific value, use $5,000/acre as the suggested H2A standard for central plants.**		
Total land costs ($)	$50,000			
Other *(add details as needed in rows below)*				
TOTAL NONDEPRECIABLE CAPITAL COSTS	$50,000			
TOTAL CAPITAL INVESTMENT	$246,255,864			

Table 18 displays the Fixed Operating and Maintenance costs. The number of full time employees was estimated from the original small-scale plant by scaling using a 0.8 exponent. Labor costs are estimated to be $15/hour with a 50% overhead rate. G&A, property taxes and miscellaneous costs for maintenance are estimated following the coal example.

Table 18 - Cost Inputs - Fixed O&M

Operating and Maintenance Costs (Inputs required in Reference Year, 2005 $)	**Base Case:**	**H2A Guidelines:**	**Comments:**	**Data source:**
Fixed O&M Costs				
Total plant staff (number of FTEs employed by plant)	266.00		scaled from 3,611 metric tonne H2/year plant estimate using a scale exponent of 0.8	
Burdened labor cost, including overhead ($/man-hr)	$ 22.50	**Without a reference to a case-specific value, use $50/hour as the suggested H2A standard for central plants.**	$15/hour labor cost is assumed with a 50% overhead rate.	
Labor cost, $/year	$12,448,800			
G&A rate (% of labor cost)	20%	**Without a reference to a case-specific value, use 20% of total labor cost as the suggested H2A standard for central plants.**		
G&A ($/year)	$2,489,760			
Property tax and insurance rate (% of total initial capital costs)	2.0%	**Without a reference to a case-specific value, use 2% of the total initial capital as the suggested H2A standard.**		
Property taxes and insurance ($/year)	$4,925,117			
Rent or lease ($/year)				
Licensing, permits, and fees ($/year)				
Material costs for maintenance and repairs ($/year)	1,107,515		0.6% of installed costs	h2a_central_coal_sequestration_current_final.xls
Other fees ($/year)				
Other fixed O&M costs ($/year)				
TOTAL FIXED O&M COSTS ($/year, year 2005 basis), excluding materials	$20,971,192			

Feedstock costs and Other Raw Materials and Utility Costs are shown in Table 19 and Table 20. Costs are estimated for the primary electrical needs assuming

10 KWhe/kg of magnesium produced in the SOM process and costs for hydrogen, oil and dispersant assuming that the oil and dispersant costs are for replacement of 5% of the oil and dispersants lost per year. There is also an estimate for the cost of electricity for pumps and fans.

Table 19 - Cost Inputs – Feedstock Costs

VARIABLE PRODUCTION COSTS (at 100% capacity, start-up year cost in reference year, (2005) dollars)				
	Base Case:	H2A Guidelines:	Comments:	Data source:
Feedstock Costs				
Type of **electricity** feedstock used	Industrial Electricity			
Use H2A electricity feedstock cost? (Enter yes or no)	No			
Enter electricity feedstock cost if NO is selected above ($/kWh)	0.029		Cost of electricity at busbar from a GT-MHR GEN IV nuclear generator	neri.ne.doe.gov/NERI2004AnnualReport_FINAL.pdf discusses the costs of nuclear produced hydrogen. Page 61 notes a cost of 1.35/kg and $1.65/kg for sales of H2 and O2 vs H2 only
Electricity feedstock consumption (kWh/kg H2)	60.2995		Based on the need for 10kWhr/kg of magnesium and the need for 1 mole of H2 per mole of Mg to make MgH2 and the recognition that 2 mole of H2 is produced per mole of MgH2.	
Electricity feedstock cost in startup year ($/year)	$212,040,384			

Table 20 - Cost Inputs – Other Raw Materials and Utility Costs

Additional Raw Material Costs *(add details as needed in rows below)*			
Hydrogen from Site Power Plant ($/kg H2)	$100,037,075		half of the hydrogen to be delivered must be reacted with Mg to produce MgH2. Assume that it will be produced by heat from power plant at 50% efficiency for a cost of $1.65/kg H2
Slurry Oil (95% recycle, 5% makeup	$13,298,910		Slurry oil will be supplied by recycling spent byproduct oil. 5% per year replacement.
Dispersant (5% makeup)	$7,507,610		Dispersant will be supplied by recycling spent byproduct oil. 5% per year replacement.
TOTAL OTHER RAW MATERIAL COSTS ($/year)	$120,843,595		
Utility Costs			
Type of **electricity** utility used	Industrial Electricity		
Use H2A Electricity utility Cost? (Enter yes or no)	No		
Enter Electricity utility Cost if NO is Selected Above ($/kWh)	0.029		
Electricity utility consumption (kWh/kg H2)	0.0		An additional 0.021kWh/kg H2 is assumed to run pumps and fans.
Electricity utility cost in startup year ($/year)	$73,846		

Working capital is assumed to be 15% of the change in operating costs. An estimate of $31,068,012 has been made for the replacement of tubes twice a year in all the SOM cells. This replacement is assumed to be carried out continuously throughout the year.

The results of the analysis are shown in Table 21. The estimated cost of hydrogen from this system is $3.893/kg of hydrogen produced.

Table 21 - Cash Flow Analysis Results

DCF CALCULATION OUTPUTS:	
Required Hydrogen Cost (Year 2005 Real Dollars/kg)	$3.893
Required Hydrogen Cost (Start-up Year (Nominal) Dollars/kg)	$3.893
After Tax Real IRR	10.0%
Pre Tax Real IRR	14.7%
After Tax Nominal IRR	12.1%
Pre Tax Nominal IRR	16.9%
After Tax Real Capital Recovery Factor	0.102
After Tax Nominal Capital Recovery Factor	0.122
Total Real Fixed Charge Rate	0.139
Total Nominal Fixed Charge Rate	0.170
NPV	$0

Specific Item Cost Contributions (Year 2005 $)		
Cost Component	Cost Contribution ($/kg)	Percentage of Cost
Capital Costs	$0.831	21%
Decommissioning Costs	$0.001	0%
Fixed O&M	$0.181	5%
Feedstock Costs	$1.834	47%
Other Raw Material Costs	$1.045	27%
Byproduct Credits	$0.000	0%
Other Variable Costs (including utilities)	$0.001	0%

5.6.3.4.2 Evaluation of SOM Based Reduction Process

The economic analysis performed using the H2A framework was extended to include some sensitivity analyses. Figure 79 displays the results of this analysis. Following is a discussion about the assumptions made in the baseline analysis and the variations selected for the sensitivity analysis.

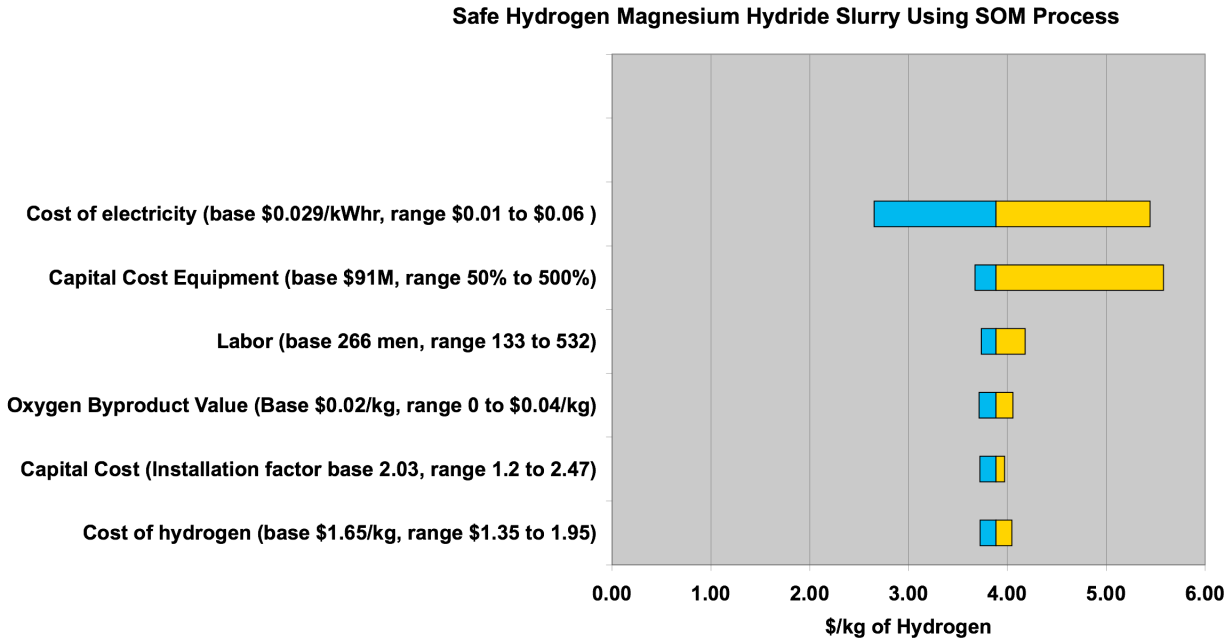

Figure 79 - Cost of Hydrogen Using H2A Framework

The primary assumption made in this analysis is that the system is a mature large-scale process scaled to consume the output of a large power plant. The scale was selected to be consistent with current power plant designs. A nuclear power plant design from the GEN IV program was used because this design study provides costs for electricity, and costs of hydrogen using a thermal conversion process. The power plant in the study is made of four 600MWth modules producing a total of 2.4GWth.

Reference 9, the Interim Status Report on the Design of the Gas Cooled Fast Reactor describes the efficiency expected from the new Gen IV nuclear reactors. The efficiency of conversion from heat to electricity is estimated to be 45%.

Reference 10, Thermochemical.pdf, from the Nuclear Energy division of the Department of Energy describes the sulfur-iodine thermochemical water splitting process and notes that it is expected to be 50% efficient.

Reference 11, Status of the GT-MHR for Electricity Production Interim Status Report for GFR describes Gen IV nuclear generators. The base design is expected to produce electricity at 42% efficiency. An alternate design is expected to have an efficiency of 45%. Cost of electricity is projected to be $0.029/kWh.

Reference 12, the Nuclear Energy Research Initiative 2004 Annual Report discusses the costs of nuclear produced hydrogen. Page 61 notes a cost of 1.35/kg and $1.65/kg for sales of H_2 and O_2 vs H_2 only.

Using the estimated efficiency of 45% for electrical production and 50% for hydrogen production, we estimated the fraction of thermal energy output of the plant that would be required to produce magnesium and the fraction required to produce hydrogen.

We assumed that the magnesium energy requirements will be 10kWhe/kg of magnesium based on the experiments and scale-up analyses performed at Boston University. The resulting magnesium plant will produce 731,174 metric ton/year. This is

about 12 times larger than the largest existing magnesium plant of 63,000 metric ton/year. It is about the same scale as some of the larger aluminum production plants. Russia has some plants that produce 800 to 900 metric tonnes per year.

Capital costs of the SOM based magnesium reduction plants are estimated to be about 16% of the cost of current magnesium chloride based magnesium reduction plants largely because they eliminate the chlorine cycle and many of the processes associated with minerals handling and extra stages of metals refining.

The sensitivity analysis found the largest effect on cost is the cost of electricity. As noted the cost of electricity is the estimated busbar cost for the GEN IV power plant. Costs of electricity from some wind energy plants have been estimated to be as low as $0.01/kWh. The H2A Framework estimates that the cost of electricity from the U.S. grid is $0.06/kWh for industrial applications.

The second largest effect on the cost of hydrogen from the slurry approach will be the capital cost of the plant. The cost of the power plant was not included in the cost of capital costs because the electric cost already included the capital cost of the plant. The capital costs were varied from half of the estimated capital costs to five times the estimated capital costs. The selection of a factor of five was arbitrary but is still less than the current cost of magnesium chloride plants.

Labor was varied from half to twice the estimated labor requirements. This was also an arbitrary variation. The capital cost installation factor was varied over the range that has been used in H2A examples. The cost of hydrogen was varied over a range of $1.35/kg to $1.95/kg. This was also an arbitrary selection but is representative of the costs that are being described by the production groups.

5.6.3.4.3 References

9. Weaver, Kevan D., Interim Status Report on the Design of the Gas-Cooled Fast Reactor (GFR), INEEL/EXT-05-02662, January 31, 2005, http://gen-iv.ne.doe.gov/documents/Interim Status Report for GFR (1-31-05).pdf page 6

10. Thermochemical Production of Hydrogen, http://www.ne.doe.gov/hydrogen/thermochemical.pdf

11. Status of the GT-MHR for Electricity Production, M.P. LaBar, A.S. Shenoy, W.A. Simon, And E.M. Campbell, World Nuclear Association Annual Symposium, London, 3-5 September 2003

12. Nuclear Energy Research Initiative 2004 Annual Report, Office of Nuclear Energy , Department of Energy, http://neri.ne.doe.gov/NERI2004AnnualReport_FINAL.pdf

5.6.3.4.4 SOM Cost Analysis Using H2A Analysis Tool

Following is an extension of the prior analysis. We extended this analysis by varying several of the variables and preparing a tornado chart to display the effects of the variations. We have prepared two tornado charts: one with a baseline assuming process electricity costs of $0.029/kWh (Figure 80); and the other assumes that the baseline costs are based on the H2A projected grid electricity costs which vary between $0.05/kWh and $0.06/kWh (Figure 81).

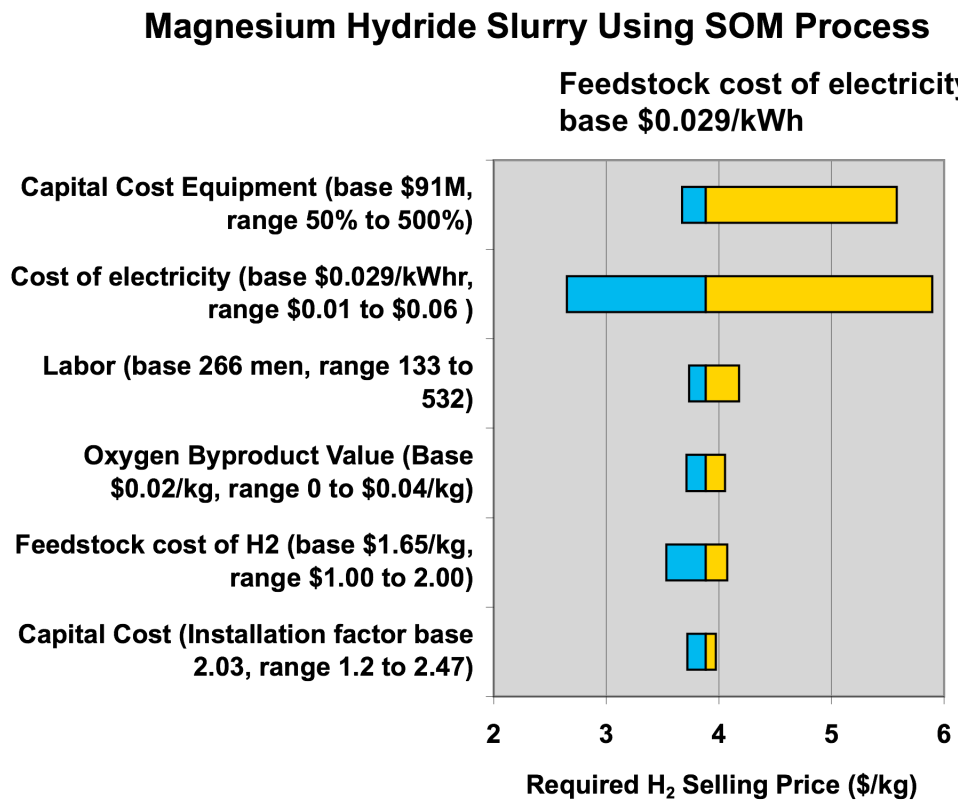

Figure 80 - Tornado Chart with Baseline Cost of Electricity of $0.029/kWh

The primary assumption of this process analysis has been that magnesium hydride slurry will be produced in large-scale processes that take advantage of large-scale economies of scale. For this analysis, we were interested in estimating the cost of a mature technology using a large processing plant to supply hydrogen to the US automotive fleet. To estimate the cost of feedstock hydrogen and electricity, we used estimates for a GEN IV nuclear power plant. (This is a DOE sponsored program that is evaluating next generation nuclear power plants. In GEN IV programs, it is assumed that cost savings in future nuclear plants will be achieved by standardizing the nuclear core design. A 600MWth module is being studied. Four modules would be ganged to produce a 2.4GWth power plant that can produce electricity at 45% efficiency and hydrogen from thermal energy at a 50% efficiency). Cost estimates for the electricity that will be produced from such a plant are $0.029/kWe and $1.65/kg H_2.

The scale of the magnesium plant that would use the output from a 2.4GWth power plant is about 12 times larger that the largest existing magnesium plants and about 7 times larger than the largest planned magnesium plants. It would comparable to the scale of many of the world's aluminum plants and smaller than some.

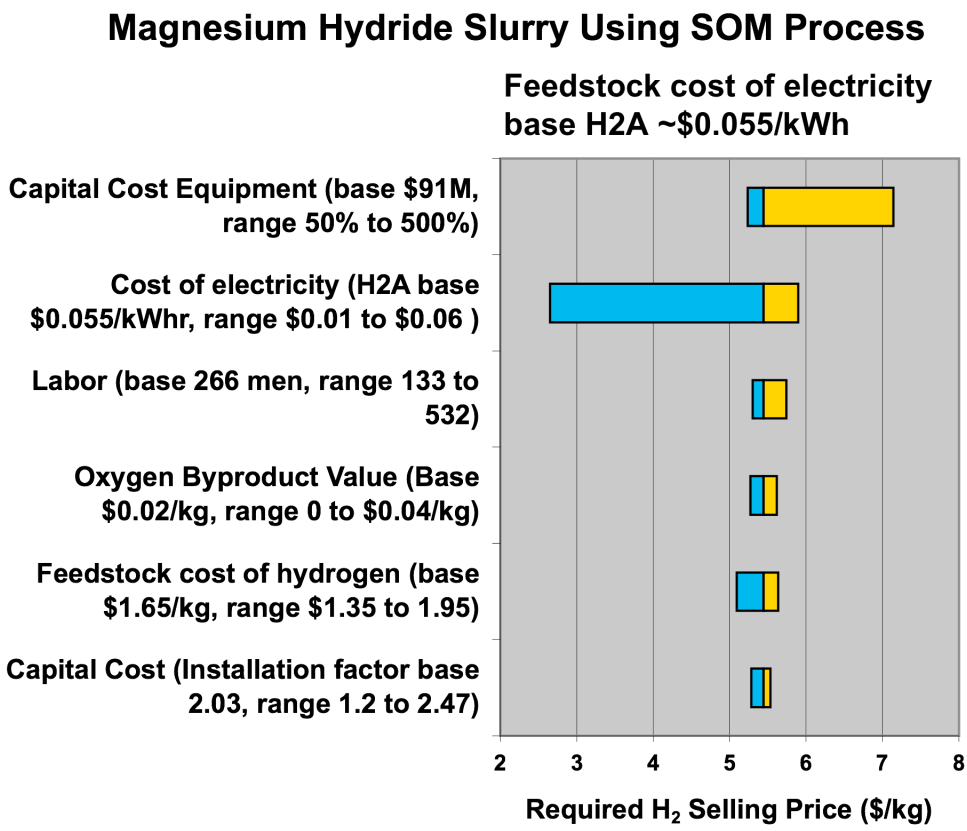

Figure 81 - Tornado Chart with Baseline Cost of Electricity of ~$0.055/kWh

The H2A analysis process has been assuming that hydrogen will be produced in plants using grid electricity. This is a situation that is not likely as even a conventional sized magnesium production plant at 63,000 metric tons/year using a SOM process will require 72 MWe which is a moderate scale power plant. A conventional magnesium chloride process at this same scale will require 115 MWe. The inclusion of a power plant in the design of the magnesium production system saves the cost and losses associated with the distribution system. Costs of electricity are also lower because the new power plant can be built as a base load power plant, which provide some of the lowest cost electricity. The grid costs include the costs associated with meeting peak loads which use higher cost electric power plants.

To determine if the capital cost estimates are reasonable, we can compare the costs estimated for the SOM electrolytic process to those of other electrolytic processes such at the production of hydrogen from electrolysis of water. The capital costs for the electrolytic reduction of water processes are estimated to be about $600/kW of electric power required (from TIAX LLC). This cost includes the transformers, current handling equipment, and other electrical components that must be part of any electrolytic process.

This cost can be contrasted with the costs of a magnesium chloride reduction plant. Current large scale plants (~63,000 metric ton/year) use about 16kWh/kg of magnesium produced and cost about $8,600/metric ton/year capacity. From this

information, we can deduce that the plant requires about 115,068 kW of electricity and that the capital cost can also be expressed as $4,709/kW.

The SOM process plant is estimated to cost about $1,345/metric ton of Mg capacity for a 63,000 metric ton per year plant. This plant is estimated to use about 10kWhr/kg Mg for a power requirement of 71,918 kW or a capital cost of $1,178/kW.

The carbothermic process plant is estimated to cost about $2,456/metric ton Mg capacity for a 90,000 metric ton per year plant. It is estimated to require about 12 kWh/kg Mg for a power requirement of 122,260 kW or a capital cost of $1,808/kW.

All three magnesium processing plants are estimated to cost more than the estimate for the water electrolysis plant. There certainly are significant differences between these electrolysis processes but the magnesium plants are estimated to all be more than 3 times the cost of the water electrolysis plant. This indicates that the capital cost estimates are probably large enough to include the electrical systems required.

5.6.3.5 Initial Magnesium Slurry Process Economic Analyses

5.6.3.5.1 Introduction

During Safe Hydrogen's initial evaluation of the costs associated with a magnesium hydride slurry system, we gathered data for past and present magnesium production systems. We were fortunate to find a study performed by the Bureau of Mines in the 1960's describing the carbothermic reduction process built and operated by the Permanente Metals Company in San Mateo, California. This study provides a bottom up analysis of the design of the plant. The problem with the analysis is that it was performed 40 years ago and does not incorporate many of the design features that make modern plants more efficient such as automatic control technology. Despite this drawback, many things can be learned about magnesium processing from such an analysis. We prepared a Safe Hydrogen Process analysis in a similar manner using information from the Bureau of Mines study to estimate the potential cost savings that a recycling system might enjoy versus the mineral ore system. We found that the Safe Hydrogen system should cost about 40% less than the carbothermic process at a scale about half that of current magnesium plants. The main reasons for this reduction in cost is the assumed lower quality magnesium needs of the Safe Hydrogen plant and the much higher quality reactants entering the magnesium reduction plant. If magnesium vapor can be condensed from the carbon/magnesium oxide reaction with less than a 1% back reaction (this is supported by recent developments in Denmark), and if the magnesium product is suitable for making magnesium hydride, then the post reduction refining step used in the Permanente plant could be eliminated. At the front end of the process, the ore handling stages can be simplified because the reactant will be a consistent quality magnesium hydroxide slurry.

Following this analysis, we gathered data on existing magnesium production plants. We found a couple studies and discussions about the magnesium chloride process. One concerned a new plant proposed to be built in Africa. Some comparative numbers were quoted in that study to define the capital, operating, and energy costs of modern magnesium reduction plants. These plants were compared with the Bureau of Mines study plant to estimate process costs not defined in the literature.

Since the magnesium hydride slurry approach is to use large-scale plants to produce the magnesium hydride slurry and then to take advantage of low cost transportation and storage of the slurry to transport the product to markets, we defined the costs of the process at scales that will be needed for a fully developed system supplying hydrogen to the U.S. automotive fleet. The current scale of magnesium production is about 60,000 metric tonnes per year. A plant this size could produce enough slurry to supply 10 million kg of hydrogen per year which in turn would supply 15,000 to 30,000 vehicles (depending on the whether they use internal combustion engines or fuel cells). The U.S. gasoline consumption is about 9 million barrels per day. On an energy equivalency basis, this demand will require about 128 million metric tonnes of hydrogen per year. To meet this demand with hydrogen stored in magnesium hydride slurry, the U.S. will need a magnesium production capacity of 768 million metric tonnes per year. This could be supplied by 1000 magnesium plants each with a capacity of 768,000 metric tonnes per year or by 100 magnesium plants each with a capacity of 7.68 million metric tonnes per year. Thus the scale of a single magnesium plant must be

increased by a factor of 10 to 100. It should be noted that aluminum smelting plants exist at a scale of 600,000 metric tonnes per year.

From this analysis, we estimate that the cost of hydrogen based on the operating costs at a scale of 60,000 metric tonnes of magnesium per year will be $7.52/kg of hydrogen. If the plant is to provide a 20% return on the capital invested, the price of hydrogen would need to be $10.34/kg of hydrogen. Assuming that the capital costs increase in a 2/3 power law rule, our projection of the costs of a magnesium hydride slurry system 100 times larger than this would be $6.35/kg of hydrogen based on the operating costs and $7.35/kg of hydrogen based on a 20% return on capital.

These costs are still higher than our targets but they show the effect of scale on the process costs. Our final evaluation was to assume some technological and energy cost improvements. This analysis concludes that hydrogen can be produced in a mature large-scale process at $2.60/kg.

The studies that the Safe Hydrogen team is performing under this task are intended to improve the estimates that are presented in section 5.6.3.5. Further discussion of the studies summarized in this introduction are discussed below.

5.6.3.5.2 Bureau of Mines Study

The cost analysis was begun using data provided by the Bureau of Mines study on carbothermic reduction of magnesium (Reference 13). The data from the report was copied to a spreadsheet and then escalated to 2002 costs using the Chemical Engineering Index and current costs for labor. The Chemical Engineering Index indicates that the cost of equipment has increased by 3.64 times between 1966 and 2002. The consumer price index indicates that prices have risen about 5.57 times over this same span of years. The labor rate increase from $2.70/hr to $15/hr is consistent with this rise. Table 22 through Table 25 display the capital cost estimates including the 1966 estimates for equipment and installation as well as the 2002 escalated estimates. The Bureau of Mines study was for a 24,000 TPY magnesium plant. Table 26 and Table 27 display the operating costs in 1966 dollars. Table 28 and Table 29 displays the operating costs using values more representative of 2002 where available and increased by inflation where not. Our study found that if costs presented in the Bureau of Mines plant are escalated to 2002 dollars, the costs of building a carbothermic magnesium reduction plant would be $195M or $8,955/tonne of installed capacity ($120M or $6,512/tonne for the magnesium plant alone). Operating costs would be expected to be $70M/yr. Based on the operating costs, the cost of magnesium would be $3.23/kg. Allowing an additional capital cost of $17.6M for working capital, the price of the magnesium would need to be $4.65/kg to achieve a 20% return on invested capital. Magnesium metal currently sells for about $2.30/kg so this carbothermic reduction plant would not be competitive. However, this design is performed at a scale that is about 3 times smaller than current design scales and the costs are based on estimates developed 40 years ago.

Table 22 - Bureau of Mines Study on Carbothermic Reduction of Magnesium – Ore Handling

	Number	Material $	Labor $	Total $	Labor rate $/hr	Labor Hours Hr	Current Labor Cost $/hr	Materials	Labor	Total
from Bureau of Mines Report on Carbothermic reduction										
Dolime Production										
Jaw crusher	1	34,300	3,400	37,700	2.70	1,259	15	124,913	18,889	143,802
Gyratory crusher	1	24,300	2,400	26,700	2.70	889	15	88,496	13,333	101,829
Calcining plant equipment		280,800	53,400	334,200	2.70	19,778	15	1,022,615	296,667	1,319,282
Screens and grizzlies	3	6,000	700	6,700	2.70	259	15	21,851	3,889	25,740
Bins and tanks	6	46,700	4,600	51,300	2.70	1,704	15	170,072	25,556	195,627
Materials handling equipment		75,000	15,500	90,500	2.70	5,741	15	273,134	86,111	359,245
total		467,100	80,000	547,100						2,145,525
Foundations				32,700						128,237
Structures				23,300						91,374
Buildings				40,900						160,395
Insulation										-
Instrumentation				12,200						47,844
Electrical work				19,300						75,688
Piping				19,800						77,648
Painting				6,400						25,098
Miscellaneous				46,700						183,140
total				201,300						789,425
Total Direct Construction				748,400						2,934,950
Indirect cost, contingency, and fee				299,360						1,173,980
Interest during construction				52,388						205,446
Total Fixed Capital				1,100,148						4,314,376
Sea Water Operation										
Centrifugal pump	4	22,600	2,300	24,900	2.70	852	15	82,304	12,778	95,082
Wood stave pipeline	1	12,600	4,400	17,000	2.70	1,630	15	45,887	24,444	70,331
Hydrotreater	2	120,600	59,500	180,100	2.70	22,037	15	439,200	330,556	769,756
Hydroseparator	2	40,200	16,800	57,000	2.70	6,222	15	146,400	93,333	239,733
Thickener	2	194,700	130,300	325,000	2.70	48,259	15	709,057	723,889	1,432,946
Thickener	2	132,200	88,900	221,100	2.70	32,926	15	481,445	493,889	975,334
Hydrotrater	1	20,100	8,400	28,500	2.70	3,111	15	73,200	46,667	119,867
Disk filter	4	72,000	7,200	79,200	2.70	2,667	15	262,209	40,000	302,209
Vacuum pmp	3	106,200	15,900	122,100	2.70	5,889	15	386,758	88,333	475,092
Flume	1	28,000	37,000	65,000	2.70	13,704	15	101,970	205,556	307,526
Rotary kiln	1	345,100	65,600	410,700	2.70	24,296	15	1,256,782	364,444	1,621,227
Electrostatic precipitator	1	56,700	14,200	70,900	2.70	5,259	15	206,490	78,889	285,378
Exhaust blower, damper, stack		14,600	1,900	16,500	2.70	704	15	53,170	10,556	63,726
Rotary cooler	1	46,400	9,300	55,700	2.70	3,444	15	168,979	51,667	220,646
Bins and tanks	7	33,400	20,100	53,500	2.70	7,444	15	121,636	111,667	233,302
Miscellaneous pumps	21	26,300	4,200	30,500	2.70	1,556	15	95,779	23,333	119,112
Materials handling equipment		46,700	8,700	55,400	2.70	3,222	15	170,072	48,333	218,405
total		1,318,400	494,700	1,813,100 -						7,549,671
Foundations				71,600						298,139
Structures				59,700						248,588
Buildings				145,500						605,856
Insulation										-
Instrumentation				34,100						141,991
Electrical work				72,800						303,136
Piping				172,600						718,699
Painting				12,500						52,049
Miscellaneous				107,600						448,042
total				676,400						2,816,501
Total Direct Construction				2,489,500						10,366,171
Indirect cost, contingency, and fee				995,800						4,146,468
Interest during construction				174,265						725,632
Total Fixed Capital				3,659,565						15,238,272

Table 23 - Bureau of Mines Study on Carbothermic Reduction of Magnesium – Magnesium Reduction

	Number	Material $	Labor $	Total $	Labor rate $/hr	Labor Hours Hr	Current Labor Cost $/hr	Materials	Labor	Total
Magnesia Reduction										
Direct Construction Cost										
Ball Mill	1	132,800	13,300	146,100	2.70	4,926	15	483,630	73,889	557,519
Briquetting press	3	102,500	10,300	112,800	2.70	3,815	15	373,284	57,222	430,506
Gas Lock	10	22,100	3,300	25,400	2.70	1,222	15	80,484	18,333	98,817
Arc Furnace	5	2,222,000	166,700	2,388,700	2.70	61,741	15	8,092,060	926,111	9,018,171
Bins and hoppers	20	51,900	5,200	57,100	2.70	1,926	15	189,009	28,889	217,898
Materials handling equipment		85,300	16,700	102,000	2.70	6,185	15	310,645	92,778	403,423
				-						
total		2,616,600	215,500	2,832,100						10,726,333
Foundations				183,100						693,475
Structures				130,800						495,394
Buildings				639,700						2,422,808
Insulation										-
Instrumentation				98,900						374,575
Electrical work				235,500						891,936
Piping				130,800						495,394
Painting				29,100						110,214
Miscellaneous				261,700						991,166
total				1,709,600						6,474,961
Total Direct Construction				4,541,700						17,201,294
Indirect cost, contingency, and fee				1,816,600						6,880,215
Interest during construction				317,900						1,204,019
Total Fixed Capital				6,676,200						25,285,527
Magnesium Quenching										
Direct Construction Cost										
Centrifugal compressor	3	139,000	20,900	159,900	2.70	7,741	15	506,209	116,111	622,320
Absorption column	2	51,200	7,700	58,900	2.70	2,852	15	186,460	42,778	229,237
Stripping column	2	28,200	4,200	32,400	2.70	1,556	15	102,699	23,333	126,032
Dehydrating tower	2	24,600	3,700	28,300	2.70	1,370	15	89,588	20,556	110,144
Miscellaneous natural gas cleaning equipment		43,800	4,400	48,200	2.70	1,630	15	159,510	24,444	183,955
Shock chilling cone	5	66,800	6,700	73,500	2.70	2,481	15	243,272	37,222	280,494
Reamer	5	99,700	19,900	119,600	2.70	7,370	15	363,087	110,556	473,642
Surge drum	5	165,800	16,600	182,400	2.70	6,148	15	603,809	92,222	696,031
Heat exchanger, 120 ft2	5	10,300	1,000	11,300	2.70	370	15	37,510	5,556	43,066
Heat exchanger, 6720 ft2	5	87,700	8,800	96,500	2.70	3,259	15	319,385	48,889	368,274
Bag filter	5	126,300	15,200	141,500	2.70	5,630	15	459,958	84,444	544,403
Gas holder	1	175,000	17,500	192,500	2.70	6,481	15	637,313	97,222	734,536
Centrifugal compressor	5	234,300	35,100	269,400	2.70	13,000	15	853,272	195,000	1,048,272
Pumps	10	13,200	1,300	14,500	2.70	481	15	48,072	7,222	55,294
Materials handling equipment		22,700	4,800	27,500	2.70	1,778	15	82,669	26,667	109,335
total		1,288,600	167,800	1,456,400						5,625,034
Foundations				90,200						348,378
Structures				64,400						248,731
Buildings				322,200						1,244,429
Insulation				38,700						149,470
Instrumentation				51,400						198,522
Electrical work				103,100						398,202
Piping				541,200						2,090,269
Painting				12,900						49,823
Miscellaneous				128,900						497,849
total				1,353,000						5,225,674
Total Direct Construction				2,809,400						10,850,708
Indirect cost, contingency, and fee				1,123,800						4,340,438
Interest during construction				196,700						759,712
Total Fixed Capital				4,129,900						15,950,857

Table 24 - Bureau of Mines Study on Carbothermic Reduction of Magnesium – Magnesium Refining

	Number	Material $	Labor $	Total $	Labor rate $/hr	Labor Hours Hr	Current Labor Cost $/hr	Materials	Labor	Total
Magnesium distillation										
Direct Construction Cost										
Pelleting press	10	192,000	38,400	230,400	2.70	14,222	15	699,224	213,333	912,557
Retort furnace	185	3,111,800	311,500	3,423,300	2.70	115,370	15	11,332,525	1,730,556	13,063,081
Vacuum plant	1	201,600	29,200	230,800	2.70	10,815	15	734,185	162,222	896,407
Crane (retort)	2	229,400	32,100	261,500	2.70	11,889	15	835,427	178,333	1,013,760
Crane (crystal recovery)	2	61,800	8,700	70,500	2.70	3,222	15	225,063	48,333	273,396
Bins and hoppers	5	12,900	1,300	14,200	2.70	481	15	46,979	7,222	54,201
Materials handling equipment		15,500	2,900	18,400	2.70	1,074	15	56,448	16,111	72,559
total		3,825,000	424,100	4,249,100						16,285,962
Foundations				267,700						1,026,041
Structures				191,300						733,215
Buildings				1,338,700						5,130,973
Insulation				76,500						293,209
Instrumentation				535,500						2,052,466
Electrical work				382,500						1,466,047
Piping				765,000						2,932,094
Painting				38,300						146,796
Miscellaneous				382,500						1,466,047
total				3,978,000						15,246,889
Total Direct Construction				8,227,100						31,532,851
Indirect cost, contingency, and fee				3,290,800						12,612,987
Interest during construction				575,900						2,207,311
Total Fixed Capital				12,093,800						46,353,149
Mobile equipment										
Retort	260	1,461,200		1,461,200			15	5,321,385	-	5,321,385
Contingency				146,100						532,066
Total mobile equipment cost				1,607,300						5,853,451
Total fixed capital cost				13,701,100						52,206,600
Magnesium melting and casting										
Direct Construction Cost										
Melting furnace	14	377,500	37,800	415,300	2.70	14,000	15	1,374,776	210,000	1,584,776
Blower	3	5,300	500	5,800	2.70	185	15	19,301	2,778	22,079
Centrifugal pump	14	18,300	1,800	20,100	2.70	667	15	66,645	10,000	76,645
Mold conveyor	2	29,000	6,400	35,400	2.70	2,370	15	105,612	35,556	141,167
Blower	8	10,500	1,100	11,600	2.70	407	15	38,239	6,111	44,350
total		440,600	47,600	488,200						1,869,018
Foundations				30,800						117,914
Structures				22,000						84,224
Buildings				264,400						1,012,225
Insulation										-
Instrumentation				30,800						117,914
Electrical work				17,700						67,762
Piping				22,000						84,224
Painting				8,800						33,690
Miscellaneous				44,100						168,832
total				440,600						1,686,786
Total Direct Construction				928,800						3,555,804
Indirect cost, contingency, and fee				371,500						1,422,245
Interest during construction				65,000						248,845
Total Fixed Capital				1,365,300						5,226,894

Table 25 - Bureau of Mines Study on Carbothermic Reduction of Magnesium - Summary

	Number	Material $	Labor $	Total $	Labor rate $/hr	Labor Hours Hr	Current Labor Cost $/hr	Materials	Labor	Total
Working Capital										
1 month supply of raw materials		225,000		225,000			15	819,403	-	819,403
1 month out of pocket expense		944,000		944,000			15	3,437,851	-	3,437,851
2 month product inventory		2,432,000		2,432,000			15	8,856,836	-	8,856,836
Total		3,601,000		3,601,000						13,114,090
Summary Totals										
Dolime Production				1,100,148						4,314,376
Sea Water Operation				3,659,565						15,238,272
Magnesia Reduction				6,676,200						25,285,527
Magnesium Quenching				4,129,900						15,950,857
Magnesium distillation				13,701,100						52,206,600
Magnesium melting and casting				1,365,300						5,226,894
Total				30,632,213						118,222,526
Nitrogen Production				130,400						474,890
Hydrogen Production				474,000						1,726,209
Dolomite										-
Total including N2 and H2 production				31,236,613						120,423,625
Plant Facilities, 10%				3,123,661						11,375,722
Plant utilities, 12%-$1 Million				2,748,394						10,009,075
Power Plant				11,000,000						40,059,701
Total Fixed Capital				48,108,668						181,868,123
Working Capital				3,601,000						13,114,090
Total				51,709,668						194,982,213
Comparisons										
Capital Cost total plant										
$/ton										8,124
$/tonne										8,955
Capital Cost Power Plant										
$/kW										801
Capital Cost Mg Plant alone										
$/ton										5,909
$/tonne										6,513

Table 26 - Bureau of Mines Study Operating Costs 1966

		Calculation Based on original report									
		Rate	Dolime Production	Sea Water Operation	Magnesia Reduction, 12,500kVA	Magnesium Quenching, Natural Gas	Magnesium Distillation, batch	Magnesium melting and casting	Nitrogen Production	Hydrogen Production	Total without Powerplant
Hours of Operation	Hrs/year	8400									
Energy Consumption											
Electric Power	MWhr										-
69 kV					296,240						296,240
2300V				3,515	3,618	30,815	52,815				90,763
440V			2,398	5,365	2,108	732	802	730	233	443	12,811
Total Electric Energy	MWhr		2,398	8,880	301,966	31,547	53,617	730	233	443	399,814
Power Required for electricity	MW		0.29	1.06	35.95	3.76	6.38	0.09	0.03	0.05	48
Natural Gas	Mcf		421,694	661,051		1,126,567		142,977	8,485	78,750	2,439,524
Resulting Gas	Mcf					1,285,385					1,285,385
Well Water	Mgal			701,040		358,120	345,708			117,936	1,522,804
Steam	1000 lb						217,350				217,350
Petroleum Coke	ton		-	-	19,427	-	-	-	-	-	19,427
Metallurgical coke	ton		-	-	1,752	-	-	-	-	-	1,752
Graphite electrodes	ton		-	-	1,680	-	-	-	-	-	1,680
Activated alumna	ton		-	-	-	9	-	-	-	-	9
Monoethanolamine	lb		-	-	-	6,786	-	-	714	3,214	10,714
Retorts	ton Mg		-	-	-	-	24,000	-	-	-	24,000
Melting Pots	ton Mg		-	-	-	-	-	24,000	-	-	24,000
Dow 230 flux	ton		-	-	-	-	-	1,277	-	-	1,277
Sulfur	ton		-	-	-	-	-	255	-	-	255
Dolomite Ore	ton		148,600								148,600
Production											
Magnesium metal	ton							24,000			24,000
Direct Cost											
Electric Power											
69 kV	$/kWhr	0.0079	-	-	2,340,296	-	-	-	-	-	2,340,296
2300V	$/kWhr	0.0084	-	29,526	30,391	258,846	443,646	-	-	-	762,409
440V	$/kWhr	0.0089	21,342	47,749	18,761	6,515	7,138	6,497	2,074	3,943	114,018
Natural Gas	$/Mcf	0.305	128,617	201,621	-	343,603	-	43,608	2,588	24,019	744,055
Resulting Gas	$/Mcf	0.065	-	-	-	83,550	-	-	-	-	83,550
Well Water	$/1000gal	0.054	-	37,856	-	19,338	18,668	-	-	6,369	82,231
Steam	$/1000 lb	0.61	-	-	-	-	132,584	-	-	-	132,584
Petroleum Coke	$/ton	11			213,700						213,700
Metallurgical coke	$/ton	23			40,300						40,300
Graphite electrodes	$/ton	560			940,800						940,800
Activated alumna	$/ton	300				2,800					2,800
Monoethanolamine	$/lb	0.28				1,900			200	900	3,000
Retorts	$/ton Mg	40					960,000				960,000
Melting Pots	$/ton Mg	5						120,000			120,000
Dow 230 flux	$/ton	143						182,600			182,600
Sulfur	$/ton	33						8,400			8,400
Dolomite Ore	$/ton	1.5	222,900								222,900
Total			372,859	316,751	3,584,248	716,552	1,562,036	361,105	4,862	35,230	6,953,643
Direct Labor											
Labor	hr		12,481	35,370	49,926	41,593	150,815	111,296	8,333	12,481	422,296
	manyears		6.0	17.0	24.0	20.0	72.5	53.5	4.0	6.0	203.0
Labor	$/hr	2.7	33,700	95,500	134,800	112,300	407,200	300,500	22,500	33,700	1,140,200
Supervision			5,100	14,300	20,200	16,800	61,100	45,100	3,400	5,100	171,100
Total			38,800	109,800	155,000	129,100	468,300	345,600	25,900	38,800	1,311,300
Plant Maintenance											
Labor			18,200	69,700	183,800	118,000	304,100	64,900	3,400	12,400	774,500
Supervision			3,700	13,900	36,800	23,600	60,800	13,000	700	2,500	155,000
Materials			23,200	80,400	183,800	118,000	152,100	129,800	3,400	12,400	703,100
Total			45,100	164,000	404,400	259,600	517,000	207,700	7,500	27,300	1,632,600
Payroll Overhead			11,300	35,800	69,500	50,100	154,100	78,300	5,600	9,900	414,600
Operating Supplies			9,100	32,800	80,900	51,900	103,400	41,500	1,500	5,500	326,600
Total direct cost			477,159	659,151	4,294,048	1,207,252	2,804,836	1,034,205	45,362	116,730	10,638,743
Indirect Cost											
Administration and Overhead			52,700	173,700	362,800	249,600	617,200	337,000	19,800	40,600	1,853,400
Fixed Cost											
Taxes and Insurance			21,000	69,700	127,100	78,700	262,500	26,000	2,500	9,000	596,500
Depreciation			55,000	183,000	333,800	206,500	637,100	62,300	6,500	23,700	1,507,900
Total			76,000	252,700	460,900	285,200	899,600	88,300	9,000	32,700	2,104,400
Total Operating Cost	$		605,859	1,085,551	5,117,748	1,742,052	4,321,636	1,459,505	74,162	190,030	14,596,543
	$/ton Mg										608
	$/lbm										0.304
	$/kg Mg										0.670
	$/tonne Mg										670
Working Capital											
1 month supply of raw materials											
1 month out of pocket expense											1,216,379
2 month product inventory											2,432,757
Total											3,649,136

Table 27 - Bureau of Mines Study Operating Costs 1966 Continued

		Calculation Based on original report Rate	Dolime Production	Sea Water Operation	Magnesia Reduction, 12,500kVA	Magnesium Quenching, Natural Gas	Magnesium Distillation, batch	Magnesium melting and casting	Nitrogen Production	Hydrogen Production	Total without Powerplant
Capital Cost			1,100,100	3,659,600	6,676,200	4,129,900	13,701,100	1,365,300	130,400	474,000	31,236,600
additional capital allocation											
Plant facilities 10%		0.1									3,123,660
Plant utilities 12%		0.12									3,748,392
Plant utilities rebate											(1,000,000)
Power Plant Capital											
Total Fixed Capital											37,108,652
working Capital											3,649,136
Total Fixed and working capital											40,757,788
return on Capital		0.2	220,020								8,151,558
Total cost	$										22,748,100
	$/ton Mg										948
	$/lbm										0.474
	$/kg										1.0448
Power Produced	kWh										
Operating Cost	$/kWh										
Energy from natural gas	GJ/yr		444,613	696,979	-	1,187,796	-	150,748	8,946	83,030	2,572,112
Calculation of fractions for the following											
Direct Labor											
Labor											
Supervision			15%	15%	14.9852%	14.9599%	15%	15%	15%	15%	15%
Total											
Plant Maintenance											
Labor			2%	2%	2.7531%	2.8572%	2%	5%	3%	3%	2.5%
Supervision			20%	20%	20.0218%	20.0000%	20%	20%	21%	20%	20%
Materials			127%	115%	100.0000%	100.0000%	50%	200%	100%	100%	91%
Total											
Payroll Overhead			18.6%	18.5%	18.5037%	18.5076%	18.5%	18.5%	18.7%	18.4%	18.5%
Operating Supplies			20%	20%	20.0049%	19.9923%	20%	20%	20%	20%	20%
Total direct cost											
Indirect Cost											
Administration and Overhead			51%	51%	51.1130%	50.8661%	50%	50%	49%	50%	50%
Fixed Cost											
Taxes and Insurance			2%	2%	1.9038%	1.9056%	2%	2%	2%	2%	2%
Depreciation			5%	5%	4.9999%	5.0001%	5%	5%	5%	5%	5%
Total											
Summary of Costs											
Materials			372,859	316,751	3,584,248	716,552	1,562,036	361,105	4,862	35,230	6,953,643
Electric Power			21,342	77,275	2,389,448	265,361	450,784	6,497	2,074	3,943	3,216,723
Natural Gas			128,617	201,621	-	343,603	-	43,608	2,588	24,019	744,055
Other			222,900	37,856	1,194,800	107,589	1,111,252	311,000	200	7,269	2,992,865
Operating Labor include supervisor			38,800	109,800	155,000	129,100	468,300	345,600	25,900	38,800	1,311,300
Plant Maintenance			45,100	164,000	404,400	259,600	517,000	207,700	7,500	27,300	1,632,600
Payroll			11,300	35,800	69,500	50,100	154,100	78,300	5,600	9,900	414,600
Operating Suppies			9,100	32,800	80,900	51,900	103,400	41,500	1,500	5,500	326,600
Administration and Overhead			52,700	173,700	362,800	249,600	617,200	337,000	19,800	40,600	1,853,400
Taxes and Insurance			21,000	69,700	127,100	78,700	262,500	26,000	2,500	9,000	596,500
Depreciation			55,000	183,000	333,800	206,500	637,100	62,300	6,500	23,700	1,507,900
Total			605,859	1,085,551	5,117,748	1,742,052	4,321,636	1,459,505	74,162	190,030	14,596,543
Materials & Energy			62%	29%	70%	41%	36%	25%	7%	19%	48%
Electric Power			4%	7%	47%	15%	10%	0%	3%	2%	22%
Natural Gas			21%	19%	0%	20%	0%	3%	3%	13%	5%
Other			37%	3%	23%	6%	26%	21%	0%	4%	21%
Operating Labor include supervisor			6%	10%	3%	7%	11%	24%	35%	20%	9%
Plant Maintenance			7%	15%	8%	15%	12%	14%	10%	14%	11%
Payroll			2%	3%	1%	3%	4%	5%	8%	5%	3%
Operating Suppies			2%	3%	2%	3%	2%	3%	2%	3%	2%
Administration and Overhead			9%	16%	7%	14%	14%	23%	27%	21%	13%
Taxes and Insurance			3%	6%	2%	5%	6%	2%	3%	5%	4%
Depreciation			9%	17%	7%	12%	15%	4%	9%	12%	10%
Total			100%	100%	100%	100%	100%	100%	100%	100%	100%

Table 28 - Bureau of Mines Study Operating Costs 2002

		Calculation using current costs	Dolime Production	Sea Water Operation	Magnesia Reduction, 12,500kVA	Magnesium Quenching, Natural Gas	Magnesium Distillation, batch	Magnesium melting and casting	Nitrogen Production	Hydrogen Production	Total without Powerplant
Hours of Operation	Hrs/year										
Energy Consumption											
Electric Power	MWhr		-	-	-	-	-	-	-	-	-
69 kV			-	-	296,240	-	-	-	-	-	296,240
2300V			-	3,515	3,618	30,815	52,815	-	-	-	90,763
440V			2,398	5,365	2,108	732	802	730	233	443	12,811
Total Electric Energy	MWhr		2,398	8,880	301,966	31,547	53,617	730	233	443	399,814
Power Required for electricity	MW		0	1	36	4	6	0	0	0	48
Natural Gas	Mcf		421,694	661,051	-	1,126,567	-	142,977	8,485	78,750	2,439,524
Resulting Gas	Mcf		-	-	-	1,285,385	-	-	-	-	1,285,385
Well Water	Mgal		-	701,040	-	358,120	345,708	-	-	117,936	1,522,804
Steam	1000 lb		-	-	-	-	217,350	-	-	-	217,350
Petroleum Coke	ton		-	-	19,427	-	-	-	-	-	19,427
Metallurgical coke	ton		-	-	1,752	-	-	-	-	-	1,752
Graphite electrodes	ton		-	-	1,680	-	-	-	-	-	1,680
Activated alumna	ton		-	-	-	9	-	-	-	-	9
Monoethanolamine	lb		-	-	-	6,786	-	-	714	3,214	10,714
Retorts	ton Mg		-	-	-	-	24,000	-	-	-	24,000
Melting Pots	ton Mg		-	-	-	-	-	24,000	-	-	24,000
Dow 230 flux	ton		-	-	-	-	-	1,277	-	-	1,277
Sulfur	ton		-	-	-	-	-	255	-	-	255
Dolomite Ore	ton		148,600	-	-	-	-	-	-	-	148,600
Production			-	-	-	-	-	-	-	-	
Magnesium metal	ton		-	-	-	-	-	24,000	-	-	24,000
			-	-	-	-	-	-	-	-	
Direct Cost			-	-	-	-	-	-	-	-	
Electric Power											
69 kV	$/kWhr	0.035	-	-	10,368,400	-	-	-	-	-	10,368,400
2300V	$/kWhr	0.035	-	123,025	126,630	1,078,525	1,848,525	-	-	-	3,176,705
440V	$/kWhr	0.035	83,930	187,775	73,780	25,620	28,070	25,550	8,155	15,505	448,385
Natural Gas	$/Mcf	3	1,265,082	1,983,153	-	3,379,701	-	428,931	25,455	236,250	7,318,572
Resulting Gas	$/Mcf	0.36199	-	-	-	465,290	-	-	-	-	465,290
Well Water	$/1000gal	0.30073	-	210,821	-	107,696	103,963	-	-	35,466	457,947
Steam	$/1000 lb	3.39709	-	-	-	-	738,358	-	-	-	738,358
Petroleum Coke	$/ton	61.259			1,190,095						1,190,095
Metallurgical coke	$/ton	128.087			224,431						224,431
Graphite electrodes	$/ton	3118.64			5,239,315						5,239,315
Activated alumna	$/ton	1670.7				15,593					15,593
Monoethanolamine	$/lb	1.55932				10,581			1,114	5,012	16,707
Retorts	$/ton Mg	222.76					5,346,240				5,346,240
Melting Pots	$/ton Mg	27.845						668,280			668,280
Dow 230 flux	$/ton	796.367						1,016,899			1,016,899
Sulfur	$/ton	183.777						46,780			46,780
Dolomite Ore	$/ton	8.3535	1,241,330								1,241,330
Total			2,590,342	2,504,774	17,222,651	5,083,006	8,065,156	2,186,440	34,724	292,234	37,979,327
Direct Labor											
Labor	hr		12,481	35,370	49,926	41,593	150,815	111,296	8,333	12,481	422,296
	manyears										-
Labor	$/hr	15	187,222	530,556	748,889	623,889	2,262,222	1,669,444	125,000	187,222	6,334,444
Supervision			28,333	79,444	112,222	93,333	339,444	250,556	18,889	28,333	950,556
Total			215,556	610,000	861,111	717,222	2,601,667	1,920,000	143,889	215,556	7,285,000
Plant Maintenance											
Labor			66,281	253,833	669,361	429,731	1,107,469	236,352	12,382	45,158	2,820,567
Supervision			13,475	50,621	134,018	85,946	221,421	47,343	2,549	9,104	564,478
Materials			84,490	292,800	669,361	429,731	553,916	472,704	12,382	45,158	2,560,543
Total			164,245	597,254	1,472,740	945,409	1,882,806	756,400	27,313	99,421	5,945,588
Payroll Overhead			54,975	169,273	307,993	228,180	726,955	407,437	29,646	49,743	1,974,202
Operating Supplies			33,140	119,451	294,621	189,009	376,561	151,134	5,463	20,030	1,189,409
Total direct cost			3,058,258	4,000,752	20,159,116	7,162,826	13,653,144	5,421,411	241,035	676,983	54,373,526
Indirect Cost											
Administration and Overhead			236,425	758,912	1,500,915	1,057,924	2,775,110	1,619,648	100,863	191,667	8,241,464
Fixed Cost											
Taxes and Insurance			76,478	253,833	462,872	286,609	955,970	94,687	9,104	32,776	2,172,328
Depreciation			200,299	666,448	1,215,630	752,030	2,320,185	226,884	23,672	86,310	5,491,457
Total			276,776	920,281	1,678,501	1,038,639	3,276,155	321,570	32,776	119,087	7,663,785
Total Operating Cost	$		3,571,460	5,679,944	23,338,533	9,259,389	19,704,410	7,362,629	374,675	987,736	70,278,775
	$/ton Mg										2,928
	$/lbm										1.464
	$/kg Mg										3.228
	$/tonne Mg										3,228
		3.64179									
Working Capital											
1 month supply of raw materials											
1 month out of pocket expense											5,856,565
2 month product inventory											11,713,129
Total											17,569,694

Table 29 - Bureau of Mines Study Operating Costs 2002 Continued

		Calculation using current costs	Dolime Production	Sea Water Operation	Magnesia Reduction, 12,500kVA	Magnesium Quenching, Natural Gas	Magnesium Distillation, batch	Magnesium melting and casting	Nitrogen Production	Hydrogen Production	Total without Powerplant
Capital Cost		3.64179	4,006,334	13,327,499	24,313,325	15,040,233	49,896,543	4,972,137	474,890	1,726,209	113,757,170
additional capital allocation											
Plant facilities 10%											11,375,717
Plant utilities 12%											13,650,860
Plant utilities rebate											(1,000,000)
Power Plant Capital											
Total Fixed Capital											137,783,748
working Capital											17,569,694
Total Fixed and working capital											155,353,441
return on Capital											31,070,688
Total cost	$										101,349,463
	$/ton Mg										4,223
	$/lbm										2.111
	$/kg										4.6549
Power Produced	kWh										
Operating Cost	$/kWh										
Energy from natural gas	GJ/yr										
Calculation of fractions for the following											
Direct Labor											
Labor											
Supervision											
Total											
Plant Maintenance											
Labor											
Supervision											
Materials											
Total											
Payroll Overhead											
Operating Supplies											
Total direct cost											
Indirect Cost											
Administration and Overhead											
Fixed Cost											
Taxes and Insurance											
Depreciation											
Total											
Summary of Costs											
Materials			2,590,342	2,504,774	17,222,651	5,083,006	8,065,156	2,186,440	34,724	292,234	37,979,327
Electric Power			83,930	310,800	10,568,810	1,104,145	1,876,595	25,550	8,155	15,505	13,993,490
Natural Gas			1,265,082	1,983,153	-	3,379,701	-	428,931	25,455	236,250	7,318,572
Other			1,241,330	210,821	6,653,841	599,160	6,188,561	1,731,959	1,114	40,479	16,667,265
Operating Labor include supervisor			215,556	610,000	861,111	717,222	2,601,667	1,920,000	143,889	215,556	7,285,000
Plant Maintenance			164,245	597,254	1,472,740	945,409	1,882,806	756,400	27,313	99,421	5,945,588
Payroll			54,975	169,273	307,993	228,180	726,955	407,437	29,646	49,743	1,974,202
Operating Suppies			33,140	119,451	294,621	189,009	376,561	151,134	5,463	20,030	1,189,409
Administration and Overhead			236,425	758,912	1,500,915	1,057,924	2,775,110	1,619,648	100,863	191,667	8,241,464
Taxes and Insurance			76,478	253,833	462,872	286,609	955,970	94,687	9,104	32,776	2,172,328
Depreciation			200,299	666,448	1,215,630	752,030	2,320,185	226,884	23,672	86,310	5,491,457
Total			3,571,460	5,679,944	23,338,533	9,259,389	19,704,410	7,362,629	374,675	987,736	70,278,775
Materials & Energy			73%	44%	74%	55%	41%	30%	9%	30%	54%
Electric Power			2%	5%	45%	12%	10%	0%	2%	2%	20%
Natural Gas			35%	35%	0%	37%	0%	6%	7%	24%	10%
Other			35%	4%	29%	6%	31%	24%	0%	4%	24%
Operating Labor include supervisor			6%	11%	4%	8%	13%	26%	38%	22%	10%
Plant Maintenance			5%	11%	6%	10%	10%	10%	7%	10%	8%
Payroll			2%	3%	1%	2%	4%	6%	8%	5%	3%
Operating Suppies			1%	2%	1%	2%	2%	2%	1%	2%	2%
Administration and Overhead			7%	13%	6%	11%	14%	22%	27%	19%	12%
Taxes and Insurance			2%	4%	2%	3%	5%	1%	2%	3%	3%
Depreciation			6%	12%	5%	8%	12%	3%	6%	9%	8%
Total			100%	100%	100%	100%	100%	100%	100%	100%	100%

5.6.3.5.3 Safe Hydrogen Process

The next step in the study was to use the Bureau of Mines carbothermic reduction process data to create a cost estimate of a magnesium hydride slurry system. Sub-processes that were not needed in the slurry plant were removed and processes that are needed but had not been included in the Bureau of Mines plant were added in a manner similar to the Bureau of Mines study. The plant analysis includes tank storage for the returned hydroxide, a solvent refining process for the recovery of the oils in the byproduct, a calcining process to decompose the hydroxide to oxide, the magnesium

oxide reduction process, the magnesium quenching process, separation equipment to separate the solids from the gases, a hydriding process, and a slurry production process. The total capital cost, Table 30 through Table 33, is estimated to be $111.6M or $3,284/tonne of magnesium of installed capacity, about half that of the Bureau of Mines magnesium plant study.

Cost savings are achieved by recycling the byproducts of the magnesium hydride slurry process rather than purchasing and processing magnesium bearing ore and by using the product of the carbothermic reduction process directly as powder rather than distilling the product, melting and casting as was done in the Bureau of Mines study. This would be achievable if the back reaction between the magnesium vapor and the carbon monoxide can be minimized and if the resulting product can be hydrided successfully. Work performed in recent years in Denmark indicates that back reactions of less than 1% can be achieved.

The operating expenses are shown in Table 34 and Table 35. Based on operating expenses alone, the Safe Hydrogen process would be expected to cost $1.94/kg of magnesium. Allowing for a 20% return on the invested capital would require a price of $2.73/kg of magnesium. These prices are half those of the magnesium plant processing magnesium ore.

The results of this analysis when compared to the results of the Bureau of Mines study indicate that a recycling system such as that proposed by Safe Hydrogen for storing and transporting hydrogen in magnesium hydride slurry might offer cost reductions of up to 50% of those anticipated for an ore processing plant.

Summaries of the Bureau of Mines study and a comparison of the updated Bureau of Mines study and the Safe Hydrogen Process Analysis are shown in Table 36 and Table 37.

Table 30 - Safe Hydrogen Slurry Process Plant Design

	Number	Material $	Labor $	Total $	Labor/Material Ratio or Rate	Labor rate $/hr	Labor Hours Hr	Current Labor Cost $/hr	Materials	Labor	Total
Tank storage- Spent Hydroxide Slurry											
Pumps	14	17,500	2,800	20,300	0.160	2.70	1,037	15	63,731	15,556	79,287
Mixers	7	7,000	3,500	10,500	0.500	2.70	1,296	15	25,493	19,444	44,937
Tanks	7	33,400	20,100	53,500	0.602	2.70	7,444	15	121,636	111,667	233,302
total		57,900	26,400	84,300							357,526
				-							
Foundations				5,227	0.062						22,167
Structures				3,709	0.044						15,731
Buildings				18,630	0.221						79,013
Insulation				2,276	0.027						9,653
Instrumentation				2,951	0.035						12,513
Electrical work				5,985	0.071						25,384
Piping				16,860	0.200						71,505
Painting				759	0.009						3,218
Miscellaneous				7,587	0.090						32,177
total				63,984							271,363
Total Direct Construction				148,284							628,889
Indirect cost, contingency, and fee				59,313	0.400						251,556
Interest during construction				10,380	0.070						44,022
Total Fixed Capital				217,977							924,467
Solvent Refining											
Tanks	7	33,400	20,100	53,500	0.602	2.70	7,444	15	121,636	111,667	233,302
Pumps	12	15,000	2,400	17,400	0.160	2.70	889	15	54,627	13,333	67,960
Disk Filter	4	72,000	7,200	79,200	0.100	2.70	2,667	15	262,209	40,000	302,209
Materials handling equipment		46,700	8,700	55,400	0.186	2.70	3,222	15	170,072	48,333	218,405
total		167,100	38,400	205,500							821,877
				-							
Foundations				12,741	0.062						50,956
Structures				9,042	0.044						36,163
Buildings				45,416	0.221						181,635
Insulation				5,549	0.027						22,191
Instrumentation				7,193	0.035						28,766
Electrical work				14,591	0.071						58,353
Piping				41,100	0.200						164,375
Painting				1,850	0.009						7,397
Miscellaneous				18,495	0.090						73,969
total				155,975							623,804
Total Direct Construction				361,475							1,445,681
Indirect cost, contingency, and fee				144,590	0.4000						578,272
Interest during construction				25,303	0.0700						101,198
Total Fixed Capital				531,368							2,125,151
Calcining											
Rotary Kiln	1	345,100	65,600	410,700	0.190	2.70	24,296	15	1,256,782	364,444	1,621,227
Electrostatic precipitator	1	56,700	14,200	70,900	0.250	2.70	5,259	15	206,490	78,889	285,378
Exhaust blower, damper, stack		14,600	1,900	16,500	0.130	2.70	704	15	53,170	10,556	63,726
Rotary cooler	1	46,400	9,300	55,700	0.200	2.70	3,444	15	168,979	51,667	220,646
Bins and tanks	7	33,400	20,100	53,500	0.602	2.70	7,444	15	121,636	111,667	233,302
Miscellaneous pumps	21	26,300	4,200	30,500	0.160	2.70	1,556	15	95,779	23,333	119,112
Materials handling equipment		46,700	8,700	55,400	0.186	2.70	3,222	15	170,072	48,333	218,405
total		569,200	124,000	693,200							2,761,796
				-							
Foundations				42,978	0.062						171,231
Structures				30,501	0.044						121,519
Buildings				153,197	0.221						610,357
Insulation				18,716	0.027						74,569
Instrumentation				24,262	0.035						96,663
Electrical work				49,217	0.071						196,088
Piping				138,640	0.200						552,359
Painting				6,239	0.009						24,856
Miscellaneous				62,388	0.090						248,562
total				526,139							2,096,203
Total Direct Construction				1,219,339							4,858,000
Indirect cost, contingency, and fee				487,736	0.4000						1,943,200
Interest during construction				85,354	0.0700						340,060
Total Fixed Capital				1,792,428							7,141,260

Table 31 - Safe Hydrogen Slurry Process Plant Design

	Number	Material $	Labor $	Total $	Labor/Material Ratio or Rate	Labor rate $/hr	Labor Hours Hr	Current Labor Cost $/hr	Materials	Labor	Total
Magnesia Reduction											
Direct Construction Cost											
Ball Mill	1	132,800	13,300	146,100	0.100	2.70	4,926	15	483,630	73,889	557,519
Briquetting press	3	102,500	10,300	112,800	0.100	2.70	3,815	15	373,284	57,222	430,506
Gas Lock	10	22,100	3,300	25,400	0.149	2.70	1,222	15	80,484	18,333	98,817
Arc Furnace	5	2,222,000	166,700	2,388,700	0.075	2.70	61,741	15	8,092,060	926,111	9,018,171
Bins and hoppers	20	51,900	5,200	57,100	0.100	2.70	1,926	15	189,009	28,889	217,898
Materials handling equipment		85,300	16,700	102,000	0.196	2.70	6,185	15	310,645	92,778	403,423
				-							
total		2,616,600	215,500	2,832,100	0.082						10,726,333
Foundations				183,100	0.065						693,475
Structures				130,800	0.046						495,394
Buildings				639,700	0.226						2,422,808
Insulation											-
Instrumentation				98,900	0.035						374,575
Electrical work				235,500	0.083						891,936
Piping				130,800	0.046						495,394
Painting				29,100	0.010						110,214
Miscellaneous				261,700	0.092						991,166
total				1,709,600							6,474,961
Total Direct Construction				4,541,700							17,201,294
Indirect cost, contingency, and fee				1,816,600	0.4000						6,880,215
Interest during construction				317,900	0.0700						1,204,019
Total Fixed Capital				6,676,200							25,285,527
Magnesium Quenching											
Direct Construction Cost											
Centrifugal compressor	3	139,000	20,900	159,900	0.150	2.70	7,741	15	506,209	116,111	622,320
Absorption column	2	51,200	7,700	58,900	0.150	2.70	2,852	15	186,460	42,778	229,237
Stripping column	2	28,200	4,200	32,400	0.149	2.70	1,556	15	102,699	23,333	126,032
Dehydrating tower	2	24,600	3,700	28,300	0.150	2.70	1,370	15	89,588	20,556	110,144
Miscellaneous natural gas cleaning equipment		43,800	4,400	48,200	0.100	2.70	1,630	15	159,510	24,444	183,955
Shock chilling cone	5	66,800	6,700	73,500	0.100	2.70	2,481	15	243,272	37,222	280,494
Reamer	5	99,700	19,900	119,600	0.200	2.70	7,370	15	363,087	110,556	473,642
Surge drum	5	165,800	16,600	182,400	0.100	2.70	6,148	15	603,809	92,222	696,031
Heat exchanger, 120 ft2	5	10,300	1,000	11,300	0.097	2.70	370	15	37,510	5,556	43,066
Heat exchanger, 6720 ft2	5	87,700	8,800	96,500	0.100	2.70	3,259	15	319,385	48,889	368,274
Bag filter	5	126,300	15,200	141,500	0.120	2.70	5,630	15	459,958	84,444	544,403
Gas holder	1	175,000	17,500	192,500	0.100	2.70	6,481	15	637,313	97,222	734,536
Centrifugal compressor	5	234,300	35,100	269,400	0.150	2.70	13,000	15	853,272	195,000	1,048,272
Pumps	10	13,200	1,300	14,500	0.098	2.70	481	15	48,072	7,222	55,294
Materials handling equipment		22,700	4,800	27,500	0.211	2.70	1,778	15	82,669	26,667	109,335
total		1,288,600	167,800	1,456,400							5,625,034
Foundations				90,200	0.062						348,378
Structures				64,400	0.044						248,731
Buildings				322,200	0.221						1,244,429
Insulation				38,700	0.027						149,470
Instrumentation				51,400	0.035						198,522
Electrical work				103,100	0.071						398,202
Piping				541,200	0.372						2,090,269
Painting				12,900	0.009						49,823
Miscellaneous				128,900	0.089						497,849
total				1,353,000							5,225,674
Total Direct Construction				2,809,400							10,850,708
Indirect cost, contingency, and fee				1,123,800	0.4000						4,340,438
Interest during construction				196,700	0.0700						759,712
Total Fixed Capital				4,129,900							15,950,857

Table 32 - Safe Hydrogen Slurry Process Plant Design

	Number	Material $	Labor $	Total $	Labor/Material Ratio or Rate	Labor rate $/hr	Labor Hours Hr	Current Labor Cost $/hr	Materials	Labor	Total
Separation Equipment											
Direct Construction Cost											
Disk Filter	4	72,000	7,200	79,200	0.100	2.70	2,667	15	262,209	40,000	302,209
Tanks	7	33,400	20,100	53,500	0.602	2.70	7,444	15	121,636	111,667	233,302
Pumps	12	15,000	2,400	17,400	0.160	2.70	889	15	54,627	13,333	67,960
Materials handling equipment		46,700	8,700	55,400	0.186	2.70	3,222	15	170,072	48,333	218,405
total		167,100	38,400	205,500							821,877
				-							
Foundations				12,741	0.062						50,956
Structures				9,042	0.044						36,163
Buildings				45,416	0.221						181,635
Insulation				5,549	0.027						22,191
Instrumentation				7,193	0.035						28,766
Electrical work				14,591	0.071						58,353
Piping				41,100	0.200						164,375
Painting				1,850	0.009						7,397
Miscellaneous				18,495	0.090						73,969
total				155,975							623,804
Total Direct Construction				361,475							1,445,681
Indirect cost, contingency, and fee				144,590	0.4000						578,272
Interest during construction				25,303	0.0700						101,198
Total Fixed Capital				531,368							2,125,151
Hydride Process											
Direct Construction Cost											
Gas Lock	10	22,100	3,300	25,400	0.149	2.70	1,222	15	80,484	18,333	98,817
Centrifugal compressor	5	234,300	35,100	269,400	0.150	2.70	13,000	15	853,272	195,000	1,048,272
Bins and hoppers	20	51,900	5,200	57,100	0.100	2.70	1,926	15	189,009	28,889	217,898
Material handling equipment		85,300	16,700	102,000	0.196	2.70	6,185	15	310,645	92,778	403,423
total		393,600	60,300	453,900							1,768,409
				-							
Foundations				28,142	0.062						109,641
Structures				19,972	0.044						77,810
Buildings				100,312	0.221						390,818
Insulation				12,255	0.027						47,747
Instrumentation				15,887	0.035						61,894
Electrical work				32,227	0.071						125,557
Piping				90,780	0.200						353,682
Painting				4,085	0.009						15,916
Miscellaneous				40,851	0.090						159,157
total				344,510							1,342,222
Total Direct Construction				798,410							3,110,631
Indirect cost, contingency, and fee				319,364	0.4000						1,244,253
Interest during construction				55,889	0.0700						217,744
Total Fixed Capital				1,173,663							4,572,628
Slurry Production											
Direct Construction Cost											
Pumps	14	17,500	2,800	20,300	0.160	2.70	1,037	15	63,731	15,556	79,287
Tanks	7	33,400	20,100	53,500	0.602	2.70	7,444	15	121,636	111,667	233,302
Grinders	14	70,000	14,000	84,000	0.200	2.70	5,185	15	254,925	77,778	332,703
Mixers	7	7,000	3,500	10,500	0.500	2.70	1,296	15	25,493	19,444	44,937
Augers	14	7,000	3,500	10,500	0.500	2.70	1,296	15	25,493	19,444	44,937
total		134,900	43,900	178,800							735,167
				-							
Foundations				11,086	0.062						45,580
Structures				7,867	0.044						32,347
Buildings				39,515	0.221						162,472
Insulation				4,828	0.027						19,849
Instrumentation				6,258	0.035						25,731
Electrical work				12,695	0.071						52,197
Piping				35,760	0.200						147,033
Painting				1,609	0.009						6,616
Miscellaneous				16,092	0.090						66,165
total				135,709							557,991
Total Direct Construction				314,509							1,293,158
Indirect cost, contingency, and fee				125,804	0.4000						517,263
Interest during construction				22,016	0.0700						90,521
Total Fixed Capital				462,329							1,900,942

Table 33 - Safe Hydrogen Slurry Process Plant Design

	Number	Material $	Labor $	Total $	Labor/Material Ratio or Rate	Labor rate $/hr	Labor Hours Hr	Current Labor Cost $/hr	Materials	Labor	Total
Mg Powder Production (needed if Mg purchased)											
Direct Construction Cost											
Melting furnace	14	377,500	37,800	415,300	0.100	2.70	14,000	15	1,374,776	210,000	1,584,776
Blower	3	5,300	500	5,800	0.094	2.70	185	15	19,301	2,778	22,079
Centrifugal pump	14	18,300	1,800	20,100	0.098	2.70	667	15	66,645	10,000	76,645
Tanks	7	7,000	3,500	10,500	0.500	2.70	1,296	15	25,493	19,444	44,937
Augers	14	7,000	3,500	10,500	0.500	2.70	1,296	15	25,493	19,444	44,937
total		415,100	47,100	462,200							1,773,374
				-							
Foundations				28,656	0.062						45,580
Structures				20,337	0.044						32,347
Buildings				102,146	0.221						162,472
Insulation				12,479	0.027						19,849
Instrumentation				16,177	0.035						25,731
Electrical work				32,816	0.071						52,197
Piping				92,440	0.200						147,033
Painting				4,160	0.009						6,616
Miscellaneous				41,598	0.090						66,165
total				350,810							557,991
Total Direct Construction				813,010							2,331,366
Indirect cost, contingency, and fee				325,204	0.4000						932,546
Interest during construction				56,911	0.0700						163,196
Total Fixed Capital				1,195,124							3,427,107
Working Capital											
1 month supply of raw materials				-				15	-	-	-
1 month out of pocket expense		1,459,185		1,459,185				15	5,622,978	-	5,622,978
2 month product inventory		2,918,371		2,918,371				15	11,245,957	-	11,245,957
Total		4,377,556		4,377,556							16,868,935
Summary Total Direct Construction Costs											
Tank storage- Spent Hydroxide Slurry				217,977	1%						924,467
Solvent Refining				531,368	3%						2,125,151
Calcining				1,792,428	12%						7,141,260
Magnesia Reduction				6,676,200	43%						25,285,527
Magnesium Quenching				4,129,900	27%						15,950,857
Separation Equipment				531,368	3%						2,125,151
Hydride Process				1,173,663	8%						4,572,628
Slurry Production				462,329	3%						1,900,942
Total Plant				15,515,231							60,025,983
Mg Powder Production (needed if Mg purchased)				1,195,124							3,427,107
Nitrogen Production				130,400	0.4%						474,890
Hydrogen Production				474,000	1.4%						1,726,209
Dolomite											-
Total including N2 and H2 production				16,119,631	47.4%						62,227,082
Plant Facilities, 10%				1,611,963	4.7%						5,870,433
Plant utilities, 12%-$1 Million				934,356	2.7%						3,402,729
Power Plant				11,000,000	32.3%						40,059,701
Total Fixed Capital				29,665,950	87.1%						111,559,945
Working Capital				4,377,556	12.9%						16,868,935
Total				34,043,507	100.0%						128,428,880
Comparisons											
Capital Cost total plant											
$/ton											5,351
$/tonne											5,899
Capital Cost Power Plant											
$/kW											801
Capital Cost Mg Plant alone											
$/ton											2,979
$/tonne											3,284

Table 34 - Safe Hydrogen Process Operating Costs

		Tank Storage	Solvent Refining	Calcining	Magnesia Reduction, 12.500MVA	Magnesium Quenching, Natural Gas	Separation
Energy Consumption							
Electric Power	MWhr	-	-	-	-	-	-
69 kV		-	-	-	296,240	-	-
2300V		-	-	-	3,618	30,815	-
440V		1,680	4,200	2,520	2,108	732	4,200
Total Electric Energy	MWhr	1,680	4,200	2,520	301,966	31,547	4,200
Power Required for electricity	MW	0	1	0	36	4	1
Natural Gas	Mcf	-	33,675	80,329	-	1,126,567	-
Resulting Gas	Mcf	-	-	-	-	1,285,385	-
Well Water	Mgal	-	-	-	-	358,120	-
Steam	1000 lb	-	-	-	-	-	-
Petroleum Coke	ton	-	-	-	19,427	-	-
Metallurgical coke	ton	-	-	-	1,752	-	-
Graphite electrodes	ton	-	-	-	1,680	-	-
Activated alumna	ton	-	-	-	-	9	-
Monoethanolamine	lb	-	-	-	-	6,786	-
Retorts	ton Mg	-	-	-	-	-	-
Melting Pots	ton Mg	-	-	-	-	-	-
Dow 230 flux	ton	-	-	-	-	-	-
Sulfur	ton	-	-	-	-	-	-
Dolomite Ore	ton	-	-	-	-	-	-
Production		-	-	-	-	-	-
Magnesium metal	ton	-	-	-	-	-	-
Direct Cost		-	-	-	-	-	-
Electric Power							
69 kV	$/kWhr	-	-	-	10,368,400	-	-
2300V	$/kWhr	-	-	-	126,630	1,078,525	-
440V	$/kWhr	58,800	147,000	88,200	73,780	25,620	147,000
Natural Gas	$/Mcf	-	101,025	240,987	-	3,379,701	-
Resulting Gas	$/Mcf	-	-	-	-	465,290	-
Well Water	$/1000gal	-	-	-	-	107,696	-
Steam	$/1000 lb	-	-	-	-	-	-
Petroleum Coke	$/ton				1,190,095		
Metallurgical coke	$/ton				224,431		
Graphite electrodes	$/ton				5,239,315		
Activated alumna	$/ton					15,593	
Monoethanolamine	$/lb					10,581	
Retorts	$/ton Mg						-
Melting Pots	$/ton Mg						
Dow 230 flux	$/ton						
Sulfur	$/ton						
Dolomite Ore	$/ton	-	-				
Total		58,800	248,025	329,187	17,222,651	5,083,006	147,000
Direct Labor							
Labor	hr	4,160	4,160	18,720	49,920	41,600	18,720
Labor	$/hr	62,400	62,400	280,800	748,800	624,000	280,800
Supervision		9,360	9,360	42,120	112,209	93,350	42,120
Total		71,760	71,760	322,920	861,009	717,350	322,920
Plant Maintenance							
Labor		15,877	36,856	130,553	669,361	429,731	38,703
Supervision		3,175	7,371	26,111	134,018	85,946	7,741
Materials		7,938	36,856	150,136	669,361	429,731	38,703
Total		26,990	81,083	306,799	1,472,740	945,409	85,146
Payroll Overhead		16,800	21,458	88,723	307,974	228,203	68,332
Operating Supplies		5,398	16,217	61,360	294,621	189,009	17,029
Total direct cost		179,748	438,543	1,108,989	20,158,995	7,162,978	640,427
Indirect Cost							
Administration and Overhead		60,474	95,259	389,901	1,500,853	1,058,001	246,714
Fixed Cost							
Taxes and Insurance		15,877	38,703	130,553	462,872	286,609	38,703
Depreciation		39,691	96,756	326,382	1,215,630	752,030	96,756
Total		55,568	135,459	456,935	1,678,501	1,038,639	135,459
Total Operating Cost	$	295,790	669,261	1,955,826	23,338,350	9,259,617	1,022,600
	$/ton Mg						
	$/kg						
Working Capital							
1 month out of pocket expense							
2 month product inventory							
Total							
Capital Cost		793,827	1,935,129	6,527,648	24,313,325	15,040,233	1,935,129
additional capital allocation							
Plant facilities 10%							
Plant utilities 12%							
Plant utilities rebate							
Power Plant Capital							
Total Fixed Capital							
working Capital							
Total Fixed and working capital							
return on Capital							
Total cost	$						
	$/ton Mg						
	$/kg						

Table 35 - Safe Hydrogen Process Operating Costs Continued

		Hydriding	Slurry Prep.	Mg Powder Production	N2 Prod.	H2 Prod.	Total
Energy Consumption							
Electric Power	MWhr	-	-	-	-	-	-
69 kV		-	-	-	-	-	296,240
2300V		-	-	-	-	-	34,433
440V		1,890	4,200	756	233	443	22,962
Total Electric Energy	MWhr	1,890	4,200	756	233	443	353,635
Power Required for electricity	MW	0	1	0	0	0	42
Natural Gas	Mcf	-	-	21,390	8,485	78,750	1,349,196
Resulting Gas	Mcf	-	-	-	-	-	1,285,385
Well Water	Mgal	-	-	-	-	117,936	476,056
Steam	1000 lb	-	-	-	-	-	-
Petroleum Coke	ton	-	-	-	-	-	19,427
Metallurgical coke	ton	-	-	-	-	-	1,752
Graphite electrodes	ton	-	-	-	-	-	1,680
Activated alumna	ton	-	-	-	-	-	9
Monoethanolamine	lb	-	-	-	714	3,214	10,714
Retorts	ton Mg	-	-	-	-	-	-
Melting Pots	ton Mg	-	-	-	-	-	-
Dow 230 flux	ton	-	-	-	-	-	-
Sulfur	ton	-	-	-	-	-	-
Dolomite Ore	ton	-	-	-	-	-	-
Production		-	-	-	-	-	
Magnesium metal	ton	-	-	24,000	-	-	24,000
Direct Cost		-	-	-	-	-	
Electric Power							
69 kV	$/kWhr	-	-	-	-	-	10,368,400
2300V	$/kWhr	-	-	-	-	-	1,205,155
440V	$/kWhr	66,150	147,000	26,460	8,155	15,505	803,670
Natural Gas	$/Mcf	-	-	64,170	25,455	236,250	4,047,588
Resulting Gas	$/Mcf	-	-	-	-	-	465,290
Well Water	$/1000gal	-	-	-	-	35,466	143,162
Steam	$/1000 lb	-	-	-	-	-	-
Petroleum Coke	$/ton						1,190,095
Metallurgical coke	$/ton						224,431
Graphite electrodes	$/ton						5,239,315
Activated alumna	$/ton						15,593
Monoethanolamine	$/lb				1,114	5,012	16,707
Retorts	$/ton Mg	-	-				-
Melting Pots	$/ton Mg			-			-
Dow 230 flux	$/ton			-			-
Sulfur	$/ton			-			-
Dolomite Ore	$/ton						-
Total		66,150	147,000	90,630	34,724	292,234	23,719,407
Direct Labor							
Labor	hr	18,720	18,720	18,720	8,320	12,480	214,240
Labor	$/hr	280,800	280,800	280,800	124,800	187,200	3,213,600
Supervision		42,120	42,120	42,120	18,720	28,080	481,679
Total		322,920	322,920	322,920	143,520	215,280	3,695,279
Plant Maintenance							
Labor		213,712	84,185	217,620	14,247	51,786	1,902,630
Supervision		42,742	16,837	43,524	2,849	10,357	380,672
Materials		106,856	84,185	217,620	14,247	51,786	1,807,419
Total		363,310	185,207	478,763	31,343	113,930	4,090,721
Payroll Overhead		107,184	78,429	108,052	29,714	51,323	1,106,193
Operating Supplies		72,662	37,041	95,753	6,269	22,786	818,144
Total direct cost		932,226	770,598	1,096,118	245,569	695,553	33,429,744
Indirect Cost							
Administration and Overhead		433,038	311,799	502,744	105,423	201,660	4,905,865
Fixed Cost							
Taxes and Insurance		85,485	33,674	87,048	9,498	34,524	1,223,544
Depreciation		213,712	84,185	217,620	23,744	86,310	3,152,818
Total		299,196	117,859	304,668	33,242	120,835	4,376,362
Total Operating Cost	$	1,664,461	1,200,257	1,903,529	384,234	1,018,047	42,711,970
	$/ton Mg						1,780
	$/kg						1.9617
Working Capital							
1 month out of pocket expense							3,559,331
2 month product inventory							7,118,662
Total							10,677,993
Capital Cost		4,274,235	1,683,704	4,352,393	474,890	1,726,209	63,056,723
additional capital allocation							
Plant facilities 10%							6,305,672
Plant utilities 12%							7,566,807
Plant utilities rebate							(1,000,000)
Power Plant Capital							
Total Fixed Capital							75,929,202
working Capital							10,677,993
Total Fixed and working capital							86,607,195
return on Capital							17,321,439
Total cost	$						60,033,409
	$/ton Mg						2,501
	$/kg						2.7573

Table 36 – Summary of Bureau of Mines Study

		Original Permanente Estimate	Fract. of Total	Updated Estimate	Fract. of Total
Year		1966		2002	
Chemical Engineering Plant Cost Index		107.2		390.4	
Cost Escalation Factor		1		3.642	
Operating Labor Cost	$/hr	2.70		15.00	
Capital Costs					
Dolime Production		1,100,148	2%	4,314,376	2%
Sea Water Operation		3,659,565	7%	15,238,272	8%
Tank storage- Spent Hydroxide Slurry					
Solvent Refining					
Calcining					
Magnesia Reduction		6,676,200	13%	25,285,527	13%
Magnesium Quenching		4,129,900	8%	15,950,857	8%
Magnesium distillation		13,701,100	26%	52,206,600	27%
Magnesium melting and casting		1,365,300	3%	5,226,894	3%
Separation Equipment		-		-	
Mg Powder Production (needed if Mg purchased)					
Hydride Process		-		-	
Slurry Production					
Total		30,632,213	59%	118,222,526	61%
		-		-	
Nitrogen Production		130,400	0%	474,890	0%
Hydrogen Production		474,000	1%	1,726,209	1%
Dolomite		-		-	
Total including N2 and H2 production		31,236,613	60%	120,423,625	62%
		-		-	
Plant Facilities, 10%		3,123,661	6%	11,375,722	6%
Plant utilities, 12%-$1 Million		2,748,394	5%	10,009,075	5%
Power Plant		11,000,000	21%	40,059,701	21%
		-		-	
Total Fixed Capital		48,108,668	93%	181,868,123	93%
Working Capital		3,601,000	7%	13,114,090	7%
Total		51,709,668	100%	194,982,213	100%
Operating Costs					
Dolime Production		605,859	4%	3,571,460	5%
Sea Water Operation		1,085,551	7%	5,679,944	8%
Tank Storage					
Solvent Refining					
Calcining					
Magnesia Reduction, 12,500kVA		5,117,748	35%	23,338,533	33%
Magnesium Quenching, Natural Gas		1,742,052	12%	9,259,389	13%
Magnesium Distillation, batch		4,321,636	30%	19,704,410	28%
Magnesium melting and casting		1,459,505	10%	7,362,629	10%
Separation					
Hydriding					
Slurry Preparation					
Mg Powder Production					
Nitrogen Production		74,162	1%	374,675	1%
Hydrogen Production		190,030	1%	987,736	1%
Total without Powerplant		14,596,543	100%	70,278,775	100%
Mg Production using Powerplant		11,165,005	77%	55,088,980	72%
Powerplant		3,285,055	23%	21,511,359	28%
Total with Powerplant		14,450,060	100%	76,600,339	100%
Comparitive Factors					
Magnesium Production	ton/yr	24,000		24,000	
Capital Cost/production rate	$/ton	2,155		8,124	
	$/tonne	2,375		8,955	
Operating Cost	$/ton	608		2,928	
	$/lb	0.304		1.464	
	$/kg	0.670		3.228	
Price for 20% ret on cap w/o powerplant	$/lb	0.474		2.111	
Price for 20% ret on cap w/ powerplant	$/lb	0.517		2.417	

Table 37 - Safe Hydrogen Recycle Plant Compared to Updated BOM Study

		Original Permanente Updated Estimate	Fract. of Total	Safe Hydrogen Recycle Plant	Fract. of Total
Year		2002		2002	
Chemical Engineering Plant Cost Index		390.4		390.4	
Cost Escalation Factor		3.642		3.642	
Operating Labor Cost	$/hr	15.00		15.00	
Capital Costs					
Dolime Production		4,314,376	2%		
Sea Water Operation		15,238,272	8%		
Tank storage- Spent Hydroxide Slurry				924,467	1%
Solvent Refining				2,125,151	2%
Calcining				7,141,260	6%
Magnesia Reduction		25,285,527	13%	25,285,527	20%
Magnesium Quenching		15,950,857	8%	15,950,857	12%
Magnesium distillation		52,206,600	27%		0%
Magnesium melting and casting		5,226,894	3%		0%
Separation Equipment		-		2,125,151	2%
Mg Powder Production (needed if Mg purchased)					
Hydride Process		-		4,572,628	4%
Slurry Production				1,900,942	1%
					0%
Total		118,222,526	61%	60,025,983	47%
		-			0%
Nitrogen Production		474,890	0%	474,890	0%
Hydrogen Production		1,726,209	1%	1,726,209	1%
Dolomite		-		-	0%
Total including N2 and H2 production		120,423,625	62%	62,227,082	48%
		-		-	0%
Plant Facilities, 10%		11,375,722	6%	5,870,433	5%
Plant utilities, 12%-$1 Million		10,009,075	5%	3,402,729	3%
Power Plant		40,059,701	21%	40,059,701	31%
		-		-	0%
Total Fixed Capital		181,868,123	93%	111,559,945	87%
Working Capital		13,114,090	7%	16,868,935	13%
Total		194,982,213	100%	128,428,880	100%
Operating Costs					
Dolime Production		3,571,460	5%		
Sea Water Operation		5,679,944	8%		
Tank Storage				295,790	1%
Solvent Refining				669,261	2%
Calcining				1,955,826	5%
Magnesia Reduction, 12,500kVA		23,338,533	33%	23,338,350	55%
Magnesium Quenching, Natural Gas		9,259,389	13%	9,259,617	22%
Magnesium Distillation, batch		19,704,410	28%		
Magnesium melting and casting		7,362,629	10%		
Separation				1,022,600	2%
Hydriding				1,664,461	4%
Slurry Preparation				1,200,257	3%
Mg Powder Production				1,575,747	4%
Nitrogen Production		374,675	1%	384,234	1%
Hydrogen Production		987,736	1%	1,018,047	2%
Total without Powerplant		70,278,775	100%	42,384,188	100%
Mg Production using Powerplant		55,088,980	72%	29,864,359	58%
Powerplant		21,511,359	28%	21,511,359	42%
Total with Powerplant		76,600,339	100%	51,375,718	100%
Comparitive Factors					
Magnesium Production	ton/yr	24,000		24,000	
Capital Cost/production rate	$/ton	8,124		5,351	
	$/tonne	8,955		5,899	
Operating Cost	$/ton	2,928		1,766	
	$/lb	1.464		0.883	
	$/kg	3.228		1.947	
Price for 20% ret on cap w/o powerplant	$/lb	2.111		1.238	
Price for 20% ret on cap w/ powerplant	$/lb	2.417		1.638	

5.6.3.5.4 Magnesium Alloy Corporation Prospectus Provides Magnesium Plant Data

The Magnesium Alloy Corporation, Reference 14, issued a prospectus with some information on an electrochemical magnesium production plant to be built in Africa. This data provides significant insights into the current costs of making magnesium. They noted:

- Break even, per year (tonnes sold) 26,000 tonnes
- SNC-Lavalin Inc has indicated that the project could supply electrical power to the company at a rate of $0.016 per kWh with a potential to reduce the rate significantly. This low power rate is critical as energy costs can account for up to 40% of the cost of magnesium production.
- Salzgitter Anlagenbau GmbH, a division of Preussag of Germany, has used these energy costs ($0.016 per kWh) and has concluded that the magnesium plant, initially rated at 60,000 tonnes per annum, could produce magnesium metal and alloys at a cash cost of $0.55 per pound.
- The electrolysis cells are huge users of electricity. Salzgitter has estimated that each tonne of magnesium produced will require 16,000 kWh of energy.
- SNC's present studies indicate that power to Mag Alloy could be provided at a rate of $0.016 per kWh. This rate may be reduced significantly with an expanded dam and a doubling of Mag Alloy's plant capacity to 120,000 tonnes of magnesium per annum. It is worthwhile noting that Norsk Hydro's Becancour plant in Quebec purchases energy at the rate of $0.022 per kWh and, to Norsk Hydro's disadvantage, the feedstock is magnesite imported from China.
- This translates to $8,571 per tonne of annual capacity. The capital cost is on par with Australian Magnesium Corporation ("AMC") and Noranda's Magnola plant. Their respective capital costs are anticipated at $8,300 to $8,600 per annual tonne. Dead Sea Magnesium Works and Norsk Hydro (Becancour) had final capital costs estimated at$17,000 to $18,200 per annual tonne.
- The total operating cash cost is estimated at $72.6 million per year or $1,210 per tonne ($0.55 per pound). This is substantially less than Magnola's and AMC's estimates of $1,700 per tonne.

5.6.3.5.5 Magnesium Chloride process evaluation

The next step in our study was an evaluation of current technology for reducing magnesium. Data for a proposed new magnesium production plant, to be built in the Kouilou region of the Republic of Congo, was found in a prospectus published by the Magnesium Alloy Corporation. In this prospectus, data was also given for Noranda's Magnola plant in Canada and for an Australian Magnesium Corporation plant. The data for these three plants were compared to current prices and evaluation parameters similar to those used in the Bureau of Mines study were determined. The first conclusion was that the evaluation parameters used by the Bureau of Mines to estimate the cost of maintenance, overhead, etc resulted in an overestimate of the reported operating costs. Operating costs for the proposed Magnesium Alloy Corporation plant are projected to be $0.55/lbm by the Magnesium Alloy Corporation. Operating costs for the Magnola plant and the Australian Magnesium Corporation plant are reported to be about $0.77/lbm (see Table 38).

Economies of scale can result in very large reductions in the cost of magnesium. To evaluate the economies of scale, capital costs were scaled using a 2/3 power law and the materials and labor using a linear extrapolation. Other operating costs were derived in the same way as was used in the Bureau of Mines study. From this evaluation, we concluded that by scaling up from 60,000 tonnes/yr to 6,000,000 tonnes/year the cost of magnesium in the Magnola plant could be reduced from $0.76/lb to $0.40/lb. The analyses are summarized in Table 39 through Table 42.

Economies of scale can be achieved both in individual larger scale plants and in the application of the technology in a large-scale implementation. In a large-scale implementation, a specific plant design can be used repeatedly because the raw material for the process is coming from the byproduct and is consistent. The plant components will also benefit from large-scale implementation because they can be standardized and factory assembled.

It must be recognized that the estimates for the carbothermic process are based on 50-year-old technology. Modern technology should be able to reduce these costs significantly through the use of automation and improved materials.

5.6.3.5.6 Business Development

A question that must be answered for any new product development is how will the venture grow. If the costs of production at small scale are too high, the business may not be able to sustain the losses required to build up its market share before sufficient sales are achieved. Magnesium hydride slurry provides an interesting solution to this question. At small scale, when the market is too small to justify the recycling of the magnesium hydroxide, the process can rely on purchased magnesium and then recover and sell the magnesium hydroxide. As the sales grow, the amount of magnesium hydroxide sales will grow until they begin to saturate the market, at which point the sales price will drop. It turns out that this point is reached after the product sales of magnesium hydride reach the level of a competitive recycle system comparable to the scale of a modern large magnesium production plant. Table 43 and Figure 82 display the effect of scale on both recycle and byproduct sale scenarios. The crossover point for recycling occurs at about the scale of a modern large-scale magnesium reduction plant.

Table 38 - Comparison of Bureau of Mines Study and Three $MgCl_2$ Plants

		BOM Permanente	BOM Permanente	Magnesium Alloy Corporation	Australian Magnesium Corporation	Noranda's Magnola plant
		1966	2002	2002	2002	2002
Source				Factors modified	Factors modified	Factors modified
Production Rate	tonne Mg/yr	21,773	21,773	60,000	63,000	63,000
	MNm3 H2/yr					
Capital Cost	$	31,236,600	113,650,860	514,000,000	522,900,000	541,800,000
	$/tonne	1,435	5,220	8,567	8,300	8,600
Electricity	kWh/tonne	18,363	18,363	16000	16,000	16,000
Electricity price	$/kWh	0.008	0.035	0.016	0.022	0.022
Reported Operating Cost	$/yr	14,596,543	70,278,775	72,600,000	107,100,000	107,100,000
	$/yr tonne	670	3,228	1,210	1,700	1,700
	$/lb Mg			0.55	0.77	0.77
Breakeven	tonne/yr			26000		
Operators	# (2080hr/yr)	203	203	150	150	150
Operator	hours	422,240	422,240	312,000	312,000	312,000
Labor Cost	$/hr	2.7	15	8	15	15
Calculation						
Capital Cost	$	31,236,600	113,650,860	514,000,000	522,900,000	541,800,000
Operating Cost	$/year	14,596,543	70,278,775	72,600,000	107,100,000	107,100,000
Materials and Utilities						
Electricity		3,216,723	13,993,490	15,360,000	22,176,000	22,176,000
Heat		827,605	7,783,862			
Other Materials		2,909,315	16,201,975	7,680,000	11,088,000	11,088,000
Direct Labor						
Operator	$/yr	1,140,048	6,333,600	2,496,000	4,680,000	4,680,000
Supervision	$/yr	171,007	950,040	374,400	702,000	702,000
Plant Maintenance						
Labor	$/yr	749,678	2,727,621	2,570,000	7,843,500	8,127,000
Supervision	$/yr	149,936	545,524	385,500	1,176,525	1,219,050
Materials	$/yr	749,678	2,727,621	2,570,000	7,843,500	8,127,000
Payroll Overhead	$/yr	408,974	1,953,005	349,554	864,122	883,683
Operating Supplies	$/yr	329,858	1,200,153	276,275	843,176	873,653
Indirect Cost						
Admin & Overhead	$/yr	1,849,590	8,218,782	4,510,865	11,976,411	12,306,193
Fixed Cost						
Taxes & Ins	$/yr	624,732	2,273,017	10,280,000	10,458,000	10,836,000
Depreciation	$/yr	1,561,830	5,682,543	25,700,000	26,145,000	27,090,000
Total Calc Operating Cost	$/yr	14,688,975	70,591,233	72,552,594	105,796,234	108,108,578
Magnesium Cost	$/tonne	675	3,242	1,209	1,679	1,716
	$/kg	0.675	3.242	1.209	1.679	1.716
	$/lbm	0.306	1.471	0.548	0.762	0.778
	$/Nm3 H2					
Working Capital						
1 month supply of raw materials						
1 month out of pocket expense		1,224,081	5,882,603	6,046,049	8,816,353	9,009,048
2 month product inventory		2,448,162	11,765,205	12,092,099	17,632,706	18,018,096
Total						
Additional Capital Allocation						
Plant Facilities 10%		3,123,660	11,365,086	-	-	-
Plant Utilities 12%		3,748,392	13,638,103	-	-	-
Power Plant Capital						
Total Fixed Capital		38,108,652	138,654,049	514,000,000	522,900,000	541,800,000
Working Capital		3,672,244	17,647,808	18,138,148	26,449,059	27,027,145
Total Fixed and Working Capital		41,780,896	156,301,857	532,138,148	549,349,059	568,827,145
Return on Capital 20%		8,356,179	31,260,371	93,124,176	68,668,632	68,259,257
Total cost	$	23,045,154	101,851,604	165,676,769	174,464,866	176,367,836
	$/tonne Mg	1,058	4,678	2,761	2,769	2,799
	$/kg	1.058	4.678	2.761	2.769	2.799
	$/lbm	0.480	2.122	1.253	1.256	1.270

Table 39 - Scaling of Bureau of Mines Process

Bureau of Mines study		BOM Permanente 2002	Scaled	Scaled	Scaled
Scale Factor		1	2.75575	27.5575	275.575
Production Rate	tonne Mg/yr	21,773	60,000	600,000	6,000,000
Capital Cost	$	113,650,860	223,391,136	1,036,889,804	4,812,816,134
	$/tonne	5,220	3,723	1,728	802
Electricity	kWh/tonne	18,363	18,363	18,363	18,363
Electricity price	$/kWh	0.035	0.035	0.035	0.035
Reported Operating Cost	$/yr	70,278,775			
	$/yr tonne	3,228			
Breakeven	tonne/yr				
Operators	# (2080hr/yr)	203	559.41725	5594.1725	55941.725
Operator	hours	422,240	1,163,588	11,635,879	116,358,788
Labor Cost	$/hr	15	15	15	15
Calculation					
Capital Cost	$	113,650,860	223,391,136	1,036,889,804	4,812,816,134
Operating Cost	$/year	70,278,775			
Materials and Utilities					
Electricity		13,993,490	38,562,560	385,625,601	3,856,256,007
Heat		7,783,862	21,450,378	214,503,777	2,145,037,771
Other Materials		16,201,975	44,648,593	446,485,926	4,464,859,261
Direct Labor					
Operator	$/yr	6,333,600	17,453,818	174,538,182	1,745,381,820
Supervision	$/yr	950,040	2,618,073	26,180,727	261,807,273
Plant Maintenance					
Labor	$/yr	2,727,621	5,361,387	24,885,355	115,507,587
Supervision	$/yr	545,524	1,072,277	4,977,071	23,101,517
Materials	$/yr	2,727,621	5,361,387	24,885,355	115,507,587
Payroll Overhead	$/yr	1,953,005	4,903,528	42,657,547	396,972,667
Operating Supplies	$/yr	1,200,153	2,359,010	10,949,556	50,823,338
Indirect Cost					
Admin & Overhead	$/yr	8,218,782	19,564,741	154,536,897	1,354,550,895
Fixed Cost					
Taxes & Ins	$/yr	2,273,017	4,467,823	20,737,796	96,256,323
Depreciation	$/yr	5,682,543	11,169,557	51,844,490	240,640,807
Total Calc Operating Cost	$/yr	70,591,233	178,993,132	1,582,808,282	14,866,702,852
Difference calc & reported Operating Cost		0.44%			
Magnesium Cost	$/tonne	3,242	2,983	2,638	2,478
	$/kg	3.242	2.983	2.638	2.478
	$/lbm	1.471	1.353	1.197	1.124
	cost ratio		0.920	0.814	0.764
Working Capital					
1 month supply of raw materials					
1 month out of pocket expense		5,882,603	14,916,094	131,900,690	1,238,891,904
2 month product inventory		11,765,205	29,832,189	263,801,380	2,477,783,809
Total					
Additional Capital Allocation					
Plant Facilities 10%		11,365,086	22,339,114	103,688,980	481,281,613
Plant Utilities 12%		13,638,103	26,806,936	124,426,776	577,537,936
Power Plant Capital					
Total Fixed Capital		138,654,049	272,537,186	1,265,005,560	5,871,635,683
Working Capital		17,647,808	44,748,283	395,702,070	3,716,675,713
Total Fixed and Working Capital		156,301,857	317,285,469	1,660,707,631	9,588,311,396
Return on Capital 20%		31,260,371	63,457,094	332,141,526	1,917,662,279
Total cost	$	101,851,604	242,450,225	1,914,949,808	16,784,365,131
	$/tonne Mg	4,678	4,041	3,192	2,797
	$/kg	4.678	4.041	3.192	2.797
	$/lbm	2.122	1.833	1.448	1.269

Table 40 - Scaling of the Magnesium Alloy Corporation Process

Magnesium Alloy Corp proposes plant		Magnesium Alloy Corporation	Scaled	Scaled	Scaled	Scaled
Scale Factor		Factors modified	0.362877667	1	10	100
Production Rate	tonne Mg/yr	60,000	21,773	60,000	600,000	6,000,000
Capital Cost	$	514,000,000	261,498,948	514,000,000	2,385,776,660	11,073,794,307
	$/tonne	8,567	12,010	8,567	3,976	1,846
Electricity	kWh/tonne	16000	16,000	16,000	16,000	16,000
Electricity price	$/kWh	0.016	0.016	0.016	0.016	0.016
Reported Operating Cost	$/yr	72,600,000				
	$/yr tonne	1,210				
Breakeven	tonne/yr	26000				
Operators	# (2080hr/yr)	150	54.43165	150	1500	15000
Operator	hours	312,000	113,218	312,000	3,120,000	31,200,000
Labor Cost	$/hr	8	8	8	8	8
Calculation						
Capital Cost	$	514,000,000	261,498,948	514,000,000	2,385,776,660	11,073,794,307
Operating Cost	$/year	72,600,000				
Materials and Utilities						
Electricity		15,360,000	5,573,801	15,360,000	153,600,000	1,536,000,000
Heat						
Other Materials		7,680,000	2,786,900	7,680,000	76,800,000	768,000,000
Direct Labor						
Operator	$/yr	2,496,000	905,743	2,496,000	24,960,000	249,600,000
Supervision	$/yr	374,400	135,861	374,400	3,744,000	37,440,000
Plant Maintenance						
Labor	$/yr	2,570,000	1,307,495	2,570,000	11,928,883	55,368,972
Supervision	$/yr	385,500	196,124	385,500	1,789,332	8,305,346
Materials	$/yr	2,570,000	1,307,495	2,570,000	11,928,883	55,368,972
Payroll Overhead	$/yr	349,554	152,713	349,554	2,545,333	21,042,859
Operating Supplies	$/yr	276,275	140,556	276,275	1,282,355	5,952,164
Indirect Cost						
Admin & Overhead	$/yr	4,510,865	2,072,993	4,510,865	29,089,394	216,539,156
Fixed Cost						
Taxes & Ins	$/yr	10,280,000	5,229,979	10,280,000	47,715,533	221,475,886
Depreciation	$/yr	25,700,000	13,074,947	25,700,000	119,288,833	553,689,715
Total Calc Operating Cost	$/yr	72,552,594	32,884,608	72,552,594	484,672,547	3,728,783,070
Difference calc & reported Operating Cost		-0.07%				
Magnesium Cost	$/tonne	1,209	1,510	1,209	808	621
	$/kg	1.209	1.510	1.209	0.808	0.621
	$/lbm	0.548	0.685	0.548	0.366	0.282
	cost ratio		1.249	1.000	0.668	0.514
Working Capital						
1 month supply of raw materials						
1 month out of pocket expense		6,046,049	2,740,384	6,046,049	40,389,379	310,731,922
2 month product inventory		12,092,099	5,480,768	12,092,099	80,778,758	621,463,845
Total						
Additional Capital Allocation						
Plant Facilities 10%		-	-	-	-	-
Plant Utilities 12%		-	-	-	-	-
Power Plant Capital						
Total Fixed Capital		514,000,000	261,498,948	514,000,000	2,385,776,660	11,073,794,307
Working Capital		18,138,148	8,221,152	18,138,148	121,168,137	932,195,767
Total Fixed and Working Capital		532,138,148	269,720,100	532,138,148	2,506,944,797	12,005,990,074
Return on Capital 20%		106,427,630	53,944,020	106,427,630	501,388,959	2,401,198,015
Total cost	$	178,980,223	86,828,628	178,980,223	986,061,506	6,129,981,085
	$/tonne Mg	2,983	3,988	2,983	1,643	1,022
	$/kg	2.983	3.988	2.983	1.643	1.022
	$/lbm	1.353	1.809	1.353	0.745	0.463

Table 41 - Scaling of the Australian Magnesium Corporation Process

Australian Magnesium Corp plant		AMC	Scaled	Scaled	Scaled	Scaled
Scale Factor		Factors modified	0.345603175	0.952380952	9.523809524	95.23809524
Production Rate	tonne Mg/yr	63,000	21,773	60,000	600,000	6,000,000
Capital Cost	$	522,900,000	257,515,747	506,165,386	2,349,411,602	10,905,002,658
	$/tonne	8,300	11,827	8,436	3,916	1,818
Electricity	kWh/tonne	16000	16,000	16,000	16,000	16,000
Electricity price	$/kWh	0.022	0.022	0.022	0.022	0.022
Reported Operating Cost	$/yr	107,100,000				
	$/yr tonne	1,700				
Breakeven	tonne/yr					
Operators	# (2080hr/yr)	150	51.84047619	142.8571429	1428.571429	14285.71429
Operator	hours	312,000	107,828	297,143	2,971,429	29,714,286
Labor Cost	$/hr	15	15	15	15	15
Calculation						
Capital Cost	$	522,900,000	257,515,747	506,165,386	2,349,411,602	10,905,002,658
Operating Cost	$/year	107,100,000				
Materials and Utilities						
Electricity		22,176,000	7,664,096	21,120,000	211,200,000	2,112,000,000
Heat						
Other Materials		11,088,000	3,832,048	10,560,000	105,600,000	1,056,000,000
Direct Labor						
Operator	$/yr	4,680,000	1,617,423	4,457,143	44,571,429	445,714,286
Supervision	$/yr	702,000	242,613	668,571	6,685,714	66,857,143
Plant Maintenance						
Labor	$/yr	7,843,500	3,862,736	7,592,481	35,241,174	163,575,040
Supervision	$/yr	1,176,525	579,410	1,138,872	5,286,176	24,536,256
Materials	$/yr	7,843,500	3,862,736	7,592,481	35,241,174	163,575,040
Payroll Overhead	$/yr	864,122	378,131	831,424	5,507,070	42,040,963
Operating Supplies	$/yr	843,176	415,244	816,192	3,788,426	17,584,317
Indirect Cost						
Admin & Overhead	$/yr	11,976,411	5,479,147	11,548,582	68,160,581	461,941,522
Fixed Cost						
Taxes & Ins	$/yr	10,458,000	5,150,315	10,123,308	46,988,232	218,100,053
Depreciation	$/yr	26,145,000	12,875,787	25,308,269	117,470,580	545,250,133
Total Calc Operating Cost	$/yr	105,796,234	45,959,688	101,757,323	685,740,556	5,317,174,753
Difference calc & reported Operating Cost		-1.22%				
Magnesium Cost	$/tonne	1,679	2,111	1,696	1,143	886
	$/kg	1.679	2.111	1.696	1.143	0.886
	$/lbm	0.762	0.957	0.769	0.518	0.402
	cost ratio		1.257	1.010	0.681	0.528
Working Capital						
1 month supply of raw materials						
1 month out of pocket expense		8,816,353	3,829,974	8,479,777	57,145,046	443,097,896
2 month product inventory		17,632,706	7,659,948	16,959,554	114,290,093	886,195,792
Total						
Additional Capital Allocation						
Plant Facilities 10%		-	-	-	-	-
Plant Utilities 12%		-	-	-	-	-
Power Plant Capital						
Total Fixed Capital		522,900,000	257,515,747	506,165,386	2,349,411,602	10,905,002,658
Working Capital		26,449,059	11,489,922	25,439,331	171,435,139	1,329,293,688
Total Fixed and Working Capital		549,349,059	269,005,669	531,604,716	2,520,846,741	12,234,296,347
Return on Capital 20%		109,869,812	53,801,134	106,320,943	504,169,348	2,446,859,269
Total cost	$	215,666,046	99,760,821	208,078,266	1,189,909,905	7,764,034,022
	$/tonne Mg	3,423	4,582	3,468	1,983	1,294
	$/kg	3.423	4.582	3.468	1.983	1.294
	$/lbm	1.553	2.078	1.573	0.900	0.587

Table 42 - Scaling of the Noranda Magnola Plant

Noranda's Magnola Plant		Magnola	Scaled	Scaled	Scaled	Scaled
Scale Factor		Factors modified	0.345603175	0.952380952	9.523809524	95.23809524
Production Rate	tonne Mg/yr	63,000	21,773	60,000	600,000	6,000,000
Capital Cost	$	541,800,000	266,823,545	524,460,520	2,434,330,094	11,299,159,381
	$/tonne	8,600	12,255	8,741	4,057	1,883
Electricity	kWh/tonne	16000	16,000	16,000	16,000	16,000
Electricity price	$/kWh	0.022	0.022	0.022	0.022	0.022
Reported Operating Cost	$/yr	107,100,000				
	$/yr tonne	1,700				
Breakeven	tonne/yr					
Operators	# (2080hr/yr)	150	51.84047619	142.8571429	1428.571429	14285.71429
Operator	hours	312,000	107,828	297,143	2,971,429	29,714,286
Labor Cost	$/hr	15	15	15	15	15
Calculation						
Capital Cost	$	541,800,000	266,823,545	524,460,520	2,434,330,094	11,299,159,381
Operating Cost	$/year	107,100,000				
Materials and Utilities						
Electricity		22,176,000	7,664,096	21,120,000	211,200,000	2,112,000,000
Heat						
Other Materials		11,088,000	3,832,048	10,560,000	105,600,000	1,056,000,000
Direct Labor						
Operator	$/yr	4,680,000	1,617,423	4,457,143	44,571,429	445,714,286
Supervision	$/yr	702,000	242,613	668,571	6,685,714	66,857,143
Plant Maintenance						
Labor	$/yr	8,127,000	4,002,353	7,866,908	36,514,951	169,487,391
Supervision	$/yr	1,219,050	600,353	1,180,036	5,477,243	25,423,109
Materials	$/yr	8,127,000	4,002,353	7,866,908	36,514,951	169,487,391
Payroll Overhead	$/yr	883,683	387,765	850,359	5,594,960	42,448,916
Operating Supplies	$/yr	873,653	430,253	845,693	3,925,357	18,219,895
Indirect Cost						
Admin & Overhead	$/yr	12,306,193	5,641,557	11,867,809	69,642,303	468,819,064
Fixed Cost						
Taxes & Ins	$/yr	10,836,000	5,336,471	10,489,210	48,686,602	225,983,188
Depreciation	$/yr	27,090,000	13,341,177	26,223,026	121,716,505	564,957,969
Total Calc Operating Cost	$/yr	108,108,578	47,098,462	103,995,664	696,130,015	5,365,398,350
Difference calc & reported Operating Cost		0.94%				
Magnesium Cost	$/tonne	1,716	2,163	1,733	1,160	894
	$/kg	1.716	2.163	1.733	1.160	0.894
	$/lbm	0.778	0.981	0.786	0.526	0.406
	cost ratio		1.261	1.010	0.676	0.521
Working Capital						
1 month supply of raw materials						
1 month out of pocket expense		9,009,048	3,924,872	8,666,305	58,010,835	447,116,529
2 month product inventory		18,018,096	7,849,744	17,332,611	116,021,669	894,233,058
Total						
Additional Capital Allocation						
Plant Facilities 10%		-	-	-	-	-
Plant Utilities 12%		-	-	-	-	-
Power Plant Capital						
Total Fixed Capital		541,800,000	266,823,545	524,460,520	2,434,330,094	11,299,159,381
Working Capital		27,027,145	11,774,615	25,998,916	174,032,504	1,341,349,587
Total Fixed and Working Capital		568,827,145	278,598,160	550,459,436	2,608,362,598	12,640,508,968
Return on Capital		65,415,122	32,038,788	63,302,835	299,961,699	1,453,658,531
Total cost	$	173,523,700	79,137,250	167,298,499	996,091,714	6,819,056,881
	$/tonne Mg	2,754	3,635	2,788	1,660	1,137
	$/kg	2.754	3.635	2.788	1.660	1.137
	$/lbm	1.249	1.649	1.265	0.753	0.516

Table 43 - Summary of Costs and Plan Costs

Slurry from Mg Metal - Mg $1.25								
Hydrogen Production Rate	MNm3/yr	1	4	40	111	400	1,106	4,000
Capital Cost	$	1,689,486	4,257,237	19,760,345	38,935,491	91,719,395	180,722,540	425,723,718
Electricity	$/kWhr	0.030	0.030	0.030	0.030	0.030	0.030	0.030
Heat	$/Mcf	3.00	3.00	3.00	3.00	3.00	3.00	3.00
Mg (Magnola plant)	$/lb	1.25	1.15	1.10	1.00	0.85	0.75	0.75
Hydrogen	$/Nm3	0.35	0.35	0.25	0.16	0.12	0.10	0.10
Mg(OH)2	$/kg	0.55	0.55	0.55	0.35	0.20	-	-
Cost of Hydrogen	$/Nm3 H2	1.29	1.09	0.90	0.97	0.94	1.05	1.04
Slurry from Mg Metal - Mg $0.60								
Hydrogen Production Rate	MNm3 H2/yr	1	4	40	111	400	1,106	4,000
Capital Cost	$	1,689,486	4,257,237	19,760,345	38,935,491	91,719,395	180,722,540	425,723,718
Electricity	$/kWhr	0.030	0.030	0.030	0.030	0.030	0.030	0.030
Heat	$/Mcf	3.00	3.00	3.00	3.00	3.00	3.00	3.00
Mg (Magnola plant)	$/lb	0.60	0.60	0.60	0.60	0.60	0.75	0.75
Hydrogen	$/Nm3	0.35	0.35	0.25	0.16	0.12	0.10	0.10
Mg(OH)2	$/kg	0.55	0.55	0.55	0.18	-	-	-
Cost of Hydrogen	$/Nm3 H2	0.51	0.44	0.30	0.70	0.89	1.05	1.04
Plan								
Hydrogen Production Rate	MNm3 H2/yr	1	4	40	111	400	1,106	4,000
Capital Cost	$	1,689,486	4,257,237	19,760,345	38,935,491	91,719,395	180,722,540	425,723,718
Electricity	$/kWhr	0.030	0.030	0.030	0.030	0.030	0.030	0.030
Heat	$/Mcf	3.00	3.00	3.00	3.00	3.00	3.00	3.00
Mg (Magnola plant)	$/lb	0.90	0.90	0.90	0.90	0.60	0.75	0.75
Hydrogen	$/Nm3	0.35	0.35	0.25	0.16	0.12	0.10	0.10
Mg(OH)2	$/kg	0.55	0.55	0.53	0.45	-	-	-
Cost of Hydrogen	$/Nm3 H2	0.87	0.80	0.69	0.73	0.89	1.05	1.04
Slurry from Recycled Mg(OH)2								
Hydrogen Production Rate	MNm3 H2/yr	1	4	40	111	400	1,106	4,000
Capital Cost	$	5,279,942	13,304,621	61,905,196	121,680,312	286,639,368	564,789,976	1,330,462,090
Electricity	$/kWh	0.030	0.030	0.030	0.030	0.030	0.030	0.030
Cost of Hydrogen	$/Nm3 H2	1.19	0.95	0.73	0.68	0.63	0.61	0.58
Plan								
Hydrogen Production Rate		1	4	40	111	400	1,106	4,000
Cost of Hydrogen		0.87	0.80	0.73	0.68	0.63	0.61	0.58

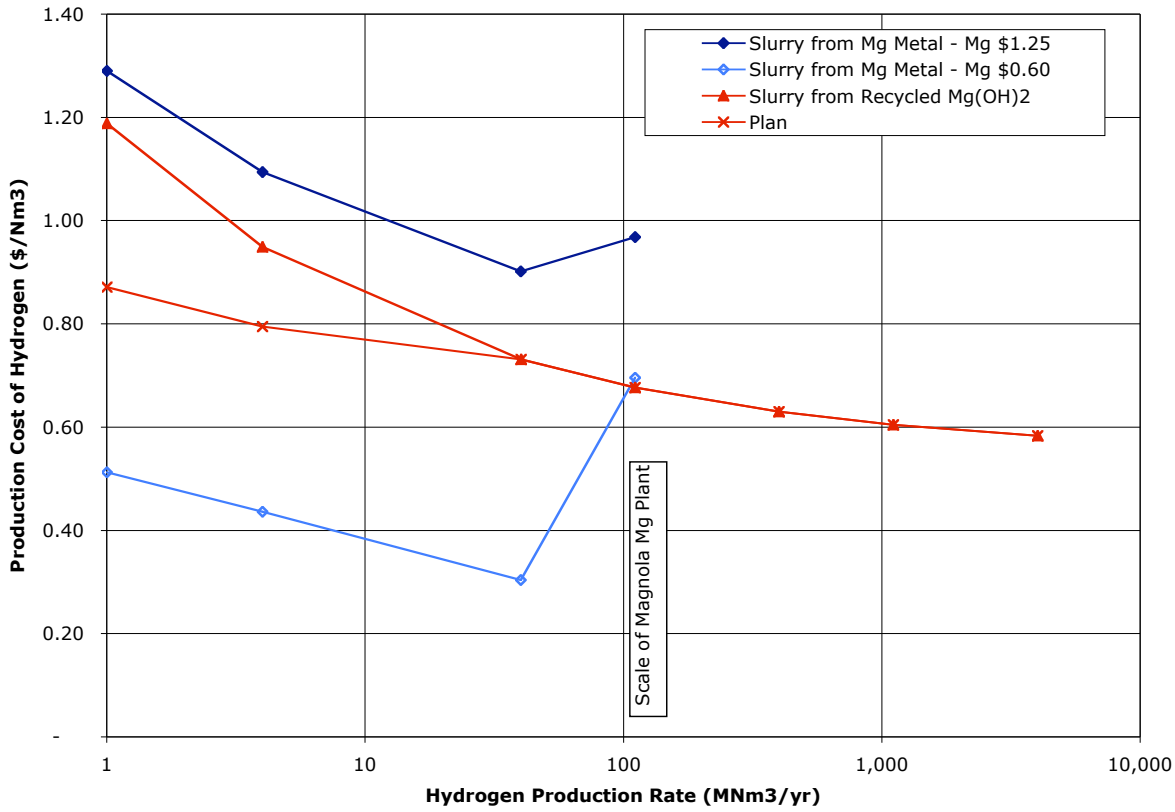

Figure 82 – Summary of Costs

5.6.3.5.7 Extrapolation to Large-Scale with Technological Improvements

Up to this point, we have been evaluating the costs associated with single plants. There are additional cost savings that can be expected from a large-scale system of production plants.

The United States currently consumes about 9 million barrels of gasoline per day (Reference 15). This is about 138 billion gallons of gasoline per year and is equivalent the consumption of 200 million 20 mile-per-gallon vehicles driving 14,000 miles per year. If these vehicles were to be supplied this energy in hydrogen, they would require about 128 billion kg of hydrogen per year. The largest hydrogen production plants currently built, produce about 558,000 kg/day or 204,000 metric tonnes/year (Krupp Uhde press release 10/12/1998). Thus, to meet this scale of demand, the U.S. would need 628 of these large steam methane reformation plants. (This assumes that the required methane is available). If MgH_2 slurry is used to carry hydrogen, 769 million tonnes per year of Mg will need to be processed. If 1000 plants are built, each would need a capacity of 769,000 tonnes/year. The largest Mg plants today have a capacity of 60,000 tonnes/year. However, aluminum plants are an order of magnitude larger in scale than Mg plants. Even larger capacity magnesium plants should be achievable.

Safe Hydrogen has estimated the cost of hydrogen from chemical hydride slurry in several steps (see Figure 83). The first two estimates are based on data for existing and past commercial scale magnesium production facilities. The following three estimates show the effect of potential technology advances.

At the 40 million Nm^3/year (3.6 million kg/year) scale, we have assumed that the byproduct slurry will be recycled for the oils and dispersants. The magnesium hydroxide will be sold as a salable byproduct. This approach will work for relatively small-scale operation until the magnesium hydroxide sales make up a large part of the existing magnesium hydroxide market. Beyond this scale, we assume that magnesium recycle from the spent magnesium hydroxide will be required.

At 4 billion Nm^3/yr (360 million kg/yr), we are assuming a large carbothermic reduction plant. This plant will only be about 4 times larger than the largest existing aluminum smelting plants however. Economies of scale result in reduced cost of magnesium. We assume that capital costs are scaled as the 2/3 power law of the scale ratio.

The 20 billion Nm^3/year (1.8 billion kg/yr) plant estimate assumes that slurry production will be achieved with many large magnesium production plants. Economies are achieved by integrating overhead functions and minimizing the duplication of functions that can be eliminated in individual plants.

The first 100 billion Nm^3/year estimate assumes the use of new technology to reduce the energy and labor requirements of the magnesium reduction process. The Solid Oxide Membrane approach under investigation at Boston University was used as a model. The SOM process has already demonstrated that it can produce magnesium from magnesium oxide at 10 kWhr/kg of magnesium. The existing electrochemical processes require 16 to 20 kWhr/kg Mg. The theoretical need is 6.9 kWh/kg Mg. So there is still room for improvement. The SOM process will eliminate the chlorine cycle and will simplify the processing so less cost will be incurred for plant and operating expenses.

The final 100 billion Nm^3/yr estimate assumes that there are some additional savings to be achieved in a fully mature industry and that the electric energy costs can be reduced from $0.03/kWhr to $0.02/kWhr when operating a modern power plant at full load continuously. Also recent conversations with wind power companies indicate that wind power can now be supplied to produce electricity at $0.025/kWhr when the equipment can be fully utilized in parts of the U.S. Midwest. We have assumed that continuing technology advances will allow us to take advantage of reduced energy costs. Co-location of the magnesium reduction plant can also reduce system costs.

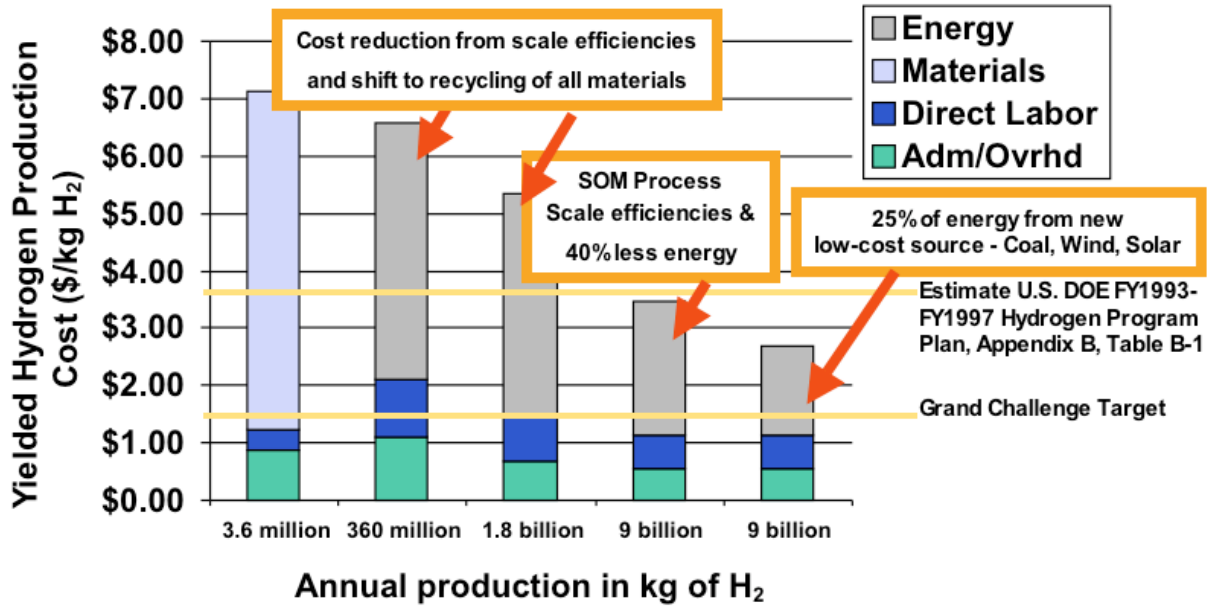

Figure 83 - Production Cost Drivers

5.6.3.5.8 References

13. Internet based prospectus for the Magnesium Alloy Corporation project planned for the Republic of Congo: http://www.magnesiumalloy.ca/project

14. Elkins, D.A., P.L. Placek, and K.C. Dean, An Economic and Technical Evaluation of Magnesium Production Methods (In Three Parts) 2. Carbothermic, United States Department of the Interior, Bureau of Mines, Bureau of Mines Report of Investigations RI 6946, May 1967, copy located at the Texas College of Arts & Industry Government Documents Depository, Kingsville, Texas [23 U43 6946]

15. Energy Information Administration/ Petroleum Supply Annual 2002, Volume 1, page 17, Table S4. Finished Motor Gasoline Supply and Disposition, 1986 – Present. This can be found in file “volume1_all-Pet Supply Annual 2003.pdf” at http://www.eia.doe.gov/oil_gas/petroleum/info_glance/gasoline.html

5.6.3.6 COMPARISON OF ANALYSES

5.6.3.6.1 Overview

This section discusses a set of analyses performed to evaluate the cost of hydrogen resulting from the use of a magnesium hydride slurry system. These analyses use the results of work performed by the team members to evaluate the capital, installation, and operating costs associated with various methods of reducing magnesium from magnesium oxide. The evaluation of the capital costs of the processes has proven more difficult than originally anticipated. Work on the estimation of capital costs is still in progress. To meet the objectives of the economic analyses, the capital costs have been based on comparing detailed analyses performed in the 1960's with the capital costs reported in the literature for magnesium chloride reduction processes.

The results of this study have been very encouraging. We conclude that the cost of hydrogen in a large-scale mature system should be below $4/kg of hydrogen. The SOM process currently provides the lowest cost hydrogen of the systems studied.

This section of the report will begin with a discussion of the basis of the analyses. In this section, assumptions will be discussed and defended.

The next section of the report will discuss the magnesium hydride slurry process and the costs associated with the various sub-processes. This will be followed by a section describing the analyses performed to estimate the cost of hydrogen.

The last section will describe the costs associated with producing, and transporting liquid hydrogen and compressed hydrogen.

5.6.3.6.2 Basis of Analysis

Assumptions

The primary contention that this study is testing is that the cost of packaged hydrogen can be significantly reduced by producing it at large-scale as chemical hydride slurry and then transporting the high-density slurry using the existing liquid fuel infrastructure. This contention relies on the recognition (and assumption of validity) that process costs have been observed to increase by the six-tenths power of the ratio of the scale increase. So if the costs can be estimated or measured for one scale, the capital costs of larger scale systems can be estimated using the six-tenths power law relationship. Several questions arise with this assumption.

What should the maximum scale of the system be?

Can magnesium be produced at larger scale with current or proposed process technologies?

How will the proposed process compare with other process options for the production and distribution of hydrogen?

Another important assumption made during this study is that the primary energy source should minimize the release of CO_2 to the atmosphere and that it should be one that can be relied upon for the long term. This assumption allows us to consider renewable energy sources, nuclear, some fossil fuel processes. Fossil fuel processes that can sequester the carbon dioxide are considered. Natural gas would appear to be a good primary energy source since it has so much energy and hydrogen per unit carbon content. However, the U.S. production rate of natural gas is at or near its peak and if it

must be imported, supply and political problems similar to those we are experiencing with oil can be expected.

Table 44 is included to summarize these and other assumptions made in the analyses.

Table 44 - Table of Assumptions

Scale capital costs using 6/10 power law	6/10
Assume some operating costs also scale using an 8/10 power law	8/10
Internal rate of return on capital	10%
Primary energy choice should minimize CO_2 release to atmosphere	
Primary energy source should have long term stability	No CH_4
Nuclear power plant efficiency (GEN IV Nuclear Generator)	45%
Thermal conversion efficiency of heat to hydrogen using GEN IV generator	50%
Cost of electricity from GT-MHR (GEN IV) Nuclear Generator	$0.029
Cost of hydrogen from GT-MHR (GEN IV) Nuclear Generator	$1.65/kg
Capital cost of GT-MHR (GEN IV) Nuclear Generator	$975/kWe

Scale of System

The system scale for supplying hydrogen for the entire U.S. automobile fleet is large. The U.S. consumed 9,000,000 barrels of oil a day in 2004 (Reference 16) to operate its automobile fleet. This is equivalent to 5 billion MWhrth of thermal energy. To provide this amount of energy with hydrogen will require 128 million metric tonnes of hydrogen per year. If this hydrogen is made by thermal processes using heat from a GEN IV nuclear power plant, 533 plants will be required. If it is produced using electrolysis, then 632 plants will be required.

To gain some perspective of the scale of this system, we can compare it to our electrical generating system. Our electrical generation system consumed 11.6 billion MWhrth of thermal energy in 2003 to produce 4 billion MWhe of electric power (Reference 17) in 16755 plants with an installed nameplate capacity of 1 million MWe. The U.S. has about 468 plants with nameplate capacity of greater than 500 MWe (Reference 18). To meet the needs of our automobile hydrogen demand, we will need to add between 576,000 and 683,000 MWe of baseload capacity.

This is a big system. It can be addressed with large-scale processes.

Scale of Project

Based on the 6/10 power law, the cost of a process per unit of product will continue to decrease with increases in scale. What is a reasonable upper limit for the scale of a process? If the process is at such a scale than only one plant is required to meet the market demand, then the process is probably too large. If the cost of the plant is larger than anything ever attempted by people, then the process is probably too large. A large project that is nearing successful completion is the Big Dig Project in Boston. This is a $14 billion project. There is a lot of criticism that the project has been

mismanaged and that costs are inflated. Perhaps this scale of project is at the limit of our current abilities. If so, the scale of individual projects should be less than $10 billion.

The Gas Turbine Modular Helium Reactor (GT-MHR) under investigation as part of the GEN IV program is estimated to cost $975/kWe (Reference 19, 20, 21). A four-module plant would produce 2,400 MWth and 1,080 MWe. The capital cost is estimated to be about $1 billion. So this power plant is about the right scale. It could perhaps be larger with some experience.

There are currently about 170,000 gasoline station sites in the U.S (Reference 22). These stations sell about 2550 gallons of gasoline per day per site. If there are 1000 plants required to produce hydrogen, then each plant will be delivering to 170 stations.

Scale of Magnesium Plant vs Aluminum Plant

The largest magnesium plants produce about 60,000 metric tonnes/year. The largest aluminum plant produces about 1,000,000 metric tonnes/year. Magnesium requires a theoretical 6.87 kWh/kg of electric power. Aluminum requires a theoretical minimum of 8.63 kWh/kg. The price at year end 2004 was $3.86/kg for magnesium and $1.81/kg for aluminum. Based on the theoretical minimum energy required, it would appear that magnesium should be cheaper. Prior to the development of the SOM process, the production of magnesium has required a more complex process and the efficiency of production has been higher for aluminum than for magnesium.

The scale of a magnesium plant to work with one of the power plants noted in the previous section will be about 733,000 metric tonnes per year. This is larger than the world production rate for magnesium in 2004 of 722,000 metric tonne per year. The production rate of aluminum was about 26,200,000 metric tonne per year in 2004 however. So if the cost of producing magnesium could be lower than that required to produce aluminum, the market for magnesium could expand rapidly.

5.6.3.6.3 Magnesium Hydride Slurry Process

The magnesium hydride slurry process is shown graphically in Figure 84. Magnesium hydride slurry is made at a large scale plant to minimize costs by taking advantage of economies of scale. The slurry is transported by the existing liquid fuel infrastructure to the market where hydrogen is produced by mixing the slurry with locally available water as hydrogen is needed. The byproduct is returned to the distributor, who returns it to the production plant in the same truck that delivers the slurry. There may be a depot between the production facility and the distributor. In this case, the slurry might be transported to the depot by barge or rail to further reduce the transportation costs. Slurry will have a shelf life sufficient to travel by rail or barge, unlike liquid hydrogen.

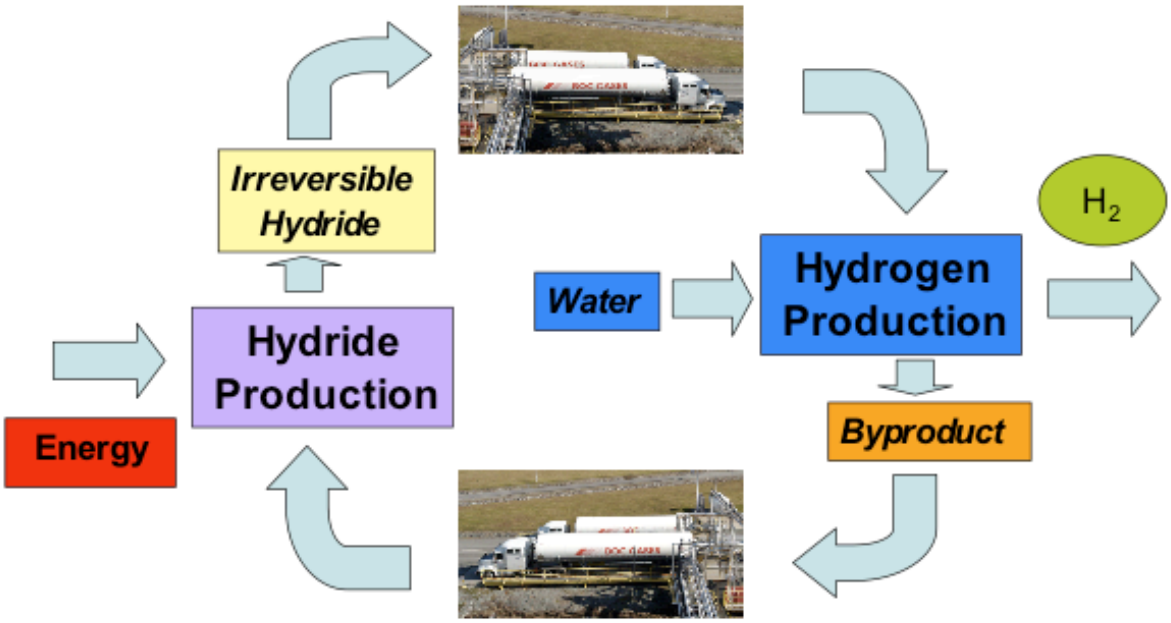

Figure 84 - Magnesium Hydride Slurry Process

At the production plant, the byproduct is separated into oils and solids. (It may turn out to be cost effective to preprocess the byproduct at a depot). Figure 85 displays the magnesium hydride slurry production process. This process is similar to the current magnesium production processes except that its reactant is a high grade magnesium hydroxide or magnesium oxide and its product probably does not have to be structural grade magnesium. The first step is to separate the oils from the solids. This can be performed using a standard solvent separation system. The oils will be reused and must be cleaned and tested prior to remixing slurry.

The second step is to calcine the magnesium hydroxide to magnesium oxide. Next, the magnesium oxide is fed to the reduction process and magnesium is produced. Then the magnesium is powdered and hydrided prior to being fed to the slurry preparation subsystem.

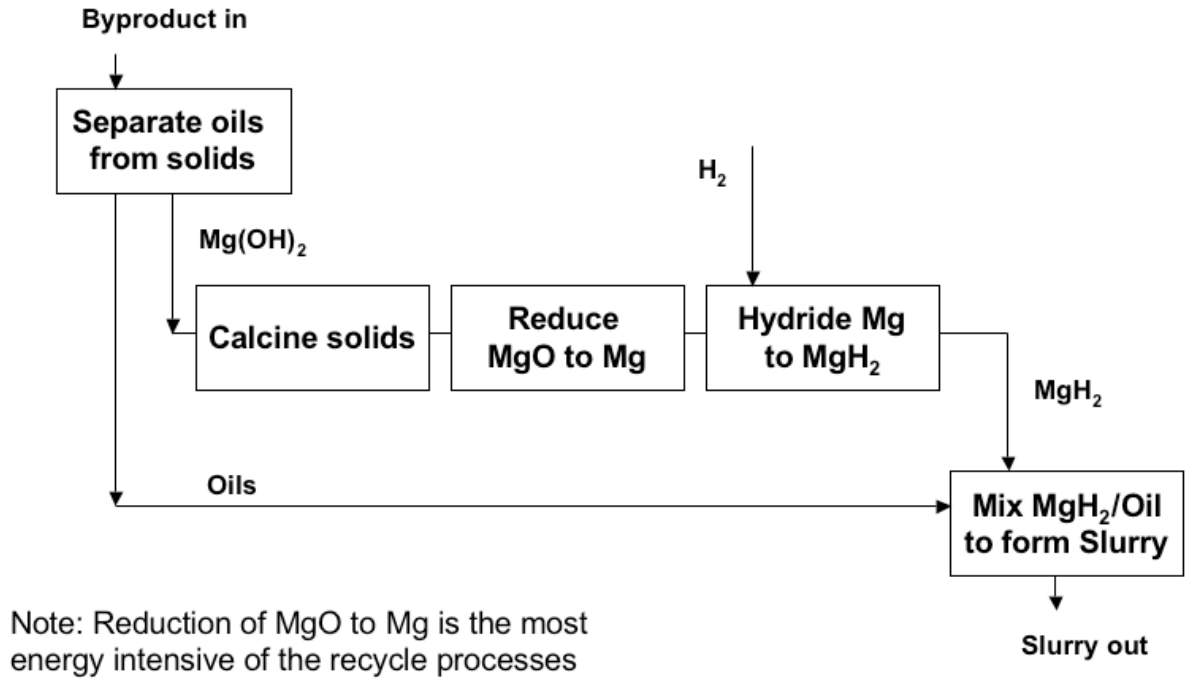

Figure 85 - Magnesium Hydride Slurry Production Process

5.6.3.6.4 *Magnesium Reduction Technologies*

There are several options for the reduction of magnesium oxide to magnesium metal. The most prevalent processes in operation today are the magnesium chloride process and the ferro-silicon process. There are several variations on the magnesium chloride process that solve the production of molten anhydrous magnesium chloride differently. Magnesium can also be produced using a carbothermic process that was used commercially in the 1940's and 1950's. Recent developments may have solved some of the problems that were observed in the earlier commercial process. A new process, invented by researchers at Boston University, uses a solid oxide membrane to separate oxygen from magnesium in an electrolysis process. This process, the Solid Oxide oxygen ion Membrane (SOM) process, passes a current through a flux containing magnesium oxide. Oxygen ions move through the membrane and are removed from the system in an anode. Magnesium is evolved as a vapor in an argon stream.

This study has made an initial estimate of the capital, installation, and operating costs of magnesium hydride slurry processes with a magnesium chloride process, a carbothermic process, and a SOM process in the magnesium oxide reduction sub-process.

Table 45 displays some of the challenges and benefits of the various magnesium oxide reduction technologies. The carbothermic process is attractive because it promises lower capital cost than the magnesium chloride process. Its drawback is that it produces carbon dioxide that will need to be sequestered.

The magnesium chloride process is attractive because of the large body of knowledge about the process. It is troubled by chlorine emissions, chlorine processing, and high energy consumption.

The SOM process promises very low capital costs, a small plant footprint, and low energy costs. Its challenge is its newness and the need to scale it to much larger operating scales.

The metallothermic ferro-silicon process uses primarily thermal energy. However, it uses ferro-silicon as a reactant that removes the oxygen from the magnesium oxide. The byproduct from the reaction must be disposed or recycled. It is currently labor intensive and like the carbothermic process, CO_2 must be sequestered.

Table 45 - Process Comparison

Process	Challenges	Benefits
Carbothermic	CO_2	Low capital cost
Magnesium Chloride	Cl emissions, Cl processing, energy consumption is high	Considerable process experience (existing primary method for reducing Mg)
Solid Oxide Membrane	Scale-up	Low energy cost, reduced footprint, potentially low capital cost
Metallothermic	Reduction of waste products, currently labor intensive, CO_2	Thermal decomposition

5.6.3.6.5 *Calculation of Costs for Processes*

The capital and installation costs can be estimated in either a top down approach or a bottom up approach. In a bottom up approach, the process is defined in as much detail as possible but at the least identifying major pieces of equipment. Then estimates are made for the installation labor. Common factors are used to estimate buildings, permits, etc. In this approach, the operating costs are estimated for each process and again common factors are used for maintenance costs, overhead, payroll, taxes, etc. The capital costs are summed to obtain an overall cost and the operating costs are summed to obtain an operating cost. Then the cost of the process is determined by calculating the income required to balance the capital and operating costs assuming an internal rate of return. This is the approach that we used to estimate the capital and operating costs of a 20,000 metric tonne per year magnesium production plant.

A top down approach can be used to determine the capital costs. In this approach a plant with a similar design is used as a model to identify the overall capital and installation costs. This approach was used to estimate the costs of the magnesium chloride process and the carbothermic process incorporating the latest technology. In the top down approach, variations in the scale are estimated using the 6/10 power law.

The magnesium chloride plant analysis used inputs from a bottom up analysis for the operating and labor costs and inputs from a top down analysis for the capital and

installation costs. Table 45 and Table 47 display the baseline analysis in the column labeled Baseline. The baseline is based on a Magnesium Alloy Corporation prospectus about Noranda's Magnola plant. This plant was designed for 63,000 metric tonne per year. It is similar to other magnesium chloride plants with a capital cost of about $8,600/metric tonne of magnesium capacity. Also shown in these tables are columns for a plant scaled to work with a GT-MHR nuclear power plant, a column at a scale five times larger, and a column for a scale comparable to the carbothermic reduction system.

Table 46 - Magnesium Chloride Process Analysis

Scale-up analysis of MgCl2 plant. Data from Magnesium Alloy Corporation prospectus about Noranda's Magnola plant.

				Baseline	Scale	Scale	Scale
Capital cost	Scale factor			1	11.63	58.17	0.35
	Mg plant Capital cost	$/metric ton Mg		8,600			
	plant capacity	metric ton/year		63,000	733,000	3,665,000	21,773
	Scale exponent				0.60	0.60	0.60
	Total Plant capital			541,800,000	2,362,093,344	6,204,103,844	286,408,323
	Additional capital cost				-	-	-
	Working capital				-	-	-
	Capital cost	$		541,800,000	2,362,093,344	6,204,103,844	286,408,323
Operating cost							
	Electricity	kWh/metric ton		16,000	10,000	10,000	10,000
	Electricity price	$/kWh		0.022	0.029	0.029	0.029
	Electricity cost	$/yr		22,176,000	212,570,000	1,062,850,000	6,314,170
	Hydrogen	mt H2/mt Mg		12.0599	12.0599	12.0599	12.0599
	Hydrogen produce	metric ton/year		5,223.92	60,779.94	303,899.70	1,805.40
	Hydrogen price	$/kg		1.65	1.65	1.65	1.65
	Hydrogen cost	$/yr		8,619,474	100,286,901	501,434,506	2,978,918
	Other materials	$/yr	5.0%	1,108,800	10,628,500	53,142,500	315,709
	Scale exponent				0.80	0.80	0.80
	Labor	manyears/year		150	1,068	3,871	64
	hours/manyear	hours		2,080	2,080	2,080	2,080
	hourly cost	$/hr		15.00	15.00	15.00	15.00
	Labor cost	$/yr		4,680,000	33,331,633	120,790,449	2,000,359
	Supervision	$/yr	15.0%	702,000	4,999,745	18,118,567	300,054
	Plant Maintenance						
	Labor	$/yr	1.5%	8,127,000	35,431,400	93,061,558	4,296,125
	Supervision	$/yr	15.0%	1,219,050	5,314,710	13,959,234	644,419
	Materials	$/yr	100.0%	8,127,000	35,431,400	93,061,558	4,296,125
	Payroll overhead	$/yr	6.0%	883,683	4,744,649	14,755,788	434,457
	Operating Supplies	$/yr	5.0%	873,653	3,808,876	10,004,117	461,833
	Indirect Cost						
	Admin & Overhead	$/yr	50.0%	12,306,193	61,531,207	181,875,636	6,216,686
	Fixed Cost						
	Taxes & Ins	$/yr	2.0%	10,836,000	47,241,867	124,082,077	5,728,166
	Depreciation	$/yr	5.0%	27,090,000	118,104,667	310,205,192	14,320,416
	Total Operating Cost	$/yr		106,748,853	673,425,555	2,597,341,183	48,307,438
		$/metric ton Mg		1,694	919	709	2,219

The results of this analysis are shown in Table 47.

Table 47 - Magnesium Chloride Hydrogen Cost Calculation

Scale-up analysis of MgCl2 plant. Data from Magnesium Alloy Corporation prospectus about Noranda's Magnola plant.

		Baseline	Scale	Scale	Scale
Scale factor		1	11.63	58.17	0.35
Mg plant Capital cost	$/metric ton Mg	8,600			
plant capacity	metric ton/year	63,000	733,000	3,665,000	21,773
Income (Use Goal Seek to make IRR=10% by changing this value)	$/yr	170,434,989	951,087,395	3,322,539,650	81,989,563
IRR	%	10%	10%	10%	10%
H2 produced from slurry	metric ton/year	10,448	121,560	607,799	3,611
Operating Cost of Mg	$/kg Mg	1.69	0.92	0.71	2.22
	$/lbm Mg	0.77	0.42	0.32	1.01
Operating Cost of H2	$/kg H2	10.22	5.54	4.27	13.38
Cost of Mg produced	$/kg Mg	2.71	1.30	0.91	3.77
	$/lbm Mg	1.23	0.59	0.41	1.71
Cost of H2 produced	$/kg H2	16.31	7.82	5.47	22.71

The cost of hydrogen using a conventional magnesium production technology is estimated to be $16.31/kg of H_2 at the current magnesium reduction scales. At the power plant scale, the cost would drop to $7.82/kg. A lower cost magnesium reduction system is needed.

Table 48 displays the design assumptions used to design the SOM Cell that might replace the magnesium chloride system shown in the previous tables.

Table 48 - SOM Cell Design Assumptions

Cell production rate	metric ton/year	730
Anode		
ZrO2 tubes	# tubes/cell	37
Cost ZrO2	$/kg	31
Material costs	% of total cost	60%
Cost of tubes/cell	$/cell	11,531
LSM coating inside tube		
mass LSM per unit area	gm/cm2	0.120
unit cost LSM	$/kg	208
Cost LSM	$/cell	4,517
Cathode		
Cathode diameter	cm	32
Cathode Length	cm	100
Cathode thickness	cm	0
Open area fraction in cathode	%	1
density of steel	gm/cm3	8
unit cost of steel	$/kg	0
Cost of steel for cell	$/cell	69
Cell container		
density insulation	gm/cm3	0.80
unit cost of insulation	$/kg	0.10
cost of insulation	$/cell	4,855
thickness steel	cm	1
cost of steel enclosure	$/cell	2,571
electrolyte		
density electrolyte	gm/cm3	3
unit cost electrolyte	$/kg	1
cost of electrolyte	$/cell	14,740
Power supply estimate		
Power Supply unit costs	$/metric ton capacity	120
Power Supply cost for cell	$	87,600
Cost summary for 1 cell		
total	$	125,884

Table 49 displays the costs of the SOM based magnesia reduction system used in the bottom up approach. Table 50 through Table 53 display comparisons between three SOM design options. The SOM – Ag Anode design uses a silver anode. Oxygen entering the silver anode bubbles out of the silver and can be captured for sale or released to the atmosphere. The SOM – Tin/H_2 anode design refers to a design in which the oxygen reacts with hydrogen in the tin anode and leaves the anode as water vapor. The SOM - LSM coated anode refers to a design that uses an LSM coating on

the inside of the membrane to combine hydrogen atoms into molecules that will either be captured or released.

The results of this analysis is shown in Table 53. The cost of hydrogen ranges from $6.54/kg to $9.81/kg with the SOM – LSM coated anode the lowest cost option. The SOM - LSM coated anode has the lowest capital and operating costs. These costs are for a relatively small plant of 21,773 metric tonne per year of magnesium. It is necessary to evaluate the costs of a larger scale unit.

Table 49 – SOM-LSM Based MgH_2 Slurry Plant Magnesium Sub-Process

Magnesia Reduction - SOM						
Direct Construction Cost						
SOM Cell - ZrO2 tubes		4,000	15	345,927	60,000	405,927
SOM Cell - LSM coating on Anode		2,000	15	119,418	30,000	149,418
SOM Cell - Steel Cathode		2,000	15	2,071	30,000	32,071
SOM Cell - Insulation		1,000	15	145,665	15,000	160,665
SOM Cell - Steel Structure		600	15	77,141	9,000	86,141
SOM Cell - Electrolyte		1,000	15	442,199	15,000	457,199
SOM Cell - Power Supply & dist		3,000	15	2,628,000	45,000	2,673,000
Gas Lock	0.149	1,222	15	80,484	18,333	98,817
Heat exchanger, 6720 ft2	0.100	3,259	15	319,385	48,889	368,274
Bag filter	0.120	5,630	15	459,958	84,444	544,403
Centrifugal compressor	0.150	13,000	15	1,100,000	195,000	1,295,000
Bins and hoppers	0.100	1,926	15	189,009	28,889	217,898
Materials handling equipment	0.196	6,185	15	310,645	92,778	403,423
total	0.139					6,892,236
Foundations	0.065					445,595
Structures	0.046					318,317
Buildings	0.226					1,556,782
Insulation	-					-
Instrumentation	0.035					240,684
Electrical work	0.083					573,116
Piping	0.046					318,317
Painting	0.010					70,818
Miscellaneous	0.092					636,877
total						4,160,505
Total Direct Construction						11,052,741
Indirect cost, contingency, and fee	0.4000					4,421,096
Interest during construction	0.0700					773,692
Total Fixed Capital						16,247,529

Table 50 - Comparison of SOM Design Options Capital Costs

Summary of SOM analyses			SOM - Ag anode	SOM - Tin/H2 anode	SOM - LSM coated anode
Production rate		ton Mg/yr	24,000	24,000	24,000
		metric ton Mg/yr	21,773	21,773	21,773
		metric ton H2 from slurry/yr	3,334	3,334	3,334
Capital Costs					
	Plant processes				
	Tank storage- Spent Hydroxide Slurry	$	924,467	924,467	924,467
	Solvent Separation	$	2,125,151	2,125,151	2,125,151
	Calcining	$	7,141,260	7,141,260	7,141,260
	Magnesia Reduction - SOM	$	72,305,543	16,959,789	16,247,529
	Hydride Process	$	4,572,628	4,572,628	4,572,628
	Slurry Production	$	1,900,942	1,900,942	1,900,942
	Total Plant	$	88,969,991	33,624,236	32,911,976
	Additional Capital costs				
	Plant Facilities, 10%	$	8,896,999	3,362,424	3,291,198
	Plant utilities, 12%		10,676,399	4,034,908	3,949,437
	Total Fixed Capital	$	108,543,389	41,021,569	40,152,611
	Working Capital	$	5,565,243	5,321,503	4,614,874
	Total	$	114,108,632	46,343,072	44,767,486
		$/(metric ton/yr)	5,241	2,128	2,056

Table 51 - Comparison of SOM Plant Design Options Operating costs

Summary of SOM analyses			SOM - Ag anode	SOM - Tin/H2 anode	SOM - LSM coated anode
Operating Costs					
	Energy Consumption				
	Electric Power	MWhr	-	-	-
	69 kV		217,727	217,727	217,727
	2300V		-	-	-
	440V		454	454	454
	Total Electric Energy	MWhr	218,181	218,181	218,181
	Power Required for electricity	MW	26	26	26
	Hydrogen for hydriding	kg/yr	1,805,379	1,805,379	1,805,379
	Hydrogen for SOM	kg/yr		1,805,379	
	Slurry oil	kg/yr	356,773	356,773	356,773
	Dispersant	kg/yr	15,512	15,512	15,512
	replacement ZrO2 tubes		2,220	2,220	2,220
	Production				
	Magnesium metal	ton	24,000	24,000	24,000
	Direct Cost				
	Electric Power				
	69 kV	$/kWhr	6,314,083	6,314,083	6,314,083
	2300V	$/kWhr	-	-	-
	440V	$/kWhr	13,166	13,166	13,166
	Hydrogen for hydriding	$/kg	2,978,875	2,978,875	2,978,875
	Hydrogen for SOM	$/kg		2,978,875	
	Slurry oil	$/kg	396,018	396,018	396,018
	Dispersant	$/kg	223,526	223,526	223,526
	replacement ZrO2 tubes		692,640	692,640	930,180
	Total		10,618,308	13,597,183	10,855,848

Table 52 - Comparison of SOM Plant Design Options Labor costs

Summary of SOM analyses			SOM - Ag anode	SOM - Tin/H2 anode	SOM - LSM coated anode
Direct Labor					
Labor		hr	33,280	33,280	33,280
		manyears	16	16	16
Labor		$/hr	499,200	499,200	499,200
Supervision			74,861	74,861	74,861
Total			574,061	574,061	574,061
Plant Maintenance					
Labor			1,023,123	992,382	1,012,894
Supervision			204,733	198,578	202,579
Materials			920,986	890,245	910,758
Total			2,148,841	2,081,205	2,126,230
Payroll Overhead			333,382	326,555	331,091
Operating Supplies			429,822	416,292	425,299
Total direct cost			14,341,955	17,232,837	14,312,530
Indirect Cost					
Administration and Overhead			1,760,801	1,715,825	1,745,761
Fixed Cost					
Taxes and Insurance			1,709,826	656,166	642,606
Depreciation			4,448,391	1,681,186	1,645,574
Total			6,158,217	2,337,352	2,288,180

Table 53 - Comparison of SOM Plant Design Options Cost of Hydrogen

Summary of SOM analyses			SOM - Ag anode	SOM - Tin/H2 anode	SOM - LSM coated anode
Calculate rate of return					
	Capital cost	$	114,049,247	46,283,687	44,739,229
	Operating Costs	$/yr	22,023,433	21,048,474	18,346,471
	Income	$/yr	35,433,679	26,484,222	23,607,473
	Internal rate of return	%	10%	10%	10%
	Cost of hydrogen	$/kg	9.81	7.33	6.54
	Mg produced	metric ton/yr	21,773	21,773	21,773
	Cost of magnesium	$/kg	1.63	1.22	1.08
		$/lb	0.74	0.55	0.49
	Energy per unit Mg produced	kWhr/kg Mg	10	10	10

5.6.3.6.6 □ *Calculation of Costs at Large Scale*

Table 54 and Table 55 describe the costs associated with a SOM – LSM Plant scaled to a GT-MHR scale and to a scale five times larger. At the power plant scale, the cost of hydrogen is estimated to be $3.91/kg. This would be a cost at the production plant.

Table 54 - Capital and Operating Costs for SOM LSM Plant

				Baseline	Scale	Scale
Capital cost						
	Scale factor			1	33.58	167.91
	Mg plant Capital cost	$/metric ton Mg		2,056		
	plant capacity	metric ton/year		21,773	731,174	3,655,870
	Scale exponent				0.60	0.60
	Total Plant capital			32,911,976	271,031,362	711,871,408
	Additional capital cost			7,240,635	59,626,900	156,611,710
	Working capital			4,614,874	38,003,665	99,817,682
	Capital cost	$		44,767,486	368,661,926	968,300,799
Operating cost						
	Electricity	kWh/metric ton		10,000	10,000	10,000
	Electricity price	$/kWh		0.029	0.029	0.029
	Electricity cost	$/yr		6,314,071	212,040,460	1,060,202,300
	Hydrogen	mt H2/mt Mg		12.0599	12.0599	12.0599
	Hydrogen produce	metric ton/year		1,805.38	60,628.53	303,142.65
	Hydrogen price	$/kg		1.65	1.65	1.65
	Hydrogen cost	$/yr		2,978,871	100,037,073	500,185,366
	MgH2 mass fraction	%		76%	76%	76%
	Slurry oil (95% recycle)	metric ton/year		357	11,981	59,906
	Slurry oil price	$/kg		1.11	1.11	1.11
	Slurry oil cost	$/yr		396,018	13,299,157	66,495,785
	Dispersant (95% recycle)	metric ton/year		16	521	2,605
	Dispersant price	$/kg		14.41	14.41	14.41
	Dispersant cost	$/yr		223,526	7,506,496	37,532,482
	production per cell			730	730	730
	Number Cells			30	1,002	5,008
	Tubes per cell			37	37	37
	Tube life	months		6	6	6
	Tube cost	$/tube		419	419	419
	Annual Tube replacement cost	$/yr		927,079	31,058,710	155,281,149
	Other materials	$/yr	0.0%	-	-	-
	Total materials	$/yr		10,839,565	363,941,897	1,819,697,081

Table 55 - Labor and Cost Estimate for SOM LSM Plant

			Baseline	Scale	Scale
Scale factor			1	33.58	167.91
Mg plant Capital cost	$/metric ton Mg		2,056		
plant capacity	metric ton/year		21,773	731,174	3,655,870
Scale exponent				0.80	0.80
Labor	manyears/year		16	266	964
hours/manyear	hours		2,080	2,080	2,080
hourly cost	$/hr		15.00	15.00	15.00
Labor cost	$/yr		499,200	8,301,604	30,084,169
Supervision	$/yr	15.0%	74,880	1,245,241	4,512,625
Plant Maintenance					
Labor	$/yr	3.00%	987,359	8,130,941	21,356,142
Supervision	$/yr	20.0%	197,472	1,626,188	4,271,228
Materials	$/yr	80.0%	789,887	6,504,753	17,084,914
Payroll overhead	$/yr	18.5%	325,399	3,571,235	11,141,471
Operating Supplies	$/yr	20.0%	394,944	3,252,376	8,542,457
Indirect Cost					
Admin & Overhead	$/yr	50.0%	1,634,570	16,316,169	48,496,503
Fixed Cost					
Taxes & Ins	$/yr	2.0%	658,240	5,420,627	14,237,428
Depreciation	$/yr	5.0%	1,645,599	13,551,568	35,593,570
Total Operating Cost	$/yr		18,047,114	431,862,599	2,015,017,590
	$/metric ton Mg		829	591	551
Income (Use Goal Seek to make					
IRR=10% by changing this value)	$/yr		23,305,930	475,161,100	2,128,892,305
IRR	%		10%	10%	10%
H2 produced from slurry	metric ton/year		3,611	121,257	606,285
Operating Cost of Mg	$/kg Mg		0.83	0.59	0.55
	$/lbm Mg		0.38	0.27	0.25
Operating Cost of H2	$/kg H2		5.00	3.56	3.32
Cost of Mg produced	$/kg Mg		1.07	0.65	0.58
	$/lbm Mg		0.49	0.29	0.26
Cost of H2 produced	$/kg H2		6.45	3.92	3.51

5.6.3.6.7 □ Transportation Costs

Table 56 summarizes the assumptions used to estimate the costs associated with transporting slurry by truck for a distance of 500 miles from the production plant. Costs range from $0.188/kg to $0.356/kg of hydrogen depending on whether the trailer carries slurry or byproduct. Since the byproduct weighs so much more than the slurry, it may be less expensive to perform some of the separation at the depot.

Table 56 - Transportation Costs

- Assumptions
  - Largest fuel truck
    - Maximum capacity 34,020 kg (75,000 lb)
    - Volume 41,640 L (11,000 gallons)
  - Cost of Truck - $90,000
  - Cost of Trailer - $100,000
  - Miles driven - 500
  - Deliveries - 353 days/year
  - Drivers - 1
  - Average speed - 50 miles/hour
  - Depreciation - 7 years
  - Working days/year - 230 days
  - Cost of Driver - $40,000
  - Overhead on Driver - 25%
  - Cost of fuel - $1.50/gallon
  - Fuel Consumption - 6 miles/gallon
- Conclusion
  - Transportation cost $0.188/kg H2 to $0.356/kg H2

5.6.3.6.8 □ References

16 Source: Energy Information Administration/ Petroleum Supply Annual 2002, Volume 1, page 17, Table S4. Finished Motor Gasoline Supply and Disposition, 1986 – Present. volume1_all-Pet Supply Annual 2003.pdf. http://www.eia.doe.gov/oil_gas/petroleum/info_glance/gasoline.html

17 Energy Information Administration Annual Energy Review 2003, From file sec8.pdf.

18 Energy Information Administration, Form EIA-860, "Annual Electric Generator Report."

19 Interim Status Report for GFR (1-31-05).pdf describes Gen IV nuclear generators. Base design is expected to produce electricity at 42% efficiency. Alternate design is expected to have an efficiency of 45%.

20 NERI2004AnnualReport_FINAL.pdf discusses the costs of nuclear produced hydrogen. Page 61 notes a cost of 1.35/kg and $1.65/kg for sales of H_2 and O_2 vs H_2 only.

21 Status of the GT-MHR for Electricity Production, M.P. LaBar, A.S. Shenoy, W.A. Simon, And E.M. Campbell, World Nuclear Association Annual Symposium, London, 3-5 September 2003, labar.pdf

22. http://www.euromonitor.com/Gasoline_Station_Retailing_in_United_States

5.6.3.7 Efficiency Comparison

During the past quarter, the efficiency of a slurry based system for carrying hydrogen to a distribution station was compared to the efficiency of doing the same process with liquid and compressed hydrogen. The Argonne National Laboratory computer program FCHTool2.0.xls was used to perform this comparison. The conclusion of this study is that if hydrogen is produced by non-fossil fuels then the efficiency difference between slurry, compressed hydrogen, and liquid hydrogen is between 3% and 14.7%.

5.6.3.7.1 Objective

The objective of this study is to compare the efficiencies of hydrogen storage systems using compressed hydrogen, liquid hydrogen, and magnesium hydride slurry.

5.6.3.7.2 Method of Analysis

The Microsoft Excel tool, FCHtool2.0b.xls, prepared by the University of Chicago and written by R.K. Ahluwalia, T.Q. Hua, and J.K. Peng, was used to evaluate the efficiencies of these options.

5.6.3.7.3 Assumptions

The process includes the production of hydrogen, the storage of the hydrogen, and the distribution of the hydrogen. Two production technologies were assumed, steam methane reformation of natural gas and thermochemical production using heat from a nuclear power plant. The SMR process represents the current primary method of making hydrogen. The thermochemical process represents a non-fossil fuel technology that may be required to control CO_2 emissions. The source of the thermal energy was assumed to be from nuclear energy though it could have been from renewable sources such as solar. However, solar energy was not an option for thermal energy in the FCHtool2.0 model and sources are available that define the expected efficiency of a nuclear powered thermochemical process. Cases were run for biofuel supplying hydrogen and electricity and for renewable energy (solar and wind) supplying hydrogen via electrolysis and supplying electricity.

ResultsTable 57 shows the assumptions that were made for the hydrogen production and storage processes. The original sample cases provided with the model are included for comparison. Set 1 makes similar assumptions to the sample cases except that the specific energy required for regeneration was assumed to be 60.3 kWh/kg H_2. The SOM process has been shown to require less than 8 kWh/kg of magnesium in laboratory experiments. Boston University has estimated that a mature SOM magnesium reduction plant will require 10 kWh/kg Mg including electrolysis energy and thermal energy. The waste heat from this system should be sufficient to supply the energy requirements of the slurry production facility except for the production

of hydrogen. Since magnesium hydride hydrolysis produces twice as much hydrogen as is stored in the magnesium hydride molecule, there are 6.03 kg of magnesium required for each kg of hydrogen produced. Thus there are:

$$6.03 \text{ kg Mg/kg } H_2 * 10 \text{ kWh/kg Mg} = 60.3 \text{ kWh/kg } H_2.$$

Table 57 - Assumptions for H_2 Production and Storage

Title	H_2 prod	H_2 storage	Sp Energy H2 Storage	Sp Energy Regen
Sample cases included with model				
Sample-cH_2	SMR	compress 350bar	1.98	0
LH_2 per sample	SMR	Liquefaction	7.1	0
Sample-MgH_2	SMR	MgH_2 chem slurry	0	80
Set 1				
cH_2-CH_4	SMR	compress 350bar	1.98	0
LH_2-CH_4	SMR	Liquefaction	7.1	0
MgH_2 Slurry-CH_4	SMR	MgH_2 chem slurry	0	60.3
Set 2				
cH_2-Nuclear	Thermochemical	compress 350bar	1.98	0
LH_2-Nuclear	Thermochemical	Liquefaction	7.1	0
MgH_2 Slurry-nuclear	Thermochemical	MgH_2 chem slurry	0	60.3
Set 3				
cH_2-Biomass	Biomass	compress 350bar	1.98	0
LH_2-Biomass	Biomass	Liquefaction	7.1	0
MgH2 Slurry-Biomass	Biomass	MgH_2 chem slurry	0	60.3
Set 4				
cH_2-Renewable	Renewable	compress 350bar	1.98	0
LH_2-Renewable	Renewable	Liquefaction	7.1	0
MgH_2 Slurry-Renewable	Renewable	MgH_2 chem slurry	0	60.3

Table 58 shows the assumptions made for the transportation of the hydrogen. The sample case for MgH_2 assumed that 4,000 kg of H_2 would be delivered by a truck.

Recent evaluations by TIAX have concluded that the maximum truck cargo is about 24,750 kg (Graham Moore, Chevron). This is based on a 9,000-gallon gasoline truck trailor.

The H2A Delivery Analysis of 10 July 2006 shows liquid hydrogen trucks carrying 3,653 kg H_2. For this analysis, we used 2,000 kg H_2, which was the default in the FCHtool2.0b model. The efficiency for a 3,653 kg case improves from 98.02% to 98.81% for the distribution efficiency and from 36.7% to 36.81% for the Well-to-Tank efficiency.

Table 58 - Transportation Assumptions

Title	Transport Distance	Transport Storage	Transport mileage
	km	kg	mpg
Sample cases included with model			
Sample-cH_2	239	330	6
LH_2 per sample	239	2000	6
Sample-MgH_2	239	4000	6
Set 1			
cH_2-CH_4	239	330	6
LH_2-CH_4	239	2000	6
MgH_2 Slurry-CH_4	239	1735	6
Set 2			
cH_2-Nuclear	239	330	6
LH_2-Nuclear	239	2000	6
MgH_2 Slurry-nuclear	239	1735	6
Set 3			
cH_2-Biomass	239	330	6
LH_2-Biomass	239	2000	6
MgH_2 Slurry-Biomass	239	1735	6
Set 4			
cH_2-Renewable	239	330	6
LH_2-Renewable	239	2000	6
MgH_2 Slurry-Renewable	239	1735	6

Table 59 displays the assumptions used for the electrical energy generation and transmission assumptions. The sample cases assume that the process will be powered by grid electricity so they include an 8% loss due to transmission. The assumption for this study is that all the cases will employ large-scale production of hydrogen and that electric power requirements will be supplied by on-site electric power production. A transmission loss for this condition of 1% is assumed.

An efficiency of 45% is assumed for the nuclear power plant option as defined by references 23 and 24. The efficiency of the biomass and renewable energy options was provided by the program.

Table 59 - Electrical Energy Generation and Transmission Assumptions

Title	Electric Generation	Transmission Efficiency	Electric Sp Energy
		Jlost/Jsupplied	Jtherm/Jelec
Sample cases included with model			
Sample-cH_2	Grid	0.08	2.86
LH_2 per sample	Grid	0.08	2.86
Sample-MgH_2	Grid	0.08	2.86
Set 1			
cH_2-CH_4	Captive process	0.01	2.22
LH_2-CH_4	Captive process	0.01	2.22
MgH_2 Slurry-CH_4	Captive process	0.01	2.22
Set 2			
cH_2-Nuclear	Captive process	0.01	2.22
LH_2-Nuclear	Captive process	0.01	2.22
MgH_2 Slurry-nuclear	Captive process	0.01	2.22
Set 3			
cH_2-Biomass	Captive process	0.01	3.03
LH_2-Biomass	Captive process	0.01	3.03
MgH_2 Slurry-Biomass	Captive process	0.01	3.03
Set 4			
cH_2-Renewable	Captive process	0.01	3.03
LH_2-Renewable	Captive process	0.01	3.03
MgH_2 Slurry-Renewable	Captive process	0.01	3.03

Table 60 displays the efficiencies of the production, storage, and distribution steps as well as the total well-to-tank efficiency of the process. With the assumptions of this analysis, the most efficient system would use compressed hydrogen. When the hydrogen must be produced by non-fossil fuel methods, the projected efficiencies are within 14.7% of one another.

Table 60 - Comparison of Efficiencies

Title	Production Efficiency	Storage Efficiency	Distribution Efficiency	Well-to-Tank Efficiency
	%	%	%	%
Sample cases included with model				
Sample-cH_2	67.8	84.4	90.6	56.7
LH_2 per sample	63.4	58.5	98.0	43.3
Sample-MgH_2	67.8	11.8	99.2	19.2
Set 1				
cH_2-CH_4	67.9	87.0	90.6	57.9
LH_2-CH_4	63.5	63.5	98.3	46.1
MgH_2 Slurry-CH_4	67.9	18.0	98.0	33.0
Set 2				
cH_2-Nuclear	48.8	88.2	90.6	43.8
LH_2-Nuclear	45.6	66.1	98.0	36.7
MgH_2 Slurry-nuclear	48.8	19.7	98.0	32.6
Set 3				
cH_2-Biomass	45.7	84.6	90.6	40.4
LH_2-Biomass	42.7	58.8	98.0	32.6
MgH_2 Slurry-Biomass	45.7	15.2	98.0	25.7
Set 4				
cH_2-Renewable	23.2	84.6	90.6	21.7
LH_2-Renewable	21.7	58.8	98.0	18.7
MgH_2 Slurry-Renewable	23.2	15.2	98.0	20.2

Table 61 displays the total energy used in the analyses and the greenhouse gas emissions of each option. The MgH_2 slurry cases all seem to be performed with twice the energy required for the other cases. We suspect that this results from the fact that twice the hydrogen is delivered when the MgH_2 is mixed with water. The large number for GHG in the nuclear option appears to result from assumptions made about the production of nuclear fuel. The MgH_2 case would use more nuclear energy than the other cases. The larger GHG emissions for the compressed option probably results from the larger transportation energy required for the compressed option.

Table 61 - Comparison of Energy Used by the Process and Greenhouse Gas Emissions

Title	Total Energy	GHGs
	MJ	g/kg H_2
Sample cases included with model		
Sample-cH_2	211	16,463
LH_2 per sample	276	21,709
Sample-MgH_2	1,072	76,547
Set 1		
cH_2-CH_4	206	16,185
LH_2-CH_4	259	20,679
MgH_2 Slurry-CH_4	724	53,329
Set 2		
cH_2-Nuclear	273	186
LH_2-Nuclear	326	152
MgH_2 Slurry-nuclear	734	1,019
Set 3		
cH_2-Biomass	296	158
LH_2-Biomass	366	37
MgH_2 Slurry-Biomass	929	92
Set 4		
cH_2-Renewable	550	153
LH_2-Renewable	638	27
MgH_2 Slurry-Renewable	1,180	29

5.6.3.7.4 References:

23. Kevan D. Weaver, “Interim Status Report on the Design of the Gas-Cooled Fast Reactor (GFR)”, INEEL/EXT-05-02662, 1 January 2005

23. M. P. LaBar, A. S. Shenoy, W. A. Simon and E. M. Campbell, “Status of the GT-MHR for Electricity Production”, World Nuclear Association Annual Symposium, 3-5 September 2003, London

5.6.4 Conclusions

Currently magnesium is produced using the metallothermic processes or magnesium chloride electrolysis processes. Based on the thermodynamics of the magnesium reduction process, it would appear that magnesium should use less energy in it reduction than is required for aluminum. This, if the primary cost of the metals is energy, the cost of magnesium should be less than that of aluminum. This is not the case because the processing of magnesium has involved more costly processes and the processing of magnesium has been performed at significantly smaller scale that the processing of aluminum.

The SOM process promises to provide a system that is as simple as the aluminum reduction system. At comparable scales, the SOM process could provide magnesium at costs lower than those of aluminum.

The magnesium hydride slurry approach will, at mature large-scale, reduce the cost of magnesium required for the slurry because it will reuse the magnesium byproducts from the water/slurry reaction. This is another significant cost reduction in the reduction of magnesium that supports the belief that magnesium reduction costs can be low enough to provide the costs that are predicted by the above studies.

Using a mature large-scale SOM process, we are estimating that hydrogen can be provided to the customer at a cost of about $4.50/kg of hydrogen. This includes costs for the reduction and rehydriding of the byproduct slurry, the cost of delivery of the slurry to the distributor, and the cost of distribution to the customer at the distributors stations. This process would be a zero carbon producing process if the trucks, trains, and barges delivering the slurry also use hydrogen as a fueling source and if the electricity required is also provided by zero carbon electricity generation processes such as wind, solar, hydroelectric, or nuclear processes.

When the true costs of using fossil fuels are actually charged to the fossil fuel user, the cost of the chemical hydride slurry system will be seen to be truly competitive.

5.7 Task 7 – Experimental Evaluation of the SOM Process – 100 g/day (Provided by Boston University)

5.7.1 Description

The SOM process offers the potential of significant reductions in the capital and operating costs of reducing magnesium. An experimental evaluation will be performed at a 100 g/day scale. The results of this evaluation will be used to design a 1-5 kg/day scale experiment. The results will also be used to update the process and economic analyses prepared in Task 6.

5.7.2 Summary

- Evaluated membrane stability during a period of 40 hours in different flux systems at two temperatures, 1150°C and 1300°C.
- Determined current-potential profile in two of the flux systems, one at 1300°C and the other at 1150°C. The former experiment was run for 20 hours and the latter was run for 80 hours.
- Determined the dissociation potential of MgO in the two flux systems.
- Determined the effect of gas bubbling on mass transfer within the system.
- Determine the effect of trace oxygen impurity on residual current.
- Measured density of all flux compositions used for experiments.
- Evaluated solubility of magnesium oxide in low temperature flux using cooling curve.
- Established 10% MgO as optimum concentration.
- Using a low temperature flux system, demonstrated that the operating temperature of the SOM cell can be lowered by 150°C to 1150°C.
- A SOM experiment with periodic addition of magnesium oxide was continuously run for two days producing at a rate in excess of 100 g/day.
- A SOM experiment without reductant was conducted, using molten silver as the liquid anode. It produced magnesium at the cathode and oxygen at the anode.
- Production of MgH_2 in the Condenser was Tested
- A 2-D electrostatics mathematical model of 3-tube scale-up cross section of the SOM reactor that is to be used for demonstrating the 1Kg scale Mg production at BU was developed using Comsol Multiphysics and convergence of the model was achieved.
- Several possible scale-up cross-section geometries were investigated.

5.7.3 Discussion

5.7.3.1 Introduction

The overall project aims at using magnesium hydride slurry as hydrogen storage materials for the transportation and the fuel cell industries. The hydrogen needed is released from these hydrides through a hydrolysis reaction that generates magnesium hydroxide as a by-product. Therefore, efficient use of these hydrides for hydrogen storage would require that the metal hydroxide by-products be reduced and the metal obtained used to regenerate the hydrides. However, current state of the art processes

for reducing large volumes of these high-energy content metal oxide by-products would have major environmental consequences apart from being highly energy consuming. The SOM (solid oxygen ion conducting membrane) process is an environmentally friendly and energy-efficient alternative technology for reducing the oxide by-products and enabling the hydrogen economy. In the SOM process, conducted between 1100-1300°C, a non-consumable flux dissolves the metal oxide byproduct and an inert oxygen-ion-conducting ceramic membrane separates the cathode from the anode. An electric potential is applied between the cathode in the flux and the anode to dissociate the magnesium oxide. The oxygen ion is pumped through the conducting ceramic membrane and the magnesium vapors reduced at the cathode are condensed in a separate chamber. By controlling the temperature gradient within the condenser, it is possible to tailor the particle size and morphology of the reduced metallic deposit. This is particularly attractive since it translates to being able to tailor the surface area of the metal that is optimum for the hydriding process. Since the process occurs at temperatures between 1100-1300°C, the electrical power requirement is lowered and efficiency increased by directly reforming hydrocarbon fuel gas over the anode to result in a byproduct that is mostly water vapor.

For the duration of this project, the scale-up potential, long-term membrane durability, and direct use of oxide by-product will be demonstrated. The information will be used to determine the cost associated with implementing this technology for high-volume reduction of the magnesium hydroxide by-product.

5.7.3.2 Initial Experiments and Results

5.7.3.2.1 Membrane Stability vs Temperature

Sections of the yttria-stabilized zirconia (YSZ) membrane tubes were placed inside the flux, contained in an iron crucible, for 40 hours at the desired temperature. It has been observed in our earlier SOM trials that the yttria in the yttria-stabilized zirconia (YSZ) membrane tubes had a tendency to slightly dissolve in the fluoride flux. However, it is possible to modify the flux to prevent the yttria dissolution. Stability experiments were conducted in two fluoride-based flux systems, MgF_2-based at 1300^0C and MgF_2-MX_2-based at 1150^0C.

The sample cross sections are shown in Figure 86 (samples 1 –4 in MgF_2-based system at 1300^0C) and Figure 87 (samples 4-8 in MX_2-MgF_2-based system at 1150^0C).

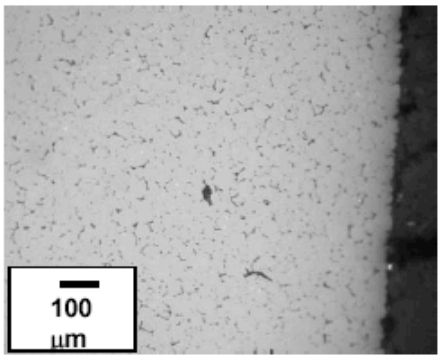

MgF_2- Based System 1
[1300 ºC for 40 hours]

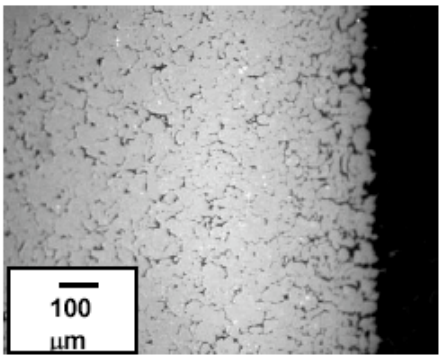

MgF_2- Based System 2
[1300 ºC for 40 hours]

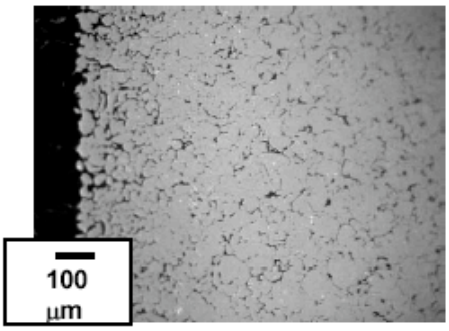

MgF_2- Based System 3
[1300 ºC for 40 hours]

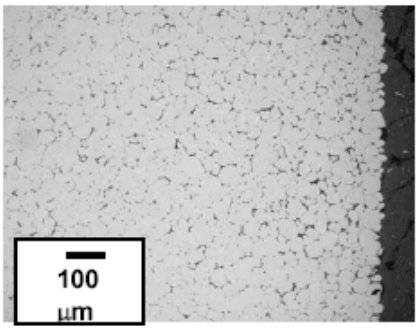

MgF_2-Based System 4 [1300 ºC for 40 hours]

Figure 86 - Cross-sections of the representative areas of the YSZ membranes in contact with the MgF_2-based flux systems at 1300°C

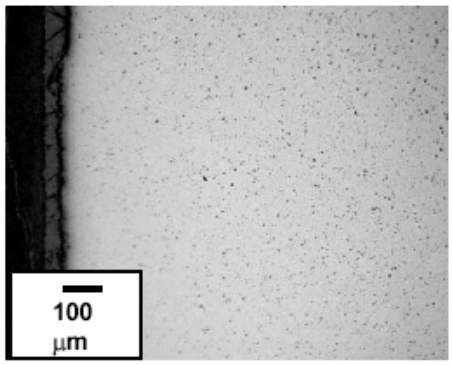

MgF_2- MX_2 Based System 1

[1150 °C for 40 hours]

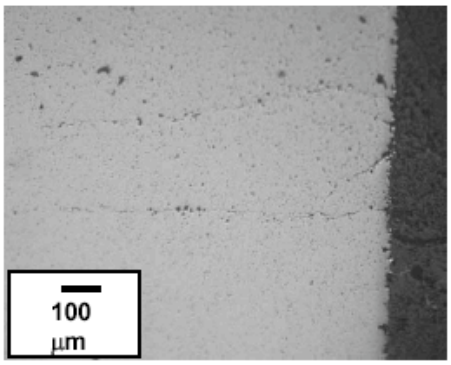

MgF_2- MX_2 Based System 2

[1150 °C for 40 hours]

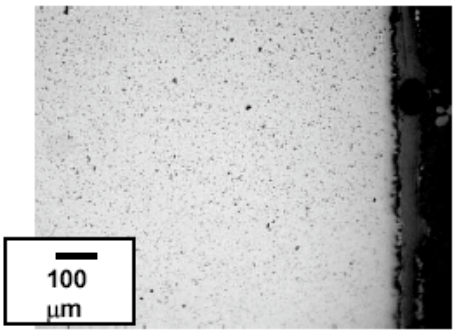

MgF_2-MX_2 Based System 3
[1150 °C for 40 hours]

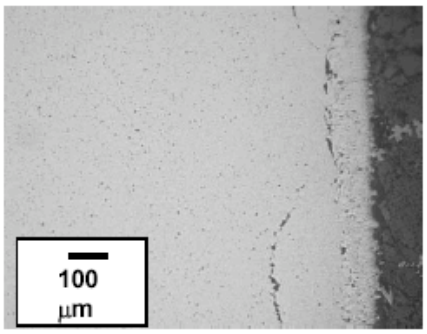

MgF_2- MX_2 Based System 4

[1150 °C for 40 hours]

Figure 87 - Cross-sections of the representative areas of the YSZ membranes in contact with the MX_2-MgF_2-based flux systems at 1150°C

It was apparent from studying the cross section of the membranes that it was most stable at 1300^{0}C in MgF_2-based System 1 and at 1150^{0}C in MX_2-MgF_2-based system 1; membranes are considered to be structurally more stable when there is less porosity and grain separation. Furthermore, the membrane was more stable at 1150°C compared to 1300°C. Detailed compositional analysis of the membrane cross-sections are being performed.

5.7.3.2.2 Current-Potential Profile of the Flux Systems

These experiments were conducted to identify the process parameters and flux systems to be used in the larger-scale experiments. To minimize experimental cost, small-scale set-up was used. The experimental arrangement is shown in Figure 88. The flux systems investigated were MgF_2- based at 1300°C and MgF_2-MX_2–based at 1150°C. The current-potential behavior of the flux system at 1300°C for different argon bubbling rates through the flux is shown in Figure 89.

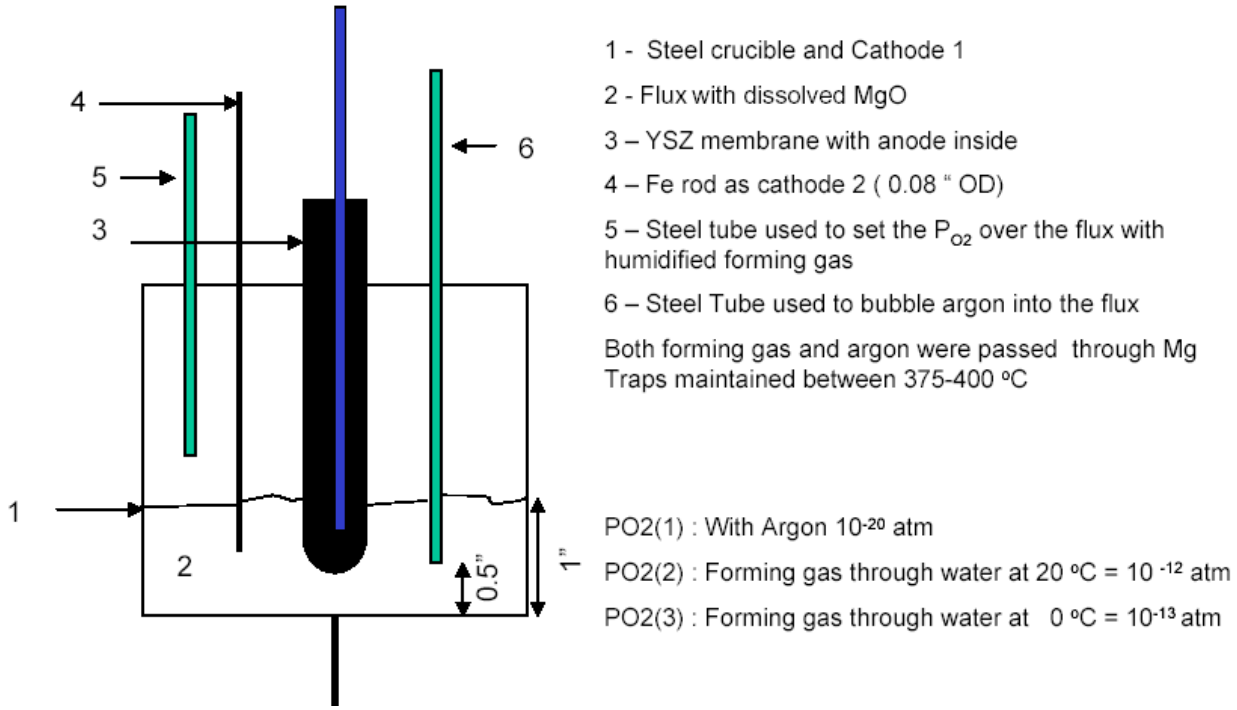

Figure 88 - Schematic of experimental apparatus for measuring current-potential profile as function of various process parameters

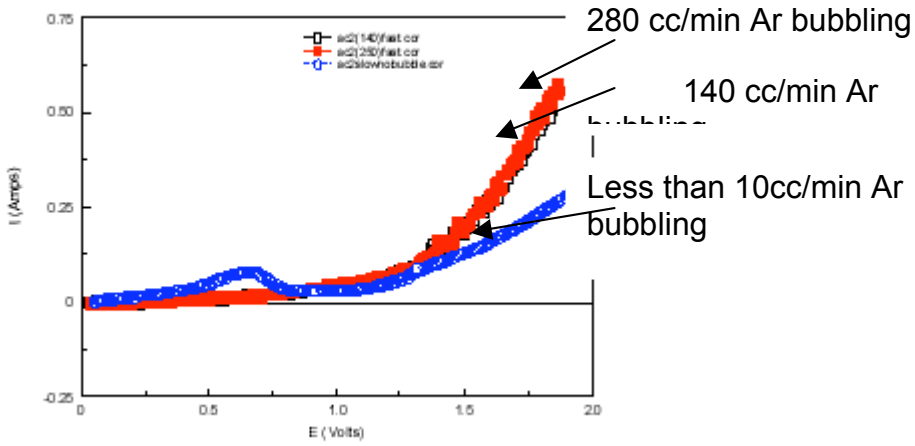

Figure 89 - Current-potential profile of thesame MgF2-MgO flux system as a function of Argon bubbling rate at 1300°C

From Figure 89, it is determined that the dissociation potential for MgO in the system at 1300°C is around 0.5 V. The lower than expected dissociation potential is likely due to the fact that in Ar the partial pressure of Mg(g) in the system is much lower than 1 atmosphere. It is also apparent that the mass-transfer in the system increases when the argon bubbling is increased from 10 cc/min. to 140 cc/min. However, above 140 cc/min. of Ar bubbling the mass-transfer does not increase much (see section

5.7.3.2.3 Analysis). The current-potential behavior in the 1150°C system is shown in Figure 90. The dissociation potential appears to be around 0.5 V. Compared to the flux system at 1300°C, the effect of increased mass transfer with Ar bubbling is not very evident. This may be due to the differences in flux viscosities.

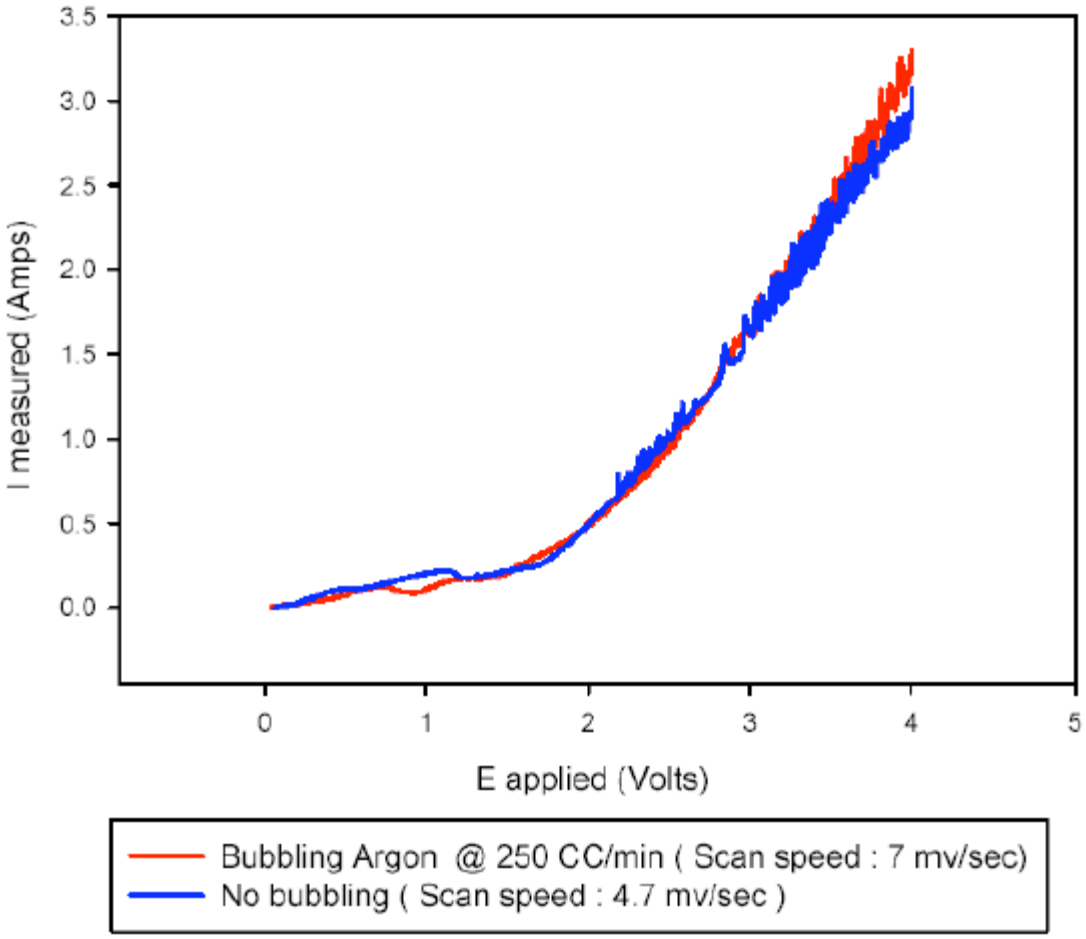

Figure 90 - Current-potential profile of the MgF_2-MX_2-MgO flux system at 1150°C

The very small residual current observed in both systems below the MgO dissociation potential (<0.5V) is due to oxygen impurity in the system. This is shown in Figure 91.

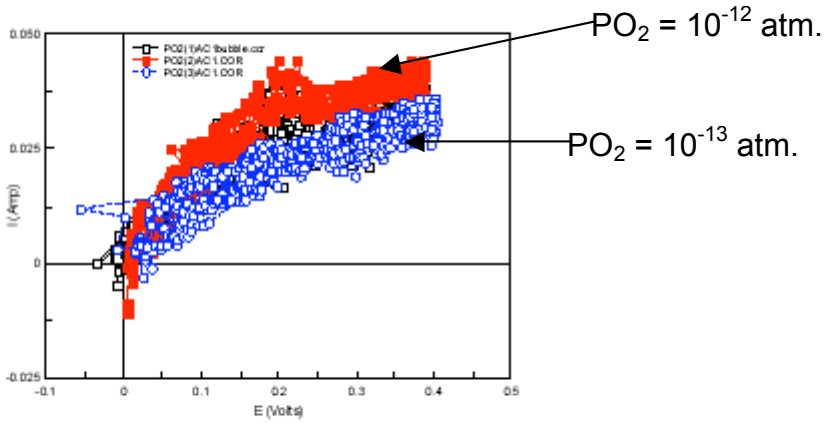

$P_{O2}(2)$: Forming gas through water at 20 °C = 10^{-12} atm
$P_{O2}(3)$: Forming gas through water at 0 °C = 10^{-13} atm

Figure 91 - Effect of oxygen partial pressure on residual current below the MgO dissociation potential for the system at 1300°C

Since the cathodic reaction below the MgO dissociation potential is due to residual oxygen impurity, the reaction can be written as:

$O_2(g) + 2e = O^{2-}$

Since the oxygen transport in the flux system was observed earlier to be rate controlling, it is expected that the residual current due to the oxygen impurity (below 0.5 V) will increase as the cathodic area is increased. This is seen in Figure 92 for the flux system at 1300°C; the same was also seen for the flux system at 1150°C.

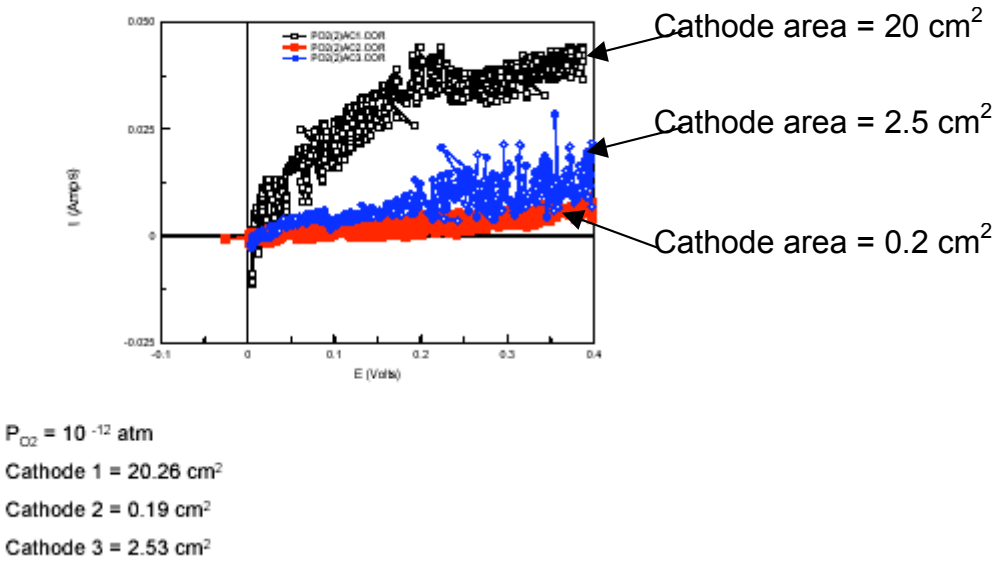

Figure 92 - Effect of cathode area on residual current below the MgO dissociation potential for the system at 1300°C

However, well above the dissociation potential (> 2V), the dominant cathodic reaction is

$Mg^{2+} + 2e = Mg(g)$

Since the magnesium ion concentration is much larger than the oxygen ion concentration, the cathodic reaction is no longer rate controlling and the process is rate limited at the flux-YSZ membrane interface:

O^{2-} (in flux) → O^{2-} (in the YSZ anode membrane)

Therefore, during the actual SOM experiments at 5 V, the contribution of the residual current to the total current will be negligible(specially when there is Mg(g)) and the process will essentially be controlled at the YSZ-anode membrane. Hence, the current density will be stated with respect to the YSZ-membrane-flux interfacial area. Preliminary estimates indicate that current density with respect to the YSZ-anodic membrane area will easily approach 0.5-1 Amp/cm^2. The experiments with the flux systems at 1300°C and 1150°C were conducted for a total duration of 20 and 80 hours, respectively. The cross-sections of the membranes from these two experiments are shown in Figure 93, and the system impedance measured during the experiment with the flux system at 1150°C is shown in Figure 94. The membranes in both experiments appeared to be stable, although the one at 1150°C appeared slightly better; this is also supported by the relatively unchanging value of the system impedance as shown in Figure 94. It is to be noted that these experiments were not conducted with the optimum flux systems.

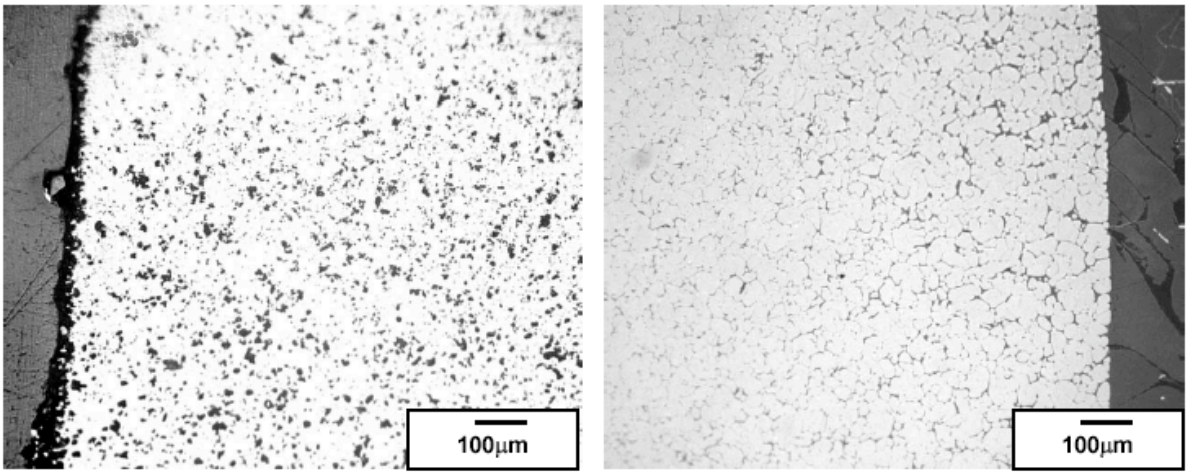

Figure 93 - Cross-sections of the membranes after the experiments conducted with the flux system at 1150°C and 1300°C

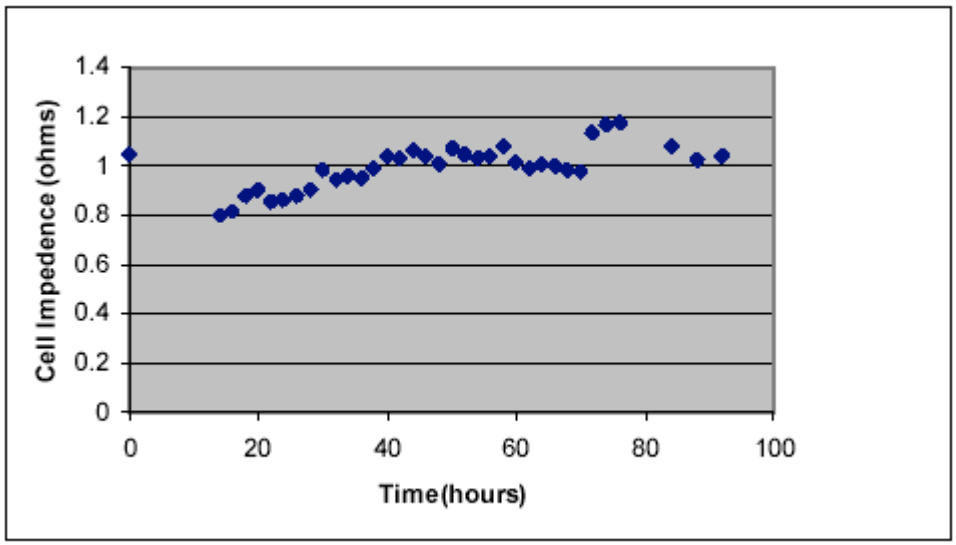

Figure 94 - Impedance of the cell system measured during the experiment with the flux system at 1150°C

Based on the experiments conducted it appears that it should be possible to run SOM experiments for more than 80 hours at 1 Amp/cm^2. This will allow us to meet and/or exceed our experimental goals. The results will also allow us to make better cost predictions.

5.7.3.2.3 Analysis of the Current-Potential Characteristic

The current-potential profile can be characterized as having two different slopes; one below and the other above the MgO dissociation potential. The first and the second slopes were determined to be due to the currents arising from the residual oxygen impurity in the system and the oxygen ions generated from MgO dissociation, respectively. The applied potential comprises contributions from the ohmic and mass-transfer polarizations along with MgO dissociation above the dissociation potential; the charge-transfer polarization is ignored since at the experimental temperatures it has been shown earlier that it is negligible compared to the other polarizations. Hence, the applied potential can be written as:

$E_{appl.} = IR_{(ohmic)} + E_{mass\text{-}transfer} + E_{MgO\ Dissociation}$ *(above the dissociation potential)*

The inverse of the slope of the current-potential profile can be written as:

$$\left(\frac{dE_{appl.}}{dI_{measured}}\right) = R_{ohmic} + R_{mass\text{-}transfer}$$

Since the mass-transfer at the anode-flux interface dominates above the dissociation potential of MgO, $R_{mass\text{-}transfer}$ at the anode can be calculated by subtracting the measured ohmic impedance from the inverse of the slope of the current-potential profile above the dissociation potential of MgO.

$$R_{mass\text{-}transfer} = \frac{dE_{appl.}}{dI_{measured}}\ (above\ dissociation\ potential\ of\ MgO) - R_{ohmic}$$

Since, the flux is stirred with Ar, it is assumed that during the short duration of the current-potential measurement, there is no chemical potential gradient of oxygen ions in the flux. Hence it is possible to express the current density (I/A) in terms of oxygen-ion conductivity and the gradient of the mass-transfer potential ($E_{mass\text{-}transfer}/\delta$).

$$\frac{I}{A} = \sigma \frac{E_{mass-transfer}}{\delta} = \frac{C_{O^{2-}} D_{O^{2-}} 4F^2}{RT} \frac{E_{mass-transfer}}{\delta}$$

or

$$R_{mass-transfer} = \frac{E_{mass-transfer}}{I} = \frac{\delta RT}{AC_{O^{2-}} D_{O^{2-}} 4F^2}$$

or

$$\frac{dE_{appl.}}{dI_{measured}} - R_{ohmic} = R_{mass-transfer} = \frac{RT}{AC_{O^{2-}} k_{mass-transfer} 4F^2}$$

or

$$k_{mass-transfer} = \frac{RT}{AC_{O^{2-}} R_{mass-transfer} 4F^2}$$

The above expression can be used to compute the mass-transfer coefficient ($k_{mass-transfer}$). Subsequently, the diffusion limited current (maximum possible current) and the corresponding E_{appl} can be determined.

5.7.3.2.4 List of symbols for the analysis

MX_2	Second Metal Halide flux constituent
$E_{appl.}$	Applied potential
$E_{MgO\ Dissociation}$	Dissociation Potential of MgO
I	Measured current
A	Anodic area
$E_{mass-transfer}$	Potential drop due to mass-transfer resistance
$E_{mass-transfer} / \delta)$	Mass-transfer potential gradient
$R_{mass-transfer}$	Mass-transfer resistance
R	Ohmic resistance in the system
$k_{mass-transfer}$	Mass-transfer coefficient
$C_{O^{2-}}$	Oxygen-ion concentration
$D_{O^{2-}}$	Oxygen-ion diffusivity
$\sigma_{O^{2-}}$	Oxygen-ion conductivity
R	Gas Constant
T	Temperature
F	Faraday constant

5.7.3.3 Characterization of Flux Properties

5.7.3.3.1 Density Measurement

The density of selected flux compositions MgF_2 -MgO, 55.5 wt% MgF_2 – CaF_2, and (55.5 wt% MgF_2 – CaF_2)-10 wt% MgO were measured in the temperature range of interest. The density was measured to accurately determine the anodic area and the current density. A known weight of the flux was heated in a steel crucible (5.6 cm OD) to the temperature of interest where it was molten. A molybdenum rod (0.3 cm OD) connected to a surface dial gauge (Least count = 0.0025 cm) was carefully lowered into the crucible. Impedance was continuously measured between the molybdenum electrode and steel crucible as the rod was being lowered into the crucible. When the electrode touched the flux, the impedance suddenly changed from an open condition to measuring a finite resistance. Thus the height of the molten flux was established and used to calculate volume and density. From Figure 95, MgF_2 - 10 wt% MgO by virtue of its higher temperature has a lower density than MgF_2 – CaF2 - MgO system. As expected, the density of 55.5 wt% MgF_2 –CaF_2 increases slightly with the addition of MgO.

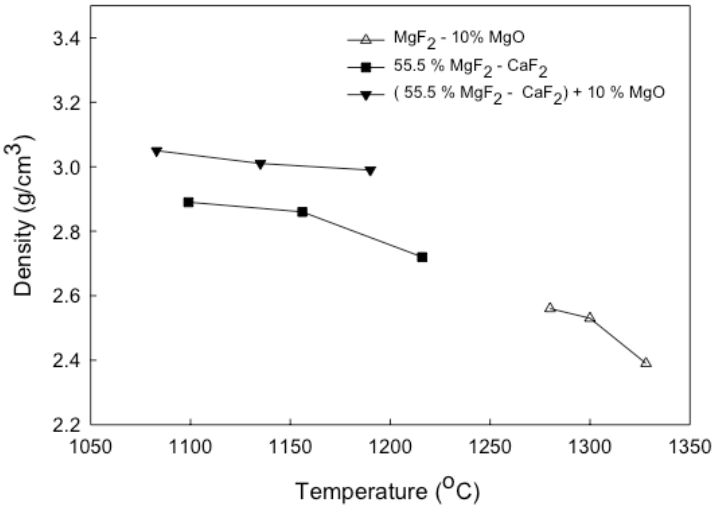

Figure 95 - Density of fluoride flux compositions

5.7.3.3.2 <u>MgF_2 -CaF_2 system</u>

During the course of this research, a flux system based on eutectic MgF_2 - CaF_2 system was investigated. From the phase diagram (Figure 96), a deep eutectic is observed for 55.5 wt% MgF_2 at 980°C. Using this flux system, the temperature of the SOM process has been lowered by 150°C.

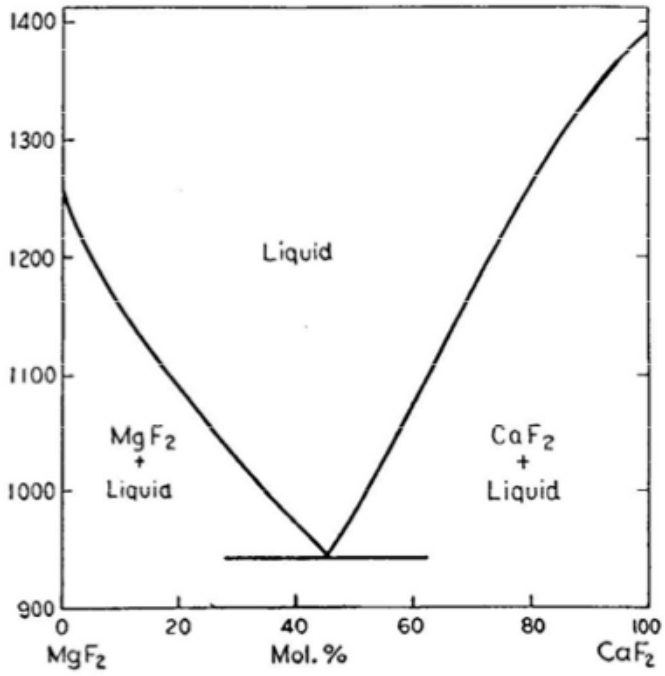

Figure 96 - - Magnesium Fluoride - Calcium Fluoride Phase diagram

5.7.3.3.3 Solubility of MgO in MgF_2-CaF_2 system

No information is available on the solubility of MgO in this flux system. Hence the effect of MgO addition on the liquidus of 55.5 wt% MgF_2 – CaF_2 was determined by analyzing cooling curves of selected flux compositions as a function of MgO concentration (2,5,7,10,15 and 20 wt%). 55.5 wt% MgF_2 – CaF_2 will be referred to as the Base composition. A steel crucible (5.6 cm OD) was used to contain the flux composition under investigation. A B-type thermocouple immersed in the flux measured the flux temperature. Another B-type thermocouple in contact with the outer wall of the crucible was used as a reference thermocouple. After equilibrating the flux at 1300 °C in the liquid state for 2 hours, the furnace was cooled at approximately 30 °C /min till the reference temperature reached 800 °C. The difference between the flux and reference temperature was plotted against flux temperature as a function of MgO concentration (Figure 97). Changes in the slope of the flux temperature versus the temperature difference with the base case indicate phase changes. From the cooling curves of base composition with varying MgO content, it is observed that the eutectic temperature for this flux system is 975°C. For 20 wt% and 15 wt% MgO, phase changes are observed at 1220 and 1160°C respectively. For MgO compositions up to 10 wt% MgO, there is no noticeable change in the cooling curve. A phase change at 1050°C is observed in all compositions. It is likely that this phase change is due to some impurity in the melt entering the system during preparation of this flux. Hence from the cooling curves, 10 wt% MgO has been found suitable for use at 1150°C. The composition (55.5 wt% MgF_2 - CaF_2) – 10 wt% MgO is referred to as Low Temperature Flux (LTF).

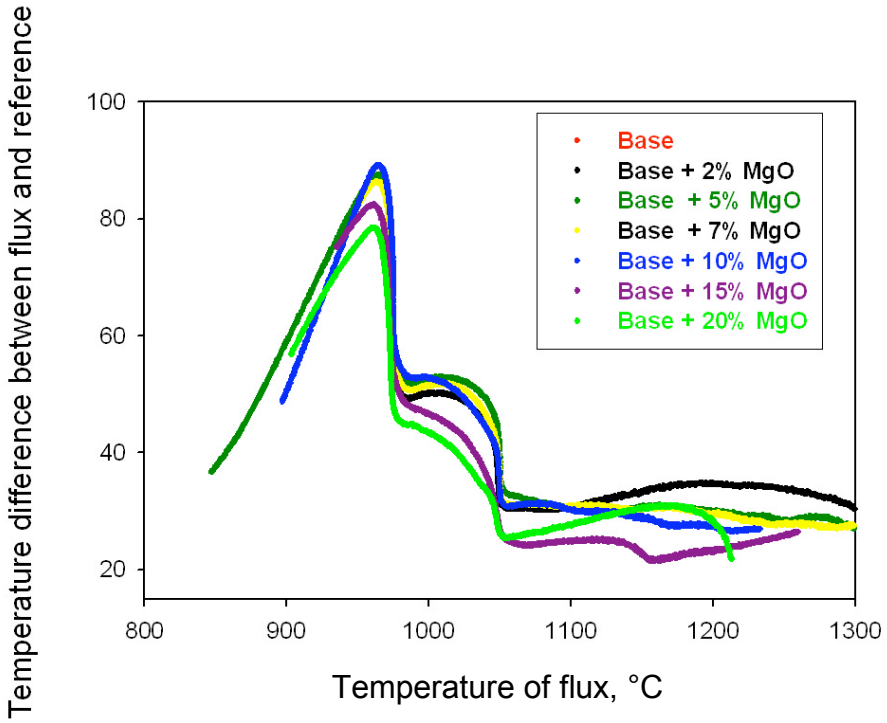

Figure 97 - Cooling curves for base composition as a function of MgO

5.7.3.4 Proof of Concept for the Low Temperature Flux (LTF) System

5.7.3.4.1 Experimental Setup

The electrolytic cell and magnesium collection apparatus (Figure 98) has been designed to produce and contain 100-200 g of magnesium metal over an extended period of operation. The electrolytic cell can reduce approximately 15 g of magnesium per hour when operated at an anode current density of 1 Amp/cm². Before ramping up to the 100 g/day scale, it was decided to validate the setup and to run the cell at 3-4 volts for an extended period (5- 10 hours) in order to collect 15 - 25 g.

Nearly all of the setup with the notable exception of the YSZ membrane and extended anode (graphite and liquid copper), is constructed of 304 stainless steel. The YSZ membrane is held in position using alumina spacers cemented together with alumina cement. The entire apparatus is contained and heated within the mullite reaction tube of a Molybdenum disilicide resistance furnace. The upper electrolysis chamber shown is approximately six inches in length, and is positioned so that the melt remains in the hot zone of the furnace. The apparatus takes advantage of the natural temperature gradient of the resistance furnace such that the electrolysis chamber is maintained at 1150°C, the lower condensation chamber can be positioned such that the temperature varies from 1100 to 500°C. In order to protect the YSZ membrane above the flux from the extremely reducing Mg vapor that is produced along the wall of the stainless steel container/cathode, argon gas is introduced into the chamber as a carrier gas and dilutant. The dilution of magnesium vapor by argon required to reduce the partial pressure of magnesium vapor in the SOM reactor in order to ensure stability of zirconia is shown in Figure 99. The argon is also bubbled through the melt with the goal of improving mass transfer in the flux by stirring the flux. The argon-magnesium gas mixture passes out of the electrolysis chamber to the lower condensation chamber, which can be maintained at a temperature such that magnesium is collected as either a liquid or solid. The remaining argon gas then passes through a baffle and exits the condensation chamber through the bottom of the furnace.

The entire setup placed inside a gas tight mullite tube is heated to the desired temperature at the rate of 3°C /min. High purity argon at the rate of 250 cc/min is passed through the mullite tube to generate an inert atmosphere around the setup. The exit gas is continuously monitored using a zirconia based oxygen sensor. After equilibrating at the desired temperature for 1 hour, the cell is characterized using impedance spectroscopy, potentio-dynamic sweeps and potentio-static holds. The electrochemical instrumentation consisted of a Princeton Applied Research (PAR) Potentiostat (Model 263 A) and Solartron impedance analyzer (Model 1250 B). A KEPCO® power booster was used to increase the current limit of the potentiostat to 10 amps. Data acquisition and control of the above instruments was achieved with CorrWare® and Zplot® (software) from Scribner Associates (Southern Pines, NC). A Hewlett Packard power supply (Model 6033A) was used to apply a constant potential to the cell for electrolysis. The applied voltage and resulting current from the cell were logged at 1 second intervals using a Fluke Hydra® data logger(Model 2635A).

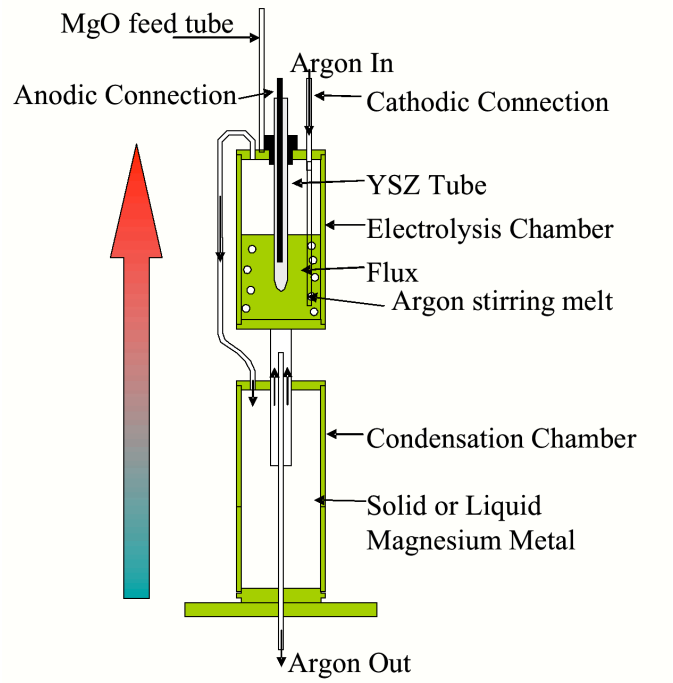

Figure 98 - Experimental Setup for SOM electrolysis for LTF system

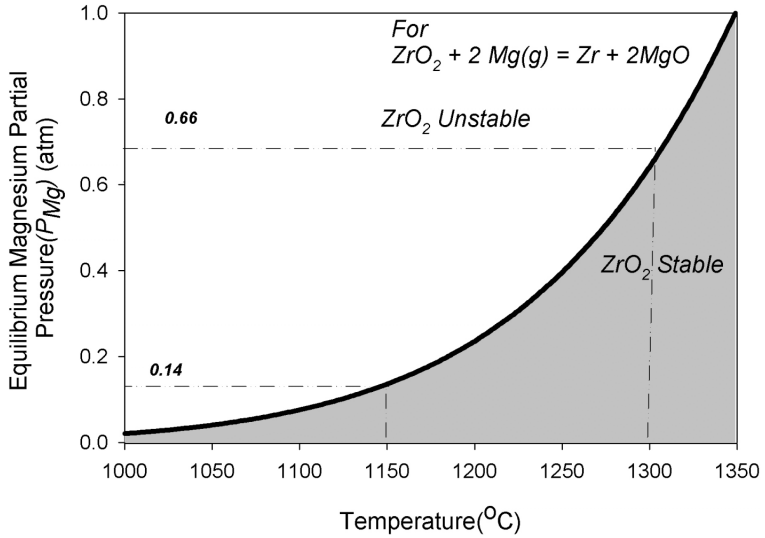

Figure 99 - Effect of Partial pressure of magnesium vapor in the SOM reactor on the stability of zirconia

5.7.3.4.2 Electrochemical Characterization and Electrolysis

In the LTF system, 10% magnesium oxide was dissolved in a eutectic magnesium fluoride-calcium fluoride flux. The SOM cell was evaluated for a period of 18 hours. During this time, 3 V was applied for 12 hours to produce Magnesium from magnesium oxide. The rest of the time was spent in electrochemically characterizing the

cell. From Figure 100, with a slow (0.5 mv/sec) potentio-dynamic sweep, the dissociation potential for magnesium oxide was calculated to be 0.63 volts. During a fast potentio-dynamic scan (Figure 101), the current through the cell steadily increases indicating that higher current densities (0.8 -1 amp/cm²) are possible. 3 volts was intentionally chosen to restrict the current density to 0.3 amp/cm². A total of 39.6 amp-hours was passed through the cell at 3 V, theoretically reducing 17-18 g of magnesium. A typical current response at 3V can be seen from Figure 102. The gradual decay in current is due to a decrease in the MgO concentration from 10 to 6 wt%. The cell impedance was measured periodically and was observed to be constant (typically 0.224 ohms) (Figure 103). The condenser showed magnesium deposited as solid lumps and fine crystals attached to the wall (Figure 104). The fine crystals are deposited at colder parts of the condenser, while the lumps are seen closer to the top of the condenser that was hotter (Figure 104a). The approximate weight of the magnesium deposited was found to correspond well with the theoretical estimate as per Faraday's law, thus indicating a high Faradic efficiency for the process. After the experiment, the YSZ membrane in contact with the flux was sectioned, polished and examined by optical microscopy. The microstructure of the as received membrane and membrane after the 18 hour experiment is compared in Figure 105. The membrane appears to be essentially unaffected after the experiment.

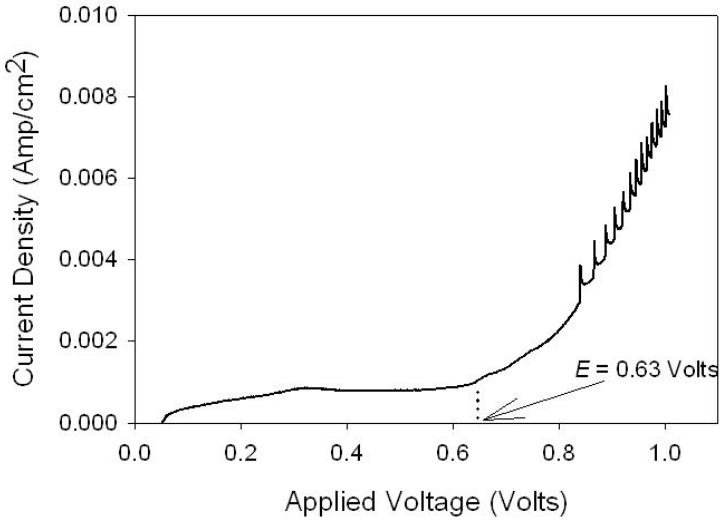

Figure 100 - Slow potentio-dynamic scan to estimate the dissociation potential of MgO in LTF system

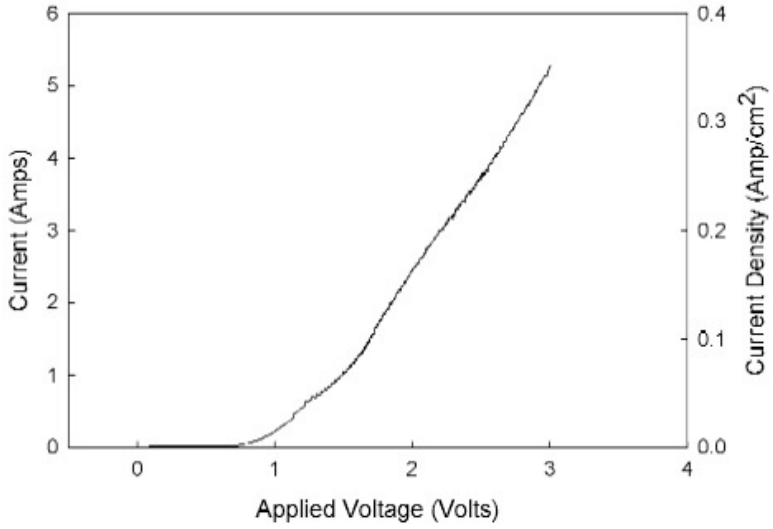

Figure 101 - Fast potentio-dynamic Scan (5mv/sec) for LTF system

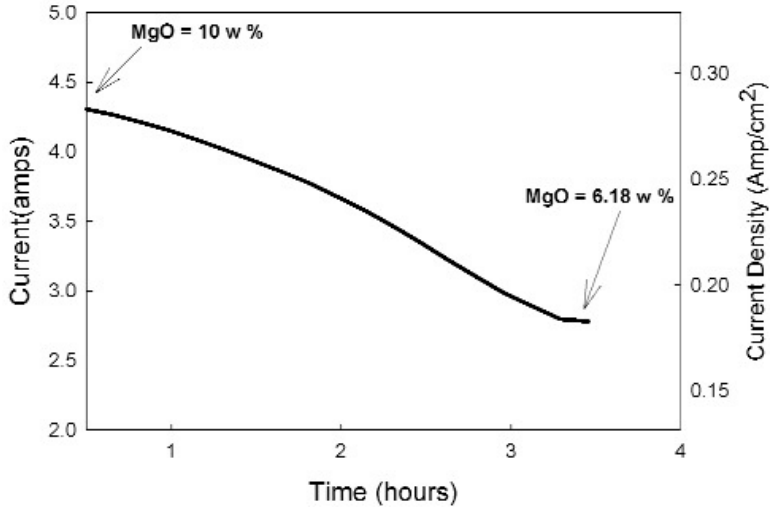

Figure 102 - Current response during electrolysis at 3 V for LTF system

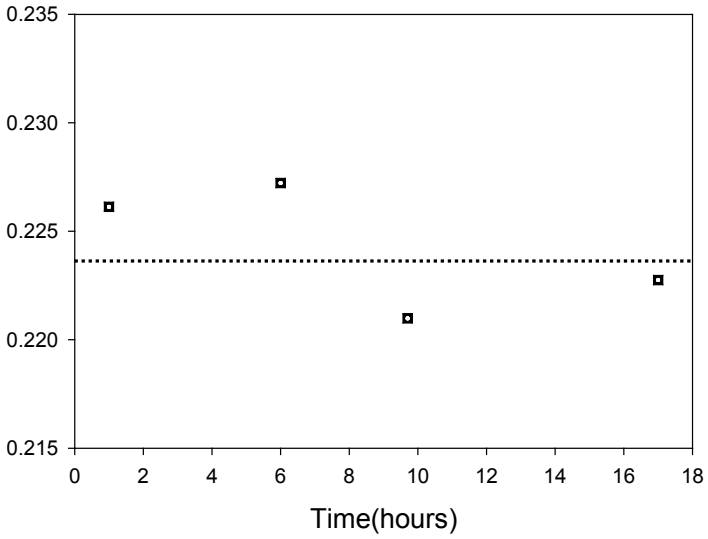

Figure 103 - Periodic Impedance measurements of cell in LTF system (The dotted line indicates the average of measured impedance values)

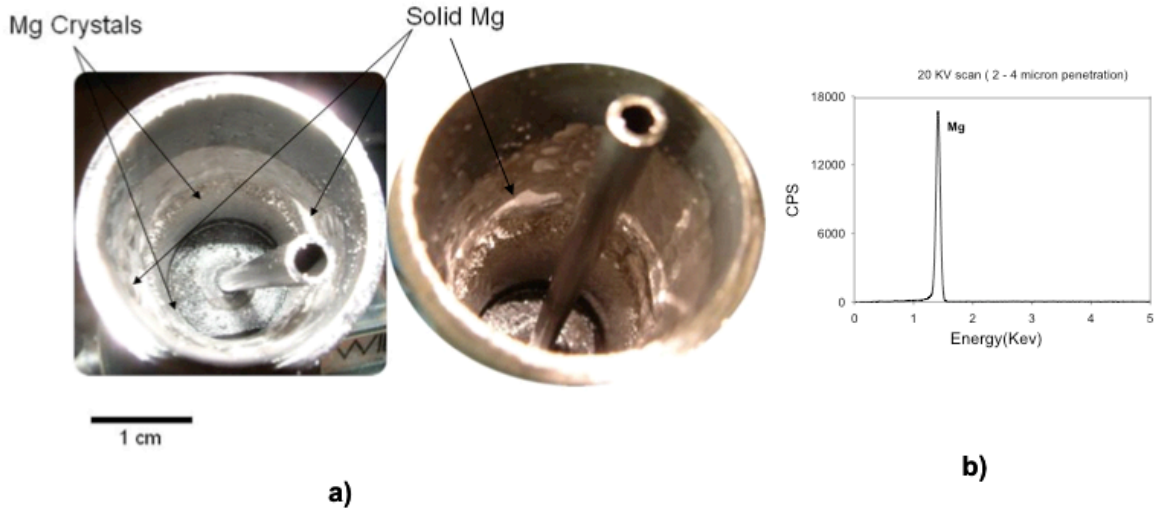

Figure 104 - a) Magnesium Deposit inside condenser b) Chemical analysis (EDAX) of Magnesium deposit in LTF system

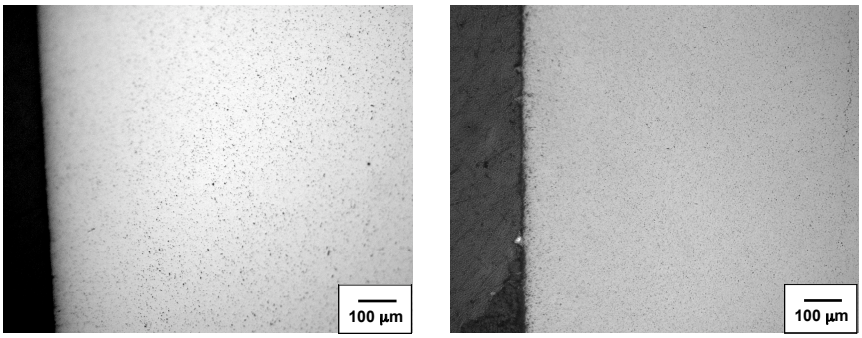

a) As Received b) After Experiment

Figure 105 - Cross-section of YSZ membrane a) before b) after experiment

Based on the experiments conducted it appears that it should be possible to run SOM experiments for more than 80 hours at 1 Amp/cm^2. This will allow us to meet and/or exceed our experimental goals. The results will also allow us to make better cost predictions.

5.7.3.5 Membrane Stability Using Flux Modification

5.7.3.5.1 Experiment

Sections of the YSZ membrane tube (6 mol% Y_2O_3-ZrO_2) were exposed (immersed) for 40 hours in selected flux compositions at desired temperatures of interest (1300°C for the HTF systems and 1150°C for the LTF systems; see Table 62) and then rapidly cooled. After the experiment, the crucible was machined leaving the YSZ membrane with the flux solidified around the membrane. The YSZ membrane tubes were then sectioned axially, and one section was polished for optical microscopy and chemical analysis. A JEOL (JXA-733) Electron Microprobe analyzer equipped with a Wavelength Dispersive Spectroscopy (WDS) Analyzer was used to chemically analyze the membrane.

Table 62 – Compositions of flux used for membrane stability experiments

Reference	Composition (w %)	Temperature (^{o}C)
HTF	MgF_2 + 10% MgO	1300
HTF + 2.5 % YF_3	(MgF_2 + 10% MgO) + 2.5 % YF_3	1300
HTF + 5 % YF_3	(MgF_2 + 10% MgO) + 5 % YF_3	1300
LTF	(55.5% MgF_2 + CaF_2) + 10% MgO)	1150
LTF + 2.5 % YF_3	(55.5% MgF_2 + CaF_2) + 10% MgO) + 2.5 % YF_3	1150
LTF+ 5 % YF_3	(55.5% MgF_2 + CaF_2) + 10% MgO) + 5 % YF_3	1150

5.7.3.5.2 Results

Grain growth was observed in samples exposed to the HTF (MgF_2 + 10% MgO) system (Figure 106) for 40 hours at 1300°C. No appreciable grain growth was observed in samples exposed to the LTF system ((55.5 w% MgF_2 + CaF_2) + 10 w% MgO) for 40 hours at 1150°C. Lower temperature appears to inhibit grain growth in the YSZ

membrane. The average yttrium content in the as- received YSZ membrane was measured by WDS to be 7.5 w% (corresponding to 10.9 w% or 6 mole% Y_2O_3). From Figure 107 and Figure 109, it is evident that when no Y is present in the flux, Y tends to diffuse from the membrane into the flux. Addition of Y in the form of yttrium fluoride minimizes the diffusion from the membrane and at higher yttrium concentration in the flux results in diffusion of Y into the membrane. For the HTF experiment, Mg tends to diffuse into the membrane and the Mg-concentration gradient is in opposite direction to the yttrium-concentration gradient. The membrane is then stabilized with both MgO and Y_2O_3. Since yttria is an expensive stabilizing oxide, and to keep the lattice constants from changing and ionic conductivity from dropping, it is essential that yttria is not lost to the flux; the ionic conductivity of yttria-doped zirconia is higher than that of magnesia doped zirconia. This is crucial since maintaining a high ionic conductivity leads to low ohmic polarization losses in the membrane. With yttrium fluoride added to the flux, Mg diffusion into the membrane can be minimized (Figure 108).

For the LTF system, Mg diffusion into the membrane is greatly reduced due to the lower temperature (Figure 110). When no yttrium fluoride is present in the flux, there is a surface depletion of yttrium (close to 0%) and the reaction layer appears to spall. It should be noted that for the HTF and LTF systems (1300 or 1150°C), there is an optimum yttrium concentration wherein the YSZ membrane is most stable. Comparing microstructures (Figure 106) and chemical analysis (Figure 107 - Figure 110), the membrane was most stable in flux compositions HTF + 2.5 w% YF_3 and LTF + 5 w% YF_3. However, the LTF system is preferred due to limited grain growth and better structural integrity of the exposed YSZ membrane.

Although, it has been established that the membrane is stable in the LTF system with 2.5 w% Y_2O_3, it was decided to analyze the bulk slag to verify there was no dissolution of zirconium. The solubility limit of zirconium in LTF system ((55.5 w% MgF_2 + CaF_2) -10 % MgO) at 1100, 1150 and 1200°C was determined by equilibrating a section of the YSZ tube with the flux for 24 hours at each temperature. After the 24-hour period, the flux samples were taken with a quartz capillary tube.

5.7.3.6 Flux Volatility, Conductivity and Viscosity Measurement

It is also necessary that the selected flux composition must have sufficiently low volatility (< 10^{-6} g/cm^2-s) for long-term operation, low viscosity (< 0.1 pa-s or 1 poise) to provide adequate mass transfer characteristics since the flux behaves as a supporting electrolyte and sufficiently high ionic conductivity (> 3 ohm-cm^{-1}) to limit ohmic polarization loss. The last two requirements are essential in order to sustain high current densities ≥ 1 A/cm^2.

The volatility and the ionic conductivity of the HTF system been measured earlier; the volatility at 1300°C is 8.6 x 10^{-7} g/cm^2-sec and the ionic conductivity at 1300°C is 3.83 ohm-cm^{-1}. The HTF system appears to have the required low volatility and high ionic conductivity values. The viscosities of the HTF and the LTF systems have been measured and are reported below:

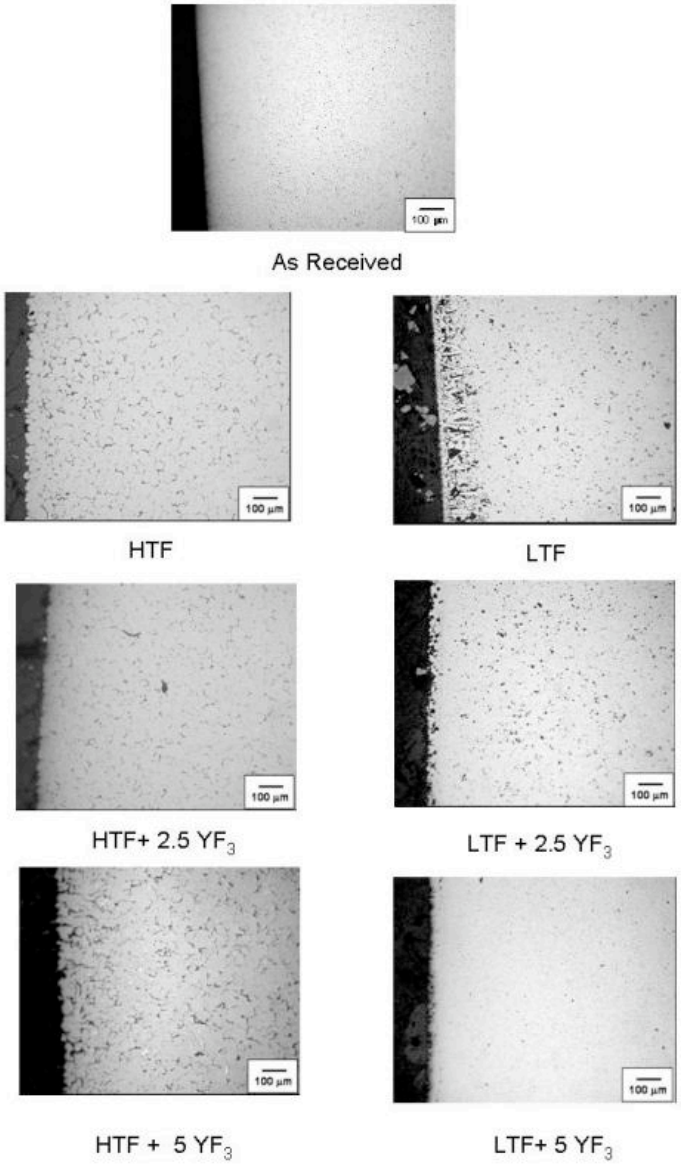

Figure 106 - Cross-sections of the representative areas of the YSZ membranes in contact with the flux compositions

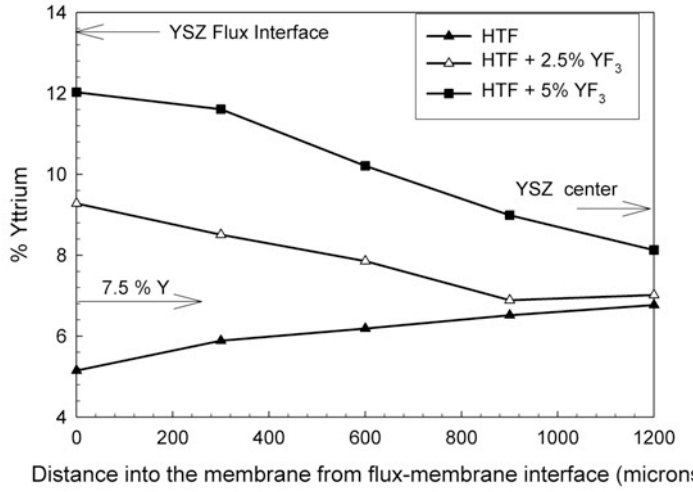

Figure 107 - WDS analysis of yttrium content across the membrane cross-section as a function of YF_3 in HTF system (MgF_2-10% MgO) exposed for 40 hours at 1300°C

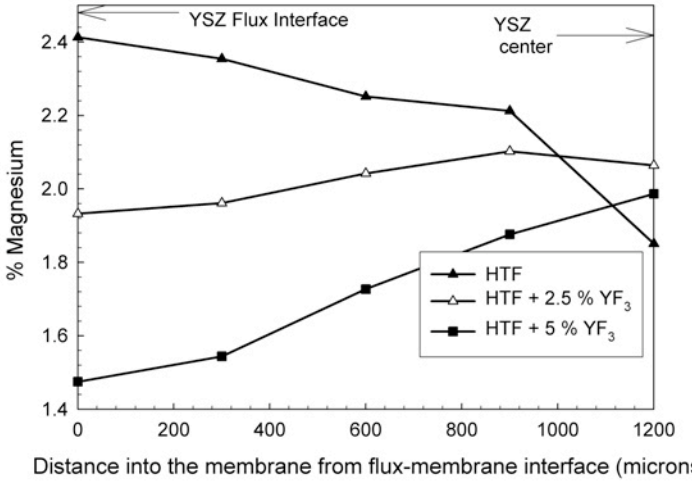

Figure 108 - WDS analysis of magnesium content across the membrane cross-section as a function of YF_3 in HTF system (MgF_2-10% MgO) exposed for 40 hours at 1300°C

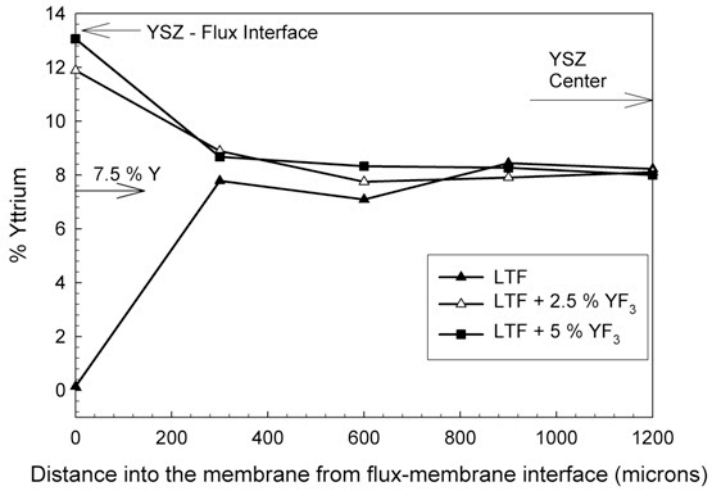

Figure 109 - WDS analysis of yttrium content across the membrane cross-section as a function of YF_3 in LTF system ({55.5% MgF_2- CaF_2} - 10% MgO) exposed for 40 hours at 1150°C

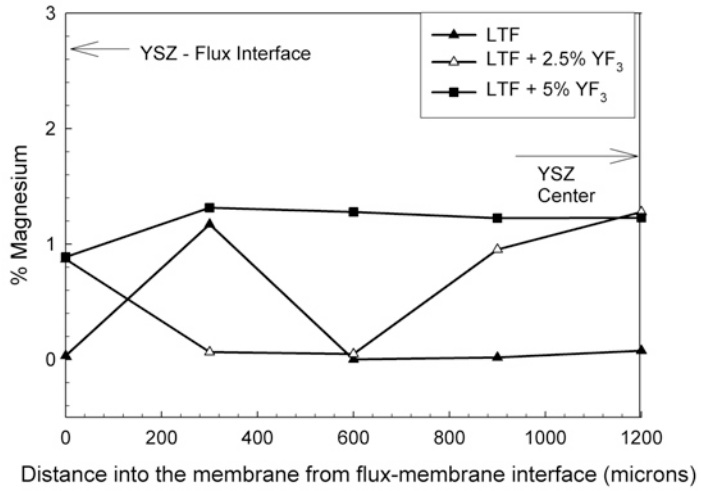

Figure 110 - WDS analysis of Magnesium content across the membrane cross-section as a function of YF_3 in LTF system ({55.5% MgF_2- CaF_2} - 10% MgO) exposed for 40 hours at 1150°C

Viscosity Measurement: The viscosity of the two flux systems, HTF (MgF_2 + 10% MgO) and LTF ((55.5% MgF_2 + CaF_2) + 10% MgO)), were measured using an inner cylinder rotation technique in a graphite crucible (Figure 111). The viscosity measurements were made as a function of temperature and the accuracy of the measurements were within ± 5 %. The pre-melted flux sample was heated to the highest temperature of interest and equilibrated for 30 minutes. Viscosity of the flux was then continuously measured using a platinum bob rotating at 300 rpm immersed in the flux, as the flux was being cooled at a rate of 3°C/min. The natural logarithm of the viscosity (η) is plotted against the inverse of temperature (1/T) in Figure 112 to depict the temperature dependence of viscosity. The measured viscosities of the two fluxes

were found to be sufficiently low; HTF @ 1300°C was 0.042 pa-s, and LTF @ 1150°C was 0.031 pa-s. Similar to the stability considerations, the LTF system is also preferred from the point of viscosity considerations since a low viscosity flux is critical to ensure rapid mass transfer in the flux. The melting points of HTF and LTF systems are 1260 and 970°C, respectively. The lower viscosity of LTF compared to that of the HTF system may be attributed to the higher temperature difference between the measurement temperature and their respective melting points. The viscosity of liquids including molten salts can be expressed as:

$$\eta = AT\exp(\frac{1000B}{T})$$

where T is the temperature in Kelvin and A and B are empirical constants.

Changes in the structure of molten fluxes affect their viscosities and it is reflected by changes in the A and B constants, particularly the B value. Extending this analysis to interpret the results of the viscosity measurements for the HTF and LTF systems (Figure 112) suggests that there are some structural changes occurring in the respective systems above 1275°C and 1100°C.

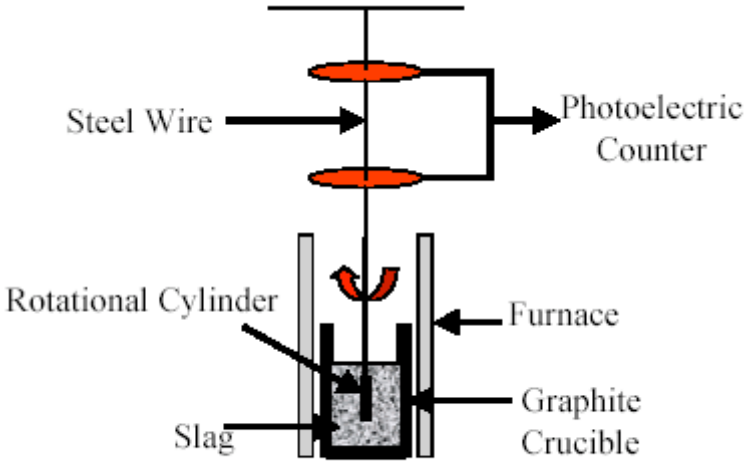

Figure 111 - Experimental setup for high-temperature viscosity measurement

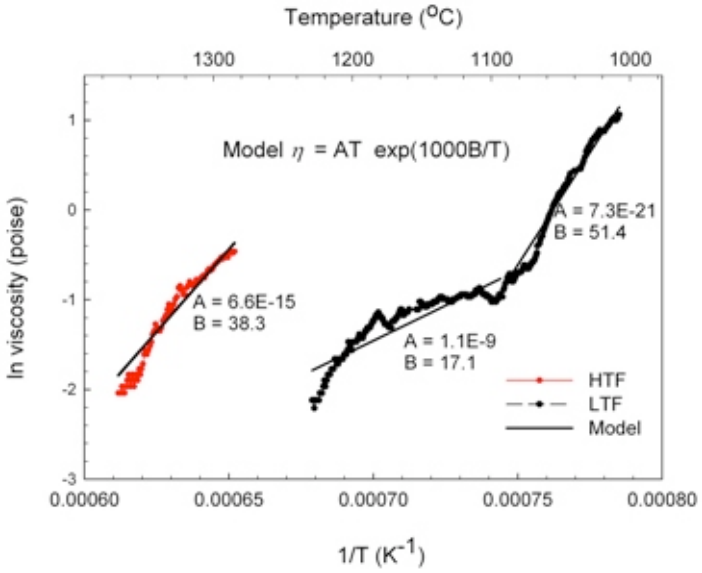

Figure 112 - Temperature dependence of viscosity of HTF and LTF system

5.7.3.7 Dissolution Rate of MgO in LTF system

It is important to determine the solubility limit of MgO in the flux system since the dissolution rate of MgO will be dependent on its solubility limit. The LF flux system (55.5 w% MgF_2 + CaF_2) was allowed to equilibrate for 24 hours with excess MgO. These experiments were performed at 1100, 1150 and 1200°C. At the end of each experiment, slag sample was taken using a quartz capillary tube and sent for ICP analysis to determine the MgO solubility limit. Experiments were then also conducted to determine the dissolution rate of MgO in the LF system as a function of temperature. In these experiments, a certain amount of small MgO particles were added to the flux and flux samples were removed as a function of time (10, 20,30, 60,90 and 120 minutes) to be analyzed using ICP. These measurements will help us determine how MgO is to be added into the SOM reactor as it is reduced during continuous operation. Furthermore, the flux system was continuously stirred with 150 cc/min. of argon to simulate the flux stirring that exists in the SOM reactor.

Analysis: Since the LTF system at 1150°C has low viscosity and the flux is stirred, it is assumed that the flux is homogeneous at all times. Furthermore, since the particle size of MgO is small, the dissolution rate is assumed to be driven by the degree of MgO saturation in the flux. The rate of change of MgO concentration in the flux can be expressed as:

$$\frac{dC_{MgO}^{\ flux}}{dt} = k\left(C_{MgO}^{\ sat} - C_{MgO}^{\ flux}\right)$$

Where $C_{MgO}^{\ sat}$, $C_{MgO}^{\ flux}$ and *k* are the MgO solubility limit, MgO concentration in the flux and the dissolution rate constant, respectively.

$$\frac{dC_{MgO}^{\ flux}}{\left(C_{MgO}^{\ sat} - C_{MgO}^{\ flux}\right)} = kdt$$

Integrating

$$\ln\left(\frac{C_{MgO}^{sat}}{C_{MgO}^{sat} - C_{MgO}^{flux}}\right) = kt$$

C_{MgO}^{sat} is the solubility limit of MgO in the flux that is measured earlier in separate experiments. Thus, by measuring the MgO concentration in the flux (C_{MgO}^{flux}) as a function of time, the dissolution rate constant of MgO can be calculated as the slope of $\ln\left(\frac{C_{MgO}^{sat}}{C_{MgO}^{sat} - C_{MgO}^{flux}}\right)$ versus *t* plot.

5.7.3.8 SOM Process Using Hydrogen Reductant and Tin Anode

5.7.3.8.1 Hydrogen as reductant

In previous proof of concept experiments, a graphite electrode immersed in molten copper (contained in the zirconia tube) was used as the anode. The role of the graphite electrode is to make an electrical connection to the cell and serve as a reductant. For long-term experiments, due to the amount of reductant required, it is cumbersome to feed the graphite electrode into the copper melt as it is being consumed and at the same time maintain good electrical contact. The anode assembly was changed from a graphite/molten copper system to a molybdenum tube/molten copper arrangement. The molybdenum tube is used to make electrical contact and hydrogen gas bubbled through it into the copper melt consumes the oxygen pumped through the zirconia membrane during electrolysis and also prevents oxidation of the Mo tube. The dissociation potential of MgO using hydrogen as a fuel was 0.78 V, measured by a slow potentio-dynamic sweep (scan rate = 0.5 mv/sec) across the electrodes in the SOM cell. In Figure 113, the dissociation potential of MgO is compared with hydrogen and carbon as reductant at 1150°C. Carbon is a more effective reductant compared to hydrogen as evident by the lower dissociation potential of the MgO-C system. However, since the process will be operated at a potential greater than 3V, the small difference in the dissociation potential between using carbon or hydrogen as a reductant will not have any significant effect on process efficiency.

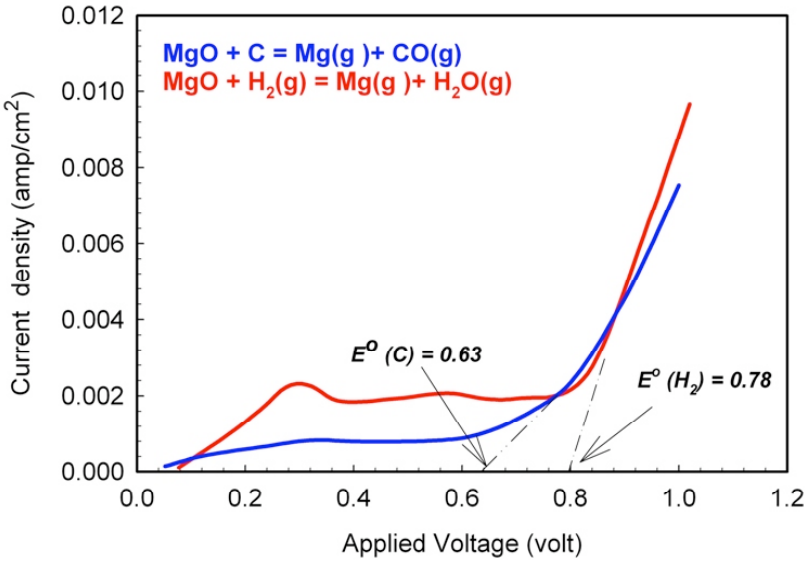

Figure 113 - - Comparison of dissociation potentials of MgO with carbon and hydrogen as reductant at 1150°C

5.7.3.8.2 Molten Sn as an extended anode instead of Molten Cu

During electrolysis, hydrogen bubbled through the molten Cu electrode and evolution of the by-product $H_2O(g)$ results in splashing of the liquid metal. The melting point of copper is 1083°C. At the current operating temperature for the SOM process (1150°C), there is a danger of partial freezing of copper due to splashing since the hot zone has a limited length. This has been avoided by the use of another lower melting liquid electrode (Sn). Tin melts at 232°C and in spite of its lower melting point, its vapor pressure at 1150°C is similar to copper (Figure 114). The oxygen solubility and diffusivity in tin are also comparable to that in copper at (1150°C). Liquid tin is therefore considered a better electrode than liquid copper at 1150°C.

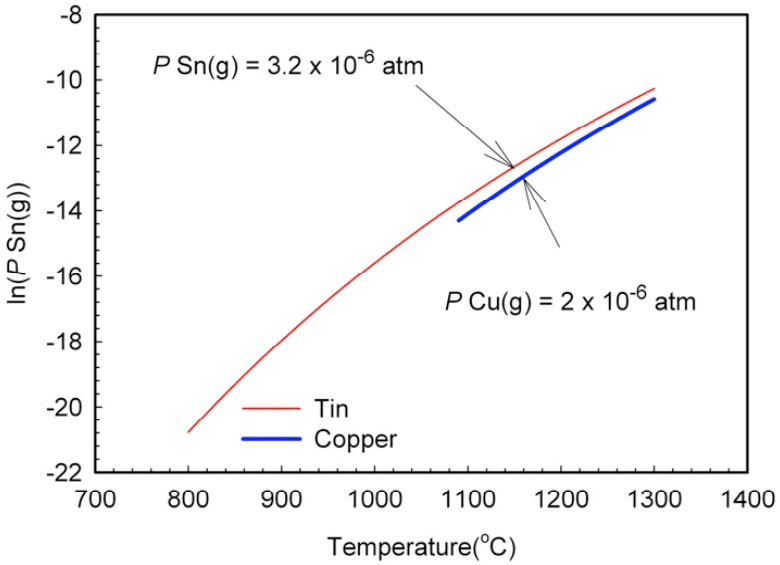

Figure 114 - Comparison of vapor pressures of liquid tin and copper

5.7.3.8.3 Periodic MgO addition

For long-term experiments, MgO is required to be periodically added in order to maintain the oxide concentration in the flux between 5-10 %. When the oxide concentration drops to 5w%, electrolysis is stopped and MgO is added to the flux through the MgO feed tube (Figure 115). Two types of MgO feeding were attempted, coarse powder and low-density pellets. It was observed that with coarse powders, there was a tendency for the powders to adhere to the walls of the feed tube during addition. To avoid this, low density (~30% porous) pellets of MgO were found suitable for making MgO additions.

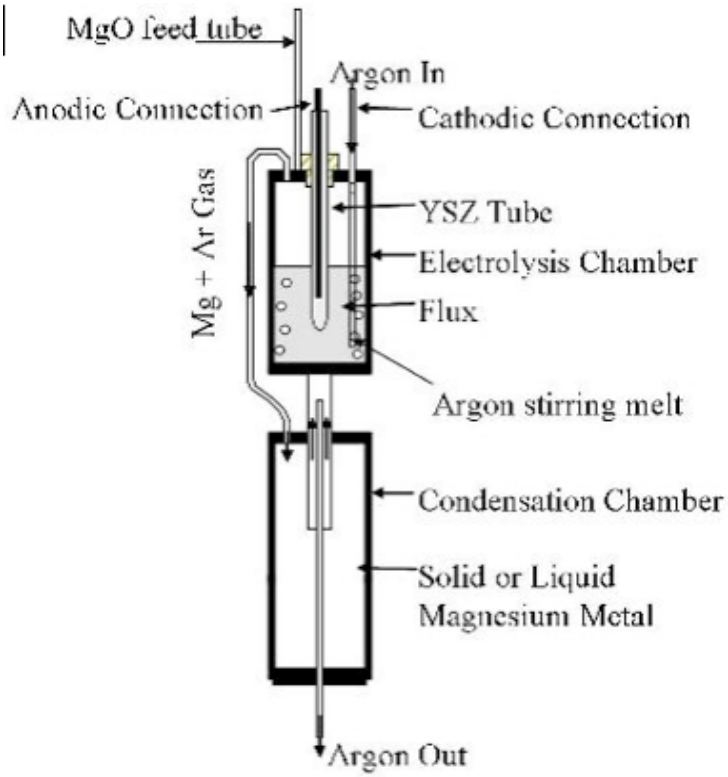

Figure 115 - Experimental setup for long-term experiments

5.7.3.8.4 Electrochemical Characterization

A) Leakage current

The leakage current i.e the current through the cell prior to dissociation of MgO is due to oxygen impurity in the SOM cell. The feed tube is opened during periodic MgO additions. Although a positive inert gas environment was maintained inside the reactor during this period, traces of oxygen (air) entry could not be completely avoided. Traces of oxygen leak into the system during this interval are responsible for increasing the oxygen impurity concentration in the cell. In order to remove this impurity from the cell prior to dissociation of MgO, a constant voltage of 0.6 V is applied across the SOM cell electrodes till the current decays below 0.02 amp/cm^2 (Figure 116). After removing the oxygen impurity traces at 0.6 V, the voltage was gradually increased and held constant at 3V for an extended period. This problem of introducing oxygen impurity in the system while adding the MgO feed can be avoided in the future by using a transfer chamber so

that the SOM cell is not partially exposed to the ambient environment even for a very brief period of time.

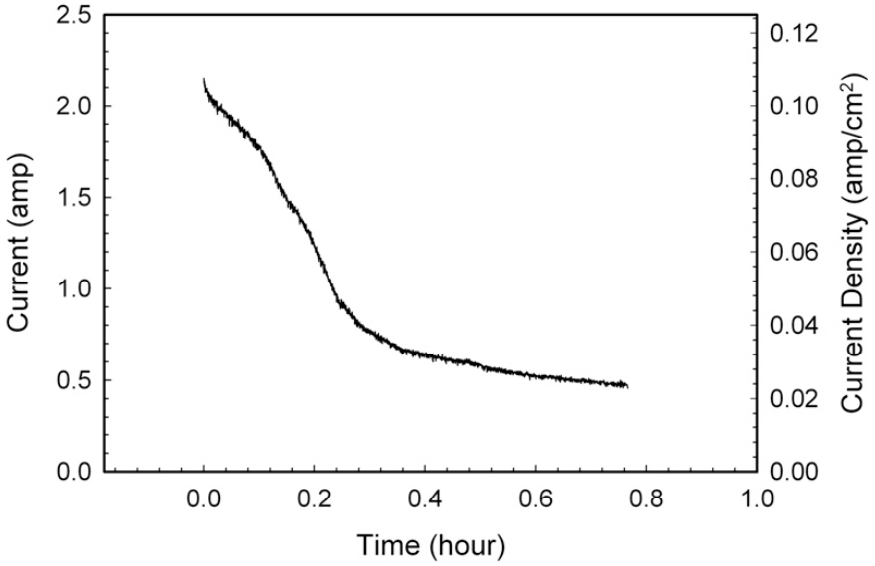

Figure 116 - Removal of oxygen impurities from the cell after MgO additions

B) Potentio-dynamic and Potentiostatic response

From Figure 117, a current density of 0.8 amp/cm^2 was achieved with the application of 4.5 volts in a SOM cell having 10 w% MgO in the flux and using H_2 as the reductant at 1150°C. In this cell the anode used was molten Sn and the H_2 was bubbled into the molten Sn through a Mo tube. It is evident that higher current densities on the order of 1 amp/cm^2 are achievable since a diffusion-limited current is not observed. The specific energy consumption for production of magnesium in the SOM cell is plotted as a function of the cell voltage. It is to be noted that at 0.8-1 A/cm^2 of the cell current, the specific energy consumption is 10-12 KWh/kg of Mg produced; this assumes 100% Faradic efficiency. Figure 118 represents a typical current response curve during electrolysis (Potentiostatic hold) at 3V. Point A on the plot represents start of electrolysis after MgO addition to the flux and removal of the trace oxygen impurities introduced in the system during the MgO addition. The current decreases as MgO in the flux is depleted over time and at point B the electrolysis is stopped for new MgO addition.

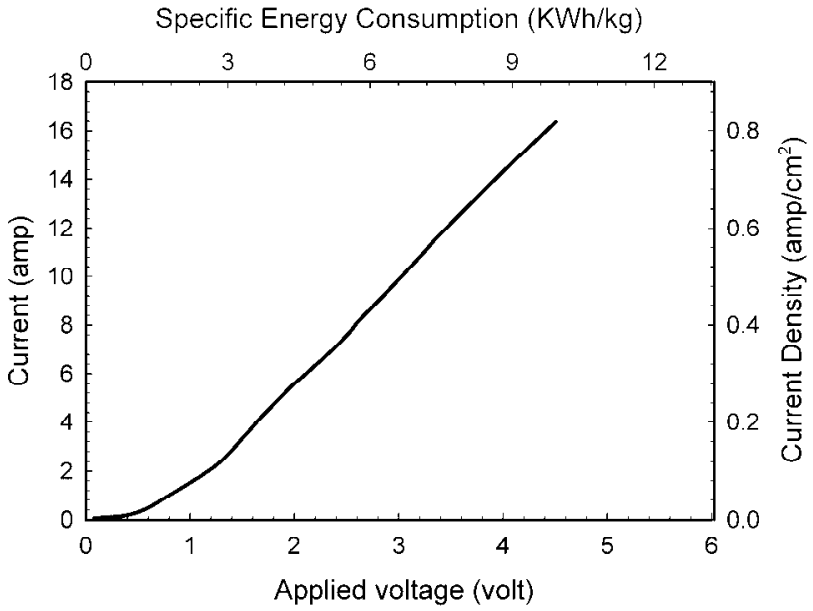

Figure 117 - Potentio-dynamic response of SOM cell with liquid Sn anode

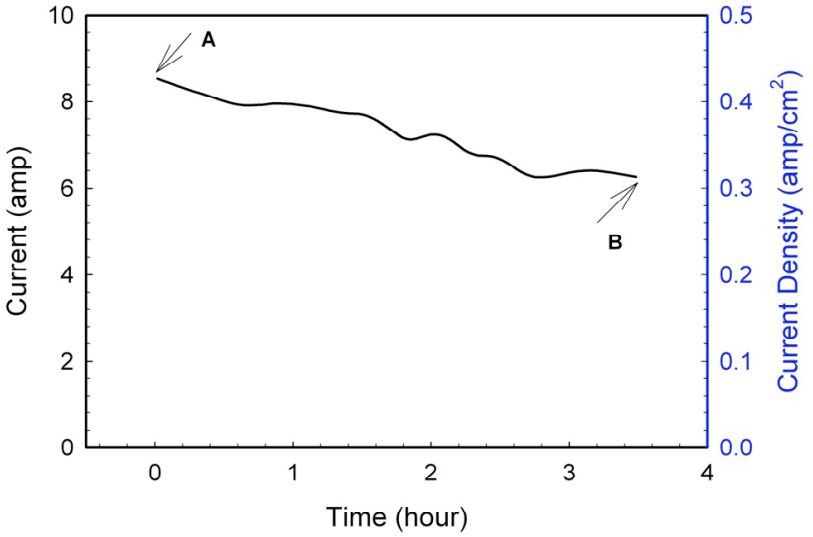

Figure 118 - Potentio-static response at 3V of SOM scale-up cell

5.7.3.8.5 Magnesium deposit

Magnesium vapor that evolves at the steel cathode condenses on a stainless steel foil placed inside the condenser. After the experiment, the condenser is cut under a protective environment of nitrogen and the stainless steel foil is removed. Figure 119 shows the stainless steel foil opened to show the deposit of magnesium. The foil contained over 24 g of magnesium. The metal deposit was analyzed by EDAX and was found to be pure magnesium (Figure 120). It is important to note that calcium was not present in the deposit.

Figure 119 - Magnesium deposit from scale-up experiment

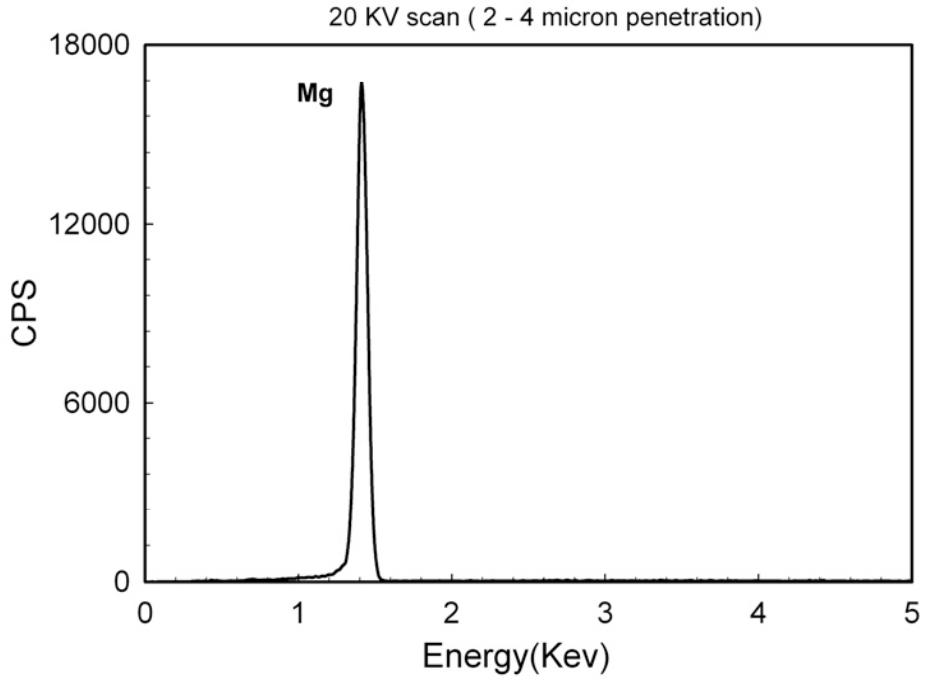

Figure 120 - Chemical analysis (EDAX) of deposit

5.7.3.8.6 Faradic (Current) Efficiency

The faradic efficiency is a critical process parameter that is required to calculate the specific energy consumption (KWh/kg of Mg produced). It is also required for estimating periodic additions of MgO needed to maintain the desired MgO concentration in the flux during the long-term SOM experiments. The faradic efficiency is defined as the ratio of actual MgO reduced to the calculated MgO reduction based on passage of known amount of charge (Faradic equivalent). It is important to note that the SOM process is inherently faradic since the zirconia membrane allows transport of oxygen ions and the ionic flux acts as an electron blocker. A sample of the molten flux (~ 5 g) was taken prior to the start of the experiment with a silica capillary tube to get an estimate of the initial MgO concentration. This is followed by electrolysis at 3V and recording the current passed through the cell as a function of time. The amount of charge (area under current versus time plot) passed through the cell during the experiment was sufficiently large (28.2 amp-hour) to get an accurate average estimate of the efficiency. The flux is again sampled at the end to get the final MgO concentration. The difference in MgO concentration in the flux samples is the actual MgO reduction and this will be used to calculate faradic efficiency.

5.7.3.9 Validation of SOM Process for Continuous Magnesium Production and SOM Process without Reductant

5.7.3.9.1 SOM experiment with periodic addition of magnesium oxide for continuous magnesium production

Periodic addition of MgO pellets

In the SOM experiment, during the electrolysis, MgO concentration in the flux (MgF_2 55.5 wt%-CaF_2) decreases gradually. In order to produce magnesium continuously in a long term SOM experiment, MgO therefore must be added periodically to the reactor. In this experiment, the initial MgO concentration was 10 wt.% and, when the MgO concentration decreased to about 5 wt.%, the electrolysis was halted and MgO was added to the flux in the reactor through the MgO feeding tube, as shown in Figure 121. This was done to restore the MgO concentration in the flux to approximately 10 wt.% before the electrolysis was resumed.

Throughout the experiment, it was found out that MgO powder tended to stick to the MgO feeding tube but that 30% porous MgO pellets could be fed easily and dissolved readily in the flux. Periodic addition of MgO introduced the issue of leakage current, which will be described later in this report.

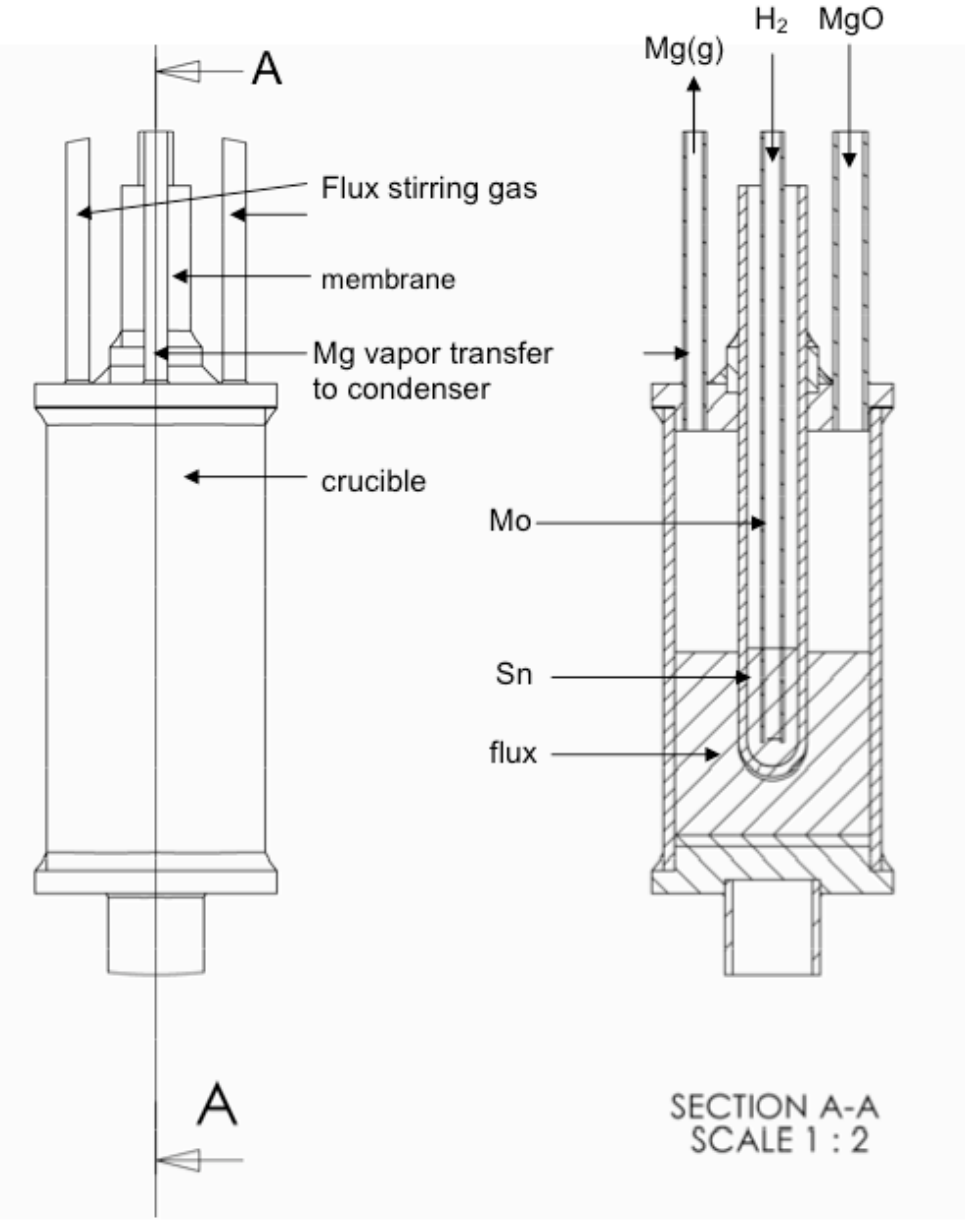

Figure 121 - Schematic of the SOM experiment reactor

Tin/molybdenum tube replaced copper/graphite in the anode

In previous proof of concept experiments, a graphite electrode immersed in copper was used as the anode. The role of the graphite electrode was to make an electrical connection to the cell and serve as a reductant. For long-term experiments, due to the amount of reductant required, it is cumbersome to feed the graphite electrode into the copper melt as it is being consumed and, at the same time, maintain good electrical contact. The anode assembly was changed from a graphite/copper system to molybdenum tube/tin arrangement. The molybdenum tube was used to make electrical contact. Hydrogen gas was bubbled through the Mo tube into the tin melt in order to

consume the oxygen being pumped through the zirconia membrane during electrolysis, thereby preventing the oxidation of the Mo tube.

The dissociation potential of MgO using hydrogen as a fuel was 0.78 V, measured by a slow potentio-dynamic sweep (scan rate = 0.5 mV/sec) across the cell. The equipment for the sweep consisted of a Princeton Applied Research (PAR) (Oak Ridge, TN) potentiostat (model 263A) and a KEPCO (Flushing, NY) power booster. The booster was used to increase the current limit of the potentiostat to 10A. Data acquisition and control was achieved using CorrWare® from Scribner Associates (Southern Pines, NC).

In Figure 122, the dissociation potential of MgO is compared with hydrogen and carbon as reductant at 1150°C. Carbon is a more effective reductant compared to hydrogen, as evidenced by the lower dissociation potential. However, since the process will be operated at a potential greater than 3V, the small difference in the dissociation potential between using carbon and hydrogen will not have any significant effect on process efficiency.

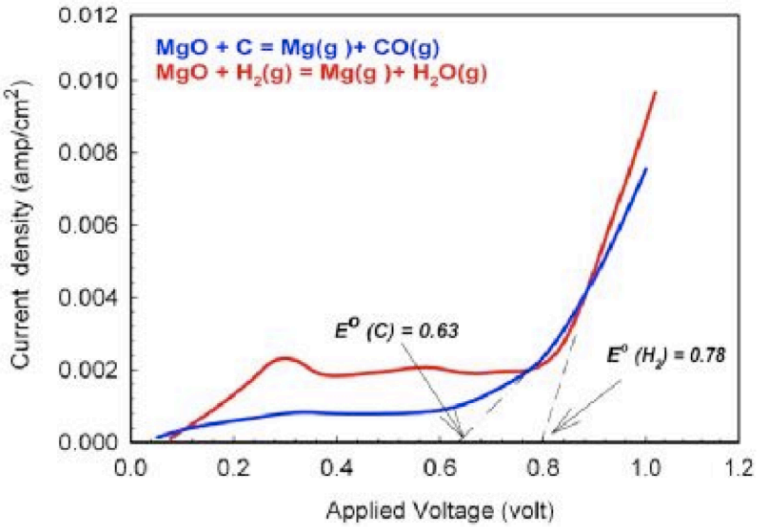

Figure 122 - Comparison of dissociation potentials of MgO with carbon and hydrogen as reductant at 1150°C

During electrolysis, hydrogen bubbled through the liquid electrode and evolution of the by-product $H_2O(g)$ results in splashing of the liquid metal. Given that the melting point of copper is 1083°C, there is great potential for the partial solidification of the liquid copper resulting from splashing, since the hot zone has a limited length. This problem was resolved by our use of a liquid electrode with a lower melting point. Tin melts at 232°C and has been found to be suitable for use as a liquid electrode. In spite of its lower melting point, its vapor pressure at 1150°C is similar to that of copper (see Figure 123). The oxygen solubility and diffusivity in tin are also comparable to copper. Liquid tin was therefore considered a better electrode material than liquid copper at 1150°C.

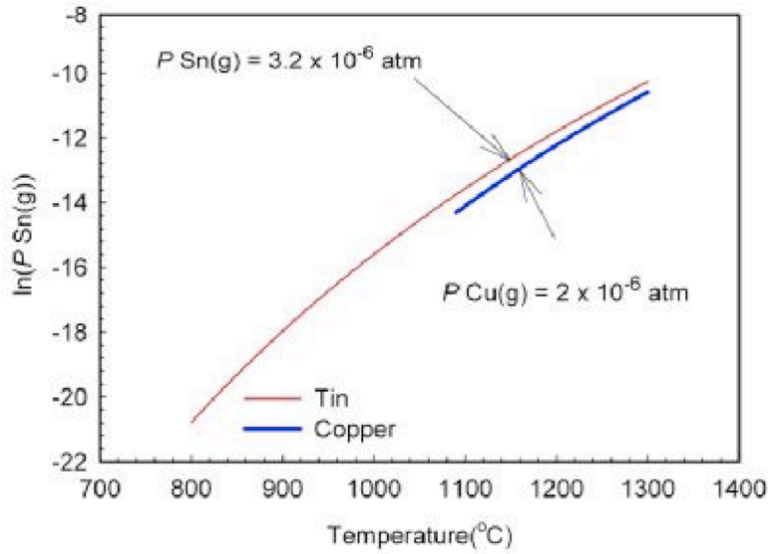

Figure 123 - Comparison of vapor pressures of liquid tin and copper Ohmic resistance of the SOM setup

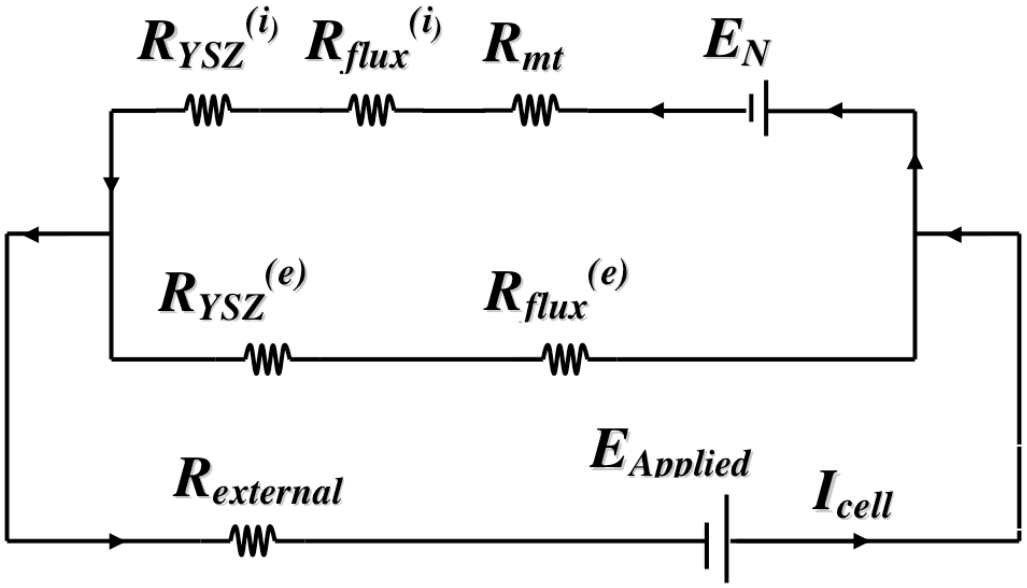

Figure 124 - Equivalent circuit of the SOM cell

The definitions of the different terms used in Figure 124 are as follows:

$R_{YSZ}^{(i)}$ = ionic resistance of the YSZ membrane
$R_{YSZ}^{(e)}$ = electronic resistance of the YSZ membrane
$R_{flux}^{(i)}$ = ionic resistance of the flux
$R_{flux}^{(e)}$ = electronic resistance of the flux
R_{mt} = mass transfer resistance of the cell
E_N = Nernst potential
$E_{applied}$ = applied voltage

$R_{external}$ = resistance outside the cell (includes resistance of the crucible, tubing, metallic support and electrical connections)

The equivalent circuit of the SOM cell is shown in Figure 124. Given that the YSZ membrane and the flux are mainly ionic conductors,

$R_{YSZ}^{(i)} << R_{YSZ}^{(e)}$ and $R_{flux}^{(i)} << R_{flux}^{(e)}$.

For a well-stirred SOM cell, R_{mt} is less than 0.1 ohms. The ohmic resistance of the cell is defined as

$R_{ohmic} = R_{flux}^{(i)} + R_{YSZ}^{(i)} + R_{external}$.

The Rohmic can be measured using impedance spectroscopy as the intercept of the real axis of the Cole-Cole plot when the frequency is high. For a SOM cell, R_{ohmic} should be around 0.3 ohms. A much smaller R_{ohmic} indicates that a membrane has broken and a much larger R_{ohmic} indicates that there are bad contacts or connections in the SOM cell. R_{ohmic} can therefore be regarded as a parameter indicating the quality of the SOM cell setup.

During the long-term SOM experiment, thirty minutes after the addition of MgO pellets, R_{ohmic} was measured. If the R_{ohmic} was within the desired range, electrolysis was resumed. The impedance spectroscopy equipment consisted of a Princeton Applied Research (PAR) (Oak Ridge, TN) potentiostat (model 263A) and Solartron impedance analyzer (Houston, TX) (model 1250B). Data acquisition and control of the above instruments was achieved with CorrWare® and Zplot® from Scribner Associates (Southern Pines, NC). The sequence of electrolysis, addition of MgO pellets, and R_{ohmic} measurement was repeated four times during the experiment. The R_{ohmic} measurement after each addition of MgO is shown in Figure 125.

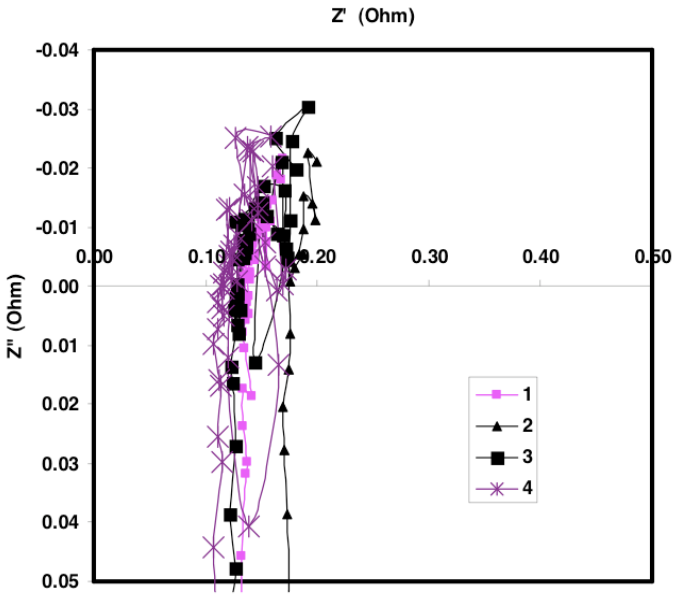

Figure 125 - Rohmic measurement results by impedance spectroscopy

The total charge passed was 101.6 Ampere.hours (corresponding to approximately 50 g).

Leakage current

A leakage current (defined as the current through the cell prior to the dissociation of MgO) results from oxygen impurity in the SOM cell. During MgO additions, the cell was opened to the outside environment. Although a positive inert gas environment was maintained inside the reactor during this period, oxygen entry could not be completely avoided. Thus, the leakage current (i_l) can be attributed to two oxygen impurity sources: (1) oxygen in the gas phase, where the oxygen is reduced at the cathode by the reaction $1/2O_2(g) + 2e^- = O^{2-}$ and (2) soluble oxygen in the flux, where the oxygen is reduced in the vicinity of cathode through the reaction $[O]+ 2e^- = O^{2-}$.

In order to minimize the effect of leakage current on the measurement of the dissociation potential of MgO, a constant voltage of 0.6 V is applied across the cell until the current decays indicate a drop in the oxygen impurity concentration. From Figure 126, it is clear that during a potentio-static hold at 0.6 V, the current quickly decayed below 0.02 amp/cm2. During a regular SOM run this step will not be necessary because during the potentio-static hold at 5V the leakage current (oxygen impurity) is expected to decay much faster (< 1 minute). Also, this problem can be avoided in the future by adding MgO through a transfer chamber so as to completely eliminate the limited exposure of the SOM cell to the ambient environment.

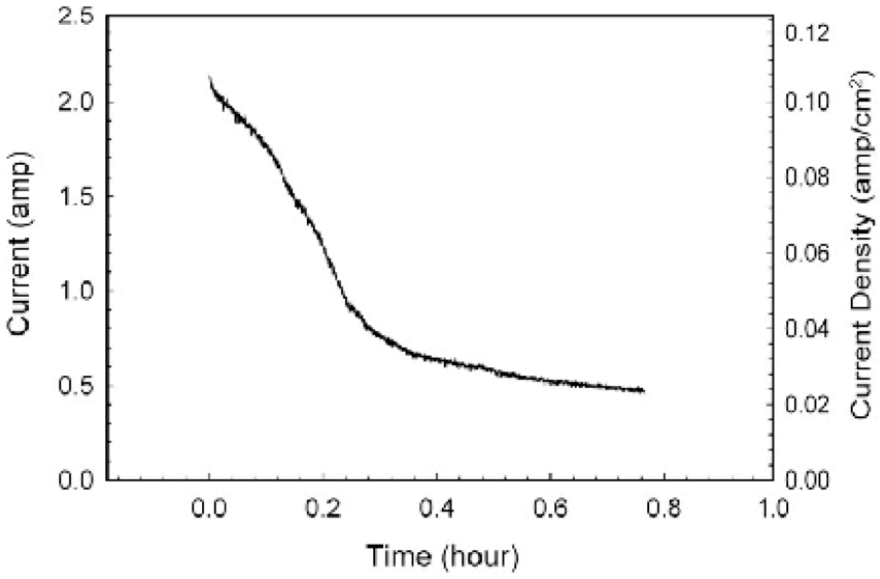

Figure 126 - Removal of oxygen impurities from the cell after MgO addition

Magnesium deposit

Magnesium vapor from the SOM experiment was condensed on a stainless steel foil placed inside the condenser. After the experiment, the condenser was sectioned under a protective environment of nitrogen and the stainless steel foil was removed. Figure 127 shows the stainless steel foil opened to show the deposit of magnesium. The foil contained the magnesium deposit. The metal deposit was analyzed by EDAX and was found to be pure magnesium (Figure 128).

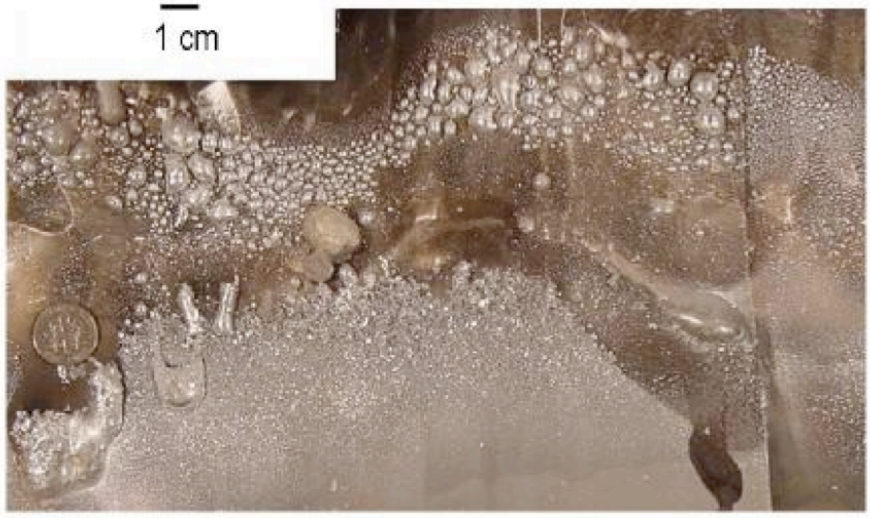

Figure 127 - Magnesium deposit from scale-up experiment

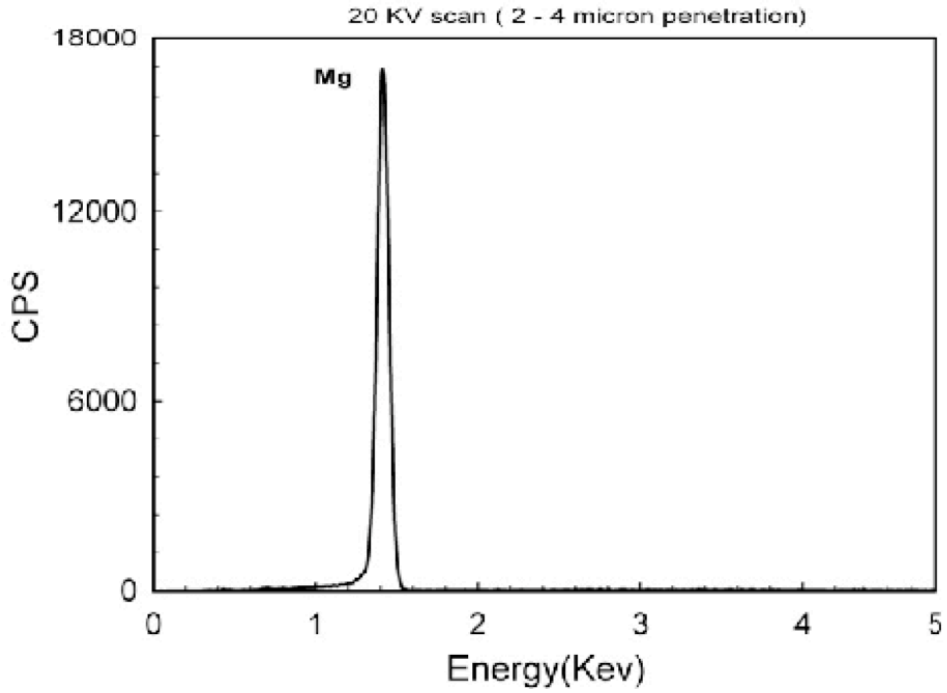

Figure 128 - Chemical analysis (EDAX) of deposit

5.7.3.9.2 Magnesium and oxygen producing SOM experiment using no reductant and molten silver as the liquid anode.

In the previous experiment, a molybdenum tube was immersed in a pool of molten tin and hydrogen was passed through it to consume the O_2 evolved during the experiment at the anode. The role of the molybdenum tube is to make an electrical connection with the cell and for use as a conduit for H_2, which worked as reductant. The molten tin ensured good connection between molybdenum tube and YSZ membrane. For continuous magnesium production, H_2 gas will have to be fed in continuously into the molten metal anode. This requirement may introduce additional challenges that pertain to hydrogen transportation, storage, and safety.

In the reported experiment, we designed and ran a magnesium production SOM experiment without any reductant feed. We have verified that magnesium can indeed be produced using the SOM process without any reductant feed. In addition, we expect that the oxygen generated at the anode can be separated from the exhaust gas flow and used for other industrial applications, further increasing the industrial merit of this green manufacturing process.

Experiment setup

This experiment used the same setup as the previous experiments, excepting liquid silver was used as the anode instead of liquid tin (see Figure 129). Silver provides several advantages over tin and copper while still retaining the qualities that make the latter elements desirable. The oxygen solubility and diffusivity in silver are comparable with that of tin and copper (see Figure 130 and Figure 131), but silver oxide is unstable at high temperatures, so oxygen can be pumped into silver without fear of oxidation. Iridium wire was used as the electrode lead.

The mechanism of magnesium production in the experiment is as follows: when the applied DC potential is greater than the dissociation potential of MgO, Mg^{2+} cations move toward the cathode, gain electrons and are reduced to Mg. At the experimental temperature 1150°C, Mg evolves as Mg gas which is condensed as before in the condenser. The O^{2-} anions in the slag are driven by the electrochemical potential difference through the YSZ membrane (an oxygen ion conductor) toward the anode. At the interface of the membrane and silver the O^{2-} ions lose electrons (oxidize) and associate with each other to form O_2 gas. This gas is subsequently carried away by the argon gas flow.

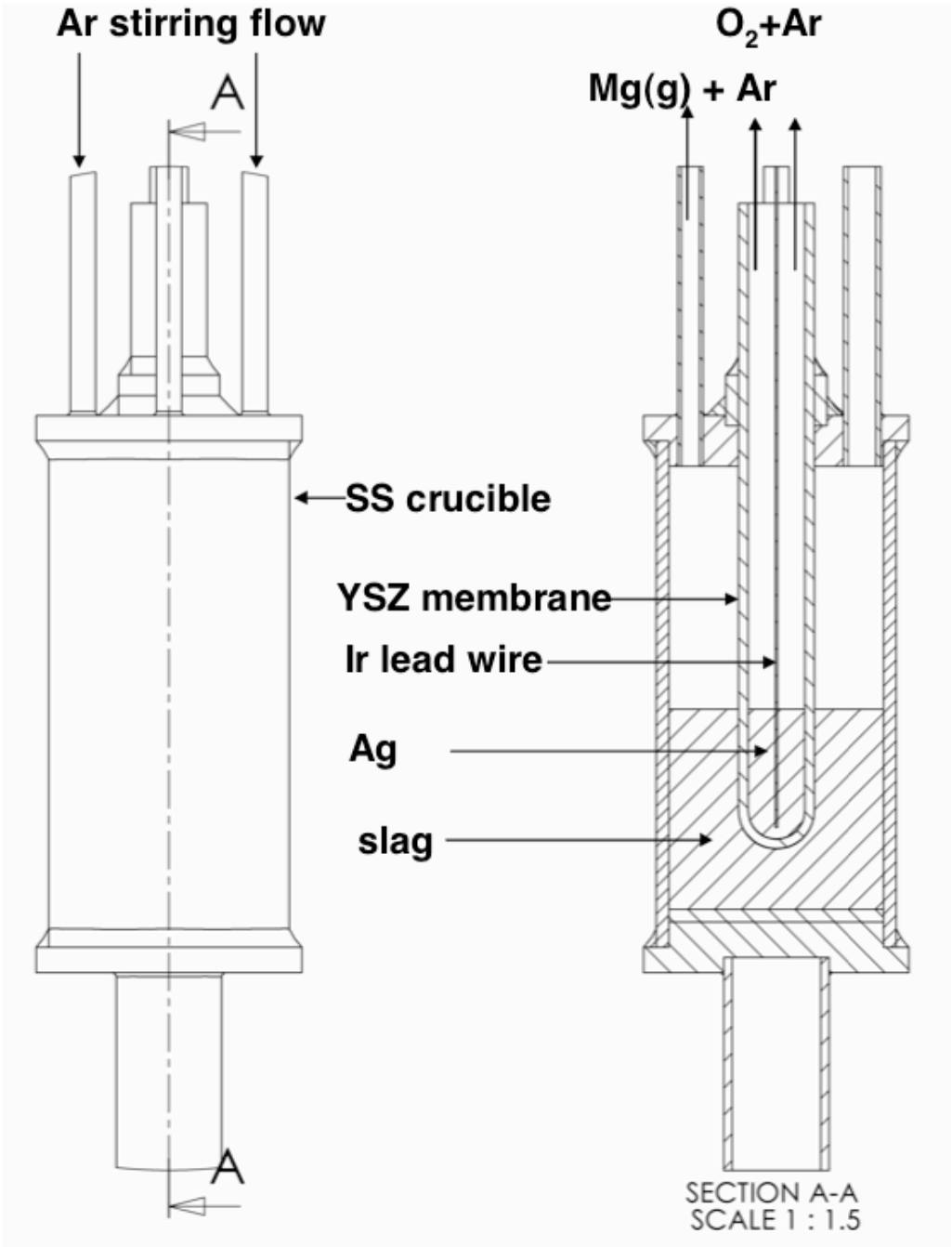

Figure 129 - Schematic of the reactor section of the experiment setup

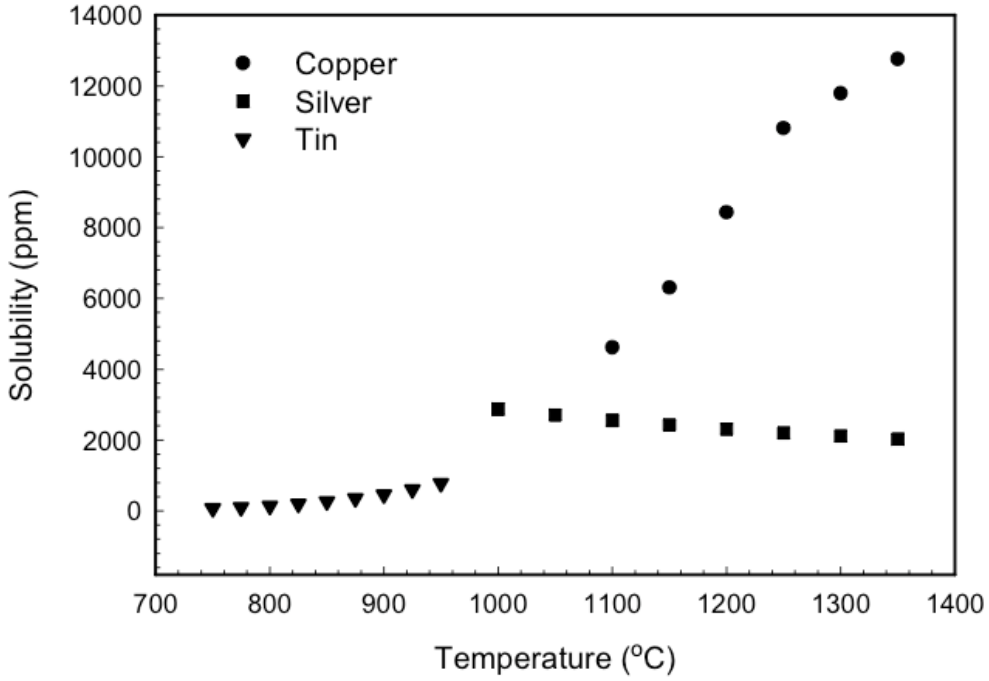

Figure 130 - Comparison of oxygen solubility in copper, tin and silver

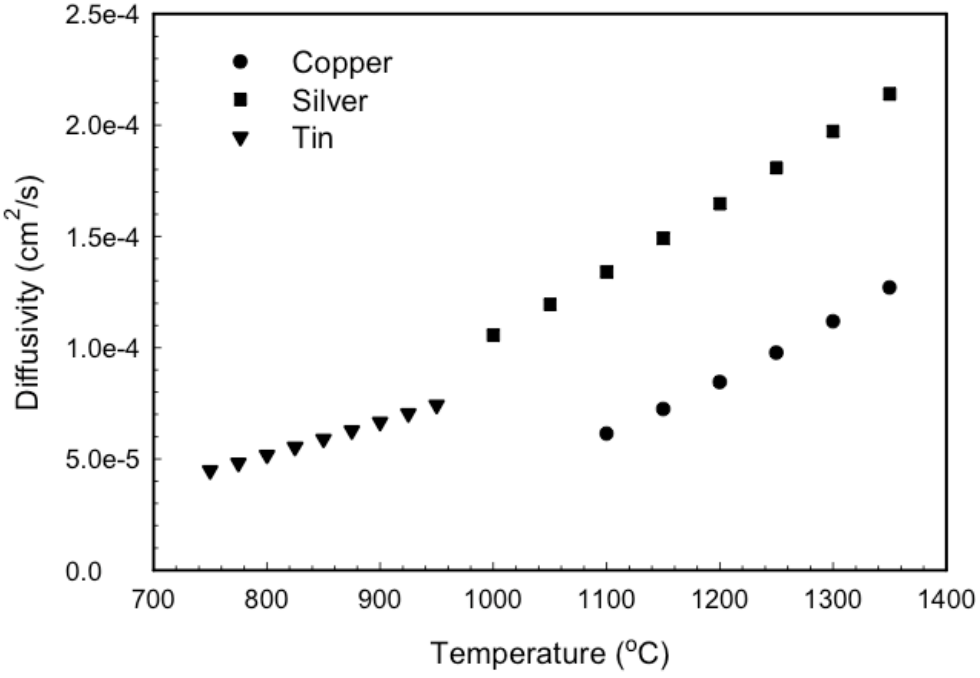

Figure 131 - Comparison of oxygen diffusivity in liquid copper, tin and silver

MgO dissociation potential measurement

The MgO dissociation potential measurement is based on the SOM cell response to the slow potentio-dynamic sweep (scan rate=0.5mV/sec) across the electrodes.

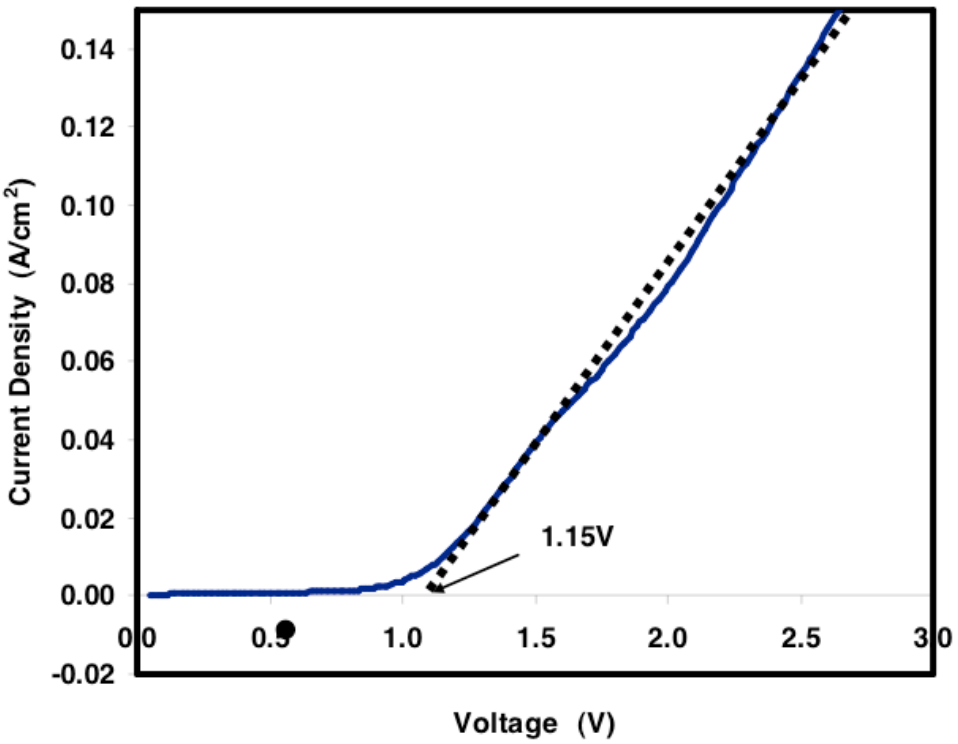

Figure 132 - Dissociation potentials of MgO without reductant at 1150°C

Figure 132 shows the results of potentio-dynamic sweep. It shows that the dissociation potential of MgO in the experiment is about 1.15V, which is about 60-80% higher than the dissociation potentials when either carbon or hydrogen is used as reductant (shown in Figure 122); in absolute terms it is only about 0.4 V to 0.5 V higher. Based on this fact, at current densities between 0.4-1 A/cm^2, about 10-15% higher electric potential has to be applied in the SOM experiment without reductant than in the experiment with either carbon or hydrogen as reductant. This implies that 10-15% more electric power has to be used in the experiment without reductant to produce the same amount of magnesium as the other that had the reductant. The savings in the carbon or hydrogen feed during magnesium production and the potential benefit of the oxygen obtained may offset this increase in electric power requirement.

Magnesium Production

During the SOM experiment, a DC voltage was applied between anode and cathode. The initial voltage was increased linearly from 0 volts to 6 volts and held at 6 volts for 6.5 hours (see Figure 133). This figure also shows, through the current density versus time curve, that the cell became stable in about three hours and the current density started decreasing after one and half hours. After the experiment, the thin stainless steel foil with the collected magnesium was removed from the condenser and the total weight of the Mg deposit was measured. After subtracting the tare weight of the steel sheet, the magnesium produced was computed to be approximately 8.1 grams. EDAX analysis reveals the product to be pure magnesium. Figure 134 shows a picture of the magnesium collected inside the condenser with the EDAX analysis results inset on the right.

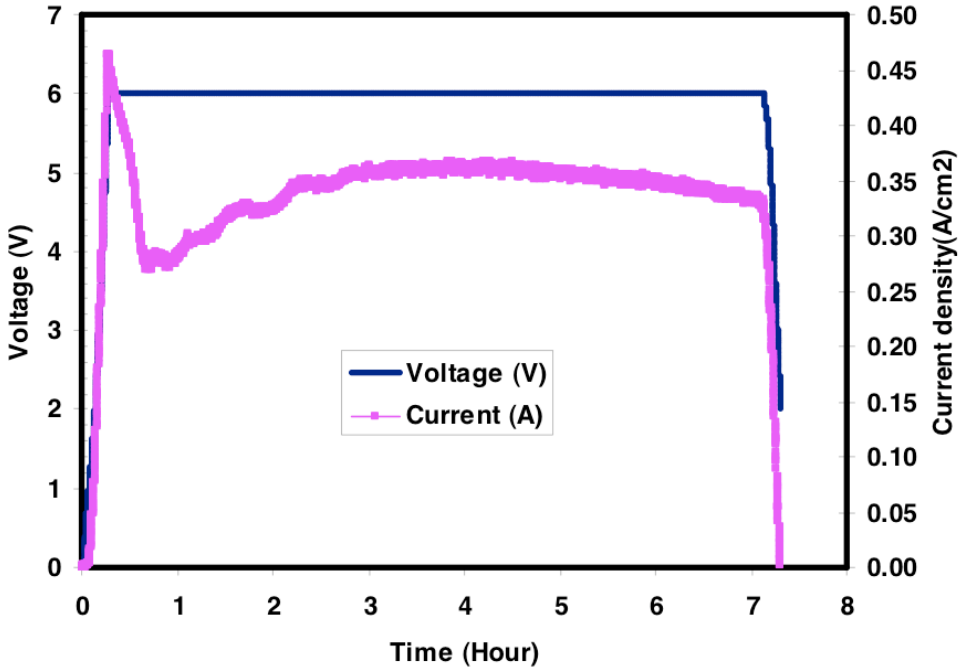

Figure 133 - Potentiostatic response of the SOM cell

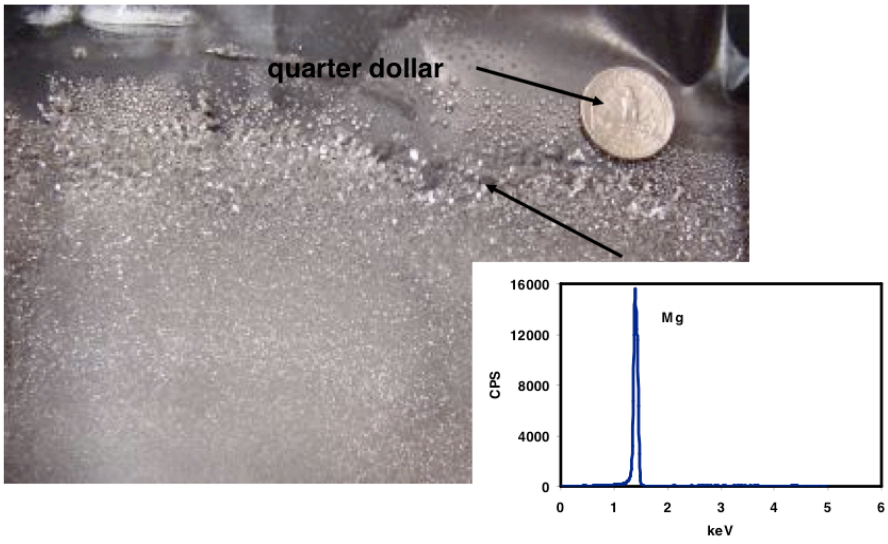

Figure 134 - Magnesium collected inside the condenser

Faraday efficiency measurement

The Faradaic efficiency ($\eta_{Faraday}$) of the SOM experiment for magnesium production is defined as the percentage of the total charge used to reduce magnesium cations to pure magnesium. ($\eta_{Faraday}$) can be expressed as:

$$\eta_{Faraday} = \frac{W_{Mg} \bullet 2 \bullet F}{M_{Mg} \bullet \int_0^t I \cdot dt}, \quad (1)$$

W_{Mg} is the weight (in grams) of pure magnesium obtained through electrolysis, M_{Mg} is the molar weight of pure magnesium (24.31g/mol), F is the Faraday constant (equals 96485.34 C/mol), I is the magnitude of the passed current (in Amperes), and t is the time duration (in seconds) used to pass the current during electrolysis.

It is difficult in practice to collect all the reduced magnesium being produced by the reactor. In the current method, a thin stainless steel foil is put on the surface inside the condenser. The weight of the foil with condensed magnesium on the surface is compared to the weight before the SOM experiment. This weight difference is regarded as the weight of the magnesium produced by SOM process. In reality, some magnesium vapor may react with the oxides on the walls of reactor as well as the magnesium vapor transfer between reactor and condenser may not be 100% efficient. In addition, it is not guaranteed that the thin stainless steel foil covers the entire surface inside the condenser where magnesium vapor deposits. So, in the current scheme, the Faradaic efficiency estimation does not provide an accurate result.

To obtain a more accurate estimation of the Faraday efficiency measurement, we plan to measure the MgO concentration change in the flux before and after the SOM electrolysis experiment. From this method, the Faradaic efficiency $\eta_{Faraday}$ can be expressed as:

$$\eta_{Faraday} = \frac{W_{flux} \bullet (C_{before} - C_{after}) \bullet 2 \bullet F}{(1 - C_{after}) \bullet M_{MgO} \bullet \int_0^t I \cdot dt}, \quad (2)$$

In this equation, W_{flux} and C_{before} are the total flux weight (in grams) and MgO concentration (by weight) before the experiment, respectively. C_{after} is the MgO concentration (by weight) after electrolysis, and M_{MgO} is the molar weight of MgO (equal to 40.304 g/mol). z, F, I, t have the same definitions used in Equation 1. During the SOM experiment, slag samples (about 5 grams each) before and after the electrolysis experiment will be obtained employing a quartz tubing inserted through the MgO feeding tube shown in Figure 121. We will use Inductively Coupled Plasma Emission Spectroscopy (ICP-ES) to measure the concentration of Ca^{2+} in the slag samples.

After weight percentages of Ca^{2+} in the slugs have been determined, the MgO concentration by weight can be calculated in the following way:

1. The concentration (by weight) of CaF_2 in the flux C_{CaF_2} can be obtained from the measured concentration (by weight) of Ca^{2+} ($C_{Ca^{2+}}$) by using Equation 3.

$$C_{CaF2} = C_{Ca^{2+}} \bullet \frac{M_{CaF_2}}{M_{Ca}} \quad (3)$$

M_{CaF_2} = molar weight of CaF_2 = 78.08 g/mol
M_{Ca} = molar weight of Ca = 40.08 g/mol

2. In the flux, the weight ratio of CaF_2 to MgF_2 equals 1:1.25. The MgF_2 concentration in the flux (C_{MgF_2}) can therefore be expressed as:

$$C_{MgF_2} = 1.25 \bullet C_{CaF_2} \quad (4)$$

3. The concentration (by weight) of MgO in the flux is $C_{MgO} = 1 - C_{CaF_2} - C_{MgF_2}$. Combining Equations 3 and 4 and the values of M_{CaF_2} and M_{Ca}, C_{MgO} can be expressed as:

$$C_{MgO} = 1 - 4.38 \bullet C_{Ca^{2+}} \quad (5)$$

The MgO concentration in the slag samples can thus be estimated by measuring the Ca^{2+} concentration in the slag.

Six flux samples with MgO concentrations of 0%, 2%, 4%, 6%, 8% and 10% by weight have been prepared as standard samples for conducting the ICP-ES analysis.

Numerical simulation of the SOM process

The objectives of the SOM process numerical simulation are to optimize process parameters to improve Mg productivity and lower process cost. By applying Computational Fluid Dynamics (CFD) technique and considering coupled fluid flow, heat transfer, and mass transfer phenomena inside the SOM reactor and condenser, a SOM process model will be setup for numerical simulation. The geometry model will be setup in Pro-Engineer®, the meshes of the model will be made in Gambit®, and the calculations will be performed using FLUENT®. The simulation results will provide technical guidelines for SOM process scale-up and evaluate the possibility of MgH_2 generation in the condenser through H_2(g) injection.

The simulation will first deal with the following aspects of SOM process:

1. Flux stirring.

   Flux stirring by argon flow can improve mass transfer in the flux, which includes making MgO concentration in the flux more homogeneous and carrying the magnesium vapor out of the flux. The argon flow will also change the partial pressure of the Mg(g) and temperature fields in the reactor and condenser. These are important variables that can affect YSZ membrane stability, flux viscosity, magnesium collection in the condenser, and the potential for synthesizing MgH_2 in the condenser through H_2(g) injection. Through simulation, the location, size of the tube for flux stirring, and the argon flow rate will be optimized.

2. Condenser design.

   For magnesium production, magnesium vapor is condensed and collected in the condenser. Through numerical simulation, condenser design will be optimized and the efficiency of magnesium collection in the

condenser will be improved. For future MgH_2 production in the condenser by H_2 injection, the simulation results will answer the following questions:

1. At steady state, what is the temperature field inside the condenser and how does hydrogen injection affect it?
2. What is the concentration distribution of the components of the gas mixture, which includes Ar, H_2, MgH_2 and Mg?
3. What are the effects of the temperature field and gas mixing on the kinetics of MgH_2 production?

The process factors considered will be:

1. Location and angle of the hydrogen injection.
2. Size of the hydrogen injection tubing.
3. H_2 flow rates.
4. Initial hydrogen flow temperature
5. Temperature distribution within the reactor

5.7.3.9.3 Other work on other related SOM projects

Titanium production from titanium oxide using the SOM process

Titanium is a high-strength, low-density metal nearly immune to corrosion, but limited in use by its high price. The high price is due not to scarcity, as titanium is the fourth most abundant metal in the earth's crust, but rather the cost of smelting and processing the ore. The Kroll process, which has dominated the reduction of titanium for over 50 years, is beset with numerous problems that keep the price of titanium metal several times higher than the sum of the costs of raw materials and dissociation energy. Our project on titanium production using the SOM process aims for a continuous production of dense billets or ingots of commercial purity (CP) titanium directly from the low-cost ore. The process consolidates nearly all of the processing steps required for the Kroll process into a single step and operates at high energy efficiency, allowing for an enormous reduction of cost for CP billet and ingot and possibly also for powder used to make titanium alloys. This project is funded by the National Science Foundation and will be done in cooperation with Professor Adam Powell, Department of Materials Science and Engineering, Massachusetts Institute of Technology.

Calcium production from calcium oxide using the SOM process

Calcium is also a relatively plentiful metallic element and composes more than three percent of the Earth's crust, making it fifth in overall abundance. In industry, calcium is used in the production of energy-efficient materials: high-strength steels, maintenance-free automotive batteries, and advanced magnetic materials. The United States accounts for over 50% of the world consumption of calcium.

The major production method used today for calcium is thermal reduction of lime with aluminum. The reactions can be expressed as:

$$6CaO + 2Al = 3CaO.Al_2O_3 + 3Ca(g)$$
$$33CaO + 14Al = 12CaO.7Al_2O_3 + 21Ca(g)$$
$$4CaO + 2Al = CaO.Al_2O_3 + 3Ca(g)$$

In the process, the reactants, lime and aluminum powder, are briquetted and charged into a high-temperature alloy retort. The reaction vessel is evacuated to 0.1 Pa

or less and heated to 1200°C. The aluminum reduces the lime to produce calcium metal vapor. The calcium vapor is then removed and condensed separately, enabling the reaction to continue in the desired direction.

High-purity grade calcium metal requires an input of highly purified lime and aluminum. A further step, vacuum distillation, is also required because the calcium produced in the reduction reaction is contaminated with aluminum. The vacuum distillation operation also reduces the level of other contaminants, such as manganese.

In the SOM process for calcium production, CaO is dissolved in MgF_2-CaF_2 slag in the crucible. This crucible will act as the cathode and the YSZ membrane with the liquid metal will work as anode. Under an applied electric potential between anode and cathode, the Ca^{2+} will be reduced and collected at cathode and the O^{2-} will pass through the oxygen conducting YSZ membrane to react at the liquid metal anode. There it is oxidized and evolved as oxygen gas or it reacts with the reductant. In the SOM process, no high purity aluminum or vacuum is required, as in the thermal reduction process, and the processing temperature is approximately 50°C lower. If we are successful in implementing the SOM process for calcium production, the price of calcium will drop and the environmental impact of its production will also be reduced. The project will be funded by Minteq Inc.

5.7.3.10 Scale-up Modeling of SOM Process for Continuous Magnesium Production

5.7.3.10.1 Numerical simulation of the SOM process

Boundary conditions used in model (refer to Figure 135):

The outer circumference and the four interior tubes (the three inert gas bubbling tubes and the slightly larger MgO feeding tube) were set as ground (cathode). The yttria-stabilized zirconia (YSZ) membrane anode ceramic tubes were assigned an electrical conductivity of 10 S/m (actual value). The electrical conductivity of the flux was assigned 383 S/m (actual value). The inner wall of the YSZ tube was assigned an electrical potential of 5 V (value expected to be used during the SOM runs).

Considerations for the 3-tube scale up design of the SOM reactor

Objective: Maximize total current and find the average current density on the YSZ tube surface by dividing the total current by the total surface area of YSZ tube immersed in the flux. Determine the current density distribution for this condition and determine if the distribution around the circumference of the YSZ tubes is uniform. Non-uniform current density around the YSZ tube may cause the tube to fail due to possible thermal gradients.

The results presented in this report are preliminary data demonstrating the viability of the modeling technique. The current densities reported in the model calculations are local current densities and refer to each cell containing the current flux. This is different from the way the current density is presented in actual experiments. In actual experiments the reported current density is the total current divided by the immersed area of the YSZ anode tubes and referred to as the anodic current density. Therefore, to obtain current density values from the model that can be compared with the experimental data one must determine the total current and divide it by the total area of the YSZ/flux interface. Also, the actual polarization losses at the electrodes and

lead wire resistance need to be incorporated in the model from the experimental data obtained while using the single cell reactor.

Modeling results to date for the 3-tube scale up design of the SOM reactor

The initial design for the 3-tube scale-up aligns the 3 ceramic YSZ membrane anodes alternated with small bubbling tubes spaced at 60-degree intervals along a circle circumference. The radius of this circle (A) was varied from 0.70” (0.0178 m) to 1.20” (0.0305m). See Figure 135.

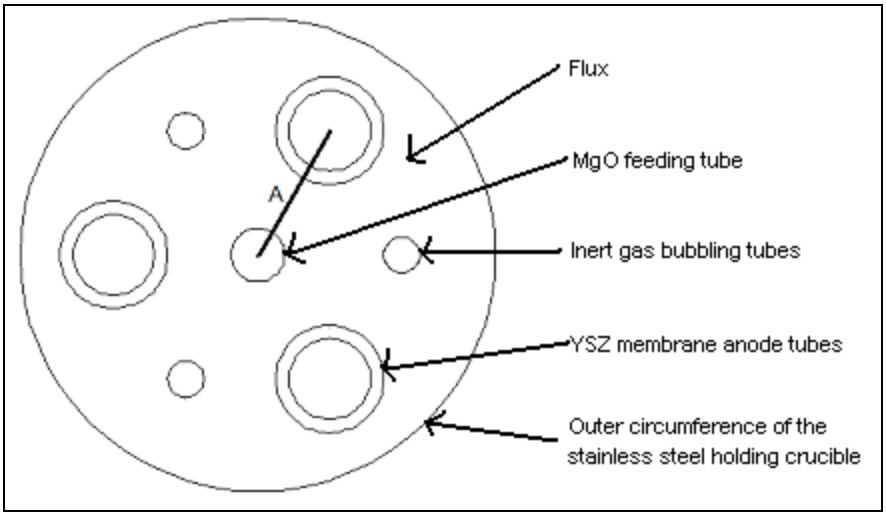

Figure 135 - Dimension A

The dimensions used to create this model are shown in Table 63.

Table 63 - Constant Model Dimensions Based on the 3-tube SOM Reactor

Component Dimensions	inches	meters
diameter of MgO feed tube (at center of circle)	0.35	0.0089
diameter of large stainless steel holding crucible	3.30	0.0838
diameter of bubbling tubes	0.25	0.0064
outer diameter of YSZ ceramic membrane	0.75	0.0191
inner diameter of YSZ ceramic membrane	0.56	0.0142

The values for the total current density maximum and minimum for each simulation are shown in Table 64.

Table 64 - Total Current Density

Figure #	A value (inches)	Total Current Density (A/m^2) Maximum (red)	Minimum (blue)
Figure 136	0.7	2.72e4x10^4	178.162
Figure 137	0.87	2.52e4x10^4	68.791
Figure 138	1	2.286e4x10^4	77.618
Figure 139	1.2	2.379e4x10^4	7.678

Figure 136, Figure 137, Figure 138, and Figure 139 show the current density distribution for each simulation.

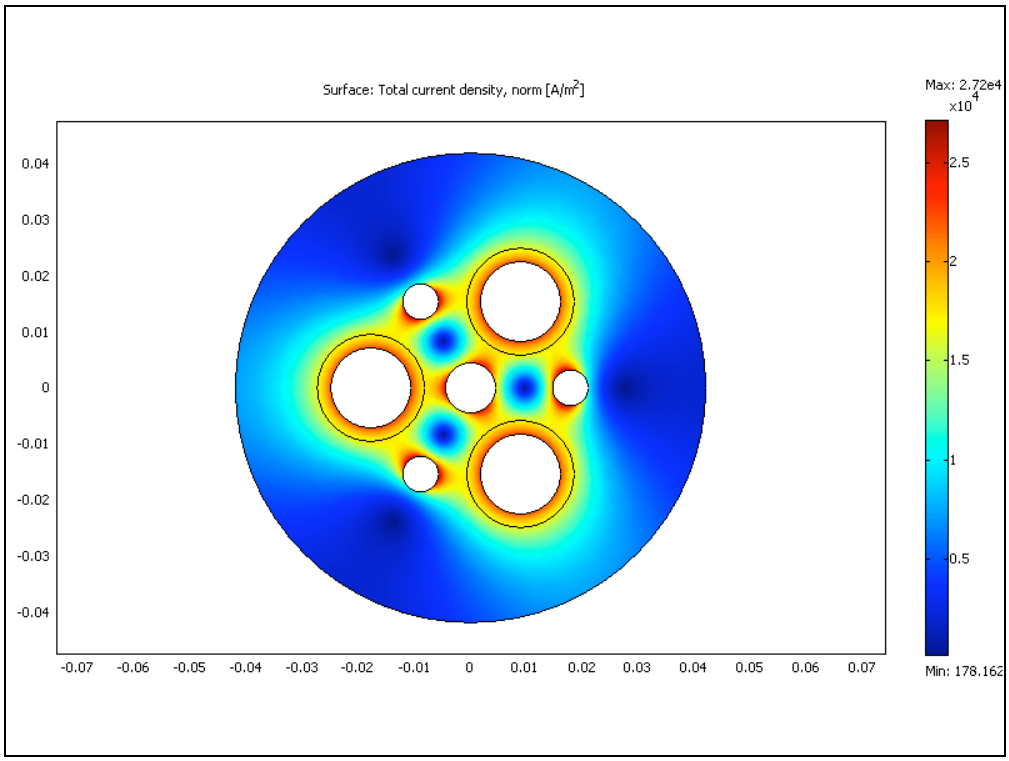

Figure 136 - Total current density for A=0.7in

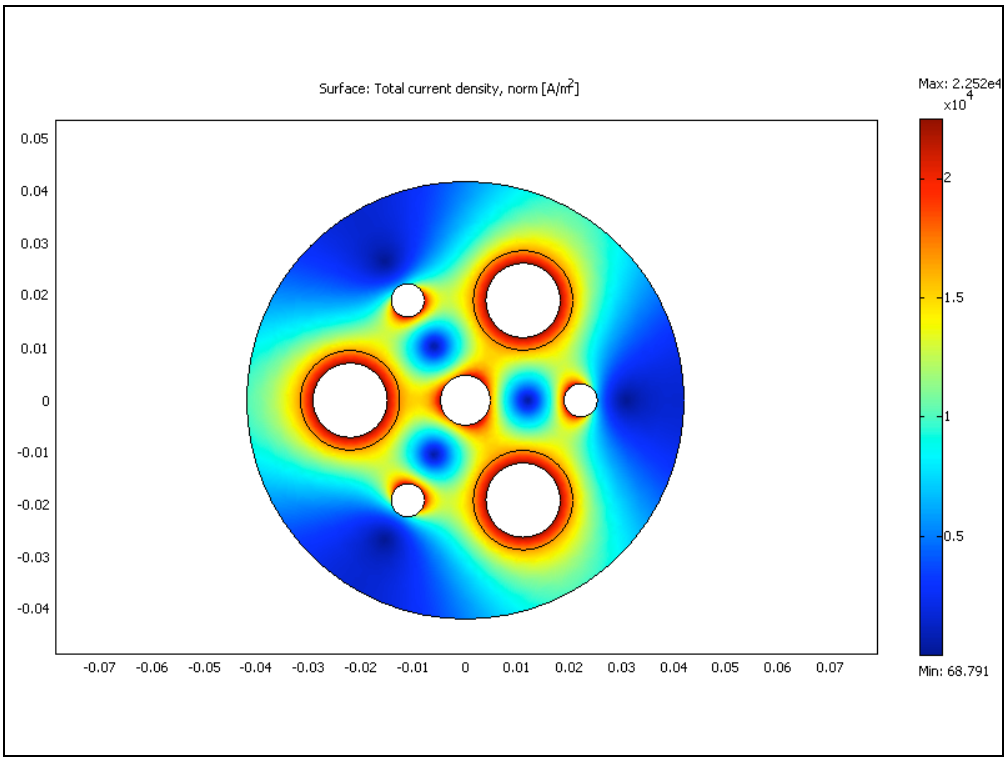

Figure 137 - Total current density for A=0.87in

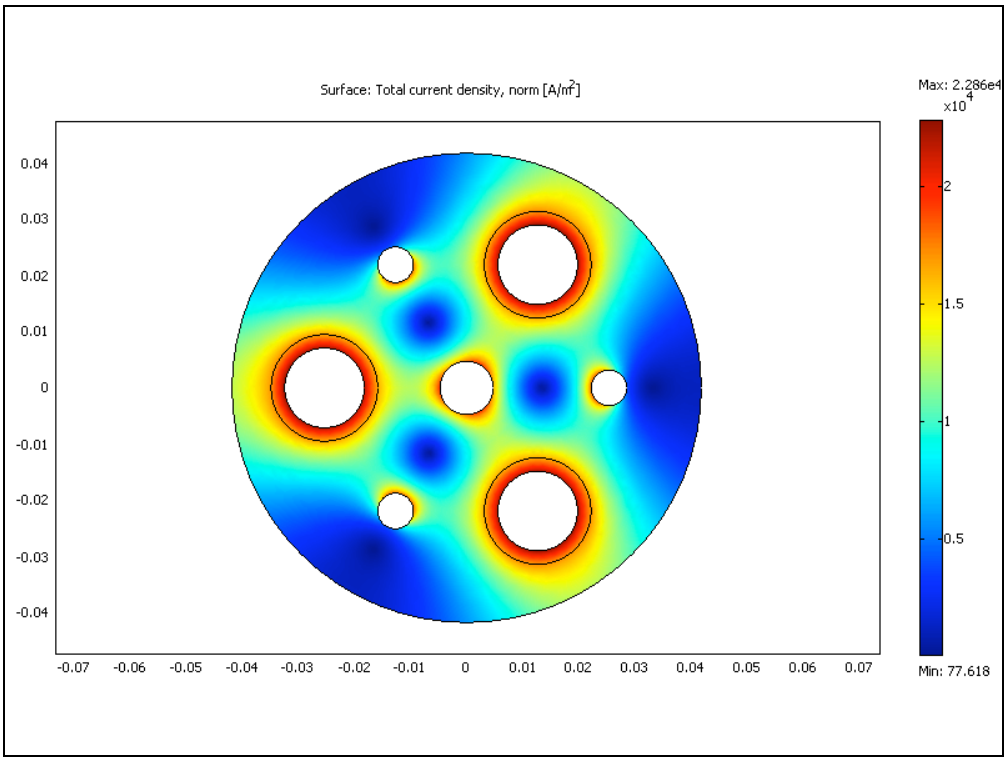

Figure 138 - Total current density for A=1.0in

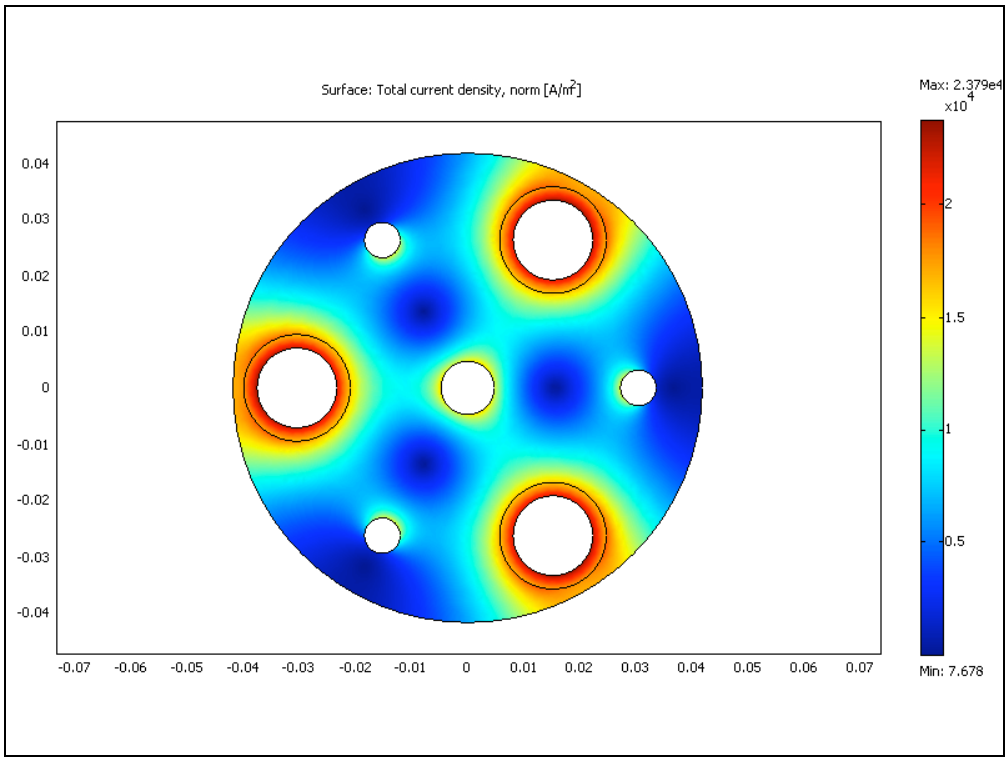

Figure 139 - Total current density for A=1.2in

5.7.3.10.2 *Conclusions:*

- It appears that for the 3-tube system, a geometry between Figure 137 and Figure 138 will result in the most uniform distribution of current density around the YSZ membrane tubes. In other words the A value needs to be between 0.87" and 1". Although, it appears that the total current is likely to be the highest when the A value is closer to 0.87" (Figure 137).
- The current density values in the YSZ membranes appear to be higher than expected. A more realistic value can be obtained if we incorporate the lead-wire resistance and the polarization losses at the electrodes. This will be done in the future work.

5.7.3.11 Modeling the 1-tube SOM cell:

Developing a model of the 1-tube SOM cell is a key step in our progress towards building the 3-tube Mg SOM scale-up. The 1-tube model will allow us to compare theoretical modeled results to previously obtained experimental results and modify the model until it approximates reality within an acceptable margin of error. Figure 140 details the dimensions used in the model of the 1-tube cell. The dimensions are similar to what was actually used in the single-cell reactor.

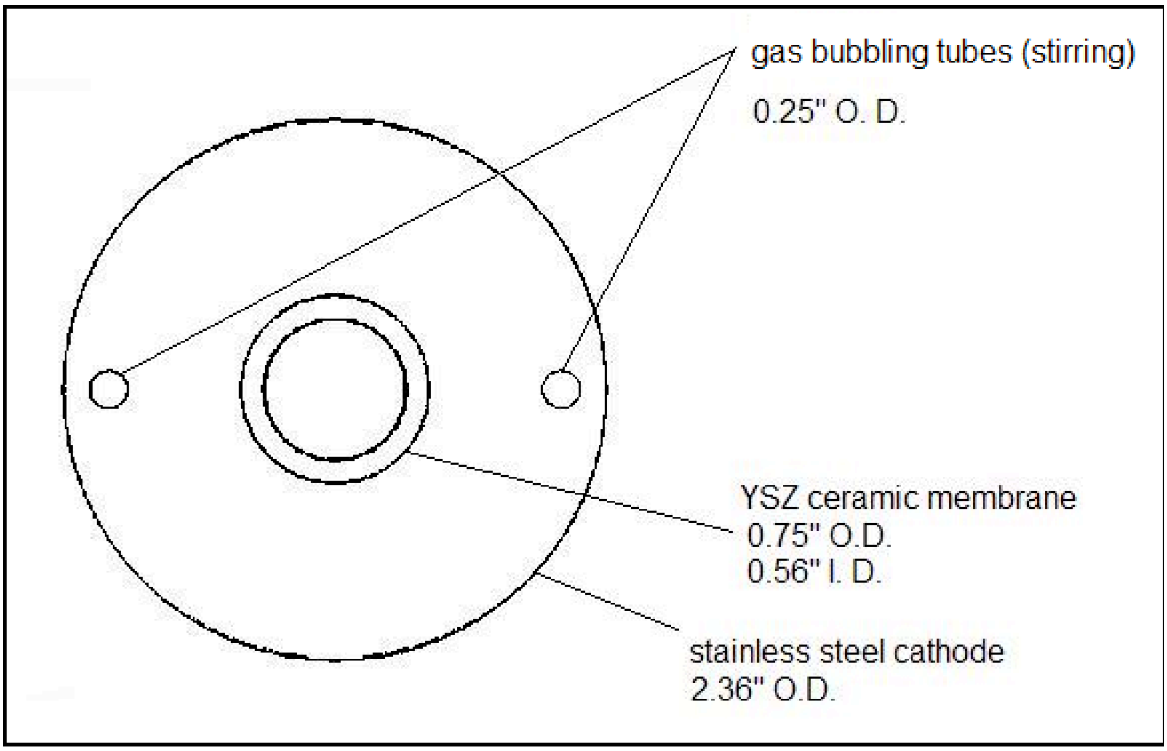

Figure 140 - Detail of the 1-tube cell simulation dimensions

5.7.3.11.1 Boundary conditions used in model:

The outer circumference of the large stainless steel tube and the interior tubes (the two inert gas bubbling tubes) were set as ground (cathode). The yttria-stabilized zirconia (YSZ) membrane anode ceramic tube was assigned an electrical conductivity of 10 S/m (actual value). The electrical conductivity of the flux was assigned 383 S/m (actual value). The inner wall of the YSZ tube was assigned an electrical potential of 5 V (value expected to be used during the SOM runs). Figure 141 shows a graph of the total current density of the 1-tube cell model.

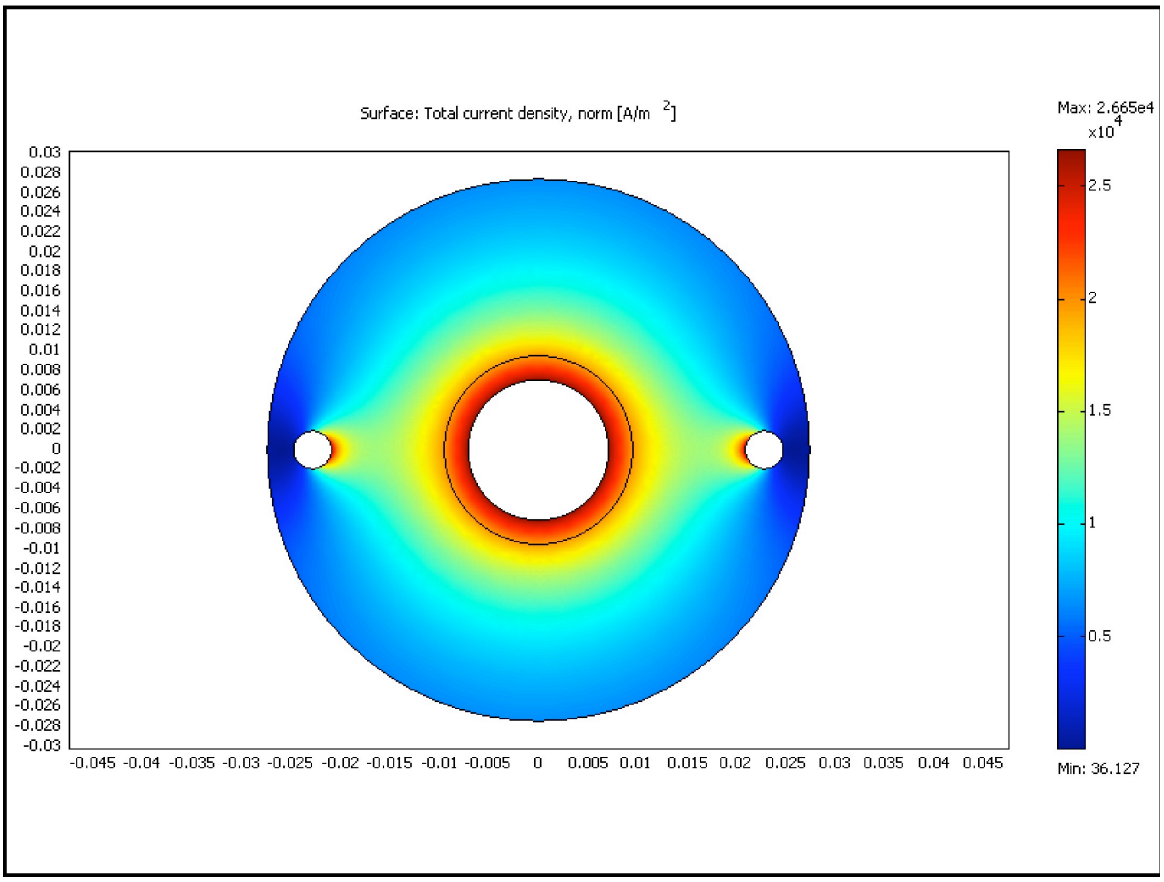

Figure 141 - Total current density in the 1-tube SOM cell model (scale to left and bottom of image in meters)

5.7.3.11.2 Considerations for modeling in the design of the SOM reactor:

The objective of the modeling project is to maximize the total current in the 3-tube cell and to determine the average current density on the YSZ tube surface. The average current density can be calculated by dividing the total current by the total surface area of YSZ tube immersed in the flux. A value of 2.54 cm was used in our calculations as the depth of immersion. Figure 142 shows a graph of the potential (V) versus the calculated total current (A) in a 1-tube Mg SOM cell.

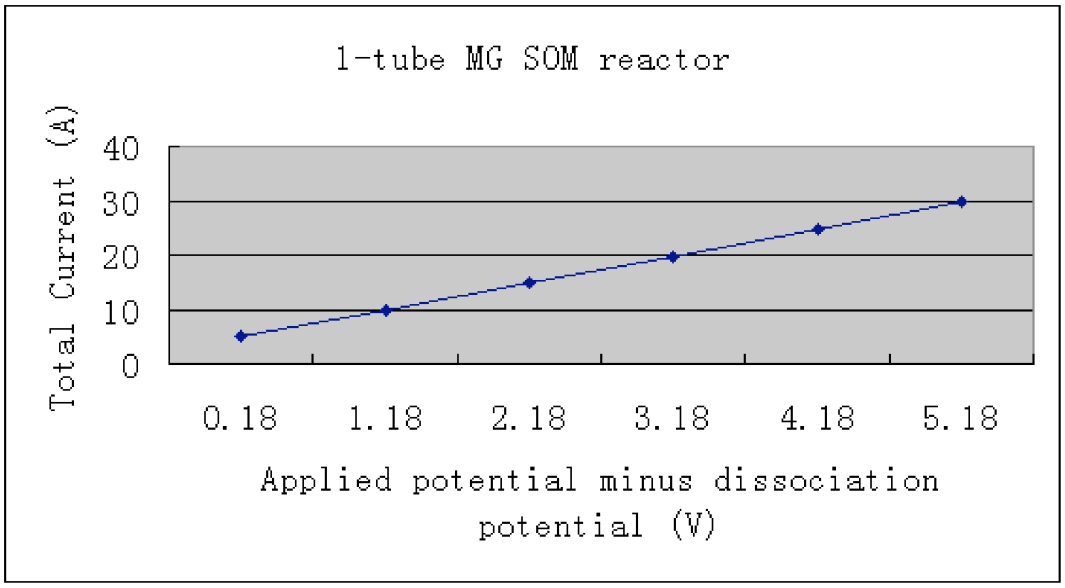

Figure 142 - A graph of potential versus calculated total current for the 1-tube Mg SOM cell

The estimated total current at a given potential was calculated by taking the average current density (A/m^2) along the inner diameter of the YSZ tube and multiplying it by the perimeter of the inner diameter of the ceramic tube (0.044 m) and the estimated immersion depth into the flux (in this case 0.0254 m). This value does not take into account the polarization and lead wire resistance. The data used to determine the values in Figure 142 are shown in Table 65.

Table 65 - Data used for Figure 142

Applied potential	Applied potential minus Dissociation potential	Current density	Total current
(V)	(V)	(A/m^2)	(A)
1	0.18	4429	4.948
2	1.18	8859	9.897
3	2.18	13290	14.847
4	3.18	17720	19.796
5	4.18	22145	24.739
6	5.18	26580	29.694
Dissociation Potential (V): 0.82			
I.D. (m): 0.014			
Perimeter (m): 0.044			
Depth of Immersion (m): 0.0254			

The polarization and lead wire resistance values are clearly a significant portion of the total current in the cell. Compare Figure 143, an example of an experimental I-V curve, to Figure 142, the I-V curve calculated from information taken from the model. If we examine a voltage value of 3 V, for example, we see a current of 5 A in the experimental system and a current of slightly less than 20 A in the modeled system. Clearly the lead wire resistance and actual polarization losses at the electrodes still need to be incorporated into the 1-tube model before the results can be extended to the 3-tube scale-up model.

In addition, determining the uniformity of the current density distribution in the YSZ tubes is important. The stability of the YSZ ceramic membrane is key to the success of the SOM method. The YSZ tube is the most expensive component of the SOM cell design. Non-uniform current density around the YSZ tube may cause the tube to fail due to possible thermal gradients. A detailed graph of the total current density of the YSZ membrane is shown in Figure 144. This image is of the same YSZ membrane shown in the graph of the total current density in Figure 141. Note that the colors shown in the different figures do not correspond with one another. Based on the 1-tube model developed, the current density distribution across the YSZ membrane varies 0.64 A/m^2 from its interior to exterior surfaces. This plot needs to be regenerated after incorporating the polarization losses and the losses due to the lead wire resistance.

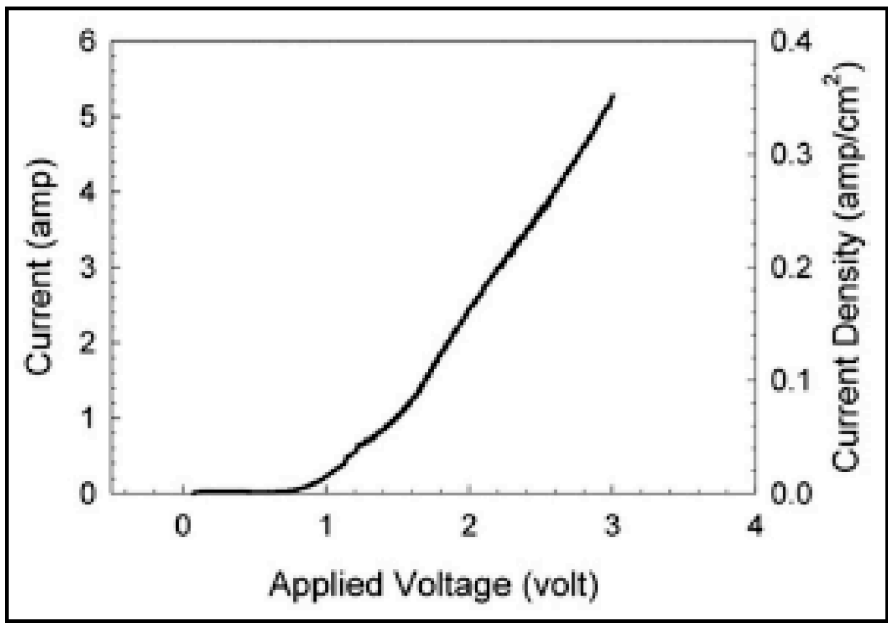

Figure 143 - Fast potentiodynamic scan (5 mv/s) of a single tube Mg SOM cell

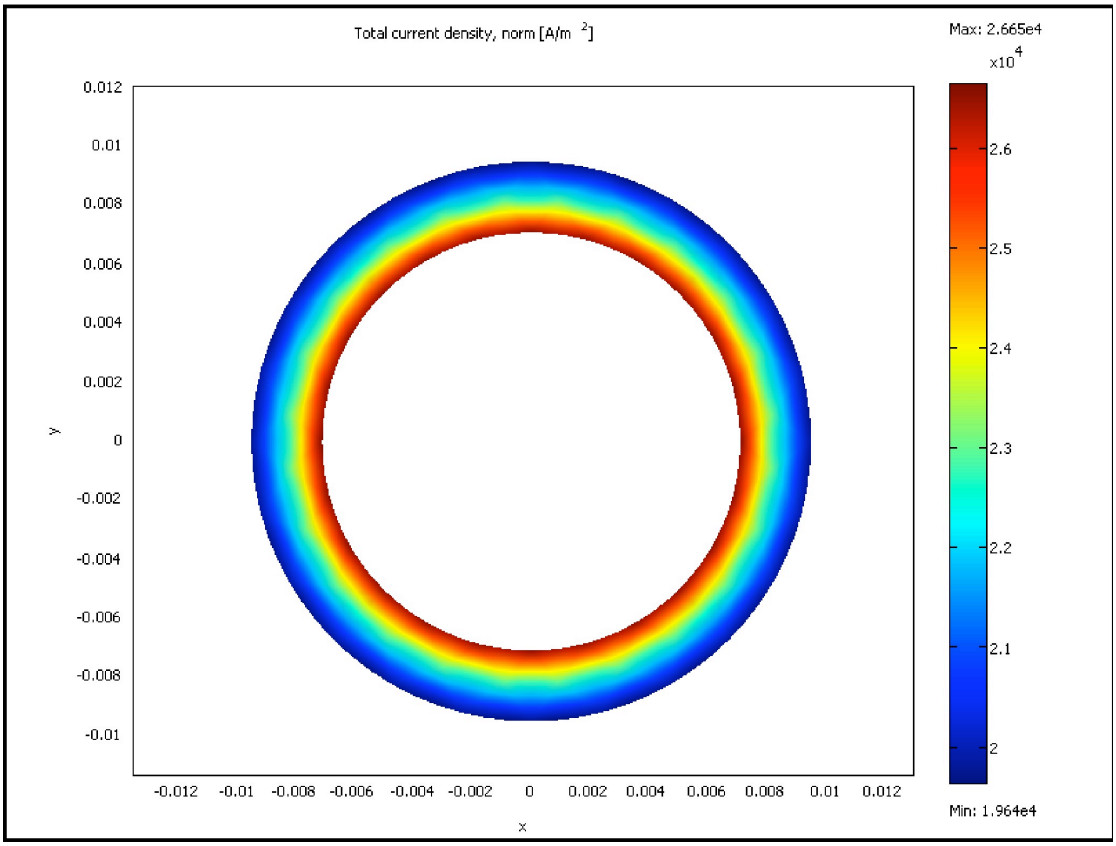

Figure 144 - A detailed image of the YSZ membrane subdomain from the 2-D model of a 1-tube Mg SOM cell (scale to left and bottom of image in meters)

5.7.3.12 Generation of MgH_2 using Mg-SOM process

5.7.3.12.1 Objective:

The ability to generate magnesium hydride using the Mg-SOM process would be a valuable method for regenerating magnesium hydride for hydrogen storage applications.

5.7.3.12.2 Considerations

A Mg-SOM setup is being explored to see if it is feasible to produce MgH_2 from the magnesium vapor before it condenses after exiting the SOM cell. A tube feeding hydrogen gas is inserted into the condenser and positioned near the exhaust for Mg vapor and argon exiting the SOM cell. Ideally, the magnesium vapor and hydrogen gas will react upon meeting to form MgH_2. Magnesium hydride decomposes into magnesium and hydrogen at temperatures greater than 327ºC, so it is important that the temperature of the gasses be fairly low. In addition, formation of the hydride requires fairly low temperatures. Specifically, if Mg vapor is reacting with hydrogen gas, the temperature must be below 600ºC before the hydride will form. If solid magnesium is reacting, the temperature must be 200ºC or below to occur. The current design of the system has the region where the two elements will be reacting at a fairly high temperature, around 1200ºC. Therefore, the major problem with the plan to generate

magnesium hydride using this setup is the temperature of the hydrogen feed gas. A method to keep it cool enough to satisfy the thermodynamic requirements of the reaction is required. Figure 145 shows a sketch of the condenser apparatus with the location of all the feed/exhaust tubes.

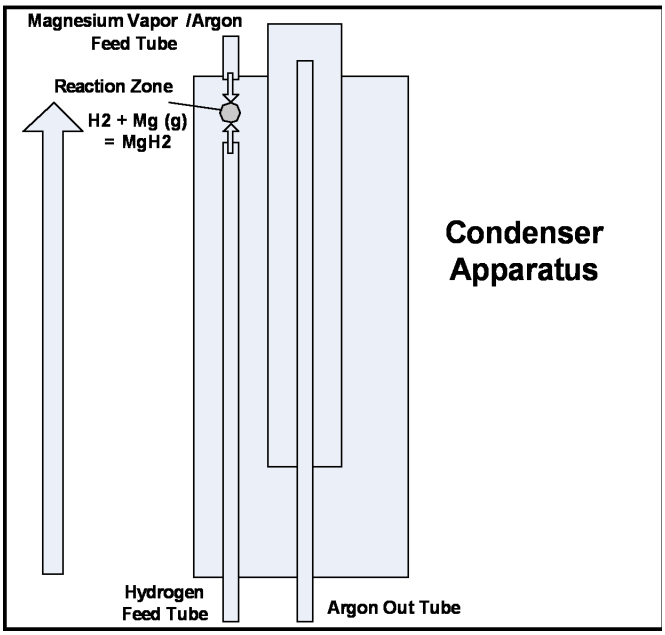

Figure 145 - Condenser Apparatus

In an attempt to lower the temperature of the hydrogen gas, the entire length of the stainless steel hydrogen feed tube was insulated with an alumina tube of approximate 0.06" thickness. Figure 146 shows the temperature profile generated from this experiment. As you can see from the graph, the temperature at the feeding end of the tube was slightly less than 800ºC. This is a decided improvement from the control experimental peak temperature measurement, which was ~1200ºC. We still have much progress to make, however, as the target temperature for the end of the hydrogen feeding tube is 200-300ºC.

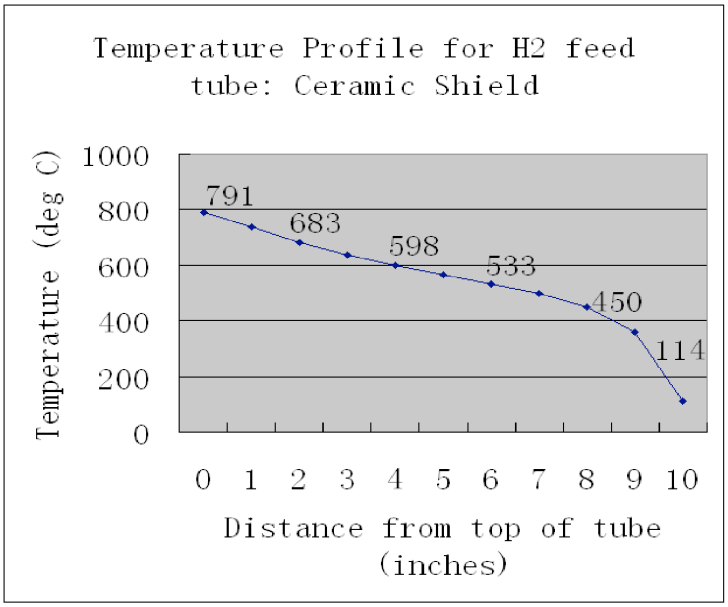

Figure 146 - Temperature Profile for the hydrogen feed tube insulated by ceramic shielding

5.7.3.12.3 *Experimental*

Magnesium hydride (solid) decomposes into magnesium (solid) and hydrogen (gas) at temperatures greater than 300 ºC. However, thermodynamically magnesium vapors can react with hydrogen gas to produce magnesium hydride at temperatures below 625 ºC. Therefore, an attempt was made to form the magnesium hydride from the vapor phases of the reactants at temperatures below 625 ºC followed by quenching the product. This requires Hydrogen gas to be passed into the condenser from the bottom using an appropriate feeding tube and making sure that the zone where the hydrogen mixes with the magnesium vapor is below 625 ºC.

Our first attempt to lower the temperature of the hydrogen gas entering the condenser involved various methods of insulating the stainless steel hydrogen feeding tube that delivers the gas to the 'reaction zone' (see Figure 148). In addition to the single alumina tube shielding described earlier, stainless steel and a double layer alumina shielding were tested. Figure 147 shows a comparison of the temperature profiles that each of these attempts yielded. None of the methods of insulating the hydrogen feeding tube resulted in a significant enough temperature reduction to enable the formation of magnesium hydride in the upper zone of the condenser. The length of the feed tube was reduced to 2.5 inches from 9 inches to put the point at which the two gases meet in a lower temperature region of the furnace (see Figure 149).

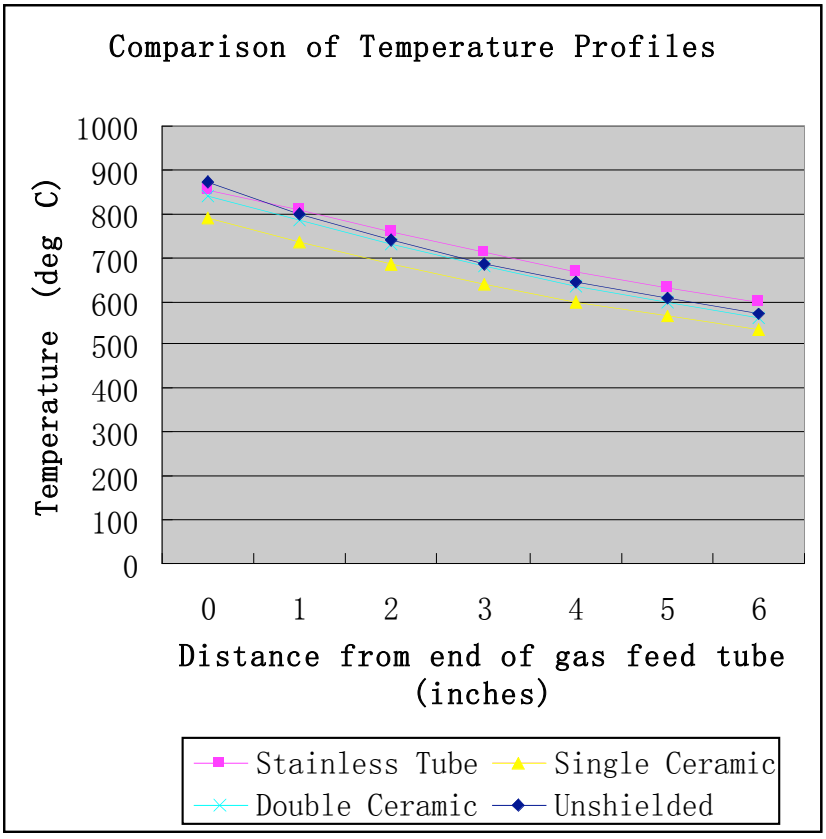

Figure 147 - Temperature Profile Comparison

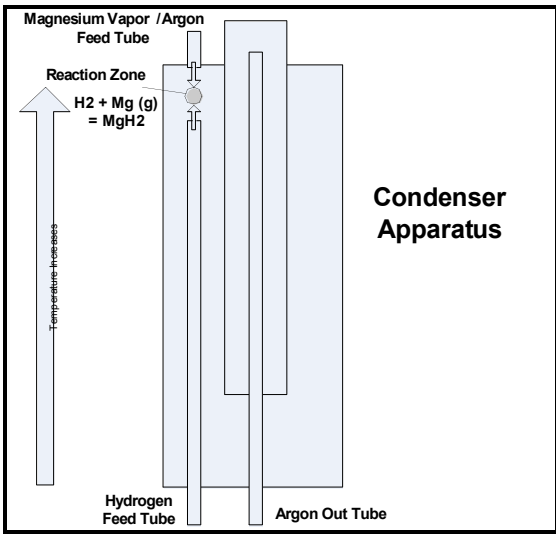

Figure 148 - Condenser Apparatus Designs - Insulated Feed Tube

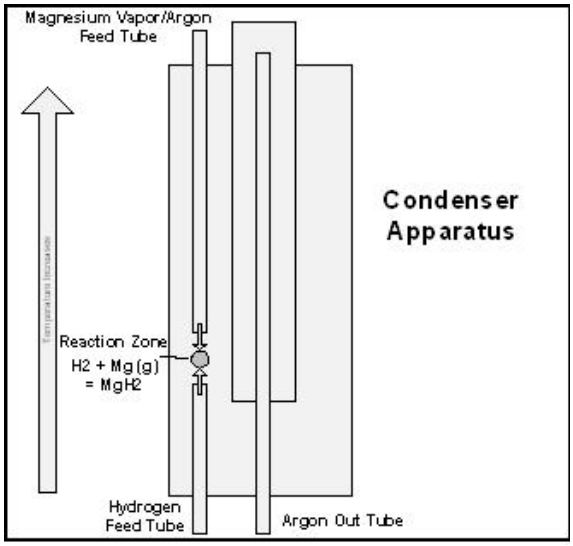

Figure 149 - Condenser Apparatus Designs - Un-insulated design

5.7.3.12.4 Integration with the SOM Process

An experiment designed to produce magnesium hydride using the modified condenser was run. The experiment was conducted using liquid tin as an anode with hydrogen gas as the reductant. The low temperature flux composition was used, with (55% MgF2-45%CaF2)-10%MgO by weight. The electrochemical cell was held at 1150ºC for the duration of the experiment. Hydrogen was pumped into the condenser in excess of that needed to react with the magnesium vapor generated during the electrolysis. In addition, hydrogen was flowed continuously during the experiment as well as during the entire cooling phase of the experiment, to maximize the chances of producing the hydride. Figure 150 shows the first potentiodynamic scan (fast) of the experiment showing the dissociation potential to be between 0.6-0.7 V. The figure is similar to scans made in previous experiments. Figure 151 shows the electrical data for the electrolysis. The relatively short electrolysis time (30 minutes) led us to expect a small amount (< 1 g) of magnesium to condense on the stainless steel foil on the inside of the condenser. When the foil was removed, a small amount of condensed magnesium was observed on the region in the cooler zone of the furnace (near end of the hydrogen gas feed tube). The foil containing the condensation was scanned using the x-ray diffractometer. Figure 152 shows the scan (in black) with superimposed peaks corresponding to magnesium hydride in blue and magnesium metal in red. By inspection, it is clear that this scan does not indicate the presence of magnesium hydride and confirms the presence of magnesium metal. It is likely that more radical alterations in the design of the condenser and perhaps reactor cell will need to be made in order to make magnesium hydride using the Mg-SOM method.

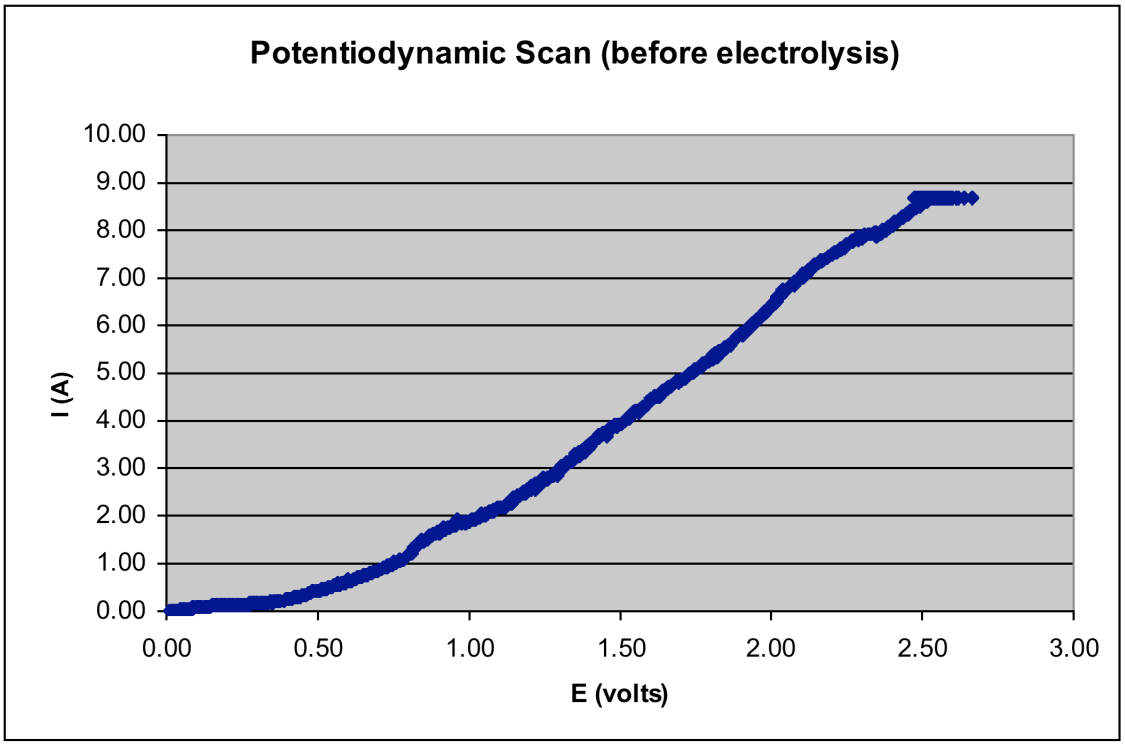

Figure 150 - Potentiodynamic Scan (before electrolysis)

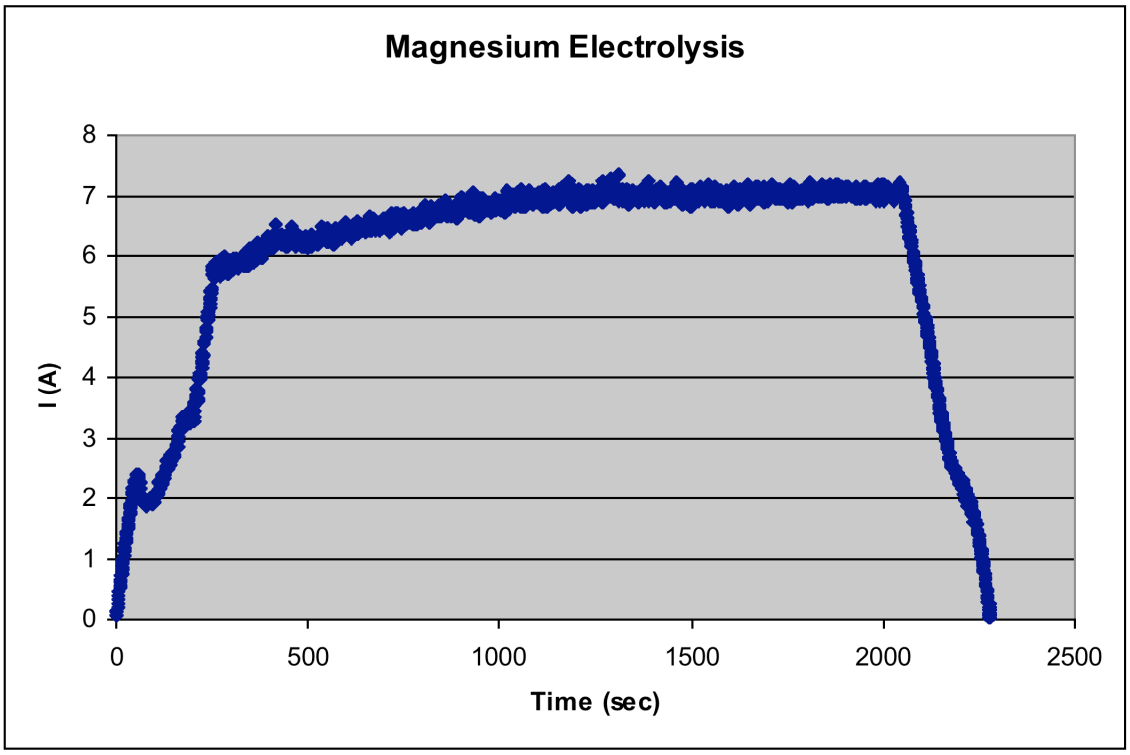

Figure 151 - Electrolysis Scan

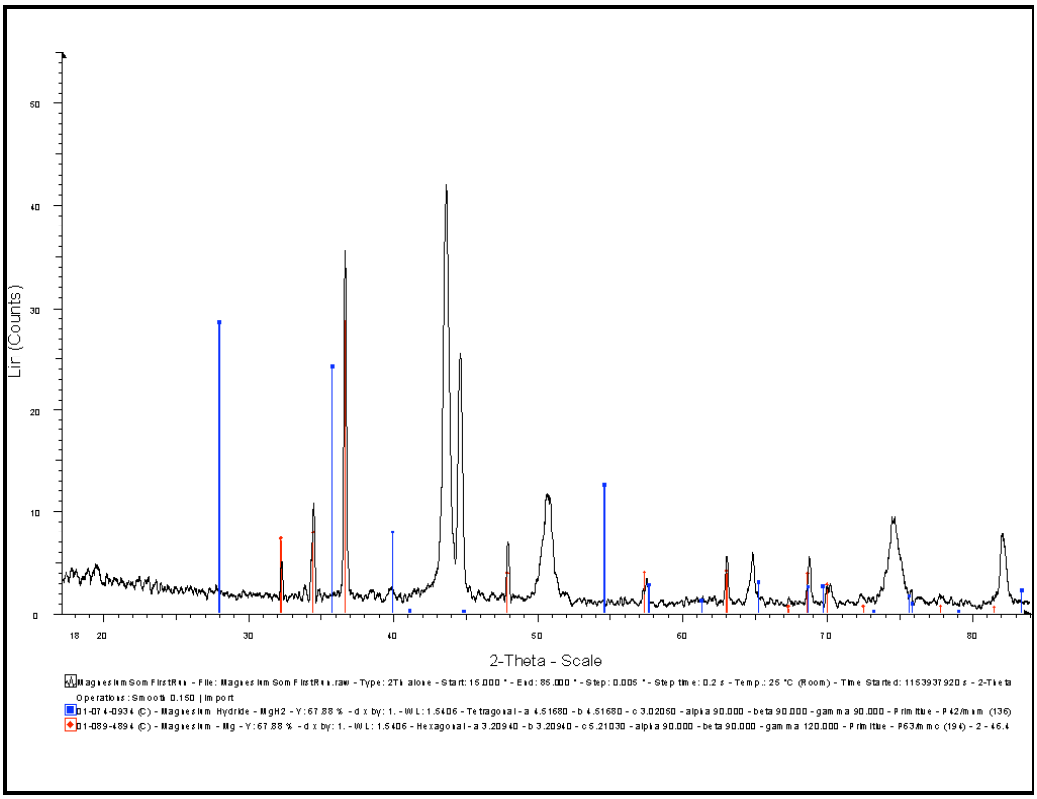

Figure 152 - XRD scan of condenser residue

5.7.3.13 Scale-up Modeling of SOM Process for Continuous Magnesium Production

5.7.3.13.1 Introduction

Two 2-D mathematical models of the Mg-SOM process were prepared previously: a single-tube simulation and a set of triple-tube simulations. These models showed the current density distribution in the cell. Four triple-tube models were created, identical except for the variation of a geometric parameter, A, in an effort to optimize the geometry for maximized total current.

5.7.3.13.2 Single Tube Cell I-V Plot:

Using the single tube model, an I-V curve for the single tube cell was generated. Figure 153 shows this plot (in blue) along with experimental data for the single tube SOM cell (in cyan). This graph compares the data gathered by a potentiodynamic scan of the cell during an experiment to one generated by evaluating different voltage boundary conditions in the model. The same anode area utilized in the experiment was used to make the calculations for the modeled curve. The anode area used for both was 15.2 cm^2. The disparity between the preliminary model I-V curve and the one generated experimentally can be accounted for by considering current losses experienced by the experimental setup. Ohmic losses in the lead wire and the electrodes and polarization losses (concentration) at the electrodes account for the difference in the I-V plot between the experiment and the model. The next phase of our model will examine these losses quantitatively.

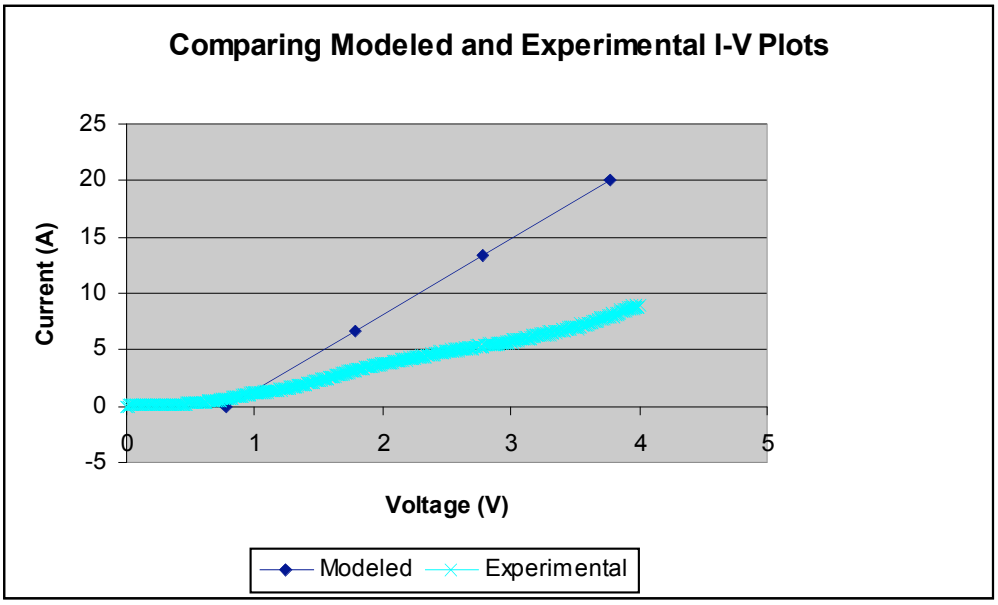

Figure 153 - Modeled and Experimental I-V Plot - Single Tube SOM Cell

5.7.3.13.3 Triple Tube Cell I-V Plot

Figure 154 shows a schematic of a 2-D cross section of the 3-tube cell. A dimension 'A' was defined to investigate several arrangements of the YSZ membranes

and gas bubbling tubes. The dimension 'A' is equal to the radius of the circle whose circumference the bubbling tubes and membranes are spaced around.

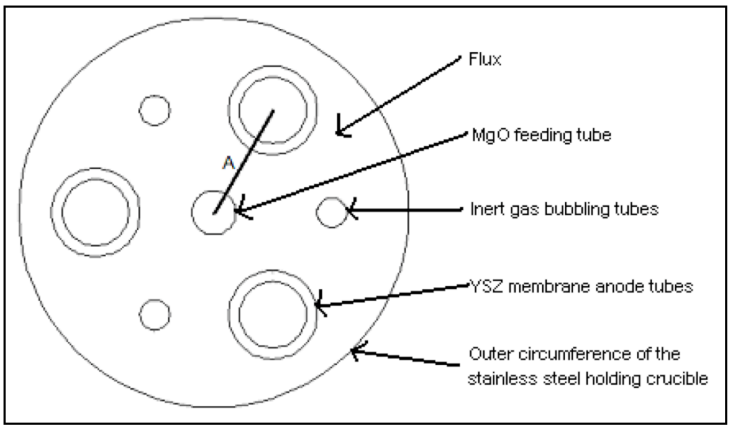

Figure 154 - Schematic of 2-D cross section of cylindrical triple tube cell geometry

Four versions of the triple tube design were made previously with the 'A' dimension assigned values of 0.7", 0.87", 1.0", and 1.2". The dimensions of every other element of the model were not changed between the four versions. That is, the membrane size and bubbling tube size are the same for each version. The anode area used for the model was 45.6 cm^2. I-V curves were generated for the different geometries for the 3-tube SOM cell. Figure 155 plots all four of the I-V curves together. Differences between these four cell geometries are not great, as is clearly seen in the plot.

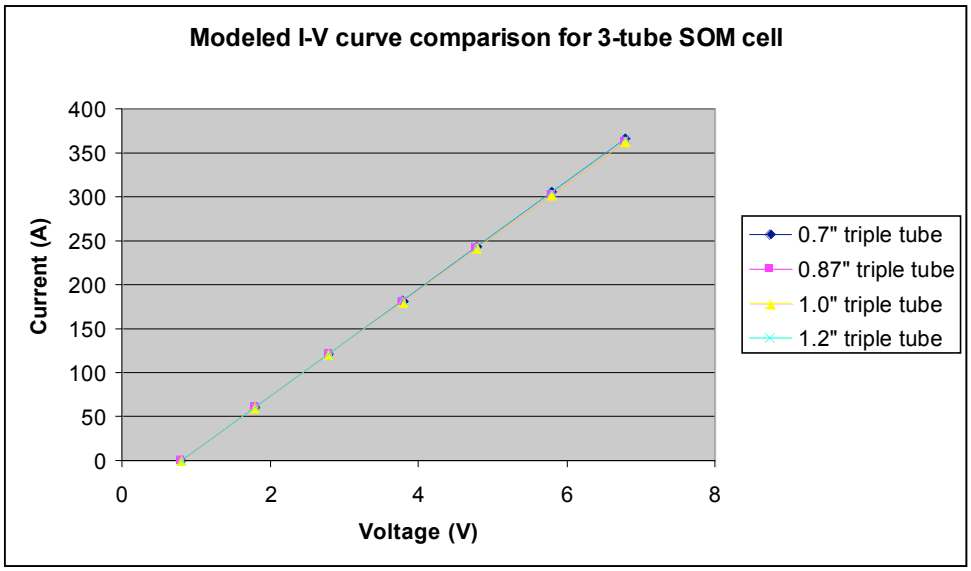

Figure 155 - Comparison of modeled I-V curves for varying 'A' values

5.7.3.13.4 *Triple tube cell model: Circle vs. Hexagonal Cathode Geometry*

Figure 156 shows a sketch of the top and side views of what we envision a scale-up SOM cell to look like. Nineteen tubes are arranged inside a honeycomb cathode

structure containing the flux and argon gas is bubbled up from the bottom to create the proper gas proportion. Magnesium vapor is removed from the top to a condensing unit elsewhere. It is important to see how a triple-tube cylinder cathode geometry compares with a triple tube hexagonal cathode geometry if we are to use the above design in our first pilot scale reactor.

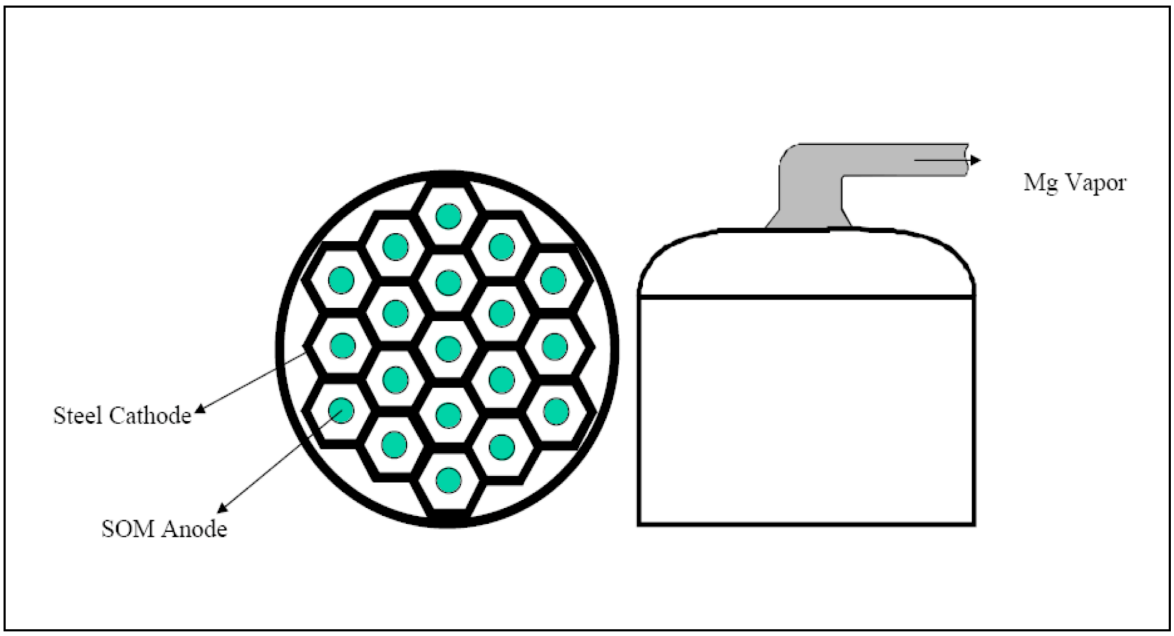

Figure 156 - Proposed SOM Reactor (Top and Side Views)

In order to determine if our cylindrical cathode mathematical model corresponds to the geometry of our anticipated large-scale reactor, we compared our current models to similarly dimensioned hexagonal models. Hexagonal geometry models were developed to correspond to the four triple tube cylindrical models. The 'A' values used for each cylindrical model version are the same for the corresponding hexagonal models (see Figure 157). Figure 158, Figure 159, Figure 160, and Figure 161 show the current density distributions of our cylindrical geometry on the left and the distributions of the hexagonal geometry on the right.

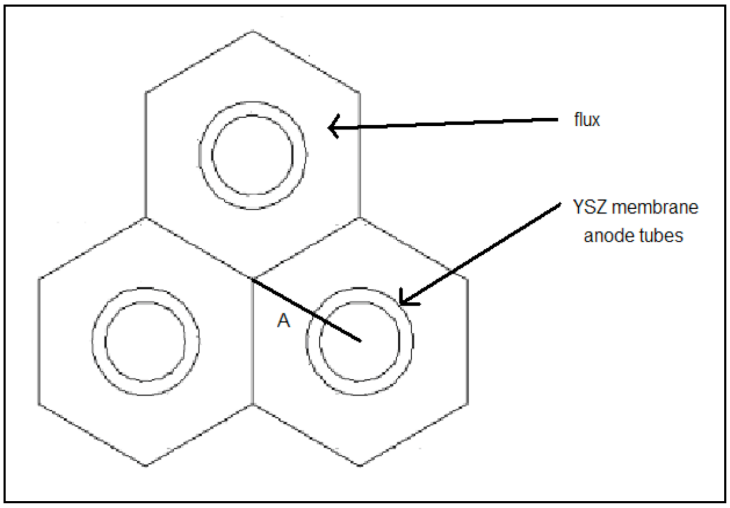

Figure 157 - Schematic of 2-D cross section of hexagonal triple tube cell geometry

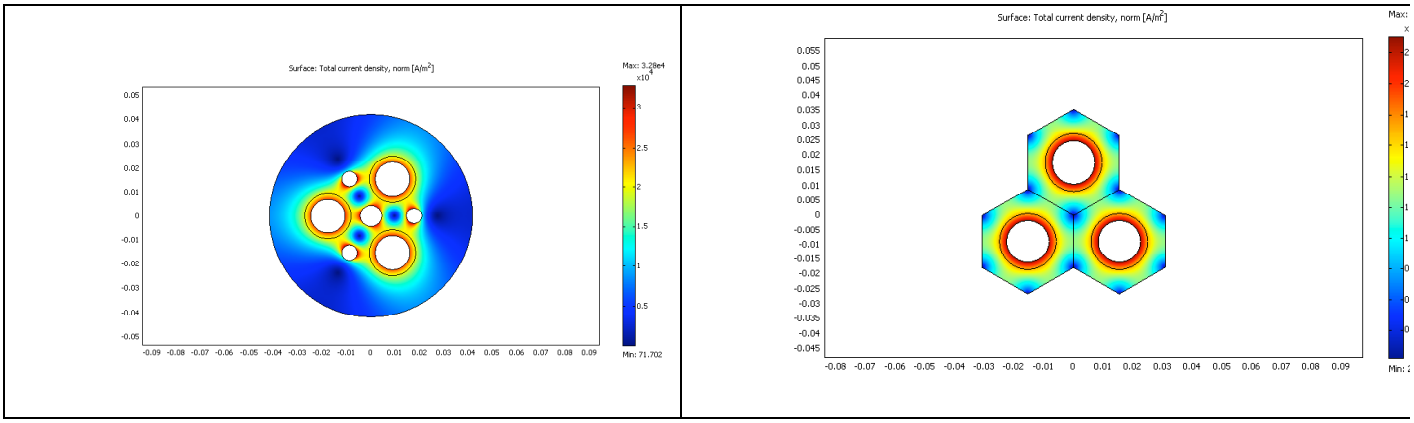

Figure 158 - Cylinder vs. Hexagonal Cathode Geometry – A = 0.7”

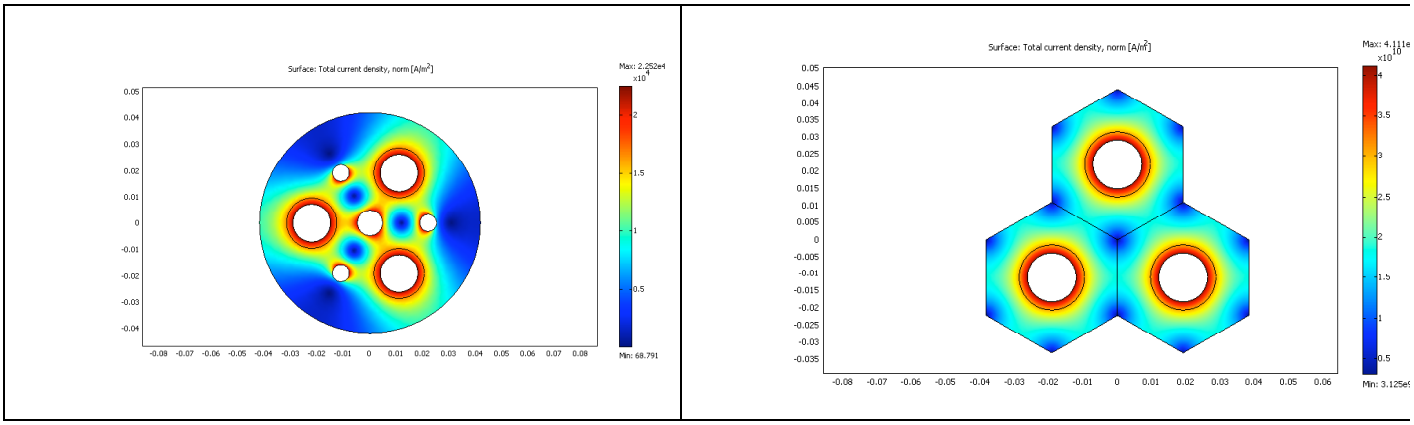

Figure 159 - Cylinder vs. Hexagonal Cathode Geometry – A = 0.87”

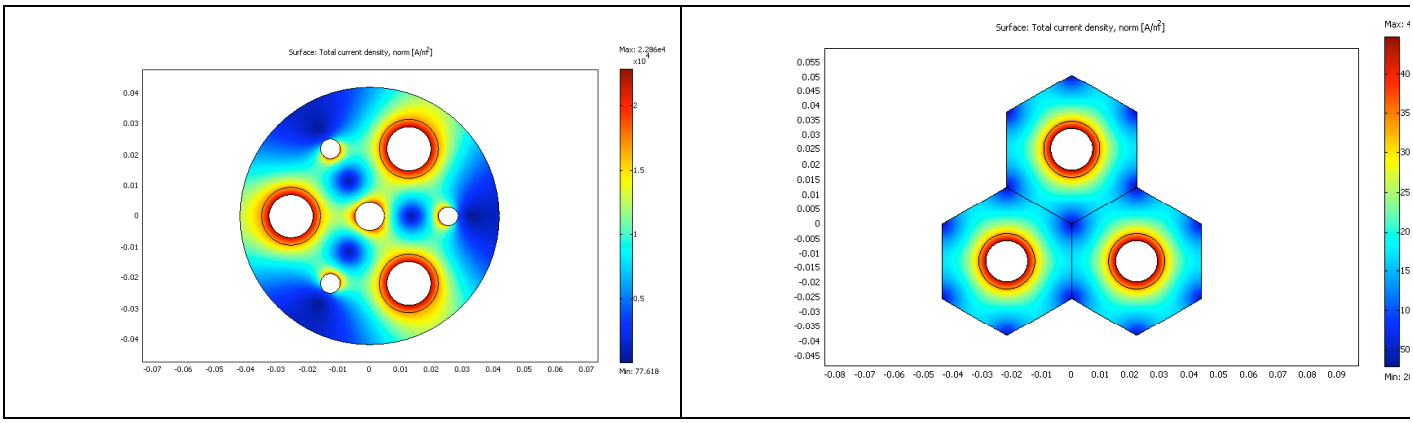

Figure 160 - Cylinder vs. Hexagonal Cathode Geometry - A = 1"

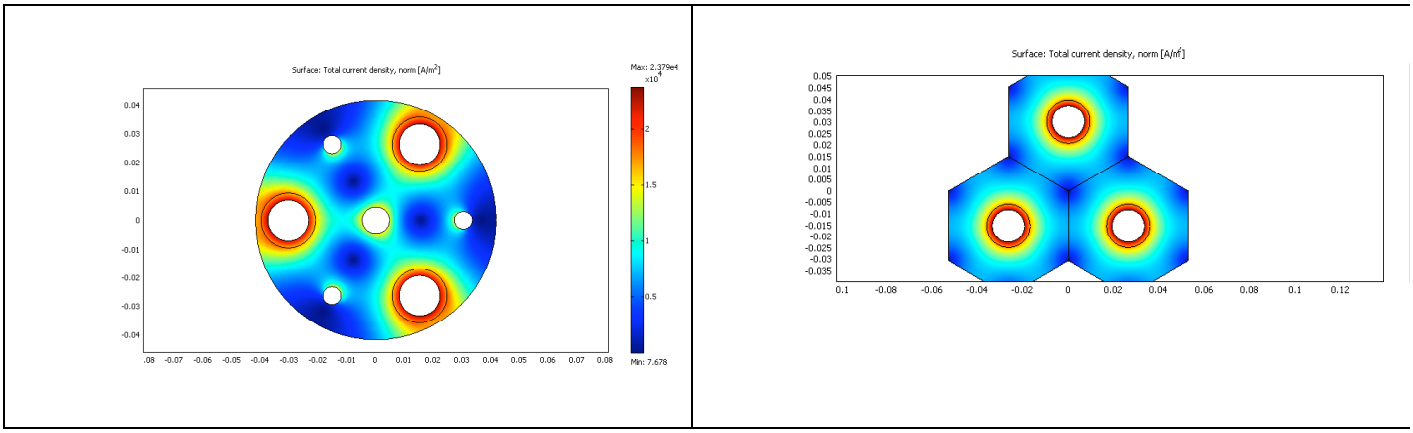

Figure 161 - Cylinder vs. Hexagonal Cathode Geometry - A = 1.2"

The total current values for each model version were calculated at a range of applied potentials. The difference between the cylinder models and their corresponding hexagonal models were calculated and plotted versus the applied potential (See Figure 162). At low potentials, there is not really a very large difference between the models. As the applied potential increases, the difference between the total current increases for three of the models. The model with the 'A' dimension of 1.0 inch stays pretty much the same over the entire range of potentials.

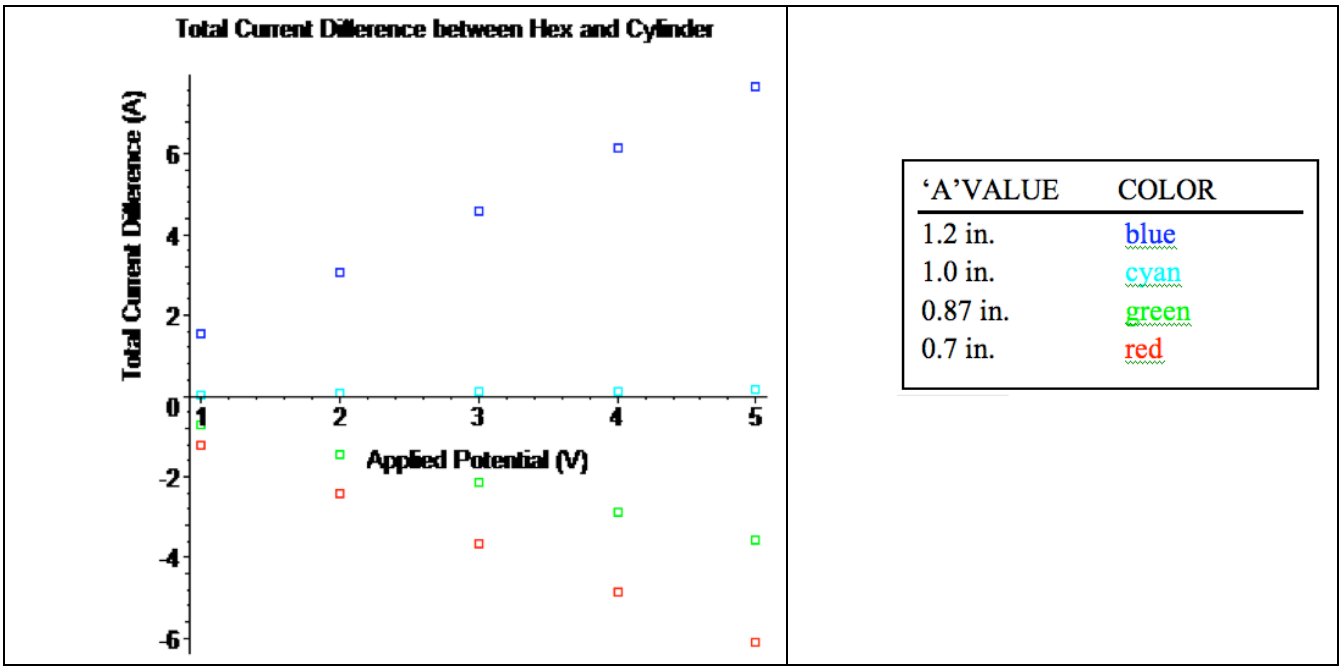

Figure 162 - Difference in Total Current between Cylindrical and Hexagonal Cathode Geometries vs. Applied Potential (V). Legend at right indicates 'A' value and corresponding color in plot

5.7.3.13.5 *Conclusions*

- The I-V curve for the triple-tube cylindrical cathode is affected very little by varying the 'A' parameter in 2-D models, as seen in Figure 155.
- A comparison of hexagonal and cylinder models supports the use of the 1.0" 'A' parameter for the most accurate correspondence of total current values, as seen in Figure 162.

5.7.3.14 Three Tube Design

5.7.3.14.1 *Design Alteration*

In the course of preparing the three-tube experiment, we found that the previously modeled design would be extremely hard to fabricate quickly with the machine shop resources available. We therefore decided to alter the design slightly in order to make it easier to build. First, we increased the inner diameter of the stainless crucible from 3.30" to 4.26". This was done because of the specific size of available stainless steel pipe stock in addition to machining constraints. Previously, we had decided to space the bubbling tubes as well as the ceramic membranes 60 degrees apart along a radius of 1.0" (Dimension 'A') (see Figure 163). Instead, we have modified the design slightly, as shown in Figure 164. The three ceramic membranes are spaced 120 degrees apart along a radius of 1.065" (Dimension 'B') and the three bubbling tubes are also spaced at 120 degree intervals (offset by 60 degrees from the ceramic membranes) at a slightly larger radius of 1.42" (Dimension 'C'). The new locations for the bubbling tubes and ceramic membranes were chosen in order to maximize the ease of machining.

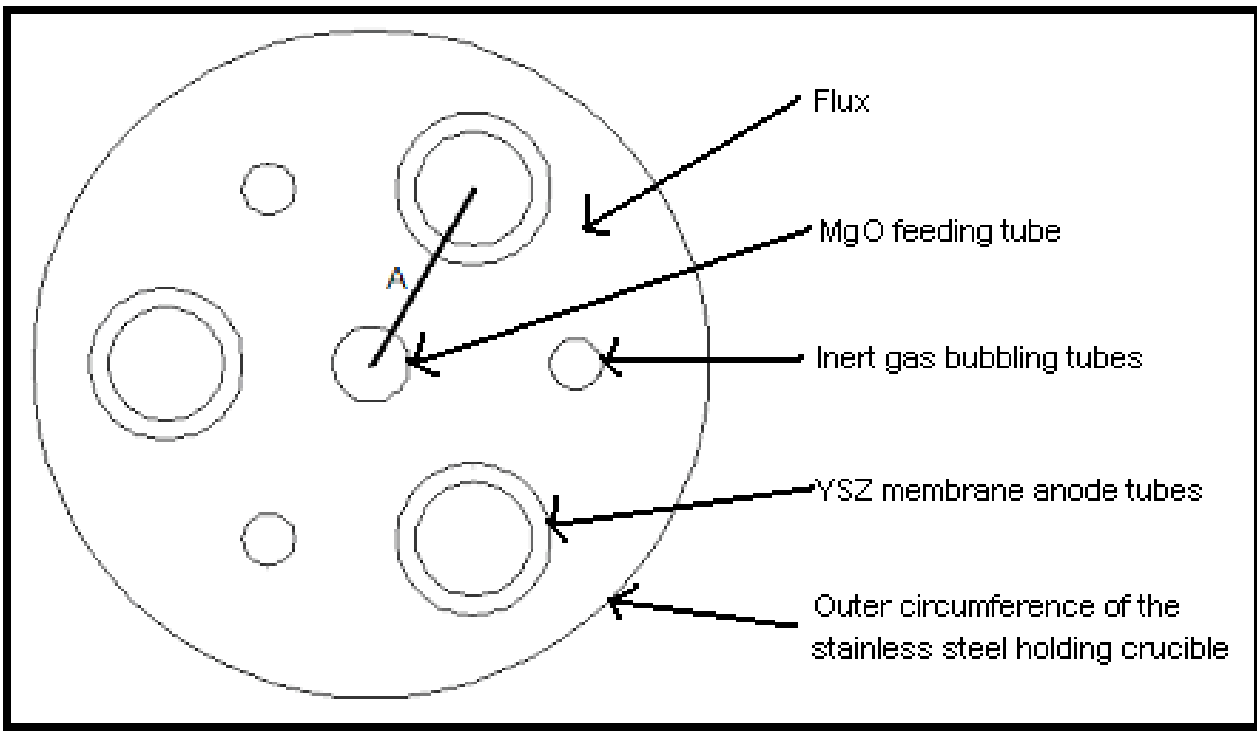

Figure 163 - Dimension 'A' in previously modeled triple-tube Mg-SOM cell design

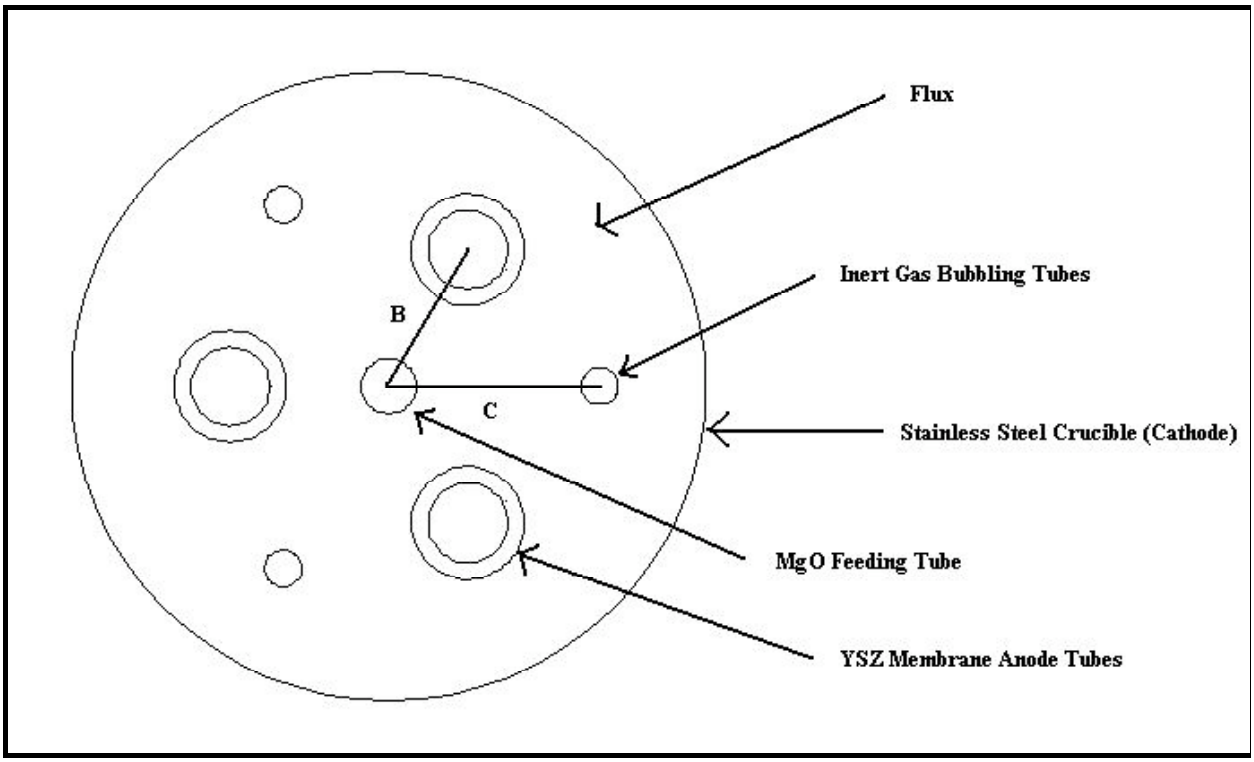

Figure 164 - Dimensions 'B' and 'C' in new triple-tube Mg-SOM cell design

Table 66 indicates the dimensions used in the new triple-tube Mg-SOM cell design.

Table 66 - Dimensions Used in Altered Cross-section Geometry

Component Dimensions	inches	meters
diameter of MgO feed tube (at center of circle)	0.375	0.0095
diameter of large stainless steel holding crucible	4.26	0.1082
diameter of bubbling tubes	0.25	0.0064
outer diameter of YSZ ceramic membrane	0.756	0.0192
inner diameter of YSZ ceramic membrane	0.533	0.0135

5.7.3.14.2 Modeling

A new 2-D mathematical model for the altered design was developed using COMSOL Multiphysics. Objectives for the scale-up design still include maximizing the total current and ensuring that the current density distribution around the circumference of the YSZ tubes is uniform. Non-uniform current density around the YSZ tube may cause the tube to fail due to possible thermal gradients. By inspection, it appears that the current density distribution around the ceramic membrane region is less distorted in the new simulation (with the different 'B' and 'C' dimensions, see Figure 165) than the previous simulation (with the single 'A' dimension, see Figure 166).

The maximum current density in the new design is ~93% of the equivalent design from previous modeling work (see Figure 165 and Figure 166). Further investigation will be required to determine if the average current density at the surface of YSZ membrane is affected significantly by the altered design.

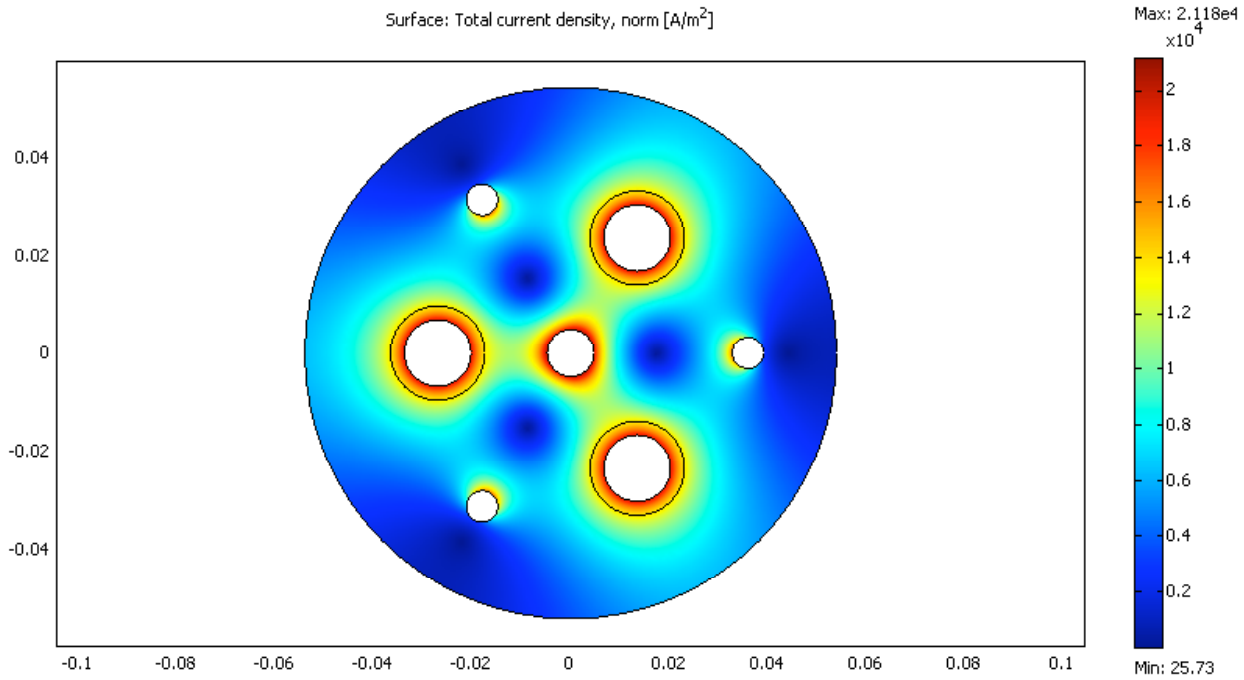

Figure 165 - Current Density Distribution at B = 1.065"and C = 1.42" (New cell design)

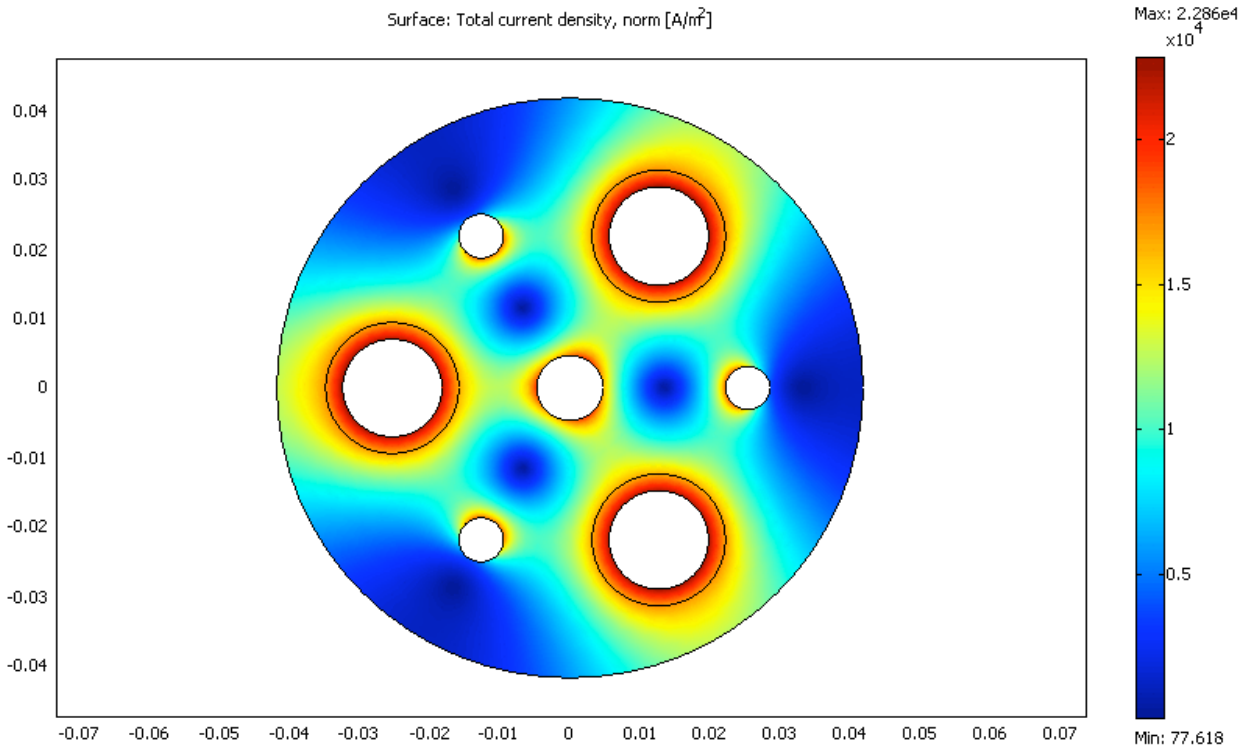

Figure 166 - Current Density Distribution at A=1.0" (Old cell design)

5.7.3.14.3 Detailed CAD/CAM drawing

A model of the modified triple-tube assembly was prepared using SolidWorks 2006. Figure 167 shows a screen shot of the exterior of the 3-D drawing. Figure 168 shows a cutaway version of the new design.

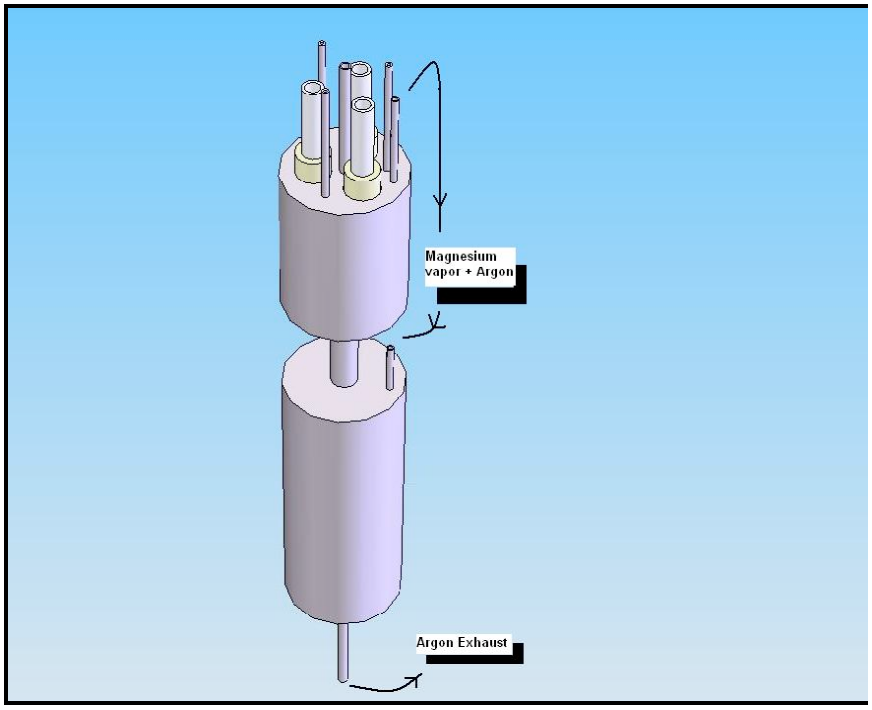

Figure 167 - Exterior of the triple-tube Mg-SOM cell assembly

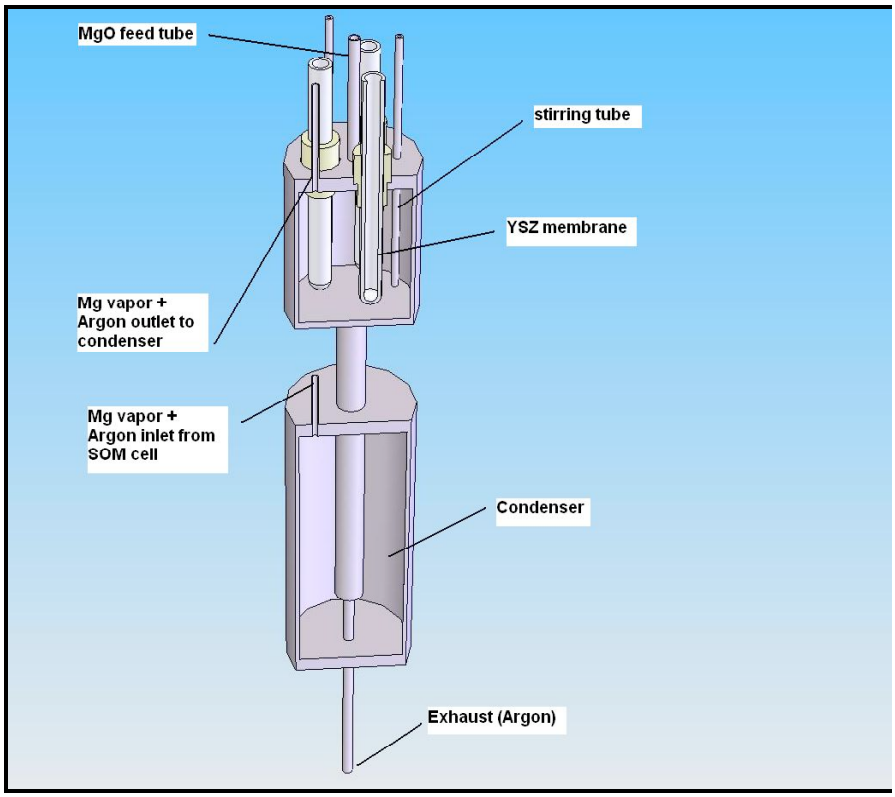

Figure 168 - Interior of the triple-tube Mg-SOM cell assembly

5.7.3.15 Lanthanum Strontium Manganite Coating (LSM) Coating Development

We are developing a lanthanum strontium manganite coating for use on the interior of the zirconia tube as the anode. Additionally, we will begin SOM experiments utilizing a triple-tube reactor.

We are making the lanthanum strontium manganite (LSM) with a composition of (La0.85Sr0.15)0.97MnO3±δ in-house by ball milling La2(CO3)3·xH_2O powder with MnO2 and SrCO3 in ethanol, drying, and firing the powder mixture at 1400ºC for 4 hours. We are then reducing the particle size of this powder by wet ball milling, dry ball milling, and sieving through a 200 size mesh. The powder produced in this way is then made into a slurry, and used to coat the interior of the zirconia tube. The coated tube is then fired once more. We are yet to decide on a current collector rod for this experiment. We plan to devise ways to lower the temperature at the current collector and experiment with using Haynes alloy and Crofer.

The use of an inert anode will allow us to evolve oxygen at the anode. The ability to evolve oxygen directly will allow us to cease use of hydrogen gas and enable the production of saleable oxygen gas as a byproduct of the SOM process. Use of the inert LSM coating rather than a liquid anode will decrease costs as well as increase the safety of our design. Liquid metal anode (tin in particular) can become hazardous if the ceramic membrane breaks during the experiment; the liquid metal leaks out and begins to react with the steel cathode and crucible. A ceramic anode will not have these safety concerns.

5.8 Task 8 – Experimental Evaluation of the SOM Process – 1-5 kg/day

5.8.1 Description

To better understand the process a 1-5 kg/day scale experiment will be fabricated and tested. The results of this experiment will be used to update the process and economic analyses prepared in Task 6. During year 2, the design and fabrication will take place with some shakedown testing. During year 3, additional testing will be performed and the economic analysis will be updated.

5.8.2 Accomplishments

- Three-Tube SOM Scale-up experiments were run and magnesium was produced
- Modeling results were tested
- Master's Thesis entitled 'Scale-up and Modeling of the Solid Oxide Membrane Process for the Direct Reduction of Magnesium from Magnesium Oxide' written and presented.

5.8.3 Discussion

In this section, we discuss the results of experiments and modeling performed on a three-tube SOM device. The three-tube SOM magnesium reformer was built to test the potential of scaling up the SOM single tube experiment. It will be necessary to employ electrolysis cells of 39 or more tubes in the commercial scale SOM magnesium plant. The three-tube SOM scale up was run several times and performed well. Magnesium metal was collected in the condenser. A mathematical model that had been prepared for the design of the new experiment was proven and additional modeling tasks were defined.

Successful modeling of an experiment of this type is extremely helpful in understanding the characteristics of the device and in testing various design options. The Boundary Element Method model, that was begun under Task 7, has been used to perform some characterization modeling of the new three-tube SOM.

5.8.3.1 Boundary Element Method (BEM) 3-D mathematical modeling

Mathematical modeling enables further understanding of the Mg-SOM system. The Boundary Element Method (BEM) is particularly suited to the three-dimensional modeling of the Mg-SOM process. BEM modeling allows one to change the geometry without remeshing, a useful feature for parametric optimization. A model is being developed to calculate the electric current density and heat generation rates for both single tube and three tube geometries of the Mg-SOM setup. The model will enable the optimization of electrode placement, first to minimize total resistance of the system, and second to maximize current density uniformity at the anode.

Code has been written to generate the 3-D geometries of both the single and triple membrane Mg-SOM cells. Figure 169 and Figure 170 show screen shots of the two geometries. Figure 169 shows the single tube geometry and Figure 170 shows the triple tube geometry. Note that the 3-D models here include only the surfaces that are in direct contact with the molten flux.

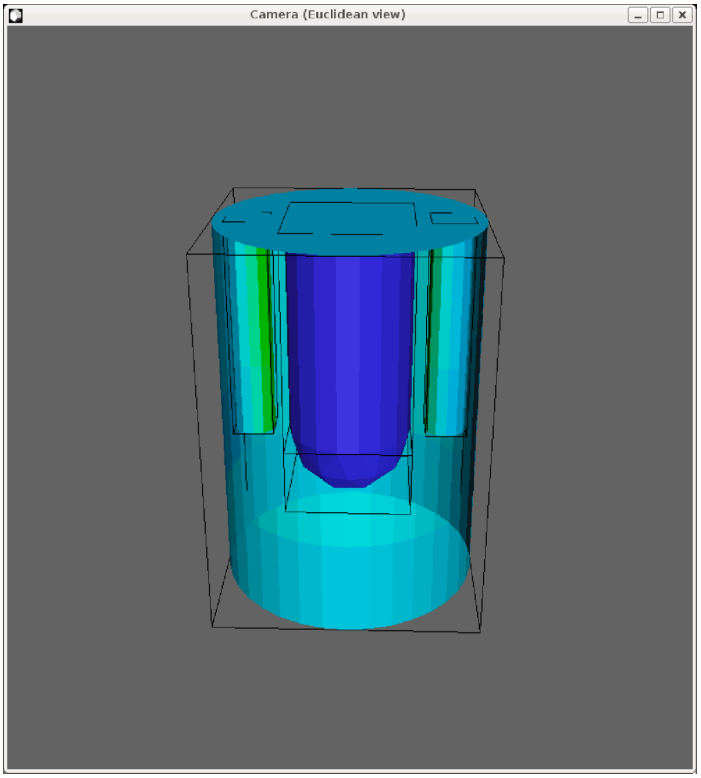

Figure 169 - Mg-SOM 3-D Model Geometry: Single Tube

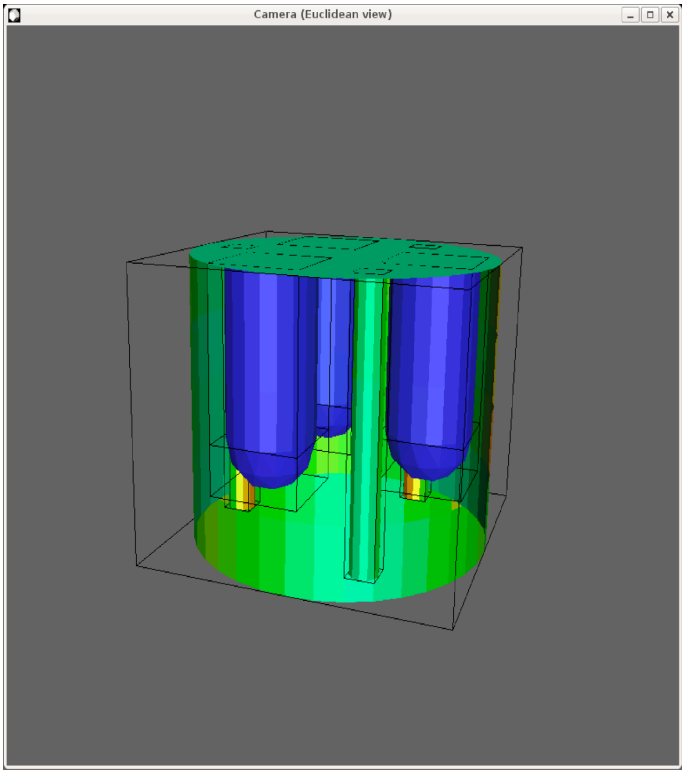

Figure 170 - Mg-SOM 3-D Model Geometry: Triple Tube

Preliminary calculations of the average current density using the BEM model fall within a realistic range. At an applied potential of 5 V the maximum calculated current density was 0.66 A/cm^2 in the single tube simulation. This calculation accounts for an estimated lead wire resistance value of 0.1 ohm and an internal resistance of 0.087 ohm. The 0.66 A/cm^2 calculated current density value is similar to the experimentally predicted value of 1 A/cm^2. Further refinement of the model will allow us to predict the values more accurately. Figure 171 shows an experimental Mg-SOM potentiodynamic scan. Figure 172 shows a plot of applied potential versus anode current values generated using the model. The dimensions used in the model are shown in Table 67.

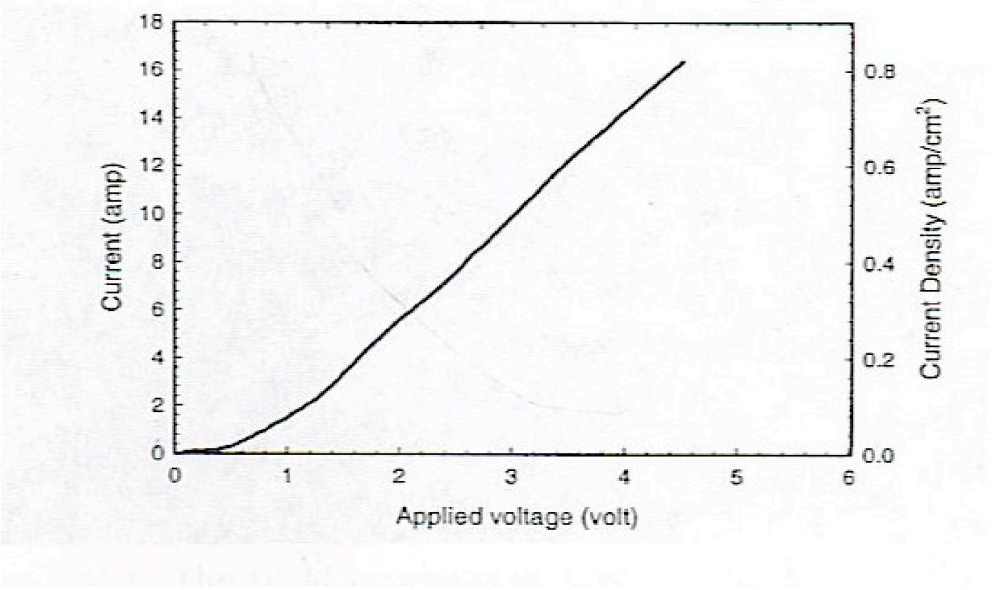

Figure 171 - Potentiodynamic Scan from Mg-SOM Experiment

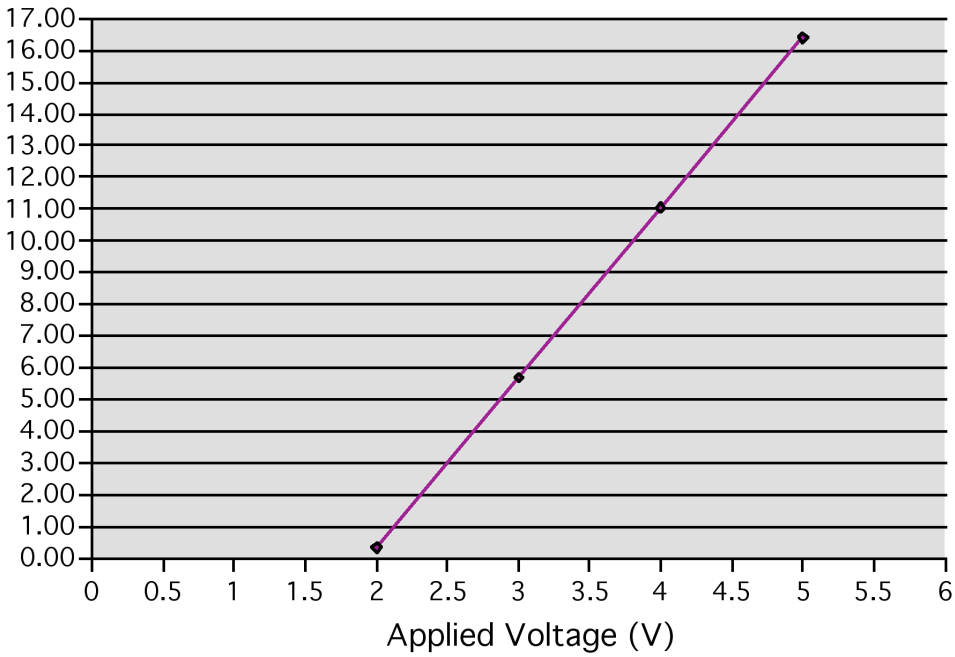

Figure 172 - Calculated Values for Anode Current using Single Tube BEM Model

Table 67 - Dimensions Used in the Single Tube Model

	Single Tube
Crucible Length	2.125”
Crucible Diameter	1.575”
Membrane Diameter	0.756”
Membrane Length	1.63”
Bubbling Tube Diameter	0.25”
Bubbling Tube Length	1.25”
Flux Conductivity	383 S/m
YSZ membrane Conductivity	10 S/m
Anode Surface Area	24.9 cm^2 (3.85 in^2)

The placement of bubbling tubes with respect to the YSZ membrane was identified as a factor affecting the current density distribution. Minimizing the current density distribution across the YSZ membrane is a factor in extending the life of the YSZ membrane. Simulations were created that varied the depth of immersion of the bubbling tube from 1 to 2 inches (in ¼ inch increments). The resulting total current density distributions were compared. Figure 173 plots the depth of immersion versus the difference between absolute values of the maximum and minimum current density values calculated by the simulation. These results indicate that a more narrow distribution can be achieved by lowering the bubbling tube closer to the bottom of the stainless steel crucible.

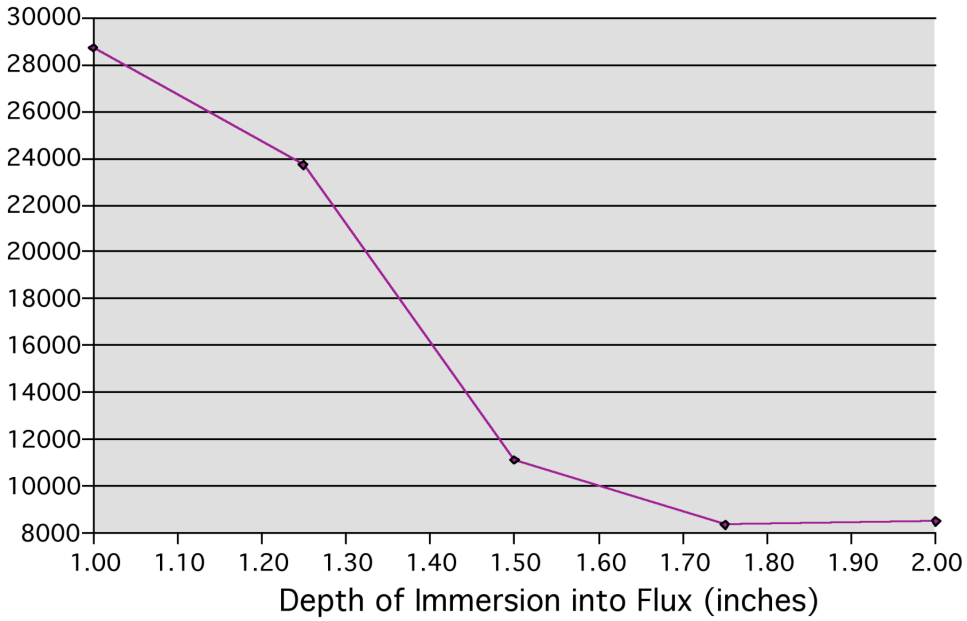

Figure 173 - Depth of Bubbling Tube Immersion vs. Current Density Difference

Figure 174 and Figure 175 show pictures of the single tube model at the minimum and maximum depths of bubbling tube immersion, respectively.

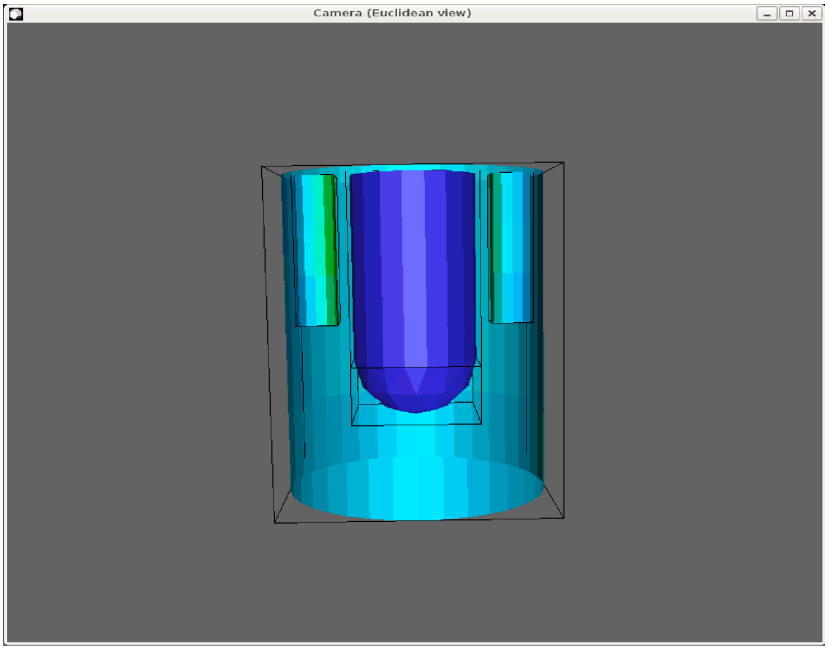

Figure 174 - Bubbling Tube at 1 inch Immersion

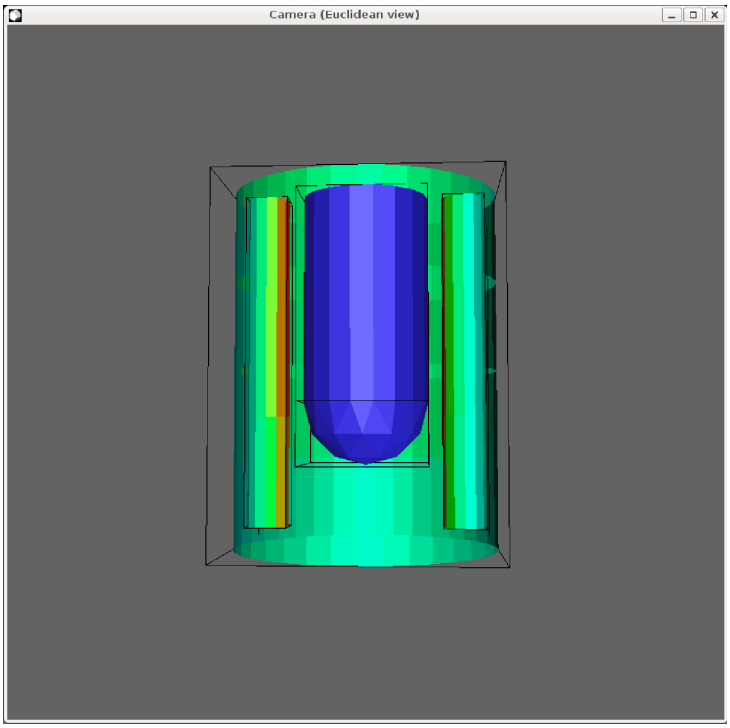

Figure 175 - Bubbling Tube at 2 inch Immersion

Development of the BEM model is being done in collaboration with Dr. Adam Powell of Veryst Engineering. Julian, an open-source BEM software package designed by Dr. Powell, is being used to develop the model.

5.8.3.2 Mg-SOM: Periodic Potentiodynamic Scans

Mg-SOM experiments were run using the low-temperature flux of MgF_2-CaF_2-MgO at 1150ºC. Potentiodynamic scans of the cell were taken every hour over the course of the electrolysis in order to better understand the electrical behavior of the cell over time. A comparison of potentiodynamic scans from one of the experiments is shown in Figure 176. In red is the initial scan, taken before the electrolysis. As can be seen in the plot, the current of this initial scan stays low until the dissociation potential of MgO is reached, then increases steadily. All potentiodynamic scans were performed at a rate of 10 mV/s. After a potential of 2.5 V was applied for 1 hour, the scans are quite different, with a marked increase in conductivity as soon as the scan begins. The plots in black are the scans taken every hour during the electrolysis. Therefore it is possible that the cell is becoming somewhat electronically conductive after the electrolysis begins.

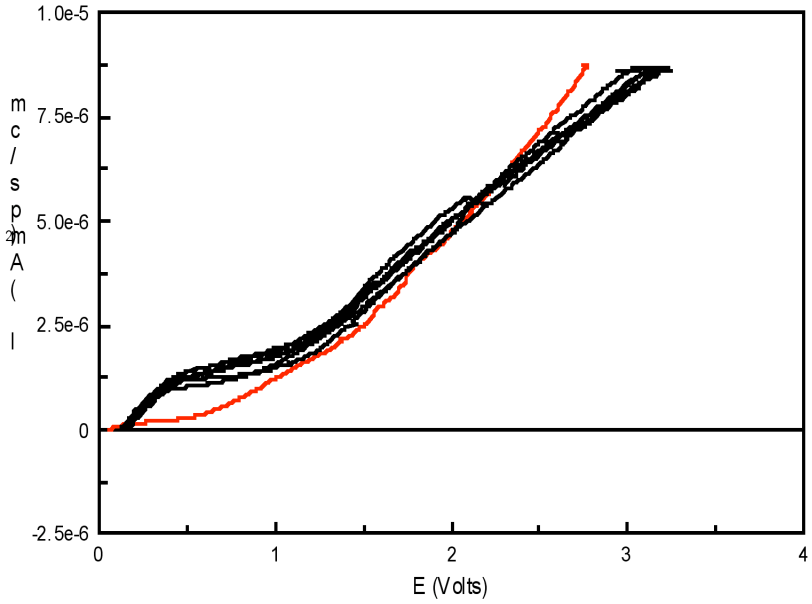

Figure 176 - Periodic Potentiodynamic Scans during Mg-SOM Electrolysis

The setup was tested for short circuits through the cooling plate and fixtures, but none were discovered. The electronic conductivity might be caused by the presence of an electronically conductive substance. Calcium metal (from the CaF_2) and/or dissolved Mg metal are possible culprits for the electrical conductivity. The flux was tested for the presence of calcium metal after the experiment. Powdered flux was mixed with water in a sealed beaker attached to a manometer. The presence of calcium would be indicated by an increase of pressure inside the beaker resulting from the creation of hydrogen gas from calcium reacting with water. The pressure inside the beaker did not increase, even after waiting two hours. It is unlikely, therefore, that calcium is being formed stably in the flux and that the electrical conductivity is the result of a calcium metal presence.

It is important to identify the source of this electronic conductivity because of the long-term stability of the membrane. The presence of an electronic current will adversely affect the membrane lifetime.

5.8.3.3 Determining the source of electronic conductivity in Mg-SOM experiments

In order to determine the cause of the electronic conductivity at low applied potentials, we will perform two experiments. The first will be an experiment using the high-temperature flux system of 90% MgF_2 - 10% MgO at 1300ºC. Potentiodynamic scans will be taken previous to the electrolysis as well as periodically throughout the electrolysis (at 2.5V) in order to compare to the previous experiment. This experiment will determine if the presence of CaF_2 has an effect on the electrical conductivity of the flux.

A second experiment will be run to determine if the high temperature causes the electronic current effect. The standard low-temperature flux ((55% MgF_2 - 45% CaF_2) -

10% MgO) will be employed, but the operating temperature will be reduced to only 1050ºC. A vacuum pump will be attached to the exhaust in order to reduce the pressure inside the cell to approximately 0.5 atm. The lower pressure will enable the magnesium to escape the flux melt, even though the boiling point of Mg metal is 1109ºC. Additionally, the use of a vacuum to reduce the operating temperature stands to increase the stability of the membrane.

An additional measure to calculate the Faradaic efficiency of the cells will be employed. Water vapor generated at the liquid anode will be captured in a condenser cooled to 0°C and measured (as well as the magnesium metal captured in the condenser) to calculate the efficiency. The collection of both these byproducts will ensure that our efficiency calculations are more accurate.

5.8.3.4 Modeling and Support Experiments

Mathematical modeling enables further understanding of the Mg-SOM system. The Boundary Element Method (BEM) is particularly suited to the three-dimensional modeling of the Mg-SOM process. BEM modeling allows one to change the geometry without remeshing, a useful feature for parametric optimization. A model is being developed to calculate the electric current density and heat generation rates for both single tube and three tube geometries of the Mg-SOM setup. The model will enable the optimization of electrode placement, first to minimize total resistance of the system, and second to maximize current density uniformity at the anode. The model was further refined by the inclusion of losses due to the lead wire resistance, which were measured experimentally.

5.8.3.4.1 Lead Wire Resistance

Lead wire resistance was determined by taking potentiodynamic scans of the individual components of the setup over a voltage range of 0 to 0.7 V and the corresponding resistance was calculated using Ohm's law. An average of the values shown in the plots from Figure 177 are shown in

Table 68. For use in modeling, we summed the average resistance values for the Lead Wires, Stainless Cathode, and Molybdenum Tube (1150°C) (0.081 ohm). Based on these values, the lead resistance for the triple tube experiment was estimated to be 0.075 ohm.

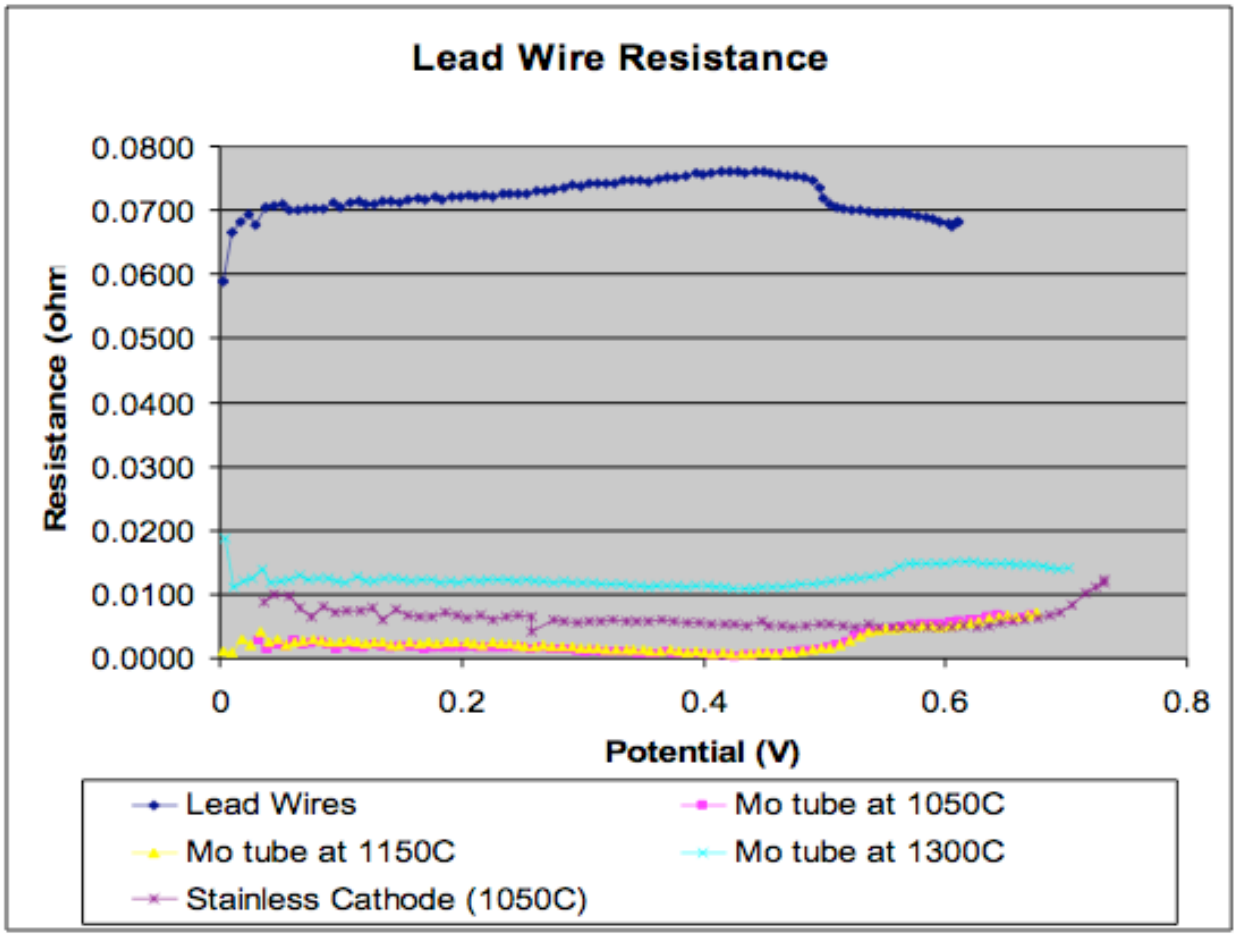

Figure 177 - Plot of Resistance of Components of Experimental Setup

Table 68 - Lead Wire Resistance Averages

	Average Resistance (ohms)	Standard Deviation
Lead Wires (connect potentiostat to anode/cathode)	0.0719	±0.0030
Stainless Steel Cathode	0.0064	±0.0017
Molybdenum Tube (1050°C)	0.0022	±0.0019
Molybdenum Tube (1150°C)	0.0027	±0.0017
Molybdenum Tube (1300°C)	0.0126	±0.0014

5.8.3.4.2 Mathematical Modeling

Assumptions

Charge transfer effects were neglected because at the high temperatures utilized in the Mg-SOM process (1150°C), these effects are negligible in comparison to electrolyte resistance. Sufficient flux stirring ensures that mass transfer is not limiting. Diffusion through the thick membrane is the most limiting. Table 69 shows the values

used to create the model's single and triple tube geometries.

Table 69 - Dimensions Used in the Single and Triple Tube Models

	Single Tube	Triple Tube
Crucible Length	2.125”	2.125”
Crucible Diameter	1.575”	4.276”
Membrane Diameter	0.756”	0.756”
Membrane Length	1.63”	1.63”
Bubbling Tube Diameter	0.25”	0.25”
Bubbling Tube Length	1.25”	1.25”
Flux Conductivity	383 S/m	383 S/m
YSZ membrane Conductivity	10 S/m	10 S/m
Anode Surface Area	24.9 cm^2(3.85 in^2)	74.7 cm^2 (11.55 in^2)

Simulated Potentiodynamic Scans for Single and Triple Tube Models

Calculations of the average current density using the BEM model fall within a realistic range. At an applied potential of 5 V the average anodic current density was calculated to be 0.9 A/cm^2 in both the single and triple tube simulations. This calculation takes into account a lead wire resistance value of 0.081 ohm and calculated flux resistance of 0.220 ohm. The 0.9 A/cm^2 calculated current density value is similar to the experimental value of 1 A/cm^2, validating the model and its assumptions. Further refinement of the model will allow us to predict the values more accurately. Figure 178 shows an experimental Mg-SOM potentiodynamic scan with modeling results from the single tube geometry. The modeled values were normalized to the 15.2 cm^2 anode area utilized in the experiment. By inspection, the experimental values for current response are somewhat lower than those calculated using the boundary element method. Figure 179 shows a plot of applied potential versus anode current values generated using the model for the triple tube geometry. The triple tube geometry plot used 74.7 cm^2 anode area.

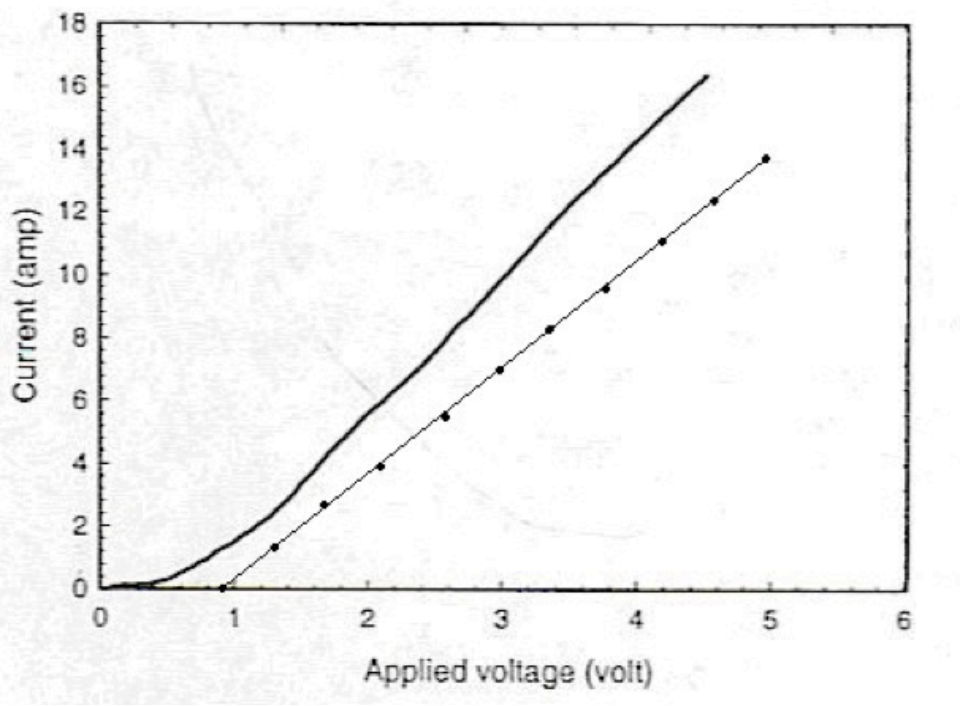

Figure 178 - Potentiodynamic Scan from Mg-SOM experiment with single-tube

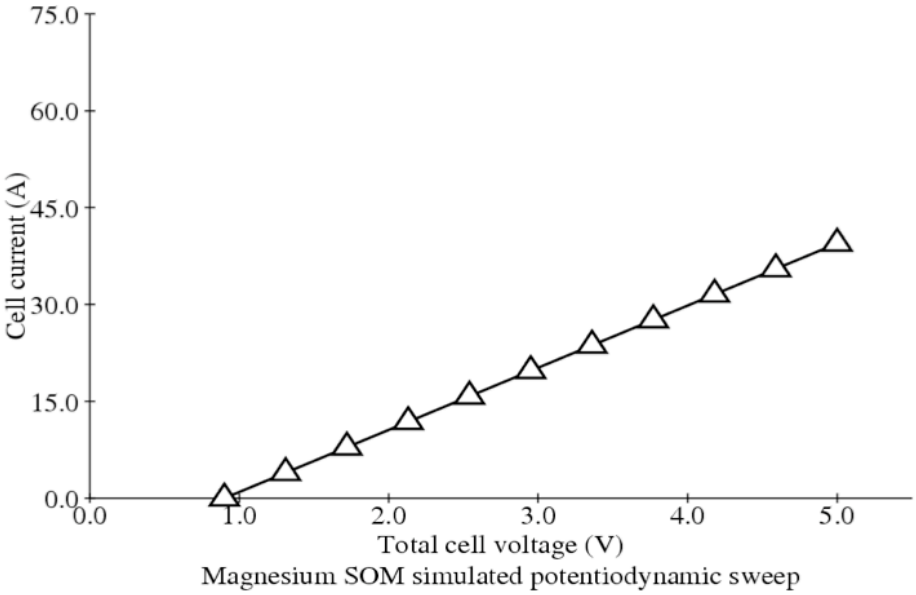

Figure 179 - Calculated Values for Anode Current using Triple Tube BEM Model

5.8.3.5 Scale-up Experiment #1

An experiment examining the feasibility of multiple-tube Mg-SOM cells has been completed. Three yttria-stabilized zirconia membranes containing tin were set into a stainless steel crucible filled with low-temperature flux (49.5 %MgF2– 40.5% CaF2 –

10% MgO) and heated to 1150°C. The cell was characterized using potentiodynamic scans as well as impedance measurements. Figure 180 and Figure 181 show photographs of the completed Mg-SOM triple-tube setup. Figure 182 shows a cutaway schematic of the interior of the triple tube Mg-SOM setup.

Figure 180 - Completed Mg-SOM Setup Furnace

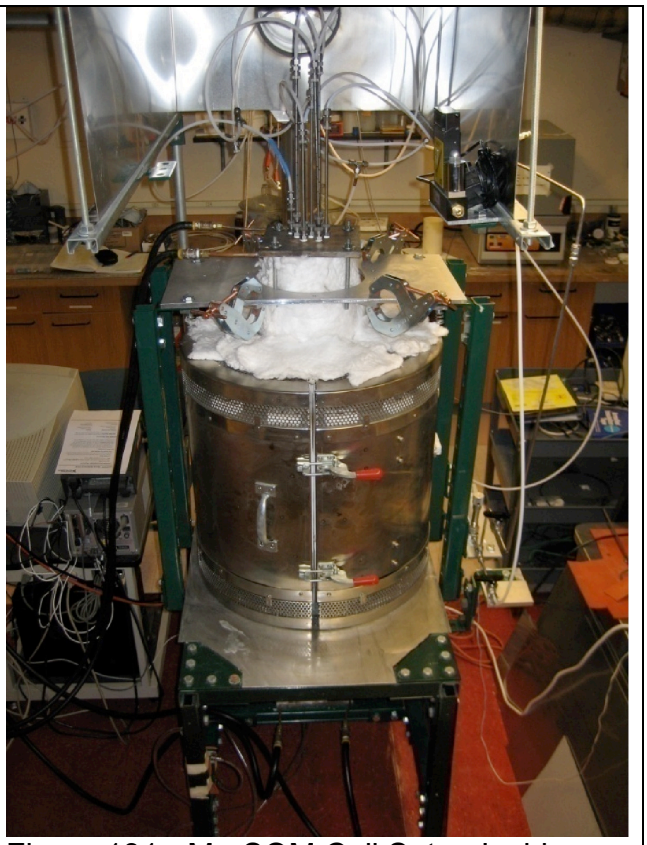

Figure 181 - Mg-SOM Cell Setup Inside

Approximately 41.6 cm^2 of anode surface area was utilized in the experiment. According to the potentiodynamic scan (Figure 183) taken before the electrolysis, this corresponds to a current density of 1.04 A/cm^2 at 4 V. This current density value is higher than expected based on previous experiments with the single-tube design. It is possible that this difference could be caused by an inaccurate calculated anode surface area. The surface area calculation does not take into account the displacement of flux due to the bubbling of hydrogen. Even so, this experiment shows that large current densities are possible using the Mg-SOM setup.

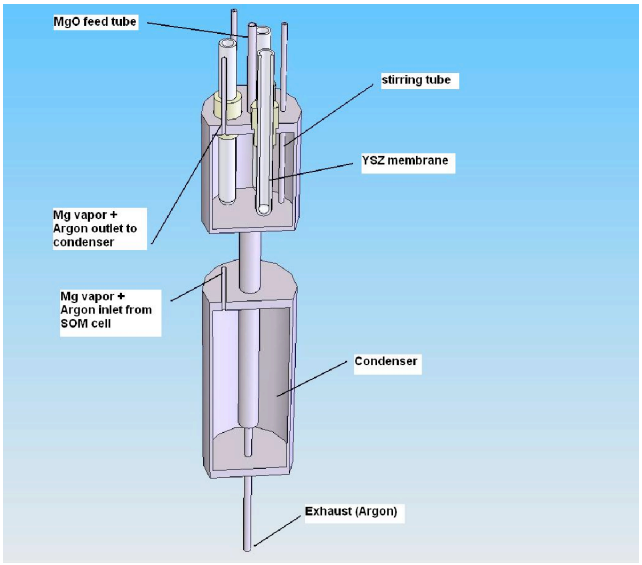

Figure 182 - Cutaway Schematic of the Triple Tube Mg-SOM Setup

Table 70 shows the dimensions used in the triple tube experiment versus those used in the single tube experiments.

Table 70 - Specifications - Comparison of Single Tube and Triple Tube Mg-SOM Experiment

	Single Tube	Triple Tube
Amount of flux used	**454 g**	**1152 g**
Anode surface area	**13.9 cm^2**	**41.56 cm^2**
Crucible inner diameter	**6.68 cm**	**10.86 cm**
Membrane ID	**1.42 cm**	**1.42 cm**
Membrane OD	**1.92 cm**	**1.92 cm**

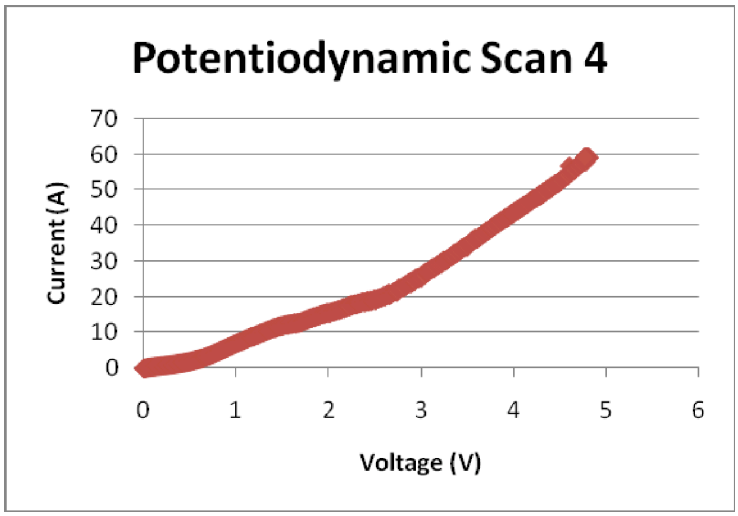

Figure 183 - Potentiodynamic Scan before Electrolysis

A potential of 4 V was applied for 2 hours for the first electrolysis. A total of 381363 C of charge was passed, theoretically resulting in the reduction of 48 g of Mg metal. The electrolysis scan is shown in Figure 184.

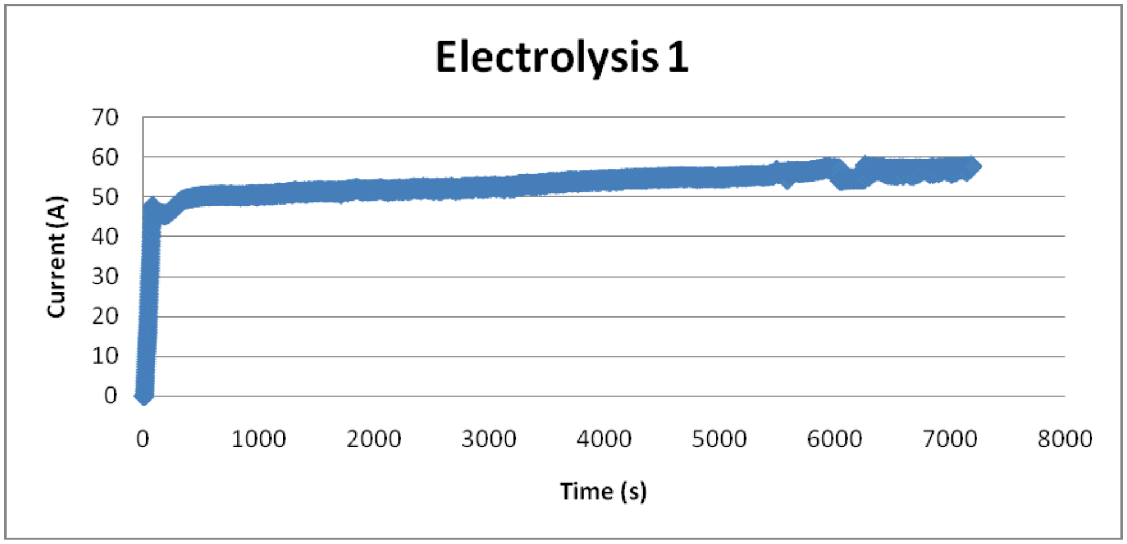

Figure 184 - Plot of Current and Time for Electrolysis

The second electrolysis scan, in Figure 185, shows a clear drop in the current after about 30 minutes. The second electrolysis utilized a smaller voltage, 3 V. The steep drop in current likely corresponds to the catastrophic failure of the tubes. The damage to the membranes was likely due to joule heating. The joule heating rate is calculated to be approximately 0.15 °K/second for an electrolysis at 4 V with a current response of 50 A. This rate could result in tube failure due to thermal shock within the timeframe of the experiment if the heat was not able to dissipate quickly enough. It was assumed that the thermocouples in the large tube furnace would be able to respond to the heat caused by the passing of current. Subsequent experiments will employ more precise temperature monitoring at the cell because it appears that the response of the furnace was not quick enough to prevent overheating the zirconia membranes.

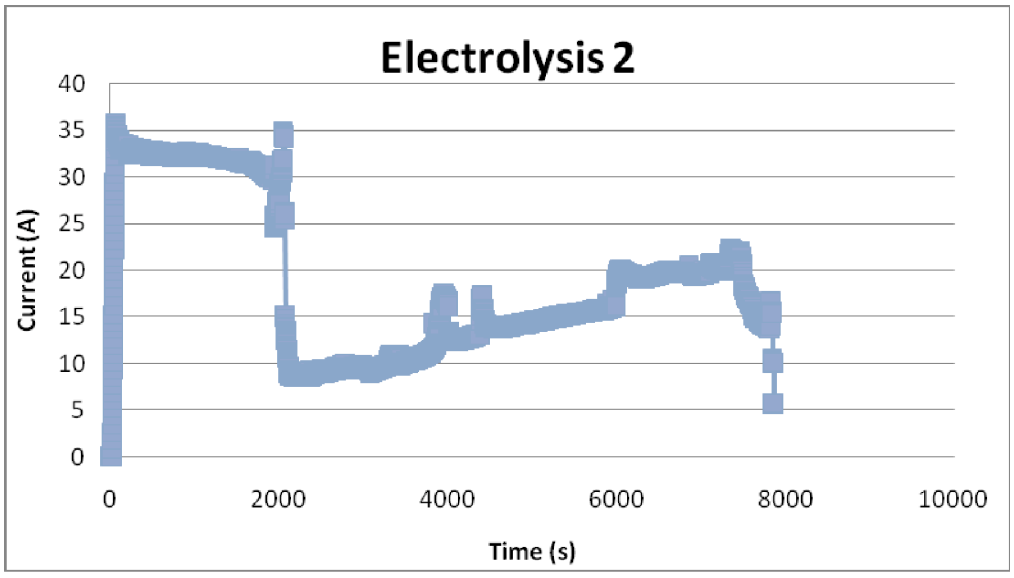

Figure 185 - Plot of Current and Time for Electrolysis 2

Figure 186 and Figure 187 show the magnesium metal recovered from the condenser chamber. Approximately 1 g was stuck to the stainless steel shim shown in Figure 186 in a fine crystalline as well as in small lump form. Figure 187 shows a deposit that appears to have been molten on the floor of the condenser chamber.

Upon examination of the experimental setup, a small amount of flux was found covering the exit from the cell to the condenser. Slight changes to the dimensions of the interior of the cell setup will prevent such clogs in future experiments.

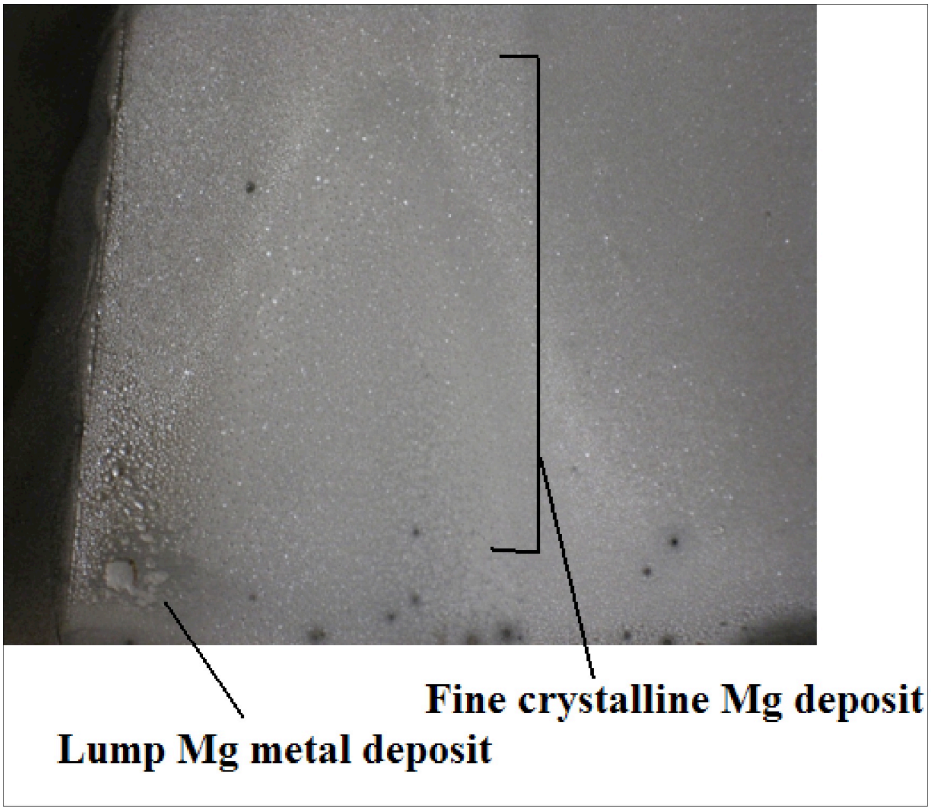

Figure 186 - Magnesium Metal Captured in Condenser

Figure 187 - Magnesium Deposit on Floor of Condenser

5.8.3.6 Scale-up Experiment #2

An experimental setup for a triple-tube Mg-SOM reactor was fabricated and tested using the low-temperature flux system [(55% MgF2-45% CaF2)-10%MgO] at 1150°C. The cell was characterized with potentiodynamic scans (scan rate = 0.05 to 0.10 V/s) and electrolysis scans. A pre-electrolysis scan was made with a potential of 0.6 V for 20 minutes to eliminate excess oxygen present in the system (Figure 188).

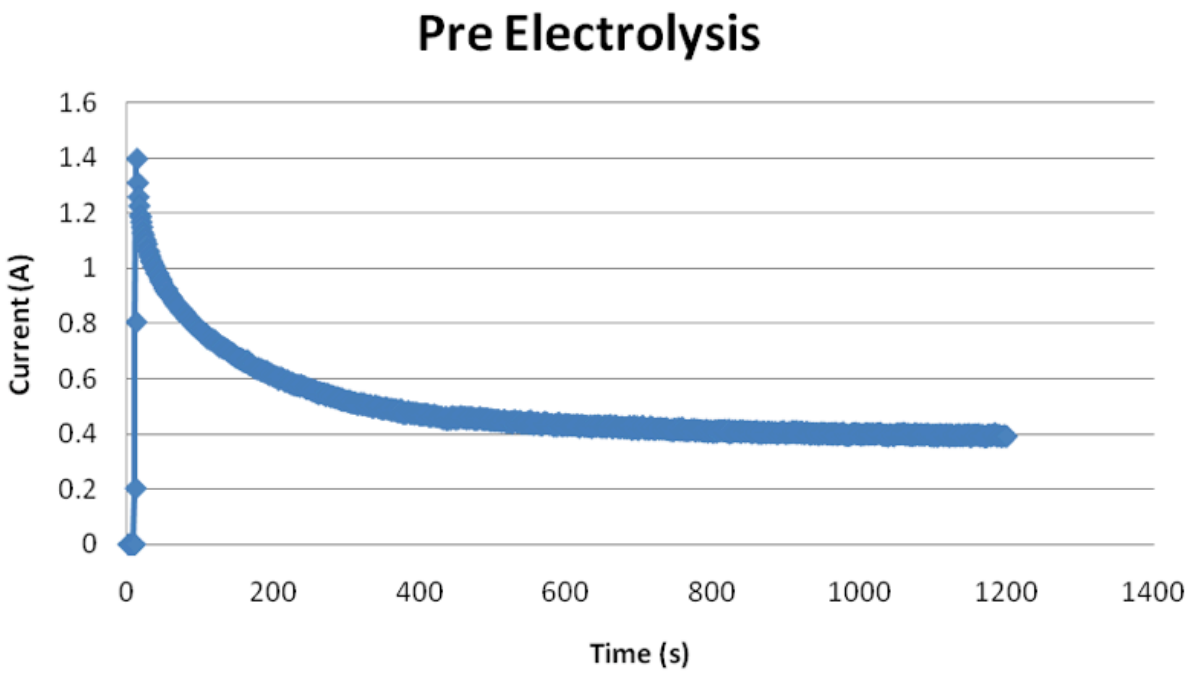

Figure 188 - Pre Electrolysis

Dissociation potential was observed around 0.6V during the initial potentiodynamic scan (Figure 189).

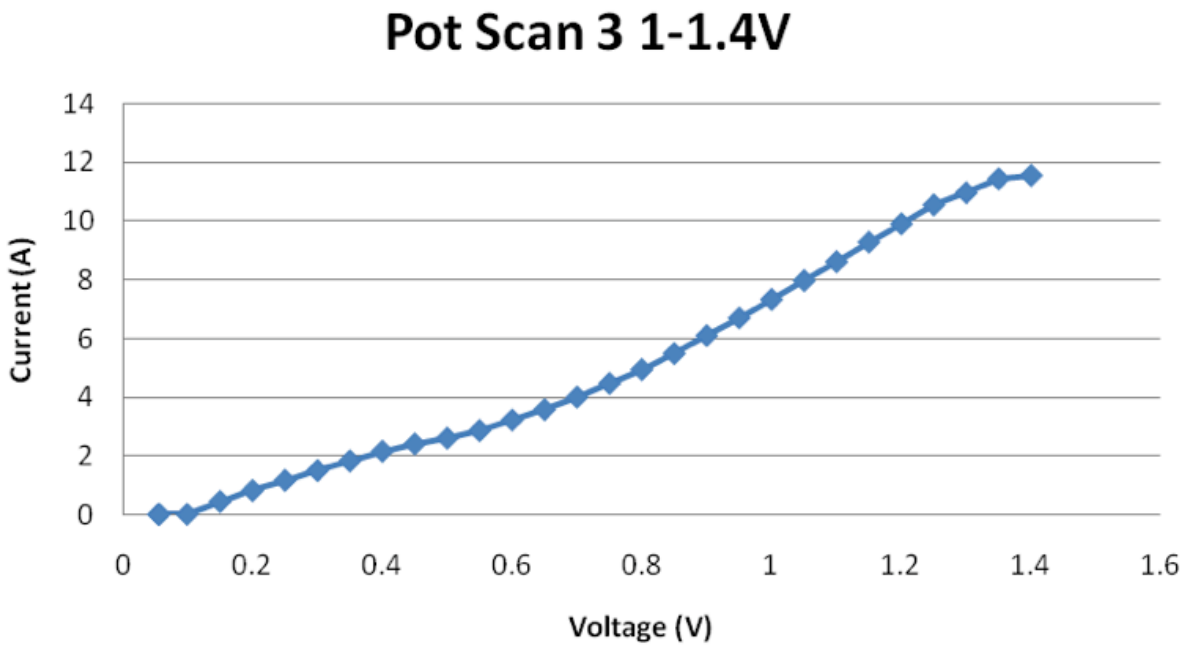

Figure 189 - Potentiodynamic Scan showing Dissociation Potential

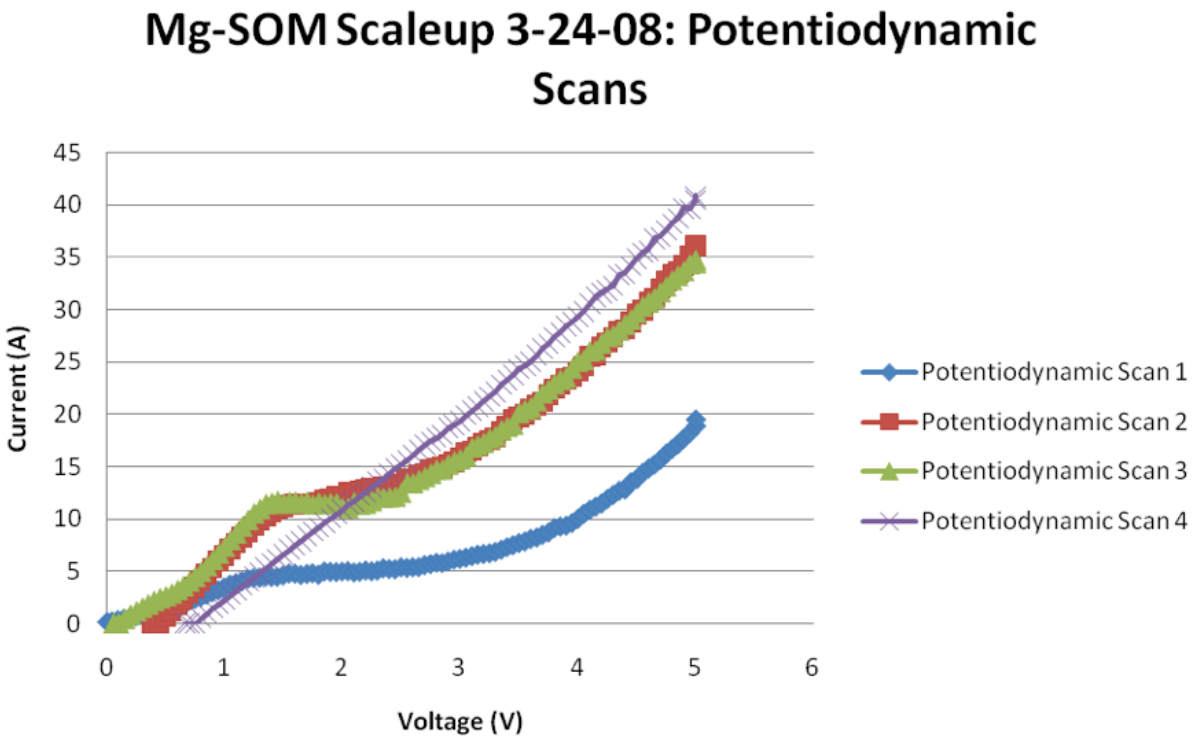

Figure 190 - Potentiodynamic Scans

Higher current observed in the potentiodynamic scan prior to the dissociation of MgO is due to the scan rate used. Potentiodynamic scans 1-3 shown in Figure 190 were taken previous to the first electrolysis. Potentiodynamic Scan 4 was taken after the last electrolysis scan and indicates only electronic conductivity (corresponds to Ohm's Law). Each electrolysis scan shown in Figure 190 resulted from applying a potential of 2.5V for 30 minutes. The system was allowed to sit for 45 minutes to 1 hour to allow residual heat built up from the high currents to dissipate. Approximately 30,000 to 33,000 C of charge were passed during each electrolysis (1 – 4), theoretically generating 18.718 g of magnesium metal.

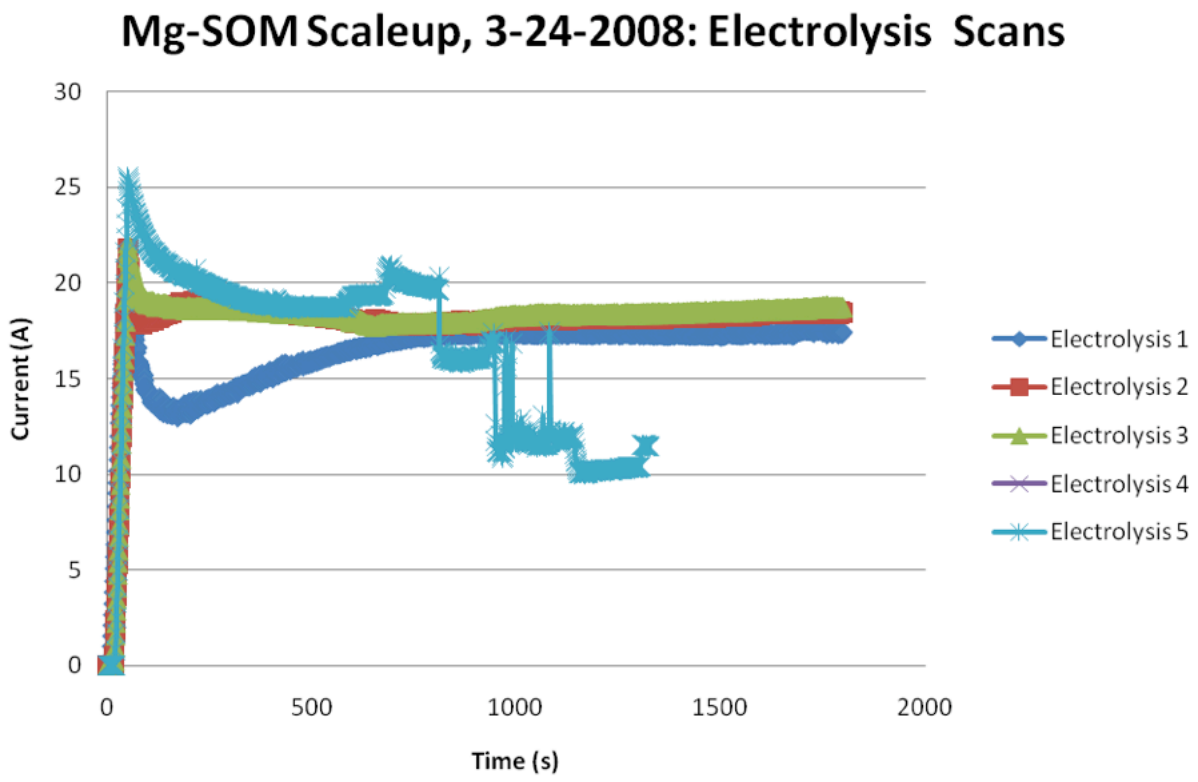

Figure 191 - Electrolysis Scans

Approximately 41.6 cm^2 of anode surface area was utilized in the experiment. According to the potentiodynamic scan (Figure 191) taken before the electrolysis, this corresponds to a current density of 0.43 A/cm^2 at 2.5 V.

The 5th electrolysis scan, in Figure 191, shows a clear drop in the current after about 13 minutes. The steep drop in current likely corresponded to the catastrophic failure of the tubes. This breakage was confirmed by visual inspection of the membranes after the entire setup was cooled down and disassembled. All three membranes were broken just below the alumina sheaths at approximately the same relative position. The breakage appears to have been caused by uncontrolled heating of the tubes caused by a large current flow through the flux to the tubes. Improvements in

the control of this system can be achieved with the addition of thermocouples in the flux to monitor the temperatures around the tubes.

5.8.3.7 Analysis

5.8.3.7.1 Joule Heating

The increase in current from Electrolysis 1-4 (Figure 4) is likely due to a steady increase in temperature resulting from the heat generated by joule heating not dissipating quickly enough. As the temperature rises, the ionic conductivity of the YSZ membrane increases, allowing an increase in current.

The damage to the membranes was also likely due to excessive heating. The joule heating rate is defined as the heat generation due to the resistance (ionic in this case) and can be calculated using the following equation:

$$heating\ rate\ \left(\frac{^{\circ}C}{s}\right) = \frac{IV}{mC_p 4.184}$$

m	=	mass of flux [g]	=	1152 g (for scale-up)
V	=	applied voltage (V – dissociation potential) [V]		
I	=	current response [A]		
C_p	=	heat capacity [ca/g˚C]	=	0.222 (for flux)

This calculation assumes uniform heating and neglects any heat loss to the crucible. Using this equation, the heating rate is calculated to be approximately 0.03 °C/s for the electrolysis at 2.5 V (with dissociation potential of 0.6V) and a current response of 18 A. The previous scale-up experiment had heating rates as high as 0.16 °C/second for an electrolysis at 4 V (assuming a dissociation potential of 0.6 V) with a current response of 50 A. Both heating rates were sufficient to cause tube failure, ending the experiments. The increase in current indicates that the heat did not dissipate as quickly as it was generated. It is possible that thermal cycling caused by allowing the large amount of time (45 min – 1 hr) for cooling between electrolyses also contributed to thermal stresses in the ceramic. Subsequent experiments will employ more precise temperature monitoring at the cell because the response of the furnace is not quick enough to prevent overheating the zirconia membranes.

5.8.3.8 Force Calculation

Another possible mechanism for the damage to the ceramic membranes is the force generated between two conductors when large amounts of current are flowing. The interaction force between two of the molybdenum tubes was examined to get an idea of the magnitudes of the forces generated due to the magnetic fields. The force per unit length between two long, parallel, current-carrying conductors can be calculated using the following equation:

$$\frac{F}{L} = \frac{\mu_0 I I'}{2\pi r}$$

F/L	=	force per unit length
μ_0	=	proportionality constant, $4\pi * 10\text{-}7\ N \cdot s^2/C^2 = 4\pi * 10^{-7}\ Wb/A \cdot m = 4\pi * 10^{-7}\ T \cdot m/A$
I, I'	=	currents carried in each of the wires
r	=	separation distance between the two wires

The force generated between the molybdenum tubes within the SOM cell will be attractive because they carry the current in the same direction. If the current carried by each of the molybdenum tubes is 50 A and the separation between the tubes 0.0528 m (2.08"), the force per unit length will be approximately 0.0095 N/m. It is unlikely that such a small force would cause a zirconia tube to break, so it the more likely explanation is the previously discussed joule heating rate.

5.8.3.9 Conclusions

Considerable knowledge has been gained from the three-tube SOM process testing. The system operated well except for the over temperature at the end of the experiment that caused the tubes to fail. There was not enough time in the project to correct the control scheme and test again.

5.8.3.10 Future Work:

- Use the BEM model to optimize electrode placement, first to minimize total resistance of the system, and second to maximize current density uniformity at the anode.
- Couple heat transfer effects to BEM model to determine temperature distribution in three dimensions.
- Perform SOM experiments to test the results of the triple-tube Mg-SOM model.
- Perform SOM experiments to test the honeycomb cathode arrangement.
- Extend analysis to larger-scale simulations.
-

5.9 Task 9 – Experimental Evaluation of the Carbothermic Process – 100 gm/day

5.9.1 Description

Based on the results of Task 6, one of the carbothermic processes will be selected for experimental evaluation. A 100 g/day laboratory scale process will be designed, fabricated, and tested to confirm the reduction operation anticipated from the Task 6 analysis. The results of this analysis will be used to prepare a design of a 1-5 kg/day scale process.

5.9.2 Discussion

This task was removed from the project due to funding changes. The planned resources were reallocated to other tasks.

5.10 Task 10 – Experimental Evaluation of the Carbothermic Process – 1-5 kg/day

5.10.1 Description

A 1-5 kg/day scale experiment will be fabricated and tested. The results of this experiment will be used to update the process and economic analyses prepared in Task 6.

5.10.2 Discussion

This task was removed from the project due to funding changes. The planned resources were reallocated to other tasks.

5.11 Task 11 – Recycling Cost Reduction Evaluation

5.11.1 Description

The objective of this task is to evaluate methods of reducing the cost of recycling. Based on the results of the preceding tasks, an evaluation will be performed to identify cost reduction opportunities yet to be investigated. These opportunities will be ranked according to their affect on their cost saving potential in the recycling process.

5.11.2 Summary

There are a number of opportunities for cost reductions in the recycling process. The primary cost component of the slurry process is the reformation of magnesium hydroxide and magnesium oxide to magnesium. There are several existing technologies currently used throughout the world to accomplish this task. Most of these processes involve multiple cycles and each cycle adds cost to the overall process.

During this project, we have evaluated two processes that provide rapid single step reduction of magnesium oxide to magnesium. The carbothermic process was used in the 1940s and 1950s to produce magnesium commercially. Modern control technology could make this a viable process again. However, the carbothermic process relies on carbon that would likely come from coal or oil though it could come from biomass. The SOM process under development by Boston University researchers is a direct reduction process using electricity that can be provided from non-carbon sources. We have recommended that the SOM process be developed, as it appears to be the most cost effective approach to producing magnesium.

In our analysis of a mature SOM process, we assumed that several issues would be solved. These include:

- the development of a highly automated process to recycle the used zirconium oxide tubes back into new zirconium oxide tubes;
- the use of LSM coatings on the interior of the zirconium oxide tubes to catalyze the recombination of oxygen atoms into oxygen molecules within the tubes to provide a byproduct of oxygen from the plant;
- the development of a compact design to maximize the use of rejected heat into feed processes that require heat, such as the calcination process for calcining magnesium hydroxide into magnesium oxide;
- the development of a magnesium condensation process to condense magnesium vapor into very small particles; and
- the development of a magnesium hydriding process based on the results of our experiments.

5.11.3 Discussion

5.11.3.1 SOM Process Description

The SOM process was discussed in sections 5.6, 5.7, and 5.8. In the SOM process, zirconium oxide tubes are dipped into a flux containing magnesium oxide. Each tube and surrounding flux bath is placed within an encircling cathode of iron or steel. Flux is allowed to move freely between and through the encircling iron cathodes.

Current passes from the cathode through the flux and through the zirconium oxide tube to the anode located inside the zirconium oxide tube. As the current moves through the flux, ions of magnesium are moved to the cathode and ions of oxygen are moved through the zirconium oxide tube to the anode. The magnesium rises from the flux as a gas aided by the flow of argon moving up through the flux and is carried with the argon to a condenser where it is condensed into a fine powder. The oxygen ions are formed into oxygen atoms at the anode and produce a second product for the plant. The magnesium powder is transported to the hydrider where it is hydrided in the presence of hydrogen. The resulting magnesium hydride is mixed with oil and dispersants to produce a slurry.

5.11.3.2 Automated Recycle of ZrO Tubes

The ZrO tubes should offer at least 6 months of life. The life may be longer or shorter depending on the thermal and electrical stresses imposed by the design. As a result, the plant cost model assumed that individual multi-tube cells would be rebuilt every 6 months. This will produce a stream of ZrO material from the plant that can likely be recycled. Since the ZrO tubes are a primary cost element of the plant and since the quantity of tubes will be high in a large scale magnesium hydride slurry hydrogen storage system, there is an opportunity for the mass production of the tubes and the reclamation of the ZrO from the used tubes. Such a system needs to be developed.

5.11.3.3 Use of LSM Coating to Produce Oxygen

During the production of magnesium with the SOM process, oxygen ions will move through the ZrO tubes and must be removed at the anode. Boston University researchers evaluated several methods of removing the oxygen. They looked at bubbling natural gas (methane) through a liquid copper anode to consume the oxygen as carbon monoxide and hydrogen. They tested a silver anode that could deliver oxygen from the process. Silver oxidizes readily but the oxide is not stable at the temperatures at which the anode will operate. These processes both worked well. Based on their experience with solid oxide fuel cells, they hypothesized that an LSM coating on the interior of the ZrO tubes could act as a catalyst to recombine the oxygen ions into oxygen molecules and thus provide a stream of oxygen from the anode much like the silver anode design. They did not test this design.

Our cost analysis indicated that the lowest cost process would be the LSM coating based on estimates of the costs of the thickness of the coating and the material required to make it. Thus further development should be performed with LSM coatings on the SOM anodes.

5.11.3.4 Design for Plant Efficiency

The SOM plant was assumed to use rejected heat from the SOM cells, and the condensation of the magnesium to supply low quality process heat to the calcination of magnesium hydroxide to magnesium oxide and to the drying of the original byproducts. The plant design will require careful design to maximize the use of the energy that is entering it.

5.11.3.5 Magnesium Condensation Process

After the SOM process produces the gaseous magnesium, the magnesium must be condensed to form small particles in the 10 to 1000 nm scale. These particles must then be transported to the hydriding process. If the particles can be produced at this size then the magnesium hydride produced should not need to be milled. The design of a condenser to achieve this size range has not yet been demonstrated.

5.11.3.6 Process Modeling

Process modeling can aid in the design process to minimize thermal, electrical, and corrosion stresses. It can provide extended life of the ZrO tubes. It can provide an inexpensive means of testing alternative configurations. It can provide information about higher current (higher throughput) operation of the process.

A process model was begun under this project. It was used to design the 3-tube experiment. The development process for the model requires model design and experimental confirmation in a series of model/experiment steps. This development process should be continued.

As the model is improved, it should be used periodically to design the large scale multi-tube design that will be used in commercial operation.

5.12 Task 12 – Program Management and Reporting

5.12.1 Description

The objective of this task is to manage the performance of the contract as well as to prepare required reports. Quarterly reports will be prepared for three quarters each year. An annual report will be prepared to describe the work performed each year. In addition, presentations will be prepared and presented at the DOE annual meeting, the DOE Annual Program Peer Review, and the annual Hydrogen Storage Technical Team review. In addition, at least one technical paper will be prepared for delivery at another meeting each year.

5.12.2 Summary

It is our belief that, with the delivery of this document, all required reports and deliverables have been forwarded to DOE.

6 Key Issues and Future Work

The purpose of the work performed during this project was to address the “show stopper” issues and to estimate the costs associated with the use of magnesium hydride slurry as a chemical hydride slurry. This has been achieved. We found no show stopper issues.

The costs associated with the process look attractive and the process continues to promise considerable safety characteristics:

- Magnesium hydride reacts very slowly at normal temperatures and pressures
- The byproduct of the reaction is benign. (Magnesium hydroxide is “milk of magnesia” and magnesium oxide is a common insulating material).
- The slurry and byproducts can use the existing liquid fuels infrastructure with modifications to the pumping systems
- Hydrogen gas need only exist for a short time between when it is produced by the slurry/water reaction and the time it is consumed by the prime mover. (It may still be attractive to have a small buffer volume to use for startup).
- Magnesium is found all over the world and occurs in relatively high concentration in seawater.
- The byproducts can be recycled using electrical or carbothermic processes that can be fueled with non-fossil fuel sources.

In this section, we have summarized what we have accomplished, some of the issues that require further development, and some suggestions for future development work.

6.1 What we have accomplished

The work proposed for this project has been completed. The results were quite encouraging. The basic issues associated with the chemical hydride slurry approach using magnesium hydride have been explored. Considerable definition of the concept has been achieved and an alternative of this concept has been identified that appears to offer an even cheaper option for hydrogen storage and delivery.

A 75% slurry has been formulated and appears to be pumpable and stable for long durations.

70% slurries have been tested with both a continuous mixing system and with a semi-continuous mixing system. No significant problems were encountered. Considerable opportunities for improvement remain.

The recycling of the byproducts has been evaluated for cost and efficiency. The recovery of oil from the slurry was found to be a conventional problem that can be achieved with conventional technologies. The reforming of magnesium oxide and magnesium hydroxide to magnesium can be performed with conventional magnesium reforming technologies or with a new technology under development by Boston University. The new technology is called the SOM (Solid-oxide Oxygen-ion-conducting Membrane) process. Using the SOM process, we estimate that the cost of hydrogen at the filling station would be about $4.50/kg of hydrogen in a mature large-scale process.

We have evaluated the process of hydriding the reformed magnesium to magnesium hydride and found patent literature that described a low cost technique. We have evaluated this technique and found it to be reliable and inexpensive.

During the process of evaluating magnesium hydride processing, we learned that magnesium hydride slurry can be used as a rechargeable slurry. We estimate that the cost of hydrogen to the consumer using this process would be about $3/kg of hydrogen. This is achievable because the high cost part of the process, the reformation of magnesium, can be done once to carry tens or hundreds of times the hydrogen that the chemical process can carry in its life. If the hydride can be cycled a hundred times, then the processing cost would be small compared to the cost of the hydrogen, the transportation, and the distribution costs. The transportation and distributions costs were estimated to be small relative to the reformation costs of the chemical hydride slurry process.

6.2 Issues and Future Work

Several issues require further development if magnesium hydride slurry is to be used as a chemical hydride for hydrogen storage.

- Water on board vehicle
- Slurry pumpability in cold climates
- Size of hydrogen release system
- Improved definition of costs for hydrogen, slurry, mixer, storage, delivery, distribution, and recycle
- Byproduct handling within the mixer
- Reuse of dispersant
- Slurry pump selection
- SOM process development
- Hydrider development

6.2.1 Water on board vehicle

Representatives from the U.S. automobile companies have expressed concern about carrying water onboard the vehicle as it could freeze in cold climates. The recognition that the reaction between water and magnesium hydride produces about equal molar portions of magnesium oxide and magnesium hydroxide, reduces the amount of water that would need to be carried. If the water could be recovered from the fuel cell or internal combustion engine, then even less water would need to be carried.

Decisions made by the automobile companies have led the development of the fuel cell toward a high air flow design that makes recovery of water from the fuel cell difficult and expensive. An alternate design concept would be to control the temperature of the fuel cell and keep it warm when not in use. Such a design for the fuel cell would allow lower air flows and higher water recovery from the exhaust. In such a design, the water required for the slurry/water reaction could be stored in the warm area of the vehicle.

The automobile representatives have stated that they want to have fuel cells that can directly replace the internal combustion engine. Over the past 10 years, the DOE design for the fuel cell has increased from 50 kWe to over 150 kWe. This desire to provide a widely variable power output from the fuel cell has driven the decisions to

provide considerably more air than is necessary for efficient operation of the fuel cell. If the design concept were to move toward an electric car concept, such as the plug-in hybrid, then the fuel cell could act as a battery charger. The smaller fuel cell could be designed to provide the air required for efficient operation of the fuel cell and the lower air requirement would allow considerably higher recovery of water from the fuel cell exhaust. The smaller fuel cell could be kept warm in an insulated vessel along with the water required for the slurry reaction.

The use of water with the magnesium hydride slurry chemical hydride approach is a requirement of the approach. Other chemical combinations could be considered but they would have other issues.

6.2.2 Slurry pumpability in cold climates

Pumping slurry is different than pumping gasoline. It is more similar to pumping diesel fuel. The viscosity of slurry is higher than that of gasoline or fuel oil. As with fuel oil, the viscosity increases as the temperature declines and can be too high to pump if the temperature of the slurry or fuel oil gets too low.

The primary issue is the flow of the slurry toward the intake of the pump. During the experiments that were performed as part of this project, the slurry was pumped at temperatures ranging from about 12°C to over 80°C.

When the slurry and water react, a considerable amount of heat is released that can be used to heat the slurry and water. Thus one strategy that could be used would be to keep a small amount of water and slurry warm so that the reaction could be initiated easily and then to use the heat produced to heat the large stored slurry.

6.2.3 Size of hydrogen release system

The size of the slurry/water mixer system required to serve the vehicle will be determined by the design decisions made for the fuel cell. If the fuel cell is large, then the mixer will need to be large. If the fuel cell is small, then the mixer can be small.

A modular mixer system has been investigated that can be readily scaled to any size. A continuous mixer system was explored that could be very small and light once perfected. We have estimated that the mixer system can meet the DOE 2010 volumetric energy density target and can nearly meet the DOE 2010 gravimetric energy density target. An actual demonstration of this design remains to be completed.

6.2.4 Improved definition of costs for hydrogen, slurry, mixer, storage, delivery, distribution, and recycle

We have estimated the costs of the processes that will be needed to produce, delivery, store, distribute, and recycle magnesium hydride slurry. We had some difficulties getting actual equipment costs and used costs reported from literature to make our capital cost estimates. Our costs for labor are also estimates.

The cost of the process continues to remain an issue for this technology. Our cost estimates, indicate that the cost could be attractive. Our cost estimates are probably close to the actual costs but they can only be confirmed by actually building prototypes of the processes required.

6.2.5 Byproduct handling within the mixer

During our testing of the modular, semi-continuous mixer apparatus, we several of the byproduct handling issues. The recovery of water and the handling of the magnesium oxide, magnesium hydroxide, water, and oil mixture resulting from the reaction appears to be achievable. We were able to filter the solids from the water and recover water for reuse. Our initial design was undersized though and we did not have time to increase its scale. We were also able to show that the oils would separate from the water so that when the water was removed through a filter, the byproduct solids and oil mixture could be removed from the recovery vessel. The demonstration of this at a proper scale remains an issue to be further developed.

6.2.6 Reuse of dispersant

The 70% and 75% magnesium hydride slurries require dispersants to achieve the high solids loading and flow ability that have been demonstrated with the slurries that we were studying. Our tests of recovered oil with new milled magnesium hydride indicate that some of the dispersants from the original slurry remained with the oil after the reaction. Further development will be required to determine how much dispersant needs to be added when the oil is recycled.

6.2.7 Slurry pump selection

During the performance of this work, we found it difficult to find some of the equipment that we needed at the scale that we needed. This is a typical problem when one is working on a new process. The primary problem area was with the pump. We tested several pumps during the development of the slurry. As the slurry has changed, some of these pump designs should be reevaluated. We settled on a piston pump design that we built rather than purchased as we could not find what we wanted. The piston pump design gave us good pressure characteristics and was pretty good at metering the slurry. The selection and development of slurry pumps at the scale of interest remains an issue for further development

6.2.8 SOM process development

The SOM process made considerable developmental progress over the course of this project. The cost of producing magnesium with the SOM process should be lower than the cost of producing aluminum with current processes. If magnesium could be produced at less expense than aluminum, it could serve both the hydrogen storage needs as well as vehicle structural needs.

The next steps in the development are improvements in the modeling of the process to be used to design the larger scale SOM electrolysis cells and to help monitor the performance of the SOM cells as they are being developed. This model will require the continued development and scale-up of the SOM process. We recommend that a joint industry and university project be set up to carry this technology from the laboratory into commercial application.

6.2.9 Hydrider development

The production of magnesium hydride requires finely divided magnesium. Our plan has been to condense gaseous magnesium coming from the SOM process and

feed this directly into the hydrider process. To scale up the production of magnesium hydride as the SOM process is being developed will require the development of a method of producing finely divided magnesium particles. A pneumatic system can be considered for this process where liquid magnesium is pneumatically sprayed into a powder that drops into a fluidized bed hydrider. This process will require some development effort but the individual processes appear to be developed already.

7 Patents:

Safe Hydrogen Patents and Applications

Patent applications and awards are broken into two categories. The first category describes the applications and awards that have proceeded from inventions made during the Thermo Power project. Safe Hydrogen purchased all rights to these inventions from Thermo Electron in 2002. The second category describes the applications filed under the current project.

I. "Storage, Generation, and Use of Hydrogen"

(a) United States: US 7,052,671 (issued 5/30/06)

(b) Canada: Appln # 2434650 (pending; examination requested; no substantive action to date)

(c) Europe: Appln # 02720786.9 (pending; response to first office action rejecting claims filed; awaiting action by European Patent Office)

(d) Taiwan: TW260344 (issued 8/21/06)

2. "Storing and Transporting Energy"

(a) United States: USSN 11/392,149 (pending; published on 10/4/07 as US 2007/0227899)

(b) PCT: PCT/US2007/0641

Boston University Patents and Applications

- A patent was filed on “Magnesiothermic SOM process for metal production from its oxides”. This would cover metals and alloys of Ti, Al, Ta, Mg, etc.
- U.S. Provisional Application No. 60/699,986, Title: Stability of Zirconia Based Inert Anodes for the SOM Process, Filed: July 15, 2005, Inventors: Uday B. Pal, Xionggang Lu, and Ajay Krishnan all of Boston University
- U.S. Provisional Application No. 60/699,970, Filed: July 15, 2005, Title: Oxygen-Producing Inert Anodes for SOM Process, Inventor: Uday B. Pal of Boston University. BU has since filed a PCT application PCT/US06/027255 on 7/14/06

8 Publications/Presentations:

1. A.W. McClaine, S.H. Tullmann, and K. Brown, “Chemical Hydride Slurry for Hydrogen Production and Storage”, Kickoff meeting with DOE Headquarters personnel, Washington D.C., 6 January 2004
2. A.W. McClaine, S.H. Tullmann, and K. Brown, “Chemical Hydride Slurry for Hydrogen Production and Storage”, DOE FreedomCAR - Hydrogen Storage Tech Team Annual Review, Detroit, MI, 19 February 2004
3. Andrew W. McClaine, “Chemical Hydride Slurry for Hydrogen Production and Storage”, 2004 DOE Hydrogen, Fuel Cells & Infrastructure Technologies Program Review, Philadelphia, PA, 25 May 2004
4. Andrew W. McClaine, Safety Discussion, prepared for the 2004 DOE Hydrogen, Fuel Cells & Infrastructure Technologies Program Review, Philadelphia, PA, 25 May 2004
5. Kenneth Brown, “Chemical Hydride Slurry for Hydrogen Storage”, presented at the “Hydrogen Generation & Storage Systems session” of the Hydrogen and Fuel Cells Summit, Worchester Polytechnic Institute, October 20, 2004.
6. Andrew W. McClaine, “Chemical Hydride Slurry for Transportation Applications” presented at the "Transportation Applications and Challenges Session” of the Hydrogen and Fuel Cells Summit, Worchester Polytechnic Institute, October 20, 2004.
7. Ajay Krishnan, Xionggang Lu, Srikanth Gopalan, Uday B Pal, of Boston University, and Andrew W McClaine of Safe Hydrogen, LLC, “Magnesium-Hydride Slurry Technology for Hydrogen Storage”, Presentation at the Materials Research Society Fall Meeting, Boston, MA, 29 November-3 December 2004
8. Robert R. Odle of Metallurgical Viability, Inc., Andrew W. McClaine of Safe Hydrogen, LLC, and Jens Frederiksen of PF&U Mineral Development ApS, “Economic Analysis of the Carbothermal Production of Magnesium”, TMS2005 134th TMS Annual Meeting Magnesium Technology 2005, San Francisco, CA, February 13-17, 2005
9. Ajay Krishnan, X. Lu, and U.B. Pal of Boston University Manufacturing Engineering Department, “Solid Oxide Membrane (SOM) for Cost Effective and Environmentally Sound Production of Magnesium Directly from Magnesium Oxide”, TMS2005 134th TMS Annual Meeting Magnesium Technology 2005, San Francisco, CA, February 13-17, 2005
10. A.W. McClaine, S.H. Tullmann, and K. Brown, “Chemical Hydride Slurry for Hydrogen Production and Storage”, Presented by K. Brown, DOE FreedomCAR - Hydrogen Storage Tech Team Annual Review, Houston, TX, 24 February 2005
11. Andrew W. McClaine, “Chemical Hydride Slurry for Hydrogen Production and Storage”, 2005 DOE Hydrogen, Fuel Cells & Infrastructure Technologies Program Review, Arlington, VA, 24 May 2005
12. A. Krishnan, U. B. Pal and X. G. Lu, “Solid Oxide Membrane Process for Magnesium Production Directly from Magnesium Oxide” in Metallurgical Transactions B, Volume 36B, pp. 463-473, August 2005

13. Andrew W. McClaine, “Chemical Hydride Slurry for Hydrogen Production and Storage”, DOE Hydrogen Production and Distribution Tech Team Annual Review, Alexandria, VA, 24 August 2005
14. A. Krishnan, “Solid Oxide Membrane Process for the Direct Reduction of Magnesium from Magnesium Oxide”, Ph.D. dissertation for Boston University, September 2005.
15. Sigmar H. Tullmann, “Chemical Hydride Slurry for Hydrogen Distribution and Storage”, AltWheels Conference, Larz Anderson Auto Museum, Brookline, MA 17-18 September 2005
16. Andrew W. McClaine, “Chemical Hydride Slurry for Hydrogen Production and Storage”, Chemical Hydrogen Storage Systems Analysis Meeting, Argonne National Laboratory, October 12, 2005
17. Uday B. Pal and Srikanth Gopalan of Boston University, “Clean Energy Research a Boston University”, Clean Energy Conference, Boston, 8 November 2005
18. Sigmar Tullmann, “Hydrogen Storage Breakthrough – The Safe Hydrogen Story”, Hydrogen and Fuel Cell Summit, Worchester Polytechnic Institute, 5 June 2006
19. Andrew W. McClaine, “Chemical Hydride Slurry for Hydrogen Production and Storage”, 2006 DOE Hydrogen, Fuel Cells & Infrastructure Technologies Program Review, Arlington, VA, 18 May 2006
20. Andrew W. McClaine, “Chemical Hydride Slurry for Hydrogen Production and Storage”, DOE Hydrogen Storage Tech Team Meeting, Detroit, MI, 22 June 2006
21. Kenneth Brown, “Materials for the Hydrogen Economy”, Presentation to the Summer School of University of Iceland, Reykjavik, June, 2006
22. Tullmann, Sigmar, “Enabling Hydrogen Energy”, Maine Hydrogen Center General Meeting, October 10, 2006, Brunswick, Maine
23. Uday B. Pal, Rachel DeLucas and Andrew McClaine, "Cost-Effective Magnesium Oxide Recycling and Economic Viability of Magnesium Hydride Slurry Technology for Hydrogen Storage", SOHN International Symposium on Advanced Processing of Metals and Materials: Principles, Technologies, and Industrial Practice, August 27-31, 2006, San Diego, CA
24. Uday Bhanu Pal, Rachel De Lucas, Guoshen Ye, and Marko Suput, "Magnesium Extraction from Magnesium Oxide Using SOM Process", SOHN International Symposium on Advanced Processing of Metals and Materials: Principles, Technologies, and Industrial Practice, August 27-31, 2006, San Diego, CA
25. Sigmar Tullmann, “Status of Hydrogen Fueled Vehicles”, Massachusetts Hydrogen Coalition and TIE joint meeting, January 10, 2007, Waltham, MA
26. Andrew W. McClaine, “Chemical Hydride Slurry for Hydrogen Production and Storage”, 2007 DOE Hydrogen, Fuel Cells & Infrastructure Technologies Program Review, Arlington, VA, 16 May 2007
27. Andrew W. McClaine, Kenneth Brown, “Chemical Hydride Slurry for Hydrogen Production and Storage”, presentation made to DOE Headquarters staff, Washington D.C., 3 August 2007

28. Adam C Powell IV, “Boundary Element Method (BEM) modeling of electrochemistry”, Materials Science and Technology 2007, COBO Center, Detroit, September 16-20, 2007.

9 Nomenclature

BEM - Boundary Element Method
BU – Boston University
DOE – Department of Energy
LLC – Limited Liability Company
g/L – grams per liter of volume
H2A framework – cost calculation framework developed by DOE H2A analysis group
H_2 – hydrogen
H_2O – water
kg – kilogram
kWhr – kilowatt hour
kWhr/kg – kilowatt hour per kilogram
kWhr/L – kilowatt hour per liter
L – Liter
LSM – Lanthanum Strontium Manganese Oxides (La(Sr)MnO3)
MgH2 – magnesium hydride
Mg(OH)2 – magnesium hydroxide
NBC – Nozzle Based Carbothermic
MgO – magnesium oxide
sL – standard Liter (0°C, 1Atm)
SOM - Solid-oxide Oxygen-ion-conducting Membrane
%H2 – percent hydrogen

10 References

1. Forsythe, W.E, Smithsonian Physical Tables (9th Revised Edition), Kovel, Apr 16, 2003

2. http://en.wikipedia.org/wiki/Abundance_of_elements_in_Earth's_crust

3. http://www.webelements.com/periodicity/abundance_seawater/

4. More Solutions to Sticky Problems, A Guide to Getting More from Your Brookfield Viscometer, Brookfield Engineering Laboratories, Inc.

5. Gasification – Versatile Solutions, Overview of Gasification Technologies, By Gary J. Stiegel, Technology Manager – Gasification, National Energy Technology Laboratory, US Department of Energy, Presented at the Global Climate and Energy Project Advanced Coal Workshop, March 15, 2005

6. CO_2 Reduction by Oxy-Fuel Combustion: Economics and Opportunities, by H. Sho Kobayashi, and Bart Van Hassel of Praxair, Inc., Presented at the GCEP Advanced Coal Workshop, Provo, Utah, March 15, 2005

7. Hydrogen Delivery Component Model prepared by researchers at National Renewable Energy Laboratory, Golden, CO. Electric Power Monthly, February 2005, Energy Information Administration, Office of Coal, Nuclear, Electric and Alternative Fuels, U.S. Department of Energy, Washing DC 20585. Available at: http://www.eia.doe.gov/cneaf/electricity/epm/epm_sum.html. Also private communications with Matthew Ringer of NREL.

8. The Annual Energy Outlook 2005 (AEO2005) prepared by the Energy Information Administration (EIA), National Energy Information Center, EI_30, Forrestal Building, Washington, DC 20585.

9. Weaver, Kevan D., Interim Status Report on the Design of the Gas-Cooled Fast Reactor (GFR), INEEL/EXT-05-02662, January 31, 2005, http://gen-iv.ne.doe.gov/documents/Interim Status Report for GFR (1-31-05).pdf page 6

10. Thermochemical Production of Hydrogen, http://www.ne.doe.gov/hydrogen/thermochemical.pdf

11. Status of the GT-MHR for Electricity Production, M.P. LaBar, A.S. Shenoy, W.A. Simon, And E.M. Campbell, World Nuclear Association Annual Symposium, London, 3-5 September 2003

12. Nuclear Energy Research Initiative 2004 Annual Report, Office of Nuclear Energy , Department of Energy, http://neri.ne.doe.gov/NERI2004AnnualReport_FINAL.pdf

13. Internet based prospectus for the Magnesium Alloy Corporation project planned for the Republic of Congo: http://www.magnesiumalloy.ca/project

14. Elkins, D.A., P.L. Placek, and K.C. Dean, An Economic and Technical Evaluation of Magnesium Production Methods (In Three Parts) 2. Carbothermic, United States Department of the Interior, Bureau of Mines, Bureau of Mines Report of Investigations RI 6946, May 1967, copy located at the Texas College of Arts & Industry Government Documents Depository, Kingsville, Texas [23 U43 6946]

15. Energy Information Administration/ Petroleum Supply Annual 2002, Volume 1, page 17, Table S4. Finished Motor Gasoline Supply and Disposition, 1986 – Present. This can be found in file “volume1_all-Pet Supply Annual 2003.pdf” at http://www.eia.doe.gov/oil_gas/petroleum/info_glance/gasoline.html

16 Source: Energy Information Administration/ Petroleum Supply Annual 2002, Volume 1, page 17, Table S4. Finished Motor Gasoline Supply and Disposition, 1986 – Present. volume1_all-Pet Supply Annual 2003.pdf. http://www.eia.doe.gov/oil_gas/petroleum/info_glance/gasoline.html

17 Energy Information Administration Annual Energy Review 2003, From file sec8.pdf.

18 Energy Information Administration, Form EIA-860, "Annual Electric Generator Report."

19 Interim Status Report for GFR (1-31-05).pdf describes Gen IV nuclear generators. Base design is expected to produce electricity at 42% efficiency. Alternate design is expected to have an efficiency of 45%.

20 NERI2004AnnualReport_FINAL.pdf discusses the costs of nuclear produced hydrogen. Page 61 notes a cost of 1.35/kg and $1.65/kg for sales of H_2 and O_2 vs H_2 only.

21 Status of the GT-MHR for Electricity Production, M.P. LaBar, A.S. Shenoy, W.A. Simon, And E.M. Campbell, World Nuclear Association Annual Symposium, London, 3-5 September 2003, labar.pdf

22. http://www.euromonitor.com/Gasoline_Station_Retailing_in_United_States

23. Kevan D. Weaver, “Interim Status Report on the Design of the Gas-Cooled Fast Reactor (GFR)”, INEEL/EXT-05-02662, 1 January 2005

23. M. P. LaBar, A. S. Shenoy, W. A. Simon and E. M. Campbell, “Status of the GT-MHR for Electricity Production”, World Nuclear Association Annual Symposium, 3-5 September 2003, London

11 Appendixes

11.1 Statement of Objectives

Statement of Objectives

Safe Hydrogen, LLC

Chemical Hydride Slurry for Hydrogen Production and Storage

Project Objectives and Goals for Year 1

The objectives of the first year of effort will be to

- Develop magnesium hydride slurry
- Improve the design and operation of the slurry/water mixing system
- Produce magnesium hydride from magnesium powder and hydrogen
- Perform process and economic analyses of four magnesium production methods
- Perform an experimental analysis of the SOM process at a 100 gm/day scale

Project Objectives and Goals for Year 2

The objectives of the second year of effort will be to

- Continue the development of magnesium hydride slurry
- Complete the design of an improved mixing system
- Test the slurry and mixer for stability, efficiency, and hydrogen purity
- Improve the continuous recycling of mineral oil and dispersant from the spent slurry
- Demonstrate stability of magnesium hydride slurry and quality of hydrogen from system
- Design and fabricate a 1-5 kg/day experimental apparatus for the SOM process

Project Objectives and Goals for Year 3

The objectives of the third year of effort will be to:

- Complete the development of magnesium hydride slurry
- Improve the slurry and mixer
- Demonstrate continuous recycling of mineral oil and dispersant from the spent slurry
- Improve the process for making magnesium hydride
- Test a 1-5 kg/day experimental apparatus for the SOM Process
- Update the economic analyses and identify opportunities for process cost reductions

Task Descriptions

Task 1 – Development of MgH_2 slurry using techniques developed for LiH slurry – Years 1, 2, and 3

The purpose of this task is to develop chemical hydride slurry based on magnesium hydride. This task will begin with a study to define the critical issues affecting the feasibility of MgH_2 slurry (ie. agglomeration of particles, hydroxide shells around hydride particles, options for assuring adequate reaction of the MgH_2). A slurry

production apparatus will be built and the slurry properties will be monitored and improved during the development effort. Slurry compositions will be evaluated and tested to achieve the same or better slurry stability as previously demonstrated with lithium hydride slurry. At the conclusion of the development effort, a design for an early commercial slurry production facility will be prepared.

Milestones

- Definition of critical issues affecting feasibility
- Design and fabrication of Slurry Production Facility
- Complete testing for composition and stability
- Complete particle size reduction testing
- System Design for Early Commercial Application

Go/No Go Decision

- Based on slurry performance decide whether to modify project for new slurry approach or to stop

Task 2 - Development of slurry mixing system for production of hydrogen – Years 1 and 2

The objective of this task will be to improve the performance of the mixing system originally prepared for lithium hydride slurry and to extend its use for magnesium hydride slurry. Specific targets are to reduce the size of the system, to improve the handling of materials within the system, and to modify the system for use with magnesium hydride slurry. Starting with the existing mixing system, an experimental development effort will be carried out to test alternate mixing technologies and material handling techniques. Two mixer designs are planned for this task. The first design will take advantage of the results of the initial experiments. The second design will improve upon the first for robustness and reliability. This task will be performed over two years. During the first year, testing of the model #3 mixing system will be completed.

Milestones

- Evaluation and selection of alternate mixing systems for tests
- Design and fabrication of model #3 mixing system complete with controls and materials handling apparatus
- Testing of model #3 mixing system to define performance capabilities and limitations
- Design and fabrication of model #4 mixing system complete with controls and materials handling apparatus incorporating more compact design
- Testing of model #4 mixing system to define performance capabilities and limitations

Go/No Go Decision

- Based on mixer performance decide whether to modify project for new mixer approach, improve existing approach, or to accept performance already demonstrated

Task 3 – Slurry and Mixer Testing – Years 2 and 3
An important issue related to the use of chemical hydride slurry is to prove its ability to supply hydrogen to fuel cells. This task will be focused on the testing of a MgH_2 slurry hydrogen storage system to measure purity of H_2, stability of the slurry, and performance of the slurry/mixer system over time. Slurry stability of at least one month is desired. The results of these tests will guide further development effort and testing to be performed on the slurry and mixer. Examples of further testing will be the use of impurities in the water supply, freeze protection, and on-board vs off-board applications.

Milestones
- Testing of hydrogen from Safe Hydrogen fuel for contaminants that might harm the fuel cell
- Testing of long term slurry stability by measuring H_2 output and purity after 1 month

Go/No Go Decision
- Based on slurry and mixer performance decide whether to modify project for new slurry or mixer approach, improve existing approach, or to stop program

Task 4 – Recycle Slurry Organics – Years 2 and 3
The first step in the recycle process is the separation of the organics contained in the spent slurry. Experiments have indicated that a solvent refining process can be used to recover the organics without damage to the oil or dispersant. A laboratory scale process will be designed, fabricated, and tested to demonstrate this process on a continuous basis. Upon successful completion of this testing, a design will be prepared for an early commercial stage process. Capital costs and operating costs will be estimated for this design. During Year 2, the first laboratory scale process will be developed. This system will be refined and an early commercial scale design will be prepared in Year 3.

Milestones
- Design of laboratory scale process
- Test of laboratory scale process
- Modified design of laboratory scale process
- Test of modified apparatus
- Design of early commercial process with capital and operating costs

Go/No Go Decision
- Based on recycle performance decide whether to modify design for new recycle approach, or improve existing approach, or decide development is complete

Task 5 – Produce Magnesium Hydride from Magnesium and Hydrogen –Years 1 and 3
Once the magnesium has been reduced from the magnesium hydroxide byproduct, it will be necessary to produce magnesium hydride. The early commercial production of

slurry may use purchased magnesium and hydrogen to make magnesium hydride for the slurry until the production needs of the process become large enough to warrant the investment in a magnesium reduction plant. The objective of this task will be to demonstrate the process that will be needed to produce magnesium hydride from magnesium and hydrogen. A laboratory scale process will be prepared and tested. The final design of this equipment will be used to produce an early commercial scale design. Capital and operating costs will be estimated from this design. During Year 1, a laboratory scale device will be tested. During Year 3, this device will be modified, tested, and a design for an early commercial device will be prepared.

Milestones

- Design of laboratory scale process
- Test results from the process
- Design of improved process
- Test results of process
- Design of early commercial process including capital and operation costs

Go/No Go Decision

- Based on hydriding system performance decide whether to modify design for new approach, or improve existing approach, or decide development is complete

Task 6 – Preliminary Designs and Economic Evaluations of $Mg(OH)_2$ Reduction Processes –Year 1 and 3

To achieve low cost hydrogen, the byproduct hydroxide from the hydrolysis process must be recycled. Recycling reduces the cost by reusing the metals used in the production of the hydrides. Several methods of recycling have been identified. Both lithium and magnesium are currently produced by melting lithium chloride or magnesium chloride and electrolytically separating the metal from the chlorine. Chlorine gas produced in the electrolysis is used to make hydrochloric acid, which in turn is used to make lithium chloride and magnesium chloride from lithium hydroxide and magnesium hydroxide.

Three alternate processes have been identified that promise significant cost reductions in the production of magnesium and lithium. Two are carbothermic reduction processes and the third is a new technology using a solid-oxide-oxygen-ion-conducting membrane (SOM) technology.

We intend to evaluate these processes for their potential cost reduction capability. This evaluation will include experimental development at the laboratory scale, design analysis at a production scale, and an economic evaluation of the cost of hydrogen resulting from each process. Information will be collected to perform a similar design and analysis of an electrochemical process so that the cost comparisons of the systems can be made.

Separation of the metal hydroxide from the oil/dispersant/water of the byproduct of the hydrolysis reaction will be a common part of each system design. Similarly, the production of hydride slurry from the reduced metal will be a common part of each design.

Milestones

- Preparation of process flow diagrams for each of the processes
- Mass and energy balances for each of the processes
- Selection of process equipment
- Price quotes for process equipment
- Estimate of operating costs for each process
- Economic evaluation of process economics

Go/No Go Decision

- Based on results of the study, decide whether MgH_2 process continues to look attractive enough to proceed with the project and if so which of the carbothermic systems to perform in Tasks 9 and 10 (No-Go, see Task 9 and 10)

Task 7 – Experimental Evaluation of the SOM Process – 100 gm/day – Years 1, 2, and 3

The SOM process offers significant reduction in the capital and operating costs of reducing magnesium. An experimental evaluation will be performed at a 100 gm/day scale. The results of this evaluation will be used to design a 1-5 kg/day scale experiment. The results will also be used to update the process and economic analyses prepared in Task 6.

Milestones

Boston University

- Fabrication of 100 gm/day reduction system
- Test of 100 gm/day reduction system

Go/No Go Decision

- Based on system performance decide whether to modify design for new reduction approach, or improve existing approach, or decide current development is sufficient

Tasks 8 – Experimental Evaluation of the SOM Process – 1-5 kg/day – Years 2 and 3

To better understand the process a 1-5 kg/day scale experiment will be fabricated and tested. The results of this experiment will be used to update the process and economic analyses prepared in Task 6. The design and fabrication will take place with some shakedown testing and later, additional testing will be performed and the economic analysis will be updated.

Milestones

- Design of process
- Fabrication of process
- Test results

Go/No Go Decision

- Based on test results, decide whether to continue testing or end task

Task 9 – Experimental Evaluation of the Carbothermic Process – 100 gm/day – Years 2 and 3

- Task removed from original SOO due to redirection in project based on economics study and recognition that similar development is taking place elsewhere

Task 10 – Experimental Evaluation of the Carbothermic Process – 1-5 kg/day – Year 3

- Task removed from original SOO due to redirection in project based on economics study and recognition that similar development is taking place elsewhere

Task 11 – Recycling Cost Reduction Evaluation – Year 3

The objective of this task is to evaluate methods of reducing the cost of recycling. Based on the results of the preceding tasks, an evaluation will be performed to identify cost reduction opportunities yet to be investigated. These opportunities will be ranked according to their affect on their cost saving potential in the recycling process.

Milestones

- Report on cost saving opportunities

Task 12 – Program Management and Reporting – Years 1, 2, and 3

The objective of this task is to manage the performance of the agreement as well as to prepare required reports. Quarterly reports will be prepared. Presentations will be prepared and presented at the DOE Annual Program Peer Review, and the annual USCAR review.

11.2 Nozzle Based Carbothermic Magnesium Process by Robert Odle PhD, Metallurgical Viability

Metallurgical Viability, Inc.

100 WEDGEMONT DRIVE
ELKTON, MD 21921
443-616-4339

Economics and Viability of the Nozzle Based Carbo-thermal (NBC) Magnesium Process

By Robert R. Odle, Ph.D.
Metallurgical Viability, Inc.
For
Andrew McClaine
Safe Hydrogen, LLC
March 2007

ABSTRACT

The carbothermal magnesium process for making magnesium has been known as a viable means of making magnesium for four decades. In this process a magnesium oxide is heated with a carbon source to produce magnesium gas and carbon monoxide according to this reaction:

$MgO + C \rightarrow Mg(g) + CO(g)$ Reaction #1

Magnesium Technology Limited (MTL) has a patented technology in which a Lavalle nozzle is used to cool the gases in a few fractions of a millisecond to condense the magnesium and separate it from the CO before the back reaction can occur. This nozzle-based carbothermal magnesium (NBC Mg) process has been demonstrated on a bench-scale where a few grams of metal were made. A furnace to demonstrate the process at the 1 kg/hour rate is currently under design by BAM, Inc. in Knoxville, TN. Techno-economic modeling has shown that the cost of producing a pound of magnesium by the nozzle-based carbothermal magnesium process could be as low as $0.30 a pound when the magnesium plant is part of an energy complex (Minimizing the Cost of Making Magnesium) with electric costs of $0.02 per kwh. Such technology could revolutionize the magnesium industry and contribute significantly to making magnesium hydride a low cost alternative for using hydrogen in automotive transportation.

A detailed capital cost estimate has been carried out for a production plant using the NBC Mg process. The estimate was incorporated into the techno-economic model. The model allows the user to select the Design Criteria for the project under consideration, including the plant capacity. The model then carries out a material and energy balance and estimates the income statement for the process and the capital costs. The model allows the optimization of the total cost of making magnesium including amortization of the facility. Amortization cost is on the order of $0.10 per pound of magnesium for a 90,000 mtpy plant.

PART 1. PRIOR DEVELOPMENT OF THE CARBO-THERMAL MAGNESIUM PROCESS

Introduction

The carbothermal method of producing magnesium has always promised to

be a low cost method of making magnesium. In concept, the process is very simple: 1) react carbon and a magnesium oxide mineral together at an elevated temperature to produce magnesium gas and carbon monoxide, then 2) cool the gases rapidly and collect the magnesium. The first step has been done and can be accomplished by those skilled in high temperature metallurgical furnaces, such as electric arc furnaces used in the steel industry. A recent patent by Engell, et al, U.S. Patent No. 5,803,947 in September 8, 1998 defines a process in which the gases from the carbothermal process are cooled rapidly by passing through a lavalle nozzle. Very high conversion rates to magnesium metal were observed in bench scale demonstrations of the process by Mineral Development International A/S (MDI), Birkerod, DK. The experimental results referred to in this report were carried out by MDI.

The methodology used by major engineering firms to evaluate new technology has been incorporated into a techno-economic model. This model has been used to bring together the design criteria, process flow diagrams, material and energy balances, and the income statement into a single format to evaluate the viability of the proposed NBC Mg Process.

In the industrialized "western" world, the majority of magnesium is currently produced by electrolytic refining of magnesium from a molten salt bath containing a significant portion of magnesium chloride. These electrolytic cells are fed with anhydrous magnesium chloride, which requires a capital-intensive process to produce a grade that will operate efficiently in modern cells. This technology also requires the handling of chlorine gas.

In recent years, a significant amount of magnesium is produced by metallo-thermic reduction of calcined dolomite. Alloys and carbides of aluminum, calcium, and silicon are good reductants of magnesium oxides and magnesium silicates. Ferro-silicon is used extensively in China, the world's largest producer. These reactions have one inherent advantage over the carbo-thermal reduction route in that only magnesium vapor (no carbon monoxide) is produced. Their inherent disadvantages are that (1) all of these reductants are expensive, (2) as batch processes under vacuum they are labor intensive, and (3) the metal is collected as a mixture of fine crystals and powder for subsequent processing into metal.

For a historical perspective, a carbothermal reduction process was operated in Permanente, USA in the late 1940's. An arc furnace was used to carry out the main reactions and large quantities of natural gas were used to quench the magnesium and carbon monoxide to reduce the back reaction. The cooling method employed frequently produced pyrophoric magnesium particles. Plants were also operated in Swansea, Wales and Konan, Korea

based on a similar approach by Austro-American Magnesite Corporation. Because of the production of pyrophoric magnesium and the difficulty of suppressing the back reaction, the carbothermal process, in any form, is not currently used for the production of magnesium.

NBC Magnesium Production

In the NBC Mg Process, a mixture of coke and magnesia, or magnesium silicate, or any other oxide based magnesium ore, is fed into the hot zone of an air-tight furnace and heated to above 1500^{O}C, typically in the range of 1800^{O}C. The carbon reacts with the magnesium oxide to produce magnesium metal and carbon monoxide in a highly endothermic reaction, see Reaction #1.

Electric arc, or submerged arc furnaces traditionally furnish this heat, but, induction furnaces, plasma arc or any other convenient means may be used. To recover the magnesium metal from this gas mixture, the gas mixture has traditionally been cooled as rapidly as possible below the freezing point of magnesium to avoid a reversal of the reaction. Past uses of carbothermal technology have never been able to cool the gases rapidly enough to avoid significant losses of magnesium by reversion to magnesia. Most approaches have involved mixing the Mg/CO mixture with large quantities of inert gases such as nitrogen or reducing gases such as methane. Such techniques depend on forming an intimate mixture of the diluting gas quickly and the transfer of heat to those gases, not a trivial task.

The new technology provides near instantaneous cooling of the gas by an adiabatic expansion of the gas through a lavalle nozzle. In prior technology, the cooled magnesium is dispersed and must be collected over a correspondingly large surface area. With the current technology, condensation is focused near the exit of the lavalle nozzle that should facilitate its collection on a cold surface or perhaps in or on a bath of liquid magnesium or fused salts. The carbon monoxide must be removed from the collection area via a vacuum, possibly maintained by steam ejectors.

A well-known phenomenon is that if a constriction is placed in a closed channel carrying a stream of fluid, there will be an increase in velocity, and an increase in kinetic energy at the point of constriction. From energy balance considerations, there must also be a reduction in pressure. If the fluid is a gas, there is a subsequent expansion and cooling of the gas after the nozzle corresponding to the pressure drop. If the pressure difference over the nozzle becomes higher than a threshold value, the gas flow through the nozzle changes from sonic to supersonic. With a given gas

composition, the amount of gas passing through the nozzle depends on the cross sectional area of the constriction and the pressure differential across the nozzle.

The pressure upstream of the nozzle is set by the vapor pressure of the magnesium and carbon monoxide, which in turn is set primarily by the temperature maintained in the reaction zone in the furnace, which in turn, is maintained by the heat input rate into the charge. The temperature of gas downstream of any given nozzle is proportional to the initial temperature of the gas and the pressure differential across the nozzle.

In the jet age, the physical chemistry and thermodynamics of how gases are cooled by adiabatic expansion through a nozzle is well understood and commonly observed.

Bench Scale Results

The nozzle was demonstrated at a rate of magnesium metal production up to a rate of 0.116 gram/min through a lavalle nozzle with a throat area of 10.18 mm^2. Forsterite, a relatively pure form of magnesium silicate ore, was used in these tests.

Aside from the desired reaction in the reaction chamber of producing Mg (v) and CO (Reaction #1), there are several other potential side reactions. If a silica or silicate is present in the magnesium feedstock, it will also react with the carbon in the bed to produce SiO according to Reaction #2 below. This reaction is more significant the higher the temperature.

$SiO2 + C \rightarrow SiO + CO$ Reaction #2

SiO gas is also evolved in the reaction chamber along with magnesium and carbon monoxide vapors. With the reaction chamber at 1500^oC, if SiO was allowed to proceed in the gas phase to the lavalle nozzle, about 1 to 3% silicon was reported to the magnesium metal. Therefore, a condenser was placed down stream from the reactor operating at 1300^oC, a lower temperature than the reaction zone. This condenser is a carbon source that converts the SiO produced to SiC according to this reaction:

$SiO + C \rightarrow SiC + CO$ Reaction #3

A potential negative effect of this condenser is that the lower temperature shifts the equilibrium for Reaction #1 slightly to the left with the possible result that some MgO(s) may condense in the second condenser if conditions in the system are not well controlled. The extent of this back

reaction can be approximated from thermodynamics. Therefore, for optimum results, the condenser must be operated above a temperature at which significant reversal of Reaction #1 will occur. Their subsequent experimental results lend support to the accuracy of their theoretical model.

Finally, there is the reaction of metals in the feedstock with carbon to produce elemental metals according to the general reaction:

$Me_XO_Y + y\ C \rightarrow x\ Me + y\ CO$ Reaction #4

Where Me can be iron, copper, nickel, phosphorus, sodium, lead, etc. Small iron droplets form and remain in the charge and contain most of the less volatile elements like nickel and copper while the vapor phase will contain all or part of the more volatile elements like zinc, lead, phosphorus, and sodium. In fact, much of the silica may also react to produce some silicon that will be dissolved in the iron droplets. Similar reactions occur in all metallothermic systems for magnesium production. The composition of the feedstock must be controlled for these volatile elements to control the quality of the magnesium metal produced.

Experimental Results with SiO Condenser in Place:

Eleven experiments were carried out with an improved bench scale reactor that included a condenser for SiO. Temperature of the reactor was varied between about 1260 to 1550oC. A nozzle with a 10.18 mm2 diameter nozzle was used, which processed about 90 to 285 grams of feed in a period ranging from about 100 to 400 minutes.

In the best test in the bench scale reactor, more than 99% of the total magnesium content of the charge was recovered as magnesium metal. In five other runs the recovery was between about 70 and 80%. These results indicate that the process is technically viable when careful attention is paid to excluding leaks from the system, a task somewhat easier in larger systems. Further, the work demonstrates the value of the lavalle nozzle for rapid cooling of magnesium and carbon monoxide to produce magnesium metal.

Quality of the Metal Produced

The bench scale reactor with the condenser produced magnesium metal with the following average impurities:

Table 1.
Impurities in the Magnesium (ppm)
Produced in the Bench Scale Reactor

Al 110	Ca 21	Zn 35	P 15
Mn 77	Na 150	Si 80*	Fe 15
K 240	Ni <5		

*Results for Si only shown for one run.

This analysis classifies the metal as meeting 9980A ASTM B92M-83 but not 9990A or higher; secondary refining may further improve metal quality. As important, on the runs with high metal yields skeletal growth of cm-sized whiskers was observed. These whiskers were not pyrophoric. The condenser appeared to remove most of the SiO from the gas phase and reduce the concentration of silicon in the magnesium. However, results for Si are only shown for one sample of metal in the report. Melting of this metal would get rid of most of the alkali metals. Iron is removable by conventional settling near the melting point.

SAFE HYDROGEN

Safe Hydrogen, Inc. is studying the feasibility of using magnesium hydride, MgH2, as a means of distributing hydrogen, primarily in the transportation sector. MgH2 in an oil slurry is reacted with water inside of an automobile to produce hydrogen, via the equation below, which is then used to power the vehicle via an internal combustion engine.

MgH2 + 2H2O --> Mg(OH)2 + 2H2 Reaction #5

The magnesium hydroxide (Mg(OH)2) produced by this reaction is returned in an oil-water slurry for reprocessing back to magnesium metal. Safe Hydrogen employs a solvent extraction process to remove most of the oil and leaving a moist, high purity magnesium hydroxide for recycling back to magnesium metal. The chemical hydride slurry has the potential of generating twice as much volume of hydrogen as a similar volume of cryogenically cooled liquid hydrogen. Liquid hydrogen is a proven method of storing hydrogen, but it takes substantial energy to liquefy the hydrogen and there is continual "boil off" of hydrogen during storage. Slurry, on the other hand, is stored at normal temperature and normal pressure.

A major cost advantage of this technology is based on the characteristics of the slurry. The slurry is a non-explosive, non-corrosive, environmentally safe, pumpable "hydrogen fuel". Slurry can be stored, transported, and pumped with existing tanks, pumps and pipelines and can therefore distribute hydrogen to the market utilizing the existing fossil fuel infrastructure. The only difference from current fuel delivery systems is that the delivery devices such as trucks or rail tankers don't return empty. They are fully loaded in both directions. They return from delivery runs, loaded with depleted slurry for recycling.

Since virtually all the magnesium would be recycled, the cost of the magnesium hydroxide that would be fed into the carbo-thermal magnesium process would only be the cost of makeup magnesium feedstock. A somewhat arbitrary cost of magnesium hydroxide was set at $2/tonne for the base case to reflect that most of the magnesium hydroxide produced by Reaction #5 would be recycled and only a nominal cost would be incurred from the inefficiencies in recycling. This affords a significant advantage, quantified subsequently, to the cost structure for the Safe Hydrogen approach compared to the normal approach where the entire feedstock has to be mined and shipped to the magnesium smelter.

The ultimate price of the Safe Hydrogen approach for delivering hydrogen economically will depend in part on the optimum placement of magnesium recycling centers near affordable power plants. In addition, a viable

system will require minimizing the transportation costs of moving the MgH2 slurry to the filling stations and the Mg(OH)2 slurry from the stations back to the magnesium recycling centers. Safe Hydrogen envisions that a mature system will be sized to use all the power from a large scale power plant thus operating the power plant as a base load plant and minimizing the distribution costs because the power plant will be part of the slurry recycling plant.

PART 2. OPERATING COSTS OF THE NOZZLE BASED CARBOTHERMAL MAGNESIUM PROCESS

TECHNO-ECONOMIC MODELING

The question arises, how would a modern carbothermal process that uses the lavalle nozzle compete with existing technology, specifically the Pidgeon Process as practiced by the Chinese. Based on prior pricing, one would expect a new process would be competitive if it could produce magnesium with operating costs in the $0.50 to $0.75 per pound range. At the low end of this range one would speculate that the Pidgeon Process could be supplanted, at the high end of this range the management of capital costs would become critical. Even lower costs have to be realized to make Safe Hydrogen's methodology for delivering hydrogen viable. The advantage Safe Hydrogen has in its approach are the lower costs possible with the economies of scale associated with very large facilities, which would be necessary with their vision.

A techno-economic model has been created that simulates all the unit operations of a magnesium facility. A complete material and energy balance is carried out for the magnesium facility based on the design criteria selected by the user of the model. This allows the model to be used for a variety of project conditions and it allows the identification of design criteria that are critical in keeping the operating costs for the facility to a minimum. The usefulness and flexibility of the model is illustrated herein by considering a project for Safe Hydrogen, Inc. With relatively small modifications, the model could be used for many other projects employing the nozzle-based carbothermal magnesium technology.

Design Criteria

The Design Criteria have been developed for the following key steps in carbothermal magnesium process:

- General
- Calcining
- Electric Arc Furnace
- Salt Box Furnace
- Ingot Casting

These are presented in Figure 1. The user can alter the "Selected Values" within the range of "Value Low" and "Value High". After making these selections and others the model is executed for these conditions to produce material and energy balances, economics, etc.

Design Criteria for the Techno-Economic Model

To execute the Techno-Economic Model or the Capital Cost Estimate, a Design Criteria must be selected. The Design Criteria impacts the material and energy balances, which impacts primarily the equipment sizes, but in some cases may also impacts operating conditions such as the temperature, and pressure, which, in the extreme, may further impact equipment costs. The Design Criteria selected for the Base Case is shown below.

Inputs

The MV Model allows the user to adjust the composition of the raw materials being fed into the process and assess the economic consequences of such changes, Figure 2A and 2B.

The user is allowed to alter the composition of the feedstock between the boundaries "Value Low" and "Value High" shown in the adjacent columns. The MV Model normalizes the analysis to 100%; this is a necessary condition to get 100% closure on the subsequent material balance. A cost for each of these raw materials will be set in worksheet called "Prices" for use in the economic analysis, as shown later.

The user of the model is also allowed to set the price of products, Figure 4, and the cost of raw materials, Figure 5.

MV Model: Carbothermal Production of Magnesium					Case Code
Modify Selected Then Press Enter Description	Value Base	Value Selected	Value Low	Value High	Units
General					
Mg Production	200,000	200,000	10,000	600,000	tonnes
Annual Operating Hours	7872.00	7872.00	6000	8,760	hr
.					.
Calcining					
Minimum Kiln Temperature	600.00	600.00	500	1,800	T C
Bag House Efficiency	99.00	99.00	95	100	%
Moisture in MgOH2	1.00	1.00	0.10	10	wt.%
Percent Dust	1.00	1.00	0.10	10	wt.%
Percent Excess Oxygen	5.00	5.00	1.00	20	%
Max Temp to Bags	200.00	200.00	105	300	T C
Coke Preheater					
Temperature of Coke Preheater	600.00	600.00	25	1,200	T C
Coke Bulk SG	2.10	2.30	1.5	4	none
.					
Modify Selected Then Press Enter Description	Value Base	Value Selected	Value Low	Value High	Units
Electric Arc Furnace					
Size of air leak, % of MgO feed	0.10	0.01	0.01	5	%
% Moisture in Coke	0.10	0.10	0.10	5	%
Target %CaO in Slag	40.00	40.00	10	80	%
Operating Temperature	1850.00	1850.00	1800	2,000	T C
Heat Loss to Surroundings	10.00	10.00	5	20	%
Power to Heat Efficiency	65.00	65.00	60.00	80	%
Electrode Consumption per tonne of Mg	5.00	5.00	1	10	kgs/tonne
Modify Selected Then Press Enter Description	Value Base	Value Selected	Value Low	Value High	Units
Ingot Casting					
SO2 Consumption	10.00	10.00	1	100	kgs/tonne
Caster capacity	10.00	10.00	1	100	mtph
Boiler					
Pressure	120.00	220.00	60	220	PSIG
Caustic Scrubber for Hot Gases					
Exit Temperature of Gas	60.00	60.00	35	80	T C
Efficiency	99.00	99.00	95	100	%
Caustic Conc	50.00	50.00	1	50	%
Precooler exit temperature	125.00	125.00	101	160	T C

Figure 1. Design Criteria for the Base Case, Part 1.

Modify Selected Then Press Enter Description	Value Base	Value Selected	Value Low	Value High	Units
Salt Box Furnace					
Pressure (abs)*	0.10	0.090	0.029999999	0.2	atm
Temperature	750.00	750.00	700	1,100	T C
Capture Efficiency	99.80	99.80	95	100	%
Salt Entrainment in Mg	0.50	0.50	0.100000001	10	%
Nozzle ID	0.20	0.20	0.01	1	meters
Nozzle Efficiency	99.00	99.00	80	100	%
%Salt Entrained in Gas Out	0.50	0.50	0.100000001	3	%
Max. Gas Velocity	20.00	20.00	1	100	meters/sec
Typical Heat Transfer Coeff.	122.00	122.00	50	200	kcal/M^2*hr*C
Length to Width Ratio	2.00	2.00	1	10	ratio
Salt Height	0.10	0.10	0.01	1	meters
Metal Melt Height	1.00	1.00	0.100000001	5	meters
Maximum Melt Capacity	200.00	200.00	50	500	tonnes
Residence Time	2.00	2.00	1	4	hrs
Program may reset Vacuum if Condensation Te					

Modify Selected Then Press Enter Description	Value Base	Value Selected	Value Low	Value High	Units
Cooling Tower					
Temperature (Dry bulb)	35.00	40.00	1	50	T C
Relative Humidity	50.00	60.00	10	95	%
Drift Loss %	0.00	0.01	0.001	1	%

Figure 2. Design Criteria for the Base Case, Part II

Given the user supplied information on Design Criteria, Raw Materials, Cost, Prices, etc., the model carries out a material and energy balance and produces an Income Statement. Since the model uses iterative techniques to establish steady state conditions, discussed later, a standalone subroutine (MB CK) checks the material balance for closure, Figure 5. The subroutine checks every element tracked in the process to verify that the same amount of each element enters and exits each unit operation. (Note, not all the elements are shown in the Figure included in this report.) It also tracks the total mass entering and leaving each unit operation. The current goal is to have the 99% closure for all elements for each unit operation. All the major elements, carbon, oxygen, magnesium, hydrogen, etc. are close to meeting this goal, some of the minor elements for example lead, phosphorus, zinc, etc. are not meeting this goal in some of the unit operations where their concentrations are very low. These are being addressed in the order that it impacts costs or product quality.

1/25/2005 6:50 AM

Carbothermal Magnesium Raw Material Analysis

Chg Sltd then Update Description	Value Base	Value Selected	Value Low	Value High	Units	Variable Name	Wt.
Mg(OH)2 from SH							
Mg(OH)2	97.87	**97.87**	80	99	Wt.%	MgOH_MgOH	97.868
C20H42	2.00	**2.0**	0.1	20	Wt.%	C20H42_MgOH	2.000
Al(OH)3	0.02	**0.02**	0.001	1	Wt.%	AlOH2_MgOH	0.020
Ca(OH)2	0.001	**0.001**	0.001	1	Wt.%	CaOH2_MgOH	0.001
Cu(OH)2	0.004	**0.004**	0.001	1	Wt.%	CuOH2_MgOH	0.004
Fe(OH)3	0.04	**0.04**	0.001	1	Wt.%	FeOH3_MgOH	0.040
Mn(OH)4	0.04	**0.04**	0.001	1	Wt.%	MnOH2_MgOH	0.035
Ni(OH)2	0.001	**0.001**	0.001	1	Wt.%	NiOH2_MgOH	0.001
P2O5	0.005	**0.005**	0.001	1	Wt.%	P2O5_MgOH	0.005
Pb(OH)2	0.005	**0.005**	0.001	1	Wt.%	PbOH2_MgOH	0.005
SiO2	0.01	**0.010**	0.001	1	Wt.%	SiO2_MgOH	0.010
Sn(OH)2	0.001	**0.001**	0.001	1	Wt.%	SnOH2_MgOH	0.001
Zn(OH)2	0.01	**0.010**	0.001	1	Wt.%	ZnOH2_MgOH	0.010
.							100.000
.							
Quick Lime							
CaO	90	**90.0**	80	99	dry wt.%	CaO_lime	92.393
Al2O3	1	**1.0**	0.1	10	dry wt.%	Al2O2_lime	1.027
CuO	0.01	**0.01**	0.01	2	dry wt.%	CuO_lime	0.010
Cr2O3	0.1	**0.1**	0.01	5	dry wt.%	Cr2O3_lime	0.103
Fe2O3	2	**2.0**	0.1	10	dry wt.%	Fe2O3_lime	2.053
PbO	0.1	**0.1**	0.1	2	dry wt.%	PbO_lime	0.103
MgO	1	**1.0**	0.1	20	dry wt.%	MgO_lime	1.027
NiO	0.1	**0.1**	0.01	2	dry wt.%	NiO_lime	0.103
SiO2	3	**3.0**	0.1	10	dry wt.%	SiO2_lime	3.080
ZnO	0.1	**0.1**	0.1	2	dry wt.%	ZnO_lime	0.103
.							100.000
.							
Salt for Collection Furnace							
MgCl2	17	**17.0**	5	50	dry wt.%	MgCl2_salt	17.000
CaCl2	25	**25.0**	5	50	dry wt.%	CaCl2_salt	25.000
MgF2	2	**2.0**	0.1	10	dry wt.%	MgF2_salt	2.000
NaCl	56	**56.0**	30	90	dry wt.%	NaCl_salt	56.000
.							100.000

Figure 3A. Raw Material Analysis

1/25/2005 6:50 AM

Carbothermal Magnesium
Raw Material Analysis

Chg Sltd then Update Description	Value Base	Value Selected	Value Low	Value High	Units	Variable Name	Wt.
Coke Analysis							
Carbon	92	**92.000**	85	96	%	C_coke	93.495
Chlorine	0.0005	**0.0005**	1E-04	0.005	%	Cl2_coke	0.001
Fluorine	0.1	**0.100**	0.01	1		F_coke	0.102
Hydrogen	2	**2.000**	0.5	5		H2_coke	2.033
Nitrogen	1	**1.000**	0.1	2		N2_coke	1.016
P2O5	0.1	**0.100**	0.01	1.00		P2O5_coke	0.102
Oxygen	0.1	**0.100**	0.01	1		O2_coke	0.102
Sulfur	0.1	**0.100**	0.01	5		S_coke	0.102
Ash	3	**3.000**	3	20		Ash_coke	3.049
.							100.000
.							
Ash_Composition							
SiO2	20	**20.0**	20	60	wt.%	SiO2_ash	21.978
Al2O3	20	20.0	10	35	wt.%	Al2O3_ash	21.978
Fe2O3	29	**29.0**	5	35	wt.%	Fe2O3_ash	31.868
CaO	10	**10.0**	1	20	wt.%	CaO_ash	10.989
MgO	3	**3.00**	0.3	4	wt.%	MgO_ash	3.297
TiO2	1	**1.0**	0.5	2.5	wt.%	TiO2_ash	1.099
Na2O	3	**3.0**	1	4	wt.%	Na2O_ash	3.297
K2O	2	**2.00**	1	4	wt.%	K2O_ash	2.198
SO3	3	**3.0**	0.1	12	wt.%	SO3_ash	3.297
.							100.000

Figure 3B Raw Material Feedstock

1/25/2005 9:13 PM

Carbothermal Magnesium

Sat

MV Model: Carbothermal Magnesium

File Updated Description	Value Base	Value Selected	Value Low	Value High	Units	Variable Name
PRICES/VALUES/LIABILITIES OF OUTPUTS						
Mg Ingots	$ 0.80	$ 0.80	$ 0.40	$ 1.30	$/lb	Mg_price
CO	$ 5.00	$ 5.00	$ 1.00	$ 10.00	$/MMBTU	CO_price
Slag	$ 5.00	$ 5.00	$ (20.00)	$ 20.00	$/tonne	Slag_value

Figure 4. Prices for Products

1/30/2005 9:28 PM | Carbothermal Magnesium | Safe Hydrogen, Inc.

MV Model: Carbothermal Magnesium

File Updated Description	Value Base	Value Selected	Value Low	Value High	Units	Variable Name
Cost of Raw Materials						
Caustic 50% solution	200.00	200.00	0.00	400.00	$/tonne	NaOH_cost
Worker Fully Loaded Cost Per Hour	26.00	26.00	10.00	50.00	$/hr	Labor_cost
Coke	50.00	50.00	20.00	200.00	$/tonne	Coke_cost
Electric Power	0.04	0.04	0.02	0.08	$/kWh	Power_cost
Fuel Oil	2.50	2.50	1.00	5.00	$/MMBTU	Fuel_cost
Limestone	30.00	40.00	10.00	100.00	$/tonne	Limestone_cost
Nitrogen	0.90	0.90	0.40	3.00	$/1000scf	N2_cost
Oxygen	0.06	0.06	0.01	0.12	$/NCM	O2_cost
H2 Gas	0.70	0.70	0.10	1.00	$/lb	H2_cost
Process Water	0.06	0.07	0.03	0.09	$/tonne	Water_cost
Sewer	0.12	0.12	0.06	0.24	$/tonne	Sewer_cost
Steam LP	10.00	10.00	3.00	15.00	$/tonne	Steam_cost
Cooling Water	7.00	7.00	4.00	90.00	$/1000 tonne	Cool_cost
Boiler Water	2.50	2.50	1.25	5.00	$/tonne	bwater_cost
DI Water	1.00	1.00	0.50	2.00	$/tonne	Diwater_cost
Waste Water	0.10	0.10	0.02	1.00	$/tonne	WWT_cost
Fluidization Costs	40.00	40.00	25.00	60.00	kWH/tonne	Fluidizing_cost
Slag	5.00	5.00	0.00	20.00	$/tonne	Slag_cost
Quick Lime	65.00	65.00	20.00	100.00	$/tonne	Lime_cost
Mg(OH)2 from SH	30.00	30.00	0.01	100.00	$/tonne	MgOH2_cost
Salt Mixture	50	50	10	200	$/tonne	Salt_cost
Methane	6	5	1	9	$/MMBTU	CH4_cost
Dross	10	10	-20	40	$/tonne	Dross_cost
Dust	20	20	0	100	$/tonne	Dust_cost
SO2	230	230	100	300	$/tonne	SO2_cost
Electrodes	250	250	100	1000	$/tonne	Electrode_cost

Figure 5. Cost of Raw Materials

Flowsheet Development

Three PFD's (process flow diagrams) for the base case were developed to describe the carbothermal magnesium process:

- Calcining Plant
- Magnesium Production Plant
- Utilities

The flowsheets underwent some evolution to minimize operating costs.

Calcining Plant

The calcining plant takes the magnesium hydroxide from Safe Hydrogen's oil/magnesium hydroxide separation plant and converts it into magnesium oxide in a rotary kiln, Figure 6. The magnesium oxide product will be conveyed to the "Magnesium Production Plant". The primary reaction in the kiln is to drive the water of hydration from the magnesium hydroxide, however, the oil left on the magnesium hydroxide from the previous step will be burnt acting as additional fuel.

The kiln uses carbon monoxide and purchased natural gas for fuel. The carbon monoxide is off-gas from the electric arc furnace and the coke pre-heater. The kiln receives the carbon monoxide that is left over from making the steam required for the vacuum ejectors. The balance of energy for the kiln is supplied by natural gas to reach the kiln temperature specified in the Design Criteria. Purchased oxygen is used to combust the fuel to allow the calcine to be preheated to very high temperatures.

Off-gases from the kiln will be run through a bag-house and then up a stack. A small amount of dust will be produced for disposal. This dust may be rich in volatile elements such as lead, and volatile compounds such as chlorides, and small particles of magnesium oxide entrained in the gas stream. The bulk of the dust is recycled, a small amount is bled off to control impurities.

There is also a coke pre-heater in this circuit. The coke is preheated by burning part of the coke to CO with oxygen. The model automatically burns enough coke to make adequate CO to make all the steam required for the vacuum steam ejectors in the Utility Plant.

1/25/2005 10:01 PM

Carbothermal Magnesium

Safe Hydrogen, Inc.

Unit Op	Date Run	Mass in	Mass out	%Acct	C In	C out	%Acct	Ca In	Ca out	%Acct	F In	F out	%Acct
Tri Kiln Feed	1/23/2005 19:54	150,718	150,718	100.0%	2,504	2,504	100.0%	1	1	100.0%	0	0	100.0%
74 into 59	1/23/2005 19:54	150,718	150,718	100.0%	2,504	2,504	100.0%	1	1	100.0%	0	0	100.0%
Calciner Part 1	1/23/2005 19:54	213,092	217,771	102.2%	17,463	17,463	100.0%	2	1	40.3%	0	0	1.2%
197 split to 195 and 7	1/23/2005 19:54	101,136	101,136	100.0%	0	0	100.0%	1	1	99.6%	0	0	100.0%
195+198=68	1/23/2005 19:54	117,646	117,646	100.0%	17,463	17,463	100.0%	0	0	100.0%	0	0	100.0%
Calciner Overall	1/23/2005 19:54	213,092	217,771	102.2%	17,463	17,463	100.0%	2	1	40.3%	0	0	1.2%
Baghouse	1/23/2005 19:54	117,646	117,646	100.0%	17,463	17,463	100.0%	0	0	99.1%	0	0	100.0%
Dust Recycle	1/23/2005 19:54	1,001	1,001	100.0%	0	0	100.0%	0	0	91.1%	0	0	99.9%
Coke Preheater	1/23/2005 19:54	41,281	41,281	100.0%	33,662	33,662	100.0%	0	0	100.0%	37	37	100.0%
Coke Preheater 2	1/23/2005 19:54	41,281	41,281	100.0%	33,662	33,662	100.0%	0	0	100.0%	37	37	100.0%
EA Furnace	1/23/2005 19:54	133,955	131,946	98.5%	30,262	30,224	99.9%	269	269	100.0%	37	0	0.0%
Salt Furnace	1/23/2005 19:54	133,118	133,386	100.2%	30,224	30,224	100.0%	172	172	100.0%	12	12	100.0%
Ingot Casting	1/23/2005 19:54	120,960	120,725	99.8%	0	0	100.0%	54	54	100.0%	4	4	100.0%
Ejectors	1/23/2005 19:54	221,623	221,610	100.0%	30,224	30,224	100.0%	118	118	100.0%	8	8	100.0%
Boiler Preheater	1/23/2005 19:54	209,705	209,705	100.0%	3,703	3,703	100.0%	0	0	100.0%	0	0	100.0%
Combust/Exhaust	1/23/2005 19:54	179,409	179,666	100.1%	19,221	19,221	100.0%	0	0	96.8%	0	0	99.4%
Boiler Water Feed Tan	1/23/2005 19:54	201,251	201,251	100.0%	0	0	103.3%	0	0	103.3%	0	0	100.6%
gascooler	1/23/2005 19:54	287,586	287,569	100.0%	33,927	33,927	100.0%	118	118	100.0%	8	8	100.0%
Scrubber Proper	1/23/2005 19:54	3,808,658	3,798,681	99.7%	33,927	33,927	100.0%	168	168	100.0%	11	11	100.0%
Scrub Tank	1/23/2005 19:54	11,736,974	11,737,280	100.0%	0	0	100.0%	167	167	100.0%	11	11	100.0%
Scrubber Overall	1/23/2005 19:54	8,511,650	8,501,862	99.9%	33,927	33,927	100.0%	118	118	100.0%	8	8	100.0%
Scrubber Proper	1/23/2005 19:54	85,799	85,799	100.0%	0	0	100.0%	0	0	100.0%	0	0	100.0%
Scrub Tank	1/23/2005 19:54	85,925	85,925	100.0%	0	0	100.0%	0	0	100.0%	0	0	100.7%
Scrubber Overall	1/23/2005 19:54	120,169	120,169	100.0%	0	0	100.0%	0	0	100.0%	0	0	100.0%
Compressor	1/23/2005 19:54	8,496,220	8,496,220	100.0%	33,927	33,927	100.0%	1	1	100.0%	0	0	100.0%
Calcining PFD	1/23/2005 19:54	253,483	258,153	101.8%	51,128	51,127	100.0%	2	1	40.1%	37	37	99.8%
Furnace PFD	1/23/2005 19:54	345,063	343,074	99.4%	30,262	30,224	99.9%	442	442	100.0%	48	12	24.3%
Utilities PFD	1/23/2005 19:54	8,967,937	8,713,301	97.2%	33,927	37,630	110.9%	118	118	100.0%	8	8	100.0%
Entire Process	1/23/2005 19:54	8,723,290	8,754,634	100.4%	36,722	40,386	110.0%	442	54	12.3%	12	4	31.4%

Figure 6. Checking Material Balance for Closure

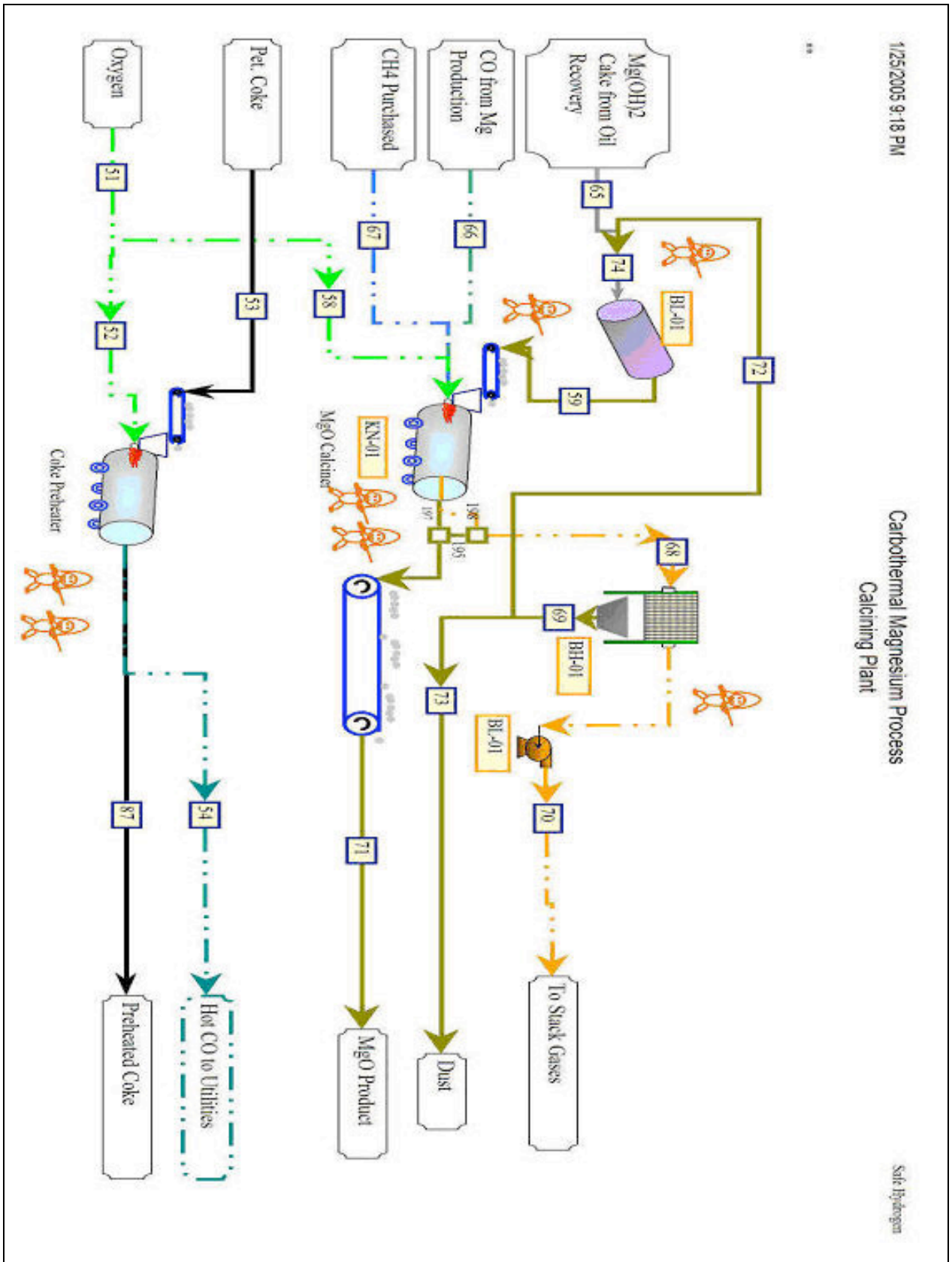

Figure 6. Calcining Plant

Magnesium Production Plant

In the Magnesium Production Plant, magnesium oxide is converted into magnesium ingots. There are three major pieces of equipment in this flowsheet, see Figure 7:

- Electric Arc Furnace
- Salt Box Collection Furnace
- Ingot Casting

A brief description of each and the assumptions used in the MV Model are outlined below.

The Electric Arc Furnace

The magnesium oxide is charged with fluxes and coke into an electric arc furnace, which is operated in excess of 1800oC. Magnesium vapors and carbon monoxide are produced and conveyed through refractory ducts to a bank of laval nozzles. The magnesium is pulled through the nozzles into a collection chamber by a vacuum on the exit side of the nozzles.

The primary reaction that occurs in the electric arc furnace is:

$$MgO(s) + C(s) \rightarrow Mg(v) + CO$$

This reaction is very endothermic and energy must be supplied by another source to make this reaction proceed. In an electric arc furnace, electric power is supplied through electrodes. In one type of furnace, a submerged arc furnace, the power is delivered by passing current through the slag utilizing its electrical resistance to produce IR heating. The exact type of furnace is not critical to modeling or cost estimation since their efficiencies are similar. The User enters a power factor that sets the efficiency in going from three phase AC power to the power delivered across the electrodes to the charge. The efficiency is on the order of 65%.

Additional heat can be brought into the furnace through sensible heat in the feedstock. For instance, the MgO and coke entering the furnace can be preheated substantially. In the current configuration of the model, the MgO enters the electric furnace hot, directly out of the calciner where it was heated to remove moisture, oils, and hydrates. The MV Model allows the user to select the temperature of this furnace and indirectly the amount of heat brought into the furnace with calcine.

The coke is also preheated, however, the temperature of the coke cannot be controlled by the user. Instead, the model controls the amount of coke burned to supply adequate fuel, CO, to the boilers in the utility circuit. The model calculates the amount of heat produced in burning part of the coke and carries out a heat balance to determine the temperature of the coke. Burning part of the coke results in a temporary shortage of coke to the electric furnace, however, the amount of incoming coke to the system is incremented upward on the next iteration of the model to meet the new demand.

Since the CO from the carbothermal reaction is burned to produce energy used in the process, there is some reduction in energy requirements for making magnesium. In preheating the calcine and coke before charging them to the furnace, thermal energy is substituted in part for the electrical energy used in the furnace.

A small amount of additional heat can also be saved by preheating the air entering the calciner with the exhaust gases from the calciner. This will be considered after the impact of energy on costs is evaluated. Currently, the hot CO gas from the coke preheater is used to preheat the water going into the boilers. The heat in the CO from the electric furnace is not recoverable since the temperature of this gas is dropped when it is expanded through the lavalle nozzles to recover the magnesium.

A small amount of inert slag will be produced since the original source of the magnesium in the circuit is high purity magnesium ingots that are converted to MgO in the production of hydrogen via MgH2 using SH's technology. The heat in the slag is lost when the slag is tapped periodically from the furnace. However, with the current source of feedstock, high purity MgO, very little slag is produced and the amount of heat lost is insignificant. The amount of heat to make magnesium should therefore approaches the theoretical requirements.

Salt Box Collection Furnace

The gases from the electric arc furnace leave the furnace through lavalle nozzles. Cooling of the magnesium and carbon monoxide mixture is accomplished by adiabatic expansion as the gases pass through the nozzle in the Salt Bath Furnace. The temperature in this chamber is controlled by the amount of adiabatic expansion. The temperature will be controlled within the range of between about 700oC (about 50 degrees above the melting point of magnesium) to about 1090oC (about the boiling point of magnesium).

The vacuum in the Salt Box Collection Furnace is maintained by steam ejectors. The steam ejectors must be physically separated from the furnace in a manner that assures that no water can find its way into the furnace and make contact with the magnesium. Commercial packages are available with

such designs. The injectors are located downstream from where the vacuum is required and connected by the appropriate ductwork. The steam ejectors are powered by steam that is produced in boilers that burn carbon monoxide, a by-product of the carbothermal reduction process.

Magnesium is pumped from the separation chamber to ingot casting machines. The liquid magnesium is covered with a sulfur dioxide/air mixture during casting to prevent oxidation and/or combustion of the metal. The off-gases from the caster are collected and scrubbed in a caustic scrubber located in the Utilities Area.

Utilities

The PFD for the Utilities is shown in Figure 8. This flowsheet presents the following functions:

- Production of Steam
- Scrubbing and Compressing of the Carbon Monoxide
- Caster Off-Gas Scrubbing

It is important for the success of the carbothermal magnesium process to effectively use the energy from combustion of the carbon monoxide to reduce the overall energy requirements for making magnesium. Therefore, careful consideration must be given to the configuration of the Utilities to maximize the energy recovered and returned to the main circuit via steam and fuel (carbon monoxide) for heating.

Currently, sensible heat is recovered from the hot CO from the coke preheater by preheating the water for the boiler. The CO from the coke preheater and the electric furnace is burned to make steam in the boilers. This steam is then used to power the ejectors that make the vacuum for the lavalle nozzles. If excess CO is available after making adequate steam for the lavalle nozzles, the balance of the CO is used in the kiln calciner. Any heat required in the calciner not furnished by the CO is supplied by purchased methane. In contrast, if enough CO is not present to make all the steam required, the amount of coke burned in the coke preheater is increased and the amount of coke charged to the process is correspondingly increased.

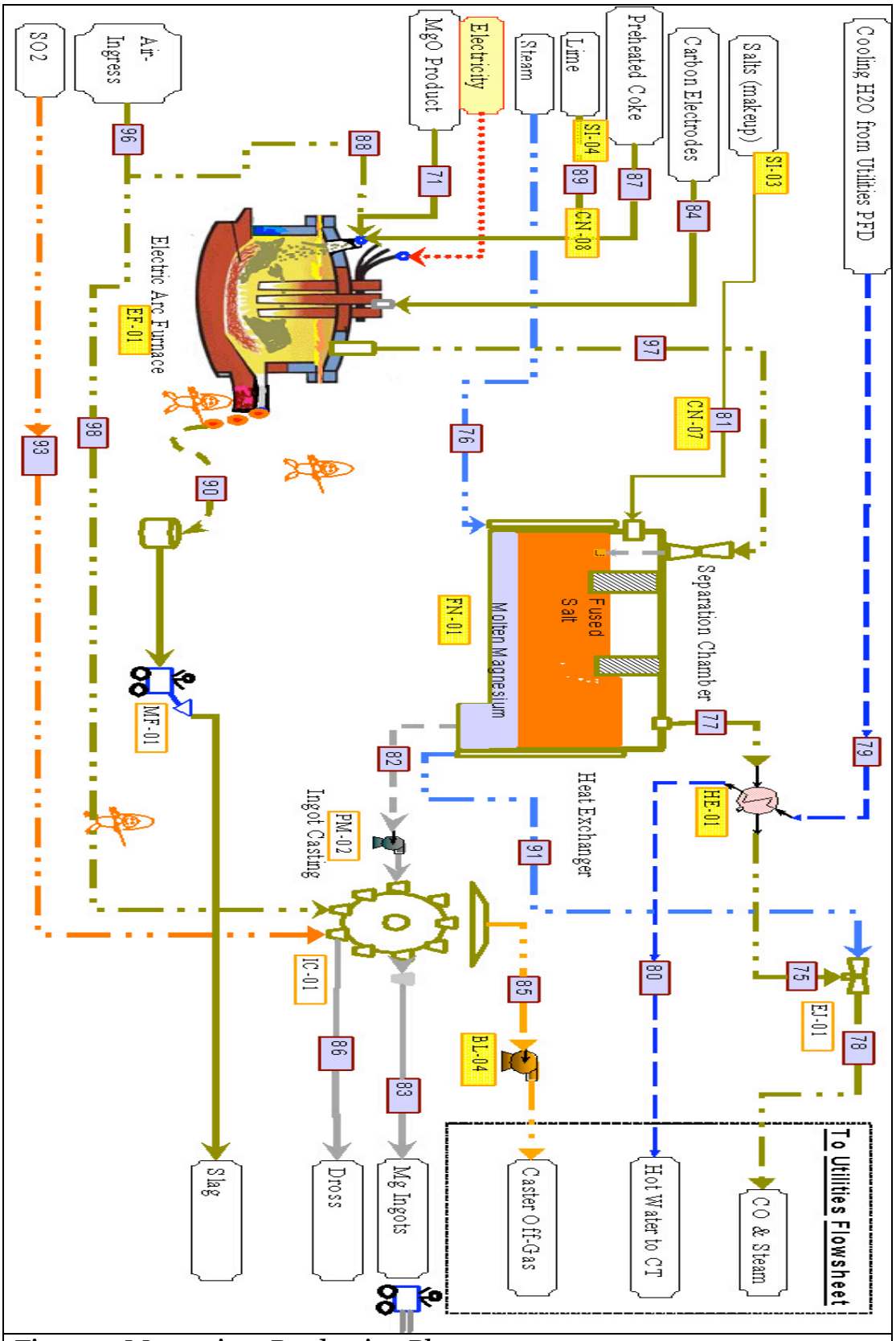

Figure 7. Magnesium Production Plant

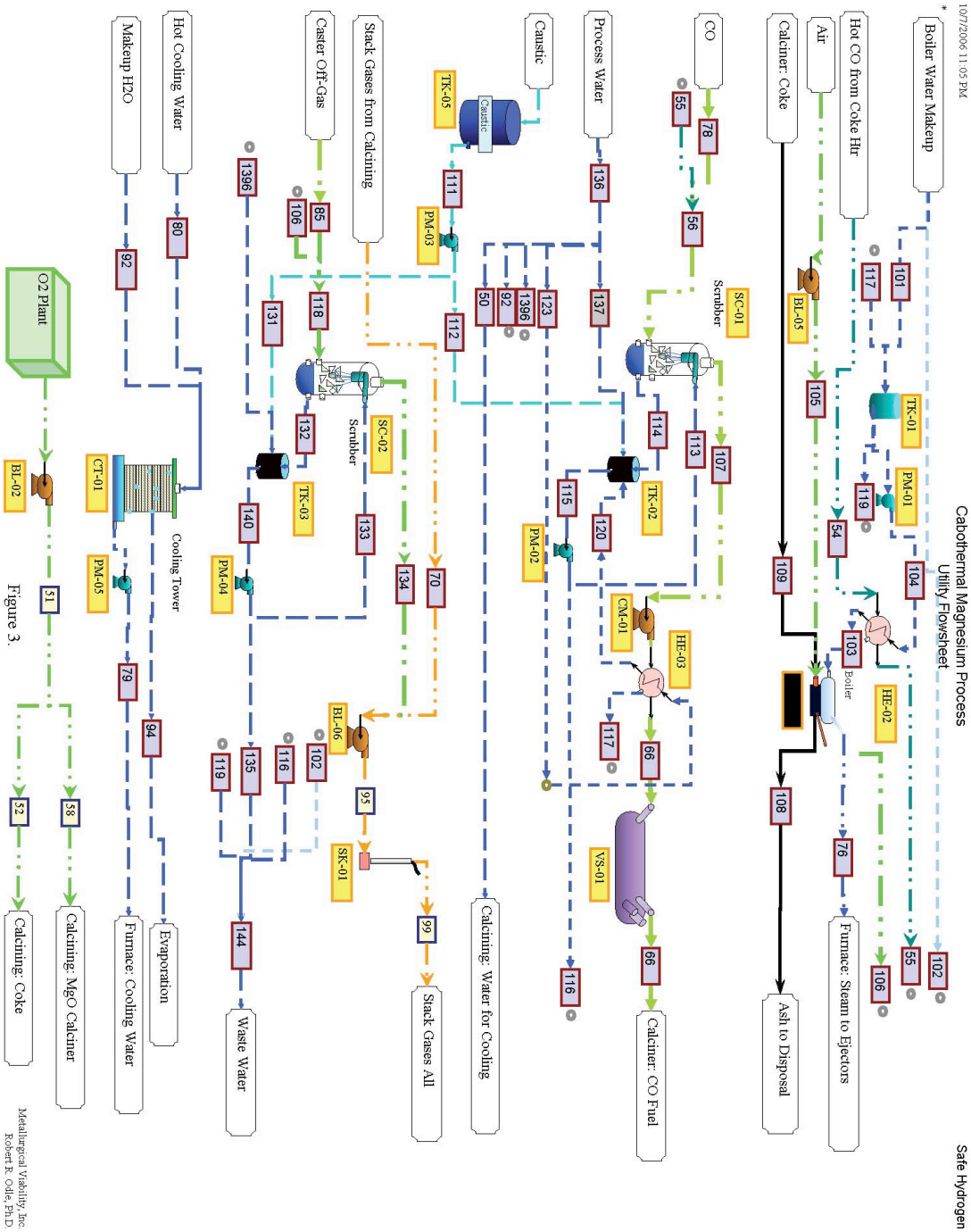

Figure 3.

Figure 8. Utilities PFD

Heat Balances

Heat balances are carried out for the energy intensive unit operations in the carbothermal process. A typical energy balance is shown for the calciner in Figure 10, for the coke preheater in Figure 11, for the electric arc furnace in Figure 12, and the Salt Box Furnace in Figure 13.

In the calciner heat balance, most of the heat is supplied by the combustion of carbon monoxide produced by the process, herein referred to as process carbon monoxide. The biggest heat consumer is the removal of water from the calciner and then the heat of reaction required to convert magnesium hydroxide to magnesium oxide. Significant heat is carried forward as sensible heat to the next unit operation in the process, the electric furnace.

In this example, about 20% of the heat required for the electric arc furnace is supplied by sensible heat of the reactants entering the furnace. About 70% of the total energy supplied is used for the endothermic reaction of reducing MgO with coke to magnesium and carbon monoxide.

Calciner: Heat Balance

Name	No.	Quant (MTPY)	Heat In (10^9kcal/yr)	Temp C
Feedstream	59	226,501	0.0	25
CO in	66	121,792	0.9	55
CH4 in	57	-	0.0	25
Heat Reactn CO + 1/2 O2-->CO2	NA	Above	294.3	55
Heat Rxtn CH4+2CO-->CO2+2H2O	na	-	0.0	25
Heat Reactn Mg(OH)2->MgO+H2O	na	220,333	-77.5	26
Oxygen	58	73,813	0.0	25
TOTAL HEAT IN	.	448,085	217.7	.
CO2 out	198	198,354	47.9	940
H2O out	198	98,970	103.9	940
O2 out	198	1,306	0.3	940
MgO_s_out	197	153,514	41.9	940
Heat Loss Surroundings	.	.	19.4	.
TOTAL HEAT OUT	.	455,623	213.5	.

Figure 10. Calciner Heat Balance

Coke Preheater: Heat Balance

Name	No.	Quant (MTPY)	Heat In (10^9kcal/yr)	Temp C
Coke to Coke Prhtr	67	56,011	0.0	25
O2 to Coke Prhtr	52	18,155	0.0	25
Heat Reactn C+O->CO	NA	.	14.9	NA
TOTALS IN	.	74,166	14.9	.
HEAT OUT				
Preheated Coke	87	47,397	9.4	630
CO from Coke Htr	54	26,769	4.2	630
Heat Loss Surroundings	.	.		
TOTALS OUT	.	74,166	15.0	.

Figure 11. Coke Pre-heater Heat Balance

Electric Arc Furnace: Heat Balance

Name	No.	Quant (MTPY)	Heat In (10^9kcal/yr)	Temp C
MgO Calcine	71	151,979	41.6	940
Coke	87	47,397	9.4	630
Lime	89	540	0.0	25
Air Leak In	88	72	0.0	25
Heat Rxn: MgO+C-->Mg(v)+CO			-448.3	
Electric Power			497.9	
TOTALS IN		199,988	100.6	
CO out	97	107,002	55.5	1850
Mg Vapor Out	97	91,091	30.2	1850
Slag	90	1,239	0.6	1850
N2 from Air Leak	97	57	5.1	1850
Heat Loss Surroundings			9.1	
TOTAL OUT		199,771	100.6	
	Power Factor %		65.0	
	Energy Per Pound of Mg KWH/lb			
		4.4	kwh/lb	
		9.6	kwh/kg	

Figure 12. Electric Arc Furnace Heat Balance

Salt Furnace: Heat Balance				
Name	**No.**	**Quant (MTPY)**	**Heat In (10^9kcal/yr)**	**Temp C**
CO	97	107,441	56	1850
Mg	97	91,091	30	1850
Steam	76	1,186,726	788	196
Salt	81	983	0	25
Heat Rxn: Mg(v)+CO-->MgO + C		incl.w Mg out	124	
TOTALS IN	.	1,386,241	999	
Name	**No.**	**Quant (MTPY)**	**Heat Out (10^9kcal/yr)**	**Temp C**
CO out	77	106,658	20	750
Mg liquid out	82	92,910	20	750
Steam Superheated	91	1,186,726	876	350
Heat Loss Surroundings			102	
TOTAL OUT		1,386,295	1018	

Figure xx. Salt Box Heat Balance

PART 3. CAPITAL COSTS ESTIMATE FOR THE NOZZLE BASED CARBOTHERMAL MAGNESIUM PROCESS

CAPITAL COST ESTIMATING

A bottom-up approach is being used to develop a capital cost model of the NBC magnesium process. The general approach taken includes these steps:

- **Selection of a Base Case.** A base case has been selected of 90,000 MTPY of magnesium. The complete Design Criteria for the Base Case is shown below. This Base Case was selected to allow comparison with the most recent estimate for an electrolytic type magnesium plant, Australian Magnesium Corporation. After the model is completed and debugged on the base case, other cases will be run.

- **Development of an Equipment List**. The process flow diagram (PFD) previous developed for the techno-economic model is used to build an equipment list.

- **Equipment Datasheet.** Using the information from the material and energy balances, a datasheet is developed for each piece of equipment.

- **Equipment Cost Estimate**. Using the equipment datasheet, an estimate was obtained from one of several sources, for the cost of each piece of equipment.

- **Algorithms for Equipment Costs as a Function of Throughput**. Given cost of the equipment at two or more sizes, an algorithm is developed to give the cost as a function of throughput for each piece of equipment.

- **Installed Cost of Basic Equipment Modules**. Factors are used to move from the cost of the individual piece of equipment to the installed cost of the equipment module. This is the installed cost of equipment if installed in an existing plant with adequate infrastructure and auxiliary plants. This cost includes engineering, project fees, the cost of labor and supplies to install equipment, and supporting equipment.

- **Installed Cost of Enhanced Equipment Modules**. Some modules are affected strongly by process conditions. The two most common factors that impact module costs are materials of construction and pressure. Additional factors are required to adjust the cost of equipment upward for more exotic materials and for high pressure operation.

- **Total Installed Equipment Cost**. The total installed cost of all equipment is obtained by adding the cost of the Equipment Modules and the cost of engineering fees for project management and contingency costs. The cost obtained is an estimate of the cost of installing equipment in a given facility with adequate infrastructure and auxiliary plants.

- **Greenfield Capital Cost.** The "Greenfield" capital cost is factored from the Total Installed Equipment Cost and allows for the cost of auxiliary equipment, infrastructure, and other project costs associated with a Greenfield site.

Each of these topics is discussed in more detail in the following sections of the report. In addition, the progress on the NBC Magnesium Plant in each of these categories is presented along with a description of the tasks required to complete the Greenfield Capital Cost estimate.

As currently written, the capital cost module is incorporated in the existing Techno-Economic Model. However, this code is executed separately after a model is executed to produce the Income Statement, material balance, energy balance, etc. The capital cost module then reads the material balance files, the design criteria, etc. and carries out the capital cost estimate as discussed in this report. As discussed below, some of the reports because of their large size are generated as text reports.

Equipment List

A master list for all the equipment in the plant was established from the PFD. Unique equipment tags were placed next to each unit operation on the PFD and these were added systematically to the Equipment List.

The goal is to include all equipment, as significant as a pump, in this list. An exception to this rule is that pipes, valves and instrumentation are estimated subsequently by parametric factors. This master list is then connected to the techno-economic model above to establish the specifications for each piece of equipment for the case under consideration. When the Capital Cost Estimate module is executed, Equipment Datasheets are produced for each piece of equipment on the Equipment List.

Equipment on this list are numbered with a four digit code, for example, PM-01, which stands for Pump-01. All pumps are numbered sequentially through out the plant. In some cases, a process stream may be so large that it cannot, for instance, be pumped by a single pump. Multiple units of identical pumps must be used. In this case, only a single entry, PM-01, for example, would be shown on the list, but multiple units would be designated under a column entitled, "No. of Units".

Equipment Datasheets

For any given Design Criteria, Equipment Datasheets are produced for each piece of equipment on the PFD which give information on the function of the equipment, materials of construction, throughputs and process conditions. The datasheet is connected to the algorithms that estimate a cost for the equipment. With information on the maximum size of equipment that is commercially available, the number of units of equipment required for the given unit operation can be calculated, see sample in Figure 1 and Appendix C.

For each piece of equipment on the PFD there are input and output streams. The model gives the amount and composition of each of these streams, as well as, the temperature and pressure of each stream. With this information, the equipment can be sized and specifications established. For example, a pump typically would have one stream coming in at a low pressure and a second stream with the same composition and temperature leaving at a higher pressure. Given the type of fluid being pumped, the quantity being pumped, and the outlet pressure, the specifications for the pump are established.

For each piece of equipment on the master list, an equipment data sheet is produced that gives all the relevant information needed to select the

correct piece of equipment for the job including its size and materials of construction. To date, this work has been completed for more than 90% of the items on the PFD's. A sample for a datasheet is shown in Figure 1. The equipment datasheets for about 55 pieces of equipment are shown in Appendix B. As mentioned, there are multiple units of equipment for some items. The total number of pieces of equipment tabulated to date is in excess of 100 items.

Estimating Equipment Cost

Once a data sheet has been produced for each piece of equipment, the cost of that equipment must be obtained. In general, equipment costs have been estimated from tabulated data from one of six sources:

References for Equipment Costs

1. Metallurgical Equipment Costs, March 2002. Mintek, Specialists in the Mineral and Metallurgical Technology, Techno-Economics Division.

2. Data from Matches, A Conceptual Process and Cost Engineering Firm. David Milligan, Principal. (http://www.matche.com). Equipment Data from 2003.

3. Gael D. Ulrich and P.T. Vasudevan. Chemical Engineering, Process Design and Economics, Practical Guide. Process Publishing, Durham, New Hampshire, 2004. For owners of the book, cost data is updated on their website, www.ulrichvasudesign.com.

4. O.P. Kharbanda and E.A. Stallworthy. Capital Cost Estimating for the Process Industries, Butterworth and Company, 1988. (This book is primarily useful for the theory; the data in the book is old and limited.)

5. Perry's Chemical Engineers' Handbook, 6th edition, Don W. Green editor, McGraw-Hill Book Company, 1984.

6. Vendor quotes, for example O.D.T. Engineering, PTY, LTD, supplied an estimate on the cost of an ingot-casting machine, and Elkem supplied a cost for the electric arc furnace.

DATASHEET

ID: SI-01 MgOH2 Blender Hopper

CATEGORY:STORAGE HOPPERS/SILOS

The function of this equipment is to take $Mg(OH)_2$ from SH and recycled dust and then release it into the blenders.

Stream No.: 74 Strm Name: Feed to Blender

MTPY:	503336	MTPH	63.94	Design MTPH	41.6
Temp.C	26.06	Pressure(atm)	1.49	MTPH per Unit	33

No.Units: 2
Bin Type: Storage HOPPER
Bin Material carbon steel Bulk SG: 1.20
Cubic Meters 107 Cubic Feet 3763
hrs storage 2.00

MgOH2 Blender Hopper $ 21828 unit cost
2 units $ 43656 cost all units

Figure 1. Sample of Data Sheet

The first three of these sources present equipment costs as a function of capacity and in some cases as a function of secondary variables like materials of construction, pressure rating, etc. Perry's Handbook is useful for understanding capital cost methodology and for obtaining factors to convert purchased equipment costs into Greenfield capital costs.

The cost data from Mintek is in Rands, the South African currency. This must be converted to U.S. dollars. Sites such as that provided by Oanda (http://www.oanda.com/convert/fxhistory) allow historical conversion of one country's currency to another's.

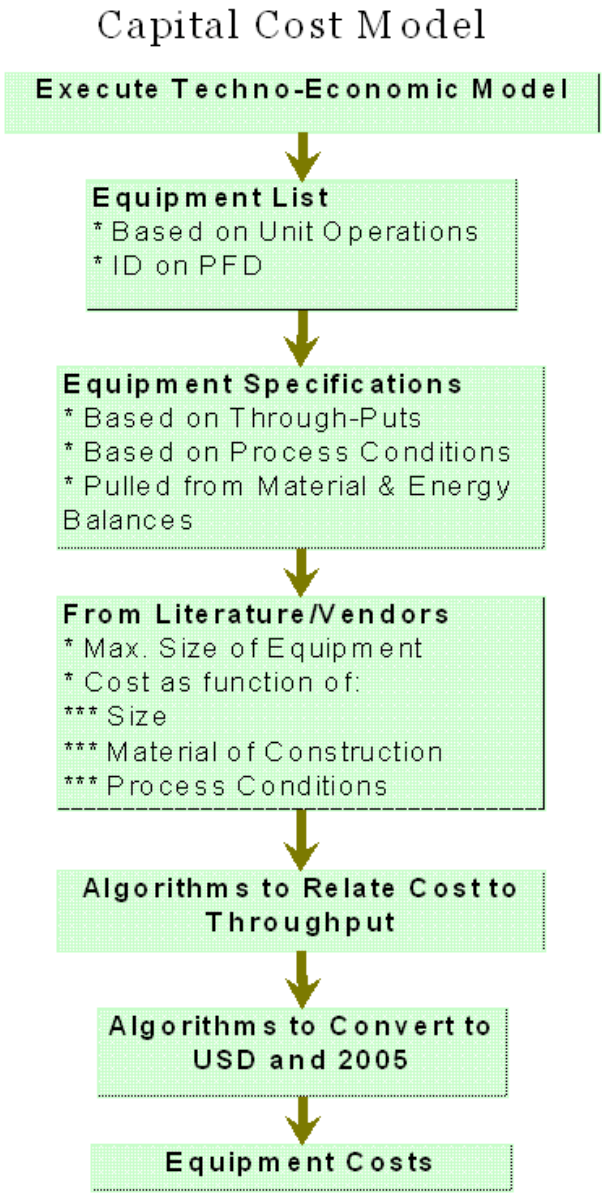

Figure 2. Development of Equipment Costs starting from the Techno-Economic Model

The process of developing the equipment costs from the Techno-Economic model is shown schematically in Figure 2 and is discussed throughout the balance of this report.

Algorithm Development for Equipment Cost as a Function of Throughput

The data, once selected for a given equipment type, is collected in a table in Excel. Two general approaches are used to convert the cost data into an algorithm that will give cost as a function of throughput.

- Multi-linear Regression Analysis
- The "Sixth Tenths Rule"

The multi-linear regression analysis, as supplied in Excel, is used to convert the costs for several differently sized pieces of a given equipment type into an algorithm that can be used to cost any that type of equipment as a function of size. For example, the data in Table 1 was collected for pumps from Matches

Table 1.
Cost of Centrifugal Pumps as a Function of Pump Discharge Size (Ref. Matches 2003)

Diameter of Outlet (inches)	Pumping Rate (Gallons/min)*	Cost ($ U.S.)

2	78	2800
4	313	4500
8	1253	7300
10	1958	8500
*Assumed 8 feet/sec pumping velocity.		

Using linear regression analysis the following relationship was obtained:

Cost of "Iron" Pump (2003 $) = 3143.1 + 2.92 * GPM (gallons/min)

This relationship is then used to estimate the cost of centrifugal pumps. The data is extrapolated out to about 10,000 GPM for cost estimation. Above this level, two pumps are required and priced accordingly. The primary advantage of using the regression analysis approach is that the cost can be a function of several independent variables instead of just one as shown in the above example.

Alternatively, the "Sixth Tenth Rule" can be used to estimate the cost of equipment when only the size of equipment is varying. The "Sixth Tenth Rule" is illustrated by this relationship:

$$C2 = C1 * (S2 / S1)^{n}$$

where

Cx is the capital cost of equipment with capacity, Sx

n = exponential factor, often about 0.60, but differs for each type of equipment.

Using Excel, a value for the exponent is selected that minimizes the error between the cost data available and the costs predicted by this relationship. This second method has become the preferred method since differences between the data and the calculated values are in general less over a broad range of values.

In Table 2, examples of algorithms developed for estimating equipment costs using the regression method are shown. In general a maximum capacity of equipment for which the relationship can be used is also given. When the cost is a function of two variables, a maximum for each of these variables is given. If a capacity is needed that falls outside the range of these algorithms, multiple pieces of equipment are used to stay within the range.

In Table 3, examples of algorithms developed for estimating equipment

costs using the sixth tenth rule are shown. In general a maximum capacity of equipment for which the relationship can be used is also given. If a capacity is needed that falls outside the range of these algorithms, multiple pieces of equipment are used.

Adjusting Cost Data for Inflation

The equipment costs shown above are valid for the year that the data was collected. The costs are corrected to 2005 by using the Chemical Engineering Plant Cost Index (CEPCI). The ratio of the index for the desired year over the year in which the data is available, is multiplied times the original cost data to adjust it for inflation. The index is published in the Chemical Engineering Magazine for about the last seven years and may be obtained from their website *www.che.com/pindex* for about the last twenty years for members. A subroutine was developed using this index to adjust the equipment costs for inflation. The subroutine requires the cost and the year for which it is valid, and then adjusts the cost for inflation for the year in question to 2005.

Installed Costs: Basic Equipment Modules

The equipment costs developed above represent the purchased price for equipment in the year it was quoted. In most cases, it is F.O.B. the plant site where the equipment is warehoused or made. However, the equipment must be transported and installed at a plant site. This requires materials of construction (foundation, buildings, connectors, paint, etc.), labor, controls, engineering, and project fees. The installed cost is typically two to four times as much as the "bare" equipment costs. The factors are different for each type of equipment.

As an example of the factors required to convert a purchased cost into a final Greenfield capital cost, Table 4 presents one example taken from Perry's[5]. With the current methodology, factors are developed for each type of equipment and applied to the purchased equipment costs. And, in some cases, factors have to be modified for an individual piece of equipment. For example, the quotation for ingot casting included instrumentation, piping, and electrical. However, it did not include off-gas handling, foundations, construction fees, etc. Therefore, a factor must be developed for ingot casting given this information.

Regression Analysis Methodology
Cost = Constant + A*X1 + B*X2

Type of Equipment	Constant	A	X1	B	X2	unit	Year	Source	X1 max	X2 max	Description
Belt Conveyors*1	-258,602	417	feet	323	cfm	$	1993	Matches	1000	1027	belt, closed w/ walkway, long
Blender Ribbon	8,325	150	cf			$	1993	Matches	320		
Blowers	-50816	10362	PSIG	3.28	cfm	$	1993	Matches	30	70000	
Heat Exchanger	32123	69	m^2	73.6	PSIG	$	1993	Matches	6000	600	shell and tube
WWTP	90113	3593	GPM								
Boiler	565,844	30.3	lbs/hr	2786	PSIG	$					stoker coal fired, field fab, 150 psi, sat.
Thickness, in	0.363	0.0442	feet	3E-04	PSIG	in	na		20	500	required thickness of wall of cylinder
Tank, 316ss	94483	435	m^3			$	1993	Matches	300		
Pumps, cast iron	3143	2.92	GPM			$	1993	Matches	2000		
Pumps, 316 ss	6204	7.23	GPM			$	1993	Matches	25000		centrifugal

*1 880 ft/sec, .33 ft depth on belt

Table 2. Examples of Equipment Costs Estimated Using Regression Analysis.

Sixth Tenth Rule Methodology

Cost = Base Cost * (New Capacity / Base Capacity) ^ Exp

Type of Equipment	Base Cost	Base Capacity	Base Unit	Exp	Unit	Description	Max	Year	Source
Cooling Tower	455386	1500	m^3/hr	0.99	Rands		2,000	1992	Mintek
Ejector	4600	8	diam in	0.61	$		12	1993	Matches
Cryogenic O2 Plant	52000000	919800	mtpy	0.66	$		1,000,000	1996	Copper Clift Copper Study
Stack Concrete	8000000	8	m	1.42	$	30 m/sec, 100 m tall	8	2004	
Kilns	5,000,000	10	tph	0.42	$		10	2003	
Ejectors steam	$ 12,600	10000	lbs/hr	0.47	$		44,000	1993	Matches
Scrubber Single Stage	3315	40000	cfm	0.57	$		43,200	1993	Matches
Scubber, 2 stage	40400	40400	cfm	0.59	$		60,602	1993	Matches
Pressure Vessels	461000	320000	lbs	0.77	$	carbon steel, horizontal, no internals	800,000	1993	Matches,
Pump Vacuum	107600	22000	cfm	0.84	$	blower, 1 stage liquid seal, not include motor, cast iron	30,000	1993	Matches
Pump Vacuum	215900	18000	cfm	0.74	$	two stage, liquid seal, cast iron, not include motor	30,000	1993	Matches
Disk Agglomerator	213600	20	feet diam	1.54	$	disk with motor, FOB gulf coast	20	1993	Matches
Bin	167800	42000	cf	0.71	$	hopper with bolted bottom	50,000	1993	Matches

Table 3. Examples of Equipment sized with the Sixth Tenth Rule.

Table 4. Typical Capital Cost Estimate for Solids-Fluid Type Plant		
Details	**Factor Assumed**	**Percentage of Total**
Equipment, delivered	1.0	23.4
Installation	0.41	9.6
Piping	0.34	8.0
Electrical	0.13	3.0
Instruments	0.13	3.0
Battery-limit building and services	0.30	7.0
Excavation and site preparation	0.15	3.5
Auxiliaries	0.52	12.2
Total Plant Physical	2.98	**69.7**
Field Expense	0.39	9.1
Engineering	0.39	9.1
Direct Plant Costs	**3.76**	**87.9**
Contractor's Fees, overhead, profits	0.13	3.0
Contingency	0.39	9.1
Total fixed-capital investment	**4.28**	**100**

Installed Costs: Enhanced or Modified Equipment Modules

Most equipment pricing is based on a basic equipment module, for equipment that does not operate under extraordinary conditions with regard to corrosion/materials, pressure, and/or temperature. For instance, equipment in the basic modules are most likely to be made out of carbon steel, copper, or other standard materials and are designed to operate near at relatively low pressures, often atmospheric, and at temperatures near room temperature. However, a boiler operating at 100 psig could be the basic module since boilers by nature operate at elevated temperatures and moderate pressures. Factors to go from purchased equipment prices to installed equipment costs are typically defined for the basic module described here.

To account for exotic materials, high pressures, etc. additional factors are introduced:

IC = fm * fp * fb * PE

Where,

IC= installed cost of equipment

fm = factor to account for the cost of exotic or corrosion resistant materials of construction

fp = factor to account for the cost of operating at higher pressures (other parameters like temperature could be handled by a similar factor)

fb = factor to convert purchased equipment cost for the basic module to installed cost

PE = purchased equipment price adjusted for throughput and inflation to the year of interest

Some examples of material factors for piping at low pressures are given below:

F-carbon steel = 1.0

F-polyvinylchloride(PVC)=0.3

F-chlorinated PVC = 0.7

F-stainless 316L = 2.0

F-fiberglass reinforced plastic = 4.9

F-Alloy 20 = 8.7

These factors vary from time to time as market conditions react to supply and demand forces.

Almost all of the equipment modules associated with the NBC Magnesium Process are basic in that they use common materials and operate at moderate pressures. Depending on how the Design Criteria is set by the user of the Techno-Economic model, a couple of exceptions to this generalization above is the boiler, which can be required to operate at relatively high pressures, and the kiln, which can be required to operate at relatively high temperatures.

Total Installed Equipment Costs/Plant Costs

In Figure 3, a schematic is shown showing the steps in going from inflation adjusted Equipment Costs to Installed Costs inside of an existing plant, and finally to the Installed Cost in a Greenfield Plant. This methodology, from G.D. Ulrich et al[3], is slightly different in approach than that shown in Table 4 from Perry, but arrives at similar costs. In the discussion above, the first three steps, up to the Modified or Enhanced Module Costs have been covered. The Module Costs include all the material costs directly related with the equipment, such things as foundations, piping, electrical supplies, etc. and even direct blue labor costs and the field engineering costs involved in installing this equipment.

Typically there are two other costs associated with installing equipment in a plant, Contingency Costs and Fees. The definition of Contingency Costs varies from one reference to the next, and from one engineering company to the next. Contingency costs exist as a result of the imperfect nature of estimating and the unknown challenges that arise in any project. One misconception is that the contingency costs are there if something unexpected arises but you are not expected to spend them if all goes well. In reality, contingency costs are expected costs for items unknown at the time of the estimate. These costs decrease as more detailed engineering is done on a project. Engineering companies keep historical records to enable them to accurately predict contingency costs as a function of the amount of engineering done on a project, even if they can not accurately predict where such money will be spent. Ulrich recommends an 18% contingency factor, which is considerably below the 30% contingency that Flour Daniel used for a project in the Feasibility Stage. There is always a tendency to lower this number despite the strong historical evidence for the need of adequate contingency costs in the estimate.

The other cost required to go from the Enhanced Module Costs to the Installed Cost is the category called "Fees". Fees represent Project Management fees. Engineering and contracting companies usually bill jobs on a cost basis for time and materials. On top of this, they had "Fees", which roughly correlate with the engineering company's profits, or as the engineering companies state, "a contribution to overhead and profits." The result of accounting for Contingency and Fees is to obtain the cost to install an equipment module in an existing plant.

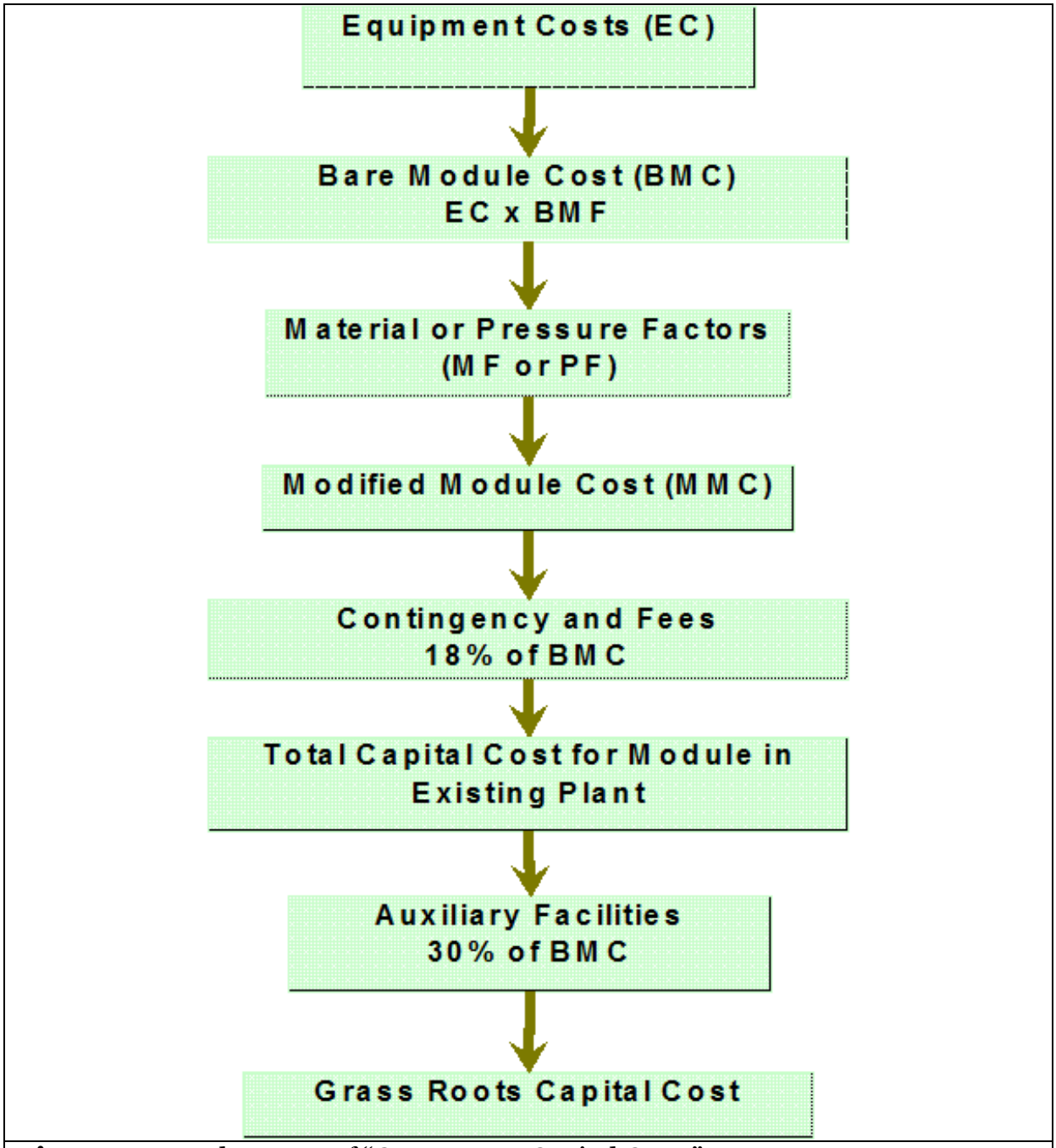

Figure 3. Development of "Grass Roots Capital Costs"

Greenfield Capital Costs

There is one set of additional costs in estimating the capital costs of the NBC Magnesium Process. In building a process plant, there are many infrastructure related costs that must be borne by the project. For instance, if a plant is built in a remote location like the Andes in Peru, infrastructure may include building an entire city next to the plant including roads, water supply, houses, etc.

Even in a developed area, such as the Gulf Coast of the United States, some typical costs include:

- Site Development
- Auxiliary Buildings
- Off-site facilities
- Power Distribution Transformers
- Rail Right-of-Way Costs
- Licensing Fees
- Startup or Operating Capital

These costs add about 30% to the Enhanced/Modified Equipment Module Costs. These costs may not all be included in the engineering estimate since they are frequently lumped in all or part under a category often called owner's costs. The first four costs above would typically be in the Engineering estimate, the last three would not be. However, the actual contract between the engineering company would define the exact boundaries. The goal in the current estimate is to include all the costs associated with a Greenfield Startup independent of whose column the costs would ultimately lie.

The Capital Cost Estimate for the NBC Magnesium Process

All of the equipment costs have been estimated for the NBC Magnesium Process. Even items that require design, such as the salt-bath furnace have been estimated by completing a preliminary design and then the cost estimated from the weight of the containment box and algorithms used for estimating the cost of low pressure vessels based on their weight.

The cost of the NBC Mg Plant could be reduced by some process changes in the Utility area of the plant. Specifically, replacing the scrubbing circuit for carbon monoxide with ESP (electrostatic precipitators) could lower the cost. This would probably also lower the operating costs slightly.

Greenfield Capital Cost

The installed equipment costs are shown in Table 5A and 5B sorted by equipment type. The most expensive equipment are the electric furnaces at $100 million, the boilers to make steam, primarily for the vacuum ejectors at $44 million, and the kilns for calcining the Mg(OH)2 at $32 million. These three items make up more than half the cost of the plant. This equipment would be optimized during engineering for any potential costs savings.

The installed equipment costs, sorted by Plant Areas, are in shown in Table 6A, 6B, and 6C. The Furnace Plant at $116 million is the most expensive, the Utilities at $80 million are the second most expensive, while the Calcining Plant costs about $26 million.

The total installed equipment cost for an NBC Magnesium Plant making 90,000 metric tons of magnesium a year is about $223 million dollars. With contingency and fees, the total plant costs are estimated at $305 million. The factored Greenfield Costs are estimated to be about $400 million, Table 7. The estimated capital costs per tonne of capacity of about $4500 compares with Alan Donaldson and Ronald Cordes estimate of $3200/metric tonne for their the rapid plasma quenching process. There are some references in the literature for the Western Pidgeon process of about $6000/metric tonne. However, none of these studies have been done as comprehensively as the present; a lack of thoroughness generally leads to an under-estimation of costs.

Table 5A. Equipment Costs Grouped by Equipment Types for the NBC Magnesium Plant, part 1.

Equipment Costs		Case No.:	2159		Capital		
Equipment Name	ID	Item Cost	No.of Units	Total Item Cost	Installa-tion Factor	Materials or Pressure Factor	Installed Cost
MgOH2/Dust Blender	BD-01A	$ 56,870	2	$ 113,739	3.0	1.00	$ 341,218
BLENDERS		Subtotal		$ 113,739			$ 341,218
Calciner Baghouse	BH-01A	$ 32,616	1	$ 32,616	1.5	3.50	$ 171,237
BAGHOUSE		Subtotal		$ 32,616			$ 171,237
Baghouse Exhaust Blower	BL-01A	$ 180,640	1	$ 180,640	3.0	1.00	$ 541,921
Oxygen Blower to Calcine Circuit	BL-02A	$ 129,525	1	$ 129,525	3.0	1.00	$ 388,576
CO Blower from Coke Preheater	BL-03B	$ 132,263	1	$ 132,263	3.0	1.00	$ 396,790
Gases from Caster Blower	BL-04B	$ 34,635	1	$ 34,635	3.0	1.00	$ 103,906
Air Blower for Boiler	BL-05C	$ 309,615	1	$ 309,615	3.0	1.00	$ 928,845
CO Compressor	CM-01B	$ 1,139,613	1	$ 1,139,613	2.5	1.00	$ 2,849,033
Stack Blower	BL-06C	$ 537,506	1	$ 537,506	3.0	1.00	$ 1,612,518
BLOWERS		Subtotal		$ 2,463,799			$ 6,821,590
Central Boiler	BP-01C	$ 8,886,069	2	$ 17,772,139	2.5	1.00	$ 44,430,347
BOILERS		Subtotal		$ 17,772,140			$ 44,430,348
MgOH2 Conveyor from SH	CN-01A	$ 194,236	1	$ 194,236	2.5	1.00	$ 485,590
MgOH2 Conveyor to Calcine	CN-02A	$ 98,558	1	$ 98,558	2.5	1.00	$ 246,395
MgO Product Conveyor	CN-03A	$ 194,236	1	$ 194,236	2.5	1.00	$ 485,590
Coke to Boiler Conveyor	CN-04C	$ 194,236	1	$ 194,236	2.5	1.00	$ 485,590
Coke to Preheater Conveyor	CN-05B	$ 98,558	1	$ 98,558	2.5	1.00	$ 246,395
Preheated Coke Conveyor	CN-06B	$ 98,558	1	$ 98,558	2.5	1.00	$ 246,395
Salts Conveyor	CN-07B	$ 98,558	1	$ 98,558	2.5	1.00	$ 246,395
Lime Conveyor	CN-08B	$ 98,558	1	$ 98,558	2.5	1.00	$ 246,395
CONVEYORS		Subtotal		$ 1,075,498			$ 2,688,744
Cooling Tower	CT-01C	$ 3,269	1	$ 3,269	2.5	1.00	$ 8,173
Cooling Tower		Subtotal		$ 3,270			$ 8,172
Ingot Casting Machine	IC-01B	$ 345,000	1	$ 345,000	1.5	1.00	$ 517,500
INGOT CASTING		Subtotal		$ 345,000			$ 517,500
Boiler Demin. Plant	DM-01C	$ 1,198,838	1	$ 1,198,838	1.5	1.00	$ 1,798,257
Demineralizer		Subtotal		$ 1,198,838	3.0	1.00	$ 1,798,256
Boiler Feedwater Pump	PM-01C	$ 8,522	1	$ 8,522	3.0	1.00	$ 25,565
CO Scrubber Pump	PM-02C	$ 22,462	11	$ 247,078	3.0	1.00	$ 741,234
Caustic Pump	PM-03C	$ 1,202	1	$ 1,202	3.0	1.00	$ 3,606
Caster Scrubber Pump	PM-04C	$ 13,289	1	$ 13,289	3.0	1.00	$ 39,868
Cooling Water Pumps	PM-05C	$ 4,877	1	$ 4,877	3.0	1.00	$ 14,632
PUMPS		Subtotal		$ 274,970	2.0	1.00	$ 824,900

Table 5B. Equipment Costs Grouped by Equipment Type for the NBC Magnesium Plant, part 2.

MgOH2 Blender Hopper	SI-01A	$ 12,285	1	$ 12,285	2.0	1.00	$ 24,571
Coke Day Bin	SI-02A	$ 20,217	1	$ 20,217	2.0	1.00	$ 40,434
Salt Week Bin	SI-03B	$ 5,340	1	$ 5,340	2.0	1.00	$ 10,681
Quick Lime Storage Bin	SI-04B	$ 4,331	1	$ 4,331	2.0	1.00	$ 8,661
Dust Transport Hoppers	HP-01A	$ 2,033	1	$ 2,033	2.0	1.00	$ 4,067
Dust Disposal Supersacks	HP-02A	$ 1,823	1	$ 1,823	2.0	1.00	$ 3,645
BINS		Subtotal		$ 46,028			$ 92,056
Plant Stack	ST-01C	$ 358,402	1	$ 358,402	2.0	1.00	$ 716,805
PLANT STACK		Subtotal		$ 358,402			$ 716,804
Vacuum Steam Ejectors	EJ-01B	$ 55,666	10	$ 556,661	2.5	1.00	$ 1,391,651
Vacuum Steam Ejectors		Subtotal		$ 556,660	2.5	1.00	$ 1,391,652
CO Gas Cooler	HX-01B	$ 57,469	1	$ 57,469	2.5	1.00	$ 143,673
Boiler H2O Preheater	HX-02C	$ 56,155	1	$ 56,155	2.5	1.00	$ 140,387
Compressed CO Cooler	HX-03C	$ 94,764	17	$ 1,610,982	2.5	1.00	$ 4,027,455
HEAT EXCHANGERS		Subtotal		$ 1,724,606	2.1	1.00	$ 4,311,516
Boiler Feedwater Tank	TK-01C	$ 92,582	2	$ 185,164	2.1	1.00	$ 388,844
CO Scrubber Tank	TK-02C	$ 130,852	22	$ 2,878,734	2.1	1.00	$ 6,045,341
Stack Scrubber Tank	TK-03C	$ 73,889	1	$ 73,889	2.1	1.00	$ 155,168
TANKS		Subtotal		$ 3,137,788			$ 6,589,352
CO Buffer Storage Vessel	VS-01C	$ 483,502	1	$ 483,502	2.1	1.00	$ 1,015,355
PRESSURE VESSELS		Subtotal		$ 483,502	3.0	1.00	$ 1,015,352
CO Scrubber	SC-01C	$ 24,626	1	$ 24,626	3.0	1.00	$ 73,877
Caster Scrubber	SC-02B	$ 42,625	1	$ 42,625	3.0	1.00	$ 127,874
SCRUBBERS		Subtotal		$ 67,250	1.0	1.00	$ 201,752
MgOH2 Calciner	KN-01A	$ 11,651,147	1	$ 11,651,147	2.0	1.00	$ 23,302,293
Coke Preheater	KN-02B	$ 4,568,909	1	$ 4,568,909	2.0	1.00	$ 9,137,819
KILNS		Subtotal		$ 16,220,054			$ 32,440,112
Salt Box Furnace	SF-01B	$ 181,458	1	$ 181,458	3.0	1.00	$ 544,373
SALT BOX FURNACE		Subtotal		$ 181,456			$ 544,376
Electric Smelting Furnace	EF-01B	$ 100,361,104	1	$ 100,361,104	1.0	1.00	$ 100,361,104
Electric Arc Furnaces		Subtotal		$ 100,361,104			$ 100,361,096
Waste Water Treatment Plant	WWTP-01C	$ 2,683,649	1	$ 2,683,649	1.5	1.00	$ 4,025,474
Wastewater Treatment Plant		Subtotal					$ 4,025,472
Cryogenic O2 Plant	OP-01C	$ 4,444,466	2	$ 8,888,931	1.5	1.00	$ 13,333,397
Cryogenic O2 Plant		Subtotal		$ 8,888,928			$ 13,333,392
Total Equipment Costs				$ 157,989,296			$ 222,624,896

Table 6A. Installed Equipment Costs by Plant Area, Calcining Plant

Equipment Costs		Case No.:	2159				
Calcining Plant Costs							
Equipment Name	**ID**	**Item Cost**	**No.of Units**	**Total Item Cost**	**Installa-tion Factor**	**Materials or Pressure Factor**	**Installed Cost**
MgOH2/Dust Blender	BD-01A	$56,870	2	$113,739	3	1	$341,218
Calciner Baghouse	BH-01A	$32,616	1	$32,616	1.5	3.5	$171,237
Baghouse Exhaust Blower	BL-01A	$180,640	1	$180,640	3	1	$541,921
Oxygen Blower to Calcine Circuit	BL-02A	$129,525	1	$129,525	3	1	$388,576
MgOH2 Conveyor from SH	CN-O1A	$194,236	1	$194,236	2.5	1	$485,590
MgOH2 Conveyor to Calcine	CN-O2A	$98,558	1	$98,558	2.5	1	$246,395
MgO Product Conveyor	CN-03A	$194,236	1	$194,236	2.5	1	$485,590
MgOH2 Blender Hopper	SI-01A	$12,285	1	$12,285	2	1	$24,571
Coke Day Bin	SI-02A	$20,217	1	$20,217	2	1	$40,434
Dust Transport Hoppers	HP-01A	$2,033	1	$2,033	2	1	$4,067
Dust Disposal Supersacks	HP-02A	$1,823	1	$1,823	2	1	$3,645
MgOH2 Calciner	KN-01A	$11,651,147	1	$11,651,147	2	1	$23,302,293
		Equip.Cost		**$12,631,055**		**Installed Cost**	**$26,035,536**

Table 6B.

Installed Equipment Costs for the NBC Magnesium Plant Area by Plant Area, Furnace Plant .

Furnace Plant Area							
Equipment Name	**ID**	**Item Cost**	**No.of Units**	**Total Item Cost**	**Installa-tion Factor**	**Materials or Pressure Factor**	**Installed Cost**
CO Blower from Coke Preheater	BL-03B	$132,263	1	$132,263	3	1	$396,790
Gases from Caster Blower	BL-04B	$34,635	1	$34,635	3	1	$103,906
CO Compressor	CM-01B	$1,139,613	1	$1,139,613	2.5	1	$2,849,033
Coke to Preheater Conveyor	CN-05B	$98,558	1	$98,558	2.5	1	$246,395
Preheated Coke Conveyor	CN-06B	$98,558	1	$98,558	2.5	1	$246,395
Salts Conveyor	CN-07B	$98,558	1	$98,558	2.5	1	$246,395
Lime Conveyor	CN-08B	$98,558	1	$98,558	2.5	1	$246,395
Ingot Casting Machine	IC-01B	$345,000	1	$345,000	1.5	1	$517,500
Salt Week Bin	SI-03B	$5,340	1	$5,340	2	1	$10,681
Quick Lime Storage Bin	SI-04B	$4,331	1	$4,331	2	1	$8,661
Vacuum Steam Ejectors	EJ-01B	$55,666	10	$556,661	2.5	1	$1,391,651
CO Gas Cooler	HX-01B	$57,469	1	$57,469	2.5	1	$143,673
Caster Scrubber	SC-02B	$42,625	1	$42,625	3	1	$127,874
Coke Preheater	KN-02B	$4,568,909	1	$4,568,909	2	1	$9,137,819
Salt Box Furnace	SF-01B	$181,458	1	$181,458	3	1	$544,373
Electric Smelting Furnace	EF-01B	$100,361,104	1	$100,361,104	1	1	$100,361,104
		Equip.Cost		**$107,823,640**		**Installed Cost**	**$116,578,647**

Table 6C. Installed Equipment Costs for the NBC Magnesium Plant by Plant Area, Utilities.

Utilities							
Equipment Name	**ID**	**Item Cost**	**No.of Units**	**Total Item Cost**	**Installa-tion Factor**	**Materials or Pressure Factor**	**Installed Cost**
Air Blower for Boiler	BL-05C	$309,615	1	$309,615	3	1	$928,845
Stack Blower	BL-06C	$537,506	1	$537,506	3	1	$1,612,518
Central Boiler	BP-01C	$8,886,069	2	$17,772,139	2.5	1	$44,430,347
Coke to Boiler Conveyor	CN-04C	$194,236	1	$194,236	2.5	1	$485,590
Cooling Tower	CT-01C	$3,269	1	$3,269	2.5	1	$8,173
Boiler Demin. Plant	DM-01C	$1,198,838	1	$1,198,838	1.5	1	$1,798,257
Boiler Feedwater Pump	PM-01C	$8,522	1	$8,522	3	1	$25,565
CO Scrubber Pump	PM-02C	$22,462	11	$247,078	3	1	$741,234
Caustic Pump	PM-03C	$1,202	1	$1,202	3	1	$3,606
Caster Scrubber Pump	PM-04C	$13,289	1	$13,289	3	1	$39,868
Cooling Water Pumps	PM-05C	$4,877	1	$4,877	3	1	$14,632
Plant Stack	ST-01C	$358,402	1	$358,402	2	1	$716,805
Boiler H2O Preheater	HX-02C	$56,155	1	$56,155	2.5	1	$140,387
Compressed CO Cooler	HX-03C	$94,764	17	$1,610,982	2.5	1	$4,027,455
Boiler Feedwater Tank	TK-01C	$92,582	2	$185,164	2.1	1	$388,844
CO Scrubber Tank	TK-02C	$130,852	22	$2,878,734	2.1	1	$6,045,341
Stack Scrubber Tank	TK-03C	$73,889	1	$73,889	2.1	1	$155,168
CO Buffer Storage Vessel	VS-01C	$483,502	1	$483,502	2.1	1	$1,015,355
CO Scrubber	SC-01C	$24,626	1	$24,626	3	1	$73,877
Plant	01C	$2,683,649	1	$2,683,649	1.5	1	$4,025,474
Cryogenic O2 Plant	OP-01C	$4,444,466	2	$8,888,931	1.5	1	$13,333,397
		Equip.Cost		**$37,534,605**		**Installed Cost**	**$80,010,737**
Totals for Entire Plant		**Ttl. Equip.Cost**		**$157,989,300**		**Ttl. Installed Cost**	**$222,624,920**

Table 7.

Greenfield Capital Costs and Unit Capital Cost for Making Magnesium via the NBC Magnesium Process

Capital Cost Estimate		**Case Code**	2159
Magnesium Production, mtpy		90,000	
Description		**Costx 10^6**	
Installed Equipment Costs		$ 223	
Contingency Cost	30%	$ 67	
Engr.Project Fees	7%	$ 16	
Total Plant Cost		$ 305	
Total Greenfield Cost/Auxilaries	30%	$ 396	
Interest rate, annual	9%		
Plant life, months	300		
Amount Financed, 90% of above	356.85	millions	
Monthly payment	($2.99)	millions	
Annual Payment	($35.94)	millions	
Amorization cost, per pound	**$ (0.18)**	**per pound**	

Unit Costs of Making Magnesium by the NBC Magnesium Process

From the previous section, the total operating cost of making magnesium was about $0.34 per pound. Coupled with the capital cost of $0.18 per pound, the total cost of making magnesium including operating and capital costs is about $0.52 per pound. The price of magnesium in 2006 ranged from about $0.90 to $1.00 per pound. This implies about a two year pay back and about a 50% return on investment for a new NBC Magnesium Plant.

Future of the NBC Magnesium Process

Obviously, the potential profitability of a NBC Magnesium Plant is either widely unknown, which is true, or taken as "to good to be true." In eight years of working on this project, there have been no serious verbal or written technical challenges to this technology. A few million have been spent illustrating poor engineering and project management can kill any project, but no serious effort

has been taken to move this promising technology from the bench scale to full production.

The next logic step in the progression of this technology is to build a pilot plant that will produce a few kilograms per hour. Tangible evidence that the process can produce metal ingots coupled with a rigorous feasibility study by a reputable engineering firm could move this technology into the mainstream.

This technology is not likely to be developed in China or India because even with its relatively low capital cost, it is still more capital intensive than the Pidgeon Process used in China. The process lends itself to automation and would be a logical fit in the United States or Europe except for the disfavor of such industries in those countries. Australia with its growing mineral's industry would be a likely candidate after it forgets the large losses it incurred in trying to develop the Australian Magnesium Corporation Process.

Perhaps the biggest hope for development of this process will come from a realization of the United States that an energy policy is critical to their long term survival. Low cost magnesium production could be helpful to that cause: (1) in providing a low weight metal helpful in reducing the weight of cars and hence their efficiency and (2) it is a viable means of containing, transporting and using hydrogen via magnesium hydride.

11.2.1 Appendix for Nozzle Based Carbothermic Magnesium Process

Metallurgical Viability, Inc.

100 WEDGEMONT DRIVE

ELKTON, MD 21921

443-616-4339

APPENDICES

Appendix A: Summary Equipment Costs

Appendix B: Detailed Equipment Costs

Appendix C: Typical Datasheets

Note, all Appendices are not for the same case, therefore costs may vary some from one Appendix to another. A few items have already been revised slightly from the values shown here from additional information/quotes received after sections of this report were already printed. The last 10% of the equipment may not represent 10% of the costs. One item not yet included is the cost of the oxygen plant, which will be significant.

APPENDIX A SUMMARY EQUIPMENT COSTS

Equipment Costs

Case No.: **1,928**

Equipment Type	**Total Item Cost**
Bins	$ 58,315
Conveyors	$ 1,075,499
Blenders	$ 9,566
Blowers	$ 4,913,984
Baghouses	$ 33,018
Plant Stack	$ 412,981
Ingot Casting	$ 500,000
Pumps	$ 8,298,492
Boilers	$ 17,772,140
Vacuum Steam Ejectors	$ 556,662
Heat Exchangers	$ 1,724,604
Tanks	$ 1,839,420

Pressure Vessels	$	483,504
Scrubbers	$	30,448
Kilns	$	16,220,056
Salt Box Furnace	$	285,456
Electric Arc Furnaces	$	62,426,696
Wastewater Treatment Plant	$	2,711,112
Cooling Tower	$	3,272
Total Equipment Costs	**$**	**119,355,224**

APPENDIX B

Detailed Equipment Costs

Equipment Costs

Case No.: 1928

Equipment Name	ID	Item Cost	No.of Units	Total Item Cost
MgOH2 Blender Hopper	SI-01	$ 12,285	2	$ 24,571
Coke Day Bin	SI-02	$ 20,217	1	$ 20,217
Salt Week Bin	SI-03	$ 5,340	1	$ 5,340
Quick Lime Storage Bin	SI-04	$ 4,331	1	$ 4,331
Dust Transport Hoppers	HP-01	$ 2,033	1	$ 2,033
Dust Disposal Supersacks	HP-02	$ 1,823	1	$ 1,823
BINS		Subtotal		$ 58,315
MgOH2 Conveyor from SH	CN-O1	$ 194,236	1	$ 194,236
MgOH2 Conveyor to Calcine	CN-O2	$ 98,558	1	$ 98,558
MgO Product Conveyor	CN-03	$ 194,236	1	$ 194,236
Coke to Boiler Conveyor	CN-04	$ 194,236	1	$ 194,236
Coke to Preheater Conveyor	CN-05	$ 98,558	1	$ 98,558
Preheated Coke Conveyor	CN-06	$ 98,558	1	$ 98,558
Salts Conveyor	CN-07	$ 98,558	1	$ 98,558
Lime Conveyor	CN-08	$ 98,558	1	$ 98,558
CONVEYORS		Subtotal		$ 1,075,499
MgOH2/Dust Blender	BD-01	$ 9,565	1	$ 9,565
BLENDERS		Subtotal		$ 9,566
Baghouse Exhaust Blower	BL-01	$ 147,405	2	$ 294,809
Oxygen Blower to Calcine Circuit	BL-02	$ 129,525	2	$ 259,051

CO Blower from Coke Preheater	BL-03	$	132,263	2	$ 264,527
Gases from Caster Blower	BL-04	$	34,635	2	$ 69,270
Air Blower for Boiler	BL-05	$	309,615	2	$ 619,230
CO Compressor	CM-01	$	1,139,613	2	$ 2,279,226
Stack Blower	BL-06	$	563,935	2	$ 1,127,870
BLOWERS		Subtotal			$ 4,913,984
Calciner Baghouse	BH-01	$	33,018	1	$ 33,018
BAGHOUSE		Subtotal			$ 33,018
Plant Stack	ST-01	$	412,981	1	$ 412,981
PLANT STACK		Subtotal			$ 412,981
Ingot Casting Machine	IC-01	$	500,000	1	$ 500,000
INGOT CASTING		Subtotal			$ 500,000
Boiler Feedwater Pump	PM-01	$	8,037	1	$ 8,037
CO Scrubber Pump	PM-02	$	826,690	10	$ 8,266,901
Caustic Pump	PM-03	$	3,627	1	$ 3,627
Caster Scrubber Pump	PM-04	$	15,437	1	$ 15,437
Cooling Water Pumps	PM-05	$	4,490	1	$ 4,490
PUMPS		Subtotal			$ 8,298,492
Central Boiler	BP-01	$	8,886,070	2	$ 17,772,140
BOILERS		Subtotal			$ 17,772,140
Vacuum Steam Ejectors	EJ-01	$	55,666	10	$ 556,661

Vacuum Steam Ejectors		Subtotal		$	556,662
CO Gas Cooler	HX-01	$ 57,469	1	$	57,469
Boiler H2O Preheater	HX-02	$ 56,155	1	$	56,155
Compressed CO Cooler	HX-03	$ 94,764	17	$	1,610,982
HEAT EXCHANGERS		Subtotal		$	1,724,604
Boiler Feedwater Tank	TK-01	$ 60,581	2	$	121,163
CO Scrubber Tank	TK-02	$ 75,911	22	$	1,670,049
Stack Scrubber Tank	TK-03	$ 48,207	1	$	48,207
TANKS		Subtotal		$	1,839,420
CO Buffer Storage Vessel	VS-01	$ 483,502	1	$	483,502
PRESSURE VESSELS		Subtotal		$	483,504
CO Scrubber	SC-01	$ 24,626	1	$	24,626
Caster Scrubber	SC-02	$ 5,823	1	$	5,823
SCRUBBERS		Subtotal		$	30,448
MgOH2 Calciner	KN-01	$ 11,651,147	1	$	11,651,147
Coke Preheater	KN-02	$ 4,568,910	1	$	4,568,910
KILNS		Subtotal		$	16,220,056
Salt Box Furnace	SF-01	$ 285,455	1	$	285,455
SALT BOX FURNACE		Subtotal		$	285,456
Electric Smelting Furnace	EF-01	$ 31,213,349	2	$	62,426,698

Electric Arc Furnaces		Subtotal		$	62,426,696
Waste Water Treatment Plant	WW-01	$ 2,711,114	1	$	2,711,114
Wastewater Treatment Plant		Subtotal		$	2,711,112
Cooling Tower	CT-01	$ 3,269	1	$	3,269
Cooling Tower		Subtotal		$	3,272
Total Equipment Costs			$		119,355,224

APPENDIX C

Typical Equipment Data Sheets

for Case No. 1944

STORAGE HOPPERS/SILOS

ID SI-01 MgOH2 Blender Hopper

The function of this equipment is to take MgOH2 from SH and recycled dust and then dump it into blender. No control just a chute.

Stream No.:	74.00	Strm Name:	Feed to Blender
MTPY:	503335.60	MTPH	63.94
Design MTPH	41.56		
Temp.C:	26.06	Pressure(atm):	1.49
Max.Avail.MTPH:	33.00		
No.Units:	2.00		
Bin Type:	Storages HOPPER/	Bin Material	carbon steel
Bulk SG:	1.20		
Cubic Meters	106.57	Cubic Feet	3763.40
hrs storage	2.00		

MgOH2 Blender Hopper		$ 25080	unit cost
2	units	$ 50161	cost all units

ID SI-02 Coke Day Bin

The function of this equipment is to take coke from front end loader and store for a day. Also dump onto conveyor belts.

Stream No.:	53.00	Strm Name:	Coke Supply
MTPY:	141302.60	MTPH	17.95
Design MTPH	23.34		
Temp.C:	25.05	Pressure(atm):	1.44
Max.Avail.MTPH:	150.00		
No.Units:	1.00		
Bin Type:	Storage Hopper	Bin Material	carbon steel
Bulk SG:	2.30		
Cubic Meters	187.30	Cubic Feet	6614.66
hrs storage	24.00		

Coke Day Bin		$ 39041 unit cost
	1 units	$ 39041 cost all units

ID SI-03 Salt Week Bin

The function of this equipment is to to store a week supply of salts for furnace

Stream No.:	81.00	Strm Name:	Salts Makeup
MTPY:	2185.09	MTPH	0.28
Design MTPH	0.36		
Temp.C:	25.40	Pressure(atm):	1.00
Max.Avail.MTPH:	5.00		
No.Units:	1.00		
Bin Type:	air-tight	Bin Material	fiber-glass
Bulk SG:	1.30		
Cubic Meters	35.87	Cubic Feet	1266.80
hrs storage	168.00		

Salt Week Bin		$ 9647	unit cost
1	units	$ 9647	cost all units

```
    ID   SI-04              Quick Lime Storage Bin

The function of this equipment is to to store a week supply of quick-lime

 Stream No.:      89.00                              Strm Name:       Lime

 MTPY:            1199.11                            MTPH             0.15
 Design MTPH      0.20

 Temp.C:          25.40                              Pressure(atm):   1.00
 Max.Avail.MTPH:  5.00

 No.Units:        1.00

 Bin Type:        live bottom                        Bin Material     carbon
steel
 Bulk SG:         1.00

 Cubic Meters     25.59                              Cubic Feet       903.74
 hrs storage      168.00

Quick Lime Storage Bin     $ 7403  unit cost
           1  units        $ 7403  cost all units
```

```
    ID   HP-01              Dust Transport Hoppers

The function of this equipment is to to take dust back to Blender BD-01

 Stream No.:     72.00                   Strm Name:      Recycle Dust

 MTPY:           3039.57                          MTPH            0.39
 Design MTPH     0.50

 Temp.C:         200.00                           Pressure(atm):  1.16
 Max.Avail.MTPH: 5.00

 No.Units:       1.00

Bin Type:       air-tight,top load, bottom unload
Bin Material    carbon steel
Bulk SG:        0.70

 Cubic Meters    2.21                             Cubic Feet      77.92
 hrs storage     4.00

Dust Transport Hoppers    $ 2298  unit cost
          1  units        $ 2298  cost all units
```

```
    ID   HP-02              Dust Disposal Supersacks

The function of this equipment is to to take waste dust off-site for
disposal


 Stream No.:      73.00                              Strm Name:       Dust to
Disposal


 MTPY:            337.73                             MTPH             0.04
 Design MTPH      0.06

 Temp.C:          200.00                             Pressure(atm):   1.16
 Max.Avail.MTPH:  1.00

 No.Units:        1.00


 Bin Type:        supersacks                         Bin Material
polyproylene
 Bulk SG:         0.70

 Cubic Meters     0.06                               Cubic Feet       2.16
 hrs storage      1.00

            Dust Disposal Supersacks  $ 1829  unit cost
                        1  units      $ 1829  cost all units
```

```
BINS                                Subtotal $: 110381
                      Accumulative Subtotal $: 110381
```

CONVEYORS

.....

ID CN-01 MgOH2 Conveyor from SH

The function of this equipment is to bring MgOH2 from SH to the SI-01 feed hopper

Stream No.:	65.00	Strm Name:	Mg(OH)2 from SH
MTPY:	500296.00	MTPH	63.55
Design MTPH	41.31		
Temp.C:	25.00	Pressure(atm):	1.49
Max.Avail.MTPH:	60.00		
No.Units:	2.00		
Conveyor Type:	belt	Belt Material	rubber
Bulk SG:	1.20		
Cubic Meters/hr	52.96	Cubic Feet/min	31.17
Length(ft)	300.00		

MgOH2 Conveyor from SH	$ 194235	unit cost
2 units	$ 388471	cost all units

ID CN-O2 MgOH2 Conveyor to Calcine

The function of this equipment is to bring the MgOH2 and recycle dust to the calciner.

Stream No.:	59.00	Strm Name:	Feed to Calciner
MTPY:	503335.60	MTPH	63.94
Design MTPH	83.12		
Temp.C:	26.06	Pressure(atm):	1.49
Max.Avail.MTPH:	100.00		
No.Units:	1.00		
Conveyor Type:	belt	Belt Material	rubber
Bulk SG:	1.20		
Cubic Meters/hr	53.28	Cubic Feet/min	31.36
Length(ft)	100.00		

MgOH2 Conveyor to Calcine		$ 98558
unit cost		
	1 units	$ 98558
cost all units		

ID CN-03 MgO Product Conveyor

The function of this equipment is to take the hot MgO product to a hopper feeding the furnace.

Stream No.:	71.00	Strm Name:	MgO Product
MTPY:	337730.30	MTPH	42.90
Design MTPH	27.89		
Temp.C:	940.00	Pressure(atm):	1.00
Max.Avail.MTPH:	50.00		
No.Units:	2.00		
Conveyor Type:	belt	Belt Material	ceramic
Bulk SG:	0.80		
Cubic Meters/hr	53.63	Cubic Feet/min	31.56
Length(ft)	300.00		

MgO Product Conveyor		$ 194235 unit cost
2	units	$ 388471 cost all units

ID CN-04 Coke to Boiler Conveyor

The function of this equipment is to take coke to the the boiler coke burner input.

Stream No.:	109.00	Strm Name:	Coke to Boiler
MTPY:	16834.72	MTPH	2.14
Design MTPH	2.78		
Temp.C:	25.40	Pressure(atm):	1.10
Max.Avail.MTPH:	100.00		
No.Units:	1.00		
Conveyor Type:	belt	Belt Material	rubber
Bulk SG:	2.30		
Cubic Meters/hr	0.93	Cubic Feet/min	0.55
Length(ft)	300.00		

Coke to Boiler Conveyor		$ 194235	unit cost
1	units	$ 194235	cost all units

ID CN-05 Coke to Preheater Conveyor

The function of this equipment is to take coke from the daybin to the preheater.

Stream No.:	67.00	Strm Name:	Coke to Coke Prhtr
MTPY:	124467.90	MTPH	15.81
Design MTPH	20.55		
Temp.C:	25.00	Pressure(atm):	1.49
Max.Avail.MTPH:	100.00		
No.Units:	1.00		
Conveyor Type:	belt	Belt Material	ceramic
Bulk SG:	2.30		
Cubic Meters/hr	6.87	Cubic Feet/min	4.05
Length(ft)	100.00		

Coke to Preheater Conveyor	$ 98558 unit cost
1 units	$ 98558 cost all units

ID CN-06 Preheated Coke Conveyor

The function of this equipment is to take preheated coke to a shoot feeding the furnace.

Stream No.:	87.00	Strm Name:	Preheated Coke
MTPY:	105326.60	MTPH	13.38
Design MTPH	8.70		
Temp.C:	630.00	Pressure(atm):	1.00
Max.Avail.MTPH:	20.00		
No.Units:	2.00		
Conveyor Type:	belt	Belt Material	ceramic
Bulk SG:	2.30		
Cubic Meters/hr	5.82	Cubic Feet/min	3.42
Length(ft)	100.00		

Preheated Coke Conveyor	$ 98558	unit cost
2 units	$ 197116	cost all units

ID CN-07 Salts Conveyor

The function of this equipment is to to deliver salts to electric furnace

Stream No.:	81.00	Strm Name:	Salts Makeup
MTPY:	2185.09	MTPH	0.28
Design MTPH	0.36		
Temp.C:	25.40	Pressure(atm):	1.00
Max.Avail.MTPH:	50.00		
No.Units:	1.00		
Conveyor Type:	belt	Belt Material	rubber or similar
Bulk SG:	1.00		
Cubic Meters/hr	0.28	Cubic Feet/min	0.16
Length(ft)	100.00		

Salts Conveyor		$ 98558 unit cost
1	units	$ 98558 cost all units

ID CN-08 Lime Conveyor

The function of this equipment is to to deliver lime to electric furnace

Stream No.:	89.00	Strm Name:	Lime
MTPY:	1199.11	MTPH	0.15
Design MTPH	0.20		
Temp.C:	25.40	Pressure(atm):	1.00
Max.Avail.MTPH:	50.00		
No.Units:	1.00		
Conveyor Type:	belt	Belt Material	rubber or similar
Bulk SG:	1.00		
Cubic Meters/hr	0.15	Cubic Feet/min	0.09
Length(ft)	100.00		

Lime Conveyor		$ 98558 unit cost
	1 units	$ 98558 cost all units

CONVEYORS Subtotal $:	1562528
Accumulative Subtotal $:	1672910

BLENDERS

ID BD-01 MgOH2/Dust Blender

The function of this equipment is to blend MgOH2 from SH and recycle dust

Stream No.:	74.00	Strm Name:	Feed to Blender
MTPY:	503335.60	MTPH	63.94
Design MTPH	41.56		
Temp.C:	26.06	Pressure(atm):	1.49
Max.Avail.MTPH:	50.00		
No.Units:	2.00		
Blender Type:		Blender Material	carbon steel
Bulk SG:	1.20		
Cubic Meters		Cubic Feet	0.00
hrs storage			

MgOH2/Dust Blender $ 9565 unit cost
2 units $ 19130 cost all units

.....

BLENDERS Subtotal $: 19130
Accumulative Subtotal $: 1692041

.....

BLOWERS

.....

ID BL-01 Baghouse Exhaust Blower

Blower Type:	Low Pressure	Blower Material	carbon steel
Bulk SG:	1.03		
Dsgn Act. CMPH	75236.15	Dsgn Act.CFM	44282.75
CMPY	915768100.00		
Dsgn Std. CMPH	50410.68	Dsgn Std.CFM	29670.89
PSIG	2.37		

The function of this equipment is to move gases from the baghouse to the stack.

Stream No.:	70.00	Strm Name:	Gases After BH
MTPY:	1001286.00	MTPH	127.20
Design MTPH	82.68		
Temp.C:	200.00	Pressure(atm):	1.16
Max.Avail.MTPH:	66.00		
No.Units:	2.00		

Baghouse Exhaust Blower		$ 136563	unit cost
2	units	$ 273126	cost all units

ID BL-02 Oxygen Blower to Calcine Circuit

Blower Type:	Low Pressure O2 Rated	Blower Material	Vendor Specified
Bulk SG:	1.11		
Dsgn Act. CMPH	12909.33	Dsgn Act.CFM	7598.22
CMPY	143226000.00		
Dsgn Std. CMPH	23652.66	Dsgn Std.CFM	13921.56
PSIG	14.70		

The function of this equipment is to supply oxygen to the MgOH2 calcining kiln and the coke preheater burners.

Stream No.:	51.00	Strm Name:	TTL O2 Supply
MTPY:	204374.20	MTPH	25.96
Design MTPH	16.88		
Temp.C:	25.00	Pressure(atm):	2.00
Max.Avail.MTPH:	33.00		
No.Units:	2.00		

Oxygen Blower to Calciner Circuit		
	$ 145265	unit cost
2 units	$ 290530	cost all units

ID BL-03 CO Blower from Coke Preheater

Blower Type:	Flamable Gases	Blower Material	carbon steel
Bulk SG:	0.84		
Dsgn Act. CMPH	15654.14	Dsgn Act.CFM	9213.77
CMPY	57316000.00		
Dsgn Std. CMPH	9465.30	Dsgn Std.CFM	5571.12
PSIG	14.70		

The function of this equipment is to move hot CO from coke preheater to CO scrubber in utilities

Stream No.:	54.00	Strm Name:	CO from Coke Htr
MTPY:	59486.32	MTPH	7.56
Design MTPH	4.91		
Temp.C:	630.00	Pressure(atm):	2.00
Max.Avail.MTPH:	10.00		
No.Units:	2.00		

CO Blower from Coke Preheater			
	$ 151350	unit cost	
2 units	$ 302700	cost all units	

ID **BL-04** **Gases from Caster Blower**

Blower Type:	Low Pressure	Blower Material	carbon steel
Bulk SG:	1.00		
Dsgn Act. CMPH	46623.99	Dsgn Act.CFM	27442.10
CMPY	517282200.00		
Dsgn Std. CMPH	42712.58	Dsgn Std.CFM	25139.91

The function of this equipment is to remove fumes from caster and area

Stream No.:	85.00	Strm Name:	Caster Off-Gases
MTPY:	665898.80	MTPH	84.59
Design MTPH	54.98		
Temp.C:	25.00	Pressure(atm):	1.00
Max.Avail.MTPH:	54.00		
No.Units:	2.00		

Gases from Caster Blower		$ 44971	unit cost
2	units	$ 89942	cost all units

ID BL-05 Air Blower for Boiler

Blower Type:	Medium Pressure	Blower Material	carbon steel
Bulk SG:	1.00		
Dsgn Act. CMPH	10814.81	Dsgn Act.CFM	6365.41
CMPY	182430300.00		
Dsgn Std. CMPH	30126.96	Dsgn Std.CFM	17732.22
PSIG	30.00		

The function of this equipment is to blower for air for boiler

Stream No.:	105.00	Strm Name:	Air to Boiler
MTPY:	234170.20	MTPH	29.75
Design MTPH	19.34		
Temp.C:	25.00	Pressure(atm):	3.04
Max.Avail.MTPH:	38.00		
No.Units:	2.00		

Air Blower for Boiler		$ 322801	unit cost
	2 units	$ 645602	cost all units

ID CM-01 CO Compressor

Blower Type:	High Pressure	Blower Material	carbon steel
Bulk SG:	0.91		
Dsgn Act. CMPH	7304.71	Dsgn Act.CFM	4299.43
CMPY	287263000.00		
Dsgn Std. CMPH	47439.27	Dsgn Std.CFM	27921.96
PSIG	100.00		

The function of this equipment is to compress the CO gas

Stream No.:	66.00	Strm Name:	CO from Compressor
MTPY:	328379.10	MTPH	41.71
Design MTPH	27.11		
Temp.C:	55.00	Pressure(atm):	7.80
Max.Avail.MTPH:	55.00		
No.Units:	2.00		

CO Compressor		$ 1148519	unit cost
2	units	$ 2297039	cost all units

ID BL-06 Stack Blower

Blower Type:	Low Pressure	Blower Material	carbon steel
Bulk SG:	1.03		
Dsgn Act. CMPH	62125.58	Dsgn Act.CFM	36566.08
CMPY	1810226000.00		
Dsgn Std. CMPH	149472.44	Dsgn Std.CFM	87976.98
PSIG	40.00		

The function of this equipment is to blow gases up the stack

Stream No.:	95.00	Strm Name:	Compressed Stack Gas
MTPY:	2174981.00	MTPH	276.29
Design MTPH	179.59		
Temp.C:	149.22	Pressure(atm):	3.72
Max.Avail.MTPH:	198.00		
No.Units:	2.00		

Stack Blower		$ 555621	unit cost
2	units	$ 1111243	cost all units

.....

BLOWERS Subtotal $: 5010184
Accumulative Subtotal $: 6702225

.....

BAGHOUSE

The function of this equipment is to to clean dust from the calciner exhaust

Basic Information
ID BH-01 Calciner Baghouse

Baghouse Type:	fan forced	Material	polypropylene
No.Units:	1.0		

Incoming Stream: Weight/time

Stream No.:	49.0	Strm Name:	Gas from Air Cooler
MTPY:	1004664.0		
MTPH	127.6	Design MTPH	165.9

Volume per unit time:

Dsgn Act.CMPH	225708.5	Dsgn Act.CFM	132848.2
CMPY	915768100.0	Dsgn Std. CMPH	151232.0
Dsgn Std.CFM	89012.7		

Temperature and Pressure

Temp.C	200.0		
P.(atm/abs):	1.2	PSIG	2.4

Dust from Baghouse:

Stream No.:	69.0	Strm Name:	Dust from BH
MTPY:	3377.3		
dust_MTPH	0.4	Design MTPH	0.6

Calciner Baghouse		$ 33017	unit cost
	1 units	$ 33017	cost all units

BAGHOUSE Subtotal $: 33018
Accumulative Subtotal $: 6735243

STACK

The function of this equipment is to distribute gases from plant into air.

Basic Information

ID	ST-01	Plant Stack	
Stack Type:	fan forced	Material	concrete
No.Units:	1.0		
Incoming Stream:	Weight/time		
Stream No.:	95.0	Strm Name:	Compressed Stack Gas
MTPY:	2174981.0		
MTPH	276.3	Design MTPH	359.2

Volume per unit time:

Dsgn Act.CMPH	124251.2	Dsgn Act.CFM	73132.2
CMPY	1810226000.0	Dsgn Std. CMPH	298944.9
Dsgn Std.CFM	175954.0		

Temperature and Pressure

Temp.C	149.2		
P.(atm/abs):	3.7	PSIG	40.0

Assumptions:

Stack Height(M)	100.0	Gas Velocity (m/s)	30.0
Stack Diam(m):	1.3		

Stack Exhaust

Stream No.:	99.0	Strm Name:	Stack Gases All
MTPY:	2174981.0		
MTPH	276.3		

Volume per unit time:

Dsgn Act.CMPH	124251.2	Dsgn Act.CFM	73132.2
CMPY	1810226000.0	Dsgn Std. CMPH	298944.9
Dsgn Std.CFM	175954.0		

Temperature and Pressure

Temp.C	149.2		
P.(atm/abs):	3.7	PSIG	40.0

Plant Stack		$ 648020	unit cost
1	units	$ 648020	cost all units

PLANT STACK Subtotal $: 648020
Accumulative Subtotal $: 7383263

INGOT CASTING

ID IC-01 Ingot Casting Machine

The function of this equipment is to to cast magnesium into ingots.

Magnesium Into Ingot Casters

Stm. No.	82.0	Strm.Name	Liquid Mg
Total Casting Through-put of Magnesium			
MTPY:	206467.7	MTPH	26.2
Design MTPH	34.1		
No.of Units	2.0		
MTPH/Unit	13.1		
SO2 Cover Gas into Caster			
Stream No.:	93.0	Strm Name:	SO2
MTPY:	2001.7		
MTPH	0.3	Design MTPH	0.3
Volume per unit time:			
Dsgn Act.CMPH:	3.09625960653648E-05		
Dsgn Act.CFM:	1.8224068000806E-05		
CMPY	0.2		
Dsgn Std. CMPH:	2.83650615529041E-05		
Design Std. Liters per hour:	2.83650615529041E-02		
Dsgn Std. CFM:	1.66952024790135E-05		
Temperature and Pressure			
Temp.C	25.0		
P.(atm/abs):	1.0	PSIG	0.0
Gas Exhaust from Casting Machine			
Stream No.:	85.0	Strm Name:	Caster Off-Gases
MTPY:	665898.8		
MTPH	84.6	Design MTPH	
Volume per unit time:			
Dsgn Act.CMPH	93248.0	Dsgn Act.CFM	54884.2
CMPY	517282200.0	Dsgn Std. CMPH	85425.2
Dsgn Std.CFM	50279.8		
Temperature and Pressure			
Temp.C	25.0		
P.(atm/abs):	1.0	PSIG	0.0

```
......... Magnesium Ingots from furnace ................

 Stream No.:      83.0                          Strm Name:      Mg Ingots
 MTPY:            200173.7
 MTPH             25.4                                Design MTPH     33.1
 Temp.C           25.0                                Pressure(atm)   1.0
 Ingots/hr        661.1                               Ingot Wt.Kg:    50.0
 Ingots/min       11.0

.........................................................................


                  Ingot Casting Machine     $ 500000  unit cost
                             1  units       $ 500000  cost all units









.........................................................................

INGOT CASTING                                    Subtotal $: 500000
                                  Accumulative Subtotal $: 7883263

.........................................................................
```

PUMPS

_____

ID PM-01 Boiler Feedwater Pump

The function of this equipment is to pump water thru HE to Boiler

Stream No.:	104.00	Strm Name:	H2O to Prhtr
MTPY:	5240876.00	MTPH	665.76
Design MTPH	865.49		
Temp.C:	25.00	Pressure(atm):	1.00
Max.Avail.MTPH:	5000.00		
No.Units:	1.00		
pump Type:	centrifugal	Pump Material	cast iron
Bulk SG:	1.00		
Cubic Meters/hr	665.76	Cubic Feet/min	391.86
GPM	2931.28		

Boiler Feedwater Pump	$ 13446	unit cost
1 units	$ 13446	cost all units

ID PM-02 CO Scrubber Pump

The function of this equipment is to circulate water thru CO scrubber via Stms 116,120,113.

Stream No.:	299.00	Strm Name:	
MTPY:	954406100.00	MTPH	121240.60
Design MTPH	7880.64		
Temp.C:	45.00	Pressure(atm):	1.00
Max.Avail.MTPH:	5000.00		
No.Units:	20.00		
pump Type:	centrifugal	Pump Material	cast iron
Bulk SG:	1.00		
Cubic Meters/hr	121235.60	Cubic Feet/min	71357.23
GPM	533787.74		

CO Scrubber Pump	$ 1794519	unit cost
20 units	$ 35890394	cost all units

ID PM-03 Caustic Pump

The function of this equipment is to add caustic to scrubber circuits via Strms 112 & 131.

Stream No.:	299.00	Strm Name:	
MTPY:	17769.42	MTPH	2.26
Design MTPH	2.93		
Temp.C:	25.00	Pressure(atm):	1.00
Max.Avail.MTPH:	5000.00		
No.Units:	1.00		
pump Type:	centrifugal	Pump Material	cast iron
Bulk SG:	1.00		
Cubic Meters/hr	2.26	Cubic Feet/min	1.33
GPM	9.94		

Caustic Pump		$ 3644	unit cost
1	units	$ 3644	cost all units

ID PM-04 Caster Scrubber Pump

The function of this equipment is to ciculate water thru Caster Scrubber, Strms 133 & 134

Stream No.:	299.00	Strm Name:	
MTPY:	9038372.00	MTPH	1148.17
Design MTPH	1492.62		
Temp.C:	30.25	Pressure(atm):	1.01
Max.Avail.MTPH:	5000.00		
No.Units:	1.00		
pump Type:	centrifugal	Pump Material	cast iron
Bulk SG:	1.00		
Cubic Meters/hr	1148.17	Cubic Feet/min	675.79
GPM	5055.26		

Caster Scrubber Pump		$ 20572 unit cost
1	units	$ 20572 cost all units

ID PM-05 Cooling Water Pumps

The function of this equipment is to circulate water thru the cooling water circuit.

Stream No.:	79.00	Strm Name:	H2O to HX
MTPY:	1040910.00	MTPH	132.23
Design MTPH	171.90		
Temp.C:	25.00	Pressure(atm):	1.00
Max.Avail.MTPH:	5000.00		
No.Units:	1.00		
pump Type:	centrifugal	Pump Material	cast iron
Bulk SG:	1.00		
Cubic Meters/hr	132.23	Cubic Feet/min	77.83
GPM	582.19		

Cooling Water Pumps	$ 5564	unit cost
1 units	$ 5564	cost all units

.....

PUMPS Subtotal $: 3.593362E+07
Accumulative Subtotal $: 4.381688E+07

.....

BOILERS

ID BP-01 Central Boiler

HX Type: coke slaker HX Material carbon steel

The function of this equipment is to make steam for the steam ejectors that pull a vacuum

Strm Name:Demin Water			
Water In:	103.0	Temp.C	34.7
Design MTPH	436.0		
Strm Name:Steam to Ht Exchgr			
Steam Made:	76.0	Temp.C	196.0
Design MTPH	435.5	Pressure(PSIG):	220.0
Strm Name:Air to Boiler			
Air In Stream:	105.0	Temp.C	25.0
Design MTPH	38.7		
Strm Name:Boiler Exhaust			
Exhaust Gas:	106.0	Temp.C	212.0
Design MTPH	42.0		

Central Boiler	$ 12512353	unit cost
3 units	$ 37537059	cost all units

.....

BOILERS Subtotal $: 3.753706E+07

Accumulative Subtotal $: 8.135394E+07

.....

STEAM EJECTORS

ID EJ-01 Vacuum Steam Ejectors

HX Type:	steam eductor	HX Material	cast iron

The function of this equipment is to pull a vacuum on the salt box furnace

Strm Name:Superheated Steam to			
Stream No.:	91.0	Temp.C	350.0
Pressure_PSIG	220.0	%CO	99.3
Total MTPH	335.0	Design MTPH	435.5
Strm Name:CO after HX			
Stmn. No.:	75.0	Temp.C	85.0
Pressure_Torr	68.4		
Ttl MTPH	29.9	Design MTPH	39.1
Strm Name:Steam & CO from Ejec			
Coolant Out:	78.0	Temp.C	328.1
Pressure	200.8		
Design MTPH	474.65		

Steam Ejector Details per Ejector

No.of Units	22.0	Steam lbs/hr design:	44100.0
Steam MTPH design	20.0		

Vacuum Steam Ejectors	$ 55666	unit cost
22 units	$ 1224653	cost all units

.....

Vacuum Steam Ejectors	Subtotal $: 1224656
	Accumulative Subtotal $: 8.25786E+07

.....

HEAT EXCHANGERS

ID HX-01 CO Gas Cooler

HX Type: tube&shell HX Material carbon steel
Bulk SG: 1.00

The function of this equipment is to cool the CO gas from the electric arc furnace before the eductor

Strm Name:H2O to HX
Coolant In: 79.00 Temp.C 25.00
Design MTPH 171.90

Strm Name:H2O from HX
Coolant Out: 80.00 Temp.C 65.00
Design MTPH 171.90

Strm Name:Gas from Salt Bath
Hot Process In: 77.00 Temp.C 750.00
Design MTPH 39.14

Strm Name:CO after HX
Process Out: 75.00 Temp.C 85.00
Design MTPH 39.00

Assumed Heat Transfer Coefficient: 122 kcal/(hr*M^2*C)

Log-Mean Temperature Differential: 256 C

Assumed Pressure Rating: 150 PSIG

Area Per HX: 219 sq.meters

CO Gas Cooler		$ 67098	unit cost
1	units	$ 67098	cost all units

ID HX-02 Boiler H2O Preheater

```
 HX Type:        tube&shell                          HX Material     carbon
steel
 Bulk SG:        1.00

The function of this equipment is to to preheat water for the boiler using
hot CO

Strm Name:H2O to Prhtr
Coolant In:     104.00                              Temp.C          25.00
Design MTPH     865.49


Strm Name:Demin Water
Coolant Out:    103.00                              Temp.C          34.70
Design MTPH     435.51

Strm Name:CO from Coke Htr
Hot Process In: 54.00                               Temp.C          630.00
 Design MTPH     9.82

Strm Name:CO after HE
Process Out:    55.00                               Temp.C          55.00
Design MTPH     9.00


Assumed Heat Transfer Coefficient: 122  kcal/(hr*M^2*C)

Log-Mean Temperature Differential: 189  C

Assumed Pressure Rating: 150  PSIG

Area Per HX: 183  sq.meters

                  Boiler H2O Preheater      $ 64178  unit cost
                            1  units        $ 64178  cost all units
```

ID HX-03 Compressed CO Cooler

```
 HX Type:        tube&shell                          HX Material     carbon
steel
 Bulk SG:        1.00

The function of this equipment is to to cool the compressed CO gas from the
scrubbers

Strm Name:Cooling H2O to CO Co
 Coolant In:     123.00                              Temp.C          25.00
 Design MTPH     14520.51

Strm Name:Hot H2O from CO Comp
 Coolant Out:    120.00                              Temp.C          45.00
 Design MTPH     14520.51


Strm Name:Scrubbed CO
 Hot Process In: 107.00                              Temp.C          322.61
Design MTPH     484.21


Strm Name:CO from Compressor
Process Out:    66.00                               Temp.C          55.00
Design MTPH     54.00


Assumed Heat Transfer Coefficient: 122  kcal/(hr*M^2*C)

Log-Mean Temperature Differential: 111  C

Assumed Pressure Rating: 150  PSIG

Area Per HX: 594  sq.meters

                     Compressed CO Cooler     $ 96966  unit cost
                               36  units      $ 3490806  cost all units

 ..........................................................................

HEAT EXCHANGERS                         Subtotal $: 3622080
                         Accumulative Subtotal $: 8.620068E+07

..........................................................................
```

TANKS

ID TK-01 Boiler Feedwater Tank

The function of this equipment is to to store feedwater for boiler.

Overall MTPY:	5240876.0	Overall MTPH:	666.0
Tk Size(CM)	288.0	No.Units	3.0
Tank Type:	water storage	Tank Material	carbon steel
SG	1.0	HRS Storage:	1.0
Cubic Feet	10188.0		

Stream In Information:

Strm.No.:	101.0	Strm.Name:	Boiler H2O Makeup
MTPY:	2637170.0	MTPH	335.0
CMPH:	335.0		
Temp.C:	25.0	Pressure(atm):	1.0
Strm.No.:	117.0	Strm.Name:	Condensate CO Compre
MTPY:	2603706.0	MTPH	331.0
CMPH:	330.8		
Temp.C:	25.0	Pressure(atm):	1.0

Boiler Feedwater Tank $ 74296 unit cost

3 units $ 222890 cost all units

ID TK-02 CO Scrubber Tank

The function of this equipment is to to store and circulate CO scrubber blow-down water

Overall MTPY:	866461248.0	Overall MTPH:	110069.0
Tk Size(CM)	298.0	No.Units	48.0
Tank Type:	Dirty Water Storage	Tank Material	carbon steel
SG	1.0	HRS Storage:	0.1
Cubic Feet	10528.0		

Stream In Information:

Strm.No.:	114.0	Strm.Name:	Scrubber Drain
MTPY:	778533952.0	MTPH	98899.0
CMPH:	98898.6		
Temp.C:	45.0	Pressure(atm):	1.0
Strm.No.:	120.0	Strm.Name:	Hot H2O from CO Comp
MTPY:	87927280.0	MTPH	11170.0
CMPH:	11169.6		
Temp.C:	45.0	Pressure(atm):	1.0
Strm.No.:	137.0	Strm.Name:	Process H2O CO Scrub
MTPY:	0.0	MTPH	0.0
CMPH:	0.0		
Temp.C:	25.0	Pressure(atm):	1.0

CO Scrubber Tank	$ 75701	unit cost
48 units	$ 3633694	cost all units

ID TK-03 Stack Scrubber Tank

The function of this equipment is to to store and circulate stack gas scrubber blowdown water

Overall MTPY:	9020640.0	Overall MTPH:	1146.0
Tk Size(CM)	149.0	No.Units	1.0
Tank Type:	dirty water storage	Tank Material	carbon steel
SG	1.0	HRS Storage:	0.1
Cubic Feet	5261.0		

Stream In Information:

Strm.No.:	**132.0**	Strm.Name:	Drain from Scubber 2
MTPY:	8100660.0	MTPH	1029.0
CMPH:	1029.0		
Temp.C:	25.0	Pressure(atm):	1.0
Strm.No.:	**131.0**	Strm.Name:	NaOH to Scrubber
MTPY:	184.0	MTPH	0.0
CMPH:	0.0		
Temp.C:	25.0	Pressure(atm):	1.0
Strm.No.:	**139.0**	Strm.Name:	Process H2O C.Scrub
MTPY:	919797.0	MTPH	117.0
CMPH:	116.8		
Temp.C:	25.0	Pressure(atm):	1.0

Stack Scrubber Tank	$ 53886	unit cost
1 units	$ 53886	cost all units

TANKS	Subtotal $: 3910472
	Accumulative Subtotal $: 9.011115E+07

.....

PRESSURE VESSELS

ID VS-01 CO Buffer Storage Vessel

The function of this equipment is to to buffer the flow of CO

Vessel Information

Overall MTPY:	328379.0	Overall MTPH:	42.0
Tk Size(CM)	244.0	No.Units	2.0
Tank Type:	Pressure Tank	Tank Material	carbon steel
Weight(lbs)	284243.2	Min. Storage:	5.0
Tank Size(CF)	8617.0		

Stream In Information:

Strm.No.:	66.0	Strm.Name:	CO from Compressor
MTPY:	328379.0	MTPH	42.0
Gas Vol(CM/min stp):	488.2	CM/min actual	75.2
Temp.C:	55.0	Pressure(atm):	7.8

CO Buffer Storage Vessel $ 483502 unit cost
2 units $ 967004 cost all units

.....

PRESSURE VESSELS Subtotal $: 967008
Accumulative Subtotal $: 9.107816E+07

.....

SCRUBBERS

ID SC-01 CO Scrubber

The function of this equipment is to to scrub the CO to remove particulates

Information of Incoming Gas Stream

Overall MTPY:	2933674.0	Overall MTPH:	373.0
CMPY:	3524589056.0	Standard CMPH:	447737.0
Actual CMPH:	67930.8	Avg.MW:	18.9
Standard CFM:	263530.8	Actual CFM:	39983.0

Information on Incoming Water Stream

MTPY water:	779830800.0	MTPH water	99063.9
Design MTPY:	1013780102.4	Design MTPH:	128783.0
GPM per unit	567070.3	Ttl Dsgn GPM	567070.3

Information on Number and Size of Each Scrubber

No.Units:	1.0	Unit CFM	51977.8
Water dMTPY:	1013780102.4	Water dMTPH:	128783.0
No.Stages:	1.0		

CO Scrubber		$ 38820 unit cost
1	units	$ 38820 cost all units

ID SC-02 Caster Scrubber

The function of this equipment is to to remove particulates and SO2 from Caster Off-Gases

Information of Incoming Gas Stream

Overall MTPY:	919797.0	Overall MTPH:	117.0
CMPY:	705870080.0	Standard CMPH:	89668.0
Actual CMPH:	100410.3	Avg.MW:	29.6
Standard CFM:	52777.4	Actual CFM:	59100.0

Information on Incoming Water Stream

MTPY water:	8118576.0	MTPH water	1031.3
Design MTPY:	10554148.2	Design MTPH:	1340.7
GPM per unit	5903.6	Ttl Dsgn GPM	5903.6

Information on Number and Size of Each Scrubber

No.Units:	1.0	Unit CFM	76829.8
Water dMTPY:	10554148.2	Water dMTPH:	1340.7
No.Stages:	2.0		

Caster Scrubber		$ 68003 unit cost
1	units	$ 68003 cost all units

SCRUBBERS Subtotal $: 106824

Accumulative Subtotal $: 9.118498E+07

KILNS

_____
ID KN-01 MgOH2 Calciner

The function of this equipment is to calcine the MgOH2 to MgO

..... Solids into Kiln .....

Stream No.:	59.00	Strm Name:	Feed to Calciner
MTPY:	503335.60	MTPH	63.94
Design MTPH	83.12		
Temp.C	26.06	Pressure(atm)	1.49
Commerc.MTPH	200.00		
No.Units:	1.00		

... Primary Fuel into Kiln ...

Stm. No.	66.00	Strm.Name	CO from Compressor
Bulk SG:	0.91		
Dsgn Act. CMPH	7304.71	Dsgn Act.CFM	4299.43
CMPY	287263000.00		
Dsgn Std. CMPH	47439.27	Dsgn Std.CFM	27921.96
PSIG	100.00	Temp.C	55.00

... Oxygen into Kiln ...

Stm. No.	58.00	Strm.Name	O2 to Calciner
MTPY:	164029.20	MTPH	20.84
Design MTPH	27.09		
Temp.C	25.00	Pressure(atm)	2.00

```
 Bulk SG:          1.11


 Dsgn Act. CMPH   10363.85                          Dsgn Act.CFM     6099.99
 CMPY             114984500.00

 Dsgn Std. CMPH   18988.80                          Dsgn Std.CFM
11176.49


 PSIG             14.70                             Temp.C           25.00


......... Solids out of Kiln .................
 Stream No.:      71.00              Strm Name:      MgO Product
 MTPY:            337730.30                         MTPH             42.90
 Design MTPH      55.77
 Temp.C           940.00                            Pressure(atm)    1.00
 No.Units:        1.00


............ Gases out of Kiln ..............

 Stm. No.         68.00                Strm.Name       Off-Gases Calciner
 MTPY:            674766.40                         MTPH             85.72
 Design MTPH      111.43
 Bulk SG:         1.22
 Dsgn Act. CMPH   370983.48            Dsgn Act.CFM    218354.69
 CMPY             505589600.00
 Dsgn Std. CMPH   83494.21             Dsgn Std.CFM    49143.30
 Temp.C           940.00


                     MgOH2 Calciner            $ 19893734  unit cost
                               1  units        $ 19893734  cost all units
```

ID KN-02 Coke Preheater

The function of this equipment is to preheat coke and make CO gas for fuel

..... Solids into Kiln .....

Stream No.:	67.00	Strm Name:	Coke to Coke Prhtr
MTPY:	124467.90	MTPH	15.81
Design MTPH	20.55		
Temp.C	25.00	Pressure(atm)	1.49
Commerc.MTPH	50.00		
No.Units:	1.00		

... Primary Fuel into Kiln ...

... Oxygen into Kiln ...

Stm. No.	52.00	Strm.Name	O2 to Coke Prhtr
MTPY:	40344.98	MTPH	5.13
Design MTPH	6.66		
Temp.C	25.00	Pressure(atm)	2.00
Bulk SG:	1.11		
Dsgn Act. CMPH	2545.48	Dsgn Act.CFM	1498.23
CMPY	28241490.00		
Dsgn Std. CMPH	4663.86	Dsgn Std.CFM	2745.07
PSIG	14.70	Temp.C	25.00

```
..... Solids out of Kiln ................

 Stream No.:      87.00                              Strm Name:
Preheated Coke

 MTPY:            105326.60                          MTPH            13.38
 Design MTPH      17.39

 Temp.C           630.00                             Pressure(atm)   1.00

 No.Units:        1.00

..... Gases out of Kiln ..............

 Stm. No.         54.00                              Strm.Name       CO from
Coke Htr

 MTPY:            59486.32                           MTPH            7.56
 Design MTPH      9.82

 Bulk SG:         0.84

 Dsgn Act. CMPH   15654.14                           Dsgn Act.CFM    9213.77
 CMPY             57316000.00

 Dsgn Std. CMPH   9465.30                            Dsgn Std.CFM    5571.12

 PSIG             14.70                              Temp.C          630.00

                                        Coke Preheater            $ 7801177
unit cost
                                                    1  units      $ 7801177
cost all units

KILNS                                 Subtotal $: 2.769491E+07
                          Accumulative Subtotal $: 1.188799E+08
```

ID SF-01 Salt Box Furnace

The function of this equipment is to collect the magnesium droplets into a pool of magnesium metal

..... Mg into Furnace with CO .....

Stm. No.	97.0	Strm.Name	Gas from E. Furnace

Furnace Through-put with Magnesium

MTPY:	202425.0	MTPH	25.7
Design MTPH	33.4		
No.of Units	1.0		
Residence Time(hrs):	2.0		

.....CO out of Furnace .....

Stm. No.	77.00	Strm.Name	Gas from Salt Bath
MTPY:	237017.50	MTPH	
Design MTPH			
Std.CMPH	23925.35	Act.CMPH	996159.00
Act.CFM	586322.58		
Act.CMPS	276.7	Dsgn Act.CMPS	359.7
P mm_Hg	68.4	Temp.C	750.0

..... salts into furnace .....

Stream No.:	81.00	Strm Name:	Salts Makeup
MTPY:	2185.09	MTPH	0.28
Design MTPH	0.36		
Temp.C	25.4	Pressure(atm)	1.0

..... Molten Magnesium out of furnace .....

Stream No.:	82.0	Strm Name:	Liquid Mg
MTPY:	206467.7		
MTPH	26.2	Design MTPH	34.1
Temp.C	750.0	Pressure(atm)	1.0

Furnace Details:

Dsgn Vol.M^3:	40.0	Cap.tonnes:	66.9

*Refers only to melt volume of furnace

Design Rate MTPH	34.1	Nominal Rate	26.2

Furnace Dimensions(meters)

Length	8.9	Width	4.5
Height	5.1	Melt Ht.	1.0
Salt Ht.	0.1	Headspace	4.0

Heat Exchanger ..Dimensions in meters:

HE Area	217.5		

*Assume CO in furnace and Steam in HX move counter-current

Temp. CO in	1850.0	Temp.Steam Out	350.0
Temp. CO out	750.0	Temp.Steam In	196.0
Pres.Steam in	16.0	Pres.Steam out	16.0
LMTD	949.7	Ht.Trans.Coeff	122.0

Heat Removed Per Hr (Kcal/hr)
24613480.2

Salt Box Furnace	$ 280242	unit cost
1 units	$ 280242	cost all units

SALT BOX FURNACE Subtotal $: 280240
Accumulative Subtotal $: 1.191601E+08

ELECTRIC ARC FURNACE

_____
ID EF-01 Electric Smelting Furnace

The function of this equipment is to heat and react MgO with coke to make Mg(v) and CO

.**..... Solids into Electric Furnace .....**

Stream No.:	71.00	Strm Name:	MgO Product
MTPY:	337730.30	MTPH	42.90
Design MTPH	25.74		
Temp.C In	940.00	Pressure(atm)	1.00
Commerc.MTPH	30.00		
No.Units:	2.00		

Metallurgical Coke Into Electric Furnace ...

Stream No.:	87.00	Strm Name:	Preheated Coke
MTPY:	105326.60	MTPH	13.38
Design MTPH	8.03		
Temp.C In	630.00	Pressure(atm)	1.00
Commerc.MTPH	30.00		

... Air into electric arc furnace ...

Stm. No.	88.00	Strm.Name	Air Ingress
MTPY:	160.83	MTPH	0.02
Design MTPH	0.01		
Temp.C	25.00	Pressure(atm)	1.00
Bulk SG:	1.00		
Dsgn Act. CMPH	10.42	Dsgn. Act.CFM	6.14
CMPY	125282.00		
Dsgn.Std. CMPH	9.55	Dsgn. Std.CFM	5.62
PSIG	0.00	Temp.C	25.00

..... Solids out of Electric Furnace .....

Stream No.:	90.00	Strm Name:	Slag Molten
MTPY:	2753.76	MTPH	0.02
Design MTPH	0.01		
Temp.C	1850.00	Pressure(atm)	1.00

..... Gases out of Electric Furnace .....

Stm. No.	97.00	Strm.Name	Gas from E. Furnace
MTPY:	441182.20	MTPH	56.04
Design MTPH	33.63		
Bulk SG:	0.97		
Dsgn Act. CMPH	112811.93	Dsgn Act.CFM	66399.22
CMPY	190327500.00		
Dsgn Std. CMPH	14506.67	Dsgn Std.CFM	8538.38
PSIG	0.00	Temp.C	1850.00
Power Factor%	65.00	Kwh/kg	9.54
# of Furnaces	2.00	MW	122.63
Mg Prod.tons	202425.00	KWH	1930741037.55

Electric Smelting Furnace $ 53295068 unit cost
2 units $ 106590137 cost all units

Electric Arc Furnaces Subtotal $: 1.065901E+08
Accumulative Subtotal $: 2.257503E+08

WASTEWATER TREATMENT PLANT

_____
ID WWTP-01 Waste Water Treatment Plant

The function of this equipment is to clean the waste water from the magnesium plant

Stream In Information:

Strm.No.:	144.0	Strm.Name:	Waste Water TTL
MTPY:	91194560.0	MTPH	11585.0
CMPH:	11584.6	GPM	2631.4
Design MTPY:		Design GPM	3157.6
Temp.C:	44.5	Pressure(atm):	1.0

Waste Water Treatment Plant $ 4542447 unit cost

1 units $ 4542447 cost all units

.....

Wastewater Treatment Plant Subtotal $: 4542448
Accumulative Subtotal $: 2.302927E+08

.....

COOLING TOWER

_____
ID CT-01 Cooling Tower

The function of this equipment is to cool the water used in various heat exchangers for cooling.

Stream In Information:

Strm.No.: from HX	80.0	Strm.Name:	H2O
MTPY:	1040910.0	MTPH	132.0
CMPH:	132.2	GPM	30.0
Design MTPY:		Design GPM	0.0
Temp.C:	65.0	Pressure(atm):	1.0

Stream Out Information:

Strm.No.: from HX		Strm.Name:	H2O
MTPY:	1040910.0	MTPH	132.0
CMPH:	132.2	GPM	30.0
Design MTPY:		Design GPM	0.0
Temp.C:	25.0	Pressure(atm):	1.0

Make-Up Water:

Strm.No.: from HX		Strm.Name:	H2O
MTPY:	104091.0	MTPH	13.0
CMPH:	13.2	GPM	3.0
Design MTPY:		Design GPM	0.0
Temp.C:	25.0	Pressure(atm):	1.0

Evaporation Water:

Strm.No.: from HX		Strm.Name:	H2O
MTPY:	104091.0	MTPH	13.0
CMPH:	13.2	GPM	3.0
Design MTPY:		Design GPM	0.0
Temp.C:	25.0	Pressure(atm):	1.0

Cooling Tower $ 7206 unit cost
1 units $ 7206 cost all units

.....

Cooling Tower Subtotal $: 7200
Accumulative Subtotal $: 2.302999E+08

.....